

APPLICATIONS OF THE ENANTIOSELECTIVE ALLYLIC ALKYLATION
TOWARD THE SYNTHESIS OF COMPLEX NATURAL PRODUCTS

Thesis by

Steven Anthony Loskot

In Partial Fulfillment of the Requirements for the Degree of
Doctor of Philosophy

CALIFORNIA INSTITUTE OF TECHNOLOGY

Pasadena, California

2019

(Defended May 3, 2019)

© 2019

Steven A. Loskot

All Rights Reserved

*To my family,
for their constant love and support*

ACKNOWLEDGEMENTS

Reflecting on the past 5 and half years of life at Caltech, I've learned that going it alone is not a possibility. There are so many people that I need to thank and acknowledge for their help and support that allowed me to reach this point in my life and achieved this surreal feat.

First I need to acknowledge Professor Brian Stoltz, my advisor, mentor, and friend. I was lucky to have such a kind and understanding advisor who knew exactly the right time to challenge and when to support me throughout my doctoral studies. It has been a pleasure working in his lab, and I would not be the scientist I am today without his guidance. It was great having such an active advisor as well. When he was in town over the summer, Brian made sure he was able to participate on our softball team "Ru-Tang Clan". Not only did he play softball, but also came out a couple times to play tennis with us as well as being our substitute for the volleyball team (we lost that game, but I'm not pointing any fingers). Needless to say, I cannot thank him enough for what he has done and the impact he has had on my life.

I would also like to thank the chair of my committee, Professor Sarah Reisman, for all her help and advice over the past five and half years at Caltech. Sarah, like Brian, always had her door open, and was willing to talk about chemistry anytime. I probably did not take advantage of this enough, but her insightful questions and advice during my formal presentation were immensely helpful and gave me a new perspective on the problems at hand. In addition, I am deeply appreciative of the valuable career advice the rest of my thesis committee, Professors Bob Grubbs and Theodor Agapie, have given me over my graduate career.

Of course, I wouldn't have even attended Caltech if it wasn't for the great mentorship and guidance I received at Seattle University from Professor Joe Langenan. Joe's passion for chemistry and teaching truly inspired me to be where I am today. At Seattle University I had the pleasure of meeting some of my closest friends, Leo Rozal and Nick Martinez, who have continued to support me through my doctoral studies. I also had the pleasure of research with Professor Neil Garg at UCLA prior to graduate school as an Amgen Scholar. Working in Neil's lab showed me firsthand what it would be like working in a top research institution and I cannot thank him enough for the opportunity and experience he gave me.

During my time at Caltech, I was extremely lucky to have had excellent mentors over the years. First I'd like to thank Rob Craig, whom I only overlapped with for about 6 months. During that time learned the Stoltz lab way and hopefully continued the tradition after he left. I'd also like to thank Matt Hesse for his constant support and willingness to talk about chemistry. Even though we were in different labs, he was always willing to set time aside and help. Finally I'd like to thank Eric Welin for his constant wisdom and seemingly endless knowledge of chemistry and sports.

During my time at Caltech, I was fortunate to be able to work with great project partners. First, I would like to thank Dr. Rob Craig, who asked me to join his project in my first year here. I need to thank Katerina Korch for working with me on the book chapter review as well as being one of the friendliest people I know. I also would like to thank Dr. David Romney and the Arnold lab for all their help in completing the total synthesis of nigelladine A. Without the use of directed evolution, the synthesis would have been significantly less impactful. Finally I'd like to thank Nick Hafeman, Chris Reimann, and

Dr. Beau Pritchett for putting up with me on the Scabtrain. Hopefully the Scabtrain will reach its final stop soon.

I'd like to thank every Stoltz group member, past and present, for their helpful discussions, thoughtfulness, and contributions to my development as a chemist. Specifically, I'd like to thank again everyone I have mention above, as well as David Schuman, Tyler Fulton, Nick Hafeman, Fa Ngamnithiporn, Austin Wright, Dr. Max Klatte, Dr. Marc Liniger, Dr. Wen-bo Liu, Dr. Jared Moore (creator of the "Dirty SAL" nickname), Dr. Gerit Potoschnig, and Dr. Marc Liniger. Moreover I'd like to thank David Schuman for being a great roommate for three-plus years and having to deal with me basically 24/7 during that time, and Tyler Fulton for being such a tolerant hoodmate.

Beyond the Stoltz lab, many thanks to the members past and present of the Reisman, Grubbs, and Fu labs for supporting the excellent collaborative atmosphere that is characteristic of the chemistry department at Caltech. I especially want to acknowledge Carson Matier, Alice Wong, Meaghan Deegan, Nina Gu, Chris Reed, and Dr. Nick Cowper for their friendship and comradery.

I want to thank all of the Caltech staff for all of their assistance and aide throughout the years, specifically Dr. Scott Virgil for all of his help maintaining the catalysis center, prepping numerous compounds, and helping me learn how to grow X-ray quality crystals. I'd also like to thank Scott and his wife Silva for hosting their Christmas party every year, which was always fun to attend. Additionally, Dr. David VanderVelde for his constant maintenance of the NMR lab as well as assistance in structure determination of a number of tricky diastereomers. I'd also like to thank Mike Takase and Larry Henling for their assistance with obtaining X-ray diffraction data, as well as Dr. Mona Shahgholi and

Naseem Torian for their tireless efforts with mass spectrometry. I would also like to thank Rick Gerhart and Jeff Groseth for their great work in the glass and electronic shops.

Finally, I need to acknowledge my family. Without them I know I would not be here completing my graduate studies. I always enjoyed when my family visited, and wished it happened more frequently than it did. I need to thank my brother for always being up for an adventure, whether it was to blow off steam and get drunk in Las Vegas or lounge around all day playing Crash Bandicoot and other video games. The life advice he has given me has helped me become the man I am today. I need to thank my mother, Annette, and late father, Victor, for being such wonderful parents. As they know I am not the most elegant writer, all I can say is that the person I am today and everything I have accomplished is because of you and your love. I also need to thank them for dealing with my late night phone calls on my walks back home from lab. I think family is the most important thing in life and I had the pleasure to expand my family during my doctoral studies by marrying the love of my life Danielle Loskot. There are no words that can describe the love and support I have received from her. Every day she is my rock and is what keeps me sane knowing that when I go home I get to see her. I also need to thank my in-laws, Thomas and Kelly Bright, for being so supportive and welcoming me into their family.

The work presented in this thesis would not have been possible without the never-ending support, friendship, and love from all of these people and many others I do not have space to name. To you all, thank you. I am eternally grateful.

ABSTRACT

The Stoltz group, and moreover the synthetic community at large, has long been interested in the development of methods for the synthesis of enantioenriched all-carbon quaternary stereocenters. This thesis present three projects all unified by the development and use of the palladium-catalyzed decarboxylative allylic alkylation to synthesize enantioenriched all-carbon quaternary stereocenter containing cyclopentanones as well as the natural product total synthesis.

An enantioselective total synthesis of the norditerpenoid alkaloid nigelladine A utilizing the asymmetric allylic alkylation to set the central all-carbon quaternary center is described. Strategically, the synthesis relies on a late-stage C–H oxidation of an advanced intermediate. While traditional chemical methods failed to deliver the desired outcome, an engineered cytochrome P450 enzyme was employed to effect a chemo- and regioselective allylic C–H oxidation in the presence of at least four oxidizable positions. The enzyme variant was readily identified from a focused library of three enzymes, allowing for completion of the synthesis without the need for extensive screening.

Lastly, we describe a unified synthetic approach toward scabrolide A. The first generation route to scabrolide A hinged upon the asymmetric allylic alkylation reaction to synthesis the key hydroxymethyl-*cis*-1,3-cyclopentenediol fragment. Ultimately, assembly of the tetracyclic scaffold is accomplished in a convergent manner from (−)-carvone and (−)-linalool. A key intramolecular Diels–Alder reaction and a photocatalytic [2+2]-ring expansion construct the [5,5,6,7] carbocyclic core of scabrolide A. Various other synthetic strategies, including transannular Diels–Alder and oxidative enolate coupling, are also discussed.

PUBLISHED CONTENT AND CONTRIBUTIONS

1. Craig, II, R. A. ‡; Loskot, S. A. ‡; Mohr, J. T.; Behenna, D. C.; Harned, A. M.; Stoltz, B. M. “Palladium-Catalyzed Enantioselective Decarboxylative Allylic Alkylation of Cyclopentanones” *Org. Lett.* **2015**, *17*, 5160–5163. DOI: 10.1021/acs.orglett.5b02376
S.A.L. participated in project design, experimental work, data acquisition and analysis, and manuscript preparation.
2. Korch, K.; Loskot, S. A.; Stoltz, B. M. (**2017**) *Asymmetric Synthesis of Quaternary Stereocenters via Metal Enolates*. In PATAI’S Chemistry of Functional Groups, Rappoport, Z. (Ed.). doi: 10.1002/9780470682531.pat0858.
S.A.L. participated in book chapter preparation, including the introduction and asymmetric allylic alkylation section. S.A.L. performed the editing process, as well as updating this review to 2018.
3. Loskot, S. A.; Romney, D. K.; Arnold, F. H.; Stoltz, B. M. “Enantioselective Total Synthesis of Nigelladine A via Late-Stage C–H Oxidation Enabled by an Engineered P450 Enzyme” *J. Am. Chem. Soc.* **2017**, *139*, 10196–10199. DOI: 10.1021/jacs.7b05196.
S.A.L. lead project design, experimental work, data acquisition and analysis, and manuscript preparation.

TABLE OF CONTENTS

Acknowledgements	iv
Abstract	viii
Published Content and Contributions	ix
Table of Contents	x
List of Figures	xvi
List of Schemes.....	xxv
List of Tables.....	xxix
List of Abbreviations	xxxiv

CHAPTER 1 1 *Asymmetric Synthesis of Quaternary Stereocenters via Metal Enolates*

1.1	Introduction	1
1.2	Enolate Types and Their Formation	3
1.2.1	Alkali and Alkaline Earth Metal Enolates	4
1.2.2	Silyl Enol Ethers	6
1.2.3	Boron Enolates.....	9
1.2.4	Transition Metal Enolates.....	11
1.3	Aldol Reaction	12
1.3.1	Introduction.....	12
1.3.2	Rhodium-Catalyzed Reactions	12
1.3.3	Palladium-, Platinum-, and Nickel-Catalyzed Reactions.....	13
1.3.4	Scandium- and Neodymium-Catalyzed Reactions	15
1.3.5	Reactions Proceeding Through Boron Enolates	17
1.4	Mannich Reaction	18
1.4.1	Introduction.....	18
1.4.2	Copper-Catalyzed Reactions.....	19
1.4.3	Palladium-Catalyzed Reactions.....	19
1.4.4	Scandium-Catalyzed Reactions.....	22
1.4.5	Nickel-Catalyzed Reactions.....	23
1.4.6	Lithium-Catalyzed Reactions	23
1.4.7	Calcium-Catalyzed Reactions	25

1.5.	Conjugate Addition and Michael Reaction	25
1.5.1	Michael Additions Involving Potassium Enolates.....	25
1.5.2	Michael Additions Involving Cobalt Enolate	26
1.5.3	Michael Additions Involving Nickel Enolates.....	28
1.5.4	Michael Additions Involving Copper Enolates.....	31
1.5.5	Michael Additions Involving Europium Enolates	32
1.5.6	Michael Additions Involving Rhodium Enolates.....	33
1.5.7	Michael Additions Using Lanthanum–BINOL Complexes.....	36
1.5.8	Michael Additions Involving Platinum and Iron Enolates.....	41
1.5.9	Michael Additions Involving Palladium Enolates.....	42
1.5.10	Michael Additions Involving Scandium and Yttrium Enolates	47
1.5.11	Michael Additions Involving Calcium Enolates	49
1.5.12	Conjugate Addition Reactions Involving Manganese Enolates	50
1.6	Allylic Alkylation.....	51
1.6.1	Introduction.....	51
1.6.2	Palladium-Catalyzed Asymmetric Allylic Alkylations of Non-Stabilized Enolates	52
1.6.3	Molybdenum-Catalyzed Asymmetric Allylic Alkylations	59
1.6.4	Iridium-Catalyzed Allylic Alkylations	60
1.6.5	Rhodium-Catalyzed Allylic Alkylations	63
1.6.6	Nickel-Catalyzed Allylic Alkylations	64
1.7	Miscellaneous Alkylations	64
1.7.1	Asymmetric Alkylations of Chromium Enolates.....	64
1.7.2	Asymmetric Alkylations of Lithium Enolates	66
1.8	α -Arylation and α -Alkenylation.....	67
1.8.1	Introduction.....	67
1.8.2	Palladium-Catalyzed Reactions.....	68
1.8.3	Nickel-Catalyzed Reactions.....	79
1.8.4	Copper-Catalyzed Reactions.....	83
1.9	Pericyclic Reactions	84
1.9.1	Claisen-Type Reactions	84
1.9.2	Conia-Ene Reactions	88
1.10	Notes and References.....	93

CHAPTER 2 **109**
Palladium-Catalyzed Enantioselective Decarboxylative Allylic Alkylation of Cyclopentanones

2.1	Introduction	109
2.2	Initial Reaction Optimization.....	111
2.3	Exploration of Reaction Scope	114
2.4	Adapting the Low Catalyst Loading Allylic Alkylation	118
2.5	Conclusion	118
2.6	Experimental Methods and Analytical Data	119
2.6.1	Materials and Methods.....	119
2.6.2	Experimental Procedures	121
2.6.3	Methods for the Determination of Enantiomeric Excess.....	154
2.6.4	Notes and References.....	156

APPENDIX 1 **161**
Spectra Relevant to Chapter 2

CHAPTER 3 **217**
Enantioselective Total Synthesis of Nigelladine A via Late-Stage C–H Oxidation Enabled by an Engineered P450 Enzyme

3.1	Introduction	217
3.2	Retrosynthetic Analysis.....	219
3.3	Synthesis of Cross-Coupling Fragments.....	220
3.4	Cross-Coupling and Elaboration to the Carbocyclic Core	222
3.5	Chemical Oxidation of Desoxy-Nigelladine A	224
3.6	Enzymatic Oxidation of Desoxy-Nigelladine A	225
3.7	Conclusion	228
3.8	Experimental Methods and Analytical Data	228
3.8.1	Materials and Methods	228
3.8.2	Protocols for Protein Expression and Lysis	230
3.8.3	Experimental Procedures	231
3.8.4	Enzymatic Screens and Enantiomer Screen.....	246
3.8.5	Chemical Oxidation Tables	248
3.8.6	Comparison of Natural and Synthetic Nigelladine A	250

3.8.7	Notes and References.....	251
APPENDIX 2 <i>Synthetic Summary of Chapter 3</i>		256
APPENDIX 3 <i>Spectra Relevant of Chapter 3</i>		258
APPENDIX 4 <i>X-Ray Crystallography Reports Relevant to Chapter 3</i>		285
A4.1	X-Ray Crystal Structure Analysis of Triene 401	286
A4.2	Notes and References.....	316
CHAPTER 4 <i>Progress Toward the Total Synthesis of Scabrolide A</i>		317
4.1	Introduction	317
4.2	Retrosynthetic Analysis; Transannular Diels–Alder.....	318
4.3	Synthesis of Convergent Coupling Fragments.....	319
4.4	Fragment Coupling and Ring Closing Metathesis.....	321
4.5	Retrosynthetic Analysis; Oxidative Enolate Coupling.....	324
4.6	Second Generation Synthesis of the Cyclopentene Diol Fragment.....	325
4.7	Alkyne Synthesis and Fragment Coupling	327
4.8	Intramolecular Diels–Alder Reaction and Late-Stage Functionalization	327
4.9	Third Generation Retrosynthetic Analysis; Ring Expansion	329
4.10	Synthesis of [2+2] Precursor.....	330
4.11	[2+2] Photocycloaddition and Ring Expansion.....	331
4.12	Future Directions.....	333
4.13	Conclusion	334
4.14	Experimental Methods and Analytical Data	334
4.14.1	Material and Methods	334
4.14.2	Experimental Procedures	336
4.14.3	Notes and References.....	369

APPENDIX 5	372
<i>Synthetic Summary for Chapter 4</i>	

APPENDIX 6	377
<i>Spectra Relevant to Chapter 4</i>	

APPENDIX 7	444
<i>X-Ray Crystallography Reports Relevant to Chapter 4</i>	

A7.1	X-Ray Crystal Structure Analysis of Tetracycle 452	445
A7.2	X-Ray Crystal Structure Analysis of Cyclobutane 465	465
A7.3	X-Ray Crystal Structure Analysis of Cyclobutane 466	485
A7.4	X-Ray Crystal Structure Analysis of Cycloheptane 468	503
A7.5	Notes and References.....	528

APPENDIX 8	529
<i>Alternative Strategy Toward the Total Synthesis of Scabrolide A</i>	

A8.1	Alternative Approach to Scabrolide A.....	529
A8.2	Synthesis of Diisopropyl Carbamate	530
A8.3	Umpolung Aldehyde Addition	531
A8.4	Experimental Methods and Analytical Data	531
A8.4.1	Materials and Methods	531
A8.4.2	Experimental Procedures	533
A8.4.3	Notes and References.....	538

APPENDIX 9	539
<i>Spectra Relevant to Appendix 8</i>	

APPENDIX 10	546
<i>Notebook Cross-Reference for New Compounds</i>	

A10.1	Contents.....	546
A10.2	Notebook Cross-Reference Tables.....	546

Comprehensive Bibliography	552
Index	581
About the Author.....	588

LIST OF FIGURES

CHAPTER 1

Asymmetric Synthesis of Quaternary Stereocenters via Metal Enolates

Figure 1.1.1. Commonly Mislabeled Tetrasubstituted C-Centers.....	2
Figure 1.1.2. Natural Products Containing Quaternary Centers Possessing Potent Biological Activities	2
Figure 1.3.2.1. Transition State of Zwitterionic (Enolato)Rhodium Intermediate	13
Figure 1.3.3.1. Scope of Palladium- and Platinum-Catalyzed Hydroxymethylation of Substituted β -Ketoesters	14
Figure 1.5.7.1 Proposed Mechanism of the Lanthanum-BINOL Complex-Catalyzed Asymmetric Michael Reaction.....	37
Figure 1.6.2.1. Representative Products of the Palladium-Catalyzed Asymmetric Allylic Alkylation Reaction Developed by Stoltz and Coworkers	55
Figure 1.6.2.2. Scope of Chiral Ferrocenylphosphine-Palladium Complex-Catalyzed Allylic Alkylation.....	59
Figure 1.8.2.1. Aminophosphine and Desamino Ligands for α -Vinylation.....	69
Figure 1.8.2.2. Proposed Mechanism of Palladium-Catalyzed Intramolecular α -Arylation Reaction Forming Oxindoles	74
Figure 1.8.2.3. NHC Ligands Screened in Intramolecular α -Arylation Reaction Reported by Kond, Aoyama, and Coworkers	76

CHAPTER 2

Palladium-Catalyzed Enantioselective Decarboxylative Allylic Alkylation of Cyclopentanones

Figure 2.1.1. Natural Products Characterized by Cyclopentane Rings Containing Chiral All-Carbon Quaternary Centers	111
---	-----

APPENDIX 1

Spectra Relevant to Chapter 2

Figure A1.1. ^1H NMR (400 MHz, CDCl_3) of compound 331	162
---	-----

Figure A1.2. Infrared spectrum (Thin Film, NaCl) of compound 331	163
Figure A1.3. ^{13}C NMR (101 MHz, CDCl_3) of compound 331	163
Figure A1.4. ^1H NMR (400 MHz, CDCl_3) of compound 332	164
Figure A1.5. Infrared spectrum (Thin Film, NaCl) of compound 332	165
Figure A1.6. ^{13}C NMR (101 MHz, CDCl_3) of compound 332	165
Figure A1.7. ^1H NMR (400 MHz, CDCl_3) of compound 336	166
Figure A1.8. Infrared spectrum (Thin Film, NaCl) of compound 336	167
Figure A1.9. ^{13}C NMR (101 MHz, CDCl_3) of compound 336	167
Figure A1.10. ^1H NMR (400 MHz, CDCl_3) of compound 339	168
Figure A1.11. Infrared spectrum (Thin Film, NaCl) of compound 339	169
Figure A1.12. ^{13}C NMR (101 MHz, CDCl_3) of compound 339	169
Figure A1.13. ^1H NMR (400 MHz, CDCl_3) of compound 346	170
Figure A1.14. Infrared spectrum (Thin Film, NaCl) of compound 346	171
Figure A1.15. ^{13}C NMR (101 MHz, CDCl_3) of compound 346	171
Figure A1.16. ^1H NMR (400 MHz, CDCl_3) of compound 347	172
Figure A1.17. Infrared spectrum (Thin Film, NaCl) of compound 347	173
Figure A1.18. ^{13}C NMR (101 MHz, CDCl_3) of compound 347	173
Figure A1.19. ^1H NMR (400 MHz, CDCl_3) of compound 348	174
Figure A1.20. Infrared spectrum (Thin Film, NaCl) of compound 348	175
Figure A1.21. ^{13}C NMR (101 MHz, CDCl_3) of compound 348	175
Figure A1.22. ^1H NMR (400 MHz, CDCl_3) of compound 349	176
Figure A1.23. Infrared spectrum (Thin Film, NaCl) of compound 349	177
Figure A1.24. ^{13}C NMR (101 MHz, CDCl_3) of compound 349	177
Figure A1.25. ^1H NMR (400 MHz, CDCl_3) of compound 351	178
Figure A1.26. Infrared spectrum (Thin Film, NaCl) of compound 351	179
Figure A1.27. ^{13}C NMR (101 MHz, CDCl_3) of compound 351	179
Figure A1.28. ^1H NMR (400 MHz, CDCl_3) of compound 353	180
Figure A1.29. Infrared spectrum (Thin Film, NaCl) of compound 353	181
Figure A1.30. ^{13}C NMR (101 MHz, CDCl_3) of compound 353	181
Figure A1.31. ^1H NMR (400 MHz, CDCl_3) of compound 354	182
Figure A1.32. Infrared spectrum (Thin Film, NaCl) of compound 354	183
Figure A1.33. ^{13}C NMR (101 MHz, CDCl_3) of compound 354	183
Figure A1.34. ^1H NMR (400 MHz, CDCl_3) of compound 355	184
Figure A1.35. Infrared spectrum (Thin Film, NaCl) of compound 355	185
Figure A1.36. ^{13}C NMR (101 MHz, CDCl_3) of compound 355	185

Figure A1.37. ^1H NMR (400 MHz, CDCl_3) of compound 359	186
Figure A1.38. Infrared spectrum (Thin Film, NaCl) of compound 359	187
Figure A1.39. ^{13}C NMR (101 MHz, CDCl_3) of compound 359	187
Figure A1.40. ^1H NMR (400 MHz, C_6D_6) of compound 361	188
Figure A1.41. Infrared spectrum (Thin Film, NaCl) of compound 361	189
Figure A1.42. ^{13}C NMR (101 MHz, C_6D_6) of compound 361	189
Figure A1.43. ^1H NMR (400 MHz, CDCl_3) of compound 363	190
Figure A1.44. Infrared spectrum (Thin Film, NaCl) of compound 363	191
Figure A1.45. ^{13}C NMR (101 MHz, CDCl_3) of compound 363	191
Figure A1.46. ^1H NMR (400 MHz, CDCl_3) of compound 364	192
Figure A1.47. Infrared spectrum (Thin Film, NaCl) of compound 364	193
Figure A1.48. ^{13}C NMR (101 MHz, CDCl_3) of compound 364	193
Figure A1.49. ^1H NMR (400 MHz, CDCl_3) of compound 365	194
Figure A1.50. Infrared spectrum (Thin Film, NaCl) of compound 365	195
Figure A1.51. ^{13}C NMR (101 MHz, CDCl_3) of compound 365	195
Figure A1.52. ^1H NMR (400 MHz, CDCl_3) of compound 366	196
Figure A1.53. Infrared spectrum (Thin Film, NaCl) of compound 366	197
Figure A1.54. ^{13}C NMR (101 MHz, CDCl_3) of compound 366	197
Figure A1.55. ^1H NMR (400 MHz, CDCl_3) of compound 367	198
Figure A1.56. Infrared spectrum (Thin Film, NaCl) of compound 367	199
Figure A1.57. ^{13}C NMR (101 MHz, CDCl_3) of compound 367	199
Figure A1.58. ^1H NMR (400 MHz, CDCl_3) of compound 370	200
Figure A1.59. Infrared spectrum (Thin Film, NaCl) of compound 370	201
Figure A1.60. ^{13}C NMR (101 MHz, CDCl_3) of compound 370	201
Figure A1.61. ^1H NMR (400 MHz, CDCl_3) of compound 377	202
Figure A1.62. Infrared spectrum (Thin Film, NaCl) of compound 377	203
Figure A1.63. ^{13}C NMR (101 MHz, CDCl_3) of compound 377	203
Figure A1.64. ^{19}F NMR (470 MHz, CDCl_3) of compound 377	204
Figure A1.65. ^1H NMR (400 MHz, CDCl_3) of compound 378	205
Figure A1.66. Infrared spectrum (Thin Film, NaCl) of compound 378	206
Figure A1.67. ^{13}C NMR (101 MHz, CDCl_3) of compound 378	206
Figure A1.68. ^1H NMR (400 MHz, CDCl_3) of compound 379	207
Figure A1.69. Infrared spectrum (Thin Film, NaCl) of compound 379	208
Figure A1.70. ^{13}C NMR (101 MHz, CDCl_3) of compound 379	208
Figure A1.71. ^1H NMR (400 MHz, CDCl_3) of compound 380	209

Figure A1.72. Infrared spectrum (Thin Film, NaCl) of compound 380	210
Figure A1.73. ^{13}C NMR (101 MHz, CDCl_3) of compound 380	210
Figure A1.74. ^1H NMR (400 MHz, CDCl_3) of compound 382	211
Figure A1.75. Infrared spectrum (Thin Film, NaCl) of compound 382	212
Figure A1.76. ^{13}C NMR (101 MHz, CDCl_3) of compound 382	212
Figure A1.77. ^1H NMR (400 MHz, CDCl_3) of compound 383	213
Figure A1.78. Infrared spectrum (Thin Film, NaCl) of compound 383	214
Figure A1.79. ^{13}C NMR (101 MHz, CDCl_3) of compound 383	214
Figure A1.80. ^1H NMR (400 MHz, CDCl_3) of compound 384	215
Figure A1.81. Infrared spectrum (Thin Film, NaCl) of compound 384	216
Figure A1.82. ^{13}C NMR (101 MHz, CDCl_3) of compound 384	216

CHAPTER 3

Enantioselective Total Synthesis of Nigelladine A via Late-Stage C–H Oxidation Enabled by an Engineered P450 Enzyme

Figure 3.1.1. Structures of Nigelladines A–C and Nigellaquinomine	218
---	-----

APPENDIX 3

Spectra Relevant of Chapter 3

Figure A3.1. ^1H NMR (400 MHz, CDCl_3) of compound 395	259
Figure A3.2. Infrared spectrum (Thin Film, NaCl) of compound 395	260
Figure A3.3. ^{13}C NMR (101 MHz, CDCl_3) of compound 395	260
Figure A3.4. ^1H NMR (500 MHz, CDCl_3) of compound 396	261
Figure A3.5. Infrared spectrum (Thin Film, NaCl) of compound 396	262
Figure A3.6. ^{13}C NMR (126 MHz, CDCl_3) of compound 396	262
Figure A3.7. ^1H NMR (500 MHz, CDCl_3) of compound 393	263
Figure A3.8. Infrared spectrum (Thin Film, NaCl) of compound 393	264
Figure A3.9. ^{13}C NMR (126 MHz, CDCl_3) of compound 393	264
Figure A3.10. ^1H NMR (500 MHz, CDCl_3) of compound 392	265
Figure A3.11. Infrared spectrum (Thin Film, NaCl) of compound 392	266
Figure A3.12. ^{13}C NMR (126 MHz, CDCl_3) of compound 392	266
Figure A3.13. ^1H NMR (400 MHz, CDCl_3) of compound 397	267
Figure A3.14. Infrared spectrum (Thin Film, NaCl) of compound 397	268
Figure A3.15. ^{13}C NMR (101 MHz, CDCl_3) of compound 397	268

Figure A3.16. ^1H NMR (400 MHz, CDCl_3) of compound 391	269
Figure A3.17. Infrared spectrum (Thin Film, NaCl) of compound 391	270
Figure A3.18. ^{13}C NMR (101 MHz, CDCl_3) of compound 391	270
Figure A3.19. ^1H NMR (400 MHz, CDCl_3) of compound 400	271
Figure A3.20. Infrared spectrum (Thin Film, NaCl) of compound 400	272
Figure A3.21. ^{13}C NMR (101 MHz, CDCl_3) of compound 400	272
Figure A3.22. ^1H NMR (400 MHz, CDCl_3) of compound 390	273
Figure A3.23. Infrared spectrum (Thin Film, NaCl) of compound 390	274
Figure A3.24. ^{13}C NMR (101 MHz, CDCl_3) of compound 390	274
Figure A3.25. ^1H NMR (400 MHz, CDCl_3) of compound 401	275
Figure A3.26. Infrared spectrum (Thin Film, NaCl) of compound 401	276
Figure A3.27. ^{13}C NMR (101 MHz, CDCl_3) of compound 401	276
Figure A3.28. ^1H NMR (400 MHz, CDCl_3) of compound 389	277
Figure A3.29. Infrared spectrum (Thin Film, NaCl) of compound 389	278
Figure A3.30. ^{13}C NMR (101 MHz, CDCl_3) of compound 389	278
Figure A3.31. ^1H NMR (400 MHz, CDCl_3) of compound 385	279
Figure A3.32. Infrared spectrum (Thin Film, NaCl) of compound 385	280
Figure A3.33. ^{13}C NMR (101 MHz, CDCl_3) of compound 385	280
Figure A3.34. ^1H NMR (400 MHz, C_6D_6) of compound 385	281
Figure A3.35. ^{13}C NMR (101 MHz, C_6D_6) of compound 385	282
Figure A3.36. ^1H NMR (400 MHz, CD_3OD) of compound 385•DCl	283
Figure A3.37. ^{13}C NMR (101 MHz, CD_3OD) of compound 385•DCl	284

APPENDIX 4

X-Ray Crystallography Reports Relevant to Chapter 3

Figure A4.1.1. X-Ray Crystal Structure of Triene 401	286
---	-----

CHAPTER 4

Progress Toward the Total Synthesis of Scabrolide A

Figure 4.1.1. Select Examples of Polycyclic Furanobutenolide-Derived
--

Norcembranoid Diterpenes.....	318
-------------------------------	-----

APPENDIX 6

Spectra Relevant to Chapter 4

Figure A6.1. ^1H NMR (500 MHz, CDCl_3) of compound 422	378
Figure A6.2. ^{13}C NMR (126 MHz, CDCl_3) of compound 422	379
Figure A6.3. ^1H NMR (500 MHz, CDCl_3) of compound ent•416	380
Figure A6.4. ^{13}C NMR (126 MHz, CDCl_3) of compound ent•416	381
Figure A6.5. ^1H NMR (400 MHz, CDCl_3) of compound 423	382
Figure A6.6. Infrared spectrum (Thin Film, NaCl) of compound 423	383
Figure A6.7. ^{13}C NMR (101 MHz, CDCl_3) of compound 423	383
Figure A6.8. ^1H NMR (400 MHz, CDCl_3) of compound 430	384
Figure A6.9. ^{13}C NMR (101 MHz, CDCl_3) of compound 430	385
Figure A6.10. ^1H NMR (400 MHz, CDCl_3) of compound 432	386
Figure A6.11. Infrared spectrum (Thin Film, NaCl) of compound 432	387
Figure A6.12. ^{13}C NMR (101 MHz, CDCl_3) of compound 432	387
Figure A6.13. ^1H NMR (400 MHz, CDCl_3) of compound 434	388
Figure A6.14. Infrared spectrum (Thin Film, NaCl) of compound 434	389
Figure A6.15. ^{13}C NMR (101 MHz, CDCl_3) of compound 434	389
Figure A6.16. ^1H NMR (400 MHz, CDCl_3) of compound 441	390
Figure A6.17. Infrared spectrum (Thin Film, NaCl) of compound 441	391
Figure A6.18. ^{13}C NMR (101 MHz, CDCl_3) of compound 441	391
Figure A6.19. ^1H NMR (400 MHz, CDCl_3) of compound 442	392
Figure A6.20. Infrared spectrum (Thin Film, NaCl) of compound 442	393
Figure A6.21. ^{13}C NMR (101 MHz, CDCl_3) of compound 442	393
Figure A6.22. ^1H NMR (400 MHz, CDCl_3) of compound 470	394
Figure A6.23. Infrared spectrum (Thin Film, NaCl) of compound 470	395
Figure A6.24. ^{13}C NMR (101 MHz, CDCl_3) of compound 470	395
Figure A6.25. ^1H NMR (400 MHz, CDCl_3) of compound 443	396
Figure A6.26. Infrared spectrum (Thin Film, NaCl) of compound 443	397
Figure A6.27. ^{13}C NMR (101 MHz, CDCl_3) of compound 443	397
Figure A6.28. ^1H NMR (400 MHz, CDCl_3) of compound 444	398
Figure A6.29. Infrared spectrum (Thin Film, NaCl) of compound 444	399
Figure A6.30. ^{13}C NMR (101 MHz, CDCl_3) of compound 444	399
Figure A6.31. ^1H NMR (400 MHz, CDCl_3) of compound 445	400
Figure A6.32. Infrared spectrum (Thin Film, NaCl) of compound 445	401
Figure A6.33. ^{13}C NMR (101 MHz, CDCl_3) of compound 445	401

Figure A6.34. ^1H NMR (400 MHz, CDCl_3) of compound 446	402
Figure A6.35. Infrared spectrum (Thin Film, NaCl) of compound 446	403
Figure A6.36. ^{13}C NMR (101 MHz, CDCl_3) of compound 446	403
Figure A6.37. ^1H NMR (400 MHz, CDCl_3) of compound 447	404
Figure A6.38. Infrared spectrum (Thin Film, NaCl) of compound 447	405
Figure A6.39. ^{13}C NMR (101 MHz, CDCl_3) of compound 447	405
Figure A6.40. ^1H NMR (400 MHz, CDCl_3) of compound 448	406
Figure A6.41. Infrared spectrum (Thin Film, NaCl) of compound 448	407
Figure A6.42. ^{13}C NMR (101 MHz, CDCl_3) of compound 448	407
Figure A6.43. ^1H NMR (400 MHz, CDCl_3) of compound 449	408
Figure A6.44. Infrared spectrum (Thin Film, NaCl) of compound 449	409
Figure A6.45. ^{13}C NMR (101 MHz, CDCl_3) of compound 449	409
Figure A6.46. ^1H NMR (400 MHz, CDCl_3) of compound 450	410
Figure A6.47. Infrared spectrum (Thin Film, NaCl) of compound 450	411
Figure A6.48. ^{13}C NMR (101 MHz, CDCl_3) of compound 450	411
Figure A6.49. ^1H NMR (400 MHz, CDCl_3) of compound 451	412
Figure A6.50. Infrared spectrum (Thin Film, NaCl) of compound 451	413
Figure A6.51. ^{13}C NMR (101 MHz, CDCl_3) of compound 451	413
Figure A6.52. ^1H NMR (400 MHz, CDCl_3) of compound 452	414
Figure A6.53. Infrared spectrum (Thin Film, NaCl) of compound 452	415
Figure A6.54. ^{13}C NMR (101 MHz, CDCl_3) of compound 452	415
Figure A6.55. ^1H NMR (400 MHz, CDCl_3) of compound 437	416
Figure A6.56. Infrared spectrum (Thin Film, NaCl) of compound 437	417
Figure A6.57. ^{13}C NMR (101 MHz, CDCl_3) of compound 437	417
Figure A6.58. ^1H NMR (400 MHz, CDCl_3) of compound 453	418
Figure A6.59. Infrared spectrum (Thin Film, NaCl) of compound 453	419
Figure A6.60. ^{13}C NMR (101 MHz, CDCl_3) of compound 453	419
Figure A6.61. ^1H NMR (400 MHz, C_6D_6) of compound 454	420
Figure A6.62. Infrared spectrum (Thin Film, NaCl) of compound 454	421
Figure A6.63. ^{13}C NMR (101 MHz, C_6D_6) of compound 454	421
Figure A6.64. ^1H NMR (400 MHz, CDCl_3) of compound 455	422
Figure A6.65. Infrared spectrum (Thin Film, NaCl) of compound 455	423
Figure A6.66. ^{13}C NMR (101 MHz, CDCl_3) of compound 455	423
Figure A6.67. ^1H NMR (400 MHz, CDCl_3) of compound 458	424
Figure A6.68. Infrared spectrum (Thin Film, NaCl) of compound 458	425

Figure A6.69. ^{13}C NMR (101 MHz, CDCl_3) of compound 458	425
Figure A6.70. ^1H NMR (400 MHz, CDCl_3) of compound 461	426
Figure A6.71. Infrared spectrum (Thin Film, NaCl) of compound 461	427
Figure A6.72. ^{13}C NMR (101 MHz, CDCl_3) of compound 461	427
Figure A6.73. ^1H NMR (400 MHz, CDCl_3) of compound 462	428
Figure A6.74. Infrared spectrum (Thin Film, NaCl) of compound 462	429
Figure A6.75. ^{13}C NMR (101 MHz, CDCl_3) of compound 462	429
Figure A6.76. ^1H NMR (400 MHz, CDCl_3) of compound 463	430
Figure A6.77. Infrared spectrum (Thin Film, NaCl) of compound 463	431
Figure A6.78. ^{13}C NMR (101 MHz, CDCl_3) of compound 463	431
Figure A6.79. ^1H NMR (400 MHz, CDCl_3) of compound 464	432
Figure A6.80. Infrared spectrum (Thin Film, NaCl) of compound 464	433
Figure A6.81. ^{13}C NMR (101 MHz, CDCl_3) of compound 464	433
Figure A6.82. ^1H NMR (400 MHz, CDCl_3) of compound 457	434
Figure A6.83. Infrared spectrum (Thin Film, NaCl) of compound 457	435
Figure A6.84. ^{13}C NMR (101 MHz, CDCl_3) of compound 457	435
Figure A6.85. ^1H NMR (400 MHz, CDCl_3) of compound 465	436
Figure A6.86. Infrared spectrum (Thin Film, NaCl) of compound 465	437
Figure A6.87. ^{13}C NMR (101 MHz, CDCl_3) of compound 465	437
Figure A6.88. ^1H NMR (400 MHz, CDCl_3) of compound 466	438
Figure A6.89. Infrared spectrum (Thin Film, NaCl) of compound 466	439
Figure A6.90. ^{13}C NMR (101 MHz, CDCl_3) of compound 466	439
Figure A6.91. ^1H NMR (400 MHz, CDCl_3) of compound 456	440
Figure A6.92. Infrared spectrum (Thin Film, NaCl) of compound 456	441
Figure A6.93. ^{13}C NMR (101 MHz, CDCl_3) of compound 456	441
Figure A6.94. ^1H NMR (400 MHz, CDCl_3) of compound 468	442
Figure A6.95. Infrared spectrum (Thin Film, NaCl) of compound 468	443
Figure A6.96. ^{13}C NMR (101 MHz, CDCl_3) of compound 468	443

APPENDIX 7

X-Ray Crystallography Reports Relevant to Chapter 4

Figure A7.1.1. X-Ray Crystal Structure of Tetracycle 452	445
Figure A7.2.1. X-Ray Crystal Structure of Cyclobutane 465	465
Figure A7.3.1. X-Ray Crystal Structure of Cyclobutane 466	485

Figure A7.4.1. X-Ray Crystal Structure of Cycloheptane 468	503
---	-----

APPENDIX 9

Spectra Relevant to Appendix 8

Figure A9.1. ^1H NMR (400 MHz, CDCl_3) of compound 476	540
Figure A9.2. Infrared spectrum (Thin Film, NaCl) of compound 476	541
Figure A9.3. ^{13}C NMR (101 MHz, CDCl_3) of compound 476	541
Figure A9.4. ^1H NMR (400 MHz, CDCl_3) of compound 475	542
Figure A9.5. Infrared spectrum (Thin Film, NaCl) of compound 475	543
Figure A9.6. ^{13}C NMR (101 MHz, CDCl_3) of compound 475	543
Figure A9.7. ^1H NMR (400 MHz, CDCl_3) of compound 473	544
Figure A9.8. ^{13}C NMR (101 MHz, CDCl_3) of compound 473	545

LIST OF SCHEMES

CHAPTER 1

Asymmetric Synthesis of Quaternary Stereocenters via Metal Enolates

Scheme 1.2.1. Zimmerman-Traxler Transition States for

Aldol Reactions of (Z)- and (E)-Enolates.....	4
---	---

Scheme 1.2.1.1. Ireland's Model for Selective Enolate Geometry Formation	5
--	---

Scheme 1.2.1.2. Selective Ester Enolate Isomer Formation.....	6
---	---

Scheme 1.2.2.1. Standard Conditions for Silyl Enol Ether Formation.....	8
---	---

Scheme 1.2.4.1. Common Methods to Form Transition Metal Enolates.....	11
---	----

Scheme 1.2.4.2. Equilibrium Between Transition Metal Enolate Coordination Sites	12
---	----

Scheme 1.3.4.1. Proposed Catalytic Cycle of Scandium-Catalyzed Aldol Reaction.....	16
--	----

Scheme 1.3.5.1. Transition State and Substrate Scope of Aldol Reaction of Aldehydes and Stereochemically Defined Tetrasubstituted Enol Borinates	18
---	----

Scheme 1.4.5.1. Nickel-Catalyzed Asymmetric Reaction.....	23
---	----

Scheme 1.5.2.1. Cobalt-Catalyzed Asymmetric Michael Reaction Reported by Brunner and Hammer.....	27
---	----

Scheme 1.5.2.2. Cobalt-Catalyzed Asymmetric Michael Reaction Reported by Botteghi and Boga.....	28
--	----

Scheme 1.5.3.1. Nickel-Catalyzed Asymmetric Michael Reaction.....	29
---	----

Scheme 1.5.7.1. Lanthanum-BINOL Complex-Catalyzed Asymmetric Michael Reaction	37
---	----

Scheme 1.5.9.1. The First Palladium Catalyzed Asymmetric Michael Reaction Forming Quaternary Centers	42
---	----

Scheme 1.5.9.2. Palladium N-Heterocyclic Carbene Diaqua Complexes in Asymmetric Michael Reaction of β -Ketoesters and Methyl Vinyl Ketone.....	45
---	----

Scheme 1.5.11.1. Calcium-Octahydro-BINOL Complex-Catalyzed Asymmetric Michael Reaction	50
---	----

Scheme 1.6.2.1. Palladium Catalyzed Asymmetric Allylic Alkylation of Non-Stabilized Enolates Bearing Other Enolizable Positions Reported by Stoltz and Coworkers.....	52
--	----

Scheme 1.6.2.2. Proposed Mechanism of the Palladium-Catalyzed Asymmetric Allylic Alkylation Reaction	53
---	----

Scheme 1.6.2.3. Asymmetric Allylic Alkylation of Cyclobutanones and Protected Lactams	54
---	----

Scheme 1.7.2.1. Asymmetric Alkylation of Cyclic Lithium Enolates Utilizing Tetradentate Amine Ligands	66
Scheme 1.7.2.2. Asymmetric Alkylation of Acyclic Acids Using Tetradentate Amines.....	67
Scheme. 1.8.1.1. α -Arylation In the Synthesis of Cephalotaxinone (218).....	67
Scheme 1.8.2.1. NHC-Palladium Complex-Catalyzed Intramolecular α -Arylation.....	75
Scheme 1.8.2.2. Palladium-Catalyzed Intramolecular α -Arylation of Aldehydes Reported by Buchwald and Coworkers.....	77
Scheme 1.8.2.3. Palladium-Catalyzed Asymmetric α -Arylation of Ketones Using Aryl Triflates.....	79
Scheme 1.8.3.1. Nickel-Catalyzed Asymmetric α -Arylation of Indanones.....	80
Scheme 1.8.4.1. Copper-Catalyzed Asymmetric α -Arylation Reported by Ma and Coworkers	84
Scheme 1.9.1.1. Corey's Synthesis of (+)- β -Elemene	85
Scheme 1.9.1.2. Enantioselective Ireland-Claisen Rearrangement in Corey's Synthesis of Dolabellatrienone.....	85
Scheme 1.9.1.3. Asymmetric Claisen-Type Reaction Using Aluminum Reported by Krebs and Kazmaier.....	86
Scheme 1.9.1.4. Generic Asymmetric Ketene-Claisen Rearrangement	87
Scheme. 1.9.1.5. Asymmetric Ketene-Claisen Rearrangement.....	88
Scheme 1.9.2.1. Mechanism of the Conia-Ene Reaction.....	88
Scheme 1.9.2.2. Proposed Mechanism of Copper-Catalyzed Asymmetric Conia-Ene Reaction	91
Scheme 1.9.2.3. Use of Cooperative Catalysis in the Asymmetric Conia-Ene Reaction.....	92
Scheme 1.9.2.4. Iron-Catalyzed Asymmetric Conia-Ene Reported by Shaw and White	93

CHAPTER 2

Palladium-Catalyzed Enantioselective Decarboxylative Allylic Alkylation of Cyclopentanones

Scheme 2.1.1. Cyclic Ketone Substrates in Transition Metal-Catalyzed Enantioselective Decarboxylative Allylic Alkylation	110
Scheme 2.3.1. Substrate Scope of Cyclopentanone Substitution in Enantioselective Allylic Alkylation	116
Scheme. 2.3.2 Enantioselective Allylic Alkylation of Indanone Substrates	117
Scheme 2.3.3. Enantioselective Allylic Alkylation of Cyclopentanone Substrates with 2-Substituted Allyl Fragments	117
Scheme 2.4.1. Low Catalyst Loading Palladium(II)-Catalyzed Enantioselective Allylic Alkylation	118

CHAPTER 3*Enantioselective Total Synthesis of Nigelladine A via Late-Stage C–H Oxidation Enabled by an Engineered P450 Enzyme*

Scheme 3.2.1. Retrosynthetic Analysis of Nigelladine A	220
Scheme 3.3.1. Synthesis of Asymmetric Allylic Alkylation Precursor	221
Scheme 3.3.2. Synthesis of Electrophilic Cross-Coupling Fragment	221
Scheme 3.3.3. Synthesis of the Nucleophilic Cross-Coupling Fragment	222
Scheme 3.4.1. Cross-Coupling of Dienone 391 and Vinyl Boronic Ester 390	223
Scheme 3.4.2. Synthesis of the Tricyclic Core of Nigelladine A.....	224
Scheme. 3.6.1. Completion of the Synthesis of Nigelladine A.....	228

APPENDIX 2*Synthetic Summary of Chapter 3*

Scheme A2.1. Synthetic Summary for Construction of Nigelladine A 385	257
---	-----

CHAPTER 4*Progress Toward the Total Synthesis of Scabrolide A*

Scheme 4.2.1. Retrosynthetic Analysis of Scabrolide A via Transannular Diels–Alder	319
Scheme 4.3.1. Synthesis of Carvone Isocarvone.....	319
Scheme. 4.3.2. Synthesis of Alkyne 423 from Carvone.....	320
Scheme 4.3.3. 1 st Generation Synthesis of Cyclopentenyl Diol ent•415	321
Scheme 4.4.1. Convergent Coupling of RCM Precursor 430	322
Scheme 4.4.2. Ring-Closing Metathesis of Ester 430	323
Scheme 4.4.3. Intramolecular Diels–Alder of Ester 430	324
Scheme 4.5.1. 2 nd Generation Retrosynthetic Analysis of Scabrolide A	324
Scheme 4.5.2. Development of Modified Synthesis of Diol 415	325
Scheme 4.6.1. Terpene-Derived Synthesis Toward Diol 415	326
Scheme 4.6.2. Synthesis of Cyclopentene Diol 415	326
Scheme 4.7.1. Synthesis of Methyl Ketone Diels–Alder Precursor	327
Scheme 4.8.1. Unexpected Aldol Condensation of Tricycle 450	328
Scheme 4.8.2. Selective Oxidation of Deprotected Tricycle 437	329

Scheme 4.9.1. 3 rd Generation Retrosynthetic Analysis Utilizing Energy of a Strained Cyclobutane Ring.....	330
Scheme 4.10.1. Convergent Esterification of Diol 415 and Ester 460	330
Scheme 4.10.2. Diels–Alder and Oxidation of Model System 458	331
Scheme 4.11.1. [2+2] Cyclization of Enone 457	332
Scheme 4.11.2. Ring Expansion of Cyclobutanol 466	333
Scheme. 4.12.1. Future Directions Toward the Completion of Scabrolide A.....	334

APPENDIX 5

Synthetic Summary for Chapter 4

Scheme A5.1. Synthetic Summary for Construction of Tricycle 434	373
Scheme A5.2. Synthetic Summary for 2 nd Generation Synthesis of Diol 415	374
Scheme A5.3 Synthetic Summary for Undesired Aldol Products 451 and 452	375
Scheme A5.4 Synthetic Summary for Late-Stage Functionalization of Diels–Alder Adduct 453	375
Scheme A5.5 Synthetic Summary for Ring Expansion Model System 458	376

APPENDIX 8

Alternative Strategy Toward the Total Synthesis of Scabrolide A

Scheme A8.1.1. Retrosynthetic Analysis of Scabrolide A	530
Scheme A8.2.1. Derivatization of Weinreb Amide ent•422 to Carbamate 475	530
Scheme A8.3.1. Coupling of Carbamate 475 and Aldehyde 444	531

LIST OF TABLES

CHAPTER 1

Asymmetric Synthesis of Quaternary Stereocenters via Metal Enolates

Table 1.2.3.1. Enolate Selectivity Due to Leaving Group, Alkyl Substituents, and Amine Base	10
Table 1.3.2.1. Substrate Scope of Rhodium-Catalyzed Aldol Reaction.....	13
Table 1.3.3.1 Scope of Nickel-Catalyzed Hydroxymethylation Reaction of Substituted β -Ketoesters	15
Table 1.3.4.1. Substrate Scope of Scandium-Catalyzed Asymmetric Aldol Reaction	16
Table 1.3.4.2. Scope of Neodymium-Catalyzed Asymmetric Aldol Reaction.....	17
Table 1.4.2.1. Substrate Scope of Copper-Catalyzed Asymmetric Mannich Reaction	19
Table 1.4.3.1. Scope of Palladium-Catalyzed Asymmetric Mannich Reaction Reported by Sodeoka, and Coworkers.....	20
Table 1.4.3.2. Scope of Palladium-Catalyzed Mannich Reaction Reported by Kim and Coworkers.....	21
Table 1.4.3.3. Palladium-Catalyzed Mannich Reaction Reported by Shi and Coworkers.....	22
Table 1.4.4.1. Scandium-Catalyzed Asymmetric Mannich Reaction.....	23
Table 1.4.6.1 Scope of Lithium BINOLate-Catalyzed Asymmetric Mannich Reaction	24
Table 1.4.7.1. Scope of Calcium-Catalyzed Asymmetric Mannich Reaction.....	25
Table 1.5.3.1. Scope of Nickel-Diamine Catalyzed Asymmetric Michael Reaction.....	30
Table 1.5.3.2. Scope of Nickel-Diamine Catalyzed Conjugate Addition of 3-Substituted Oxindoles and Nitroolefins	31
Table 1.5.4.1. Copper(II)-Catalyzed Reaction of Methyl Vinyl Ketone and Methyl 1-Oxo-2-Indanecarboxylate	32
Table 1.5.6.1. Scope of the First Asymmetric Michael Reaction using Chiral Rhodium Catalysts.....	33
Table 1.5.6.2. Rhodium-Catalyzed Asymmetric Michael Reaction of α -Cyano Weinreb Amides.....	34
Table 1.5.6.3. Scope of Rhodium-Catalyzed Asymmetric Michael Reaction of α -Cyanocarboxylates	35
Table 1.5.6.4. First Example of Rhodium-Catalyzed Asymmetric Michael Reaction with β -Ketoesters	36

Table 1.5.7.1. LSB-Catalyzed Asymmetric Michael Reaction	38
Table 1.5.7.2. Lanthanum NR-Linked-BINOL-Catalyzed Asymmetric Michael Reaction	40
Table 1.5.7.3. Scope of Michael Reaction of Cyclic β -Ketoesters and Methyl Vinyl Ketone Using Podand-Type Alkali Metal 2'-Substituted 1,1'-Binaphthalene-2-Oxides.....	41
Table 1.5.9.1. Palladium Pincer Complex-Catalyzed Asymmetric Michael Reaction.....	43
Table 1.5.9.2. Palladium-Catalyzed Michael Reaction Reported by Sodeoka and Coworkers	44
Table 1.5.9.3. Palladium Diaqua Complex-Catalyzed Michael Reaction with α -Quinone Methides	46
Table 1.5.10.1. Chiral Scandium- N,N' -Dioxide-Catalyzed Asymmetric Michael Reaction	48
Table 1.5.10.2. Asymmetric Michael Reaction of 4-Substituted-5-Pyrazolones and 1,4-Dicarbonyl But-2-enes	49
Table 1.5.12.1. Homodinuclear Manganese-Schiff Base Complex-Catalyzed Conjugate Addition Reaction.....	51
Table 1.6.2.1. Asymmetric Allylic Alkylation of β -Ketoesters Using LDA, Palladium, and the Trost Ligand	56
Table 1.6.2.2. Formation of Aryl Substituted Cyclic Ketones Using NaHMDS, Allylpalladium(II) Chloride Dimer, a Trost Ligand, and Allyl Acetate	57
Table 1.6.2.3. Asymmetric Allylic Alkylation of Lithium Enolates in the Presence of a Tin Lewis Acid, Palladium Source, and a Trost Ligand	57
Table 1.6.2.4. 3-Aryloxindoles In the Asymmetric Allylic Alkylation Reaction.....	58
Table 1.6.2.5. Allyl Enol Carbonates In the Asymmetric Allylic Alkylation Reaction Using Trost Ligand 182	59
Table 1.6.3.1. Molybdenum-Catalyzed Asymmetric Allylic Alkylation	60
Table 1.6.4.1. Iridium-Catalyzed Intramolecular Allylic Alkylation Generating Six-Membered Rings.....	61
Table 1.6.4.2. Iridium-Catalyzed Intramolecular Allylic Alkylation Generating Five-Membered Rings.....	61
Table 1.6.4.3 Intermolecular Iridium-Catalyzed Allylic Alkylation to Generate Compounds Bearing Vicinal Quaternary and Tertiary Stereocenters	62
Table 1.6.5.1. Scope of the Rhodium-Catalyzed Asymmetric Allylic Alkylation of Acyclic Aldehydes.....	64
Table 1.7.1.1. Scope of Asymmetric Alkylation of Cyclic Tin Enolates Using Chromium Complexes.....	65
Table 1.7.1.2. Scope of Asymmetric Alkylation of Acyclic Tine Enolates Using Chromium Complexes	65

Table 1.8.2.1. Scope of Palladium BINAP-Catalyzed α -Arylation Reaction.....	68
Table 1.8.2.2. Scope of Palladium-Catalyzed α -Vinylation Reaction	70
Table 1.8.2.3. Scope of Palladium MOP-Derived Ligand-Catalyzed α -Arylation	71
Table 1.8.2.4. Scope of Palladium P-Chirogenic Binaphthyl Monophosphine Ligand-Catalyzed α -Arylation and α -Vinylation Reactions.....	71
Table 1.8.2.5. Scope of Palladium-Catalyzed α -Arylation and α -Vinylation of 3-Substituted Oxindoles	72
Table 1.8.2.6. Scope of Palladium-Catalyzed Intramolecular α -Arylation Reaction to Form Oxindoles.....	73
Table 1.8.2.7. Scope of Palladium Carbene Ligand-Catalyzed Intramolecular α -Arylation Reaction to Form Oxindoles	74
Table 1.8.2.8. Ligand Screen for Palladium-Catalyzed Intramolecular α -Arylation Reaction Reported by Kündig and Coworkers.....	76
Table 1.8.2.9. Scope of Asymmetric Intramolecular α -arylation of Aldehydes Forming Indanes.....	78
Table 1.8.3.1. Nickel-Catalyzed Intermolecular α -Heteroarylation of Cyclic Ketones	81
Table 1.8.3.2. Asymmetric α -Arylation of Lactones Using Nickel BINAP Catalysts	82
Table 1.8.3.3. Asymmetric Nickel Catalyzed α -Arylation Reaction Using P-Phos Ligand	83
Table 1.9.2.1. Scope of Palladium DTBM-SEGPHOS 64 Catalyzed Conia-Ene Reaction	89
Table 1.9.2.2. Scope of Copper-Catalyzed Asymmetric Conia-Ene Reaction	90

CHAPTER 2

Palladium-Catalyzed Enantioselective Decarboxylative Allylic Alkylation of Cyclopentanones

Table 2.2.1. PHOX Ligand Screen	112
Table 2.2.2. Solvent Effect on Enantiomeric Excess of Cyclopentanone Product (<i>S</i>)- 332	114

CHAPTER 3

Enantioselective Total Synthesis of Nigelladine A via Late-Stage C–H Oxidation Enabled by an Engineered P450 Enzyme

Table 3.5.1. Attempted Chemical Oxidations	225
Table 3.6.1. Screening of Focused Library for Allylic Oxidation	227
Table 3.8.5.1. Oxidations of Imine 389	248

Table 3.8.5.2. Oxidations of Enone 397	249
Table 3.8.6.1. Comparison of Synthetic and Natural Nigelladine A	250

APPENDIX 4

X-Ray Crystallography Reports Relevant to Chapter 3

Table A4.1.1. Experimental Details for X-Ray Structure Determination of Triene 401	287
Table A4.1.2. Crystal Data and Structure Refinement for Triene 401	288
Table A4.1.3. Atomic Coordinates ($\times 10^4$) and Equivalent Isotropic Displacement Parameters ($\text{\AA}^2 \times 10^3$) for Triene 401	289
Table A4.1.4. Bond Lengths [\AA] and angles [°] for Triene 401	291
Table A4.1.5. Anisotropic Displacement Parameters ($\text{\AA}^2 \times 10^3$) for Triene 401	306
Table A4.1.6. Hydrogen Coordinates ($\times 10^4$) and Isotropic Displacement Parameters ($\text{\AA}^2 \times 10^3$) for Triene 401	308
Table A4.1.7. Torsion Angles [°] for Triene 401	311
Table A4.1.8. Hydrogen Bonds for Triene 401 [\AA and °]	315

APPENDIX 7

X-Ray Crystallography Reports Relevant to Chapter 4

Table A7.1.1. Experimental Details for X-Ray Structure Determination of Tetracycle 452	446
Table A7.1.2. Crystal Data and Structure Refinement for Tetracycle 452	447
Table A7.1.3. Atomic Coordinates ($\times 10^4$) and Equivalent Isotropic Displacement Parameters ($\text{\AA}^2 \times 10^3$) for Tetracycle 452	448
Table A7.1.4. Bond Lengths [\AA] and angles [°] for Tetracycle 452	450
Table A7.1.5. Anisotropic Displacement Parameters ($\text{\AA}^2 \times 10^3$) for Tetracycle 452	457
Table A7.1.6. Hydrogen Coordinates ($\times 10^4$) and Isotropic Displacement Parameters ($\text{\AA}^2 \times 10^3$) for Tetracycle 452	459
Table A7.1.7. Torsion Angles [°] for Tetracycle 452	461
Table A7.1.8. Hydrogen Bonds for Tetracycle 452 [\AA and °]	464
Figure A7.2.1. X-Ray Crystal Structure of Cyclobutane 465	466
Table A7.2.2. Crystal Data and Structure Refinement for Cyclobutane 465	467
Table A7.2.3. Atomic Coordinates ($\times 10^4$) and Equivalent Isotropic Displacement Parameters ($\text{\AA}^2 \times 10^3$) for Cyclobutane 465	468
Table A7.2.4. Bond Lengths [\AA] and angles [°] for Cyclobutane 465	470

Table A7.2.5. Anisotropic Displacement Parameters ($\text{\AA}^2 \times 10^3$) for Cyclobutane 465	476
Table A7.2.6. Hydrogen Coordinates ($\times 10^4$) and Isotropic Displacement Parameters ($\text{\AA}^2 \times 10^3$) for Cyclobutane 465	478
Table A7.2.7. Torsion Angles [°] for Cyclobutane 465	480
Table A7.2.8. Hydrogen Bonds for Cyclobutane 465 [\AA and °]	484
Table A7.3.1. Experimental Details for X-Ray Structure Determination of Cyclobutane 466	486
Table A7.3.2. Crystal Data and Structure Refinement for Cyclobutane 466	487
Table A7.3.3. Atomic Coordinates ($\times 10^4$) and Equivalent Isotropic Displacement Parameters ($\text{\AA}^2 \times 10^3$) for Cyclobutane 466	488
Table A7.3.4. Bond Lengths [\AA] and angles [°] for Cycloheptane 466	490
Table A7.3.5. Anisotropic Displacement Parameters ($\text{\AA}^2 \times 10^3$) for Cyclobutane 466	496
Table A7.3.6. Hydrogen Coordinates ($\times 10^4$) and Isotropic Displacement Parameters ($\text{\AA}^2 \times 10^3$) for Cyclobutane 466	497
Table A7.3.7. Torsion Angles [°] for Cyclobutane 466	499
Table A7.3.8. Hydrogen Bonds for Cyclobutane 466 [\AA and °]	502
Table A7.4.1. Experimental Details for X-Ray Structure Determination of Cyclobutane 468	504
Table A7.4.2. Crystal Data and Structure Refinement for Cycloheptane 468	505
Table A7.4.3. Atomic Coordinates ($\times 10^4$) and Equivalent Isotropic Displacement Parameters ($\text{\AA}^2 \times 10^3$) for Cycloheptane 468	506
Table A7.4.4. Bond Lengths [\AA] and angles [°] for Cycloheptane 468	508
Table A7.4.5. Anisotropic Displacement Parameters ($\text{\AA}^2 \times 10^3$) for Cycloheptane 468	518
Table A7.4.6. Hydrogen Coordinates ($\times 10^4$) and Isotropic Displacement Parameters ($\text{\AA}^2 \times 10^3$) for Cycloheptane 468	520
Table A7.4.7. Torsion Angles [°] for Cycloheptane 468	522
Table A7.4.8. Hydrogen Bonds for Cycloheptane 468 [\AA and °]	527

APPENDIX 10

Notebook Cross-Reference for New Compounds

Table A10.2.1. Notebook Cross-Reference For Compounds in Chapter 2	546
Table A10.2.2. Notebook Cross-Reference For Compounds in Chapter 3	548
Table A10.2.3. Notebook Cross-Reference For Compounds in Chapter 4	549
Table A10.2.4. Notebook Cross-Reference For Compounds in Appendix 8.....	551

LIST OF ABBREVIATIONS

$[\alpha]_D$	specific rotation at wavelength of sodium D line
°C	degrees Celsius
Å	Ångstrom
Ac	acetyl
Acac	acetylacetone
AcOH	acetic acid
ADH	alcohol dehydrogenase
Adm	adamantyl
ALB	aluminum-lanthanum-BINOL complex
All	allyl
An	anisole
APCI	atmospheric pressure chemical ionization
app	apparent
aq	aqueous
Ar	aryl
atm	atmosphere
BINAP	2,2'-bis(diphenylphosphino)-1,1'-binaphthyl
BINOL	1,1-binaphthol
bmim	1-Butyl-3-methylimidazolium
Bn	benzyl
Boc	<i>tert</i> -butyloxycarbonyl
BOX	bis(oxazoline)
bp	boiling point
br	broad

Bu	butyl
Bz	benzoyl
<i>c</i>	concentration for specific rotation measurements (g/100 mL)
ca.	about (Latin circa)
calc'd	calculated
cat	catalytic
CDI	1,1'-carbonyldiimidazole
cm ⁻¹	wavenumber(s)
cod	1,5-cyclooctadiene
Cp	cyclopentadienyl
Cp*	pentamethyl-cyclopentadienyl
CSA	camphorsulfonic acid
Cy	cyclohexyl
d	doublet
D	deuterium
DABCO	1,4-diazabicyclo[2.2.2]octane
dba	dibenzylideneacetone
DBU	1,8-diazabicyclo[5.4.0]undec-7-ene
DCC	<i>N,N'</i> -Dicyclohexylcarbodiimide
DCE	1,2-dichloroethane
DCM	dichloromethane
DDQ	2,3-dichloro-5,6-dicyano- <i>p</i> -benzoquinone
DIBAL	diisobutylaluminum hydride
DIC	<i>N,N'</i> -Diisopropylcarbodiimide
DIFLUORPHOS	5,5'-Bis(diphenylphosphino)-2,2,2',2'-tetrafluoro- 4,4'-bi-1,3-benzodioxole

DIPEA	<i>N,N</i> -diisopropylethylamine
DMA	<i>N,N</i> -dimethylacetamide
DMAP	4-dimethylaminopyridine
dmdba	bis(3,5-dimethoxybenzylidene)acetone
DMDO	dimethyldioxirane
DME	1,2-dimethoxyethane
DMF	<i>N,N</i> -dimethylformamide
DMP	Dess–Martin periodinane
DMPU	<i>N,N'</i> -Dimethylpropyleneurea
DMS	dimethyl sulfide
DMSO	dimethyl sulfoxide
DPPA	diphenyl phosphoryl azide
dr	diastereomeric ratio
DTBM	di- <i>t</i> -butyl-methoxy
e.g.	for example (Latin exempli gratia)
EDC	<i>N</i> -(3-dimethylaminopropyl)- <i>N'</i> -ethylcarbodiimide
EDCI	1-ethyl-3-(3-dimethylaminopropyl)carbodiimide
<i>ee</i>	enantiomeric excess
EI+	electron impact
equiv	equivalent(s)
ESI	electrospray ionization
Et	ethyl
EtOAc	ethyl acetate
EWG	electron withdrawing group
FAB	fast atom bombardment
Fu	furanyl
g	gram(s)

G-I	Grubbs catalyst 1 st generation
G-II	Grubbs catalyst 2 nd generation
GC	gas chromatography
gCOSY	gradient-selected correlation spectroscopy
h	hour(s)
HG-II	Hoveyda-Grubbs catalyst 2 nd generation
hmim	2-methylimidazole
HMBC	heteronuclear multiple bond correlation
HMDS	1,1,1,3,3,3-hexamethyldisilazane
HMPA	hexamethylphosphoramide (HMPT)
HPLC	high-performance liquid chromatography
HRMS	high-resolution mass spectroscopy
HSQC	heteronuclear single quantum correlation
Hz	hertz
<i>hν</i>	light
<i>i-</i>	<i>iso-</i>
<i>i</i> -Pr	isopropyl
i.e.	that is (Latin id est)
IBX	2-iodoxybenzoic acid
IL-6	interleukin 6
IPA	isopropanol, 2-propanol
Ipc	diisopinocampheyl
IR	infrared (spectroscopy)
<i>J</i>	coupling constant
K	Kelvin(s) (absolute temperature)
kcal	kilocalorie
KP _{<i>i</i>}	potassium phosphate

L	liter; ligand
L*	chiral ligand
LDA	lithium diisopropylamide
LG	leaving group
lit.	literature value
LSB	lanthanum-sodium-BINOL
m	multiplet; milli
<i>m</i>	meta
M	metal; molar; molecular ion; Mega
<i>m</i> -CPBA	<i>meta</i> -chloroperoxybenzoic acid
<i>m/z</i>	mass to charge ratio
Me	methyl
mg	milligram(s)
min	minute(s)
MM	mixed method
MOC	methoxycarbonyl
mol	mole(s)
MOP	2-(diphenylphosphino)-2'-methoxy-1,1'-binaphthyl
mp	melting point
Ms	methanesulfonyl (mesyl)
MS	molecular sieves
MTBE	methyl <i>tert</i> -butyl ether
n	nano
N	normal
<i>n</i> -	<i>normal</i> -
NADP	nicotinamide adenine dinucleotide phosphate
Naph	naphthyl

NBS	<i>N</i> -bromosuccinimide
NHC	<i>N</i> -heterocyclic carbene
NMO	<i>N</i> -methylmorpholine <i>N</i> -oxide
NMR	nuclear magnetic resonance
Nu	nucleophile
<i>o</i>	ortho
<i>p</i>	para
P450	cytochrome P450
Pd/C	palladium on carbon
pen	pentyl
Ph	phenyl
pH	hydrogen ion concentration in aqueous solution
PHOX	phosphinoxazoline
Pin	2,3-dimethylbutane-2,3-diol (pinacol)
Piv	trimethylacetyl, pivaloyl
p <i>K</i> <i>a</i>	p <i>K</i> for association of an acid
pmdba	bis(4-methoxybenzylidene)acetone
PMP	<i>para</i> -methoxy phenyl
ppm	parts per million
PPTS	pyridinium <i>p</i> -toluenesulfonate
Pr	propyl
Proton sponge	1,8-bis(dimethylamino)naphthalene
Py	pyridine
q	quartet
R	generic for any atom or functional group
RCM	ring-closing metathesis
Ref.	reference

R_f	retention factor
RRCM	relay ring-closing metathesis
s	singlet
s-	<i>sec-</i>
sat.	saturated
SEGPPOS	5,5'-Bis(diphenylphosphino)-4,4'-bi-1,3-benzodioxole
SFC	supercritical fluid chromatography
Solv	solvent
t	triplet
<i>t</i> -	<i>tert</i> -
T-Hydro	70% TBHP in water
TBAF	tetrabutylammonium fluoride
TBAI	tetrabutylammonium iodide
TBAT	tetrabutylammonium difluorotriphenylsilicate
TBD	1,3,4-triazabicyclo[4.4.0]dec-5-ene
TBDPS	<i>tert</i> -butyldiphenylsilyl
TBHP	<i>tert</i> -butyl hydroperoxide
TBS	<i>tert</i> -butyldimethylsilyl
TES	triethylsilyl
Tf	trifluoromethanesulfonyl (triflyl)
TFA	trifluoroacetic acid
TFAA	trifluoroacetic anhydride
TFE	2,2,2-trifluoroethanol
THF	tetrahydrofuran
TIPS	triisopropylsilyl
TLC	thin-layer chromatography

TMEDA	<i>N,N,N',N'</i> -tetramethylethylenediamine
TMS	trimethylsilyl
TMP	tetramethylpiperidine
TOF	time-of-flight
Tol	tolyl
<i>t</i> R	retention time
TRAP	2,2"-bis[1 -(diphenylphosphino)ethyl]-1,1"-biferrocene
TRIS	tris(hydroxymethyl)aminomethane
Ts	<i>p</i> -toluenesulfonyl (tosyl)
UV	ultraviolet
<i>v/v</i>	volume to volume
Val	valine
w	weak
<i>w/v</i>	weight to volume
X	anionic ligand or halide
XPhos	2-dicyclohexylphosphino-2',4',6'-triisopropylbiphenyl
λ	wavelength
μ	micro

CHAPTER 1

Asymmetric Synthesis of

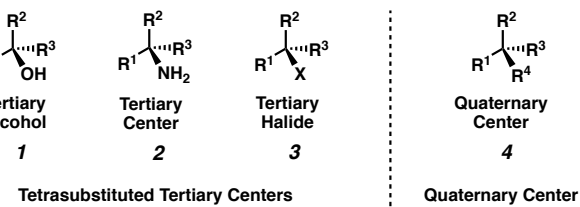
Quaternary Stereocenters via Metal Enolates[†]

1.1 INTRODUCTION

By definition, a quaternary center is a carbon atom bonded to four other carbon atoms by single bonds.^{1,2} Due to the multitude of names for quaternary centers—all-carbon quaternary centers, all-carbon quaternary carbon, quaternary compound, and quaternary carbon—some functional groups have been falsely labeled as quaternary centers in the literature. Common moieties that are misrepresented as quaternary centers include tertiary alcohols (**1**) and tertiary centers bonded to other heteroatoms (**2,3**). Quaternary centers as used in this chapter must have the general structure of compound **4**, where R¹–R⁴ are any carbon substituted group (Figure 1.1.1).

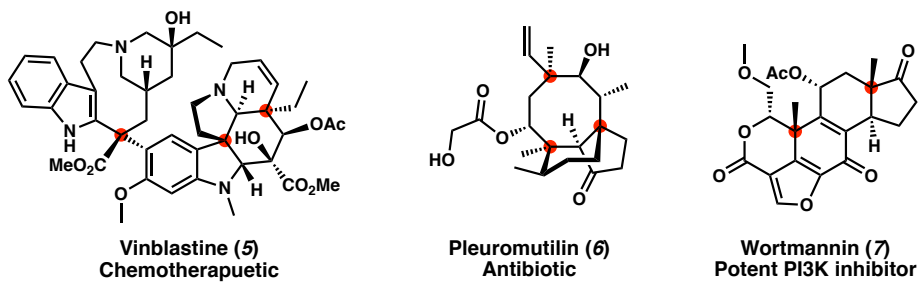
[†] This research was performed in collaboration with Katerina Korch, an alumni of the Stoltz group. Additionally, this research has been published and adapted with permission Korch, K. M., Loskot, S. A. and Stoltz, B. M. (2017). Asymmetric Synthesis of Quaternary Stereocenters via Metal Enolates. In PATAI'S Chemistry of Functional Groups, Z. Rappoport (Ed.). doi:10.1002/9780470682531.pat0858

Figure 1.1.1. Commonly Mislabeled Tetrasubstituted C-Centers



The ubiquitous nature of quaternary centers in pharmaceuticals and biologically active natural products (**5–7**) creates the need for their efficient and stereoselective synthesis.³ Because of their significance, the synthesis of chiral quaternary centers has garnered much attention in chemical research (Figure 1.1.2). Although great advances have been made, quaternary center synthesis remains an active research topic due to the difficulty of synthesizing and functionalizing these centers.⁴

Figure 1.1.2. Natural Products Containing Quaternary Centers Possessing Potent Biological Activities



Since all the substituents on a quaternary center are carbon-linked, there is a large steric encumbrance during the C–C bond-forming event compared to less substituted centers. Elevated steric congestion creates high-energy transition states that must be overcome with the use of harsh forcing conditions or catalytic methods. To accomplish this stereospecificity, an endogenous (e.g., chiral auxiliary) or exogenous (e.g., chiral catalyst) chiral source is needed.

In most cases, metal enolates are sufficiently strong nucleophiles to overcome the energy barrier required to form sterically hindered quaternary centers. Because of this, metal enolates are commonly employed in the asymmetric formation of quaternary centers at the α -position of a ketone, aldehyde, ester, or amide (α -quaternary centers). Moreover, enolates strongly coordinate with Lewis acids, thereby facilitating stereoinduction through the use of chiral Lewis acids. This chapter will review common methods to prepare metal enolates and, more importantly, the stereoselective synthesis of α -quaternary centers that they facilitate.

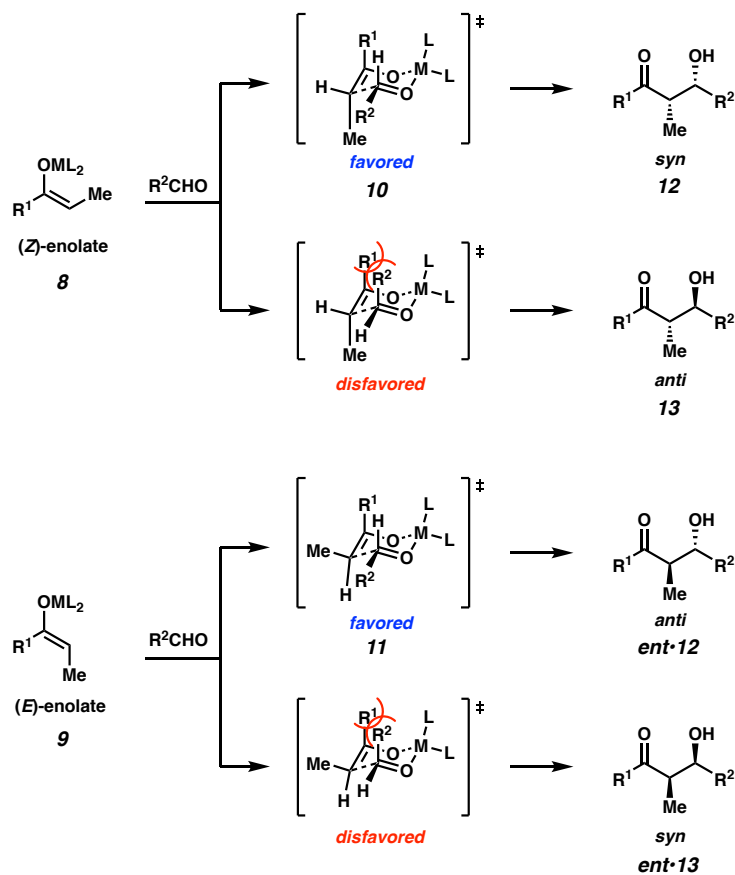
1.2 ENOLATE TYPES AND THEIR FORMATION

The most common method used to form enolates is through the α -deprotonation of a carbonyl compound. With an asymmetric ketone in hand, a regioselective deprotonation can occur depending on the conditions used.⁵ If the reaction is performed at low, typically below 0 °C, in aprotic ethereal solvents, and over short reaction times, deprotonation will occur at the most accessible position (i.e., lowest transition state energy) to obtain the so-called '*kinetic*' enolate. On the other hand, if the deprotonation is performed at warmer temperatures, in protic solvents, and over increased reaction times, the deprotonation is allowed to reach equilibrium and will form the thermodynamically stable enolate. Other factors must be taken into account when considering the stereoselectivity in enolate formation.

Metal enolates can exist in either the (Z)- or (E)- configuration (8 and 9 respectively, Scheme 1.2.1). Each stereoisomer has its own unique steric and electronic characteristics that dictate reactivity. Over the past several decades, the conditions needed to dictate enolate geometry have been extensively studied, particularly for the

diastereoselective aldol reaction.⁶ Both enolates form different Zimmerman–Traxler transition states, in order to minimize 1,3-diaxial interactions (**10** and **11**), ultimately resulting in the production of *syn*- (**12**) and *anti*- (**13**) diastereomers. Thermodynamic enolates predominantly exist in the *Z* conformation excluding the small- and mid-sized rings, in order to minimize A^{1,3}-strain.⁷ Kinetic enolates, on the other hand, depend on an array of variables, including base, solvent, counterion, co-solvents, and various additives.

Scheme 1.2.1. Zimmerman–Traxler Transition States for Aldol Reactions of (Z)- and (E)-Enolates

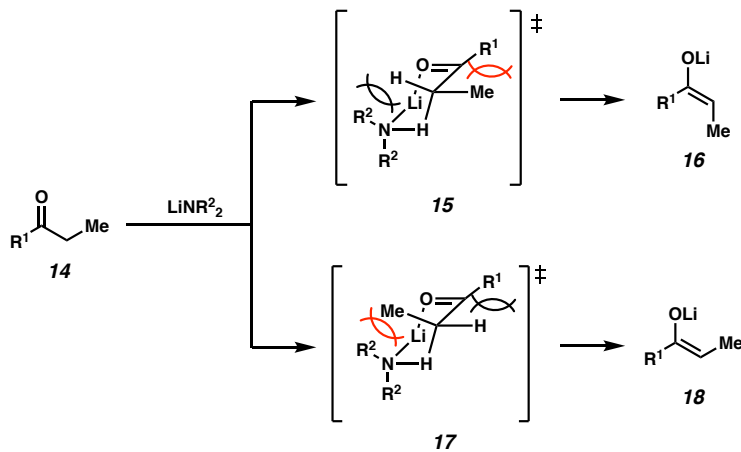


1.2.1 ALKALI AND ALKALINE EARTH METAL ENOLATES

Alkali metal bases are one of the most common reagents used to form kinetic enolates. Typical conditions employ subzero temperatures (-78°C), ethereal solvents, and

strong amide bases or metal hydrides. Common alkali bases include lithium diisopropylamide (LDA), lithium hexamethyldisilazide (LiHMDS), lithium 2,2,6,6-tetramethylpiperidine (LiTMP), lithium *t*-butyl-*t*-octyl amide (LOBA), lithium bis(dimethylphenylsilyl)amide, and *N*-*t*-butyl-*N*-tritylamide, as well as their sodium and potassium analogs. The first model used to describe the inherent selectivity of enolate formation was postulated by Ireland in 1975,⁸ and stated that the deprotonation occurred through a closed, chair-like transition state (Scheme 1.2.1.1). Ireland demonstrated that treating ketones **14** with strong bases LiNR²₂ can result in two potential closed transition states. When R¹ is small and R² is large, the steric interaction between R² and the methyl (Me) is greater than the interaction between R¹ and Me (transition state **15**). Consequently, the (*E*)-enolate **16**, is favored. On the other hand if R² is small and R¹ is large, the steric interaction between R¹ and Me is greater than the interaction between R² and Me (transition state **17**), and the (*Z*)-enolate **18** is favored.

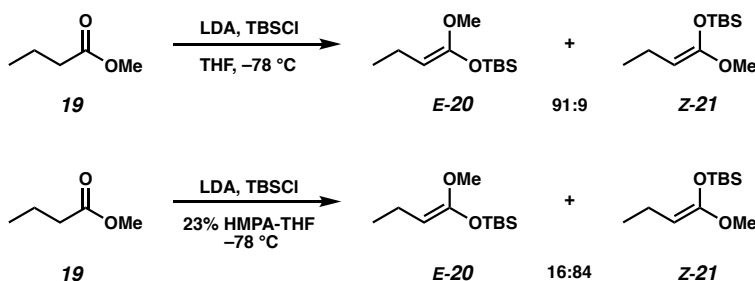
Scheme 1.2.1.1. Ireland's Model for Selective Enolate Geometry Formation



While the Ireland model is predictive for most systems, it is important to realize that it is a simple model. In reality, lithium amide bases can form aggregates in solutions;

usually di-, tetra-, or hexameric structures.⁹ Treatment of esters (e.g. **19**) and amides, with a strong alkali base, tends to result in the *E*- (**20**) and *Z*-enolates (**21**), respectively. It is possible, however, to reverse the selectivity of esters by adding a strong solvating co-solvent (i.e., HMPA), which can reverse this trend by disturbing the aggregates (Scheme 1.2.1.2), albeit with diminished selectivity.¹⁰

Scheme 1.2.1.2. Selective Ester Enolate Isomer Formation.



While alkali metal (Group 1) enolates are commonly used, their counterparts, alkali earth metal (Group 2) enolates, are far less common, largely due to their attenuated reactivity. These enolates can be formed by the same methods as the alkali enolates, using strong basic amides like bromomagnesium diisopropylamide.¹¹ Other methods of alkaline earth metal enolate formation include the transmetalation of lithium enolate by addition of a magnesium(II) salt,¹² the Cu-catalyzed conjugate addition of a Grignard reagent to an α,β -unsaturated ketone,¹³ or the insertion into an α -bromoketone.¹⁴

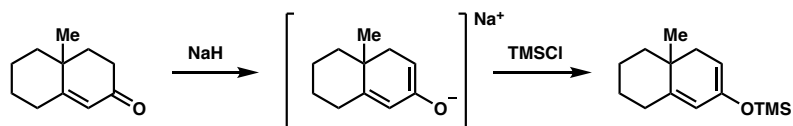
1.2.2 SILYL ENOL ETHERS

Silyl enol ethers are considered masked enolate equivalents. The increased stability allows these trapped or protected enolates to be carried through multiple steps in a synthesis.¹⁵ Another advantage is that silyl enol ether can be purified by distillation or column chromatography over neutralized silica. Because of the versatility of silyl enol ethers, chemists have developed various methods for their synthesis, under a variety of

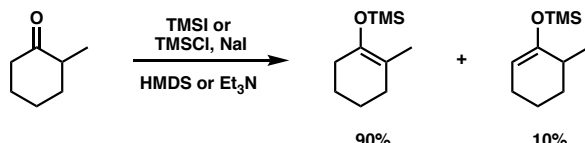
conditions, using a wide range of silyl sources (Scheme 1.2.2.1). These methods include silylation of enolates,¹⁶ silylation of enols,¹⁷ hydrosilylation of α,β unsaturated ketones,¹⁷ trapping the intermediate enolate formed during a 1,4-conjugate addition to an α,β -unsaturated ketone,¹⁸ isomerization of allyl silyl ethers,¹⁹ reaction of vinylolithiums with silyl peroxides,²⁰ simultaneous carbonylation and silylation of alkyl acetates,²¹ and Brook-like rearrangements.²² Common silylating reagents include silyl chlorides, silyl iodides (often formed *in situ*), and silyl triflates.

Scheme 1.2.2.1. Standard Conditions for Silyl Enol Ether Formation

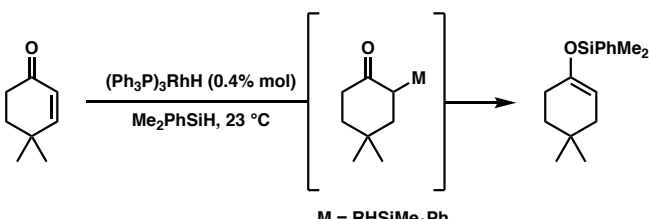
Enolate Silylation



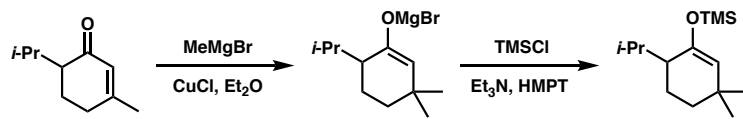
Enol Silylation



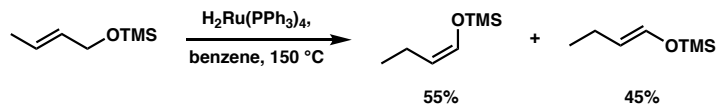
Enone Hydrosilylation



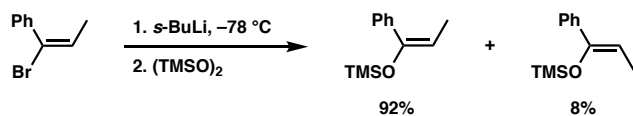
Enolate Trapping



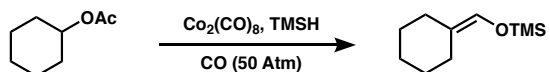
Olefin Isomerization



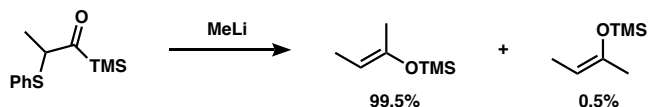
Vinyl Anion Quenching with Silyl Peroxide



Reductive Carbonylation



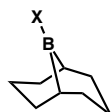
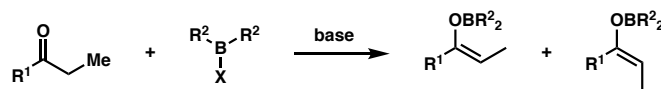
Brook-Type Rearrangement



1.2.3 BORON ENOLATES

While the versatility of boron enolates is significantly decreased compared to silyl vinyl ethers, boron enolates are heavily relied on in aldol, and aldol-like reactions.²³ The breadth of boron enolates has been extensively explored by Evans, Masamune, Mukaiyama, and Brown with their use in aldol chemistry, which shows excellent diastereo- and enantioselectivity. A considerable amount of research, performed by Evans, Masamune, Mukaiyama, and Brown, has enabled stereoselective boron enolate formation. Numerous factors play a role in forming boron enolates stereoselectively, including substituents on the ketone and boron precursor, the leaving group X on the latter, and the amine base (Table 1.2.3.1).²⁴

Table 1.2.3.1. Enolate Selectivity Due to Leaving Group, Alkyl Substituents, and Amine Base



22



23

Boron Source	X	R ¹	Base	Yield (%)	Z (%)	E (%)
22	OTf	t-Bu	NEt ₃	90	10	90
	Ms	t-Bu	NEt ₃	87	<3	>97
	I	t-Bu	NEt ₃	95	>97	<3
	Br	t-Bu	NEt ₃	94	<3	>97
	Cl	t-Bu	NEt ₃	94	<3	>97
	OTf	Ph	NEt ₃	97	>97	<3
	Ms	Ph	NEt ₃	96	>97	<3
	I	Ph	NEt ₃	98	>97	<3
	Br	Ph	NEt ₃	96	83	17
23	Cl	Ph	NEt ₃	97	52	48
	OTf	t-Bu	NEt ₃	85	<3	>97
	Ms	t-Bu	NEt ₃	66	<3	>97
	I	t-Bu	NEt ₃	96	>97	<3
	Br	t-Bu	NEt ₃	82	10	90
	Cl	t-Bu	NEt ₃	60	<3	>97
	OTf	Ph	NEt ₃	96	67	33
	OTf	Ph ^a	Hunigs	ND	>99	<1
	Ms	Ph	NEt ₃	95	62	38
	I	Ph	NEt ₃	97	>97	<3

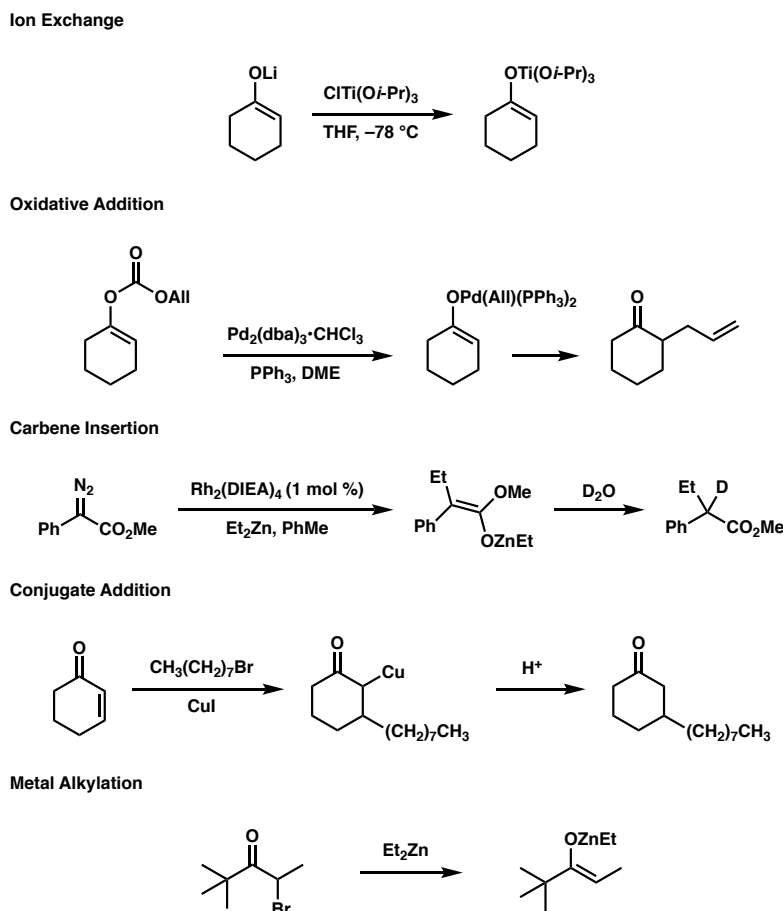
^a Aldol product with benzaldehyde, *syn:anti* = 5:95. ^b Aldol

product with benzaldehyde, *syn:anti* = 98:2.

1.2.4 TRANSITION METAL ENOLATES

Research on transition metal enolates has gained much attention over the past several years. At least 23 different transition metal enolates have been prepared²⁵ and used in organic synthesis, especially those of palladium, zinc, copper, titanium, and nickel. Transition metal enolates are synthesized using a wide variety of methods²⁶ including ion exchange, oxidative addition, carbene insertion, conjugate addition, and metal alkylation (Scheme 1.2.4.1).

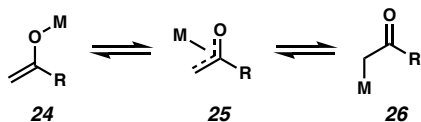
Scheme 1.2.4.1. Common Methods to Form Transition Metal Enolates



The three main types of binding modes that transition metal enolates can adopt are η^1 -*O*-bound (**24**), η^3 -oxa- π -allyl (**25**), or η^1 -*C*-bound (**26**, Scheme 1.2.4.2). All three

configurations are capable of interconversion, but each complex has a preferred one, depending on multiple factors, including the hardness or softness of the metal, the steric and electronic environments of the ligands, and the solvent. Although there are exceptions, the general trend for preferred enolate configurations is that early transition metals tend to primarily adopt the η^1 -O-bound configuration (**24**), while late transition metals primarily adopt the η^1 -C-bound (**26**).²⁷ Since transition metals generally have higher coordination numbers, chiral ligands can be used to control the stereochemical outcome.

Scheme 1.2.4.2. Equilibrium Between Transition Metal Enolate Coordination Sites



1.3 ALDOL REACTION

1.3.1 INTRODUCTION

First discovered in 1872 by Wurtz,²⁸ the aldol reaction has long served as an important method of carbon–carbon bond formation. Due to the highly organized cyclic transition state, diastereoselective aldol methodologies including those utilizing chiral auxiliaries²⁹ have long been employed in organic synthesis.³⁰ More recently catalytic asymmetric aldol reactions relying on organic catalysts³¹ or metal complex catalysts have been explored. Although many examples of metal-catalyzed asymmetric aldol reactions exist in the literature, few methods tolerate the construction of quaternary centers.

1.3.2 RHODIUM-CATALYZED REACTIONS

First reported in 1998 by Kuwano and Ito, the asymmetric aldol reaction of aldehydes (**27**) with 2-cyanopropionates (**28**) catalyzed by trans-chelating chiral diphosphine ligands (*R,R*)-TRAP (**29**)–rhodium(I) complex generates β -hydroxy- α -

cyanocarboxylate products (**30** and **31**) bearing two vicinal stereocenters, one of which is quaternary (Table 1.3.2.1).³² Good *anti* to *syn* ratios were achieved only for a few substrates although with poor to good enantioselectivities.

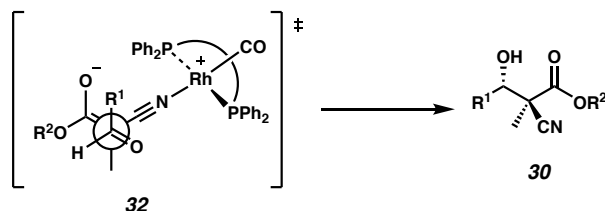
Table 1.3.2.1. Substrate Scope of Rhodium-Catalyzed Aldol Reaction

R ¹	R ²	time (h)	Yield (%)	anti/syn	ee-anti	ee-syn
Me	Et	24	63	45/55	31	23
Me	i-Pr	24	61	47/53	55	50
Me	CH(i-Pr) ₂	24	67	81/19	86	33
Et	CH(i-Pr) ₂	48	76	75/25	57	10
CO ₂ Et	CH(i-Pr) ₂	40	88	68/32	91	63

(*R,R*)-TRAP (29)

In order to explain the *anti*-selectivity of their system, Kuwano and Ito propose several possible transition state structures of the zwitterionic (enolato)rhodium intermediate and suggest that an antiperiplanar transition state (**32**) in which the steric interaction between the aldehyde substituent (R¹) and the alkyl group (R²) of the ester is minimized is most likely (Figure 1.3.2.1).

Figure 1.3.2.1. Transition State of Zwitterionic (Enolato)Rhodium Intermediate

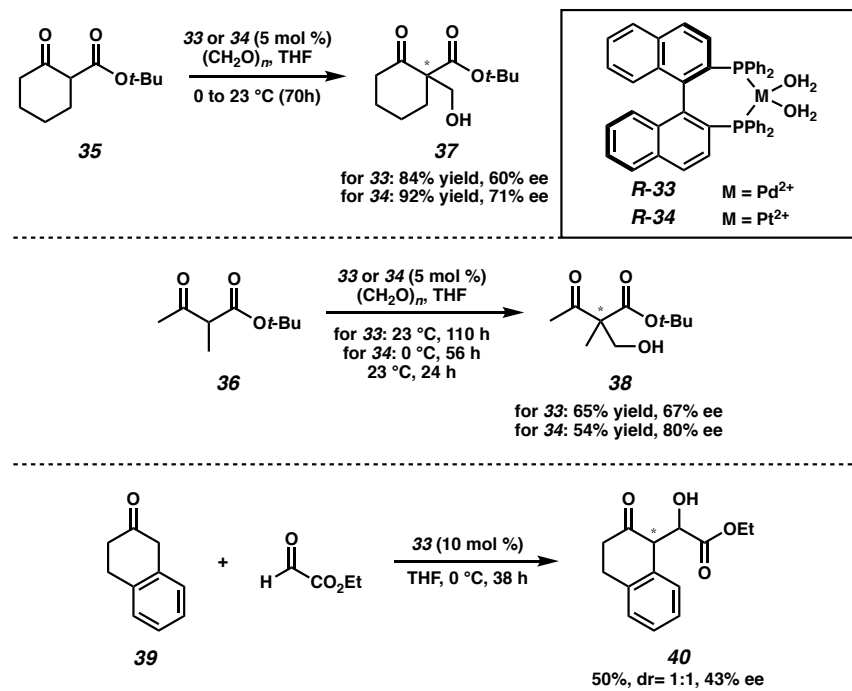


1.3.3 PALLADIUM- PLATINUM- AND NICKEL-CATALYZED REACTIONS

Sodeoka and coworkers have reported an asymmetric hydroxymethylation of substituted β -ketoesters with formaldehyde produced *in situ*, using chiral palladium or platinum bisphosphine catalysts (**33** and **34**).³³ They also found that chiral platinum

bisphosphine catalysts were able to affect the same reactivity. Their proposed mechanism for the reaction proceeds through the enolization of the substituted β -ketoester (**35** and **36**) to form a chiral palladium enolate that reacts with the highly electrophilic aldehyde in a selective fashion to produce the chiral quaternary center containing products (**37** and **38**) in good yield (up to 92% yield) and enantioselectivity (up to 80% ee, Scheme 1.3.3.1). The reaction was also found to work for less acidic ketones such as β -tetralone (**39**), with more electrophilic aldehydes such as ethyl glyoxalate, albeit only to form tertiary centers (**40**).

Figure 1.3.3.1. Scope of Palladium- and Platinum-Catalyzed Hydroxymethylation of Substituted β -Ketoesters



In 2009, Matsunaga and Shibasaki reported the synthesis of asymmetric hydroxymethylated derivatives (**43**) of substituted β -ketoesters with formaldehyde, but their catalyst was a homodinuclear Ni²⁺-Schiff base complex (**42**).³⁴ With relatively low catalyst loading (0.1–1.0 mol %) they were able to obtain a variety of hydroxymethylated,

quaternary carbon containing products in modest to good yields, featuring enantioselectivities of 66% ee or better (Table 1.3.3.1).

Table 1.3.3.1 Scope of Nickel-Catalyzed Hydroxymethylation Reaction of Substituted β -Ketoesters

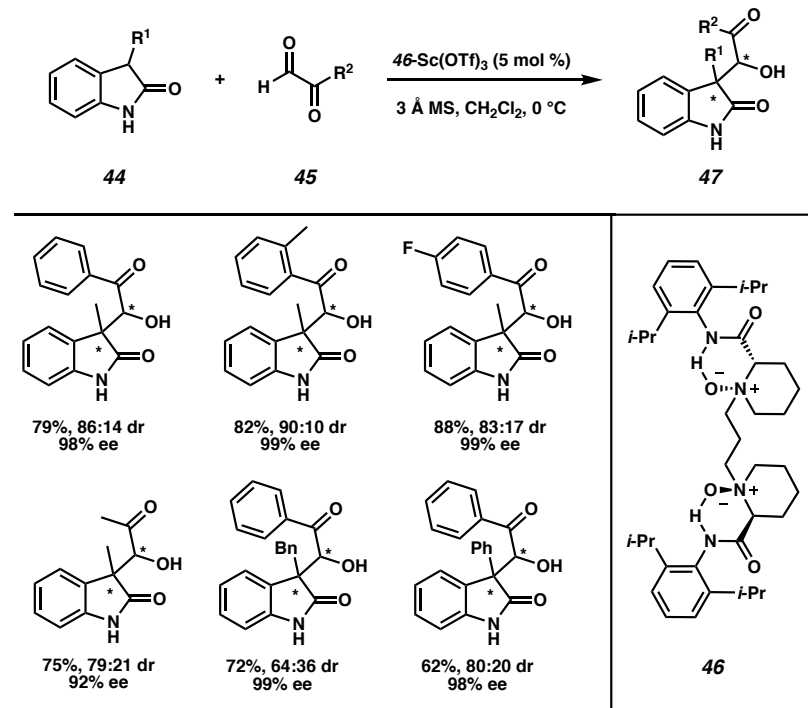
R ¹	R ²	Yield (%)	ee (%)
-(CH ₂) ₃ -		94	93
-(CH ₂) ₄ -		91	85
-(CH ₂) ₅ -		81	66
Me	Me	79	81
Me	Et	79	89
Me	Bn	84	90
Ph	Me	40	89

(R)-42

1.3.4 SCANDIUM- AND NEODYMIUM-CATALYZED REACTIONS

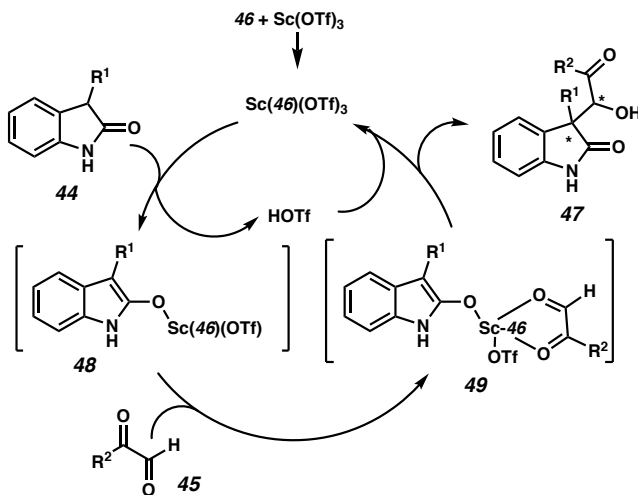
Feng and coworkers, in 2010, disclosed an asymmetric aldol reaction where a Sc(OTf)₃ complex, formed from chiral ligand **46**, catalyzes the reaction of 3-substituted-2-oxindoles (**44**) and glyoxal derivatives (**45**) to form enantioenriched 3-(α -hydroxy- β -carbonyl)oxindoles (**47**).³⁵ The reaction's mild conditions tolerate a variety of substituents on both the glyoxal electrophile as well as on the oxindole substrate with yields ranging from 62% to 92%, enantioselectivities ranging from 82% to 99%, and diastereoselectivities as high as 99:1 (Table 1.3.4.1). They also found that the reaction was scalable with no major loss in yield, ee, or dr.

Table 1.3.4.1. Substrate Scope of Scandium-Catalyzed Asymmetric Aldol Reaction



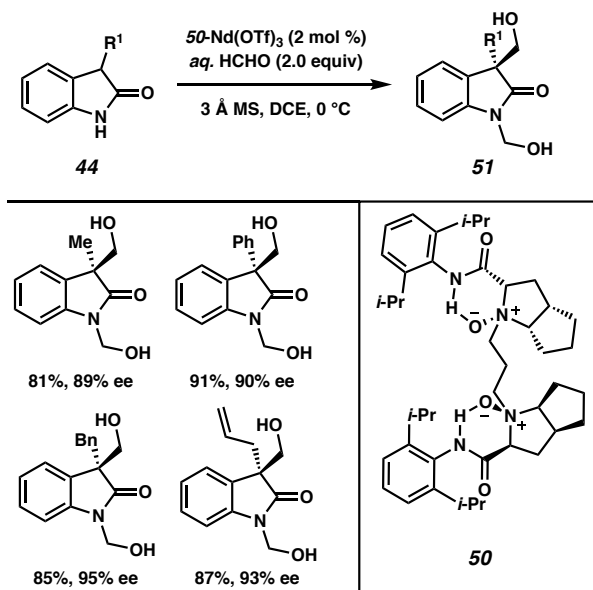
The mechanism proposed feature a scandium enolate (**48**) which serves to coordinate the glyoxal electrophile in a bidentate fashion (**49**), thereby allowing the aldol reaction to form the enantioenriched products (**47**) with vicinal stereocenters (Figure 1.3.4.1).

Scheme 1.3.4.1. Proposed Catalytic Cycle of Scandium-Catalyzed Aldol Reaction



In another report, Feng and coworkers disclosed the use of chiral neodymium catalysts in the asymmetric aldol reaction of 3-substituted-2-oxindoles and formalin.³⁶ Again, *N,N'*-dioxide ligands were utilized, and the optimal ligand for this transformation was found to be **50**. Good yields ranging from 60% to 93% and excellent enantioselectivities all above 87% were obtained, producing enantioenriched 1,3-bis(hydroxymethyl)-2-oxindoles (**51**, Table 1.3.4.2).

Table 1.3.4.2. Scope of Neodymium-Catalyzed Asymmetric Aldol Reaction

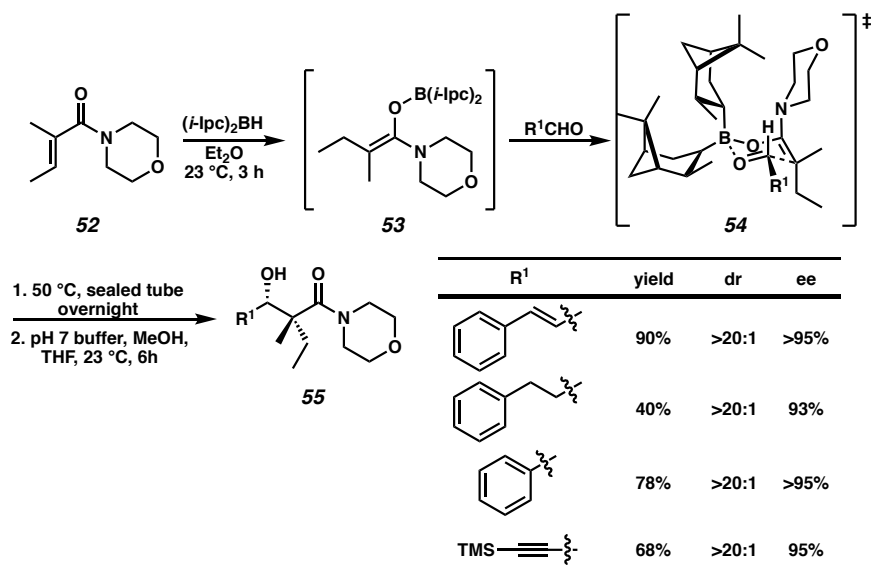


1.3.5 REACTIONS PROCEEDING THROUGH BORON ENOLATES

The aldol reaction of aldehydes and stereochemically defined tetrasubstituted enol borinates generated by the 1,4-hydroboration of α,β -unsaturated morpholine carboxamides with diisopinocampheylborane, (L-Ipc)₂BH, has been reported by Roush and coworkers in 2013.³⁷ Based on the stereochemistry of product (**55**), they propose that the reaction proceeds through an organized six-membered transition state (**54**) of a *Z*(*O*)-enolborinate (**53**, Scheme 1.3.5.1). Depending on the configuration of the starting acrylamide (**52**), both

syn and *anti* products could both be predictably obtained. Moderate to good yields (40 to 90%) were obtained for almost all of the quaternary carbon containing products with diastereoselectivities greater than 20:1 and enantioselectivities above 92%.

Scheme 1.3.5.1. Transition State and Substrate Scope of Aldol Reaction of Aldehydes and Stereochemically Defined Tetrasubstituted Enol Borinates



1.4 MANNICH REACTION

1.4.1 INTRODUCTION

A C–C bond forming reaction that has been used by chemists since the nineteenth century is the aminoalkylation reaction known as the *Mannich reaction*, named after German chemist Carl Mannich, who played a pivotal role in developing this reaction for broad synthetic use. The Mannich reaction produces β -amino carbonyl compounds by nucleophilic attack of an enol or enolate on a α electrophilic iminium salt.³⁸ This reaction has been employed in the synthesis of several bioactive compounds³⁹ and a number of asymmetric variants have been developed utilizing organic catalysts⁴⁰ or metal-based

catalysts.⁴¹ To date, direct asymmetric Mannich reactions employing transition metal catalysts are limited to stabilized enolates (1,3-dicarbonyl, β -keto nitriles, or oxindoles).

1.4.2 COPPER-CATALYZED REACTIONS

Jørgensen and coworkers first reported the direct catalytic asymmetric Mannich reaction of malonates and β -ketoesters in 2003.⁴² They found that by using Cu(OTf)₂ and the (*S*)-*t*-Bu-BOX ligand (**57**) in the reaction between substituted β -ketoesters (**41**) and *N*-tosyl- α -imino ester (**56**), they could obtain the quaternary carbon-containing products (**58**) in modest to good yields, diastereoselectivities as high as 99:1, and enantioselectivities ranging from 86% to 95% (Table 1.4.2.1). Although the best enantioselectivities were observed at -20 °C, these reactions were also plagued with low yields. The yields could be greatly improved upon warming to room temperature with only a slight decrease in ee.

Table 1.4.2.1. Substrate Scope of Copper-Catalyzed Asymmetric Mannich Reaction

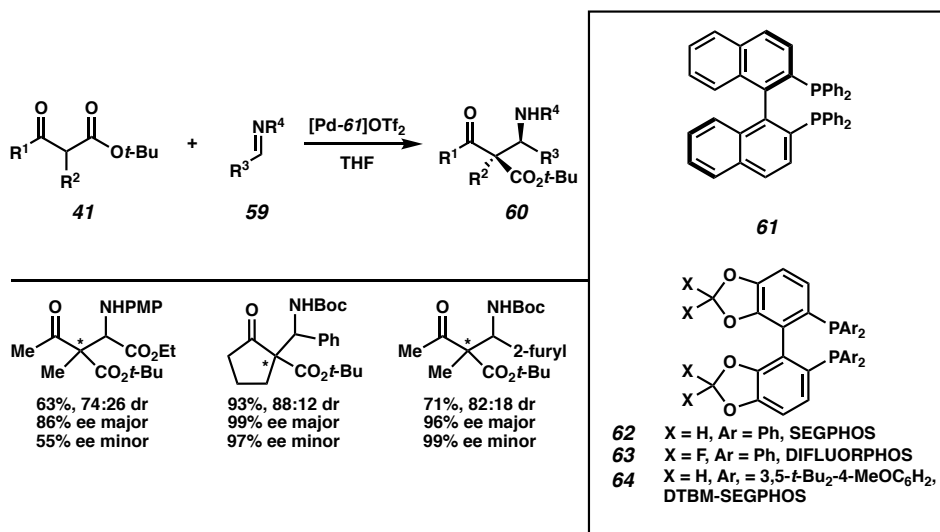
R ¹	R ²	T (°C)	yield (%)	dr	ee (%)
Me	Me	-20	55	97:3	95
Et	Me	-20	17	98:2	93
i-Pr	Me	-20	15	84:16	92
Me	Me	23	87	93:7	88
Et	Me	23	80	98:2	92
i-Pr	Me	23	55	84:16	91
-(CH ₂) ₄ -		23	89	99:1	86
Bn	Me	23	83	96:4	93
i-Pr	All	23	69	92:8	87

1.4.3 PALLADIUM-CATALYZED REACTIONS

Chiral palladium enolates have also found use in the asymmetric Mannich reaction, such as one reported by Jørgensen, Sodeoka and coworkers for β -ketoesters.⁴³ However, they utilize palladium catalysts and are able to extend their reaction to a variety of imine

electrophiles. Two palladium catalysts one with BINAP ligand (**61**) and the other with SEGPHOS ligand (**62**), were used to optimize their substrate scope that features a variety of β -ketoesters and imines (Table 1.4.3.1). Good to excellent yields of the vicinal quaternary and secondary stereocenter-containing products (**60**) could be obtained with good diastereoselectivity for most β -ketoester/imine combinations. The enantioselectivity of the reaction is also excellent, with enantioselectivities as high 99%. After assigning the absolute stereochemistry of their products by comparison to previously published results, they propose that the excellent enantioselectivity comes from the face selection of the chiral palladium-enolate.

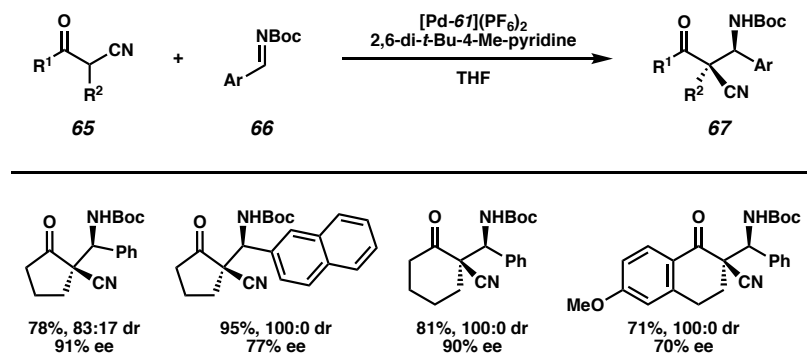
Table 1.4.3.1. Scope of Palladium-Catalyzed Asymmetric Mannich Reaction Reported by Sodeoka, and Coworkers



Another Pd-BINAP catalyst system utilized in an asymmetric Mannich reaction was reported by Kim and coworkers in 2009.⁴⁴ This time the targeted substrates were α -cyanoketones (**65**) and *N*-Boc protected aldimines (**66**). The reaction was tolerant of a variety of aromatic substituted aldimines as well as a number of cyclic α -cyanoketones

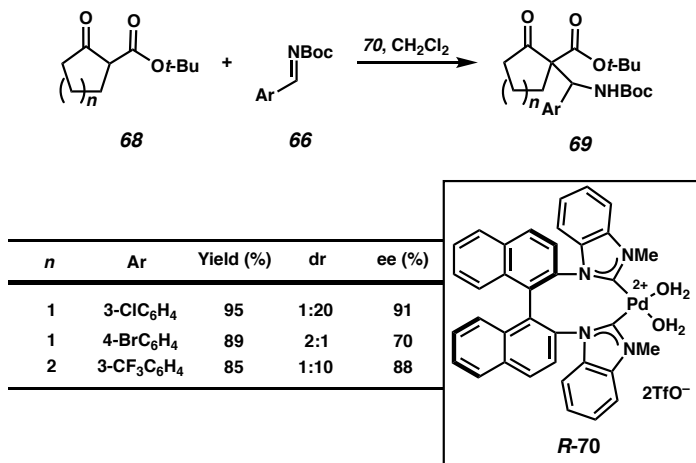
with yields ranging from 71–95% (Table 1.4.3.2). The enantioselectivity of the reaction was also good with enantioselectivities as high as 91%. Several products could be obtained with complete diastereoselectivity, selective for the *syn* product.

Table 1.4.3.2. Scope of Palladium-Catalyzed Mannich Reaction Reported by Kim and Coworkers



N-heterocyclic carbene Pd²⁺ diaqua complex (**70**) has been utilized as a catalyst by Shi and coworkers, who found that under mild conditions cyclic β -ketoesters (**68**) and *N*-Boc imines (**66**) could be reacted with these complexes to form Mannich adducts (**69**) in good yield (80–95%) and good enantioselectivity (70–96%, Table 1.4.3.3).⁴⁵ The reaction, however, was not very diastereoselective for many of the substrate combinations; the diastereoselectivities ranged from 2:1 to 1:20. They propose a mechanism almost identical to that of Sodeoka⁴³ with the reaction proceeding through a chelated palladium enolate, which directs the stereochemical outcome of the nucleophilic addition through an open transition state.

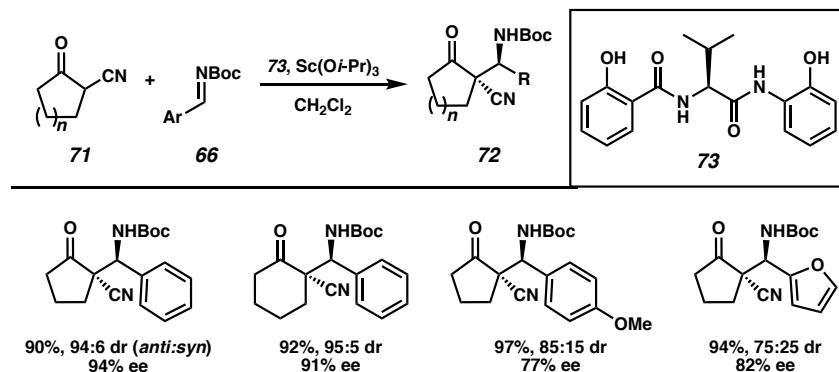
Table 1.4.3.3. Palladium-Catalyzed Mannich Reaction Reported by Shi and Coworkers



1.4.4 SCANDIUM-CATALYZED REACTIONS

Prior to Kim and coworkers' report⁴⁴ on the asymmetric Mannich reaction of α -cyanoketones and *N*-Boc protected aldimines, a similar reaction was reported by Shibasaki and coworkers.⁴⁶ Unlike Kim and coworkers, Shibasaki's conditions were able to preferentially form the *anti*-product. By using scandium complex with amide ligand (73), the quaternary carbon-containing products (72) could be obtained in good to excellent yields (80–99% and good to excellent enantioselectivities for most substrate combinations (77–96%) at a broad range of temperatures (Table 1.4.4.1). The *anti*-selectivity of the reaction was excellent, with diastereoselectivities as high as 97:3. Mechanistic investigations were not conclusive and suggested that the catalyst exists in solution as a conglomerate without order or regularity that must dissociate in order to form the highly ordered transition state necessary for the high enantioselectivity and diastereoselectivity observed in the reaction.

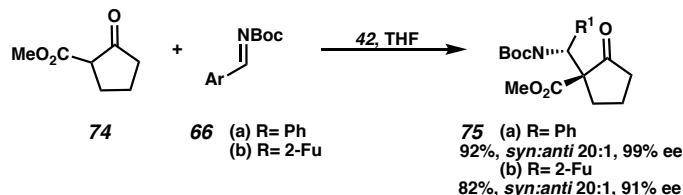
Table 1.4.4.1. Scandium-Catalyzed Asymmetric Mannich Reaction



1.4.5 NICKEL-CATALYZED REACTIONS

Shibasaki and Matsunaga reported a second asymmetric Mannich reaction of *N*-Boc protected aldimines in 2008.⁴⁷ However this reaction utilized a homodinuclear nickel Schiff base complex catalyst instead of a scandium complex. The targeted nucleophilic partner in this reaction was substituted nitroacetates resulting in tertiary stereocenter-containing products, but they also showed two examples of a β -ketoester **74** with aldimine (**66**) resulting in quaternary stereocenter-containing products. These two products (**75**) were obtained in good yields (82% and 92%) and with great enantioselectivities (91% and 99%, Scheme 1.4.5.1).

Scheme 1.4.5.1. Nickel-Catalyzed Asymmetric Reaction



1.4.6 LITHIUM-CATALYZED REACTIONS

An asymmetric Mannich reaction of cyclic and acyclic 1,3-dicarbonyl compounds (**76**) and *N*-Boc aldimines (**77**) using BINOL (**79**) lithium salts as the chiral catalyst was

reported by Ishihara and coworkers.⁴⁸ All products (**78**) were obtained in good yield (above 90%), good diastereoselectivity (most greater than 9:1), and good to excellent enantioselectivities (82%–97%, Table 1.4.6.1). Interestingly they found that the *syn/anti* selectivity of the reaction and the absolute stereochemistry at the newly formed amino-carbon stereocenter switched depending on whether the 1,3-dicarbonyl substrate was cyclic or acyclic. Cyclic substrates resulted in high *syn* selectivities whereas acyclic substrates exhibited high *anti* selectivity with the exception of the ketolactone. Two mechanistic pathways were proposed for the reaction. In pathway A, the aldimine is activated by the Lewis acidic lithium center, allowing for the conformational flexibility preferred by acyclic substrates, and in pathway B the pronucleophile is activated as a lithium enolate, forming a more rigid structure promoting chelation by the 1,3-dicarbonyl. Pathway A would most likely result in attack of the pronucleophile, coordinated by a naphtholate oxygen, on the *re* face of the lithium-coordinated aldimine resulting in *anti*-products, whereas in the pathway B the aldimine is activated by the naphthol proton and the lithium enolate attacks the aldimine on the *si* face resulting in *syn* products.

Table 1.4.6.1 Scope of Lithium BINOLate-Catalyzed Asymmetric Mannich Reaction

$$\begin{array}{c} \text{O} \\ \parallel \\ \text{R}^1 - \text{C}(\text{R}^2) - \text{CH}_2 - \text{C}(=\text{O})\text{R}^3 \end{array} + \begin{array}{c} \text{NR}^4 \\ || \\ \text{Ar} \end{array} \xrightarrow[\substack{\text{t-BuOH, toluene}}]{\substack{\text{79, } n\text{-BuLi}}} \begin{array}{c} \text{O} \\ \parallel \\ \text{R}^1 - \text{C}(\text{R}^2) - \text{CH}(\text{NHR}^4) - \text{C}(=\text{O})\text{R}^3 \\ \text{Ar} \end{array}$$

76 **77** **78**

R-79

R¹	R²	R³	R⁴	Ar	Yield (%)	dr	ee (%)
-(CH ₂) ₄ -	CO ₂ Me	Boc	Ph	98	88:12	91	
-(CH ₂) ₄ -	CO ₂ Me	Boc	p-An	95	96:4	95	
-(CH ₂) ₄ -	CO ₂ Me	CBz	Ph	91	95:5	87	
-OCH ₂ CH ₂ -	Ac	Boc	Ph	>99	39:61	85	
-(CH ₂) ₂ S(CH ₂) ₂ -	CO ₂ Me	Boc	Ph	90	88:12	93	
Me	H	CO ₂ Me	Boc	Ph	97	5:95	85
Me	H	CONMe ₂	Boc	p-An	93	9:91	97

1.4.7 CALCIUM-CATALYZED REACTIONS

Kobayashi and coworkers reported an asymmetric Mannich reaction of 3-substituted oxindoles (**80**) and *N*-Boc-imines (**59**) in 2015.⁴⁹ Their optimized conditions utilized catalytic triethylamine, CaI₂, and a PyBOX ligand (**83**) to generate 3-tetrasubstituted oxindoles (**81**, **82**) with vicinal quaternary and secondary stereocenters. Yields as high as 99% and enantioselectivities greater than 99% could be obtained for some substrate combinations (Table 1.4.7.1). The diastereoselectivity of the reaction was excellent, ranging from 93:7 to 98:2 with preferential formation of diastereomer **81**.

Table 1.4.7.1. Scope of Calcium-Catalyzed Asymmetric Mannich Reaction^a

R ¹	R ²	yield (%)	dr XX:XX	ee XX
Me	Ph	87	95:5	98
Me	2-tol	93	97:3	97
Me	i-Bu	99	94:6	84
Bn	2-thi	84	96:4	98
n-Pr	Et	43	97:3	72
i-Pr	Ph	80	95:5	>99

S,S-83

^a R³ = Boc.

1.5. CONJUGATE ADDITION AND MICHAEL REACTION

1.5.1 MICHAEL ADDITIONS INVOLVING POTASSIUM ENOLATES

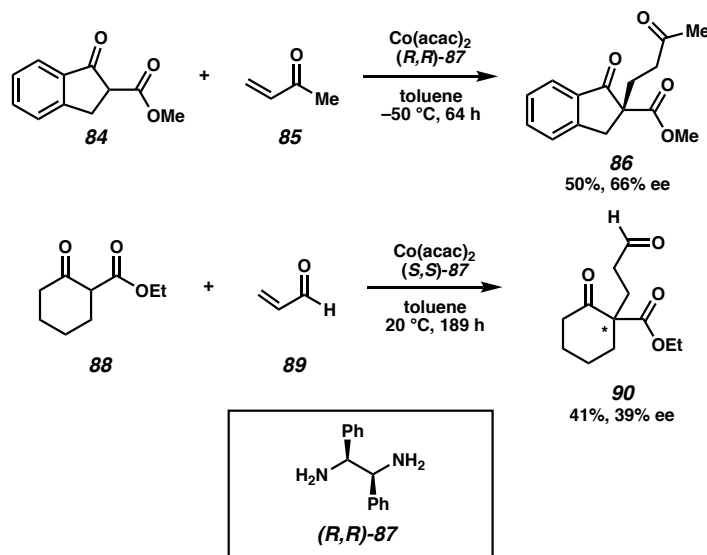
The earliest example of an asymmetric Michael reaction⁵⁰ resulting in the formation of a quaternary center was published in 1973 by Långström and Bergson,⁵¹ relying on the use of 2-(hydroxymethyl)-quinuclidine enantiomer as the chiral organic catalyst to obtain optically active products. Their substrate scope was very limited and no conclusions could be reached regarding the mechanism of asymmetric induction. In 1981, the first example

of an asymmetric Michael reaction proceeding through a metal enolate was reported by Cram and Sogah,⁵² using potassium enolates in conjunction with chiral crown ethers to effect this transformation. Although the enantioselectivity of the products was fair (low 60's) for most reactant combinations, one exceptional case resulted in an enantioselectivity of 99%. The chiral crown ether hosts could be recovered and reused many times.

1.5.2 MICHAEL ADDITIONS INVOLVING COBALT ENOLATES

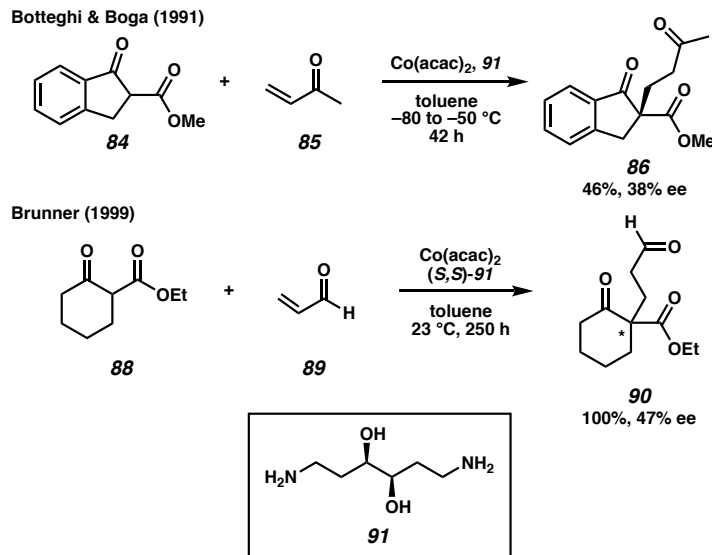
The use of cobalt catalysts in the asymmetric Michael reaction first appears in the literature in 1984, where Brunner and Hammer, investigated the Michael reaction of cyclic- β -ketoesters and methyl vinyl ketone with Co(acac)₂ in the presence of enantiomeric diamines (e.g. 87, Scheme 1.5.2.1).⁵³ Subzero temperatures were required to obtain modest enantioselectivities (up to 66%). However, lowered temperatures also resulted in diminished yields. The highest enantioselectivity obtained corresponded to only a 50% yield at -50 °C. In a subsequent publication the substrate scope of this reaction was of this reaction was explored and it was found that substrate architecture played an enormous role in the selectivity of the reaction.⁵⁴ The highest enantioselectivity obtained in the substrate scope study was only 39%, which was the result for the reaction of cyclohexanone derived β -ketoester with acrolein at 20 °C.

Scheme 1.5.2.1. Cobalt-Catalyzed Asymmetric Michael Reaction Reported by Brunner and Hammer



In 1991, Botteghi, Boga, and coworkers reported the asymmetric Michael reaction using cobalt catalysts derived from a number of ligand architectures (Scheme 1.5.2.2).⁵⁵ For the formation of the quaternary carbon-containing product the optimal ligand was found to be a tetradentate diaminodiol ligand **91**. Under optimized conditions the reaction only proceeded with 38% enantioselectivity accompanied by a low 46% yield. Higher yields could be achieved but only at the cost of lowered enantioselectivity. Brunner revisited the asymmetric Michael reaction again in 1999. In this report a number of chiral transition metal complexes are utilized as the catalyst.⁵⁶ Although cobalt was only one of several metals tested, its complex with 1,2-diphenylethylenediamine gave the highest enantioselectivity (47%) for this reaction.

Scheme 1.5.2.2. Cobalt-Catalyzed Asymmetric Michael Reaction Reported by Botteggi and Boga

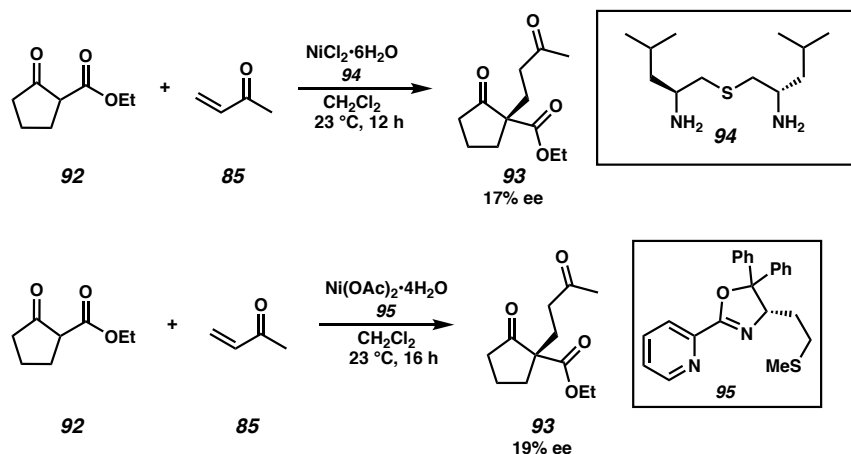


1.5.3 MICHAEL ADDITIONS INVOLVING NICKEL ENOLATES

Chiral nickel complexes of various ligand architectures have found use in asymmetric Michael reactions since the early 1990s. Botteggi and coworkers first reported the use of nickel chiral Schiff base complexes in a Michael addition of methyl vinyl ketone and ethyl 2-methylacetooacetate with slight asymmetric induction topping out at 6% for the quaternary carbon-containing product.⁵⁷ Their intention was not to optimize the reaction conditions but rather to study the mechanism of the reaction which they propose proceeds through a chelated nickel enolate intermediate. The use of tridentate ligands in coordination with nickel centers in the asymmetric Michael reaction has been explored by Christoffers and coworkers. A series of tridentate diamino thioethers (**94**), diimino thioethers, and oxazolines (**95**)⁵⁸ were screened with a variety of metal salts in reaction of 1,3-dicarbonyl (e.g. **92**) with methyl vinyl ketone (Scheme 1.5.3.1).⁵⁹ They concluded that the nickel complexes with diamino thioether ligand **94** and pyridine, or the methionine derived

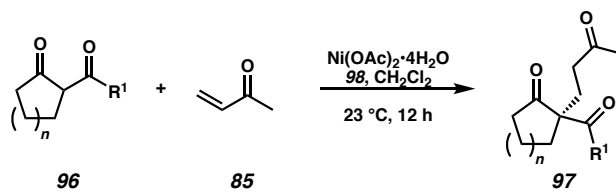
oxazoline ligand **95** produced the best results in terms of both conversion and enantioselectivity. However enantioselectivities of the product **93** did not exceed 19% for any of the tested combinations and optimized reaction conditions with these ligands.

Scheme 1.5.3.1. Nickel-Catalyzed Asymmetric Michael Reaction



Instead Christoffers and coworkers have reported mild conditions utilizing nickel diamine complexes for the asymmetric Michael reaction of cyclic β -ketoesters and methyl vinyl ketone.⁶⁰ The enantioselectivity of the reaction was hugely dependent on the ring size of the cyclic β -ketoester; the cyclohexanone derived product could be obtained in 91% ee but the cycloheptanone derived product was nearly racemic with an ee of only 2% (Table 1.5.3.1). The other disadvantage of this reaction is that the chiral diamine is not catalytic, but the authors note that some of the auxiliary can be recovered after workup.

Table 1.5.3.1. Scope of Nickel-Diamine Catalyzed Asymmetric Michael Reaction

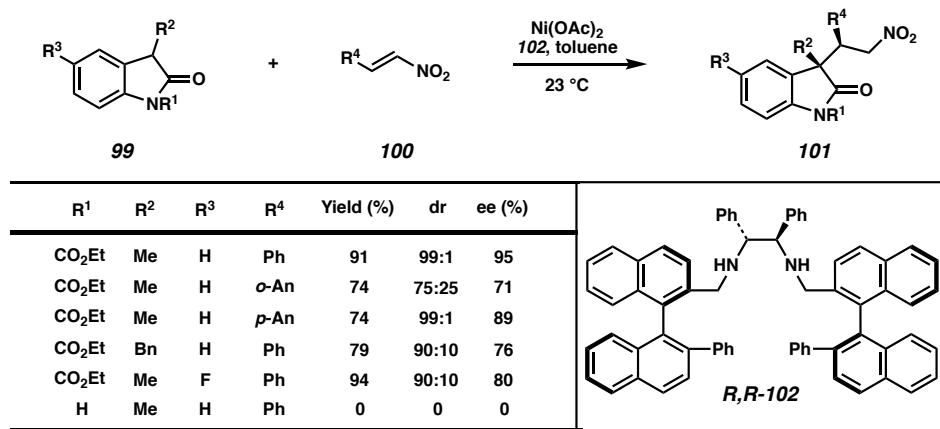


n	R¹	ee (%)	
2	OEt	91	
1	O <i>t</i> -Bu	74	
1	O <i>i</i> -Pr	6	
3	OMe	2	
2	Me	41	

R,R-98

More recently chiral diamine complexes have also been utilized in the conjugate addition of 3-substituted oxindoles (**99**) and nitroolefins (**100**).⁶¹ These mild conditions employ $\text{Ni}(\text{OAc})_2$ with ligand **102** and deliver the products (**101**) in good yield, diastereoselectivity, and enantioselectivity for a range of substrates (Table 1.5.3.2). Aliphatic nitroolefins were note tolerated and the oxindole nitrogen needed to be substituted as a carbamate; free N–H oxindole as well as *N*-benzyl substituted oxindole produced no reaction. This suggests that the 1,3-dicarbonyl motif is critical for reactivity and the reaction likely proceeds through a chelated nickel enolate.

Table 1.5.3.2. Scope of Nickel-Diamine Catalyzed Conjugate Addition of 3-Substituted Oxindoles and Nitroolefins

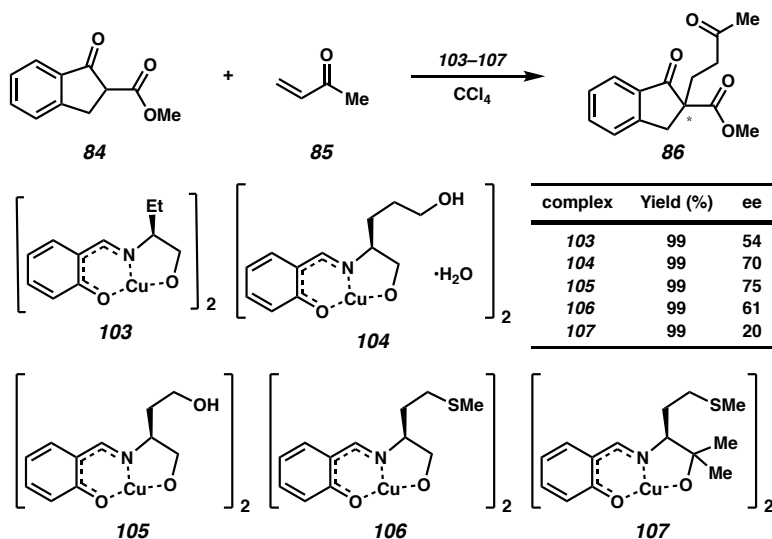


1.5.4 MICHAEL ADDITIONS INVOLVING COPPER ENOLATES

Chiral copper(II) complexes (**103–107**) were used by Desimoni and coworkers⁶² in the reaction of methyl 1-indanone-2-carboxylate (**84**) and methyl vinyl ketone **85** to yield the chiral Michael adduct **86** (Table 1.5.4.1). Initially tridentate Schiff base ligands bearing ethyl or phenyl substituents were investigated along with various solvents and it was found that the ethyl-substituted ligand (**103**) gave the highest ee when carbon tetrachloride was used as the solvent. Based on these results, they reasoned that catalysts with increased rigidity would result in higher ee's and thus tetradentate ligands should be investigated. Two tetradentate ligands, one derived from (*S*)-2-amino-1,5-pentandiol (**104**) and the other derived from (*S,S*)-2-amino-1,3-propandiol, were screened with a variety of solvents; although there was no clear difference between the two ligands and that the highest ee's were obtained from reactions carried out in carbon tetrachloride. The highest ee obtained was 70% which corresponded to a stoichiometric use of the copper catalyst; although the catalyst loading could be dropped to 10 mol % with only a minor loss of enantioselectivity. Subsequent work in the Desimoni group focused on designing new ligands to improve the

efficiency of the copper catalyzed asymmetric Michael reaction.⁶³ Eight new Schiff base ligands were investigated and the ligand **105** derived from (*S*)-aspartic acid gave the highest ee value of 75% which outperformed the ligands investigated in their previous publication. Unlike **104** and **105**, the methionine derived methyl thiol (**106**) and its *gem*-dimethyl analog (**107**) result in enantioselectivities equal to or worse than the original ligand **103**, suggesting the pendant alcohol acts as an axial coordinating ligand. It was concluded that minor modifications in the ligand structure will not be enough to significantly improve the enantioselectivity of the reaction and alternative avenues will need to be investigated to obtain better results.

Table 1.5.4.1. Copper(II)-Catalyzed Reaction of Methyl Vinyl Ketone and Methyl 1-Oxo-2-Indanecarboxylate



1.5.5 MICHAEL ADDITIONS INVOLVING EUROPIUM ENOLATES

Scettri and coworkers reported in 1993⁶⁴ an early example of the Michael reaction of a 1,3-dicarbonyl compound and methyl vinyl ketone to produce various quaternary carbon-containing products, using the commercially available europium(III) tris(3-

(trifluoromethylhydroxymethylene-*d*-camphorate)) as the catalyst under very mild conditions. The yields were modest to good but only with modest enantioselectivities up to 36%.

1.5.6 MICHAEL ADDITIONS INVOLVING RHODIUM ENOLATES

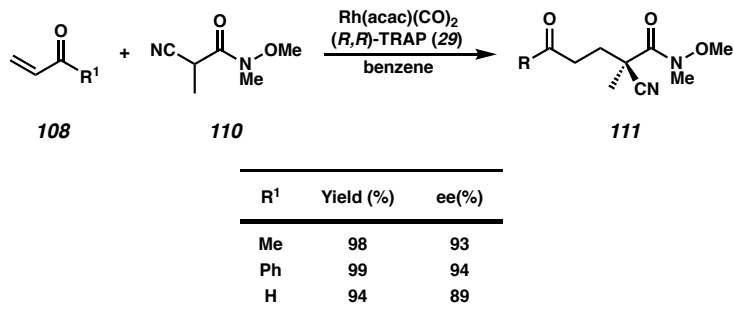
Ito and coworkers reported in 1992⁶⁵ the first asymmetric Michael reaction of vinyl ketones (**108**) using chiral rhodium–TRAP (**29**) catalysts. The products (**109**) were in quantitative yields and enantioselectivities as high as 89% (Table 1.5.6.1). The nucleophilic partner in this reaction was an α -cyanocarboxylate (**28**) which they propose is key to the selectivity of the reaction because of coordination of the cyano group to the rhodium center forming a cationic rhodium species, which serves as the counterion for the enolate. The *cis*-chelating TRAP ligand⁶⁶ (**29**) was also essential to the selectivity of the reaction as *cis*-chelating chiral diphosphines such as BINAP produced very little asymmetric induction.

Table 1.5.6.1. Scope of the First Asymmetric Michael Reaction using Chiral Rhodium Catalysts

108	28	$\text{RhH}(\text{CO})(\text{PPh}_3)_3$ <i>(R,R)-TRAP (29)</i> benzene	109	
R ¹	R ²	Time (h)	Yield (%)	ee (%)
Me	Me	10	99	72
Me	<i>i</i> -Pr	10	99	84
<i>p</i> -An	<i>i</i> -Pr	1.5	99	89
4-ClC ₆ H ₄	<i>i</i> -Pr	4	98	85
Ph	<i>i</i> -Pr	1.5	95	83
H	<i>i</i> -Pr	2.5	88	87
Me	<i>t</i> -Bu	10	95	81
Me	CH(<i>i</i> -Pr) ₂	23	99	93
H	CH(<i>i</i> -Pr) ₂	3.5	88	92

In a followup publication, addition substrates were investigated and enantioselectivities up to 93% were obtained.⁶⁷ Considering the potential synthetic use of the quaternary carbon containing Michael adducts, subsequent product elaborations were also conducted. The use of α -cyano Weinreb amides (**110**) as the nucleophilic partner was also investigated and enantioselectivities up to 94% could be obtained (Table 1.5.6.2).⁶⁸ These highly useful enantioenriched products (**111**) could also be further elaborated.

Table 1.5.6.2. Rhodium-Catalyzed Asymmetric Michael Reaction of α -Cyano Weinreb Amides



Takaya and coworkers⁶⁹ reported about the rhodium catalyzed asymmetric Michael addition of α -cyanocarboxylates (**112**). They used a bisphosphine ligand (**114**) with large bite angles capable of forming trans-chelating metal complexes to obtain good yields of the quaternary carbon-containing products (**113**, Table 1.5.6.3). Temperature played a large role in the enantioselectivity of the reaction, with the best enantioselectivities (up to 73% ee) were obtained at 0 °C. Interestingly, lower temperatures resulted in sluggish reactions with decreased enantioselectivities.

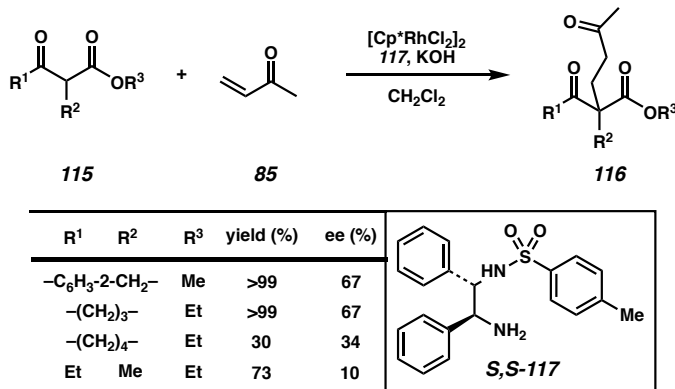
Table 1.5.6.3. Scope of Rhodium-Catalyzed Asymmetric Michael Reaction of α -Cyanocarboxylates

R^1	R^2	R^3	Solvent	Temp (°C)	Time (h)	Yield (%)	ee (%)
Me	Et	Me	PhH	30	4	90	55
Me	Et	Me	PhMe	0	13	86	73
Me	Et	Me	PhMe	-30	20	88	11
Et	Et	Me	PhH	30	13	89	14
Me	Et	OMe	PhH	30	212	0	ND
Me	i-Pr	Me	PhH	0	6	93	72
Me	t-Bu	Me	PhMe	0	11	95	66

R-114

Suzuki and Torii⁷⁰ in early 2000's reported another rhodium-catalyzed asymmetric Michael reaction yielding products bearing quaternary centers that likely proceeded through a metal enolate. This was the first example of a Michael reaction with a β -ketoester (**115**) rather than an α -cyanocarboxylate serving as the nucleophilic partner in conjunction with a rhodium catalyst (Table 1.5.6.4). Using a chiral rhodium complex, prepared *in situ* from $[\text{Cp}^*\text{RhCl}_2]_2$ and partially sulfonated diamine **117**, enantioenriched products (**116**) were obtained from cyclic β -ketoesters and methyl vinyl ketone in quantitative yield with enantioselectivities as high as 67%. Acyclic β -ketoesters also exhibited good reactivity but very poor selectivity. Iridium and osmium catalysts were also investigated in this report, but provided inferior yields and enantioselectivities.

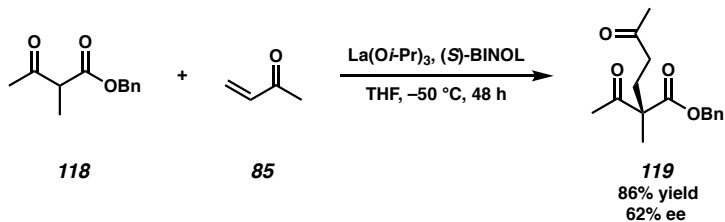
Table 1.5.6.4. First Example of Rhodium-Catalyzed Asymmetric Michael Reaction with β -Ketoesters



1.5.7 MICHAEL ADDITIONS USING LANTHANUM–BINOL COMPLEXES

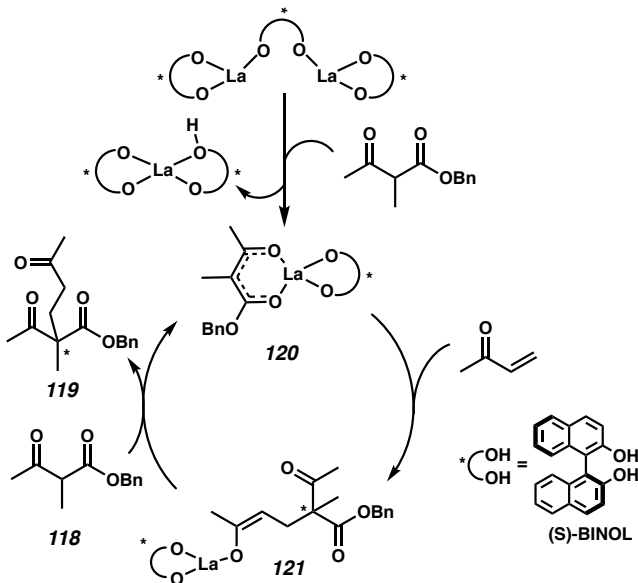
Lanthanum–BINOL complexes,⁷¹ initially developed by Shibasaki and coworkers for the asymmetric nitroaldol reaction,⁷² have found use in the asymmetric Michael reaction of malonates and β -ketoesters.⁷³ First reported in 1994, the asymmetric Michael reaction of several symmetrical malonates with cyclic enones using lithium-free lanthanum BINOL catalysts proceeds in up to quantitative yield and up to 95% ee.⁷⁴ In this initial report, one example of a quaternary carbon-containing product (**119**) is shown; the reaction of methyl vinyl ketone with benzyl 2-methyl-3-oxobutanoate (**118**) proceeds in good yield (86%) but with only a 62% ee; the lowest value reported in the initial publication (Scheme 1.5.7.1).

Scheme 1.5.7.1. Lanthanum-BINOL Complex-Catalyzed Asymmetric Michael Reaction



The proposed mechanism for this reaction features a chelated lanthanum enolate (**120**) that undergoes the conjugate addition to yield lanthanum enolate product (**121**) that is then turned over by deprotonating 1,3-dicarbonyl (**118**, Figure 1.5.7.1)

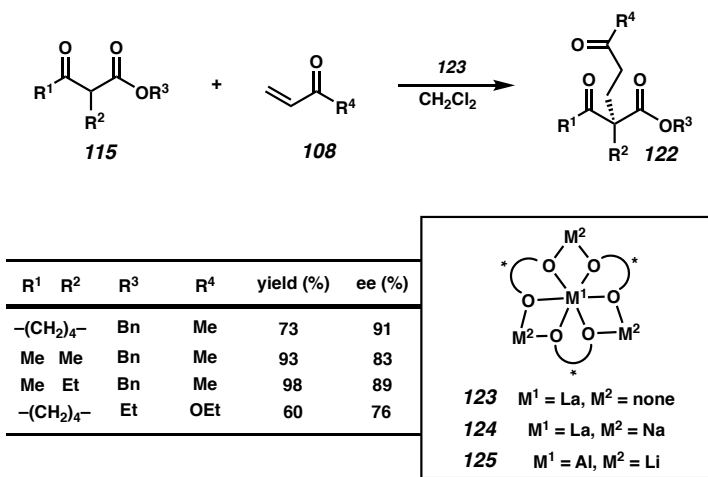
Figure 1.5.7.1 Proposed Mechanism of the Lanthanum-BINOL Complex-Catalyzed Asymmetric Michael Reaction



The asymmetric Michael addition of β-ketoesters (**115**) with vinyl ketones (**108**) producing quaternary carbon-containing products (**122**) was the focus of a later report from the Shibasaki group.⁷⁵ Of their three lanthanum-BINOL catalysts developed at the time (the alkali metal free La–BINOL complex (**123**), the La–Na–BINOL complex (**124**, LSB),

and the Al–Li–BINOL complex (**125**, ALB)), the highest enantioselectivities were observed when using the LSB catalyst. The catalyst loading could be decreased from 10 to 5 mol % and an increased enantioselectivity of 91% could be observed when using dichloromethane as the solvent, without the slow substrate addition necessary for high enantioselectivities when using toluene as the solvent (Table 1.5.7.1). The reaction was not very sensitive to the choice of rare earth metal and praseodymium, samarium, gadolinium, and dysprosium could all be substituted for the lanthanum with only minor drops in yield and enantioselectivity. Cyclic and acyclic β -ketoesters were both tolerated in this reaction and methyl vinyl ketone as well as acrylates were competent Michael electrophiles, all proceeding in good yield and enantioselectivity. The proposed mechanism of this reaction proceeds through a chelated sodium enolate rather than a lanthanum enolate, as was suggested for the reaction using alkali metal-free lanthanum–BINOL catalyst (**123**).

Table 1.5.7.1. LSB-Catalyzed Asymmetric Michael Reaction



In efforts to improve the stability and reusability of the lanthanum–BINOL catalysts, Shibasaki and coworkers prepared in 2000⁷⁶ a lanthanum complex from La(*i*-PrO)₃ and the amino-linked BINOL ligand **129**, which exhibits no deliquescence and can

be stored under air with no decrease in enantioselectivity after four weeks of storage. At 10 mol % catalyst loading, 97% yield and 75% ee can be obtained from the reaction of methyl vinyl ketone and ethyl 2-oxocyclohexane-1-carboxylate. Thanks to solubility differences between the catalyst and the Michael adducts the catalyst can easily be recovered and reused. Very minor decreases in enantioselectivity were observed upon using recycled catalyst.

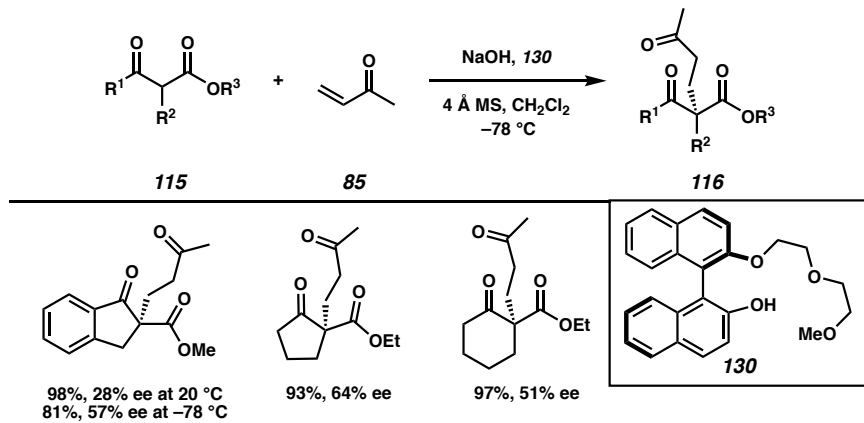
In 2005, Shibasaki and coworkers reported an enantioselective diastereoselective Michael reaction of substituted β -ketoesters (**126**) and cyclic enones (**127**) yielding products (**128**) containing vicinal tertiary and quaternary stereocenters (Table 1.5.7.2).⁷⁷ After optimization of the amino-linked BINOL ligand (**129**), modest to excellent yields (37–100%) were obtained for a diverse array of substrates. The diastereoselectivity also was somewhat substrate dependent with dr's ranging from 68:32 up to 86:14. The enantioselectivity of the reaction was good for a few substrates with ee's as high as 86% for the major isomer but many substrate combinations result in enantioselectivities around 60% with some as low as 39% for the major isomer.

Table 1.5.7.2. Lanthanum NR-Linked-BINOL-Catalyzed Asymmetric Michael Reaction

n	R ¹	R ²	Yield (%)	dr	ee major (%)	ee minor (%)
0	Me	Me	100	76:24	79	73
0	Me	All	86	77:23	56	63
0	i-Pr	Me	71	86:14	63	16
1	Me	Me	92	86:14	86	80
1	Me	(CH ₂) ₃ Ph	37	68:32	56	86
1	i-Pr	Me	42	84:16	80	35
2	Me	Me	89	86:14	82	82
2	Me	All	69	74:26	42	72
2	Me	(CH ₂) ₃ Ph	45	81:19	39	67

The use of chiral alkali metal base catalysts in the asymmetric Michael reaction to form quaternary centers extends beyond the work of Shibasaki. Tamai and Miyano reported the asymmetric Michael addition of cyclic-β-ketoesters (**115**) and methyl vinyl ketone using podand-type alkali metal 2'-substituted 1,1'-binaphthalene-2-oxides (Table 1.5.7.3).⁷⁸ A number of alkali metals were investigated but sodium provided the products (**116**) in the highest yields and enantioselectivities in combination with the optimized oligoether bearing ligand **130**. Cooling the reaction to -78 °C provided an additional boost in enantioselectivity up to 64%.

Table 1.5.7.3. Scope of Michael Reaction of Cyclic β -Ketoesters and Methyl Vinyl Ketone Using Podand-Type Alkali Metal 2'-Substituted 1,1'-Binaphthalene-2-Oxides



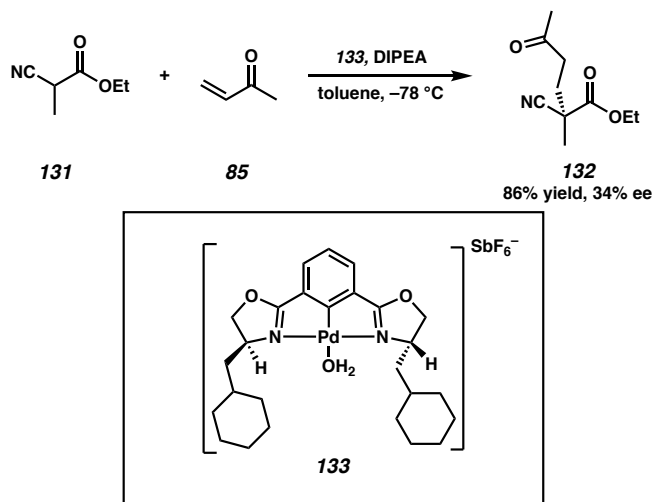
1.5.8 MICHAEL ADDITIONS INVOLVING PLATINUM AND IRON ENOLATES

Williams and coworkers have reported the use of platinum catalysts in the asymmetric Michael reaction. Although the major focus of their report was the synthesis and characterization of novel platinum phosphino-oxazoline complexes, they did demonstrate the use of two cationic platinum complexes in the asymmetric Michael addition of ethyl cyanopropionate and methyl vinyl ketone.⁷⁹ Although good yields were obtained, the reaction proceeded with low enantioselectivity (up to 25%). Iron has also found use in the asymmetric Michael reaction of β -ketoesters and methyl vinyl ketone with the use of a dipeptide ligand.⁸⁰ Although several metals work to catalyze this reaction, the highest enantioselectivity, 18%, was observed using iron(III). This was a surprising result because at the time iron was not typically used in enantioselective transformations.⁸¹

1.5.9 MICHAEL ADDITIONS INVOLVING PALLADIUM ENOLATES

One metal that has found widespread use in a symmetric addition reactions is palladium.⁸² The first palladium catalyzed asymmetric Michael reaction forming quaternary stereocenters was reported in 2000 by Richards and coworkers.⁸³ A number of cationic palladium pincer complexes were screened in the reaction of α -cyanocarboxylates and methyl vinyl ketone. Modest to good yields of **132** were obtained in most reactions however the enantioselectivities were generally low. The best ee obtained was 34% for the reaction of ethyl 2-cyanopropanoate **131** and methyl vinyl ketone, in the presence of DIPEA, catalyzed by **133** (Scheme 1.5.9.1).

Scheme 1.5.9.1. The First Palladium Catalyzed Asymmetric Michael Reaction Forming Quaternary Centers



The use of palladium pincer complexes in the asymmetric Michael reaction was further explored by Uozumi and coworkers in 2004.⁸⁴ They also investigated the asymmetric Michael reaction of vinyl ketones (**108**) and α -cyanocarboxylates (**28**), but

their palladium pincer complexes had pyrroloimidazolone coordinating groups. With low loading of their optimal catalyst **134** (0.5 mol %), they were able to obtain enantioenriched products (**ent•109**) in up to 91% yield and 83% ee (Table 1.5.9.1). The use of palladium pincer complexes was revisited again in 2007 by Fossey and coworkers.⁸⁵ They used chiral palladium bis-aldimine NCN–pincer complexes in the reaction of vinyl ketones and α -cyanocarboxylates. Although the reaction proceeded in nearly quantitative yield the product was completely racemic due to the conformational flexibility of the halide-abstacted catalyst.

Table 1.5.9.1. Palladium Pincer Complex-Catalyzed Asymmetric Michael Reaction

R ¹	R ²	Yield (%)	Time (h)	ee (%)
Et	Me	89	4	81
i-Pr	Me	90	4	80
CH(i-Pr) ₂	Me	93	24	80
i-Pr	Et	91	4	83

134

The first highly enantioselective palladium catalyzed Michael reaction was reported in 2002 by Sodeoka and coworkers.⁸⁶ They targeted β -diketones as their nucleophilic partner in the reaction because no work prior had attempted to utilize this type of dicarbonyl compound. The reaction of ketone **76** and **135**, which proceeds through a chelated chiral palladium enolate,⁸⁷ as evidenced by NMR and ESI-MS, is promoted by triflic acid and capable of generating product **136** in good yield and enantioselectivity at 10 mol % catalyst loading (**33**, Table 1.5.9.2). They extended their optimized conditions to

β -ketoesters and their substrate scope features both cyclic and acyclic β -ketoesters bearing bulky *t*-butyl or phenyl groups on the ester. Yields ranging from 69% to 93% and ee's narrowly ranging from 86% to 93% were obtained for several substrate combinations. Revealed in a subsequent full paper, the reaction is somewhat sensitive to substitution on the β -ketoester with some substrates proceeding in yields as low as 8% and ee's as low as 30%.⁸⁸ β -substituted *trans*-enones were also competent substrates in combination with *t*-butyl-2-oxocyclopentane-1-carboxylate, yielding vicinal stereocenter-containing products in good yield and excellent enantioselectivity as high as 99% for the major isomer with diastereoselectivities of 3.6:1 for (*E*)-4-phenylbut-3-en-2-one and 8:1 for (*E*)-pent-3-en-2-one. Good enantioselectivities but poor diastereoselectivities were observed for β -substituted *cis*-enones.

Table 1.5.9.2. Palladium-Catalyzed Michael Reaction Reported by Sodeoka and Coworkers

The reaction scheme shows the palladium-catalyzed Michael addition of a β -ketoester (76) to a substituted α,β -unsaturated carbonyl compound (135) in THF at -20°C using catalyst 33. Product 136 is a trisubstituted product where the β -ketoester has added across the double bond of the enone, resulting in a new chiral center with substituents R⁴ and R⁵.

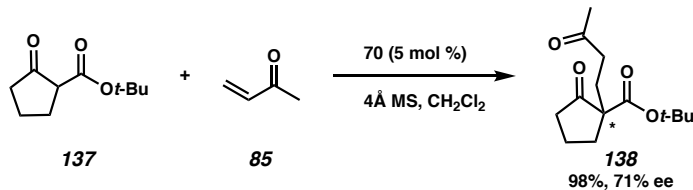
R ¹	R ²	R ³	R ⁴	R ⁵	Yield (%)	dr	ee, major (%)
$-(\text{CH}_2)_3-$	$\text{CH}_2\text{t-Bu}$	H	Me	Me	89	ND	90
Me	Me	O <i>t</i> -Bu	H	Me	88	ND	90
Me	Me	OPh	H	Me	69	ND	93
$-(\text{CH}_2)_3-$	O <i>t</i> -Bu	H	Me	92	ND	92	
$-(\text{CH}_2)_4-$	O <i>t</i> -Bu	H	Me	92	ND	90	
$-(\text{CH}_2)_3-$	O <i>t</i> -Bu	H	Et	84	ND	88	
$-(\text{CH}_2)_3-$	O <i>t</i> -Bu	Ph	Me	83	3.6:1	97	
$-(\text{CH}_2)_3-$	O <i>t</i> -Bu	Me	Me	89	8:1	99	
Et	Me	O <i>t</i> -Bu	H	Me	8	ND	35
Me	$-(\text{CH}_2)_2-$	H	Me	88	ND	30	

In a follow-up paper, Sodeoka and coworkers report the use of their palladium catalysts immobilized in ionic liquids in the asymmetric Michael reaction, allowing for

catalyst recycling.⁸⁹ The optimal ionic liquid for single use was 1-hexyl-3-methylimidazolium tetrafluoroborate ([hmim][BF₄]), generating products with yields as high as 97% and ee's as high as 88%, which is comparable to the results obtained in usual organic solvents. The optimal ionic liquid for recycling was found to be 1-butyl-3-methylimidazolium trifluoromethanesulfonate ([bmim][OTf]); unfortunately, the catalyst could be recycled only once before a significant drop in reaction rate took place. They could preserve the reactivity by using a palladium catalyst recycled previously in an asymmetric fluorination reaction, but only five cycles could be completed with this pretreated catalyst before a significant drop in reaction rate was observed.

Shi and coworkers demonstrated the use of palladium(II)-N-heterocyclic carbene-diaqua complexes in the asymmetric Michael reaction of β-ketoesters (**137**) and methyl vinyl ketone.⁴⁵ Using complex **70** they were able to obtain enantioenriched products (**138**) in up 98% yield and 71% ee (Scheme 1.5.9.2). They did not broadly explore the substrate scope of the asymmetric Michael reaction but instead investigated the use of complex **70** in the asymmetric Mannich reaction. (See Section 1.4).

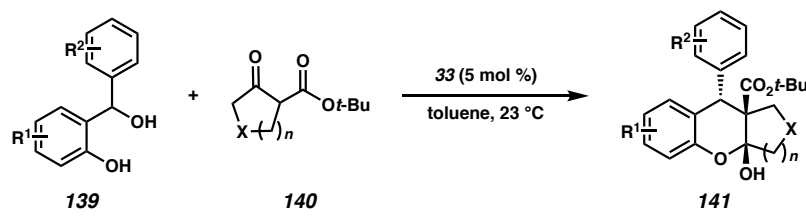
Scheme 1.5.9.2. Palladium N-Heterocyclic Carbene Diaqua Complexes in Asymmetric Michael Reaction of β-Ketoesters and Methyl Vinyl Ketone



More recently in 2018, Schneider and coworkers were able to utilize a palladium-aqua-BINAP complex **33** in order to perform an asymmetric Michael reaction with ortho-quinone methides and cyclic β-ketoesters.⁹⁰ The reaction of cyclic phenol **139** and β-

ketoesters **140** is believed to proceed through a chelated chiral palladium enolate which is then capable of undergoing a conjugate addition to *ortho* quinone methide, generated *in situ* with trifluoromethyl sulfonic acid, to form tricyclic chroman cores bearing vicinal tertiary and quaternary stereocenters (Table 1.5.9.3). The enantioenriched chroman products **141** were obtained in excellent yield (up to 99%), enantioselectivity (as high as 99%), and diastereoselectivity (as great as 95:5). Mechanistically, the reaction is believed to progress through a stepwise process. Palladium coordinated complex **33** first undergoes a conjugate addition to the *Re*-face of *ortho*-quinone methide through an open transition state. The initial addition product can then rearomatize through the hemi-ketalization to form the desired chroman core **141**.

Table 1.5.9.3. Palladium Diaqua Complex-Catalyzed Michael Reaction with o-Quinone Methides

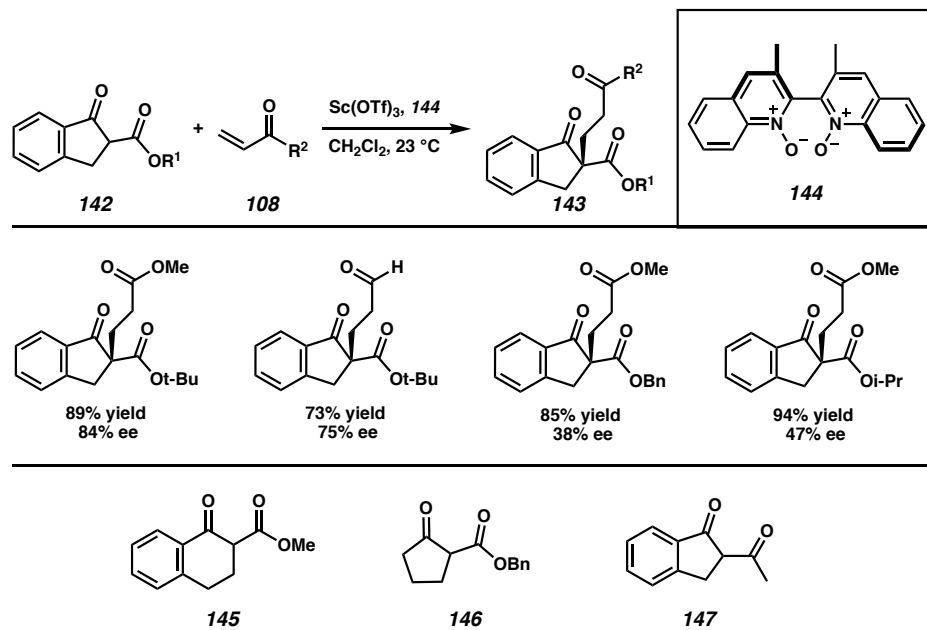


R ¹	R ²	X	n	Yield (%)	dr	ee (%)
H	p-OMe	O	1	95	90:10	98
H	p-Me	O	1	99	89:11	98
p-OMe	H	O	1	96	90:10	>99
p-t-Bu	Thi	CH ₂	2	94	88:12	99
H	p-OMe	S	1	83	88:12	99
p-t-Bu	p-OMe	S	1	92	>95:5	>99
p-OMe	p-OMe	NMoc	1	78	87:13	>99
H	p-OMe	CH ₂	1	99	84:16	99
p-t-Bu	H	CH ₂	1	93	86:14	99

1.5.10 MICHAEL ADDITIONS INVOLVING SCANDIUM AND YTTRIUM ENOLATES

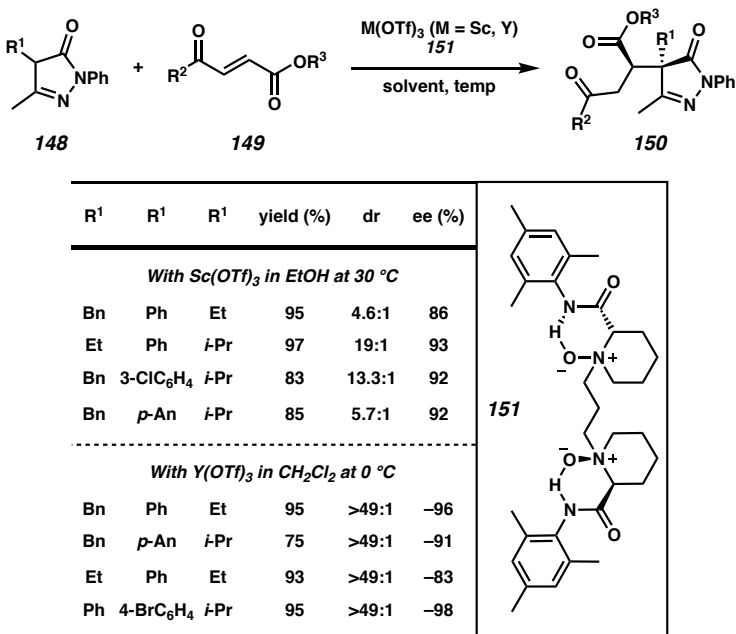
Chiral *N,N'*-dioxides have been used in a number of asymmetric transformations as organic catalysts or as tetradentate ligands for metal-catalyzed reactions.⁹¹ Nakajima and coworkers in 2001⁹² first utilized chiral *N,N'*-dioxides in the scandium-catalyzed asymmetric Michael reaction of indanone-2-carboxylates (**142**) and methyl vinyl ketone. By using a 1:1 mixture of ligand **144** and Sc(OTf)₃ in dichloromethane the enantioenriched products **143** could be obtained in good yield but with variable enantioselectivities. The highest ee observed was for the reaction of **142** and methyl acrylate, which proceeded with 89% yield and 84% ee although ee's as low as 38% were observed for some indan-2-carboxylate substrate combinations (Table 1.5.10.1).⁹³ The indanone-2-carboxylate skeleton appears to be important in the enantiocontrol of the reaction, as using substrate **145–147** instead of **142** afforded good yields of totally racemic products.

Table 1.5.10.1. Chiral Scandium-*N,N'*-Dioxide-Catalyzed Asymmetric Michael Reaction



Feng and coworkers utilized scandium *N,N'*-dioxide complexes in the asymmetric Michael reaction and their targeted substrates were 4-substituted-5-pyrazolones (**148**) and 4-aryl-4-oxo-butenoic esters (**149**, Table 1.5.10.2).⁹⁴ Interestingly, they were able to use one enantiomer of their optimized (*S*)-pipelicolic acid-derived ligand **151** to obtain either enantiomer of the Michael adduct by switching the metal from scandium to yttrium. With scandium yields ranging from 83–97% and enantioselectivities from 86–95%. The diastereoselectivity of the reaction was also good with dr's as high as 19:1, with yttrium the yields ranged from 75–95% and enantioselectivities from –83 to –98% with significantly improved diastereoselectivity, usually greater than 49:1. This reaction was also scalable up to gram-scale without loss of reactivity or selectivity.

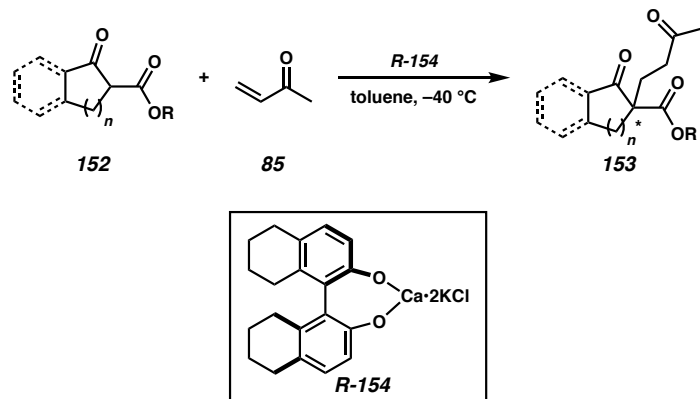
Table 1.5.10.2. Asymmetric Michael Reaction of 4-Substituted-5-Pyrazolones and 1,4-Dicarbonyl But-2-enes



1.5.11 MICHAEL ADDITIONS INVOLVING CALCIUM ENOLATES

An example of a calcium catalyzed Michael addition that generates products bearing quaternary stereocenters comes from Kumaraswamy and coworkers.⁹⁵ Their calcium–octahydro-BINOL complex **154** catalyzed the addition of a variety of cyclic β -ketoesters **152** to methyl vinyl ketone **85** in good yield and moderate to good enantioselectivities (Scheme 1.5.11.1).

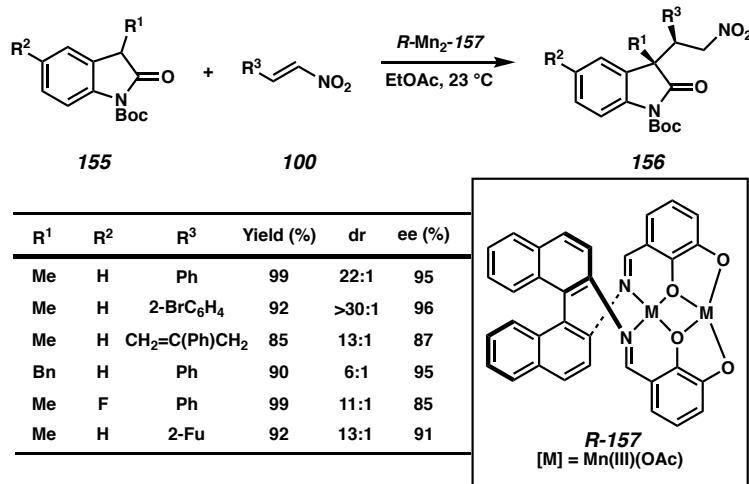
Scheme 1.5.11.1. Calcium-Octahydro-BINOL Complex-Catalyzed Asymmetric Michael Reaction



1.5.12 CONJUGATE ADDITION REACTIONS INVOLVING MANGANESE ENOLATES

An Asymmetric conjugate addition reaction of 3-substituted oxindoles **155** and nitroolefins **100**, similar to that in Table 1.5.3.2 was reported by Shibasaki and coworkers in 2009.⁹⁶ A homodinuclear manganese–Schiff base complex (**157**) catalyzed the conjugate addition of a variety of substrate combinations in high yields and excellent enantioselectivities ranging from 87–96% (Table 1.5.12.1). The diastereoselectivity of the reaction was also good with dr's ranging from 5:1 to greater than 30:1.

Table 1.5.12.1. Homodinuclear Manganese-Schiff Base Complex-Catalyzed Conjugate Addition Reaction



1.6 ALLYLIC ALKYLATION

1.6.1 INTRODUCTION

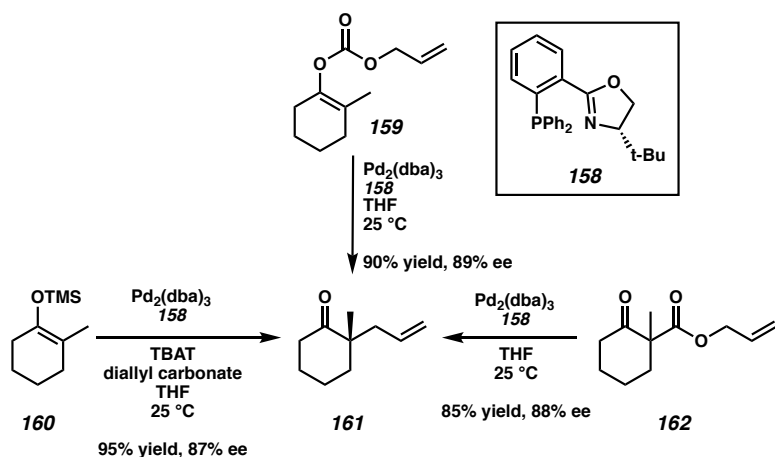
Asymmetric transition metal-catalyzed allylic alkylation has been an area of interest to many organic chemists.⁹⁷ Specifically, the use of palladium catalyzed allylic alkylation to asymmetrically generate stereocenters has received much attention over the last 30 years, but the generation of quaternary stereocenters using this strategy has only been utilized in the last 20 years.⁹⁸ In 1992, Ito and coworkers published a palladium-catalyzed asymmetric allylation of β -diketones using chiral phosphine ligands modified by crown ethers. Enantioselectivities up to 75% were obtained for a limited number of substrates.⁹⁹ Similarly in 2000, Tenaglia, Buono, and coworkers published a palladium-catalyzed asymmetric allylic alkylation reaction that generated a quaternary stereocenter using a chiral QUIPHOS ligand and a stabilized prochiral nucleophile derived from β -ketoesters.¹⁰⁰ Good yields and enantioselectivities were obtained for some select substrate combinations but in general their conditions resulted in poor enantioselectivities. Hamada

and coworkers were able to get consistently good enantioselectivities for the palladium-catalyzed allylic alkylation of their β -ketoester substrates using *P*-chirogenic diaminophosphine oxide ligands.¹⁰¹

1.6.2 PALLADIUM-CATALYZED ASYMMETRIC ALLYLIC ALKYLATION OF NON-STABILIZED ENOLATES

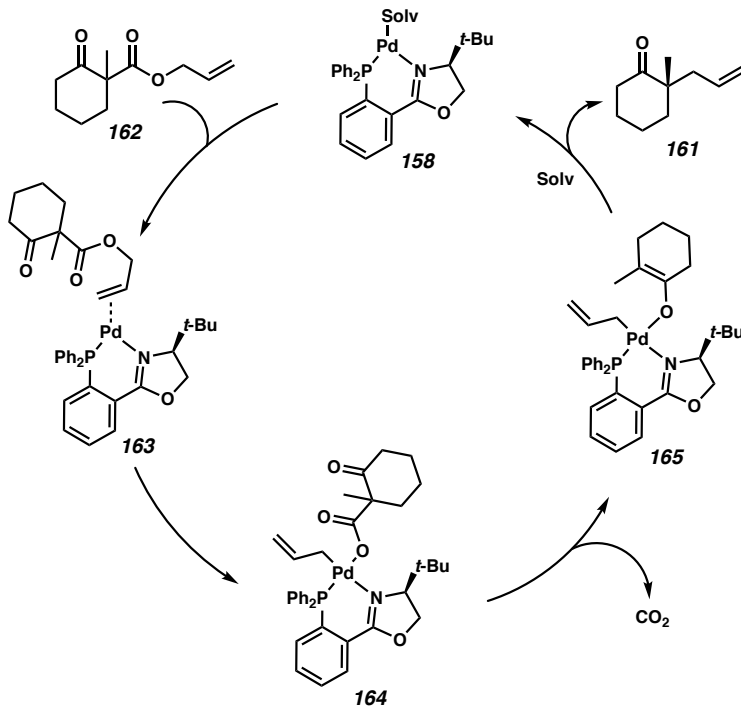
The first example of palladium-catalyzed asymmetric allylic alkylation of non-stabilized enolates bearing other enolizable positions was reported by Behenna and Stoltz in 2004.¹⁰² In this initial report, both cyclic enol carbonates (**159**) and cyclic silyl enol ethers (**160**), in the presence of TBAT, a diallyl carbonate, a palladium(0) complex, and *t*-butyl-PHOX ligand **158** to give the enantioenriched product **161** in good yields and enantioselectivities (Scheme 1.6.2.1). This work was later extended to include β -ketoesters substrates **162** as well.¹⁰³

Scheme 1.6.2.1. Palladium Catalyzed Asymmetric Allylic Alkylation of Non-Stabilized Enolates Bearing Other Enolizable Positions Reported by Stoltz and Coworkers



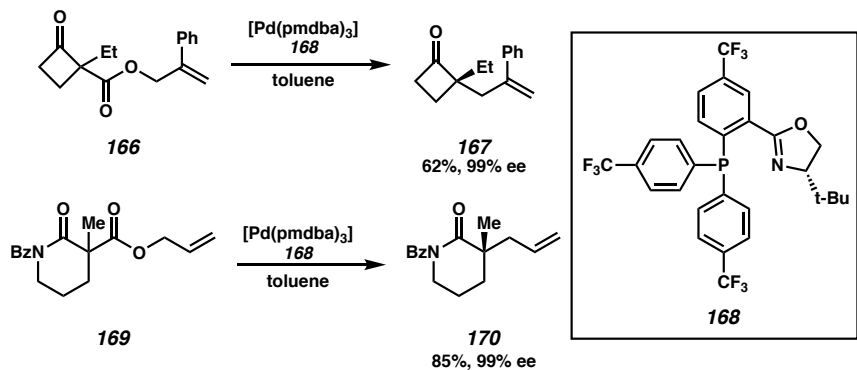
The proposed mechanism for the enantioselective decarboxylative allylic alkylation of a racemic allyl β -ketoester (**162**) to a chiral α -allyl ketone (**161**) catalyzed by Pd-phosphine complex **158**, proceeds through a number of intermediate steps (Scheme 1.6.2.2). Initial π -coordination of the allyl moiety to Pd generates complex (**163**), which then allows for oxidative insertion of the ester bond to form Pd(II) complex (**164**). Complex **164** is then able to undergo decarboxylation to form chiral Pd-enolate (**165**) followed by an inner-sphere sigmatropic reductive elimination to generate the desired product.¹⁰⁴

Scheme 1.6.2.2. Proposed Mechanism of the Palladium-Catalyzed Asymmetric Allylic Alkylation Reaction.



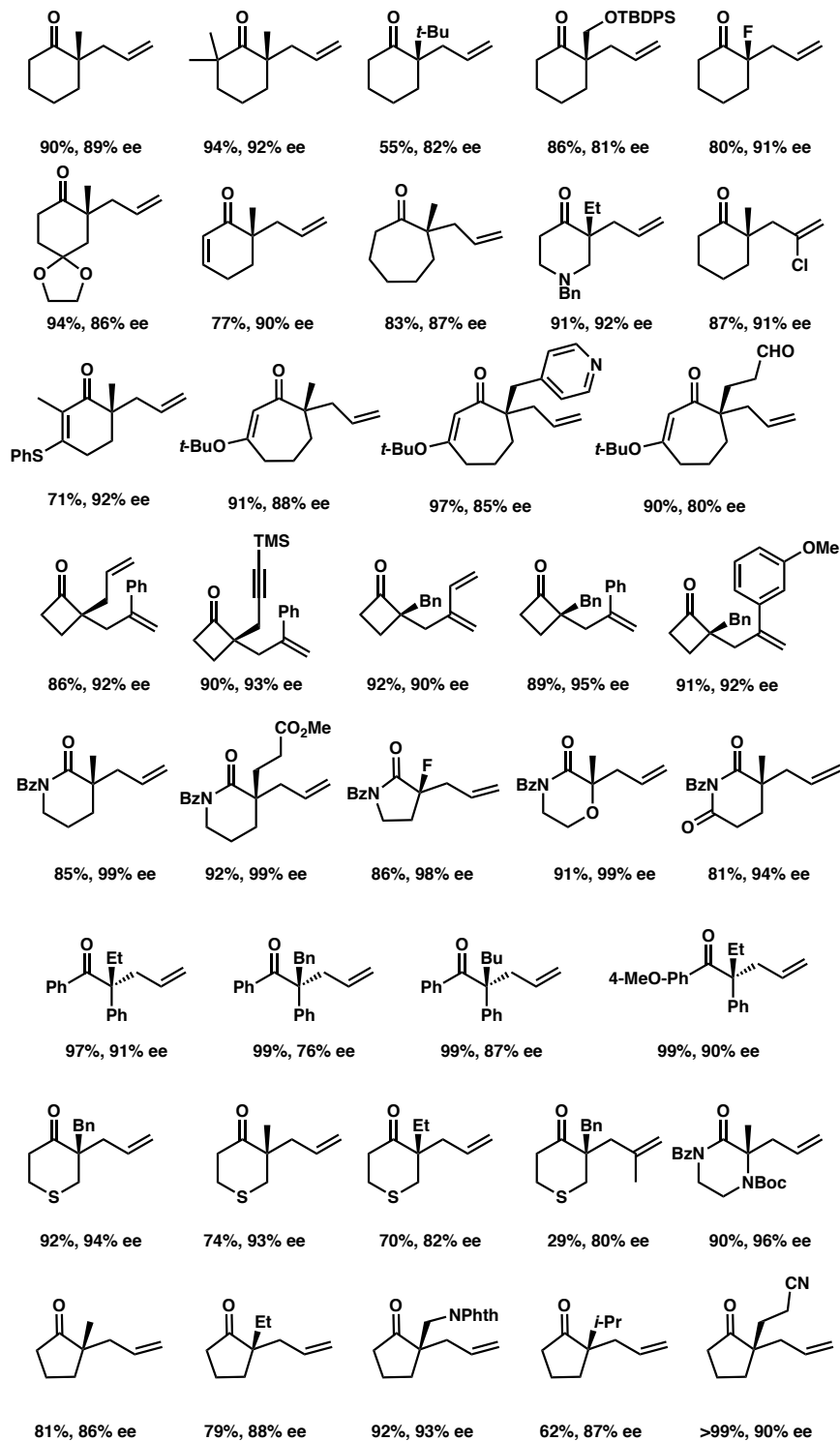
Stoltz and coworkers also found that the use of the more electron deficient $(\text{CF}_3)_3-$ *t*-Bu-PHOX (**168**) was found to give excellent yields and enantioselectivities with benzoyl-protected lactam substrates (e.g. **169**) as well as strained cyclobutanones (e.g. **166**) (Scheme 1.6.2.3).^{105,106s}

Scheme 1.6.2.3. Asymmetric Allylic Alkylation of Cyclobutanones and Protected Lactams



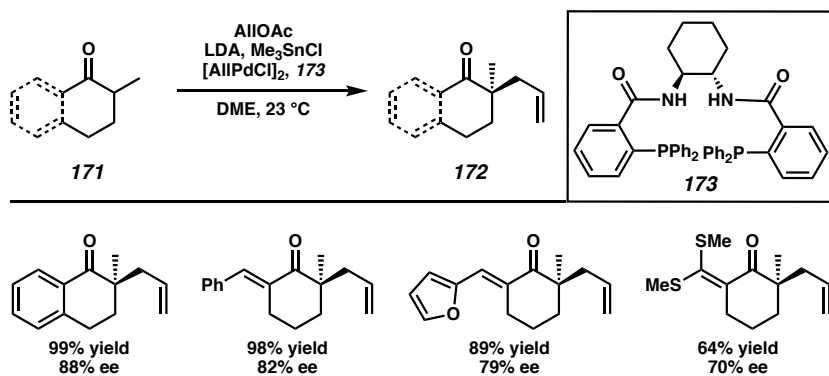
Utilize the PHOX ligand scaffold the Stoltz group has been able to perform the asymmetric decarboxylative allylic alkylation on a wide variety of substrates exhibiting great functional group tolerance (Figure 1.6.2.1). Recently the Stoltz group has been able to expand the scope of the asymmetric allylic alkylation chemistry to encompass Mannich adduct products,¹⁰⁷ as well as create chiral acyclic quaternary centers for the first time from stabilized palladium enolates utilizing the PHOX ligand scaffold.¹⁰⁸ Moreover, the catalyst loading could be dropped as low as 0.125 mol % Pd(OAc)₂ without greatly diminishing the yield or enantioselectivity of the reaction.¹⁰⁹

Figure 1.6.2.1. Representative Products of the Palladium-Catalyzed Asymmetric Allylic Alkylation Reaction Developed by Stoltz and Coworkers



Work by Trost and coworkers in the area of palladium catalyzed allylic alkylation to form quaternary stereocenters was first published in 1997.¹¹⁰ Their initial work was on the asymmetric allylic alkylation through stabilized enolates of tetralone-derived β -ketoesters using palladium and the Trost ligand **173**. In 1999, they pursued ketone substrates that would give non-stabilized enolate intermediates.¹¹¹ LDA was used to generate the lithium enolate *in situ* in the presence of the Lewis acid trimethyltin chloride, allyl acetate, a palladium source, and the Trost ligand **173**. An α -blocking group was required but thioacetals, benzylidene, furanylidene, and tetralones were all tolerated and generated their corresponding quaternary centered products (Table 1.6.2.1).

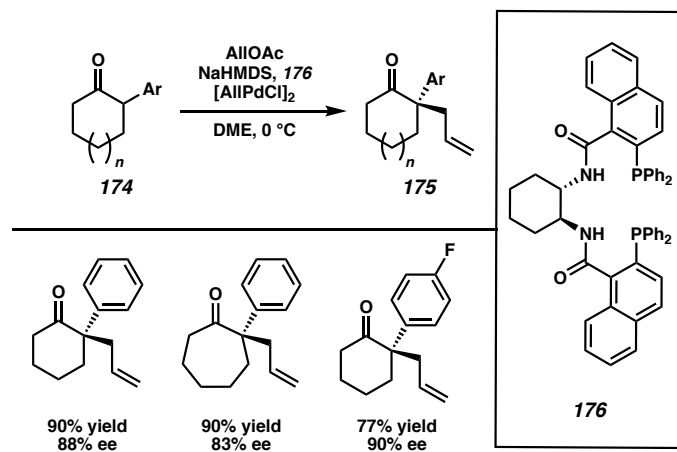
Table 1.6.2.1. Asymmetric Allylic Alkylation of β -Ketoesters Using LDA, Palladium, and the Trost Ligand



In 2002, Trost showed that aryl substituted cyclic ketones (**174**) could be subjected to a base like NaHMDS in the presence of allylpalladium(II) chloride dimer, a Trost ligand **176**, and allyl acetate to give good yields and enantioselectivities of the allyl-substituted enantioenriched product (**175**, Table 1.6.2.2).¹¹²

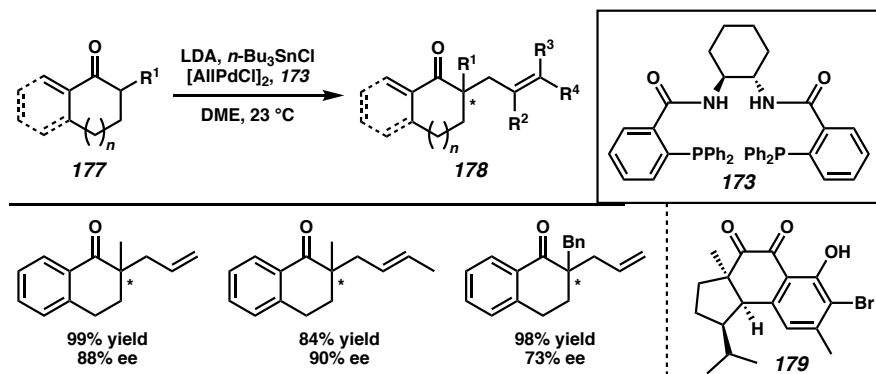
Table 1.6.2.2. Formation of Aryl Substituted Cyclic Ketones Using NaHMDS,

Allylpalladium(II) Chloride Dimer, a Trost Ligand, and Allyl Acetate



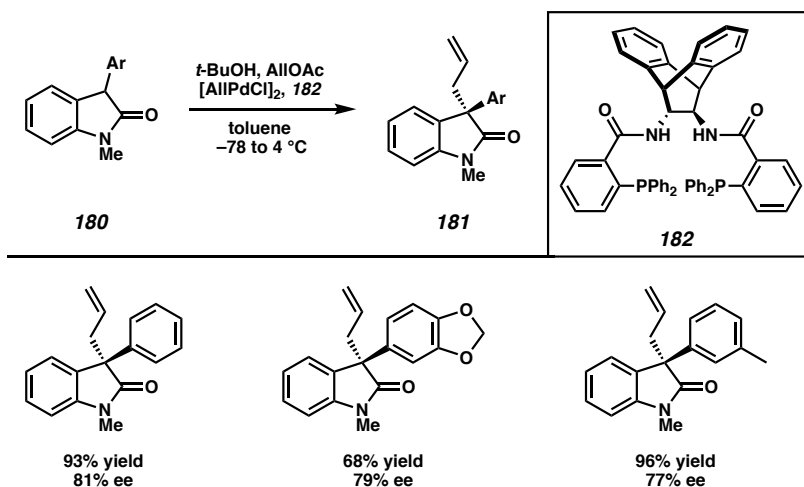
In 2005, Trost demonstrated that lithium enolates could be generated *in situ* in the presence of a tin Lewis acid, palladium source, and a Trost Ligand **173** to effect the asymmetric allylic alkylation of a variety of substituted tetralones.¹¹³ Good yields and enantioselectivities were obtained for a variety of allyl sources and for a variety of substituted tetralones **177** (Table 1.6.2.3).¹¹⁴ Other substrates with blocking groups were also tolerated including the dithioacetal. This method was featured in the synthesis of hamigeran B **179**.

Table 1.6.2.3. Asymmetric Allylic Alkylation of Lithium Enolates in the Presence of a Tin Lewis Acid, Palladium Source, and a Trost Ligand



Trost investigated the use of 3-aryloxindoles (**180**) as substrates for asymmetric allylic alkylation.¹¹⁵ The anthracenyl-Trost ligand **182** was found to be optimal, with no need to form the lithium enolate in order to obtain good yield and enantioselectivity of the corresponding products (**181**, Table 1.6.2.4).

Table 1.6.2.4. 3-Aryloxindoles In the Asymmetric Allylic Alkylation Reaction

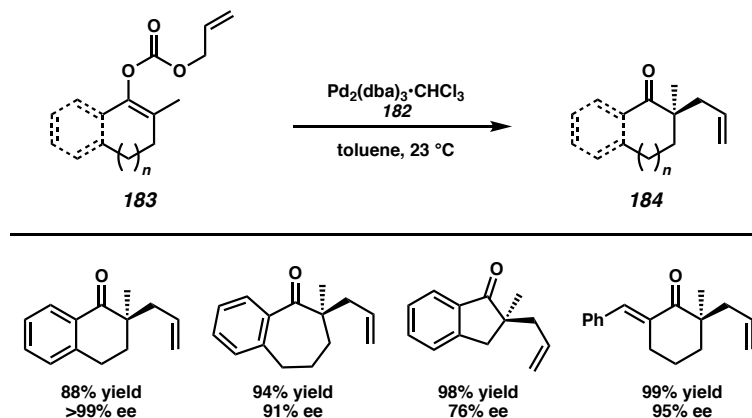


This work has also been extended to β -ketoesters and allyl enol carbonates (**183**).¹¹⁶

For the latter, Trost Ligand **182** was found to be optimal although α -blocking groups were necessary to obtain good yields of the quaternary stereocenter-containing product, for example, as in the 2,3-benzo cyclic ketones (Scheme 1.6.2.5), or in 2-benzylidenehexanone undergoing the same process (yields 99%, 95% ee). Allylated products bearing tertiary stereocenters could also be generated using these reaction conditions from unsubstituted all enol carbonates. Vinyllogous esters were also found to be good substrates for this chemistry.¹¹⁷

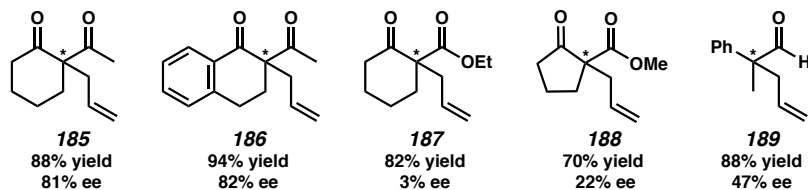
Table 1.6.2.5. Allyl Enol Carbonates In the Asymmetric Allylic Alkylation Reaction

Using Trost Ligand 182



Hayashi and coworkers found that sodium enolates could be subjected to chiral ferrocenylphosphine-palladium complexes and allyl acetate to form quaternary stereocenters bearing allyl substituents in good yields and modest enantioselectivities.¹¹⁸ Unfortunately, no ee's exceeding 82% were observed for any of the substrates tested and some of them yielded nearly racemic products (**185–189**, Figure 1.6.2.2).

Figure 1.6.2.2. Scope of Chiral Ferrocenylphosphine-Palladium Complex-Catalyzed Allylic Alkylation



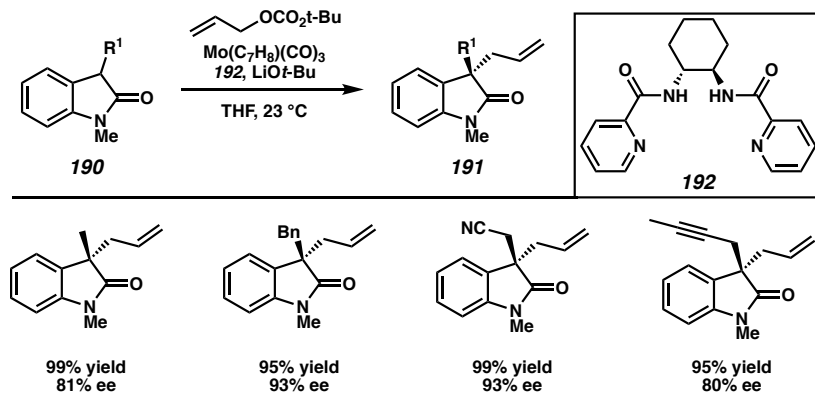
1.6.3 MOLYBDENUM-CATALYZED ASYMMETRIC ALLYLIC ALKYLATIONS

In 2006, the first example of molybdenum-catalyzed asymmetric allylation of oxindoles (**190**) to create quaternary stereocenters was reported by Trost.¹¹⁹ A variety of quaternary stereocenter-containing oxindoles **191** were obtained in good yields and

enantioselectivities when using catalyst $[\text{Mo}(\text{C}_7\text{H}_8)(\text{CO})_3]$ and ligand **192** (Table 1.6.3.1).

This method was also applied in the formal synthesis of (–)-physostigmine.

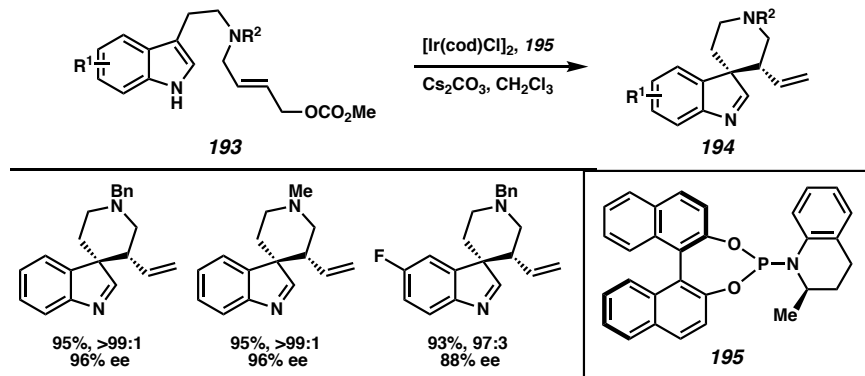
Table 1.6.3.1. Molybdenum-Catalyzed Asymmetric Allylic Alkylation



1.6.4 IRIDIUM-CATALYZED ALLYLIC ALKYLATIONS

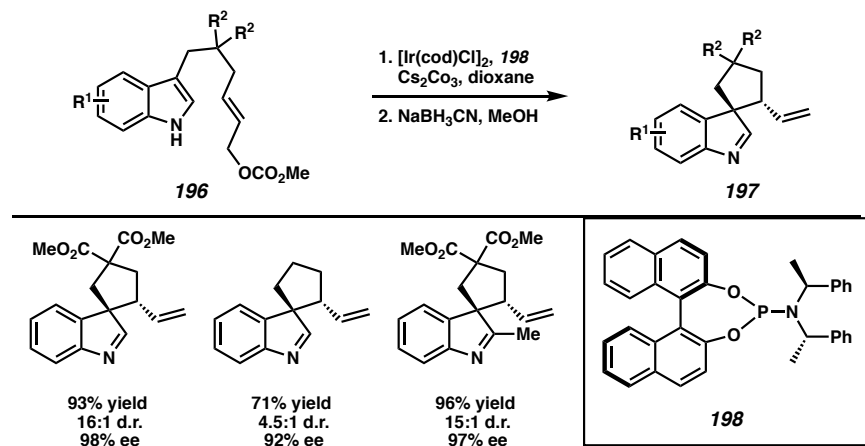
You and coworkers have reported in 2010¹²⁰ on the iridium-catalyzed intramolecular allylic alkylation reaction generating vicinal quaternary and tertiary stereocenters. Using $[\text{Ir}(\text{cod})\text{Cl}]_2$, phosphoramidite ligand **195** and cesium carbonate in dichloromethane they were able to transform indoles (**193**) into spirocyclic quaternary stereocenter-containing products (**194**) with good yields, diastereoselectivities, and enantioselectivities (Table 1.6.4.1).

Table 1.6.4.1. Iridium-Catalyzed Intramolecular Allylic Alkylation Generating Six-Membered Rings



You and coworkers also targeted Spirocyclic products (**197**) bearing five-membered rings in 2012. These products originated from indoles (**196**), this time using a BINOL-phosphoramidite derived ligand (**198**, Table 1.6.4.2).¹²¹

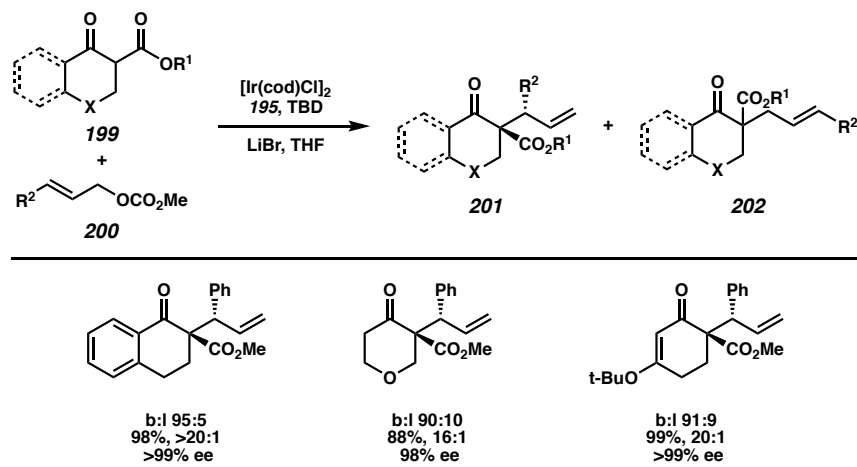
Table 1.6.4.2. Iridium-Catalyzed Intramolecular Allylic Alkylation Generating Five-Membered Rings



Initial work in the area of intermolecular iridium-catalyzed allylic alkylation by Takemoto and coworkers was focused on the generation of products bearing a tertiary stereocenter vicinal to a quaternary one.¹²² Stoltz and coworkers used iridium catalysis in the asymmetric allylic alkylation of cyclic β -ketoesters (**199**) to generate on reaction with

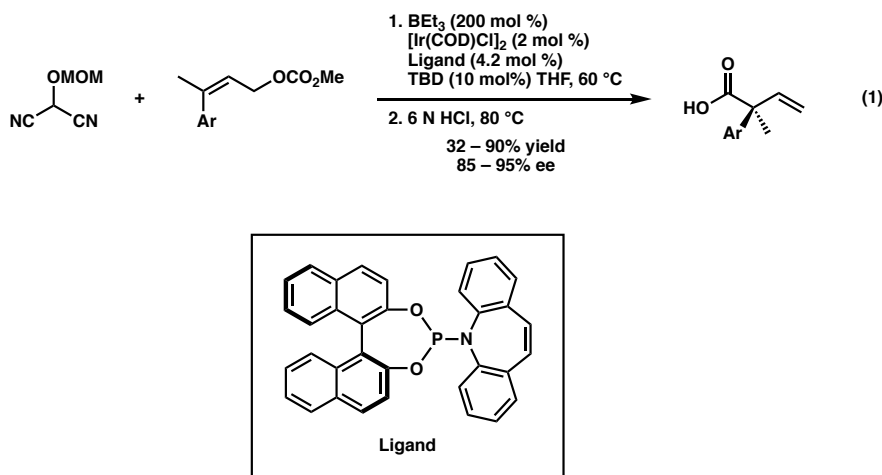
3-phenylallyl acetate compounds bearing vicinal quaternary and tertiary stereocenters (**201**, **202**, Table 1.6.4.3).¹²³ $[\text{Ir}(\text{cod})\text{Cl}]_2$ and phosphoramidite ligand **195** in the presence of the TBD base were used to preferentially generate these branched products by electrophilic attack of position 3 of the allyl group with good regio-, diastereo-, and enantioselectivity. Linear allylation products **202** were also obtained but as minor byproducts. Branched to linear ratios as high as 95:5, diastereoselectivities greater than 20:1 and enantioselectivities exceeding 99% ee were obtained. Acyclic substrates were targeted in a later publication with some products being obtained in >99% ee and 20:1 diastereoselectivity.¹²⁴

Table 1.6.4.3 Intermolecular Iridium-Catalyzed Allylic Alkylation to Generate Compounds Bearing Vicinal Quaternary and Tertiary Stereocenters



Hartwig and coworkers have reported on an intermolecular iridium-catalyzed allylic alkylation reaction of tetralones and cyclohexanones and allylcarbonates using $\text{Ba}(\text{Ot}-\text{Bu})_2$ in tetrahydrofuran. The vicinal quaternary and tertiary stereocenter-containing products were obtained in diastereoselectivities up to >20:1 and enantioselectivities up to >99% ee using a preformed iridium phosphoramidite catalyst.

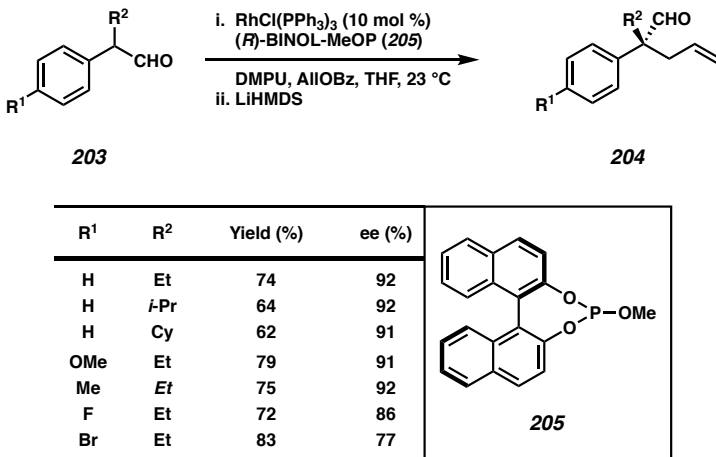
Finally Stoltz and coworkers reported the enantioselective synthesis of acyclic α -quaternary-containing carboxylic acid derivatives through iridium-catalysis (equation 1).¹²⁵ Masked acyl cyanides were used as the stabilized nucleophile to add into the Ir π -allyl complex formed from allylic carbonates and a phosphoramidite ligand. After an acidic workup, α -quaternary-center containing carboxylic acids were obtained in high yields and enantioselectivities.



1.6.5 RHODIUM-CATALYZED ALLYLIC ALKYLATIONS

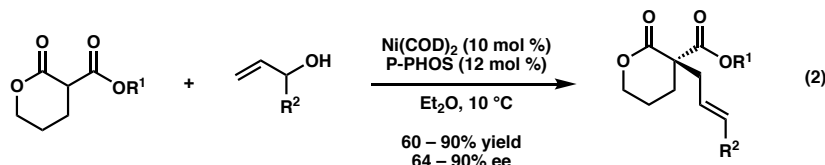
In 2016, Evans and coworkers reported the first example of a rhodium-catalyzed allylic alkylation of acyclic α -alkyl-benzaldehydes to form a quaternary center.¹²⁶ Utilizing a BINOL-derived phosphite ligand (**205**), DMPU additive, and LiHMDS, Evans and coworkers successfully generated α,α' -disubstituted benzaldehydes in excellent yields and enantioselectivities (Table 1.6.5.1). While the substrate scope is fairly limited, reaction conditions tolerate a variety of steric bulk α - to the aldehyde as well as electron rich and deficient benzyl substitutions.

Table 1.6.5.1. Scope of the Rhodium-Catalyzed Asymmetric Allylic Alkylation of Acyclic Aldehydes



1.6.6 NICKEL-CATALYZED ALLYIC ALKYLATION

In 2018, the Stoltz group reported the first example of a nickel-catalyzed intermolecular allylic alkylation of β -ketoesters with allyl alcohols (equation 2).¹²⁷ Utilizing P-PHOS and Ni(COD)₂ in Et₂O at 10 °C Stoltz and coworkers successfully generated α -quaternary-center containing δ -valerolactone in moderate yield and excellent yields. This method was further explored with benzoyl protected δ -valerolactams to afford excellent yields and enantioselectivities.



1.7 MISCELLANEOUS ALKYLATIONS

1.7.1 ASYMMETRIC ALKYLATIONS OF CHROMIUM ENOLATES

The first asymmetric alkylation of cyclic tin enolates using chromium complexes to generate quaternary stereocenters was reported in 2004 by Jacobsen.¹²⁸ Preformed tin

enolates (**206**) were exposed to an alkyl halide (bromide or iodide) electrophile and a chiral salen-chromium complex catalyst (**208**) in benzene at 0 °C to give the enantioenriched alkylated cyclic ketone product (**207**) in good yield and enantioselectivity (Table 1.7.1.1).

Table 1.7.1.1. Scope of Asymmetric Alkylation of Cyclic Tin Enolates Using Chromium Complexes

n	R ¹	R ²	yield (%)	ee (%)
1	Me	CH ₂ CCH	81	96
1	Me	Bn	91	93
2	Me	Et	43	90
2	CH ₂ CO ₂ Et	Et	72	89
2	Me	Bn	80	85

R,R-208

This work was extended to acyclic tin enolates (**209**) in 2007.¹²⁹ Using a modified chiral (salen)-chromium complex catalyst (**211**), to generate a variety of linear quaternary stereocenter-containing products (**210**) in good yield and enantioselectivity, although the latter were not as high as those observed in the cyclic case (Table 1.7.1.2).

Table 1.7.1.2. Scope of Asymmetric Alkylation of Acyclic Tin Enolates Using Chromium Complexes

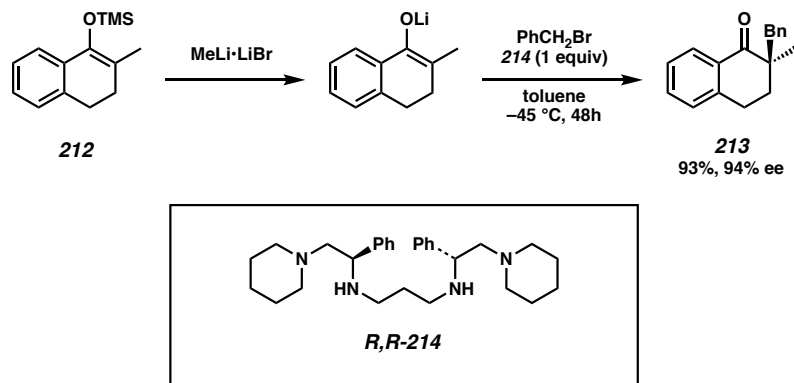
R ¹	R ²	yield (%)	ee (%)
Et	Bn	86	81
Et	CH ₂ CO ₂ Et	73	76
<i>n</i> -Bu	Bn	83	86
<i>n</i> -Bu	CH ₂ CCSiMe ₃	97	78

R,R-211

1.7.2 ASYMMETRIC ALKYLATION OF LITHIUM ENOLATES

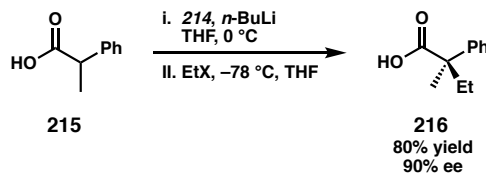
Asymmetric alkylation to construct quaternary stereocenters has also been achieved from achiral lithium enolates using chiral tetradentate ligands. Reported in 1999 by Koga and coworkers, Lithium enolates were generated from the silyl enol ethers (**212**) and were subjected to a chiral tetradentate amine ligand (**214**) and a bromide electrophile to achieve the asymmetric alkylation product (**213**) in good yield and enantioselectivity for some of the ligands tested (Scheme 1.7.2.1).¹³⁰ The scope of the reaction was not investigated in detail and although catalytic conditions were investigated, the best yields and enantioselectivities were observed when using the chiral ligand in stoichiometric ratio.

Scheme 1.7.2.1. Asymmetric Alkylation of Cyclic Lithium Enolates Utilizing Tetradentate Amine Ligands



In 2017, Zakarian and coworkers utilized similar conditions to perform the asymmetric alkylation of carboxylic acid **215** with various electrophiles to generate all-carbon quaternary center containing products **216**.¹³¹ Double deprotonation of the acid **215** by *n*-BuLi in the presence of stoichiometric chiral amine **214** followed by addition of the electrophile generated the products **216** in good yield (80%) and enantioselectivity (90%, Scheme 1.7.2.2).

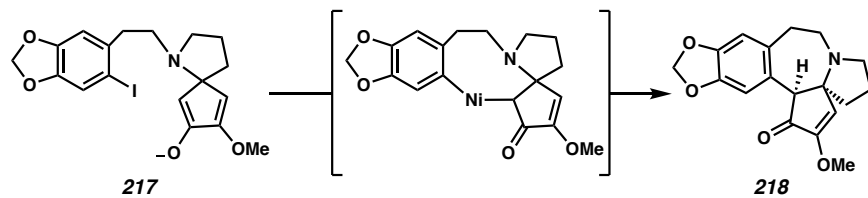
Scheme 1.7.2.2. Asymmetric Alkylation of Acyclic Acids Using Tetradentate Amines



1.8 α -ARYLATION AND α -ALKENYLATION

1.8.1 INTRODUCTION

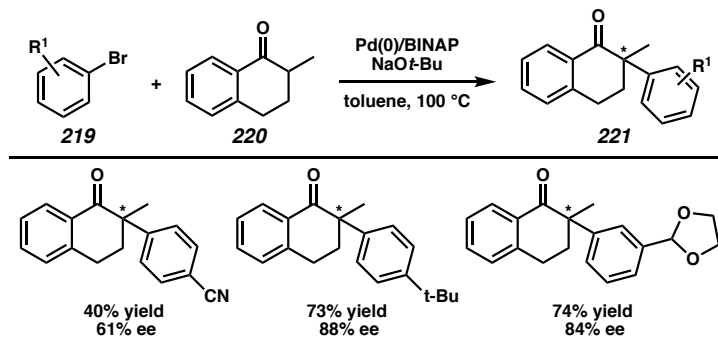
The first metal-catalyzed α -arylation reaction¹³² of a carbonyl compound was reported in 1973 by Semmelhack and coworkers,¹³³ using $[\text{Ni}(\text{cod})_2]$ to effect the ring-closure of **217** to obtain cephalotaxinone (**218**) in 25–30% yield (Scheme 1.8.1.1). In 1992 Musco, Santi, and coworkers reported the first asymmetric α -arylation reaction,¹³⁴ using palladium–(*R*)-BINAP complex generated *in situ* to obtain in 68% yield and 54% ee from a silyl ketene acetal and bromobenzene. Other chiral phosphine ligands provided reduced enantioselectivities. In 1997 Muratake and Natsume¹³⁵, Buchwald,¹³⁶ Hartwig,¹³⁷ and Miura¹³⁸ independently reported palladium-catalyzed catalyzed α -arylation reactions that produced racemic or achiral products from readily available ketones; these methods served as a foundation for the development of an asymmetric α -arylation reaction that forms asymmetric quaternary stereocenters.

Scheme 1.8.1.1. α -Arylation In the Synthesis of Cephalotaxinone (**218**)

1.8.2 PALLADIUM-CATALYZED REACTIONS

In 1998, the first asymmetric α -arylation reaction of ketone enolates yielding quaternary stereocenter-containing products was reported by Buchwald and coworkers.¹³⁹ Using 10–20 mol % of a palladium(0)–(*R*)-BINAP complex catalyst in toluene at elevated temperatures, 2-methyl- α -tetralone (**220**) could be α -arylated with a variety of aryl bromides giving modest to good yields (40–74%) and enantioselectivities (61–88% ee) of the quaternary stereocenter-containing products **224** (Table 1.8.2.1). 2-Methyl-1-indanone and 2-methylcyclopentanone derivative could also be obtained in high yields and enantioselectivities. Interestingly, α -arylated 2-methylcyclohexanone derivative could only be obtained with low enantioselectivity and no clear explanation was provided for this phenomenon. An intramolecular variation of this method was applied in Zhang's synthesis of physovenine albeit proceeding in extremely low enantioselectivity and only moderate yield.¹⁴⁰

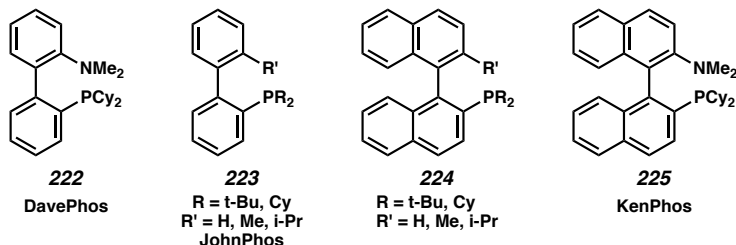
Table 1.8.2.1. Scope of Palladium BINAP-Catalyzed α -Arylation Reaction



Buchwald and coworkers extended this methodology to the asymmetric α -vinylation of ketone enolates.¹⁴¹ Considering that the palladium–BINAP catalyst led to the desired product in low yield and enantioselectivity, additional ligands were investigated. Prior work¹⁴² on the racemic α -arylation reaction identified 2aminophosphine ligand **222**

and simpler desamino ligands **223** and **224** as efficient ligands for α -arylation (Figure 1.8.2.1).

Figure 1.8.2.1. Aminophosphine and Desamino Ligands for α -Vinylation



Therefore, enantiomerically pure analogs of these ligands were synthesized and screened in the asymmetric α -vinylation reaction. Aminophosphine ligand **225** was found to provide the best yields and enantioselectivities in the synthesis of asymmetric vinylated ketones **228**, in combination with [Pd₂(dba)₃] for the reaction of cyclic ketones **226** ($R^1 = \text{Me}$) and *trans*-1-bromopropene (**227**, $R^2 = \text{H}$, $R^3 = \text{Me}$, Table 1.8.2.2). Lower temperatures provided increased enantioselectivities, but room temperature was found to provide the best balance of reactivity and selectivity. The scope of the reaction was quite broad with, α -vinylated derivates of 2-alkylcyclopentanones, 2-methylcyclohexanone, 2-methyl- α -tetralone (**229**), and 2-methyl-1-indanone (**230**) all being obtained in good to excellent yields (76–96%) and modest to good enantioselectivities (50–92%).

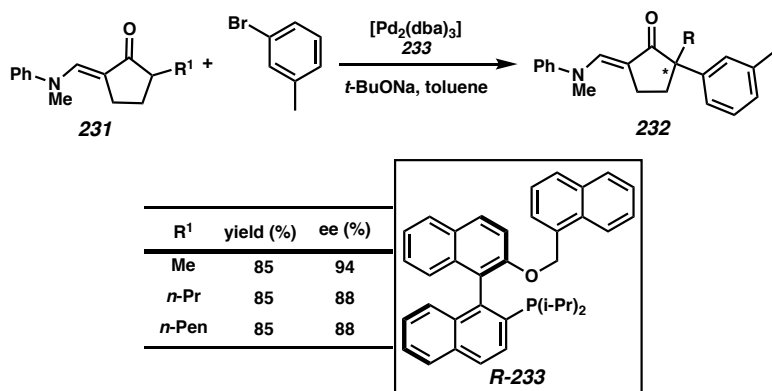
Table 1.8.2.2. Scope of Palladium-Catalyzed α -Vinylation Reaction

<i>n</i>	R ¹	R ²	R ³	yield (%)	ee (%)
1	Me	H	Me	95	90
1	Me	H	Ph	92	89
1	Me	H	H	94	92
1	Me	Me	Me	95	71
1	<i>n</i> -Pr	H	H	86	90
1	<i>n</i> -Pen	H	H	84	92
2	Me	H	H	78	50

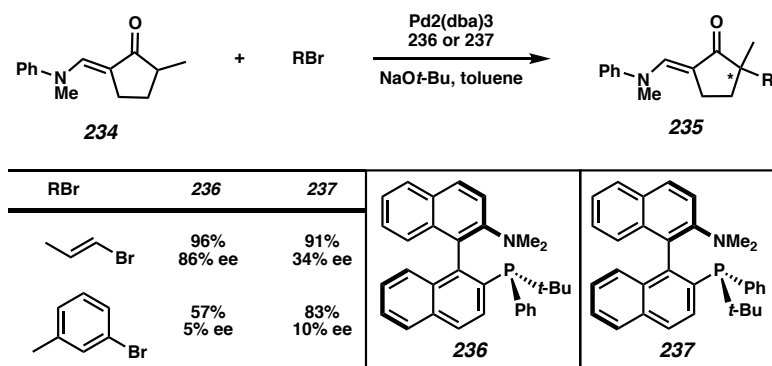
229
96% yield
80% ee

230
95% yield
74% ee

Following the success of enantiomerically pure aminophosphine and desamino phosphine ligands in the asymmetric α -vinylation reaction, they were also utilized in the asymmetric α -arylation reaction.¹⁴³ Aminophosphine ligand **233**, the optimal ligand found for the asymmetric α -vinylation reaction, was found to give the highest combined yield and enantioselectivity in the α -arylation reaction. The reaction with aminophosphine ligand **225** could be conducted at room temperature rather than the elevated temperatures required in the initial system, and a lower catalyst loading was also possible. Some ligands that were not previously screened in the asymmetric α -vinylation reaction, namely MOP-derived ligands, were also tested in the α -arylation reaction. Ligand **233** outperformed aminophosphine ligand **225** in the α -arylation reaction of cyclopentanone **231** with 3-bromotoluene, consistently giving higher yields and better enantioselectivities (up to 94% ee) under the same mild conditions (Table 1.8.2.3).

Table 1.8.2.3. Scope of Palladium MOP-Derived Ligand-Catalyzed α -Arylation

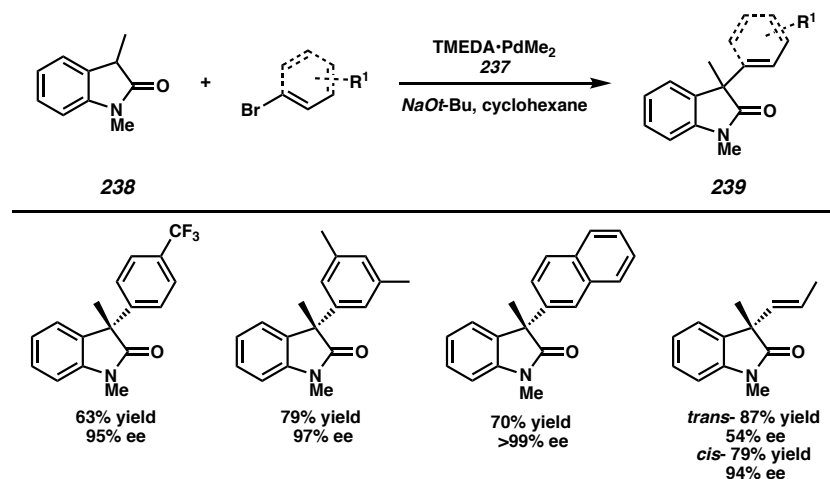
Further work by Buchwald and coworkers investigated *P*-chirogenic binaphthyl substituted monophosphine ligands in palladium-catalyzed asymmetric α -arylation and α -vinylation reactions.¹⁴⁴ Diastereomeric ligand **236** was found to give similar results as **225** for the α -vinylation reaction of **234** but reactions with **236** or its diastereomer **237** tested in the α -arylation of **234** were unable to exceed 10% ee of ketone **235** (Table 1.8.2.4)

Table 1.8.2.4. Scope of Palladium *P*-Chirogenic Binaphthyl Monophosphine Ligand-Catalyzed α -Arylation and α -Vinylation Reactions

These ligands were studied again in the context of palladium-catalyzed α -arylation and α -vinylation of 3-substituted oxindoles with more satisfying results.¹⁴⁵ For the α -

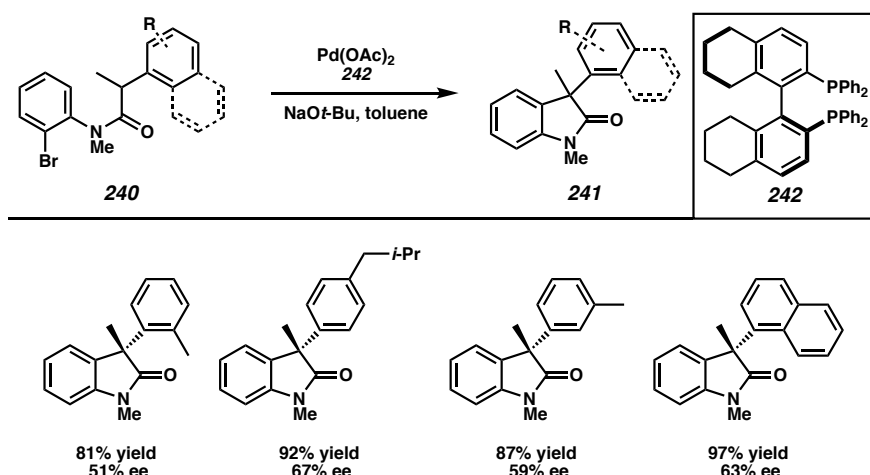
arylation reaction of oxindoles (e.g. **238**) using **237** as the chiral ligand, good yields and ee values greater than 99% could be obtained of **239** (Table 1.8.2.5).

Table 1.8.2.5. Scope of Palladium-Catalyzed α -Arylation and α -Vinylation of 3-Substituted Oxindoles



Enantioenriched 3-alkyl-3-aryloxindoles (**240**) were also the targeted products of Aoyama and coworkers. however, they were interested in an asymmetric intramolecular α -arylation reaction to close the oxindole ring in *N*-arylamides (**241**) rather than intermolecular arylation on an existing oxindole skeleton.¹⁴⁶ Using palladium and the (*S*)-H₈-BINAP ligand (**242**), they were able to effect this ring closing reaction (Table 1.8.2.6) in good yields (up to 97%) but only moderate enantioselectivities (51–67%) for a small collection of substrates.

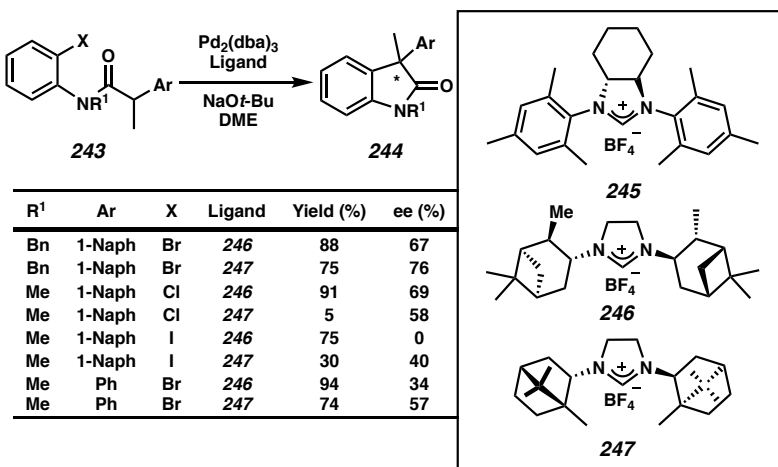
Table 1.8.2.6. Scope of Palladium-Catalyzed Intramolecular α -Arylation Reaction to Form Oxindoles



In addition to the success of phosphine and aminophosphine ligands, carbene ligands have also found widespread use in the palladium catalyzed asymmetric α -arylation reaction (Table 1.8.2.7). The first report of carbene ligands in a palladium-catalyzed asymmetric α -arylation reaction generating quaternary stereocenter-containing products is by Lee and Hartwig in 2001,¹⁴⁷ who investigated *N*-heterocyclic carbene (NHC) ligands **245–247** in the intramolecular α -arylation reaction of *N*-(2-bromophenyl)- α -arylpropionamides (**243**) to form enantioenriched 3,3-disubstituted oxindoles **244** (Table 1.8.2.7). Ligand **245**, derived from *trans*-1,2 diaminocyclohexane, performed as well as the phosphine ligands that were also investigated, although the enantioselectivities for both did not exceed 61%. Ligands **246** and **247**, derived from (–)isopinocampheylamine and (+)-bornylamine respectively, gave slightly higher enantioselectivities. Additionally, reactions with ligand **247** proceeded quite rapidly at room temperature allowing for even greater selectivities. After optimization of the base and solvent, the substrate scope was investigated for ligands **246** and **247**. Good yields and enantioselectivities ranging from

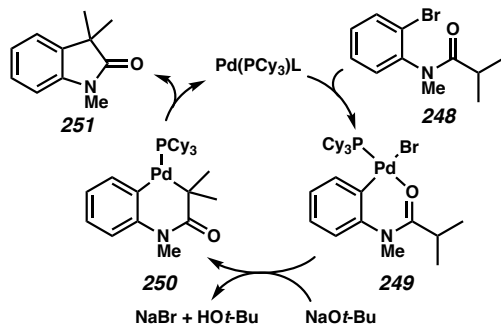
33% to 69% were obtained when using ligand **246** at room temperature or above. Ligand **247** performed slightly better, with enantioselectivities ranging from 40% to 76% at room temperature or below, but yields were highly variable, ranging from 5% to 95%.

Table 1.8.2.7. Scope of Palladium Carbene Ligand-Catalyzed Intramolecular α -Arylation Reaction to Form Oxindoles



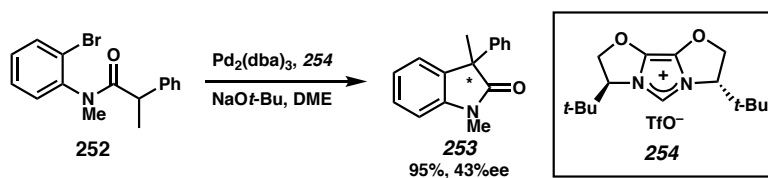
Further studies suggest the mechanism consists of oxidative addition of the catalyst to form palladacycle **249**, base-mediated formation of a C-bound palladium enolate (**250**), and reductive elimination to form the achiral product (**251**, Figure 1.8.2.2).

Figure 1.8.2.2. Proposed Mechanism of Palladium-Catalyzed Intramolecular α -Arylation Reaction Forming Oxindoles



The use of chiral carbene ligands in the palladium-catalyzed intramolecular α -arylation reaction to form enantioenriched 3,3-disubstituted oxindoles has also been investigated by Glorius and coworkers.¹⁴⁸ Although the major focus of this report was the synthesis and characterization of enantioenriched oxazoline-derived imidazolium salts, their subsequent deprotonation, and coordination to palladium, they also demonstrate the use of their novel NHC-palladium complex in the enantioselective synthesis of oxindole **253** (Scheme 1.8.2.1). Compound **253** has been previously synthesized by Lee and Hartwig, also via a palladium-catalyzed intramolecular α -arylation reaction, using 5 mol % of their palladium/NHC (**247**) catalyst to obtain a 74% yield of **253** with 57% ee at room temperature. Glorius and coworker's oxazoline-derived imidazolinium triflate **254** in combination with $\text{Pd}_2(\text{dba})_3$ and sodium *tert*-butoxide was able to catalyze the formation of **253** in an improved 95% yield but with slightly diminished 43% ee at room temperature.

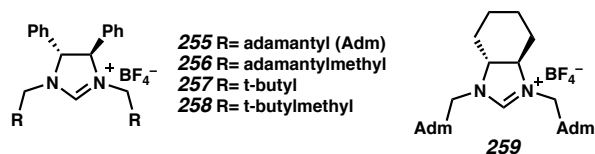
Scheme 1.8.2.1. NHC-Palladium Complex-Catalyzed Intramolecular α -Arylation



An asymmetric palladium-catalyzed intramolecular α -arylation reaction to form enantioenriched 3,3-disubstituted oxindoles using carbene ligands was also reported by Kondo, Aoyama, and coworkers.¹⁴⁹ They screened a number of NHC ligands **255** and **256** in the synthesis of **253**, a product targeted by Hartwig and Glorius. Using **255** as the NHC ligand precursor and sodium *tert*-butoxide as the base, they were able to obtain the product in 67% ee, but the yield was only 14%. The yield could be increased to 62% by switching the

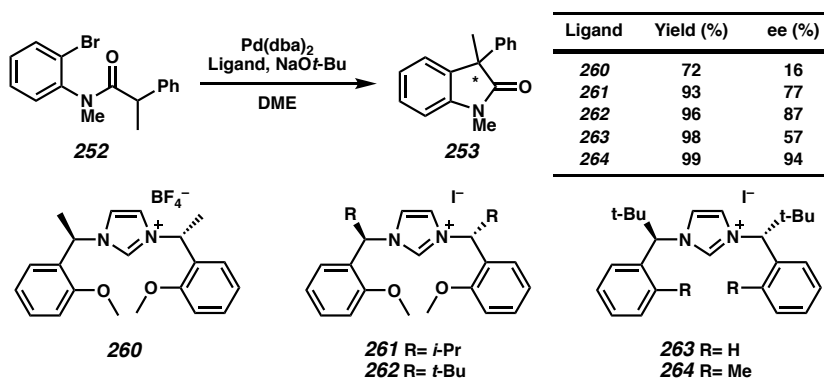
base to lithium *t*-butoxide but the enantioselectivity was slightly diminished to 61% ee (Figure 1.8.2.3).

Figure 1.8.2.3. NHC Ligands Screened in Intramolecular α -Arylation Reaction Reported by Kond, Aoyama, and Coworkers



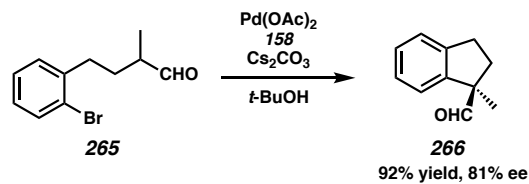
In 2007, Kündig and coworkers¹⁵⁰ synthesized five novel imidazolium salts **260–264** and screened them in the palladium-catalyzed ring-closing reaction of **252** to form **253** (Table 1.8.2.8). Previously the highest enantioselectivity seen in this reaction was 67% by using Kondo and Aoyama's **255** as the NHC ligand precursor. Kündig and coworker's NHC ligand precursor **264** in combination with Pd(dba)₂ and sodium *tert*-butoxide was able to catalyze the formation of **253** in 94% ee and quantitative yield. The scope of this reaction was also investigated and found to be quite broad, with only *ortho*- or electron-withdrawing substituents on the aniline ring resulting in low reactivity.

Table 1.8.2.8. Ligand Screen for Palladium-Catalyzed Intramolecular α -Arylation Reaction Reported by Kündig and Coworkers



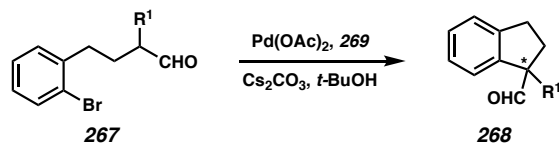
The asymmetric α -arylation of aldehydes was first reported in 2008 by Buchwald and coworkers.¹⁵¹ Initial optimization of reaction conditions concluded that the use of *t*-Bu-PHOX ligand **158** in *t*-BuOH with Pd(OAc)₂ and excess Cs₂CO₃ provided the highest yield (92%) and best enantioselectivity (81% ee) for the cyclization product (**266**) of **265** (Scheme 1.8.2.2).

Scheme 1.8.2.2. Palladium-Catalyzed Intramolecular α -Arylation of Aldehydes Reported by Buchwald and Coworkers



Additional PHOX ligands with varied steric and electronic properties were screened. No clear trend in ligand electronics could be seen but steric factors did play a major role in selectivity; bulky substituents on the phosphine leading to reduced enantioselectivities. Using *t*-Bu-PHOX ligand **269** a number of enantioenriched indane derivatives **268** bearing alkyl or aryl substituents were obtained in moderate to good yields and good to excellent enantioselectivities from aryl bromide **267** (Table 1.8.2.9). Tetrahydronaphthalene derivatives proved to be more challenging products to obtain in high enantioselectivities using these conditions.

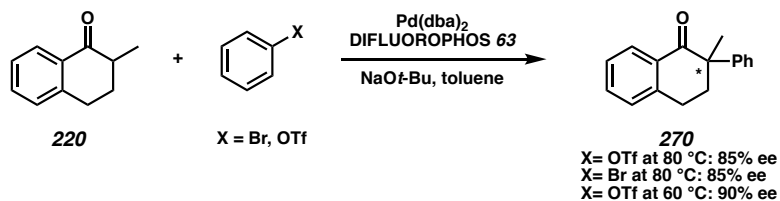
Table 1.8.2.9. Scope of Asymmetric Intramolecular α -arylation of Aldehydes Forming Indanes



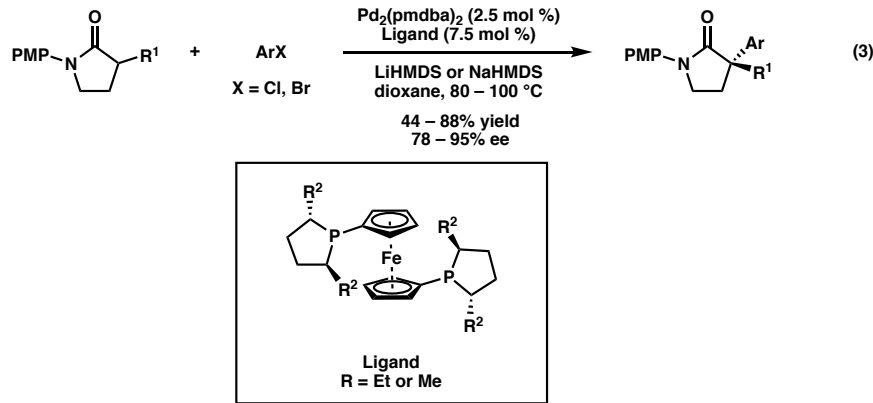
R ¹	Yield (%)	ee (%)	
Me	64	87	
i-Pr	86	94	
t-Bu	88	96	
Cy	87	96	
Ph	81	98	

Hartwig and coworkers were the first to report on the α -arylation of ketones using aryl triflates rather than aryl halides.¹⁵² Using DIFLUOROPHOS ligand and Pd(dba)₂ catalyst in the presence of two equivalents of sodium *tert*-butoxide, the arylation of tetralone **220** using bromobenzene or phenyl trifluoromethanesulfonate was investigated (Scheme 1.8.2.3). Although both reactions yielded product in 85% ee at 80 °C, the reaction of the aryl triflate proceeded faster allowing this reaction to be carried out at a lower temperature. At 60 °C, arylation of tetralone **220** with phenyl triflate provided the product in 90% ee. These optimized conditions were then applied in a substrate scope study. A variety of cyclic ketones were α -arylated with electron-rich and electron-neutral aryl triflates yielding quaternary stereocenter-containing products in good yields and enantioselectivities. α -Arylation using electron-poor aryl triflates required switching the palladium(0) catalyst to Ni(cod). Tetralone **220** and the analogous indanone were α -arylated under these nickel-catalyzed conditions to yield products in moderate to good yields and good to excellent enantioselectivities.

Scheme 1.8.2.3. Palladium-Catalyzed Asymmetric α -Arylation of Ketones Using Aryl Triflates



Finally in 2019, Stoltz and coworkers reported the first enantioselective α -arylation γ -lactams (equation 3).¹⁵³ Using dialkylferrocenane type ligands with $\text{Pd}_2(\text{pmdba})_3$ and a strong base in dioxane, α -quaternary containing γ -lactams were obtained in moderate to good yield and great enantioselectivities. Interestingly depending on the choice of base both aryl chlorides and aryl bromides could successfully undergo the desired transformation.

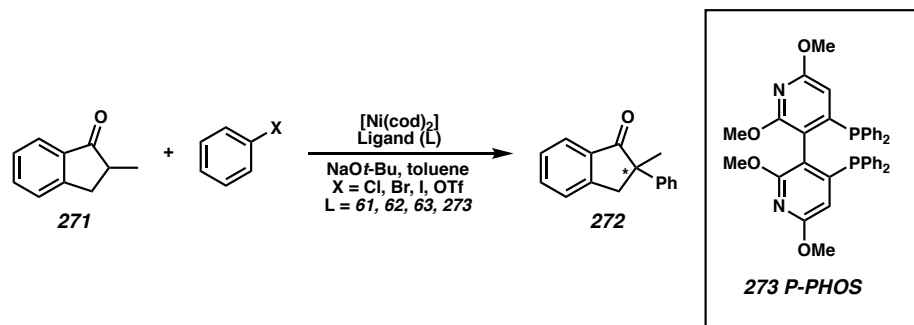


1.8.3 NICKEL-CATALYZED REACTIONS

In addition to the nickel-catalyzed α -arylation using electron-poor aryl triflates discussed in relation to Scheme 1.8.5.3, Hartwig and coworkers have utilized nickel also in the catalytic asymmetric intermolecular α -arylation and heteroarylation of ketones using aryl chlorides.¹⁵⁴ Aryl halides and triflates were investigated in the nickel-catalyzed α -

arylation of indanone **271** to form **272** using a variety of bidentate phosphine ligands (Scheme 1.8.3.1). For all ligands tested the yields and enantioselectivities of the reactions using phenyl chloride ($X = Cl$) exceeded the results obtained for the other electrophiles ($X = Br, I, OTf$). BINAP (**61**), SEGPHOS (**62**), DIFLUORPHOS (**63**), and P-PHOS (**273**) complexes of nickel were all able to catalyze the formation of **272** with yields ranging from 67% to 80% and enantioselectivities from 93% to 96%. Because of its availability and low cost, BINAP was selected as the ligand in further substrate scope studies.

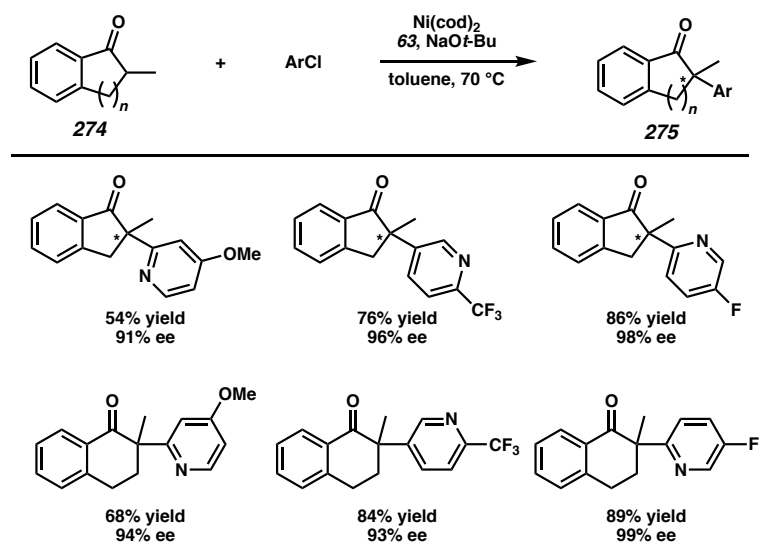
Scheme 1.8.3.1. Nickel-Catalyzed Asymmetric α -Arylation of Indanones



Electron-neutral, electron-rich, and electron-poor aryl chlorides were all competent substrates for the α -arylation of alkyl-substituted indanones and tetralones **274** with yields ranging from 58% to 89% and enantioselectivities from 90% to 99%. When heteroaryl bromides were investigated, no product was observed with BINAP (**61**) as the ligand; however, switching to DIFLUORPHOS (**63**) recovered the reactivity, albeit only in moderate yield and enantioselectivity (Table 1.8.3.2). Switching from heteroaryl bromides to heteroaryl chlorides boosted the yield and enantioselectivity dramatically. Several chloropyridine derivatives bearing electron-donating and electron-withdrawing groups, as well as 3-chlorothiophene, were successfully coupled with methyl-substituted indanone and tetralone **274** with moderate to good yields (54–93%) and moderate to excellent

enantioselectivities (81–99%). Reactions of 2-chloro-6-methoxypyridine proceeded in low enantioselectivity presumably due to chelation to the nickel center and two of the electron-deficient 2-chloropyridines proceeded in low enantioselectivity due to competing uncatalyzed nucleophilic aromatic substitution.¹⁵⁴

Table 1.8.3.1. Nickel-Catalyzed Intermolecular α -Heteroarylation of Cyclic Ketones



Prior to Hartwig's work on the asymmetric α -arylation of ketones using nickel–BINAP complex catalysts and aryl chlorides, Buchwald and coworkers reported the asymmetric α -arylation of γ -lactones (**276**) using nickel–BINAP complex catalysts and both aryl bromides and aryl chlorides.¹⁵⁵ The optimized conditions included the use of catalytic $[\text{Ni}(\text{cod})_2]$, BINAP, and ZnBr_2 along with 2.3 equiv of NaHMDS and an excess of the lactone in toluene–THF (3:1) solution at elevated temperatures. It is postulated that the ZnBr_2 acts as a Lewis acid facilitating halide abstraction generating a cationic nickel complex that undergoes transmetalation more rapidly resulting in the observed rate increase as well as the improved yield. The scope of this reaction was studied and it was found that *o*-substitution on the aryl halide is not tolerated, but both electron-rich and

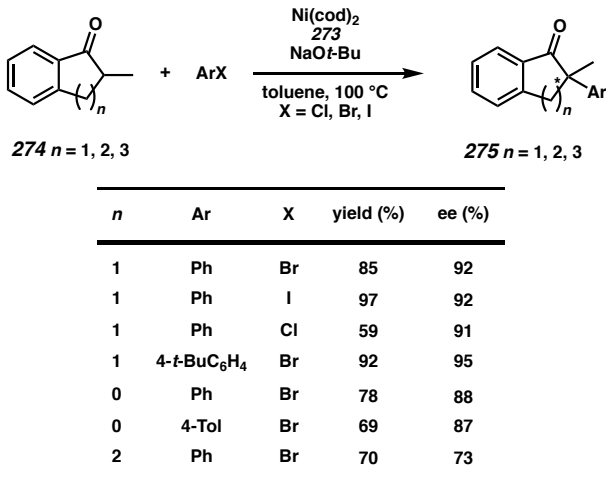
electron-poor aryl halides can be coupled with yields of γ -lactones (**277**) ranging from 57% to 95% and enantioselectivities ranging from 90% to 99% (Table 1.8.3.2). Various alkyl substitution on the lactone were tolerated with yields as high as 91% and enantioselectivities up to 98%.

Table 1.8.3.2. Asymmetric α -Arylation of Lactones Using Nickel BINAP Catalysts

276		ArX	$\xrightarrow[\text{ZnBr}_2]{\text{Ni}(\text{cod})_2, \text{BINAP, NaHMDS}}$	277	
R¹				yield (%)	ee (%)
Me	2-Naph	Br		33	98
Me	2-Naph	Cl		95	94
Me	3-Me ₂ N	Cl		81	>97
Me	3-CO ₂ Bu-t	Br		58	93
Bn	2-Naph	Cl		91	96
All	2-Naph	Cl		80	89
Bn	3-Me ₂ N	Cl		58	96
i-Pr	Ph	Cl		84	98

The asymmetric nickel-catalyzed α -arylation reaction leading to quaternary stereocenters (Table 1.8.3.3) was reported by Kwong, Chan, and coworkers in 2006.¹⁵⁶ The P-PHOS (**273**)–nickel complex in combination with sodium *t*-butoxide in toluene was able to effect the α -arylation of tetralone **274** with bromobenzene in 85% yield and 92% ee at elevated temperatures. Bromobenzene, chlorobenzene, and iodobenzene were all competent aryl coupling partners although yields were diminished when using chlorobenzene. A variety of *meta*- and *para*-substituted aryl bromides could be coupled in moderate to good yield and good to excellent enantioselectivities. Indanone **274** and benzosuberone containing a cycloheptanone moiety were also competent substrates.

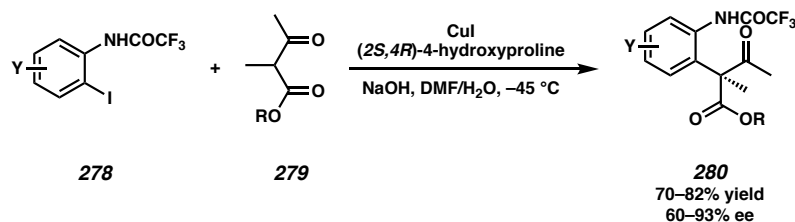
Table 1.8.3.3. Asymmetric Nickel Catalyzed α -Arylation Reaction Using P-Phos Ligand



1.8.4 COPPER-CATALYZED REACTIONS

One example of an asymmetric copper-catalyzed α -arylation was reported by Ma and coworkers in 2006.¹⁵⁷ This Ullman-type reaction involves the use of CuI and *trans*-4-hydroxy-l-proline, the chiral ligand, with sodium hydroxide as the base and aqueous DMF as the optimal solvent (Scheme 1.8.4.1). Notably these reactions are performed at low temperatures which is rare for Ullman-type reactions. Substituted β -ketoester **279** could be α -arylated with aryl iodides **278** under optimized conditions to generate **280** in yields ranging from 70% to 82% and enantioselectivities ranging from 60% to 93%. The NHCOCF₃ group on the aryl iodide is necessary as it promotes the Ullman-type reaction. Additional substitution on the aryl ring is tolerated although aryl iodides bearing electron-withdrawing groups require increased temperatures to ensure complete conversion and suffer from reduced yields due to competing reductive homo-coupling. Ethyl, isopropyl, and *t*-butyl ester substituents were also well tolerated, although the scope of the reaction in regards to the α -substituent on the β -ketoester was not examined.

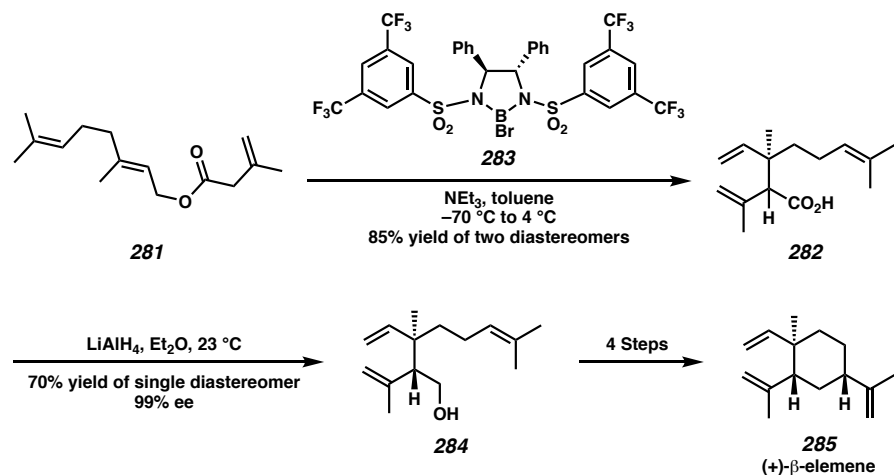
Scheme 1.8.4.1. Copper-Catalyzed Asymmetric α -Arylation Reported by Ma and Coworkers



1.9 PERICYCLIC REACTIONS

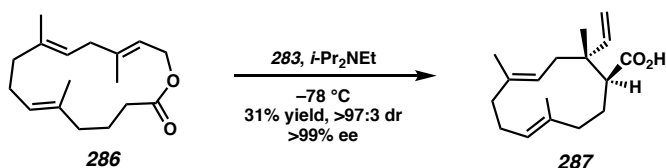
1.9.1 CLAISEN-TYPE REACTIONS

Pericyclic reactions have long served as important carbon-carbon bond forming reactions especially for the generation of quaternary centers. The Claisen rearrangement, discovered in 1912,¹⁵⁸ has seen over 100 years of use and many variations have been developed, including asymmetric methods.¹⁵⁹ Three asymmetric Claisen-type reactions yielding quaternary stereocenter-containing products that proceed through a metal enolate intermediate have been reported. The first one was reported by Corey and coworkers in 1995.¹⁶⁰ Their enantioselective Ireland-Claisen rearrangement relies on the use of chiral boron reagent **283**, which provides good control over the geometry of the intermediate boron enolate. Previous work with this reagent found that use of triethylamine as the base in toluene resulted in the formation of the (*Z*)-boron enolate.¹⁶¹ Corey applied this method to the synthesis of (+)- β -elemene (**283**). Compound **284** was treated with chiral boron reagent **283** and triethylamine in toluene to yield **282** as a mixture of two diastereomers (Scheme 1.9.1.1). After reduction of the carboxylic acid to a primary alcohol and purification to separate the two diastereomers, **284** was obtained in 70% yield and >99% ee.

Scheme 1.9.1.1. Corey's Synthesis of (+)- β -Elemene

Corey also applied this method in the synthesis of dolabellatrienone in which 286 was reacted with chiral boron reagent 283 and Hünig's base affording 287 in >97:3 dr and >99% ee but only a 31% yield (Scheme 1.9.1.2).¹⁶² The yield could be increased to 86% with no major loss in enantioselectivity or diastereoselectivity by switching to the more hindered base penta-isopropylguanidine.

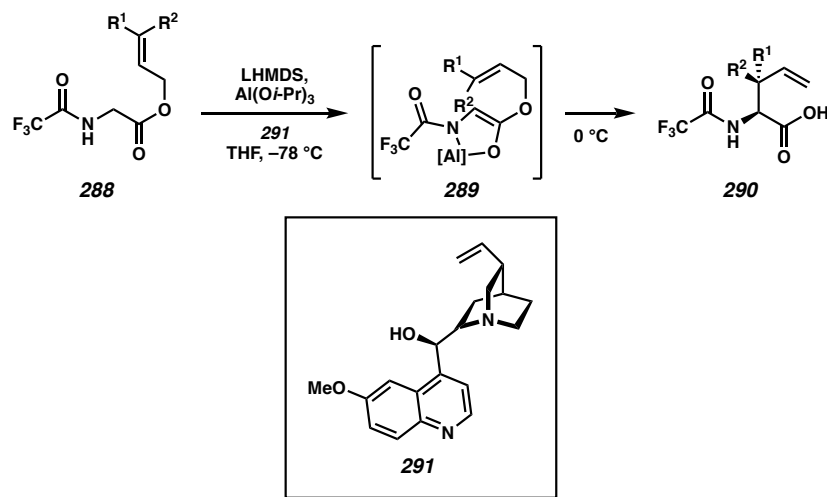
Scheme 1.9.1.2. Enantioselective Ireland-Claisen Rearrangement in Corey's Synthesis of Dolabellatrienone



The second example of an asymmetric Claisen-type reaction yielding quaternary stereocenter-containing products that proceeds through a metal enolate was reported by Krebs and Kazmaier in 1996.¹⁶³ Addition of LHMDS and excess Al(Oi-Pr)_3 to trifluoroacetyl-protected disubstituted allylic glycine ester 288 in the presence of quinine (291) in THF at $-78\text{ }^\circ\text{C}$ results in the formation of chiral chelated aluminum enolate 289

which, upon warming to room temperature undergoes an ester enolate Claisen rearrangement forming enantioenriched amino acid **290** (Scheme 1.9.1.3), containing a β -quaternary carbon stereocenter in high diastereoselectivity and good enantioselectivity. A variety of alkyl and aryl substituents were tolerated at the R^1 position with diastereoselectivities ranging from 9:1 to 49:1 dr and enantioselectivities from 81% to 93%, although the yields were quite low with none exceeding 51% and some as low as 12%. The only substituent investigated at the R^2 position was methyl because Z-configured esters failed to give the desired rearranged product, indicating that large cis-oriented substituents sterically crowd the quinine ligand in the coordination sphere.

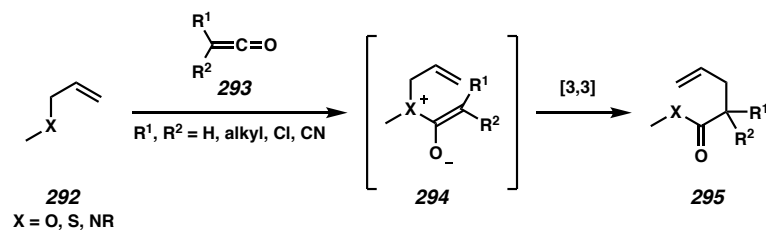
Scheme 1.9.1.3. Asymmetric Claisen-Type Reaction Using Aluminum Reported by Krebs and Kazmaier



The third example is an asymmetric ketene-Claisen rearrangement, also known as a *Belluš-Claisen rearrangement*, reported by MacMillan and coworkers in 2001. The Belluš-Claisen rearrangement, discovered in 1978,¹⁶⁴ is the reaction of an allylic ether, thioether, or amine (**292**) with a ketene (**293**), producing a zwitterionic intermediate (**294**) that undergoes a [3,3] sigmatropic bond reorganization yielding an *E* unsaturated ester,

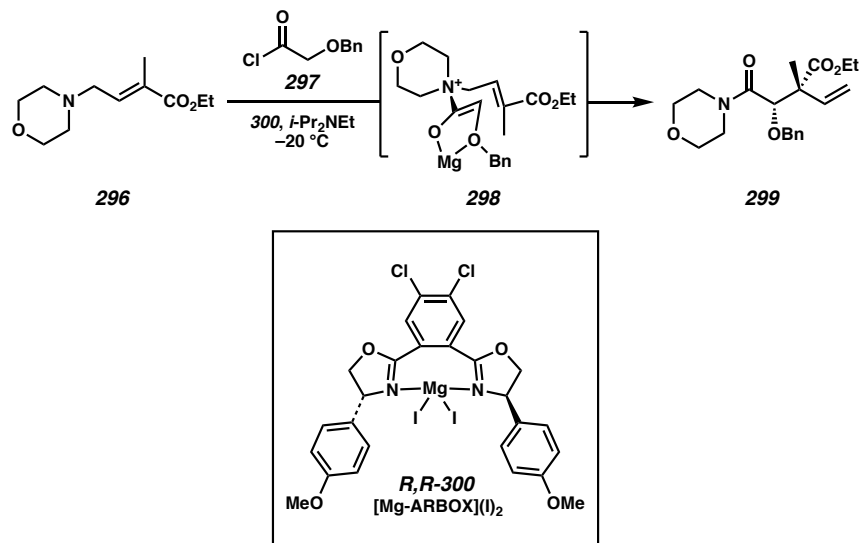
thioester, or amide (**295**) (Scheme 1.9.1.4).¹⁶⁵ Prior work by MacMillan and coworkers found that Lewis acids could serve to coordinate and activate the *in situ* formed ketene resulting in high yields and excellent diastereoselectivities of racemic rearranged products.¹⁶⁶ They envisioned that chiral Lewis acids may be able to effect enantioinduction in this rearrangement and in a subsequent publication they reported an asymmetric ketene-Claisen rearrangement.¹⁶⁷

Scheme 1.9.1.4. Generic Asymmetric Ketene-Claisen Rearrangement



Optimized reaction conditions of the acyl-Claisen rearrangement using *N*-allylmorpholines (e.g. **296**) included the use of an excess of chiral Lewis acid [Mg-ARBOX](I)₂ complex **300** in CH₂Cl₂ with Hünig's base and acid chloride **297** serving as the ketene surrogate (Scheme 1.9.1.5).¹⁶⁷ The -OBn group of **297** was crucial to obtaining good yields and enantioselectivities of the rearranged products as it serves to chelate the magnesium center in the intermediate magnesium enolate **298**. Although the reaction optimization was conducted on substrates yielding enantioenriched products bearing tertiary stereocenters, these conditions were also readily applied to 3,3-disubstituted allyl morpholine **271** which undergoes the acyl-Claisen rearrangement with acid chloride **297** to yield quaternary stereocenter-containing **299** in 75% yield, 97% ee, and 94:6 *syn:anti* diastereoselectivity.

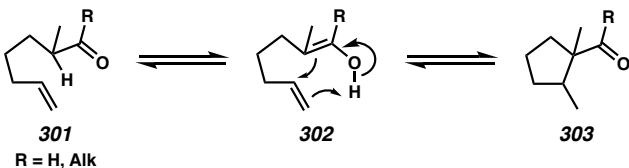
Scheme 1.9.1.5. Asymmetric Ketene-Claisen Rearrangement



1.9.2 CONIA-ENE REACTION

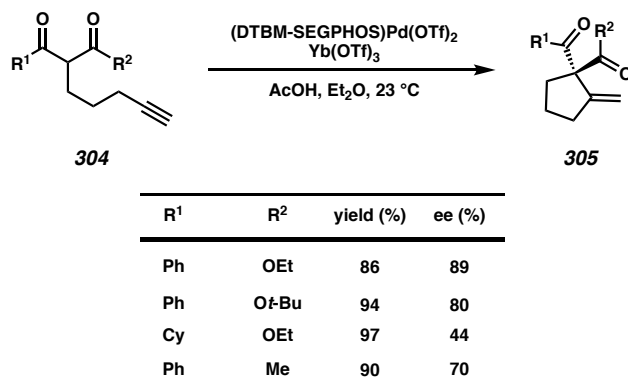
The Conia-ene reaction was first reported in 1968 by Conia and coworkers as the thermal intramolecular cyclization of a ketone or aldehyde with a tethered terminal alkene or alkyne.¹⁶⁸ Mechanistically, the reaction proceeds by two distinct steps (Scheme 1.9.2.1): first the ketone or aldehyde (**301**) is tautomerized at elevated temperatures to form the enol (**302**), which then undergoes a hydrogen shift from the enol group to the terminal double or triple bond with simultaneous formation of the new carbon–carbon bond (**303**).¹⁶⁹ A number of metals have been utilized in the asymmetric Conia-ene reaction including palladium, copper, lanthanum, and iron.

Scheme 1.9.2.1. Mechanism of the Conia-Ene Reaction



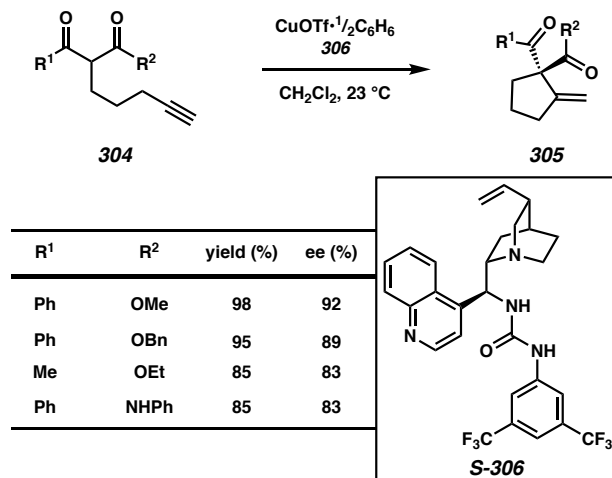
Toste and coworkers reported the first palladium-catalyzed Conia-ene reaction in 2005.¹⁷⁰ Stemming from their interest in the gold(I)-catalyzed intramolecular addition of β -ketoesters to alkynes,¹⁷¹ they envisioned that a chiral gold complex may be able to catalyze an asymmetric Conia-ene reaction. Although good yields were observed for this gold-catalyzed transformation the product was racemic. A screen of other metals identified the palladium complex with DTBM-SEGPHOS (**64**) as a competent catalyst for this reaction with moderate enantioselectivity, although the yield was low and the reaction proceeded slowly. Further optimization identified Yb(OTf)₃ as a co-catalyst which boosted the rate of the reaction and excess acetic acid as an additive which improved the asymmetric Conia-ene reactivity with good yields of **305** ranging from 70% to 97% and enantioselectivities ranging from 70% to 94%, with the exception of the aliphatic β -ketoester **305** ($R^1 = Cy$, $R^2 = OEt$), which proceeded in only 44% ee (Table 1.9.2.1). Mechanistically they propose the reaction proceeds through a palladium enolate that undergoes Lewis acid-promoted addition to the alkyne.

*Table 1.9.2.1. Scope of Palladium DTBM-SEGPHOS **64** Catalyzed Conia-Ene Reaction*



Dixon and coworkers reported a copper-catalyzed asymmetric Conia-ene reaction in 2009.¹⁷² Their cooperative catalysis approach aimed to utilize a cinchona-derived bifunctional catalyst (**306**) as well as a “soft” transition-metal ion. After optimization copper(I) triflate in combination with **306** was found transform **305** to β -ketoester **305** yielding up to a 92% ee and 98% conversion (Table 1.9.2.2). A number of pentynyl β -ketoesters with varying substituents on the ester and ketone groups were subjected to this reaction. Aliphatic, electron-rich, and electron-poor aromatic substrates were all competent participants in the cyclization reaction, with yields ranging from 67% to 98% and enantioselectivities ranging from 79% to 93%. β -Ketoamides were also found to be good substrates. Homologation of the carbon chain leading to the terminal alkyne was not tolerated in the reaction and products bearing six- or seven-membered rings could not be generated. Detailed kinetic and computational studies were completed in order to elucidate the mechanism of this transformation.¹⁷³

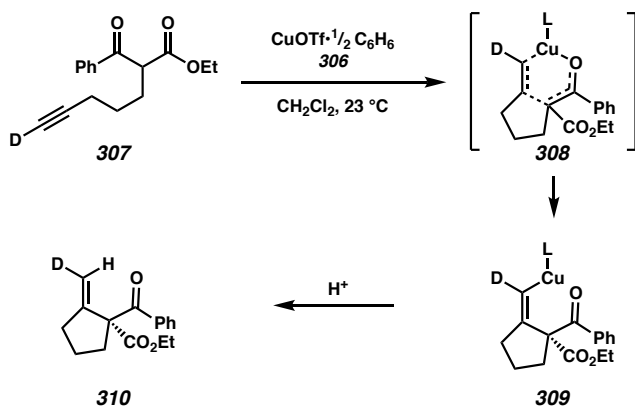
Table 1.9.2.2. Scope of Copper-Catalyzed Asymmetric Conia-Ene Reaction



The proposed mechanism (Scheme 1.9.2.2) begins with rate-determining enolization of the β -ketoester **307** forming copper enolate **308**. Coordination of the

cinchona-derived pre-catalyst to the copper center is followed by the stereo-determining *syn*-carbocupration generating **309**, which undergoes protonation–demetallation to form the product **310** and regenerate the catalyst.

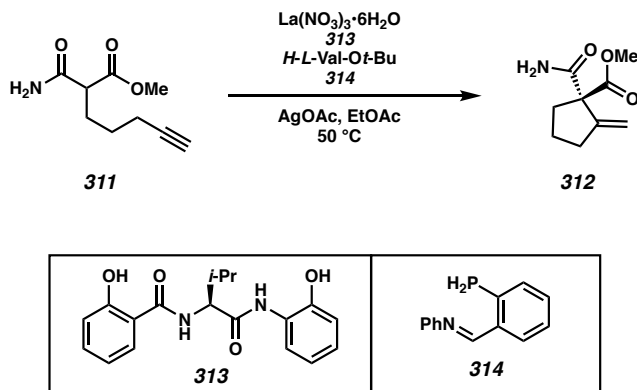
Scheme 1.9.2.2. Proposed Mechanism of Copper-Catalyzed Asymmetric Conia-Ene Reaction



Another example of the use of cooperative catalysis in the asymmetric Conia-ene reaction of malonic ester amide **311** comes from Kumagai, Shibasaki, and coworkers.¹⁷⁴ Their initial catalyst system used the combination of $\text{La}(\text{NO}_3)_3$, an amide-based chiral ligand **313**, and the protonated amino acid ester H-l-Val-Ot-Bu, in 1:1:3 ratio, in the presence of a soft Lewis acid. Screening of soft Lewis acids found that AgOAc in the presence of phosphine ligand **314** gave the desired product **312** in 55% yield, albeit with only slight enantioinduction (Scheme 1.9.2.3). The selectivity of the reaction was improved by modifying the metal to ligand ratios, switching from **314** to triphenylphosphine, and cooling the reaction down to 0 °C. With optimized conditions in hand a variety of substrates were subjected to the asymmetric Conia-ene reaction. Yields ranging from 63% up to 100% and enantioselectivities ranging from 83% to 96% were obtained for a variety

of substrates, with the exception of one bearing an electron-donating methoxy substituent which gave only 26% yield despite extended reaction time.

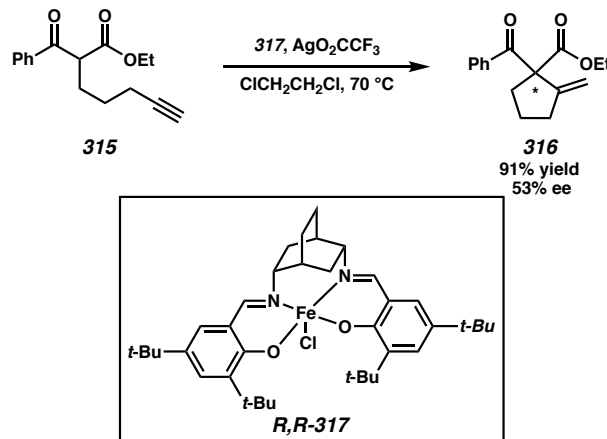
Scheme 1.9.2.3. Use of Cooperative Catalysis in the Asymmetric Conia-Ene Reaction



Shaw and White recently reported an iron-catalyzed asymmetric Conia-ene reaction with a broader substrate scope than that of the previous reports.¹⁷⁵ Their initial screen of metal-salen complexes identified iron salen complex **317** as able to catalyze the transformation of **315** to **316** in moderate yield and selectivity. Addition of silver trifluoroacetate or silver triflate boosted the yields of these reactions; however, the enantioselectivity of the reaction remained unsatisfactory (Scheme 1.9.2.4). New salen ligands were synthesized and investigated in this reaction and the optimal reaction conditions were found to be 7.5 mol% **317** in chloroform. A variety of β -ketoesters, thioesters, and ketones bearing the pentynyl group were found to be good substrates for this reaction, forming the products in good yields and excellent enantioselectivities. Unlike any previous asymmetric method, β -ketoesters bearing hexynyl and heptynyl groups at the α -position could be cyclized to give the *exo*-methylenecyclohexene and *exo*-methylenecycloheptene with no loss of reactivity or selectivity. Even a β -ketoesters

bearing a butynyl group at that position could be cyclized to yield the cyclobutane, although the yield and ee were somewhat diminished.

Scheme 1.9.2.4. Iron-Catalyzed Asymmetric Conia-Ene Reported by Shaw and White



1.10 NOTES AND REFERENCES

1. This chapter includes reported research up to and including the year 2018.
2. A. Jay in *Dictionary of Chemistry*, 2nd Edition (Ed. E Geller), McGraw-Hill, 2003, p. 317.
3. (a) Sears, J. E.; Boger, D. L. *Acc. Chem. Res.* **2015**, *48*, 653–662. (b) Giner, J.-L.; Kehbein, K. A.; Cook, J. A.; Smith, M. C.; Vlahos, C. J.; Badwey, J. A. *Bioorg. Med. Chem. Lett.* **2006**, *16*, 2518–2521. (c) Egger, H.; Reinshagen, H. *J. Antibiot.* **1976**, *29*, 923–927.
4. For reviews see: (a) Prakash, J.; Marek, I. *Chem. Commun.* **2011**, *47*, 4593–4623. (b) Douglas, C. J.; Overman, L. E. *Proc. Natl. Acad. Sci.* **2004**, *101*, 5363–5367. (c) Minko, Y.; Pasco, M.; Lercher, L.; Botoshansky, M.; Marek, I. *Nature* **2012**, *490*, 522–526.
5. d'Angelo J. *Tetrahedron* **1976**, *32*, 2979–2990.

-
6. Evans, D. A.; Nelson, J. V.; Taber, T. R., *Top. Stereochem.*, **13**, 1 (1982); Heathcock, C. H. in *Asymmetric Synthesis*, Vol. 3 (Ed. J. D. Morrison), Chap. 2, Academic Press, 1984, p. 111–212.
 7. Mekelburger, H. B.; Wilcox, C. S. in *Comprehensive Organic Synthesis*, 2nd Edition (Eds. Knochel, P. and Molander, G. A.), Chap. 2, Elsevier, 2014, p. 243–272.
 8. (a) Ireland, R. E.; Willard, A. K. *Tetrahedron Lett.* **1975**, *16*, 3975–3978. (b) Ireland, R. E.; Wipf, P. (c) Armstrong, J. D. III, *J. Org. Chem.* **1991**, *56*, 650–657.
 9. Seebach, S. *Angew. Chem. Int. Ed. Engl.* **1988**, *27*, 1624–1654.
 10. Ireland, R. E.; Mueller, R. H.; Willard, A. K. *J. Am. Chem. Soc.* **1976**, *98*, 2868–2877.
 11. Frostick, F. C.; Hauser, C. R. *J. Am. Chem. Soc.* **1949**, *71*, 1350–1352.
 12. Boechman, Jr., R. K.; Chinn, R. L. *Tetrahedron* **1985**, *26*, 5005–5008.
 13. Taylor, R. J. K. *Synthesis* **1985**, 364–392.
 14. Collman, J. P. *J. Org. Chem.* **1961**, *26*, 3162–3166.
 15. Jung, M. E.; Nishimura, N. *Org. Lett.* **2001**, *3*, 2113–2115.
 16. House, H. O.; Czuba, L. J.; Gall, M.; Olmstead, H. D. *J. Org. Chem.* **1969**, *34*, 2324–2336.
 17. (a) Cazeau, P.; Moulines, F.; Laporte, O.; Duboudin, F. *J. Organomet. Chem.* **1980**, *201*, C9–C13. (b) Miller, R. D.; McKean, D. R. *Synthesis* **1979**, 730–732. (c) Chan, T. H.; Zheng, G. Z. *Tetrahedron Lett.* **1993**, *34*, 3095–3098.
 18. Shrestham R.; Dorn, S. C. M.; Weix, D. J. *J. Am. Chem. Soc.* **2013**, *135*, 751–762.
 19. Suzuki, H.; Koyama, Y. *Tetrahedron Lett.* **1979**, *20*, 1415–1418.

-
20. Davis, F. A.; Lal, G. S.; Wei, J. *Tetrahedron Lett.* **1988**, *29*, 4269–4272.
 21. Chantani, N. Murai, S.; Sonoda, N. *J. Am. Chem. Soc.* **1983**, *105*, 1370–1372.
 22. Reich, H. J.; Holtan, R. C.; Borkowsky, S. L. *J. Org. Chem.* **1987**, *52*, 312–314.
 23. (a) T. Mukaiyama and J.-I. Matsuo in *Modern Aldol Reactions*, 1st Edition (Ed. R. Mahrwald), Chap. 3, Wiley, 2004, p. 127–160. (b) C. J. Cowden and I. Paterson in *Organic Reactions*, Vol. 51, Chap. 1, Wiley, 1997, p. 1–200. (c) Masamune, S.; Choy, W.; Kerdsky, F. A. J.; Imperiali, B. *J. Am. Chem. Soc.* **1981**, *103*, 1566–1568.
 24. (a) Brown H. C.; Ganesan, K.; Dhar, R. K. *J. Org. Chem.* **1993**, *58*, 147–153. (b) Brown, H. C.; Dhar, R. K.; Bakshi, R. K.; Pandiarajan, P. K.; Singaram, B. *J. Am. Chem. Soc.* **1989**, *111*, 3441–3442.
 25. (a) Streuff, J.; White, D. E.; Virgil, S. C.; Stoltz, B. M. *Nature Chem.* **2010**, *2*, 192–196. (b) Hama, T.; Culkin, D. A.; Hartwig, J. F. *J. Am. Chem. Soc.* **2006**, *128*, 4976–4985. (c) Ohtsuka, Y.; Ikeno, T.; Yamada, T. *Tetrahedron: Asymmetry* **2003**, *14*, 967–970. (d) Hirano, M.; Ito, Y.; Hirai, M.; Fukuoka, A.; Komiya, S. *Chem. Lett.* **1993**, *22*, 2057–2060. (e) Burkhardt, E. R.; Bergman, R. G.; Heathcock, C. H. *Organometallics* **1990**, *9*, 30–44. (f) Yanagisawa, A.; Lin, Y.; Miyake, R.; Yoshida, K. *Org. Lett.* **2014**, *16*, 86–89. (g) Herrmann, A. T.; Smith, L. L.; Zakarian, A. *J. Am. Chem. Soc.* **2012**, *134*, 6976–6979. (h) Kalek, M.; Himo, F. *J. Am. Chem. Soc.* **2012**, *134*, 19159–19169. (i) Noda, D.; Sunada, Y.; Hatakeyama, T.; Nakamura, M.; Nagashima, H. *Chem. Commun.* **2012**, *48*, 12231–12233. (j) Yoshikai, N.; Zhang, S.-L.; Yamagata, K.-I.; Tsuji, H.; Nakamura, E. *J. Am. Chem. Soc.* **2009**, *131*, 4099–4109. (k) Trost, B. M.; Zhang, Y. *J. Am. Chem. Soc.* **2007**, *129*, 14548–

-
14549. (l) Sibi, M. P.; Tatamidani, H.; Patil, K. *Org. Lett.* **2005**, *7*, 2571–2573. (m) Ishikawa, S.; Hamada, T.; Manabe, K.; Kobayashi, S. *J. Am. Chem. Soc.* **2004**, *126*, 12236–12237. (n) Oisaki, K.; Suto, Y.; Kanai, M.; Shibasaki, M. *J. Am. Chem. Soc.* **2003**, *125*, 5644–5645. (o) Murahashi, S.-I.; Take, K.; Naota, T.; Takaya, H. *Synlett* **2000**, 1016–1018. (p) Fujimura, O. *J. Am. Chem. Soc.* **1998**, *120*, 10032–10039. (q) Nerz-Stormes, M.; Thornton, E. R. *J. Org. Chem.* **1991**, *56*, 2489–2498. (r) Meyer, T. Y.; Garner, L. R.; Baenziger, N. C.; Messerie, L. *Inorg. Chem.* **1990**, *29*, 4045–4050. (s) Masahiro, M.; Masahiko, I.; Michinori, S.; Yoshihiko, I. *Bull. Chem. Soc. Jpn.* **1988**, *61*, 3649–3652. (t) Bassner, S. L.; Morrison, E. D.; Geoffroy, G. L.; Rheingold, A. L. *J. Am. Chem. Soc.* **1986**, *108*, 5358–5359. (u) Evans, W. J.; Dominguez, R.; Hanusa, T. P. *Organometallics* **5**, 1291–1296.
26. (a) Reetz, M. T.; Peter, R. *Tetrahedron Lett.* **1981**, *22*, 4691–4694. (b) Tsuji, J.; Minami, I.; Shimizu, I. *Tetrahedron Lett.* **1983**, *24*, 1793–1796. (c) Panish, R.; Selvaraj, R.; Fox, J. M. *Org. Lett.* **2015**, *17*, 3978–3981. (d) Wehmeyer, R. M.; Rieke, R. D. *J. Org. Chem.* **1987**, *52*, 5056–5057. (e) Hansen, M. M.; Bartlett, P. A.; Heathcock, C. H. *Organometallics* **1987**, *6*, 2069–2074.
27. Burkhardt, E. R.; Doney, J. J.; Slough, G. A.; Stack, J. M.; Heathcock, C. H.; Bergman, R. G. *Pure Appl. Chem.* **1998**, *60*, 1–6.
28. Wurtz, A. C. *Bull. Soc. Chim. Fr.* **1872**, *17*, 436–442.
29. (a) Heravi, M. M.; Zadsirjan, V. *Tetrahedron: Asymmetry* **2013**, *24*, 1149–1188. (b) Heravi, M. M.; Zadsirjan, V. *Tetrahedron: Asymmetry* **2014**, *25*, 1061–1090.

-
30. (a) Brodmann, T.; Lorenz, M.; Schäckel, R.; Simsek, S.; Kalesse, M. *Synlett* **2009**, 174–192. (b) Schetter, B.; Mahrwald, R. *Angew. Chem. Int. Ed.* **2006**, *45*, 7506–7525.
31. (a) Heravi, M. M.; Asadi, S. *Tetrahedron: Asymmetry* **2012**, *23*, 1431–1465. (b) Bhanushali, M.; Zhao, C.-G. *Synthesis* **2011**, 1815–1830. (c) Dalko, P. I.; Moisan, L. *Angew. Chem. Int. Ed.* **2004**, *43*, 5138–5175. (d) Mukherjee, S.; Yang, J. W.; Hoffmann, S.; List, B. *Chem. Rev.* **2007**, *107*, 5471–5569. (e) Notz, W.; Tanaka, F.; Barbas, C. F. *Acc. Chem. Res.* **2004**, *37*, 580–591. (f) Bisai, V.; Bisai, A.; Singh, V. K. *Tetrahedron* **2012**, *68*, 4541–4580.
32. (a) Kuwano, R.; Miyazaki, H.; Ito, Y. *J. Organomet. Chem.* **2000**, *603*, 18–29. (b) Kuwano, R.; Miyazaki, H.; Ito, Y. *Chem. Commun.* **1998**, 71–72.
33. Fukuchi, I.; Hamashima, Y.; Sodeoka, M. *Adv. Synth. Catal.* **2007**, *349*, 509–512.
34. Mouri, S.; Chen, Z.; Matsunaga, S.; Shibasaki, M. *Chem. Commun.* **2009**, 5138–5140.
35. Shen, K.; Liu, X.; Zheng, K.; Li, W.; Hu, X.; Lin, L.; Feng, X. *Chem. Euro. J.* **2010**, *16*, 3736–3742.
36. Shen, K.; Liu, X.; Wang, W.; Wang, G.; Cao, W.; Li, W.; Hu, X.; Lin, L.; Feng, X. *Chem. Sci.* **2010**, *1*, 590–595.
37. Allais, C.; Tsai, A. S.; Nuhant, P.; Roush, W. R. *Angew. Chem. Int. Ed.* **2013**, *52*, 12880–12891.
38. Arend, M.; Westermann, B.; Risch, N. *Angew. Chem. Int. Ed.* **1998**, *37*, 1044–1070.
39. Subramaniapillai, S. G. *J. Chem. Sci.* **2013**, *125*, 467–482.

-
40. (a) A. Córdova, in *Stereoselective Organocatalysis: Bond Formation Methodologies and Activation Modes*, 1st Edition (Ed. R. R. Torres), Chap. 4, Wiley, 2013, p. 129–146 (b) Verkade, J. M. M.; van Hemert, L. J. C.; Quaedflieg, P. J. L. M.; Rutjes, F. P. J. T. *Chem Soc. Rev.* **2008**, *37*, 29–41. (c) Ting, A.; Schaus, S. E. *Eur. J. Org. Chem.* **2007**, 5797–5815.
41. (a) Arrayás, R. G.; Carretero, J. C. *Chem. Soc. Rev.* **2009**, *38*, 1940–1948. (b) Manuel, M.; Marques, M. B. *Angew. Chem. Int. Ed.* **2006**, *45*, 348–352. (c) Karimi, B.; Ender, D.; Jafari, E. *Synthesis* **2013**, *45*, 2769–2812. (d) Córdova, A. *Acc. Chem. Res.* **2004**, *37*, 102–112. (d) Kobayashi, S.; Mori, Y.; Fossey, J. S.; Salter, M. M. *Chem. Rev.* **2011**, *111*, 2626–2704. (e) Greco, S. J.; Lacerda, V. Jr.; dos Santos, R. B. *Aldrichimica Acta* **2011**, *44*, 15–24.
42. Marigo, M.; Kjærsgaard, A.; Juhl, K.; Gathergood, N.; Jørgensen, K. A. *Chem. Eur. J.* **2003**, *9*, 2359–2367.
43. Hamashima, Y.; Sasamoto, N.; Hotta, D.; Somei, H.; Umebayashi, N.; Sodeoka, M. *Angew. Chem. Int. Ed.* **2005**, *44*, 1525–1529.
44. Kim, E. J.; Kang, Y. K.; Kim, D. Y. *Bull. Korean Chem. Soc.* **2009**, *30*, 1437–1438.
45. Liu, Z.; Shi, M. *Organometallics* **2010**, *29*, 2831–2834.
46. Nojiri, A.; Kumagai, N.; Shibasaki, M. *J. Am. Chem. Soc.* **2008**, *130*, 5630–5631.
47. Chen, Z.; Morimoto, H.; Matsunaga, S.; Shibasaki, M. *J. Am. Chem. Soc.* **2008**, *130*, 2170–2171.
48. Hatano, M.; Horibe, T.; Ishihara, K. *J. Am. Chem. Soc.* **2010**, *132*, 56–57.
49. Shimizu, S.; Tsubogo, T.; Xu, P.; Kobayashi, S. *Org. Lett.* **2015**, *17*, 2006–2008.

-
50. For reviews on the asymmetric Michael reaction see: (a) Christoffer, J.; Baro, A. *Angew. Chem. Int. Ed.* **2003**, *42*, 1688–1690. (b) Krause, N.; Hoffmann-Röder, A. *Synthesis* **2001**, 171–196. (c) Sibi, M. P.; Manyem, S. *Tetrahedron* **2000**, *56*, 8033–8061. (d) Leonard, J.; Díez-Barra, E.; Merino, S. *Eur. J. Org. Chem.* **1998** 2051–2061. (e) Christoffers, J. *Eur. J. Org. Chem.* **1998**, 1259–1266.
51. Långström, B.; Göran, B. *Acta Chem. Scand.* **1973**, *27*, 3118–3119.
52. Cram, D. J.; Sogah, G. D. Y. *J. Chem. Soc., Chem. Commun.* **1981**, 625–628.
53. Brunner, H.; Hammer, B. *Angew. Chem. Int. Ed.* **1984**, *23*, 312–313.
54. Brunner, H.; Kraus, J. *J. Mol. Catal.* **1989**, *49*, 133–142.
55. Botteghi, C.; Paganelli, S.; Schionate, A; Boga, C; Fava, A. *J. Mol. Catal.* **1991**, *66*, 7–21.
56. Brunner, H.; Krumey, C. *J. Mol Catal. A: Chem.* **1999**, *142*, 7–15.
57. Botteghi, C.; Schionanto, A.; Rosini, C.; Salvadori, R. P. *J. Mol. Catal.* **1990**, *63*, 155–165.
58. For a review on thioether ligands see: Masdeu-Bultó, A. M.; Diéguez, M.; Martin, E.; Gómez, M. *Coord. Chem. Rev.* **2003**, *242*, 159–201.
59. (a) Christoffers, J.; Mann, A. *Eur. J. Org. Chem.* **1999**, 1475–1479. (b) Christoffers, J.; Mann, A.; Pickardt, J. *Tetrahedron* **1999**, *55*, 5377–5388.
60. Christoffers, J.; Rößler, U.; Werner, T. *Eur. J. Org. Chem.* **2000**, 701–705.
61. Han, Y.-Y.; Wu, Z.-J.; Chen, W.-B.; Du, X.-L.; Zhang, X.-M.; Yuan, W.-C. *Org. Lett.* **2011**, *13*, 5064–5067.
62. Desimoni, G.; Quadrelli, P.; Righetti, P. P. *Tetrahedron* **1990**, *46*, 2927–2934.

-
63. Desimoni, G.; Dusi, G.; Faita, G.; Quadrelli, P.; Righetti, P. P. *Tetrahedron* **1995**, *51*, 4131–4144.
64. Bonadies, F.; Lattanzi, A.; Orelli, L. R.; Pesci, S.; Scettri, A. *Tetrahedron Lett.* **1993**, *34*, 7649–7650.
65. Sawamura, M.; Hamashima, H.; Ito, Y. *J. Am. Chem. Soc.* **1992**, *114*, 8295–8296.
66. Freixa, Z.; van Leeuwen, P. W. N. M. *Coord. Chem. Rev.* **2008**, *252*, 1755–1786.
67. Sawamura, M.; Hamashima, H.; Ito, Y. *Tetrahedron* **1994**, *50*, 4439–4454.
68. Sawamura, M.; Hamashima, H.; Shinoto, H.; Ito, Y. *Tetrahedron Lett.* **1995**, *36*, 6479–6482.
69. Inagaki, K.; Nozaki, K.; Takaya, H. *Synlett* **1997**, 119–120.
70. Suzuki, T.; Torii, T. *Tetrahedron: Asymmetry* **2001**, *12*, 1077–1081.
71. For a review on lanthanide complexes in asymmetric catalysis see: Shibasaki, M.; Yoshikawa, N. *Chem Rev.* **2002**, *102*, 2187–2210.
72. (a) Sasai, H.; Suzuki, T.; Arai, S.; Arai, T.; Shibasaki, M. *J. Am. Chem. Soc.* **1992**, *114*, 4418–4420. (b) Sasai, H.; Suzuki, T.; Itoh, N.; Shibasaki, M. *Tetrahedron Lett.* **1993**, *34*, 851–854. (c) Sasai, H.; Itoh, N.; Suzuki, T.; Shibasaki, M. *Tetrahedron Lett.* **1993**, *34*, 855–858. (d) Sasai, H.; Suzuki, T.; Itoh, N.; Arai, S.; Shibasaki, M. *Tetrahedron Lett.* **1993**, *34*, 2657–2660. (e) Sasai, H.; Suzuki, T.; Itoh, N.; Tanaka, K.; Date, T.; Okamura, K.; Shibasaki, M. *J. Am. Chem. Soc.* **1993**, *115*, 10372–10373.
73. For reviews on heterobimetallic catalysts see: (a) Shibasaki, M.; Sasai, H.; Arai, T. *Angew. Chem. Int. Ed.* **1997**, *36*, 1236–1256. (b) Matsunaga, S.; Ohshima, T.; Shibasaki, M. *Adv. Synth. Catal.* **2002**, *344*, 3–15.

-
74. Sasai, H.; Arai, T.; Shibasaki, M. *J. Am. Chem. Soc.* **1994**, *116*, 1571–1572.
 75. Sasai, H.; Emori, E.; Arai, T.; Shibasaki, M. *Tetrahedron Lett.* **1996**, *37*, 5561–5564.
 76. Kim, Y. S.; Matsunaga, S.; Das, J.; Sekine, A.; Ohshima, T.; Shibasaki, M. *J. Am. Chem. Soc.* **2000**, *122*, 6506–6507.
 77. Majima, K.; Tosaki, S.-Y.; Ohshima, T.; Shibasaki, M. *Tetrahedron Lett.* **2005**, *46*, 5377–5381.
 78. Yasufumi, T.; Atsushi, K.; Eiji, K.; Sotaro, M. *Chem. Lett.* **1995**, *24*, 957–958.
 79. Blacker, A. J.; Clarke, M. L.; Loft, M. S.; Mahon, M. F.; Williams, J. M. *Organometallics* **1999**, *18*, 2867–2873.
 80. Christoffers, J. *Prakt. Chem. (Weinheim, Ger.)*, **1999**, *341*, 495.
 81. For a review on chiral iron catalysts see: Gopalaiah, K. *Chem. Rev.* **2013**, *113*, 3248–3296.
 82. For a review on palladium catalyzed asymmetric addition reactions see: Sun, Y.-W.; Zhu, P.-L.; Xu, Q.; Shi, M. *RSC Adv.* **2013**, *3*, 3153–3168.
 83. Stark, M. A.; Jones, G.; Richards, C. J. *Organometallics* **2000**, *19*, 1282–1291.
 84. (a) Takenaka, K.; Uozumi, Y. *Org. Lett.* **2004**, *6*, 1833–1835. (b) Takenaka, K.; Minakawa, M.; Uozumi, Y. *J. Am. Chem. Soc.* **2005**, *127*, 12273–12281.
 85. Fossey, J. S.; Russell, M. L.; Malik, K. M. A.; Richards, C. J. *J. Organomet. Chem.* **2007**, *692*, 4843–4848.
 86. (a) Hamashima, Y.; Hotta, D.; Sodeoka, M. *J. Am. Chem. Soc.* **2002**, *124*, 11240–11241. (b) Mikiko, S.; Yoshitaka, H. *Bull. Chem. Soc. Jpn.* **2005**, *78*, 941–956.

-
87. For a review on the use of chiral palladium enolates in asymmetric reactions see:
Hamashima, Y.; Sodeoka, M. *Chem. Rec.* **2004**, *4*, 231–242.
88. Hamashima, Y.; Hotta, D.; Umebayahi, N.; Tsuchiya, Y.; Suzuki, T.; Sodeoka, M. *Adv. Synth. Catal.* **2005**, *347*, 1576–1586.
89. Hamashima, Y.; Takano, H.; Hotta, D.; Sodeoka, M. *Org. Lett.* **2003**, *5*, 3225–3228.
90. Görlicke, F.; Schneider, C. *Angew. Chem. Int. Ed.* **2018**, *57*, 14736–14741.
91. Liu, X.; Lin, L.; Feng, X. *Acc. Chem. Res.* **2011**, *44*, 574–587.
92. Nakajima, M.; Yamaguchi, Y.; Hashimoto, S. *Chem. Commun.* **2001**, 1596–1597.
93. Nakajima, M.; Yamamoto, S.; Yamaguchi, Y.; Nakamura, S.; Hashimoto, S. *Tetrahedron* **2003**, *59*, 7307–7313.
94. Wang, Z.; Yang, Z.; Chen, D.; Liu, X.; Lin, L.; Feng, X. *Angew. Chem. Int. Ed.* **2011**, *50*, 4928–4932.
95. Kumaraswamy, G.; Jena, N.; Sastry, M. N. V.; Padmaja, M.; Markondaiah, B. *Adv. Synth. Catal.* **2005**, *347*, 867–871.
96. Kato, Y.; Furutachi, M.; Chen, Z.; Mitsunuma, H.; Matsunaga, S.; Shibasaki, M. *J. Am. Chem. Soc.* **2009**, *131*, 9168–9169.
97. (a) Trost, B. M.; Van Vranken, D. L. *Chem. Rev.* **1996**, *96*, 395–422. (b) Trost, B. M. *J. Org. Chem.* **2004**, *69*, 5813–5837.
98. You, S.-L.; Dai, L.-X. *Angew. Chem. Int. Ed.* **2006**, *45*, 5246–5248.
99. Sawamura, M.; Nagata, H.; Sakamoto, H.; Ito, Y. *J. Am. Chem. Soc.* **1992**, *114*, 2586–2592.
100. Brunel, J. M.; Tenaglia, A.; Buono, G. *Tetrahedron: Asymmetry* **2000**, *11*, 3585–3590.

-
101. Nemoto, T.; Matsumoto, T.; Masuda, T.; Hitoma, T.; Hatano, K.; Hamada, Y. *J. Am. Chem. Soc.* **2004**, *126*, 3690–2691.
 102. Behenna, D. C.; Stoltz, B. M. *J. Am. Chem. Soc.* **2004**, *126*, 15044–15045.
 103. Mohr, J. T.; Behenna, D. C.; Harned, A. M.; Stoltz, B. M. *Angew. Chem. Int. Ed.* **2005**, *44*, 6924–6927.
 104. (a) Sherden, N. H.; Behenna, D. C.; Virgil, S. C.; Stoltz, B. M. *Angew. Chem. Int. Ed.* **2009**, *48*, 6840–6843. (b) Keith, J. A.; Behenna, D. C.; Mohr, J. T.; Ma, S.; Marinescu, S. C.; Oxgaard, J.; Stoltz, B. M.; Goddard, W. A. *J. Am. Chem. Soc.* **2007**, *129*, 11876–11877.
 105. Behenna, D. C.; Liu, Y.; Yurino, T.; Kim, J.; White, D. E.; Virgil, S. C.; Stoltz, B. M. *Nature Chemistry* **2012**, *4*, 130–133.
 106. Reeves, C. M.; Eidamshaus, C.; Kim, J.; Stoltz, B. M. *Angew. Chem. Int. Ed.* **2013**, *52*, 6718–6721.
 107. Numajiri, Y.; Pritchett, B. P.; Chiyoda, K.; Stoltz, B. M. *J. Am. Chem. Soc.* **2015**, *137*, 1040–1043.
 108. Alexy, E. J.; Zhang, H.; Stoltz, B. M. *J. Am. Chem. Soc.* **2018**, *140*, 10109–10112.
 109. (a) Marziale, A. N.; Duquette, D. C.; Craig, II, R. A.; Kim, K. E.; Liniger, M.; Numajiri, Y.; Stoltz, B. M. *Adv. Synth. Catal.* **2015**, *357*, 2238–2245. (b) Hong, A. Y.; Bennett, N. B.; Krout, M. R.; Jensen, T.; Harned, A. M.; Stoltz, B. M. *Tetrahedron* **2011**, *67*, 10234–10248. (c) Petrova, K. V.; Mohr, J. T.; Stoltz, B. M. *Org. Lett.* **2009**, *11*, 292–295. (d) Craig, II, R. A.; Loskot, S. A.; Mohr, J. T.; Behenna, D. C.; Harned, A. M.; Stoltz, B. M. *Org. Lett.* **2015**, *17*, 5160–5163.

-
110. Trost, B. M.; Radinov, R.; Grenzer, E. M. *J. Am. Chem. Soc.* **1997**, *119*, 7879–7880.
 111. Trost, B. M.; Schroeder, G. M. *J. Am. Chem. Soc.* **1999**, *121*, 6759–6760.
 112. Trost, B. M.; Schroeder, G. M.; Kristensen, J. *Angew. Chem. Int. Ed.* **2002**, *41*, 3492–3495.
 113. Trost, B. M.; Schroeder, G. M. *Chem. Eur. J.* **2005**, *11*, 174–184.
 114. Trost, B. M.; Pissot-Soldermann, C.; Chen, I. *Chem. Eur. J.* **2005**, *11* 951–959.
 115. Trost, B. M.; Frederiksen, M. U. *Angew. Chem. Int. Ed.* **2005**, *44*, 308–310.
 116. Trost, B. M.; Xu, J.; Schmidt, T. *J. Am. Chem. Soc.* **2009**, *131*, 18343–18357.
 117. Trost, B. M.; Bream, R. N.; Xu, J. *Angew. Chem. Int. Ed.* **2006**, *45*, 3109–3112.
 118. Hayashi, T.; Kanehira, K.; Hagihara, T.; Kumada, M. *J. Org. Chem.* **1988**, *53*, 113–120.
 119. Trost, B. M.; Zhang, Y. *J. Am. Chem. Soc.* **2006**, *128*, 4590–4591.
 120. Wu, Q.-F.; He, H.; Liu, W.-B.; You, S.-L. *J. Am. Chem. Soc.* **2010**, *132*, 11418–11419.
 121. Wu, Q.-F.; Zheng, C.; You, S.-L. *Angew. Chem. Int. Ed.* **2012**, *51*, 1680–1683.
 122. Kanayama, T.; Yoshida, K.; Miyabe, H.; Takemoto, Y. *Angew. Chem. Int. Ed.* **2003**, *42*, 2054–2056.
 123. Liu, W.-B.; Reeves, C. M.; Virgil, S. C.; Stoltz, B. M. *J. Am. Chem. Soc.* **2013**, *135*, 10626–10629.
 124. Liu, W.-B.; Reeves, C. M.; Stoltz, B. M. *J. Am. Chem. Soc.* **2013**, *135*, 17298–17301.

-
125. Shockley, S. E.; Hethcox, J. C.; Stoltz, B. M. *Angew. Chem. Int. Ed.* **2017**, *56*, 11545–11548.
126. Wright, T. B.; Evans, P. A. *J. Am. Chem. Soc.* **2016**, *138*, 1503–15306.
127. Ngamnithiporn, A.; Jette, C. I.; Bachman, S.; Virgil, S. C.; Stoltz, B. M. *Chem. Sci.* **2018**, *9*, 2547–2551.
128. Doyle, A. G.; Jacobsen, E. N. *J. Am. Chem. Soc.* **2005**, *127*, 62–63.
129. Doyle, A. G.; Jacobsen, E.N. *Angew. Chem. Int.* **2007**, *46*, 3701–3705.
130. Yamashita, Y.; Odashima, K.; Koga, K. *Tetrahedron Lett.* **1999**, *40*, 2803–2806.
131. Yu, K.; Jackson, J. J.; Nguyen, T. D.; Alvatado, J.; Stivala, C. E.; Ma, Y.; Mack, K. A.; Hayton, T. W.; Collum, D. B.; Zakarian, A. *J. Am. Chem. Soc.* **2017**, *139*, 527–533.
132. For reviews on α -arylation see: (a) Johansson, C. C. C.; Colacot, T. J. *Angew. Chem. Int. Ed.* **2010**, *49*, 676–707. (b) Bellina, F.; Rossi, R. *Chem. Rev.* **2010**, *110*, 1082–1146. (c) Mazet, C. *Synlett*, **2012**, *23*, 1999–2004. (d) Burtoloso, A. C. B. *Synlett* **2009**, 320–327.
133. (a) Semmelhack, M. F.; Stauffer, R. D.; Rogerson, T. D. *Tetrahedron Lett.* **1973**, *14*, 4519–4522. (b) Semmelhack, M. F.; Chong, B. P.; Stauffer, R. D.; Rogerson, T. D.; Chong, A.; Jones, L. D. *J. Am. Chem. Soc.* **1975**, *97*, 2507–2516.
134. Galarini, R.; Musco, A.; Pontellini, R.; Santi, R. *J. Mol. Catal.* **1992**, *72*, L11–L13.
135. (a) Muratake, H.; Natsume, M. *Tetrahedron Lett.* **1997**, *38*, 7581–7582. (b) Muratake, H.; Hayakawa, A.; Natsume, M. *Tetrahedron Lett.* **1997**, *38*, 7577–7580.
136. Palucki, M.; Buchwald, S. L. *J. Am. Chem. Soc.* **1997**, *119*, 11108–11109.
137. Hamann, B. C.; Hartwig, J. F. *J. Am. Chem. Soc.* **1997**, *119*, 12382–12383.

-
138. Satoh, T.; Kawamura, Y.; Miura, M.; Nomura, M. *Angew. Chem. Int. Ed.* **1997**, *36*, 1740–1742.
139. Åhman, J.; Wolfe, J. P.; Troutman, M. V.; Palucki, M.; Buchwald, S. L. *J. Am. Chem. Soc.* **1998**, *120*, 1918–1919.
140. Zhang, T. Y.; Zhang, H. *Tetrahedron Lett.* **2002**, *43*, 1363–1365.
141. Chieffi, A.; Kamikawa, K.; Åhman, J.; Fox, J. M.; Buchwald, S. L. *Org. Lett.* **2001**, *3*, 1897–1900.
142. Fox, J. M.; Huang, X.; Chieffi, A.; Buchwald, S. L. *J. Am. Chem. Soc.* **2000**, *122*, 1360–1370.
143. Hamada, T.; Chieffi, A.; Åhman, J.; Buchwald, S. L. *J. Am. Chem. Soc.* **2002**, *124*, 1261–1268.
144. Hamada, T.; Buchwald, S. L. *Org. Lett.* **2002**, *4*, 999–1001.
145. Taylor, A. M.; Altman, R. A.; Buchwald, S. L. *J. Am. Chem. Soc.* **2009**, *131*, 9900–9901.
146. Arao, T.; Kondo, K.; Aoyama, T. *Chem. Pharm. Bull.* **2006**, *54*, 1743–1744.
147. (a) Lee, S.; Hartwig, J. F. *J. Org. Chem.* **2001**, *66*, 3402–3415. (b) Culkin, D. A.; Hartwig, J. F. *Acc. Chem. Res.* **2003**, *36*, 234–245.
148. Glorius, F.; Altenhoff, G.; Goddard, R.; Lehmann, C. *Chem. Commun.* **2002**, 2704–2705.
149. Arao, T.; Kondo, K.; Aoyama, T. *Tetrahedron Lett.* **2006**, *47*, 1417–1420.
150. Kündig, E. P.; Seidel, T. M.; Jia, Y.; Bernardinelli, G. *Angew. Chem. Int. Ed.* **2007**, *46*, 8484–8487.
151. García-Fortanet, J.; Buchwald, S. L. *Angew. Chem. Int. Ed.* **2008**, *47*, 8108–8111.

-
152. Liao, X.; Weng, Z.; Hartwig, J. F. *J. Am. Chem. Soc.* **2008**, *130*, 195–200.
153. Jette, C. I.; Geibel, I.; Bachman, S.; Hayashi, M.; Sakurai, S.; Shimizu, H.; Morgan, J. B.; Stoltz, B. M. *Angew. Chem. Int. Ed.* **2019**, *58*, 1–6.
154. Ge, S.; Hartwig, J. F. *J. Am. Chem. Soc.* **2011**, *133*, 16330–16333.
155. (a) Spielvogel, D. J.; Buchwald, S. L. *J. Am. Chem. Soc.* **2002**, *124*, 3500–3501. (b) Spielvogel, D. J.; Davis, W. M.; Buchwald, S. L. *Organometallics* **2002**, *21*, 3833–3836.
156. Chen, G.; Kwong, F. Y.; Chan, H. O.; Yu, W.-Y.; Chan, A. S. C. *Chem. Commun.* **2006**, 1413–1415.
157. Xie, X.; Chen, Y.; Ma, D. *J. Am. Chem. Soc.* **2006**, *128*, 16050–16051.
158. Claisen, L. *Chem. Ber.* **1912**, *45*, 3157–3166.
159. For reviews on the Claisen rearrangement see: (a) Rehbein, J.; Hiersemann, M. *Synthesis* **2013**, *45*, 1121–1159. (b) Castro, A. M. M. *Chem. Rev.* **2004**, *104*, 2939–3002. (c) Ito, H.; Taguchi, T. *Chem. Soc. Rev.* **1999**, *28*, 43–50. (d) Enders, D.; Knopp, M.; Schiffers, R. *Tetrahedron: Asymmetry* **1996**, *7*, 1847–1882. (e) Ziegler, F. E. *Chem. Rev.* **1988**, *88*, 1423–1452.
160. Corey, E. J.; Roberts, B. E.; Dixon, B. R. *J. Am. Chem. Soc.* **1995**, *117*, 193–196.
161. Corey, E. J.; Lee, D. H. *J. Am. Chem. Soc.* **1991**, *113*, 4026–4028.
162. Corey, E. J.; Kania, R. S. *J. Am. Chem. Soc.* **1996**, *118*, 1229–1230.
163. Krebs, A.; Kazmaier, U. *Tetrahedron Lett.* **1996**, *37*, 7945–7946.
164. (a) Malherbe, R.; Belluš, D. *Helv. Chim. Acta* **1978**, *61*, 3096–3099. (b) Malherbe, R.; Rist, G.; Belluš, D. *J. Org. Chem.* **1983**, *48*, 860–869.

-
165. For a review on the Belluš–Claisen rearrangement see: Gonda, J. *Angew. Chem. Int. Ed.* **2004**, *43*, 3516–3524.
166. Yoon, T. P.; Dong, V. M.; MacMillan, D. W. C. *J. Am. Chem. Soc.* **1999**, *121*, 9726–9727.
167. Yoon, T. P.; MacMillan, D. W. C. *J. Am. Chem. Soc.* **2001**, *123*, 2911–2912.
168. Bloch, R.; Le Perche, P.; Rouessac, F.; Conia, J.-M. *Tetrahedron* **1968**, *24*, 5971–5989.
169. Conia, J.-M.; Le Perche, P. *Synthesis* **1975**, 1–19.
170. Corkey, B. K.; Toste, F. D. *J. Am. Chem. Soc.* **2005**, *127*, 17168–17169.
171. (a) Kennedy-Smith, J. J.; Staben, S. T.; Toste, F. D. *J. Am. Chem. Soc.* **2004**, *126*, 4526–4527. (b) Staben, S. T.; Kennedy-Smith, J. J.; Toste, F. D. *Angew. Chem. Int. Ed.* **2004**, *43*, 5350–5352.
172. Yang, T.; Ferrali, A.; Sladojevich, F.; Campbell, L.; Dixon, D. J. *J. Am. Chem. Soc.* **2009**, *131*, 9140–9141.
173. Sladojevich, F.; Fuentes de Arriba, Á. L.; Ortín, I.; Yang, T.; Ferrali, A.; Paton, R. S.; Dixon, D. J. *Chem. Eur. J.* **2013**, *19*, 14286–14295.
174. Matsuzawa, A.; Mashiko, T.; Kumagai, N.; Shibasaki, M. *Angew. Chem. Int. Ed.* **2011**, *50*, 7616–7619.
175. Shaw, S.; White, J. D. *J. Am. Chem. Soc.* **2014**, *136*, 13578–13581.

CHAPTER 2

Palladium-Catalyzed Enantioselective Decarboxylative Allylic Alkylation of Cyclopentanones[†]

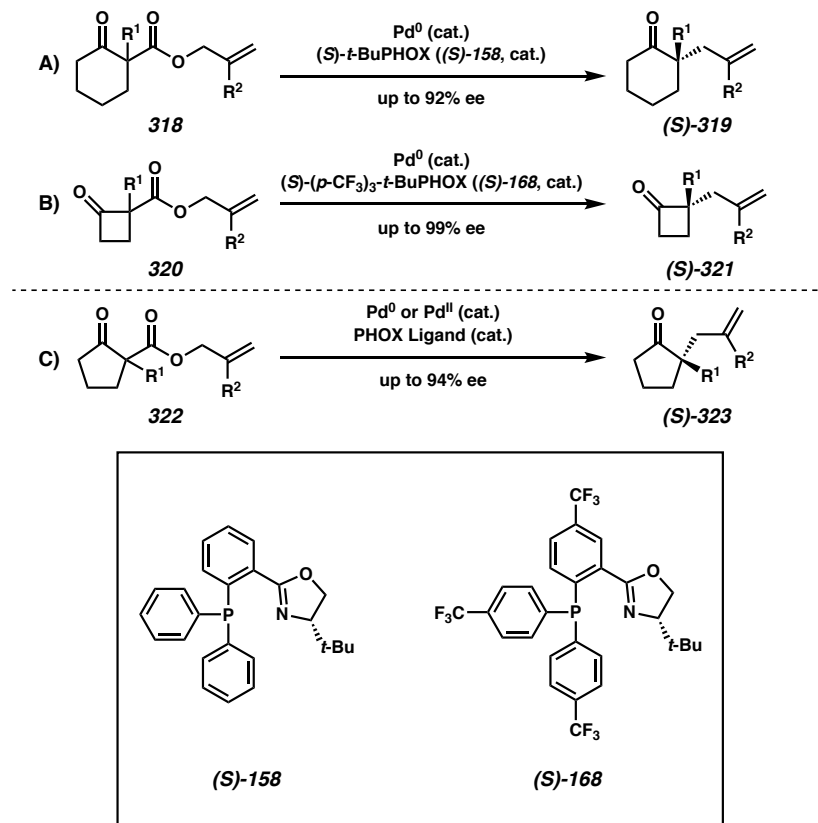
2.1 INTRODUCTION

The efficient construction of all-carbon quaternary centers remains a challenge for the modern synthetic chemist.¹ The difficulty associated with forming all-carbon quaternary centers arises from the inherent steric congestion during the C–C bond forming event. Toward this end, our laboratory disclosed the first palladium-catalyzed enantioselective decarboxylative allylic alkylation for the construction of all-carbon quaternary centers of non-stabilized enolates.² Over the past decade we have continued to explore the breadth of our reaction manifold,³ including the development of new ligands based on the original PHOX scaffold.⁴ Cyclic ketones generally represent the most explored class of substrates, from the initially reported cyclohexanones (Scheme 2.1.1A),^{2,5}

[†] This research was performed in collaboration with Robert A. Craig, II, Justin T. Mohr, Douglas C. Behenna, and Andrew M. Harned, all alumni of the Stoltz group. Additionally, this research has been published and adapted with permission Craig, II, R. A.; Loskot, S. A.; Mohr, J. T.; Behenna, D. C.; Harned, A. M.; Stoltz, B. M. *Org. Lett.* **2015**, *17*, 5160–5163. R.A.C. and S.A.L. contributed equally.

cycloheptanones,^{2,3d,5b,c} and cyclooctanones^{2,3d,5b} to the highly strained cyclobutanones (Scheme 2.1.1B).⁶

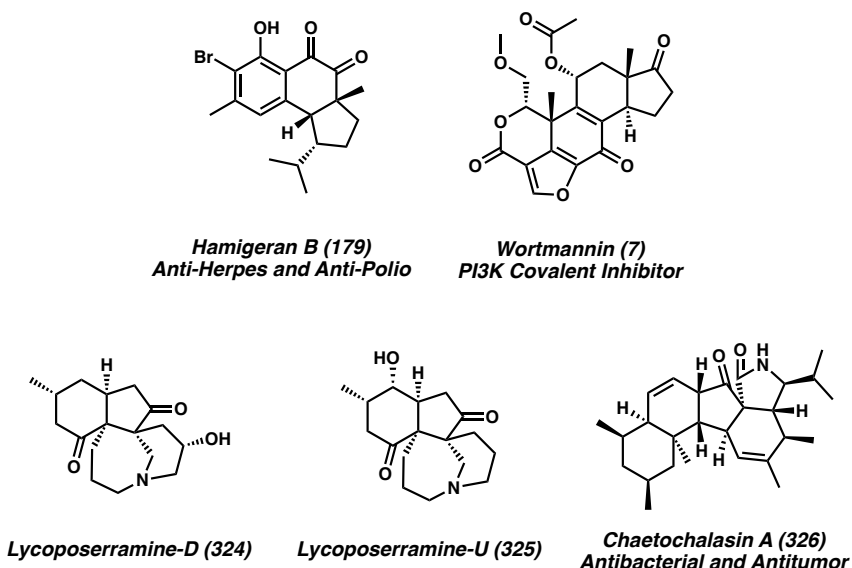
Scheme 2.1.1. Cyclic Ketone Substrates in Transition Metal-Catalyzed Enantioselective Decarboxylative Allylic Alkylation



Interestingly, cyclopentanones have typically performed worse than the corresponding 6-membered substrates, often furnishing the α -quaternary ketone products in comparatively reduced yields and ee.^{3d} Only a few examples with limited substrate scope exist for the formation of α -quaternary cyclopentanones by transition metal-catalyzed enantioselective allylic alkylation.⁷ Yet cyclopentanes containing enantioenriched quaternary centers characterize a number of biologically pertinent and chemically fascinating natural products, including polycyclic terpenoids⁸ **179**⁹ and **7**¹⁰ as well as

alkaloids **324**,¹¹ **325**,¹¹ and **326**¹² (Figure 2.1.1). As part of our continued efforts to extend the utility of our reaction methodology, we revisited the problematic cyclopentanone substrate class, striving to develop the first general method for the construction of α -quaternary center cyclopentanones and 5-membered cyclic ketone substrates by transition metal-catalyzed enantioselective decarboxylative allylic alkylation (Scheme 2.1.1C).

Figure 2.1.1. Natural Products Characterized by Cyclopentane Rings Containing Chiral All-Carbon Quaternary Centers



2.2 INITIAL REACTION OPTIMIZATION

Initial reaction development employed *p*-Me-benzyl-substituted β -ketoester **327**, using catalytic $\text{Pd}_2(\text{dba})_3$ at 20 °C in toluene in the presence of a chiral PHOX ligand, affording enantioenriched α -quaternary cyclopentanone **328** (Table 2.2.1).^{13,14} Using the classic (*S*)-*t*-BuPHOX ligand ((*S*)-**158**), cyclopentanone (*S*)-**340** was provided in 87% *ee* (entry 1). Switching to the electron-deficient (*S*)-(*p*-CF₃)₃-*t*-BuPHOX ((*S*)-**168**) furnished product (*S*)-**340** in an improved 89% *ee* (entry 2). The recently disclosed, cost-effective

alternative to **168**, (R) - $(p\text{-CF}_3)_3\text{-}i\text{-PrPHOX}^{\text{Me}^2}$ (***R***-**329**) provided cyclic ketone **(R)**-**340** in a decreased 83% *ee* (entry 3).^{4a} Similarly to **(R)**-**329**, geminally disubstituted valine-derived (S) - $(p\text{-CF}_3)_2\text{-}i\text{-PrPHOX}^{\text{Ph}^2}$ (***S***-**330**) afforded ketone **(S)**-**340** with nearly equivalent *ee* (82%, entry 4). Switching to ester-substituted β -ketoester **331**, we confirmed (S) - $(p\text{-CF}_3)_3\text{-}t\text{-BuPHOX}$ (***S***-**168**) was indeed the optimal ligand for the desired enantioselective decarboxylative allylic alkylation, providing enantioenriched α -quaternary cyclopentanone **(S)**-**332** in 91% *ee* (entry 6). The remaining PHOX ligands **(S)**-**158**, **(R)**-**329**, and **(S)**-**330** furnished the desired product (**332**) in reduced *ee*'s, ranging between 80% and 82% (entries 5, 7, and 8, respectively).

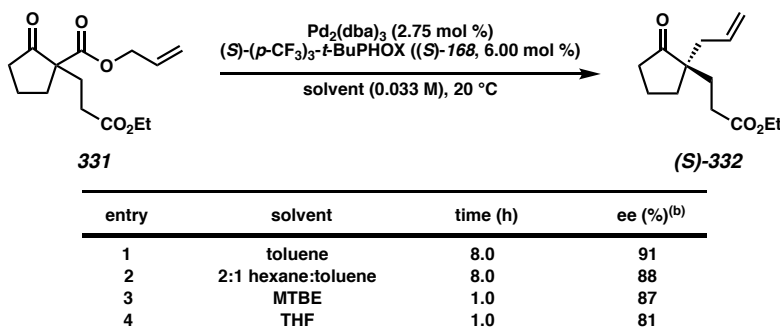
Table 2.2.1. PHOX Ligand Screen

entry	R ¹	product	ligand	ee (%) ^b
1	p-Me-C ₆ H ₄ CH ₂ -	(<i>S</i>)-340	(<i>S</i>)-158	87
2	p-Me-C ₆ H ₄ CH ₂ -	(<i>S</i>)-340	(<i>S</i>)-168	89
3	p-Me-C ₆ H ₄ CH ₂ -	(<i>S</i>)-340	(<i>R</i>)-329	83
4	p-Me-C ₆ H ₄ CH ₂ -	(<i>S</i>)-340	(<i>S</i>)-330	82
5	EtO ₂ CCH ₂ CH ₂ -	(<i>S</i>)-332	(<i>S</i>)-158	82
6	EtO ₂ CCH ₂ CH ₂ -	(<i>S</i>)-332	(<i>S</i>)-168	91
7	EtO ₂ CCH ₂ CH ₂ -	(<i>S</i>)-332	(<i>R</i>)-329	82
8	EtO ₂ CCH ₂ CH ₂ -	(<i>S</i>)-332	(<i>S</i>)-330	80

(*S*)-329 **(*S*)-330**

^a Conditions: β -Ketoester **331** (0.19 mmol), $\text{Pd}_2(\text{dba})_3$ (2.75 mol %), **(*S*)-168** (6.00 mol %), toluene (5.8 mL). ^b Measured by analytical chiral SFC.

Having identified the optimal ligand for the enantioselective decarboxylative allylic alkylation, we next examined the solvent effect using β -ketoester **331** (Table 2.2.2). Employing identical reaction conditions from our ligand screen, using toluene as the solvent, we isolated α -quaternary center cyclopentanone (*S*)-**332** in 91% ee, achieving complete consumption of starting material **331** in 8.0 h (entry 1). Switching to the less polar solvent mixture 2:1 hexanes:toluene, which has previously provided increased ee's for other α -quaternary cyclic ketones constructed through palladium-catalyzed enantioselective decarboxylative allylic alkylation,¹⁵ did not affect the reaction time, but furnished ketone (*S*)-**332** in a diminished 88% ee (entry 2). Changing to ethereal solvents (entries 3 and 4) drastically decreased the reaction time, facilitating the full consumption of β -ketoester **331** in 1.0 h. While the use of MTBE (entry 3) afforded cyclopentanone (*S*)-**332** in nearly identical ee to the mixed nonpolar solvent system (entry 2), switching to THF (entry 4) proved deleterious. Ultimately, the use of Pd₂(dba)₃ (2.75 mol %) with (*S*)-(*p*-CF₃)₃-*t*-BuPHOX ((*S*)-**168**, 6.00 mol %) in toluene (0.033 M in β -ketoester **331**) at 20 °C proved optimal.

Table 2.2.2. Solvent Effect on Enantiomeric Excess of Cyclopentanone Product (*S*)-332^a

^a Conditions: β -ketoester **331** (0.19 mmol), $\text{Pd}_2(\text{dba})_3$ (2.75 mol %), $(\text{S})\text{-168}$ (6.00 mol %), toluene (5.8 mL).

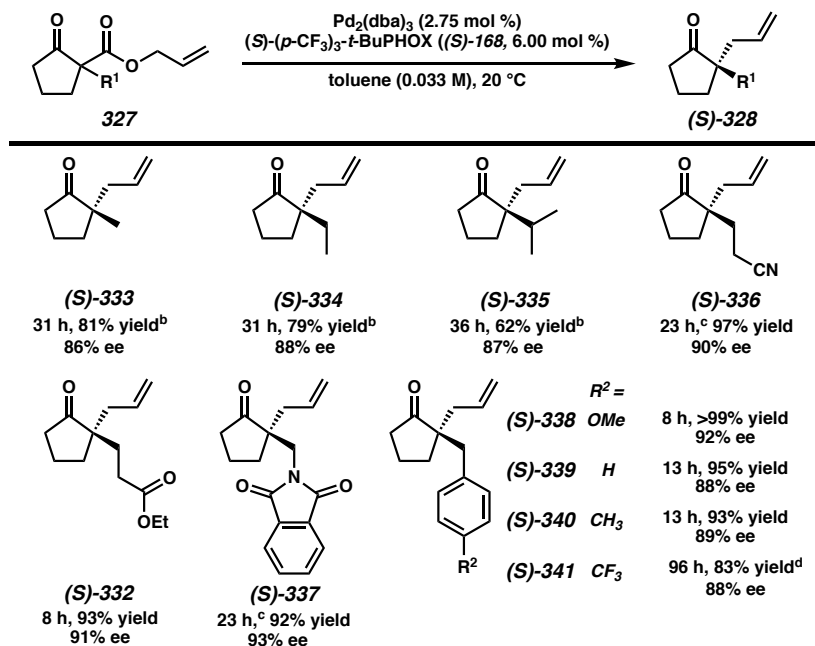
^b Measured by analytical chiral SFC.

2.3 EXPLORATION OF REACTION SCOPE

Subsequently, we explored the substrate scope of the enantioselective allylic alkylation of cyclopentanones. We found that our reaction manifold was tolerant of a variety of substitution at the α -position of the cyclopentanone (Scheme 2.3.1).¹⁶ Alkyl-substituted α -quaternary cyclopentanones (**S**-333, **S**-334, and **S**-335) were each produced over reaction times greater than 30 hours with ee's ranging from 86% to 88%, providing the more sterically congested cyclopentanone (**S**-335) over a slightly longer reaction time.¹³ Along with ester-substituted cyclopentanone (**S**-332), nitrile (**S**-336) and phthalimide (**S**-337) were both produced quite rapidly at 20 °C in excellent yield with good ee (2.5 h, 97% yield, 87% ee and 3 h, 93% yield, 88% ee, respectively). We found that we could increase the ee of these two products significantly by lowering the temperature without any deleterious effect on the yield, providing cyclopentanones (**S**-336) and (**S**-337) in an improved 90% ee and 93% ee, respectively, at 0 °C over 23 h. This result represents a dramatic improvement in the formation of (**S**-337) compared to our previously reported

system, employing THF as the solvent with (*S*)-**158** as the ligand, which provided (*S*)-**337** in only 67% yield with 48% ee.^{3d} Comparatively, benzyl-substituted cyclopentanones proved to have a correlation between the electronics of the aryl substituent and the overall reaction time. Electron rich *p*-OMe-benzyl cyclopentanone (*S*)-**338** was furnished in only 8 h, while the electron neutral benzyl and *p*-Me-benzyl products ((*S*)-**339** and (*S*)-**340**) were each produced over a slightly extended reaction time (13 h). Interestingly, the reaction producing electron poor *p*-CF₃-benzyl-substituted (*S*)-**341** failed to proceed to full conversion over 96 h, affording the product in a reduced 56% overall yield (83% yield based on recovered β -ketoester). Interestingly, despite the variable reaction times, the ee of the benzyl-substituted cyclopentanone products was largely consistent (88%–89% ee), with a slight boost for the electron-rich *p*-OMe-benzyl product ((*S*)-**338**) to 92% ee.

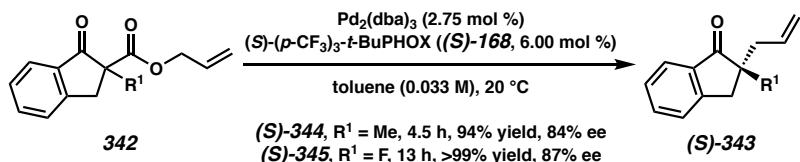
Scheme 2.3.1. Substrate Scope of Cyclopentanone Substitution in Enantioselective Allylic Alkylation



Unless otherwise noted, all reported yields are isolated yields. Enantiomeric excess (ee) was determined by either analytical chiral SFC or HPLC. ^a Conditions: β -ketoester **327** (0.19 mmol), $\text{Pd}_2(\text{dba})_3$ (2.75 mol %), (*S*)-**168** (6.00 mol %), toluene (5.8 mL). ^b Cyclopentanone product was volatile, resulting in a reduced isolated yield compared to other substrates. ^c Reaction performed at 0 °C. ^d Isolated yield was 56%.

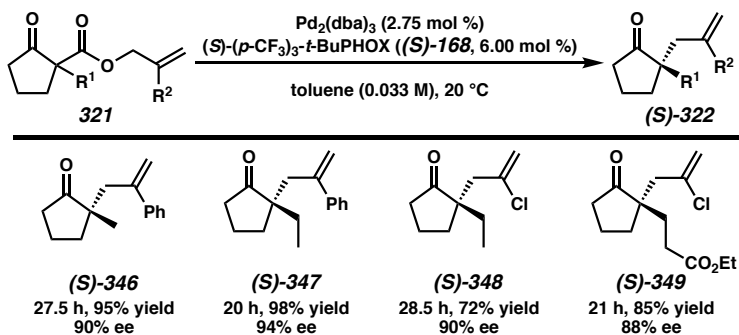
Additionally, we found that indanones were competent substrates within our reaction manifold (Scheme 2.3.2).^{3d,5a,d,7g} Methyl-substituted indanone product (**S**-344) was furnished over a greatly shortened 4.5 h compared to the methyl-substituted cyclopentanone product ((*S*)-333, see Scheme 2.3.1). Additionally, bicyclic (**S**-344) was provided in 94% yield with 84% ee. Comparatively, the fluorinated analog (**S**-345) was produced in an improved >99% yield and 87% ee, albeit over a longer reaction time (13 h).

Scheme. 2.3.2 Enantioselective Allylic Alkylation of Indanone Substrates



Having investigated the tolerance of our reaction manifold to a variety of substitution on the cyclopentanone ring, we next evaluated the potential to use 2-substituted allyl fragments in the enantioselective allylic alkylation of cyclopentanones (Scheme 2.3.3). Methyl- and ethyl-substituted cyclopentanone products **(S)-346** and **(S)-347** containing a 2-phenylallyl fragment were both produced in excellent yield and with 90% and 94% ee, respectively. Comparatively, cyclopentanones **(S)-348** and **(S)-349**, each containing a 2-chloroallyl fragment, were produced with similar ee's in slightly reduced yield. Interestingly, each of the alkyl-substituted cyclopentanone products possessing a 2-substituted allyl fragment were produced over a shorter reaction time than the same substrates containing an unsubstituted allyl fragment (see Scheme 2.3.1).

Scheme 2.3.3. Enantioselective Allylic Alkylation of Cyclopentanone Substrates with 2-Substituted Allyl Fragments^a

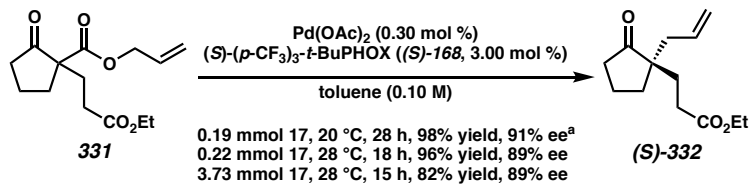


^a All reported yields are isolated yields. Enantiomeric excess (ee) was determined by analytical chiral SFC. Conditions: β -ketoester **321** (0.19 mmol), $\text{Pd}_2(\text{dba})_3$ (2.75 mol %), (S)-168 (6.00 mol %), toluene (5.8 mL).

2.4 ADAPTING THE LOW CATALYST LOADING ALLYLIC ALKYLATION

Lastly, we examined the potential to apply our recently disclosed palladium(II) low catalyst loading protocol for enantioselective decarboxylative allylic alkylation to this new substrate class.¹⁷ We discovered that on small scale, ester-substituted cyclopentanone (*S*)-**332** was provided in an identical 91% ee and an improved 98% yield at 20 °C using only 0.15 mol % palladium catalyst (Scheme 2.4.1) compared to our palladium(0)-mediated reaction conditions, which employ 5.50 mol % palladium (vide supra). Increasing the scale of the reaction slightly (0.22 mmol) as well as the temperature (28 °C) and catalyst loading (0.30 mol % Pd) furnished (*S*)-**332** over a reduced 18 h in 96% yield with 89% ee. Using these reaction conditions and increasing the scale 17 times (3.73 mmol) provided (*S*)-**332** with identical 89% ee, although in a slightly diminished 82% yield.

Scheme 2.4.1. Low Catalyst Loading Palladium(II)-Catalyzed Enantioselective Allylic Alkylation



All reported yields are isolated yields. Enantiomeric excess (ee) was determined by analytical chiral SFC. ^a Pd(OAc)₂ (0.15 mol %), (*S*)-**168** (1.50 mol %) used.

2.5 CONCLUSION

In conclusion, we have disclosed the first general method for the construction of α -quaternary-containing cyclopentanones by enantioselective palladium-catalyzed decarboxylative allylic alkylation. The reaction manifold proved optimal when electron-deficient (*S*)-(p-CF₃)₃-t-BuPHOX ((*S*)-**168**) was employed, providing a variety of

substituted cyclopentanone products in up to near-quantitative yield and with up to 94% ee. Additionally, the enantioselective allylic alkylation was found to be tolerant of allyl fragments substituted at the 2-position. Employment of low-catalyst loading, palladium(II)-mediated reaction conditions was successfully accomplished, facilitating the synthesis of α -quaternary cyclopentanones on increased scale in a cost-effective manner. Currently, our lab is pursuing the further development of this technology through substrate scope extension and application in natural product synthesis.

2.6 EXPERIMENTAL METHODS AND ANALYTICAL DATA

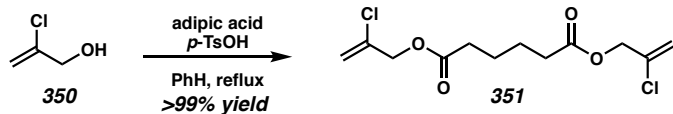
2.6.1 MATERIALS AND METHODS

Unless stated otherwise, reactions were performed at ambient temperature (23 °C) in flame-dried or oven-dried glassware under an argon or nitrogen atmosphere using dry, deoxygenated solvents (distilled or passed over a column of activated alumina).¹⁸ Commercially obtained reagents were used as received with the exception of Pd(OAc)₂, Pd₂(dba)₃, tetrakis(triphenylphosphine)palladium(0), and TBAT, which were stored in a nitrogen-filled glovebox. (S)-*t*-BuPHOX,^{4c} (S)-(CF₃)₃-*t*-BuPHOX,^{4b} (R)-(CF₃)₃-*i*-PrPHOX^{Me2, 4a, 19} (S)-(CF₃)₂-*i*-PrPHOX^{Ph2, 20} allyl 2-oxocyclopentanecarboxylate,²¹ 2-phenylallyl alcohol,²² 2-(*p*-methylbenzyl)-cyclopentanone,²³ and 2,2-dimethyl-5-oxo-cyclopentanecarboxylic acid methyl ester²⁴ were prepared by known methods. Reactions requiring external heat were modulated to the specified temperatures using an IKAmag temperature controller. Reaction progress was monitored by TLC, which was performed using E. Merck silica gel 60 F254 precoated glass plated (0.25 mm) and visualized by UV fluorescence quenching, potassium permanganate, or *p*-anisaldehyde staining. Silicycle

SiliaFlash® P60 Academic Silica gel (particle size 40-63 nm) was used for column chromatography. ^1H and ^{13}C NMR spectra were recorded on a Varian Inova 500 (500 MHz and 126 MHz, respectively), Varian Mercury 300 spectrometer (300 MHz and 75 MHz, respectively), and a Bruker AV III HD spectrometer equipped with a Prodigy liquid nitrogen temperature cryoprobe (400 MHz and 101 MHz, respectively) and are reported in terms of chemical shift relative to CHCl_3 (δ 7.26 and δ 77.16, respectively). ^{19}F NMR spectra were recorded on a Varian Inova 500 spectrometer (470 MHz) and are reported in terms of absolute chemical shift according to IUPAC standard recommendations from CFCl_3 .²⁵ Data for ^1H NMR are reported as follows: chemical shift (δ ppm) (multiplicity, coupling constant (Hz), integration). Multiplicities are reported as follows: s = singlet, d = doublet, t = triplet, q = quartet, p = pentet, sept = septet, m = multiplet, and br s = broad singlet. Infrared (IR) spectra were recorded on a Perkin Elmer Paragon 1000 spectrometer using thin films deposited on NaCl plates and are reported in frequency of absorption (cm^{-1}). Optical rotations were measured with a Jasco P-2000 polarimeter operating on the sodium D-line (589 nm), using a 100 mm path-length cell and are reported as: $[\alpha]_D^T$ (concentration in g/100 mL, solvent). Analytical SFC was performed with a Mettler SFC supercritical CO_2 analytical chromatography system utilizing Chiralpak (AD-H) or Chiracel (OD-H, OJ-H or OB-H) columns (4.6 mm x 25 cm) obtained from Daicel Chemical Industries, Ltd. Analytical chiral HPLC was performed with an Agilent 1100 Series HPLC utilizing chiralcel OD-H or OJ (4.6 mm x 25 cm) obtained from Daicel Chemical Industries, Ltd., with visualization at 254 and 210 nm. High resolution mass spectra were obtained from the Caltech Mass Spectral Facility using a JEOL JMS-600H

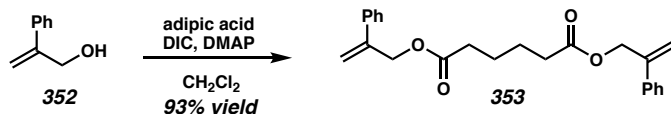
High Resolution Mass Spectrometer in fast atom bombardment (FAB+) ionization mode or a Agilent 6200 Series TOF with an Agilent G1978A Multimode source in electrospray ionization (ESI+), atmospheric pressure chemical ionization (APCI+), or mixed (ESI/APCI) ionization mode. Julabo Presto LH45 was used to control reaction temperatures inside the nitrogen-filled glovebox.

2.6.2 EXPERIMENTAL PROCEDURES



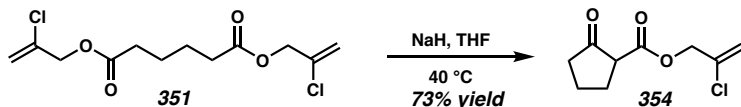
2-Chlorodiallyl adipate (351): Esterification using alcohol S1 was adapted from the literature.^{3d} Adipic acid (800 mg, 5.47 mmol, 1.00 equiv), 2-chloroallyl alcohol (**350**, 1.30 mL, 16.4 mmol, 3.00 equiv), and *p*-TsOH (3.0 mg, 0.03 mmol, 0.03 equiv) were added to a flask and diluted in benzene (8.00 mL, 0.68 M). The flask was then fitted with a Dean-Stark trap filled with additional benzene. The reaction flask was heated to reflux with stirring for 16 h, at which time the starting material had been completely consumed (determined by TLC analysis, 9:1 Pentane:Et₂O). The reaction solution was cooled to 23 °C, washed with saturated aqueous NaHCO₃ (10 mL), dried over Na₂SO₄, filtered, and concentrated in vacuo. The crude oil was purified by column chromatography (SiO₂, 10% Et₂O in pentane) to afford ester **351** (1.62 g, >99% yield) as a pale yellow oil; R_f = 0.21 (9:1 Pentane:Et₂O); ¹H NMR (400 MHz, CDCl₃) δ 5.49–5.38 (m, 4H), 4.68–4.63 (m, 4H), 2.46–2.37 (m, 4H), 1.78–1.65 (m, 4H); ¹³C NMR (101 MHz, CDCl₃) δ 172.5 (C), 136.1 (C), 115.2 (CH₂), 66.1 (CH₂), 33.8 (CH₂), 24.4 (CH₂); IR (thin film, NaCl) 2943, 2873,

1740, 1637, 1419, 1374, 1134, 1077, 899, 720, 640 cm⁻¹; HRMS (FAB+) m/z calc'd for C₁₂H₁₆Cl₂O₄ [M+H]⁺: 295.0504, found: 295.0516.



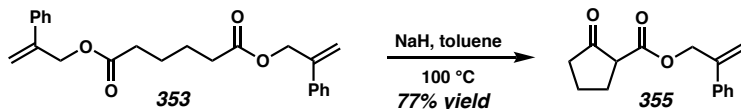
2-Phenylidallyl adipate (353): Esterification of **352** was adapted from the literature.^{3d} A flask charged with alcohol **352** (5.10 g, 38.0 mmol, 1.90 equiv), adipic acid (2.93 g 20.0 mmol, 1.00 equiv), and 4-(dimethylamino)-pyridine (DMAP, 1.88 g, 15.4 mmol, 0.77 equiv), was evacuated and filled with argon (3 x 5 minutes). Dichloromethane (77 mL, 0.26 M) was added and the solution was cooled to 0 °C (ice/H₂O bath) with stirring. Diisopropylcarbodiimide (DIC, 6.20 mL, 39.6 mmol, 1.98 equiv) was added dropwise and the reaction mixture was allowed to stir for 5 minutes. The cooling bath was then removed and the solution was allowed to warm to ambient temperature (ca. 23 °C). After 11 h, the consumption of starting material was complete (as determined by TLC analysis, 12:1 hexanes:EtOAc) and the reaction was filtered through filter paper and then diluted with dichloromethane (200 mL). The solution was washed with 0.1 M aqueous HCl (200 mL), saturated aqueous NaHCO₃ (100 mL), and brine (100 mL). The combined organics were dried over MgSO₄, filtered, and concentrated in vacuo. The crude residue was purified by column chromatography (SiO₂, 7.7% EtOAc in hexanes) to provided diallyladipate **353** (7.06 g, 93% yield) as a pale orange oil; R_f = 0.15 (12:1 hexanes:EtOAc); ¹H NMR (400 MHz, CDCl₃) δ 7.45–7.37 (m, 4H), 7.41–7.24 (m, 6H), 5.54 (d, J = 0.9 Hz, 2H), 5.35 (q, J = 1.2 Hz, 2H), 4.98 (d, J = 1.2 Hz, 4H), 2.36–2.23 (m, 4H), 1.61–1.56 (m, 4H); ¹³C NMR (101 MHz, CDCl₃) δ 173.0 (C), 142.6 (C), 138.0 (C), 128.5 (CH), 128.1 (CH), 126.0 (CH),

115.3 (CH₂), 65.6 (CH₂), 33.9 (CH₂), 24.3 (CH₂); IR (thin film, NaCl) 2943, 1734, 1631, 1496, 1444, 1387, 1165, 1076, 1026, 910, 709, 778 cm⁻¹; HRMS (FAB+) m/z calc'd for C₂₄H₂₆O₄ [M+H]⁺: 379.1904, found: 379.1908.



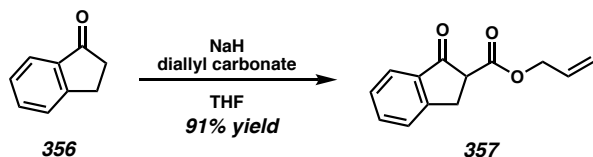
2-Chloroallyl 2-oxocyclopentanecarboxylate (354): Dieckmann condensation was adapted from the literature.²¹ A flask was charged with NaH (60% dispersion in mineral oil, 140 mg, 3.5 mmol, 1.04 equiv) and subsequently evacuated and re-filled with argon (3 x 5 minutes). THF (17 mL, 0.20 M) was added followed by 2-chlorodiallyl adipate (**351**, 1.00 g, 3.40 mmol, 1.00 equiv). The reaction was then placed into a preheated 40 °C oil bath. After 16 h, the consumption of starting material was complete (as determined by TLC analysis, 9:1 hexanes:EtOAc) and the reaction was removed from the heating bath and allowed to cool to ambient temperature (ca. 23 °C). After cooling, the reaction was quenched with 1.0 M aqueous HCl (20 mL). The resultant solution was extracted with EtOAc (3 x 30 mL). The combined organics were washed with brine (90 mL), dried over Na₂SO₄, filtered, and concentrated in vacuo. The crude product was purified by column chromatography (SiO₂, 10% EtOAc in hexanes) to furnish β-ketoester **354** (502 mg, 73% yield) as a clear colorless oil; R_f = 0.27 (9:1 hexanes:EtOAc); ¹H NMR (400 MHz, CDCl₃) δ 5.56 (q, J = 1.4 Hz, 1H), 5.44 (dd, J = 1.9, 0.9 Hz, 1H), 4.74 (qt, J = 13.9, 1.0 Hz, 2H), 3.35–3.17 (m, 1H), 2.45–2.27 (m, 4H), 2.19 (ddq, J = 13.2, 7.8, 5.3 Hz, 1H), 2.01–1.82 (m, 1H); ¹³C NMR (101 MHz, CDCl₃) δ 211.9 (C), 168.6 (C), 135.3 (C), 115.1 (CH₂), 66.5 (CH₂), 54.7 (CH), 38.2 (CH₂), 21.1 (CH₂); IR (thin film, NaCl) 2971, 2883, 1757, 1734,

1730, 1656, 1639, 1405, 1333, 1295, 1248, 1179, 1108, 1003, 961, 901, 833 cm⁻¹; HRMS (FAB+) m/z calc'd for C₉H₁₂O₃Cl [M+H]⁺: 203.0475, found: 203.0470.

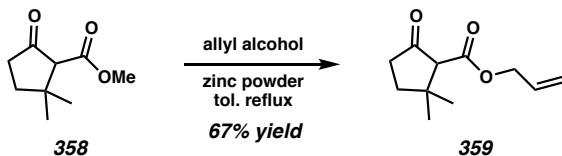


2-Phenylallyl 2-oxocyclopentanecarboxylate (355): Dieckmann condensation was adapted from the literature.^{3d} A flask was charged with NaH (60% dispersion in mineral oil, 216 mg, 9.02 mmol, 1.10 equiv) and subsequently evacuated and re-filled with argon (3 x 5 minutes). Toluene (31.0 mL, 0.26 M) was added followed by 2-phenyldiallyl adipate (**353**, 3.10 g, 8.20 mmol, 1.00 equiv). The reaction was then placed in a preheated 100 °C oil bath. After 16 h, the consumption of starting material was complete (as determined by TLC analysis, 8:2 hexanes:EtOAc) and the reaction was removed from the heating bath and allowed to cool to ambient temperature (ca. 23 °C). After cooling, the reaction was quenched with 1 M HCl (12.5 mL) and saturated aqueous NH₄Cl (25 mL). The resultant solution was extracted with Et₂O (3 x 30 mL). The combined organics were washed with a 50:50 mixture of H₂O and brine (90 mL), dried over Na₂SO₄, filtered, and concentrated in vacuo. The crude solution was purified by column chromatography (SiO₂, 20% EtOAc in hexanes) to afford β-ketoester **355** (1.54 g, 77% yield) as a faint pink oil; R_f = 0.42 (8:2 hexanes:EtOAc); ¹H NMR (400 MHz, CDCl₃) δ 7.45–7.40 (m, 2H), 7.39–7.28 (m, 3H), 5.56 (d, J = 0.9 Hz, 1H), 5.40 (q, J = 1.2 Hz, 1H), 5.12–4.96 (m, 2H), 3.28–3.06 (m, 1H), 2.38–2.18 (m, 4H), 2.15–1.98 (m, 1H), 1.93–1.76 (m, 1H); ¹³C NMR (101 MHz, CDCl₃) δ 212.2 (C), 169.2 (C), 142.2 (C), 138.0 (C), 128.6 (CH), 128.2 (CH), 126.2 (CH), 115.5 (CH₂), 66.6 (CH₂), 54.9 (CH), 38.2 (CH₂), 27.5 (CH₂), 21.1 (CH₂); IR (thin film, NaCl)

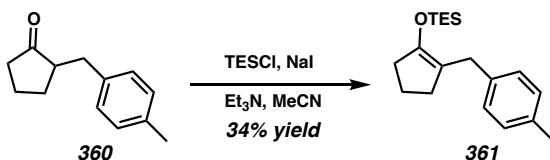
3467, 3083, 3056, 2962, 1725, 1574, 1496, 1450, 1400, 1341, 1294, 1249, 1180, 1106, 1025, 959, 914, 833, 778, 708 cm^{-1} ; HRMS (APCI/ESI) m/z calc'd for $\text{C}_{15}\text{H}_{17}\text{O}_3$ [M+H] $^+$: 245.1182, found: 245.1173.



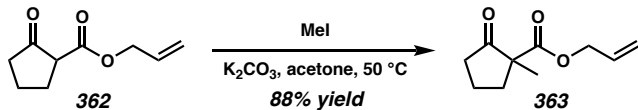
Allyl 1-oxo-2,3-dihydro-1H-indene-2-carboxylate (357): Acylation of **356** was adapted from the literature.^{3d} A flask was charged with NaH (60% dispersion in mineral oil, 500 mg, 20.8 mmol, 2.50 equiv) and subsequently evacuated and re-filled with argon (3 x 5 minutes). THF (10.8 mL, 1.92 M) was added and the resultant solution was cooled to 0 °C (ice/H₂O bath). A solution of 1-indanone (**356**, 1.10 g, 8.30 mmol, 1.00 equiv) in THF (2.6 mL, 3.20 M) was added dropwise. The solution was allowed to warm to room temperature (ca. 23 °C). After 15 minutes, diallyl carbonate (1.79 mL, 12.5 mmol, 1.50 equiv) was added dropwise. After 16 h, the consumption of starting material was complete (as determined by TLC analysis, 12:1 hexanes:EtOAc) and the solution was quenched with saturated aqueous NH₄Cl and extracted with EtOAc (3 x 20 mL). The combined organics were dried over Na₂SO₄, filtered, and concentrated in vacuo. The crude product was purified by column chromatography (SiO₂, 7.7% EtOAc in hexanes) to provided β-ketoester **357** (1.62 g, 91% yield) as a purple oil; $R_f = 0.25$ (12:1 hexanes:EtOAc). β-ketoester **357** was carried on without any further characterization.



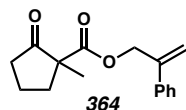
Allyl 2,2-dimethyl-5-oxocyclopentane-1-carboxylate (359): A solution of **358** (400 mg, 2.35 mmol, 1.00 equiv) in toluene (1.96 mL, 1.20 M) was added zinc powder (31 mg, 0.47 mmol, 0.20 equiv) and allyl alcohol (799 μ L, 11.8 mmol, 5.00 equiv). The reaction mixture was allowed to stir at reflux. After 24 h the consumption of starting material was complete (as determined by TLC analysis, 9:1 hexanes:EtOAc). The crude solution was directly purified by column chromatography (SiO_2 , 10% Et_2O in hexanes) to furnish cyclopentanone **359** (309 mg, 67% yield) as a clear colorless oil; $R_f = 0.24$ (9:1 hexanes: Et_2O); ^1H NMR (400 MHz, CDCl_3) δ 5.91 (ddt, $J = 17.2, 10.4, 5.8$ Hz, 1H), 5.34 (dq, $J = 17.2, 1.5$ Hz, 1H), 5.25 (dq, $J = 10.4, 1.2$ Hz, 1H), 4.62 (ddt, $J = 5.9, 3.0, 1.4$ Hz, 2H), 2.97–2.91 (m, 1H), 2.55–2.31 (m, 2H), 2.01 (ddd, $J = 12.8, 9.1, 5.7$ Hz, 1H), 1.82–1.65 (m, 1H), 1.22 (s, 3H), 1.10 (s, 3H); ^{13}C NMR (101 MHz, CDCl_3) δ 213.0 (C), 168.6 (C), 131.8 (CH), 118.9 (CH₂), 65.8 (CH), 65.7 (CH₂), 41.0 (C), 36.8 (CH₂), 36.1 (CH₂), 29.1 (CH₃), 24.1 (CH₃); IR (thin film, NaCl) 2959, 2872, 1757, 1761, 1734, 1729, 1647, 1610, 1616, 1458, 1390, 1370, 1363, 1319, 1234, 1219, 1190, 1159, 1112, 1032, 991, 934, 810, 772, 736 cm^{-1} ; HRMS (APCI/ESI) m/z calc'd for $\text{C}_{11}\text{H}_{16}\text{O}_3$ [M+H]⁺: 197.1172, found 197.1169.



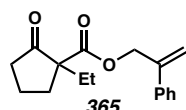
2-(*p*-methylbenzyl)-1-triethylsiloxy-1-cyclopentene (361): To a solution of cyclopentanone **360** (300 mg, 1.59 mmol, 1.00 equiv) and sodium iodide (310 mg, 2.00 mmol, 1.30 equiv) in acetonitrile (2.65 mL, 0.60 M) had Et₃N (357 μL, 2.54 mmol, 1.60 equiv) added dropwise. After 5 minutes of stirring, TESCl (347 μL, 2.07 mmol, 1.30 equiv) was added dropwise. After 6 hours of stirring, consumption of starting was complete (as determined by TLC analysis, 19:1 hexanes:Et₂O). Crude solution was extracted with pentane (4 x 5 mL), the combined organic layers were washed with brine, dried over Na₂SO₄, filtered, and concentrated in vacuo. The crude product was purified by flash chromatography (SiO₂, 0.5% Et₃N, 1% Et₂O in hexanes) to provide silyl enol ether **361** (164 mg, 34%) as a pale yellow oil; R_f = 0.62 (19:1 hexanes:Et₂O); ¹H NMR (400 MHz, C₆D₆) δ 7.21 (d, *J* = 7.9 Hz, 2H), 7.03 (d, *J* = 7.7 Hz, 2H), 3.52 (s, 2H), 2.30 (dd, *J* = 8.6, 7.3, 3.4, 1.7 Hz, 2H), 2.19 (dd, *J* = 9.5, 7.2, 3.0, 1.3 Hz, 2H), 2.13 (s, 3H), 1.72 – 1.61 (m, 2H), 1.01 (t, *J* = 7.9 Hz, 9H), 0.65 (q, *J* = 7.8 Hz, 6H); ¹³C NMR (101 MHz, C₆D₆) δ 147.6 (C), 138.2 (C), 135.1 (C), 129.3 (CH), 129.0 (CH), 115.8 (C), 34.2 (CH₂), 33.0 (CH₂), 31.2 (CH₂), 21.1 (CH₃), 20.1 (CH₂), 7.1 (CH₃), 5.9 (CH₂); IR (thin film, NaCl) 3044, 2954, 2876, 2845, 1895, 1681, 1512, 1458, 1412, 1378, 1341, 1306, 1240, 1107, 1045, 1016, 974, 888, 859, 746, 680 cm⁻¹; HRMS (FAB+) m/z calc'd for C₁₉H₃₀OSi [M]⁺: 302.2066, found 302.2075.

General Procedure A: α -Quaternary β -Ketoester Cyclopentanone Synthesis

The alkylation β -ketoester **362** was adapted from the literature.^{3d} β -ketoester **262** (500 mg, 2.97 mmol, 1.00 equiv) was added to a suspension of anhydrous K_2CO_3 (822 mg, 5.95 mmol, 2.00 equiv) in acetone (3.00 mL, 1.00 M). To the reaction mixture was added iodomethane (0.370 mL, 5.95 mmol, 2.00 equiv). The resultant solution was placed in a preheated 50 °C oil bath. After 14 h, the consumption of starting material was complete (as determined by TLC analysis, 9:1 Pentane:Et₂O) and the reaction was removed from the heating bath and allowed to cool to ambient temperature (ca. 23 °C). After cooling, the solution was filtered with grade 4 filter paper and concentrated in vacuo. The crude product was purified by column chromatography (SiO_2 , 10% Et₂O in pentane) to furnish β -ketoester **363** (477 mg, 88% yield) as a clear colorless oil; $R_f = 0.23$ (9:1 Pentane:Et₂O); ¹H NMR (400 MHz, CDCl_3) δ 5.88 (ddt, $J = 17.3, 10.5, 5.6$ Hz, 1H), 5.29 (dq, $J = 17.2, 1.6$ Hz, 1H), 5.23 (dq, $J = 10.5, 1.3$ Hz, 1H), 4.60 (dq, $J = 5.6, 1.4$ Hz, 2H), 2.61–2.38 (m, 2H), 2.39–2.26 (m, 1H), 2.14–1.98 (m, 1H), 2.02–1.80 (m, 2H), 1.33 (s, 3H); ¹³C NMR (101 MHz, CDCl_3) δ 215.8 (C), 172.0 (C), 131.7 (CH), 118.3 (CH₂), 65.8 (CH₂), 56.0 (C), 37.7 (CH₂), 36.2 (CH₂), 19.6 (CH₃), 19.5 (CH₂). IR (thin film, NaCl) 3462, 3086, 2973, 2886, 1752, 1731, 1648, 1457, 1406, 1375, 1316, 1273, 1153, 1064, 976, 939, 842, 814, 770 cm⁻¹; HRMS (FAB+) m/z calc'd for $\text{C}_{10}\text{H}_{15}\text{O}_3$ [M+H]⁺: 183.1021, found 183.1022.

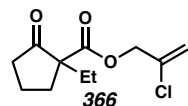


2-Phenylallyl 1-methyl-2-oxocyclopentanecarboxylate (364): Prepared by using general procedure A above from 2-phenylallyl 2-oxocyclopentanecarboxylate (**355**, 1.64 mmol), using iodomethane as the electrophile, and purified by column chromatography (SiO₂, 10% Et₂O in pentane) to afford β -ketoester **364** (292 mg, 69% yield) as a clear colorless oil; R_f = 0.25 (9:1 Pentane:Et₂O); ¹H NMR (400 MHz, CDCl₃) δ 7.43–7.28 (m, 5H), 5.52 (q, J = 0.8 Hz, 1H), 5.33 (q, J = 1.3 Hz, 1H), 5.06 (ddd, J = 13.4, 1.5, 0.7 Hz, 1H), 4.96 (ddd, J = 13.3, 1.3, 0.7 Hz, 1H), 2.46–2.34 (m, 1H), 2.31–2.18 (m, 2H), 1.94–1.74 (m, 3H), 1.29 (s, 3H); ¹³C NMR (101 MHz, CDCl₃) δ = 215.8 (C), 172.1 (C), 142.5 (C), 138.0 (C), 128.6 (CH), 128.2 (CH), 126.2 (CH), 115.4 (CH₂), 66.6 (CH₂), 56.1 (C), 37.7 (CH₂), 36.3 (CH₂), 19.61 (CH₃), 19.59 (CH₂); IR (thin film, NaCl) 3467, 2972, 1750, 1729, 1496, 1457, 1405, 1374, 1316, 1262, 1230, 1150, 1063, 1027, 973, 911, 840, 778, 709 cm⁻¹; HRMS (FAB+) m/z calc'd for C₁₆H₁₉O₃ [M+H]⁺: 259.1334, found: 259.1347.

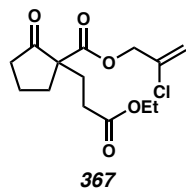


2-Phenylallyl 1-ethyl-2-oxocyclopentanecarboxylate (365): Prepared by using general procedure A above from 2-phenylallyl 2-oxocyclopentanecarboxylate (**355**, 1.63 mmol), using iodoethane as the electrophile, and purified by column chromatography (SiO₂, 10% Et₂O in pentane) to provide β -ketoester **365** (288 mg, 65% yield) as a clear colorless oil; R_f = 0.29 (9:1 Pentane:Et₂O); ¹H NMR (400 MHz, CDCl₃) δ 7.42–7.28 (m, 5H), 5.52 (d, J = 0.8 Hz, 1H), 5.34 (q, J = 1.3 Hz, 1H), 5.04 (ddd, J = 13.3, 1.4, 0.7 Hz, 1H), 4.99 (ddd, J =

= 13.4, 1.3, 0.6 Hz, 1H), 2.50–2.32 (m, 1H), 2.32–2.11 (m, 2H), 1.94 (dq, J = 14.1, 7.5 Hz, 1H), 1.89–1.78 (m, 3H), 1.62 (dq, J = 14.0, 7.4 Hz, 1H), 0.83 (t, J = 7.5 Hz, 3H); ^{13}C NMR (101 MHz, CDCl_3) δ 215.0 (C), 170.9 (C), 142.6 (C), 138.1 (C), 128.6 (CH), 128.2 (CH), 126.2 (CH), 115.5 (CH₂), 66.5 (CH₂), 61.0 (C), 38.2 (CH₂), 32.3 (CH₂), 26.9 (CH₂), 19.6 (CH₂), 9.3(CH₃); IR (thin film, NaCl) 3460, 2968, 2881, 1749, 1725, 1635, 1496, 1457, 1405, 1318, 1294, 1223, 1142, 1078, 1027, 977, 915, 824, 779, 709 cm⁻¹; HRMS (FAB+) m/z calc'd for $\text{C}_{17}\text{H}_{21}\text{O}_3$ [M+H]⁺: 273.1491, found: 273.1480.

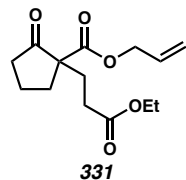


2-Chloroallyl 1-ethyl-2-oxocyclopentanecarboxylate (366): Prepared by using general procedure A above from 2-chloroallyl 2-oxocyclopentanecarboxylate (**354**, 0.99 mmol), using iodoethane as the electrophile, and purified by column chromatography (SiO_2 , 5% Et_2O in pentane) to furnish β -ketoester **366** (228 mg, 80% yield) as a clear colorless oil; R_f = 0.3 (8:2 Pentane: Et_2O); ^1H NMR δ 5.46 (q, J = 1.4 Hz, 1H), 5.39 (dd, J = 1.8, 0.8 Hz, 1H), 4.75–4.59 (m, 2H), 2.60–2.49 (m, 1H), 2.49–2.38 (m, 1H), 2.34–2.21 (m, 1H), 2.14–1.90 (m, 4H), 1.67 (dq, J = 13.9, 7.4 Hz, 1H), 0.92 (t, J = 7.4 Hz, 3H); ^{13}C NMR (101 MHz, CDCl_3) δ 214.7 (C), 170.4 (C), 135.5 (C), 115.3 (CH₂), 66.5 (CH₂), 61.0 (C), 38.3 (CH₂), 32.3 (CH₂), 26.9 (CH₂), 19.7 (CH₂), 9.3 (CH₃); IR (thin film, NaCl) 3466, 3115, 2970, 2882, 1755, 1732, 1639, 1458, 1405, 1382, 1319, 1294, 1222, 1132, 1082, 1030, 904, 820, 797, 765, 705, 643 cm⁻¹; HRMS (FAB+) m/z calc'd for $\text{C}_{11}\text{H}_{16}\text{O}_3\text{Cl}$ [M+H]⁺: 231.0788, found: 231.0794.



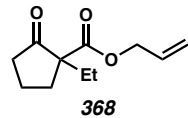
2-Chloroallyl 1-(3-ethoxy-3-oxopropyl)-2-oxocyclopentanecarboxylate (367):

Prepared by using general procedure A above from 2-chloroallyl 2-oxocyclopentanecarboxylate (**354**, 0.99 mmol), using ethyl acrylate as the electrophile, and purified by column chromatography (SiO_2 , 20% Et_2O in pentane) to afford β -ketoester **367** (132 mg, 44% yield) as a clear colorless oil; $R_f = 0.1$ (8:2 Pentane: Et_2O); ^1H NMR δ 5.46 (dt, $J = 2.2, 1.2$ Hz, 1H), 5.43–5.39 (m, 1H), 4.75–4.61 (m, 2H), 4.12 (q, $J = 7.1$ Hz, 2H), 2.58–2.47 (m, 2H), 2.47–2.39 (m, 1H), 2.39–2.19 (m, 3H), 2.13–1.88 (m, 4H), 1.24 (t, $J = 7.1$ Hz, 3H); ^{13}C NMR (101 MHz, CDCl_3) δ 214.1 (C), 173.0 (C), 170.3 (C), 135.4 (C), 115.7 (CH_2), 66.7 (CH_2), 60.7 (CH_2), 59.4 (C), 38.1 (CH_2), 33.8 (CH_2), 29.9 (CH_2), 28.5 (CH_2), 19.8 (CH_2), 14.3 (CH_3); IR (thin film, NaCl) 3459, 2978, 1730, 1638, 1448, 1377, 1180, 1109, 1023, 905, 642 cm^{-1} ; HRMS (FAB+) m/z calc'd for $\text{C}_{14}\text{H}_{20}\text{O}_5\text{Cl}$ $[\text{M}+\text{H}]^+$: 303.0999, found: 303.0986.

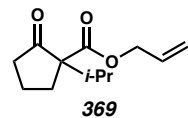


Allyl 1-(3-ethoxy-3-oxopropyl)-2-oxocyclopentanecarboxylate (331): Prepared by using general procedure A above from allyl 2-cyclopentanonecarboxylate (**362**, 8.97 mmol), using ethyl acrylate as the electrophile, and purified by column chromatography (SiO_2 , 10% Et_2O in pentane) to provide β -ketoester **331** (1.83 g, 76% yield) as a clear

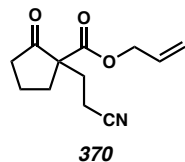
colorless oil; $R_f = 0.20$ (8:2 Pentane:Et₂O); ¹H NMR (400 MHz, CDCl₃) δ 5.83 (ddt, $J = 17.2, 10.4, 5.6$ Hz, 1H), 5.33–5.11 (m, 2H), 4.55 (dt, $J = 5.6, 1.4$ Hz, 2H), 4.06 (q, $J = 7.2$ Hz, 2H), 2.54–2.38 (m, 2H), 2.36 (ddd, $J = 8.7, 6.3, 1.1$ Hz, 1H), 2.32–2.12 (m, 3H), 2.08–1.77 (m, 4H), 1.19 (t, $J = 7.1$ Hz, 3H); ¹³C NMR (101 MHz, CDCl₃) δ 214.2 (C), 172.9 (C), 170.7 (C), 131.5 (CH), 118.6 (CH₂), 65.9 (CH₂), 60.6 (CH₂), 59.3 (C), 37.9 (CH₂), 33.7 (CH₂), 29.8 (CH₂), 28.4 (CH₂), 19.6 (CH₂), 14.2 (CH₃); IR (thin film, NaCl) 3453, 3086, 2979, 1731, 1648, 1451, 1377, 1182, 1113, 1025, 985, 939, 852 cm⁻¹; HMRS (APCI) m/z calc'd for C₁₄H₂₁O₅ [M+H]⁺: 269.1384, found: 269.1389.



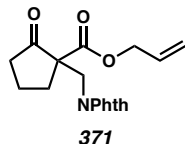
Allyl 1-ethyl-2-oxocyclopentanecarboxylate (368): Prepared by using general procedure A above from allyl 2-cyclopentanonecarboxylate (**362**, 9.17 mmol), using iodoethane as the electrophile, and purified by column chromatography (SiO₂, 10% Et₂O in hexanes) to afford β -ketoester **368** (1.53 g, 85% yield) as a clear colorless oil; $R_f = 0.23$ (9:1 hexanes:Et₂O); characterization data match known literature values.^{3d}



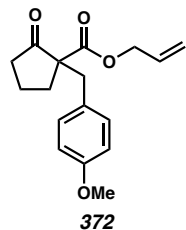
Allyl 1-isopropyl-2-oxocyclopentanecarboxylate (369): Prepared by using general procedure A above from allyl 2-cyclopentanonecarboxylate (**362**, 8.99 mmol), using 2-iodopropane as the electrophile, and purified by column chromatography (SiO₂, 10% to 30% Et₂O in hexanes) to provide β -ketoester **369** (1.55 g, 82% yield) as a clear colorless oil; $R_f = 0.32$ (10:1 hexanes:EtOAc); characterization data match known literature values.^{3d}



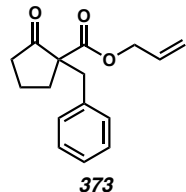
Allyl 1-(cyanomethyl)-2-oxocyclopentanecarboxylate (370): Prepared by using general procedure A above from allyl 2-cyclopentanonecarboxylate (**362**, 2.66 mmol), using acrylonitrile as the electrophile, and purified by column chromatography (SiO₂, 50% Et₂O in pentane) to afford β -ketoester **370** (589 mg, 30% yield) as a clear colorless oil; R_f = 0.20 (8:2 Pentane:Et₂O); ¹H NMR (400 MHz, CDCl₃) δ 5.96–5.76 (m, 1H), 5.37–5.20 (m, 2H), 4.67–4.54 (m, 2H), 2.67–2.41 (m, 4H), 2.41–2.26 (m, 1H), 2.26–2.15 (m, 1H), 2.14–1.88 (m, 4H); ¹³C NMR (101 MHz, CDCl₃) δ 213.7 (C), 170.1 (C), 131.2 (CH), 119.4 (C), 119.3 (CH₂), 66.4 (CH₂), 58.7 (C), 37.9 (CH₂), 34.1 (CH₂), 29.5 (CH₂), 19.8 (CH₂), 13.2 (CH₂); IR (thin film, NaCl) 2962, 2247, 1748, 1726, 1648, 1451, 1362, 1261, 1232, 1164, 1115, 938, 824 cm⁻¹; HMRS (ESI+) m/z calc'd for C₁₂H₁₆O₃N [M+H]⁺: 222.1125, found: 222.1127.



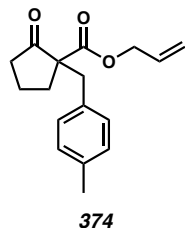
Allyl 1-((1,3-dioxoisindolin-2-yl)methyl)-2-oxocyclopentanecarboxylate (371): Prepared by using general procedure A above from allyl 2-cyclopentanonecarboxylate (**362**, 8.83 mmol), using (N-chloromethyl)phthalimide as the electrophile, and purified by column chromatography (SiO₂, 20% to 30% EtOAc in hexanes) to furnish β -ketoester **371** (1.56 g, 54% yield) as a white amorphous solid; R_f = 0.27 (6:3 hexanes:EtOAc); characterization data match known literature values.^{3d}



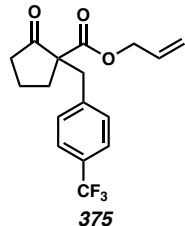
Allyl 1-(4-methoxybenzyl)-2-oxocyclopentanecarboxylate (372): Prepared by using general procedure A above from allyl 2-cyclopentanonecarboxylate (**362**, 8.88 mmol), using 4-methoxybenzyl chloride as the electrophile, and purified by column chromatography (SiO_2 , 9% EtOAc in hexanes) to provide β -ketoester **372** (2.56 g, 95% yield) as a clear colorless oil; $R_f = 0.17$ (11:1 hexanes:EtOAc); characterization data match known literature values.^{3d}



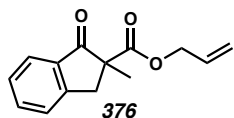
Allyl 1-benzyl-2-oxocyclopentanecarboxylate (373): Prepared by using general procedure A above from allyl 2-cyclopentanonecarboxylate (**362**, 8.86 mmol), using benzyl bromide as the electrophile, and purified by column chromatography (SiO_2 , 10% Et₂O in pentane) to furnish β -ketoester **373** (824 mg, 36% yield) as a clear colorless oil; $R_f = 0.17$ (9:1 Pentane:Et₂O); characterization data match known literature values.²⁶



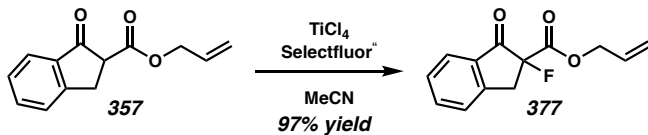
Allyl 1-(4-methylbenzyl)-2-oxocyclopentanecarboxylate (374): Prepared by using general procedure A above from allyl 2-cyclopentanonecarboxylate (**362**, 8.79 mmol), using 4-methylbenzyl bromide as the electrophile, and purified by column chromatography (SiO_2 , 10% Et_2O in pentane) to afford β -ketoester **374** (2.13 g, 89% yield) as a clear colorless oil; $R_f = 0.20$ (9:1 Pentane: Et_2O); characterization data match known literature values.^{3d}



Allyl 2-oxo-1-(4-(trifluoromethyl)benzyl)cyclopentanecarboxylate (375): Prepared by using general procedure A above from allyl 2-cyclopentanonecarboxylate (**362**, 9.10 mmol), using 4-trifluoromethylbenzyl bromide as the electrophile, and purified by column chromatography (SiO_2 , 10% Et_2O in pentane) to furnish β -ketoester **375** (1.93 g, 65% yield) as an amorphous solid; $R_f = 0.20$ (9:1 Pentane: Et_2O); characterization data match known literature values.^{3d}

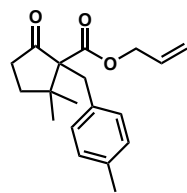


Allyl 2-methyl-1-oxo-2,3-dihydro-1H-indene-2-carboxylate (376): Prepared by using general procedure A above from allyl 1-oxo-2,3-dihydro-1H-indene-2-carboxylate (357, 1.84 mmol), using iodomethane as the electrophile, and purified by column chromatography (SiO_2 , 7.7% EtOAc in hexanes) to provide β -ketoester 376 (361 mg, 85% yield) as a pale yellow oil; $R_f = 0.23$ (12:1 hexanes:EtOAc); characterization data match known literature values.²⁶



Allyl 2-fluoro-1-oxo-2,3-dihydro-1H-indene-2-carboxylate (377): TiCl_4 (18 μL , 167 μmol , 0.09 equiv) was added to a solution of indanone 357 (400 mg, 1.85 mmol, 1.00 equiv) in acetonitrile (18.5 mL, 0.10 M). After 10 minutes, Selectfluor[®] (786 mg, 2.22 mmol, 1.20 equiv) was added. After 3 h, the starting material had been completely consumed (determined by TLC analysis, 8:2 Pentane:Et₂O). The solution was partitioned between H₂O (100 mL) and Et₂O (25 mL), extracted with Et₂O (3 x 30 mL). The combined organics were dried over MgSO₄, filtered, and concentrated in vacuo. Crude product was filtered through a silica plug (Et₂O) to provide β -ketoester 377 (421 mg, 97% yield) as an amorphous orange solid; $R_f = 0.23$ (8:2 Pentane:Et₂O); ¹H NMR (400 MHz, CDCl₃) δ 7.84 (dt, $J = 7.7, 1.0$ Hz, 1H), 7.70 (td, $J = 7.5, 1.3$ Hz, 1H), 7.59–7.39 (m, 2H), 5.84 (ddt, $J = 17.2, 10.5, 5.7$ Hz, 1H), 5.35–5.16 (m, 2H), 4.70 (dq, $J = 5.7, 1.3$ Hz, 2H), 3.92–3.72 (m, 1H), 3.59–3.32 (m, 1H); ¹⁹F NMR (470 MHz, CDCl₃) δ -164.6 (dd, $J = 11.6, 23.2$ Hz); ¹³C

NMR (101 MHz, CDCl₃) δ 195.2 (d, *J* = 18.2 Hz, C), 167.1 (d, *J* = 28.0 Hz, C), 150.9 (d, *J* = 3.7 Hz, C), 136.9 (CH), 133.4 (C), 130.8 (CH), 128.8 (CH), 126.7 (d, *J* = 1.5 Hz, CH), 125.8 (CH), 119.4 (CH₂), 94.7 (d, *J* = 201.8 Hz, C), 66.8 (CH₂), 38.4 (d, *J* = 23.7 Hz, CH₂); IR (thin film, NaCl) 3585, 3435, 3078, 2943, 1761, 1720, 1603, 1465, 1423, 1363, 1272, 1181, 1155, 1067, 994, 917, 806, 751, 721, 692 cm⁻¹; HRMS (ESI+) m/z calc'd for C₁₃H₁₂FO₃ [M+H]⁺: 235.0765, found: 235.0768.

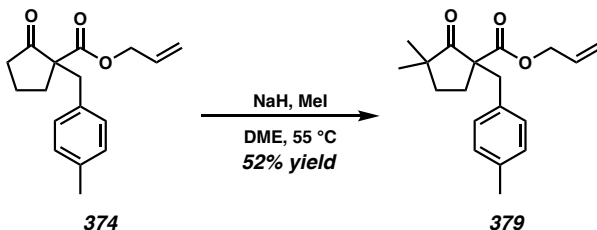


378

Allyl 2,2-dimethyl-1-(4-methylbenzyl)-5-oxocyclopentane-1-carboxylate (378):

Prepared by using general procedure A above from allyl 2,2-dimethyl-5-oxocyclopentane-1-carboxylate (**359**, 1.48 mmol) and using 4-methylbenzyl chloride as the electrophile.

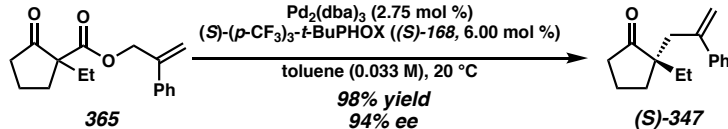
Purified by column chromatography (SiO₂, 10% Et₂O in hexanes) to furnish β-ketoester **378** (61 mg, 14% yield) as a clear colorless oil; R_f = 0.12 (9:1 hexanes:Et₂O); ¹H NMR δ 7.29 (d, *J* = 8.1 Hz, 2H), 7.18 (d, *J* = 7.8 Hz, 2H), 5.99 (ddt, *J* = 17.2, 10.6, 5.4 Hz, 1H), 5.35 (dq, *J* = 17.2, 1.7 Hz, 1H), 5.19 (dq, *J* = 10.5, 1.5 Hz, 1H), 5.08 (s, 2H), 4.68 (dt, *J* = 5.4, 1.6 Hz, 2H), 2.60 (t, *J* = 7.5 Hz, 2H), 2.37 (s, 3H), 1.69 (t, *J* = 7.4 Hz, 2H), 1.24 (s, 6H); ¹³C NMR (101 MHz, CDCl₃) δ 167.7 (C), 165.0 (C), 137.8 (CH), 133.9 (CH), 133.0 (CH), 129.3, 127.0, 117.3 (CH₂), 113.4 (C), 71.5 (CH₂), 64.1 (CH₂), 43.0 (C), 37.2 (CH₂), 29.1 (CH₂), 27.9 (CH₃), 21.3 (CH₃); IR (thin film, NaCl) 2948, 1685, 1617, 16517, 1457, 1370, 1356, 1283, 1224, 1170, 1087, 1047, 1020, 994, 929, 801, 788 cm⁻¹; HRMS (FAB+) m/z calc'd for C₁₉H₂₅O₃ [M+H]⁺: 301.1798, found 301.1803.



Allyl 3,3-dimethyl-1-(4-methylbenzyl)-2-oxocyclopentane-1-carboxylate (379): The alkylation of **374** was adapted from the literature.²⁷ A flask was charged with sodium hydride (60% dispersion in mineral oil, 61.7 mg, 1.54 mmol, 3.00 equiv) and subsequently evacuated and re-filled with argon (3 x 5 minutes). DME (6 mL, 0.63 M) was added followed by methyliodide (0.16 mL, 2.57 mmol, 5.00 equiv) and β -ketoester **374** (140 mg, 0.514 mmol, 1 equiv). The heterogeneous solution was heated to 55 °C with stirring. After 2 hours, the consumption of starting was complete (as determined by TLC analysis, 9:1 Pentane:Et₂O). The solution was poured into water, and extracted with Et₂O (3 x 5 mL), dried over MgSO₄, filtered, and concentrated in vacuo. The crude solution was purified by flash chromatography (SiO₂, 5% Et₂O in hexanes) to afford β -ketoester **379** (80 mg, 52% yield) as a clear colorless oil; R_f = 0.60 (9:1 Pentane:Et₂O); ¹H NMR δ 7.05 (d, *J* = 7.9 Hz, 2H), 7.01 (d, *J* = 8.1 Hz, 2H), 5.89 (ddt, *J* = 17.2, 10.4, 5.7 Hz, 1H), 5.32 (dq, *J* = 17.2, 1.5 Hz, 1H), 5.24 (dq, *J* = 10.4, 1.3 Hz, 1H), 4.62 (ddt, *J* = 5.6, 2.7, 1.4 Hz, 2H), 3.14 (s, 2H), 2.38–2.31 (m, 1H), 2.30 (s, 3H), 1.97 (ddd, *J* = 13.6, 8.5, 7.2 Hz, 1H), 1.78 (ddd, *J* = 12.8, 8.4, 7.2 Hz, 1H), 1.41 (ddd, *J* = 12.7, 7.2, 5.4 Hz, 1H), 1.08 (s, 3H), 0.70 (s, 3H); ¹³C NMR (101 MHz, CDCl₃) δ 218.5 (C), 171.3 (C), 136.6 (C), 133.5 (C), 131.7 (CH), 130.6 (CH), 129.1 (CH), 118.8 (CH₂), 66.2 (CH₂), 62.4 (C), 46.2 (C), 39.1 (CH₂), 35.5 (CH₂), 28.1 (CH₂), 25.1 (CH₃), 24.0 (CH₃), 21.2 (CH₃); IR (thin film, NaCl) 2963, 2870, 1747, 1726,

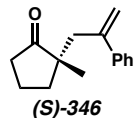
1515, 1457, 1380, 1361, 1315, 1252, 1197, 1183, 1130, 1061, 993, 977, 931, 888, 817, 775
 cm^{-1} ; HRMS (FAB+) m/z calc'd for $\text{C}_{19}\text{H}_{25}\text{O}_3$ [$\text{M}+\text{H}$]⁺: 301.1798, found 301.1808.

General Procedure B: Pd-Catalyzed Enantioselective Allylic Alkylation

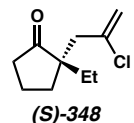


In a nitrogen-filled glovebox, separate stock solutions of $\text{Pd}_2(\text{dba})_3$ (2.50 mg/mL), (*S*)-(CF₃)₃-*t*-Bu-PHOX (**(S)-168**, 10.0 mg/mL), and β -ketoester **365** (100. mg/mL) in toluene were prepared. $\text{Pd}_2(\text{dba})_3$ (1.92 mL, 4.8 mg, 5.20 μmol , 0.0275 equiv) and (*S*)-(CF₃)₃-*t*-Bu-PHOX (**(S)-168**, 0.67 mL, 6.7 mg, 11.4 μmol , 0.06 equiv) were added to a 20 mL scintillation vial and placed in a pre-chilled 20 °C stirrer. After 20 minutes, the solution was diluted with toluene (2.69 mL, 20 °C) followed by β -ketoester **365** (0.517 mL, 51.7 mg, 0.19 mmol, 1.00 equiv) in one portion (total volume 5.8 mL, 0.033 M). After 20 h, the consumption of starting material was complete (as determined by TLC analysis, 19:1 Pentane:Et₂O). The crude solution was directly purified by column chromatography (SiO₂, 100% pentane then 5% Et₂O in pentane) to furnish cyclopentanone (**(S)-347**) (43 mg, 98% yield) as a clear colorless oil; R_f = 0.20 (19:1 Pentane:Et₂O); ¹H NMR (400 MHz, CDCl₃) δ 7.37–7.26 (m, 5H), 5.26 (d, J = 1.7 Hz, 1H), 5.07 (dt, J = 1.8, 0.9 Hz, 1H), 2.77 (dd, J = 13.8, 1.1 Hz, 1H), 2.62 (d, J = 13.8 Hz, 1H), 2.17–2.04 (m, 1H), 1.99–1.84 (m, 1H), 1.82–1.66 (m, 3H), 1.66–1.60 (m, 1H), 1.51–1.31 (m, 2H), 0.79 (t, J = 7.5 Hz, 3H); ¹³C NMR (101 MHz, CDCl₃) δ 223.2 (C), 146.1 (C), 142.3 (C), 128.3 (CH), 127.6 (CH), 126.8 (CH), 117.4 (CH₂), 52.8 (C), 40.0 (CH₂), 38.4 (CH₂), 31.9 (CH₂), 28.8 (CH₂), 18.8 (CH₂), 8.8 (CH₃); IR (thin film, NaCl) 3079, 3054, 2963, 2879, 1734, 1623, 1572, 1491, 1457, 1405,

1380, 1306, 1268, 1160, 1083, 1028, 902, 778, 700 cm^{-1} ; HRMS (APCI/ESI) m/z calc'd for $\text{C}_{16}\text{H}_{21}\text{O}$ [M+H]⁺: 229.1587, found 229.1589; $[\alpha]_D^{25} -40.78$ (*c* 0.510, CHCl_3 , 94% ee).

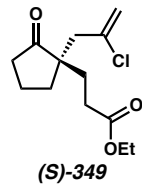


2-(2-Phenyl)allyl-2-methylcyclopentanone ((S)-346): Prepared by using general procedure B from β -ketoester **364** (0.19 mmol), reaction time = 27.5 h. Purified by column chromatography (SiO_2 , 5% Et_2O in pentane) to provide cyclopentanone **(S)-346** (39 mg, 95% yield) as a clear colorless oil; $R_f = 0.11$ (19:1 Pentane: Et_2O); ¹H NMR (400 MHz, CDCl_3) δ 7.37–7.26 (m, 5H), 5.27 (d, *J* = 1.7 Hz, 1H), 5.08 (dt, *J* = 1.8, 1.0 Hz, 1H), 2.74 (dd, *J* = 13.7, 1.1 Hz, 1H), 2.62 (d, *J* = 13.8 Hz, 1H), 2.29–2.14 (m, 1H), 2.04–1.90 (m, 1H), 1.88–1.65 (m, 3H), 1.51–1.37 (m, 1H), 0.91 (s, 3H); ¹³C NMR (101 MHz, CDCl_3) δ 223.3 (C), 146.1 (C), 142.5 (C), 128.4 (CH), 127.6 (CH), 126.8 (CH), 117.3 (CH₂), 49.0 (C), 41.8 (CH₂), 37.6 (CH₂), 35.4 (CH₂), 22.6 (CH₃), 18.8 (CH₂); IR (thin film, NaCl) 3078, 2960, 1734, 1623, 1491, 1457, 1405, 1160, 1061, 900, 778, 701 cm^{-1} ; HRMS (APCI/ESI) m/z calc'd for $\text{C}_{15}\text{H}_{19}\text{O}$ [M+H]⁺: 215.21436, found 215.21430; $[\alpha]_D^{25} -99.32$ (*c* 0.445, CHCl_3 , 90% ee).

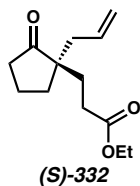


2-(2-Chloro)allyl-2-ethylcyclopentanone ((S)-348): Prepared by using general procedure B from β -ketoester **366** (0.19 mmol), reaction time = 28.5 h. Purified by column chromatography (SiO_2 , 10% Et_2O in pentane) to furnish cyclopentanone **(S)-348** (26 mg, 72% yield) as a clear colorless oil; $R_f = 0.71$ (8:2 Pentane: Et_2O); ¹H NMR (400 MHz,

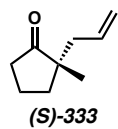
CDCl_3) δ 5.24 (t, $J = 0.9$ Hz, 1H), 5.15 (t, $J = 1.1$ Hz, 1H), 2.61 (dd, $J = 14.4, 1.1$ Hz, 1H), 2.49 (d, $J = 14.4$ Hz, 1H), 2.34–2.21 (m, 2H), 2.16–2.00 (m, 1H), 1.98–1.79 (m, 3H), 1.48 (qd, $J = 7.4, 3.1$ Hz, 2H), 0.84 (t, $J = 7.5$ Hz, 3H); ^{13}C NMR (101 MHz, CDCl_3) δ 222.1 (C), 139.5 (C), 116.3 (CH_2), 51.8 (C), 44.1 (CH_2), 38.2 (CH_2), 32.1 (CH_2), 28.6 (CH_2), 18.9 (CH_2), 8.6 (CH_3); IR (thin film, NaCl) 2965, 1734, 1629, 1458, 1405, 1382, 1260, 1158, 1115, 1085, 886 cm^{-1} . HRMS (FAB+) m/z calc'd for $\text{C}_{10}\text{H}_{16}\text{ClO}$ [M+H] $^+$: 187.0890, found 187.0897; $[\alpha]_D^{25} -38.57$ (c 0.165, CHCl_3 , 90% ee).



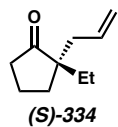
2-(2-Chloro)allyl-2-(3-ethoxy-3oxopropyl)cyclopentanone ((S)-349): Prepared by using general procedure B from β -ketoester **367** (0.19 mmol), reaction time = 21 h. Purified by column chromatography (SiO_2 , 20% Et_2O in pentane) to afford cyclopentanone **(S)-349** (42 mg, 85% yield) as a clear colorless oil $R_f = 0.32$ (8:2 Pentane: Et_2O); ^1H NMR (400 MHz, CDCl_3) δ 5.33–5.23 (m, 1H), 5.18 (t, $J = 1.2$ Hz, 1H), 4.11 (q, $J = 7.1$ Hz, 2H), 2.59 (dd, $J = 14.4, 1.1$ Hz, 1H), 2.51 (d, $J = 14.4$ Hz, 1H), 2.40–2.21 (m, 4H), 2.19–2.05 (m, 1H), 2.03–1.72 (m, 5H), 1.24 (t, $J = 7.1$ Hz, 3H); ^{13}C NMR (101 MHz, CDCl_3) δ 221.1 (C), 173.3 (C), 138.9 (C), 116.7 (CH_2), 60.7 (CH_2), 50.7 (C), 43.9 (CH_2), 37.8 (CH_2), 33.5 (CH_2), 30.1 (CH_2), 29.1 (CH_2), 18.8 (CH_2), 14.3 (CH_3); IR (thin film, NaCl) 2962, 1734, 1629, 1375, 1304, 1267, 1191, 1025, 888 cm^{-1} ; HRMS (ESI) m/z calc'd for $\text{C}_{13}\text{H}_{20}\text{ClO}_3$ [M+H] $^+$: 259.1095, found 259.1108; $[\alpha]_D^{25} -26.99$ (c 0.255, CHCl_3 , 88% ee).



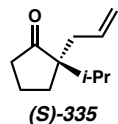
2-Allyl-2-(3-ethoxy-3-oxopropyl)cyclopentanone ((S)-332): Prepared by using general procedure B above from β -ketoester **331** (0.19 mmol), reaction time = 8 h. Purified by column chromatography (SiO_2 , 20% Et_2O in pentane) to provide cyclopentanone **(S)-332** (40 mg, 93% yield) as a clear colorless oil; $R_f = 0.30$ (8:2 Pentane: Et_2O); ^1H NMR (400 MHz, CDCl_3) δ 5.66 (ddt, $J = 16.4, 10.6, 7.4$ Hz, 1H), 5.11–5.01 (m, 2H), 4.09 (q, $J = 7.1$ Hz, 2H), 2.39–2.10 (m, 6H), 1.95–1.67 (m, 4H), 1.23 (t, $J = 7.1$ Hz, 3H); ^{13}C NMR (101 MHz, CDCl_3) δ 221.9 (C), 173.5 (C), 133.4 (CH), 118.7 (CH_2), 60.6 (CH_2), 50.9 (C), 39.1 (CH_2), 38.3 (CH_2), 33.3 (CH_2), 29.7 (CH_2), 29.2 (CH_2), 18.7 (CH_2), 14.3 (CH_3); IR (thin film, NaCl) 3076, 2961, 1734, 1639, 1445, 1406, 1376, 1303, 1252, 1190, 1096, 1028, 919 cm^{-1} ; HRMS (FAB+) m/z calc'd for $\text{C}_{13}\text{H}_{21}\text{O}_3$ [$\text{M}+\text{H}]^+$: 225.1491, found 225.1498; $[\alpha]_D^{25} -18.69$ (c 1.950, CHCl_3 , 91% ee).



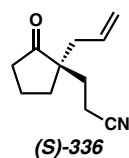
2-Allyl-2-methylcyclopentanone ((S)-333): Prepared by using general procedure B from β -ketoester **363** (0.38 mmol), reaction time = 31 h. Purified by column chromatography (SiO_2 , 5% Et_2O in pentane) to furnish cyclopentanone **(S)-333** (43 mg, 81% yield) as a clear colorless oil; $R_f = 0.24$ (19:1 Pentane: Et_2O); $[\alpha]_D^{25} -72.21$ (c 0.245, CHCl_3 , 86% ee); characterization data match known literature values.⁷ⁱ



2-Allyl-2-ethylcyclopentanone ((S)-334): Prepared by using general procedure B from β -ketoester **368** (0.38 mmol), reaction time = 31 h. Purified by column chromatography (SiO_2 , 7% Et_2O in pentane) to afford cyclopentanone **(S)-334** (69 mg, 79% yield) as a clear colorless oil; $R_f = 0.44$ (10:1 hexanes: EtOAc); $[\alpha]_D^{25} -20.22$ (c 0.340, Et_2O , 88% ee); characterization data match known literature values.^{3d}

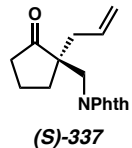


2-Allyl-2-isopropylcyclopentanone ((S)-335): Prepared by using general procedure B from β -ketoester **369** (0.38 mmol), reaction time = 36 h. Purified by column chromatography (SiO_2 , 5% Et_2O in pentane) to provide cyclopentanone **(S)-335** (39 mg, 62% yield) as a clear colorless oil; $R_f = 0.44$ (10:1 hexanes: EtOAc); $[\alpha]_D^{25} +33.57$ (c 0.315, CHCl_3 , 87% ee); characterization data match known literature values.^{3d}

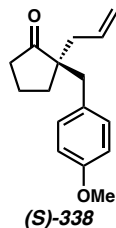


2-Allyl-2-(cyanomethyl)cyclopentanone ((S)-336): Prepared by using general procedure B from β -ketoester **370** (0.19 mmol), except catalyst pre-stir ran for 40 minutes (20 minutes at 30 °C followed by another 20 minutes at 0 °C) and the reaction was run at 0 °C, reaction time = 23 h. Purified by column chromatography (SiO_2 , 40% Et_2O in pentane) to afford cyclopentanone **(S)-336** (35 mg, 97% yield) as a clear colorless oil; $R_f = 0.32$ (1:1

hexanes:Et₂O); ¹H NMR (400 MHz, CDCl₃) δ 5.68 (ddt, *J* = 16.9, 10.2, 7.4 Hz, 1H), 5.26–5.07 (m, 2H), 2.52–2.21 (m, 4H), 2.18 (dt, *J* = 7.4, 1.2 Hz, 2H), 2.10–1.79 (m, 6H); ¹³C NMR (101 MHz, CDCl₃) δ 221.0 (C), 132.4 (CH), 119.7 (C), 119.5 (CH₂), 50.6 (C), 38.4 (CH₂), 38.0 (CH₂), 33.2 (CH₂), 30.2 (CH₂), 18.6 (CH₂), 12.3 (CH₂); IR (thin film, NaCl) 2961, 2246, 1731, 1444, 1159, 921 cm⁻¹; HRMS (EI+) m/z calc'd for C₁₁H₁₅NO [M]⁺: 177.1154, found 177.1171; [α]_D²⁵ −13.41 (*c* 0.450, CHCl₃, 90% ee).

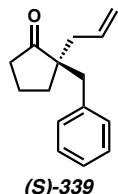


2-Allyl-((1,3-dioxoisooindolin-2-yl)methyl)cyclopentanone ((S)-337): Prepared by using general procedure B from β-ketoester **371** (0.19 mmol), except catalyst pre-stir ran for 40 minutes (20 minutes at 30 °C followed by another 20 minutes at 0 °C) and the reaction was run at 0 °C, reaction time = 23 h. Purified by column chromatography (SiO₂, 20% Et₂O in pentane) to afford cyclopentanone **(S)-337** (48 mg, 93% yield) as a white amorphous solid; R_f = 0.50 (1:1 Pentane:Et₂O); [α]_D²⁵ −25.16 (*c* 0.305, CHCl₃, 92% ee); characterization data match known literature values.^{3d}

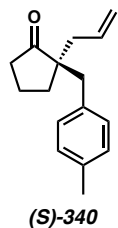


2-Allyl-2-(4-methoxybenzyl)cyclopentanone ((S)-338): Prepared by using general procedure B from β-ketoester **372** (0.19 mmol), reaction time = 8 h. Purified by column chromatography (SiO₂, 10% Et₂O in pentane) to provide cyclopentanone **(S)-338** (46 mg,

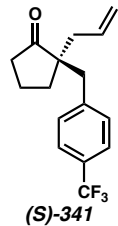
>99% yield) as a clear colorless oil; $R_f = 0.25$ (9:1 Pentane:Et₂O); $[\alpha]_D^{25} +6.40$ (*c* 0.275, CHCl₃, 92% ee); characterization data match known literature values.^{3d}



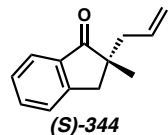
2-Allyl-2-benzylcyclopentanone ((S)-339): Prepared by using general procedure B from β -ketoester **373** (0.19 mmol), reaction time = 13 h. Purified by column chromatography (SiO₂, 7% Et₂O in pentane) to furnish cyclopentanone **(S)-339** (39 mg, 95% yield) as a clear colorless oil; $R_f = 0.41$ (9:1 Pentane:Et₂O); ¹H NMR (400 MHz, CDCl₃) δ 7.32–7.15 (m, 3H), 7.16–7.08 (m, 2H), 5.75 (dddd, *J* = 17.0, 10.2, 7.8, 6.9 Hz, 1H), 5.18–5.05 (m, 2H), 2.94 (d, *J* = 13.3 Hz, 1H), 2.62 (d, *J* = 13.3 Hz, 1H), 2.31 (ddt, *J* = 13.8, 7.0, 1.3 Hz, 1H), 2.24–2.11 (m, 2H), 2.07–1.93 (m, 1H), 1.97–1.81 (m, 2H), 1.75 (ddq, *J* = 12.8, 8.7, 7.0 Hz, 1H), 1.56–1.41 (m, 1H); ¹³C NMR (101 MHz, CDCl₃) δ 223.0 (C), 137.9 (C), 133.8 (CH), 130.4 (CH), 128.3 (CH), 126.5 (CH), 118.8 (CH₂), 53.3 (C), 41.8 (CH₂), 41.0 (CH₂), 39.0 (CH₂), 31.1 (CH₂), 18.8 (CH₂); IR (thin film, NaCl) 3027, 2960, 1733, 1639, 1495, 1453, 1404, 1156, 997, 920, 757 cm⁻¹; HRMS (FAB+) m/z calc'd for C₁₅H₁₉O [M+H]⁺: 215.1436, found 215.1433; $[\alpha]_D^{25} +6.88$ (*c* 1.950, CHCl₃, 88% ee).



2-Allyl-2-(4-methylbenzyl)cyclopentanone ((S)-340): Prepared by using general procedure B from β -ketoester **374** (0.19 mmol), reaction time = 13 h. Purified by column chromatography (SiO_2 , 5% Et_2O in pentane) to afford cyclopentanone **(S)-340** (50 mg, 93% yield) as a clear colorless oil; $R_f = 0.39$ (9:1 Pentane: Et_2O); $[\alpha]_D^{25} +12.78$ (c 0.835, CHCl_3 , 89% ee); characterization data match known literature values.^{3d}

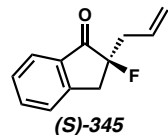


2-Allyl-2-(4-(trifluoromethyl)benzyl)cyclopentanone ((S)-341): Prepared by using general procedure B from β -ketoester **375** (0.19 mmol), reaction time = 96 h. Purified by column chromatography (SiO_2 , 7% Et_2O in pentane) to furnish cyclopentanone **(S)-341** (30 mg, 54% yield (83% yield based on recovered starting material **375**) as a clear colorless oil; $R_f = 0.59$ (6:3 Pentane: Et_2O); $[\alpha]_D^{25} +10.22$ (c 0.540, CHCl_3 , 88% ee); characterization data match known literature values.^{3d}

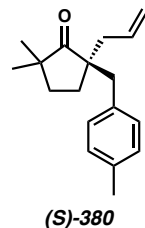


2-Allyl-2-methyl-2,3-dihydro-1H-inden-1-one ((S)-344): Prepared by using general procedure B from β -ketoester **376** (0.19 mmol), reaction time = 4.5 h. Purified by column

chromatography (SiO_2 , 10% Et_2O in pentane) to afford cyclopentanone **(S)-344** (33 mg, 93% yield) as a clear colorless oil; $R_f = 0.36$ (9:1 hexanes: EtOAc); $[\alpha]_D^{25} -59.24$ (c 0.595, CHCl_3 , 84% ee); characterization data match known literature values.^{3d}



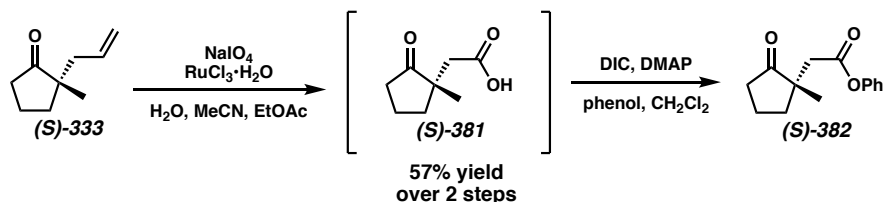
2-Allyl-2-Fluoro-2,3-dihydro-1H-inden-1-one ((S)-345): Prepared by using general procedure B above from β -ketoester **377** (0.19 mmol), reaction time = 13 h. Purified by column chromatography (SiO_2 , 5% Et_2O in pentane) to provide cyclopentanone **(S)-345** (36 mg, >99% yield) as a clear colorless oil; $R_f = 0.19$ (19:1 Pentane: Et_2O); $[\alpha]_D^{25} -75.79$ (c 0.585, CHCl_3 , 87% ee); characterization data match known literature values.^{7g}



(S)-2-allyl-5,5-dimethyl-2-(4-methylbenzyl)cyclopentan-1-one ((S)-380): Prepared by using general procedure B from β -ketoester **379** (0.19 mmol), reaction time = 48 h. Purified by column chromatography (SiO_2 , 3% Et_2O in hexanes) to afford cyclopentanone **(S)-380** (32 mg, 66% yield) as a clear colorless oil $R_f = 0.24$ (19:1 hexanes: Et_2O); ^1H NMR (400 MHz, CDCl_3) δ 7.07–7.03 (m, 2H), 6.97 (d, $J = 8.0$ Hz, 2H), 5.73 (dd, $J = 17.0, 10.1$, 7.8, 7.0 Hz, 1H), 5.14–5.01 (m, 2H), 2.87 (d, $J = 13.3$ Hz, 1H), 2.55 (d, $J = 13.3$ Hz, 1H), 2.30 (s, 3H), 2.26 (ddt, $J = 13.7, 7.0, 1.3$ Hz, 1H), 2.17 – 2.10 (m, 1H), 1.89–1.72 (m, 2H), 1.63 (dt, $J = 12.8, 7.2$ Hz, 1H), 1.39 (ddd, $J = 12.8, 7.3, 6.3$ Hz, 1H), 0.98 (s, 3H), 0.67 (s,

3H); ^{13}C NMR (101 MHz, CDCl_3) δ 136.1 (C), 134.8 (C), 134.1 (CH), 130.6 (CH), 128.9 (CH), 118.7 (CH₂), 54.5 (C), 45.6 (C), 41.7 (CH₂), 41.6 (CH₂), 35.0 (CH₂), 27.4 (CH₂), 24.7 (CH₃), 23.9 (CH₃), 21.2 (CH₃); IR (thin film, NaCl) 2958, 2867, 1731, 1513, 1459, 1379, 1061, 997, 916, 812, 752 cm^{-1} ; HRMS (ESI) m/z calc'd for $\text{C}_{18}\text{H}_{25}\text{O}$ [M+H]⁺: 257.1900, found 275.1901; $[\alpha]_D^{25} +13.67$ (*c* 0.58, CHCl_3 , 73% ee).

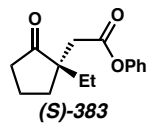
General Procedure C: Phenyl Ester Derivative Synthesis



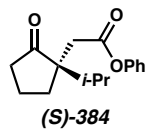
Ketone **(S)-333** (34 mg, 0.25 mmol, 1.00 equiv) was diluted in H_2O (2.34 mL, 0.11 M), acetonitrile (1.50 mL, 0.160 M), and EtOAc (1.50 mL, 0.16 M). Sodium periodate (NaIO_4 , 342 mg, 1.60 mmol, 6.40 equiv) and ruthenium(III) trichloride (RuCl_3 , 4.7 μL , 0.1 M solution in H_2O , 0.019 equiv) were added in single portions. The reaction was allowed to stir at ambient temperature (ca. 23 °C) for 4 h, at which time consumption of starting material was complete (as determined by TLC analysis, 19:1 Pentane:Et₂O). Crude reaction mixture was filtered through a celite plug and extracted with a saturated solution of NaHCO_3 . The aqueous solution was acidified to pH 1 with 1 M HCl. Acidified aqueous solution was extracted with dichloromethane, dried over Na_2SO_4 , filtered, and concentrated in vacuo. Crude solution was carried on with no further purification.

A flask charged with carboxylic acid **(S)-381** (0.25 mmol, 1.00 equiv), phenol (14 mg, 0.27 mmol, 1.10 equiv), and 4-(dimethylamino)-pyridine (DMAP, 14 mg, 0.11 mol, 0.45 equiv) was evacuated and re-filled with argon (3 x 5 minutes). Dichloromethane (946 μL , 0.26

M) was added and the solution was cooled to 0 °C (ice/H₂O bath). Diisopropylcarbodiimide (DIC, 42.0 μL, 0.27 mmol, 1.10 equiv) was added dropwise and allowed to stir for 5 minutes. The cooling bath was then removed and the solution was allowed to warm to ambient temperature (ca. 23 °C). After 11 h, the consumption of starting material was complete (as determined by TLC analysis, 9:1 hexanes:EtOAc) and the reaction was filtered through filter paper and then diluted with dichloromethane (200 mL). The solution was washed with 0.1 M aqueous HCl (200 mL), 1 M aqueous NaOH, saturated aqueous NaHCO₃ (100 mL), and brine (100 mL). The combined organics were dried over MgSO₄, filtered, and concentrated in vacuo. The crude residue was purified by column chromatography (SiO₂, 10% hexanes in EtOAc) to provide ester (**S**)-382 (33 mg, 57% yield over 2 steps) as a clear colorless oil; R_f = 0.24 (9:1 hexanes:EtOAc); ¹H NMR (400 MHz, CDCl₃) δ 7.42–7.31 (m, 2H), 7.22 (ddt, J = 7.9, 6.9, 1.2 Hz, 1H), 7.09–6.99 (m, 2H), 2.92 (d, J = 16.6 Hz, 1H), 2.72 (d, J = 16.6 Hz, 1H), 2.45–2.30 (m, 2H), 2.27–2.13 (m, 1H), 2.09–1.94 (m, 1H), 1.97–1.81 (m, 2H), 1.13 (s, 3H); ¹³C NMR (101 MHz, CDCl₃) δ 221.7 (C), 170.2 (C), 150.5 (C), 129.6 (CH), 126.1 (CH), 121.6 (CH), 46.5 (C), 41.6 (CH₂), 37.3 (CH₂), 35.1 (CH₂), 22.8 (CH₃), 18.9 (CH₂); IR (thin film, NaCl) 3459, 3066, 2964, 2873, 1756, 1738, 1592, 1493, 1456, 1404, 1375, 1350, 1317, 1266, 1242, 1193, 1162, 1127, 1070, 1023, 1006, 969, 925, 896, 817, 800, 772, 749, 772, 722, 698, 687 cm⁻¹; HRMS (FAB+) m/z calc'd for C₁₄H₁₇O₃ [M+H]⁺: 233.1178, found 233.1176; [α]_D²⁵ -45.05 (c 0.280, CHCl₃, 86% ee).



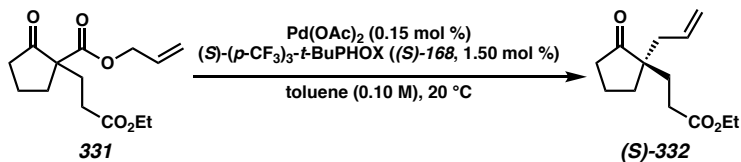
(1-Ethyl-2-oxo-cyclopentyl)-acetic acid phenyl ester ((S)-383): Prepared by using general procedure C from cyclopentanone (**S**-334) (0.25 mmol). Purified by column chromatography (SiO₂, 10% EtOAc in hexanes) to furnish ester (**S**-383) (46 mg, 75% yield over 2 steps) as an amorphous solid; R_f = 0.28 (9:1 hexanes:EtOAc); ¹H NMR (400 MHz, CDCl₃) δ 7.39–7.33 (m, 2H), 7.21 (tt, J = 7.1, 1.1 Hz, 1H), 7.07–7.02 (m, 2H), 2.90 (d, J = 16.7 Hz, 1H), 2.73 (d, J = 16.7 Hz, 1H), 2.48–2.27 (m, 2H), 2.14 (ddd, J = 13.1, 10.3, 7.8 Hz, 1H), 2.06–1.94 (m, 2H), 1.95–1.80 (m, 1H), 1.53 (p, J = 7.4 Hz, 2H), 0.93 (t, J = 7.5 Hz, 3H); ¹³C NMR (101 MHz, CDCl₃) δ 221.8 (C), 170.5 (C), 150.5 (C), 129.6 (CH), 126.0 (CH), 121.6 (CH), 50.0 (C), 39.5 (CH₂), 37.6 (CH₂), 32.4 (CH₂), 28.6 (CH₂), 18.8 (CH₂), 8.6 (CH₃); IR (thin film, NaCl) 3455, 3066, 2965, 2881, 1733, 1592, 1492, 1456, 1404, 1383, 1349, 1262, 1238, 1190, 1161, 1125, 1024, 1006, 951, 926, 895, 810, 768, 721, 688 cm⁻¹; HRMS (APCI/ESI) m/z calc'd for C₁₅H₁₉O₃ [M+H]⁺: 247.1329, found 247.1327; $[\alpha]_D^{25}$ +2.45 (*c* 0.445, CHCl₃, 88% ee).



(1-(1-Methylethyl)-2-oxo-cyclopentyl)-acetic acid phenyl ester ((S)-384): Prepared by using general procedure C from cyclopentanone (**S**-335) (0.20 mmol). Purified by column chromatography (SiO₂, 10% EtOAc in hexanes) to afford ester (**S**-384) (27 mg, 52% yield over 2 steps) as an amorphous white solid; R_f = 0.36 (9:1 hexanes:EtOAc); ¹H NMR (400 MHz, CDCl₃) δ 7.40 – 7.33 (m, 2H), 7.21 (dd, J = 7.0, 1.1 Hz, 1H), 7.08–7.01 (m, 2H),

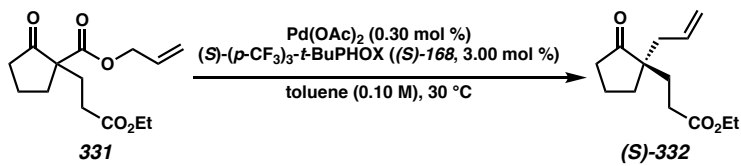
2.94 (d, $J = 16.6$ Hz, 1H), 2.73 (d, $J = 16.6$ Hz, 1H), 2.56–2.42 (m, 1H), 2.33–2.20 (m, 1H), 2.20–1.80 (m, 5H), 0.95 (d, $J = 6.9$ Hz, 3H), 0.90 (d, $J = 6.8$ Hz, 3H); ^{13}C NMR (101 MHz, CDCl_3) δ 223.1 (C), 170.8 (C), 150.5 (C), 129.6 (CH), 126.0 (CH), 121.6 (CH), 52.9 (C), 39.8 (CH₂), 38.5 (CH₂), 33.4 (CH), 29.7 (CH₂), 18.9 (CH₂), 18.4 (CH₃), 17.6 (CH₃); IR (thin film, NaCl) 2963, 1757, 1734, 1592, 1492, 1404, 1389, 1372, 1350, 1271, 1237, 1193, 1162, 1127, 1069, 1023, 932, 898, 818, 764, 719, 687 cm⁻¹; HRMS (FAB+) m/z calc'd for $\text{C}_{16}\text{H}_{21}\text{O}_3$ [M+H]⁺: 261.1491, found 261.1495; $[\alpha]_D^{25} -45.05$ (c 0.280, CHCl_3 , 88% ee).

Low-Catalyst Loading, Pd(II)-Catalyzed Enantioselective Allylic Alkylation



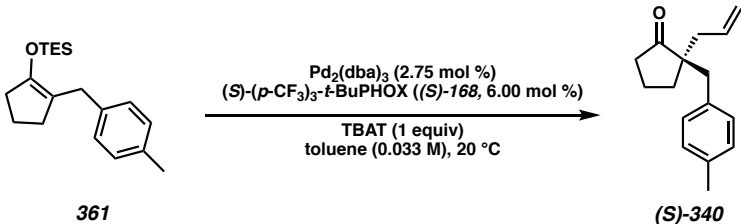
In a nitrogen-filled glovebox, stock solutions of $\text{Pd}(\text{OAc})_2$ (1.00 mg/mL), (S)-(CF₃)₃-t-BuPHOX ((S)-168, 10.0 mg/mL), and β -ketoester **331** (100. mg/mL) in toluene were prepared. $\text{Pd}(\text{OAc})_2$ (64.0 μL , 0.064 mg, 0.285 μmol , 0.0015 equiv) and (S)-(CF₃)₃-t-BuPHOX (0.17 mL, 1.69 mg, 2.85 μmol , 0.015 equiv) were added to a 20 mL scintillation vial and placed in a pre-chilled 20 °C stirrer. After 40 minutes, the solution was diluted with toluene (1.16 mL, 20 °C) followed by β -ketoester **331** (0.51 mL, 51.0 mg, 0.19 mmol, 1.00 equiv) in one portion (total volume 1.9 mL, 0.10 M). After 28 h, the consumption of starting material was complete (as determined by TLC analysis, 19:1 Pentane:Et₂O). The crude solution was directly purified by column chromatography (SiO₂, 100% pentane then 20% Et₂O in pentane) to furnish **(S)-332** (42 mg, 98% yield) as a clear colorless oil; $R_f = 0.30$ (8:2 Pentane:Et₂O); characterization data match those that are reported above.

Large Scale Low-Catalyst Loading, Pd(II)-Catalyzed Enantioselective Allylic Alkylation



In a nitrogen filled glovebox, $\text{Pd}(\text{OAc})_2$ (2.49 mg, 11.1 μmol , 0.003 equiv) and (S) -(CF_3)₃-*t*-Bu-PHOX **168** (65.7 mg, 0.111 μmol , 0.03 equiv) were added to a flask and diluted with toluene (37.3 mL, 0.10M). The solution stirred in the ambient glovebox atmosphere (ca. 30 °C) for 40 minutes. β -ketoester **331** (1.00 g, 3.73 mmol, 1.00 equiv) was then added in one portion. After 15 h, the consumption of starting material was complete (as determined by TLC analysis, 19:1 Pentane:Et₂O). The crude solution was directly purified by column chromatography (SiO_2 , 100% pentane then 20% Et₂O in pentane) to furnish **(S)-332** (682 mg, 82% yield, 89% ee) as a clear colorless oil; $R_f = 0.30$ (8:2 Pentane:Et₂O); characterization data match those that are reported above.

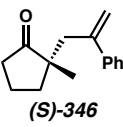
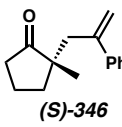
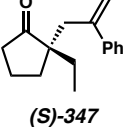
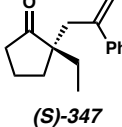
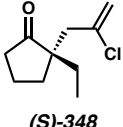
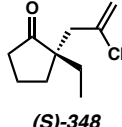
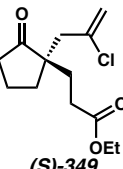
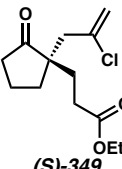
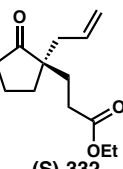
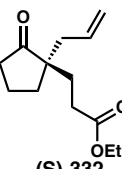
Fluoride Triggered, Pd(0)-Catalyzed Enantioselective Allylic Alkylation

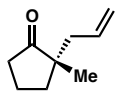
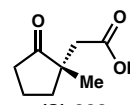
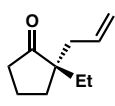
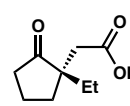
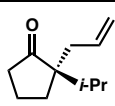
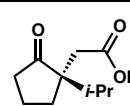
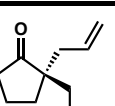
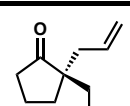
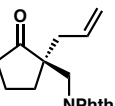
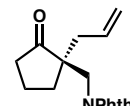
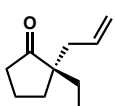
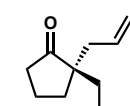


In a nitrogen-filled glovebox, separate stock solutions of $\text{Pd}_2(\text{dba})_3$ (2.50 mg/mL), (S) -(CF_3)₃-*t*-Bu-PHOX (**(S)-168**, 10.0 mg/mL), and silyl enol ether **361** (100. mg/mL) in toluene were prepared. $\text{Pd}_2(\text{dba})_3$ (1.92 mL, 4.8 mg, 5.20 μmol , 0.0275 equiv), (S) -(CF_3)₃-*t*-Bu-PHOX (**(S)-168**, 0.67 mL, 6.7 mg, 11.4 μmol , 0.06 equiv), and TBAT (103 mg, 0.19

mmol, 1.00 equiv) were added to a 20 mL scintillation vial and placed in a pre-chilled 20 °C well with stirring. After 20 minutes, the solution was diluted with toluene (2.69 mL, 20 °C) followed by the addition of diallyl carbonate (28.7 µL, 0.20 mmol, 1.05 equiv) and silyl enol ether **361** (0.574 mL, 57.4 mg, 0.19 mmol, 1.00 equiv) in one portion (total volume 5.8 mL, 0.033 M). After 48 h, the consumption of starting material appeared stalled (as determined by TLC analysis, 19:1 Pentane:Et₂O). The crude solution was directly purified by column chromatography (SiO₂, 100% hexanes then 5% Et₂O in hexanes) to furnish cyclopentanone (*S*)-**340** (17 mg, 40% yield, 75% ee) as a clear colorless oil; characterization data match those that are reported above.

2.6.3 METHODS FOR THE DETERMINATION OF ENANTIOMERIC EXCESS

entry	product	compound assayed	assay conditions	retention time of major isomer (min)	retention time of minor isomer (min)	% ee
1			SFC Chiracel OJ-H 2% IPA isocratic 2.5 mL/min	7.11	8.59	90
2			SFC Chiracel OJ-H 1% IPA isocratic 2.5 mL/min	8.03	10.18	94
3			SFC 2 Chiraldak AD-H 3% IPA isocratic 2.5 mL/min	5.40	5.14	90
4			SFC Chiraldak AD-H 3% IPA isocratic 2.5 mL/min	5.05	6.35	88
5			SFC Chiraldak AD-H 3% IPA isocratic 2.5 mL/min	3.57	4.58	91

entry	product	compound assayed	assay conditions	retention time of major isomer (min)	retention time of minor isomer (min)	% ee
6			SFC Chiracel OB-H 5% IPA isocratic 2.5 mL/min	11.37	7.36	86
7			SFC Chiracel OB-H 3% IPA isocratic 2.5 mL/min	12.19	11.18	88
8			SFC Chiracel OB-H 5% IPA isocratic 2.5 mL/min	7.35	6.65	88
9			SFC Chiracel OD-H 10% IPA isocratic 2.5 mL/min	2.87	2.48	90
10			HPLC Chiracel OD-H 4% IPA in hexanes isocratic; 1 mL/min	20.82	27.11	92
11			SFC Chiracel OJ-H 1% IPA isocratic 2.5 mL/min	9.87	9.20	92

entry	product	compound assayed	assay conditions	retention time of major isomer (min)	retention time of minor isomer (min)	% ee
12			HPLC Chiracel OJ 0.1% EtOH in hexanes isocratic; 1 mL/min	14.61	13.26	88
13			HPLC Chiracel OJ 0.1% EtOH in hexanes isocratic; 1 mL/min	12.90	11.43	89
14			SFC Chiraldpak AD-H 1% IPA isocratic 2.5 mL/min	5.61	6.03	88
15			SFC Chiraldpak AD-H 2% IPA isocratic 2.5 mL/min	7.17	6.30	84
16			SFC Chiracel OB-H 2% IPA isocratic 2.5 mL/min	7.18	4.46	87
17			SFC Chiraldpak IC 3% IPA isocratic 2.5 mL/min	9.50	6.12	73

2.6.4 NOTES & REFERENCES

1. (a) Liu, Y.; Han, S. J.; Lui, W. B.; Stoltz, B. M. *Acc. Chem. Res.* **2015**, *48*, 740–751. (b) Minko, Y.; Pasco, M.; Lercher, L.; Botoshansky, M.; Marek, I. *Nature* **2012**, *490*, 522–526. (c) Das, J. P.; Marek, I. *Chem. Commun.* **2011**, *47*, 4593–4623.

-
- (d) Weaver, J. D.; Recio, A.; Grenning, A. J.; Tunge, J. A. *Chem. Rev.* **2011**, *111*, 1846–1913. (e) Douglas, C. J.; Overman, L. E. *Proc. Natl. Acad. Sci. U.S.A.* **2004**, *101*, 5363–5367. (f) Martin, S. F. *Tetrahedron* **1980**, *36*, 419–460.
2. Behenna, D. C.; Stoltz, B. M. *J. Am. Chem. Soc.* **2004**, *126*, 15044–15045.
3. (a) Korch, K. M.; Eidamshaus, C.; Behenna, D. C.; Nam, S.; Horne, D.; Stoltz, B. M. *Angew. Chem. Int. Ed.* **2015**, *54*, 179–183. (b) Numajiri, Y.; Pritchett, B. P.; Chiyoda, K.; Stoltz, B. M. *J. Am. Chem. Soc.* **2015**, *137*, 1040–1043. (c) Reeves, C. M.; Behenna, D. C.; Stoltz, B. M. *Org. Lett.* **2014**, *16*, 2314–2317. (d) Behenna, D. C.; Mohr, J. T.; Sherden, N. H.; Marunescu, S. C.; Harned, A. M.; Tani, K.; Seto, M.; Ma, S.; Novak, Z.; Krout, M. R.; McFadden, R. M.; Roizen, J. L.; Enquist Jr., J. A.; White, D. E.; Levine, S. R.; Petrova, K. V.; Iwashita, A.; Virgil, S. C.; Stoltz, B. M. *Chem. – Eur. J.* **2011**, *17*, 14199–14223.
4. (a) Craig, II, R. A.; Stoltz, B. M. *Tetrahedron Lett.* **2015**, *56*, 4670–4673. (b) McDougal, N. T.; Streuff, J.; Mukherjee, H.; Virgil, S. C.; Stoltz, B. M. *Tetrahedron Lett.* **2010**, *51*, 5550–5554. (c) Krout, M. R.; Mohr, J. T.; Stoltz, B. M. *Org. Synth.* **2009**, *86*, 181–205. (d) Sprinz, J.; Helmchen, G. *Tetrahedron Lett.* **1993**, *34*, 1769–1772. (e) Dawson, G. J.; Frost, C. G.; Williams, J. M. J.; Coote, S. J. *Tetrahedron Lett.* **1993**, *34*, 3149–3150. (f) Von Matt, P.; Pfaltz, A. *Angew. Chem., Int. Ed. Engl.* **1993**, *32*, 566–568.
5. (a) Trost, B. M.; Xu, J.; Schmidt, T. *J. Am. Chem. Soc.* **2009**, *131*, 18343–18357. (b) Burger, E.; Barron, B.; Tunge, J. *Synlett* **2006**, *17*, 2824–2826. (c) Mohr, J. T.;

-
- Behenna, D. C.; Harned, A. M.; Stoltz, B. M. *Angew. Chem. Int. Ed.* **2005**, *44*, 6924–6927. (d) Trost, B. M.; Xu, J. *J. Am. Chem. Soc.* **2005**, *127*, 2846–2847.
6. Reeves, C. M.; Eidamshaus, C.; Kim, J.; Stoltz, B. M. *Angew. Chem. Int. Ed.* **2013**, *52*, 6718–6721.
7. (a) Trost, B. M. *Tetrahedron* **2015**, *71*, 5708–5733. (b) Nahra, F.; Macé, Y.; Boreux, A.; Billard, F.; Riant, O. *Chem. – Eur. J.* **2014**, *20*, 10970–10981. (c) Rambla, M.; Duroure, L.; Chabaud, L.; Guillou, C. *Eur. J. Org. Chem.* **2014**, 7716–7720. (d) Nahra, F.; Macé, Y.; Lambin, D.; Riant, O. *Angew. Chem. Int. Ed.* **2013**, *52*, 3208–3212. (e) Huang, J. Z.; Jie, X. K.; Wei, K.; Zhang, H.; Wang, M. C.; Yang, Y. R. *Synlett* **2013**, *24*, 1303–1306. (f) Nahra, F.; Macé, Y.; Lambin, D.; Riant, O. *Angew. Chem. Int. Ed.* **2013**, *52*, 3208–3212. (g) Nakamura, M.; Hajra, A.; Endo, K.; Nakamura, E. *Angew. Chem. Int. Ed.* **2005**, *44*, 7248–7251. (h) Trost, B. M.; Pissot-Soldermann, C.; Chen, I. *Chem. – Eur. J.* **2005**, *11*, 951–959. (i) Doyle, A. G.; Jacobsen, E. N. *J. Am. Chem. Soc.* **2005**, *127*, 62–63. (j) Sawamura, M.; Nagata, H.; Sakamoto, H.; Ito, Y. *J. Am. Chem. Soc.* **1992**, *114*, 2586–2592.
8. Asai, R.; Mitsuhashi, S.; Shigetomi, K.; Miyamoto, T.; Ubukata, M. *J. Antibiot.* **2011**, *64*, 693–696.
9. Wellington, K. D.; Cambie, R. C.; Rutledge, P. S.; Bergquist, P. R. *J. Nat. Prod.* **2000**, *63*, 79–85.
10. Abbas, H. K.; Mirocha, C. J. *Appl. Environ. Microbiol.* **1988**, *54*, 1268–1274.
11. Takayama, H.; Katakawa, K.; Kitajima, M.; Yamaguchi, K.; Aimi, N. *Tetrahedron Lett.* **2002**, *43*, 8307–8311.

-
12. Oh, H.; Swenson, D. C.; Gloer, J. B.; Wicklow, D. T.; Dowd, P. F. *Tetrahedron Lett.* **1998**, *39*, 7633–7636.
 13. Absolute stereochemistry of cyclopentanone (*S*)-333 was determined by comparison of optical rotation of the methyl ketone Wacker product to the known literature value, see: Thominiaux, C.; Roussé, S.; Desmaële, D.; d'Angelo, J.; Riche, C. *Tetrahedron: Asymmetry* **1999**, *10*, 2015–2021. The absolute stereochemistry of all other products generated herein was assigned by analogy to the absolute stereochemistry of (*S*)-333.
 14. Additionally, silyl enol ether derivatives of cyclopentanones were found to be suitable enolate precursors for the formation of α -quaternary cyclopentanones under similar reaction conditions with an external allyl electrophile.
 15. McDougal, N. T.; Virgil, S. C.; Stoltz, B. M. *Synlett* **2010**, *11*, 1712–1716.
 16. Additionally, α' , α' -disubstituted cyclopentanones were suitable substrates within the disclosed reaction manifold, albeit generally giving the α -quaternary cyclopentanone products in reduced yields and with slightly diminished ee. α,α -disubstituted cyclopentanones were not suitable substrates under the optimized conditions.
 17. Marziale, A. N.; Duquette, D. C.; Craig, II, R. A.; Kim, K. E.; Liniger, M.; Numajiri, Y.; Stoltz, B. M. *Adv. Synth. Catal.* **2015**, *357*, 2238–2245.
 18. Pangborn, A. M.; Giardello, M. A.; Grubbs, R. H.; Rosen, R. K.; Timmers, F. J. *Organometallics* **1996**, *15*, 1518–1520.
 19. Craig, II, R. A.; Stoltz, B. M. *Tetrahedron Lett.* **2015**, *56*, 4670–4673.

-
20. McDougal, N. T.; Virgil, S. C.; Stoltz, B. M. *Synlett* **2010**, 1712–1716.
 21. Doran, R.; Guiry, P. J. *J. Org. Chem.* **2014**, *79*, 9112–9124.
 22. Garzan, A.; Jaganathan, A.; Salehi Marzijarani, N.; Yousefi, R.; Whitehead, D. C.; Jackson, J. E.; Borhan, B. *Chem. – Eur. J.* **2013**, *19*, 9015–9021.
 23. Corbin, N. C.; Fraher, P.; McChesney, J. D. *J. Pharm. Sci.* **1979**, *68*, 1501–1504.
 24. Zou, Y.; Millar, J. G. *J. Org. Chem.* **2009**, *74*, 7207–7209.
 25. (a) Harris, R. K.; Becker, E. D.; Cabral de Menezes, S. M.; Granger, P.; Hoffman, R. E.; Zilm, K. W. *Pure Appl. Chem.* **2008**, *80*, 59–84. (b) Harris, R. K.; Becker, E. D.; Cabral de Menezes, S. M.; Goodfellow, R.; Granger, P. *Pure Appl. Chem.* **2001**, *73*, 1795–1818.
 26. Marinescu, S. C.; Nishimata, T.; Mohr, J. T.; Stoltz, B. M. *Org. Lett.* **2008**, *10*, 1039–1042.
 27. Keana, J. F.; Seyedrezai, S. E. *J. Org. Chem.* **1982**, *42*, 347–352.

APPENDIX 1

Spectra Relevant to Chapter 2:

Palladium-Catalyzed Enantioselective

Decarboxylative Allylic Alkylation of

Cyclopentanones

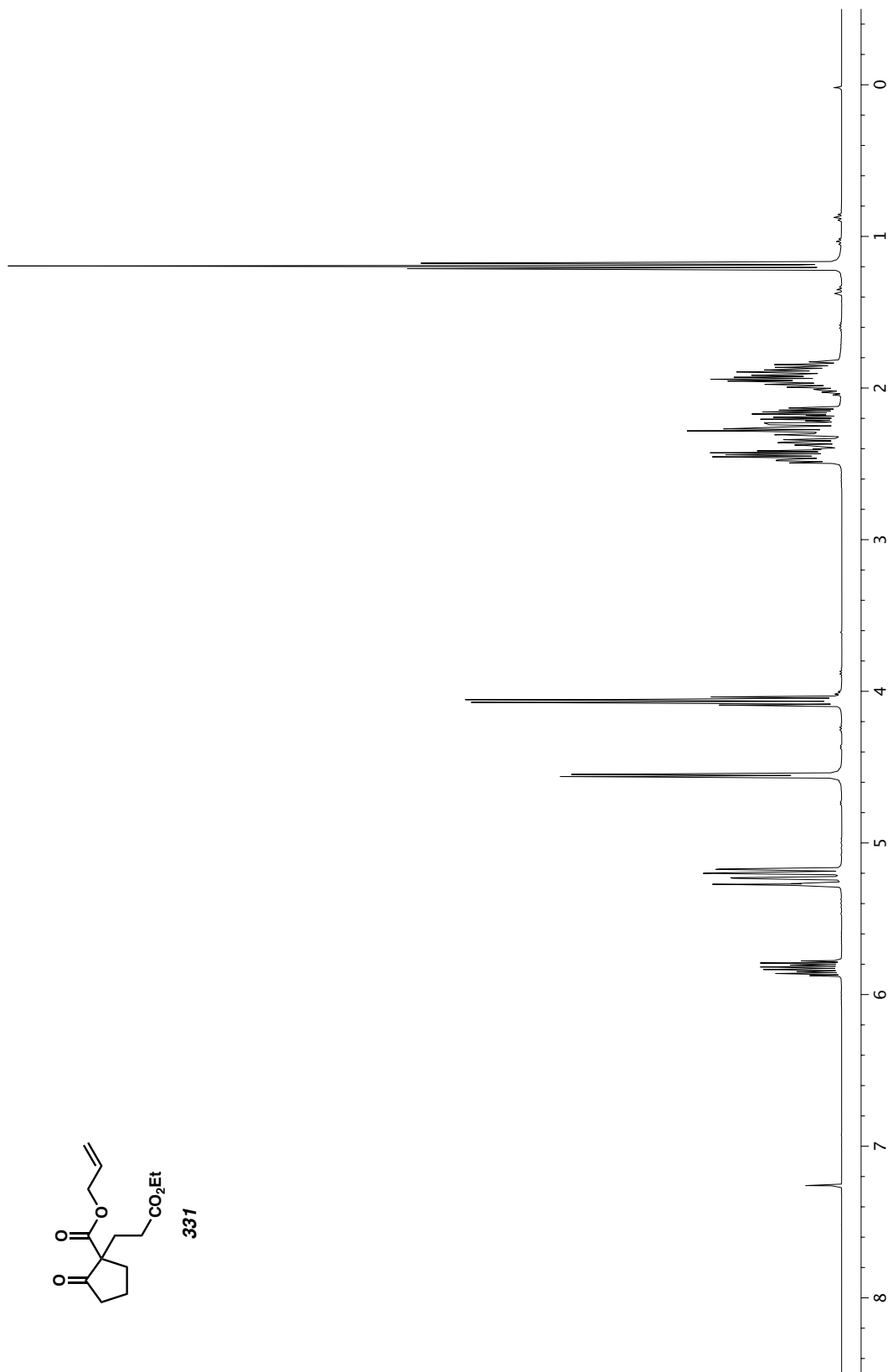
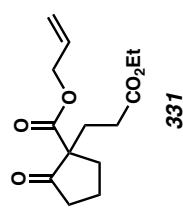


Figure A1.1. ^1H NMR (400 MHz, CDCl_3) of compound 331.

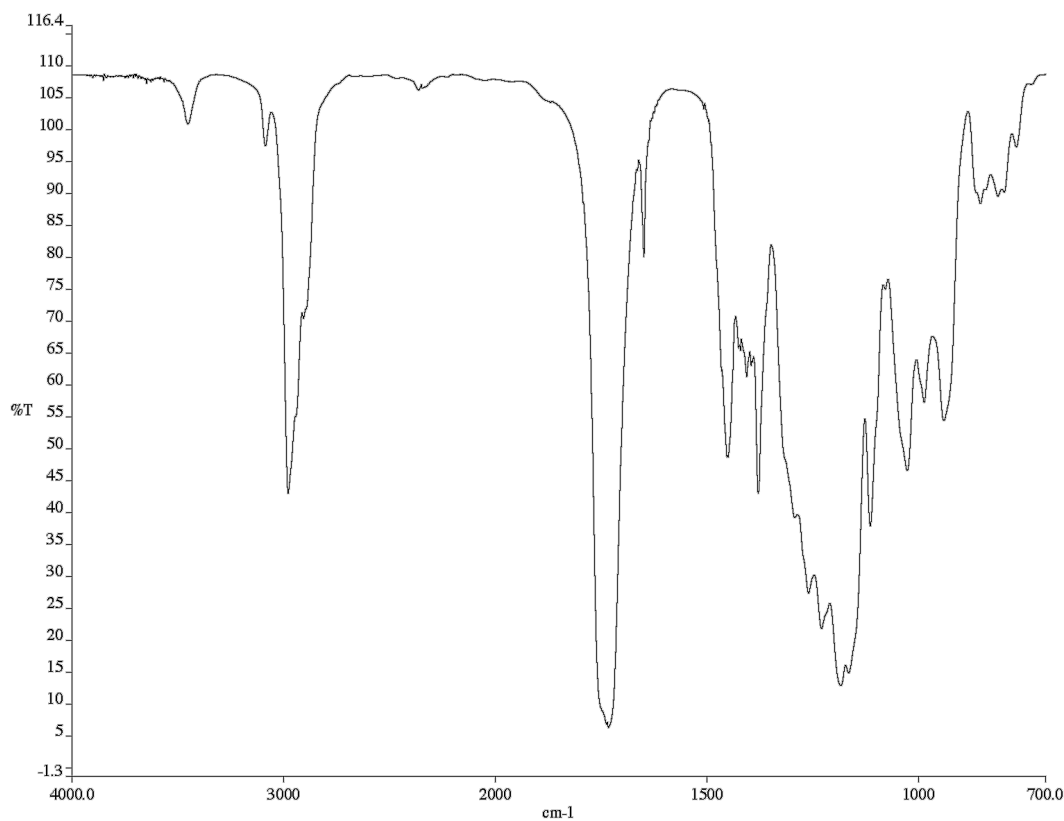


Figure A1.2. Infrared spectrum (Thin Film, NaCl) of compound 331.

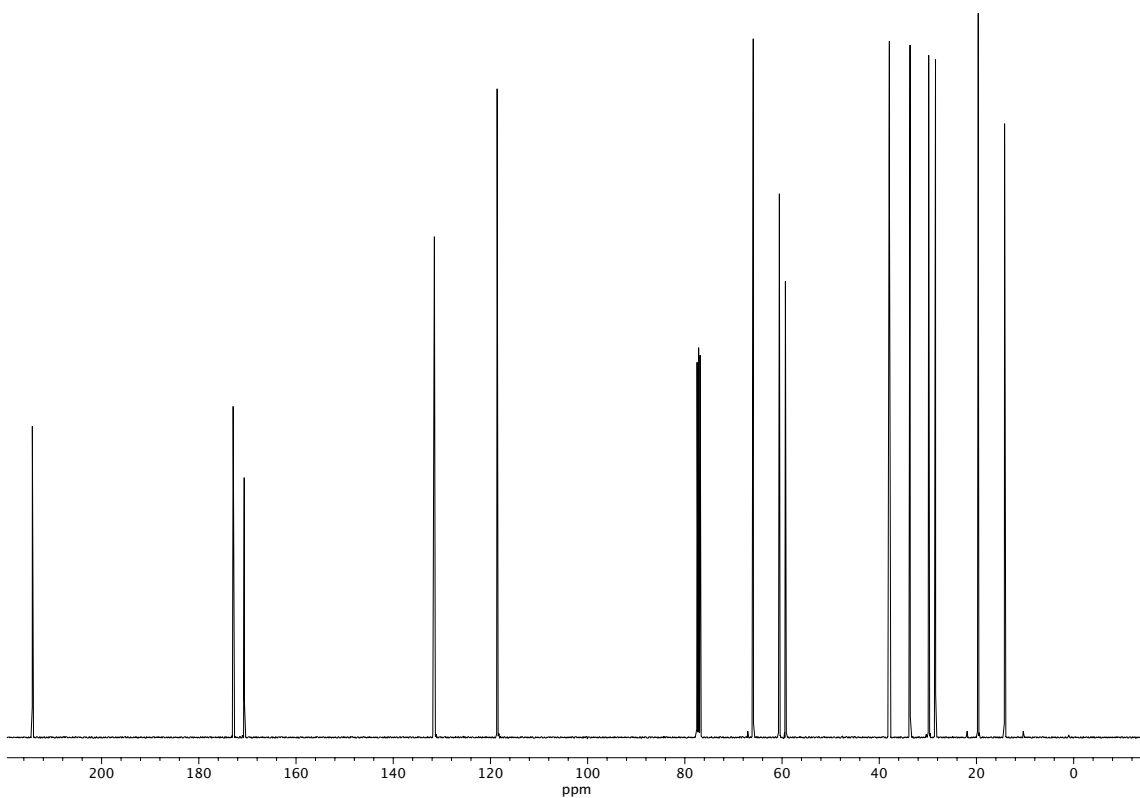
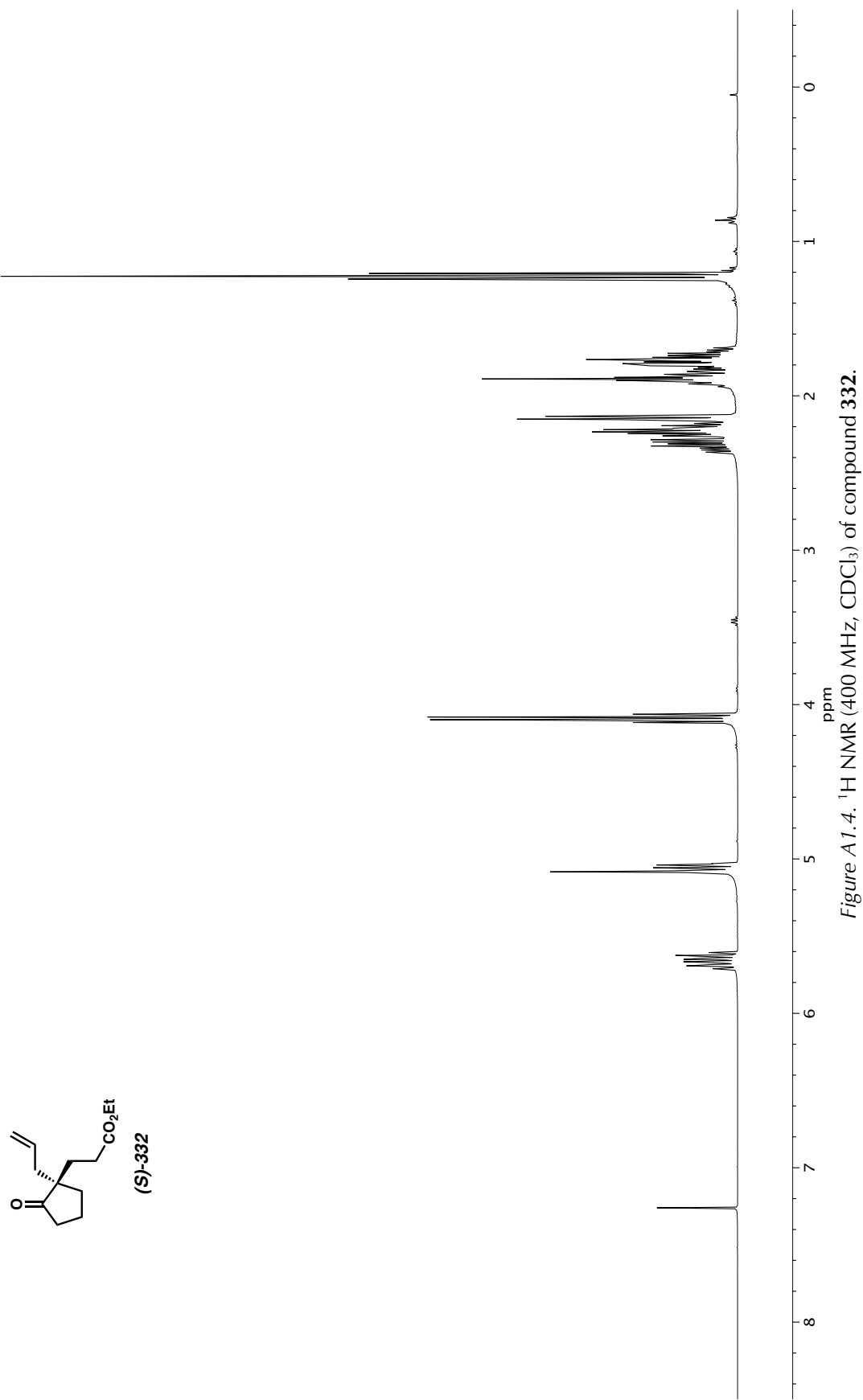


Figure A1.3. ^{13}C NMR (101 MHz, CDCl_3) of compound 331.



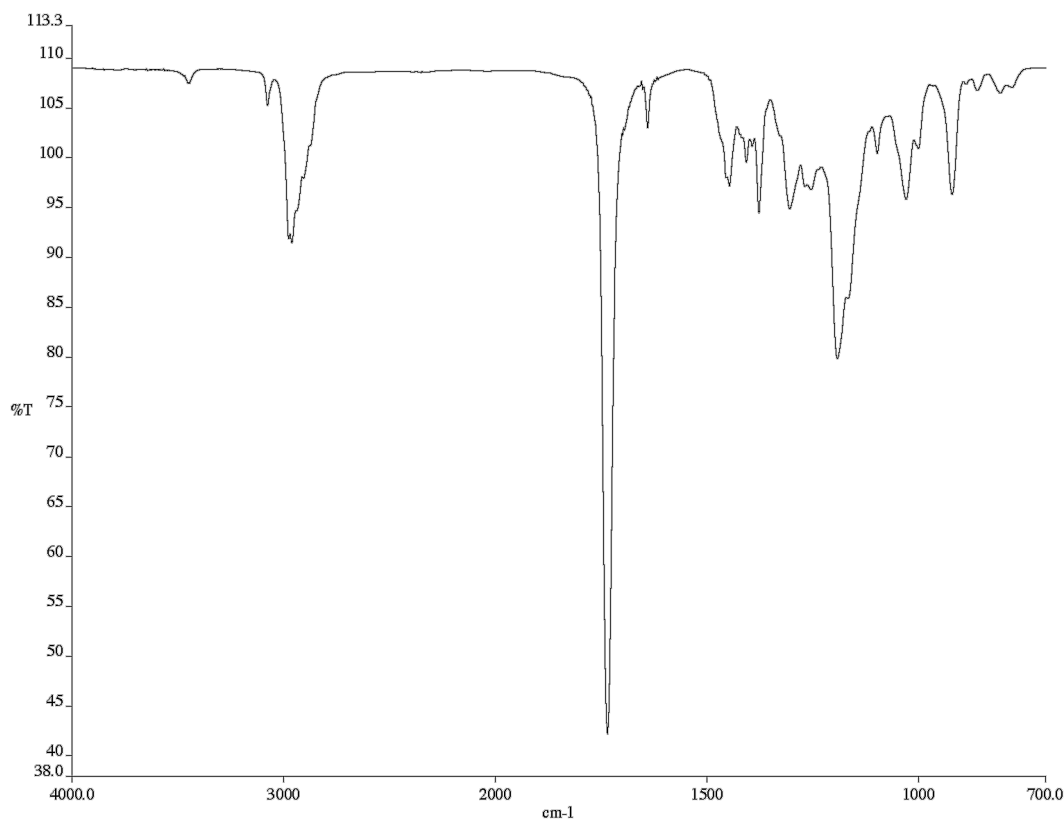


Figure A1.5. Infrared spectrum (Thin Film, NaCl) of compound 332.

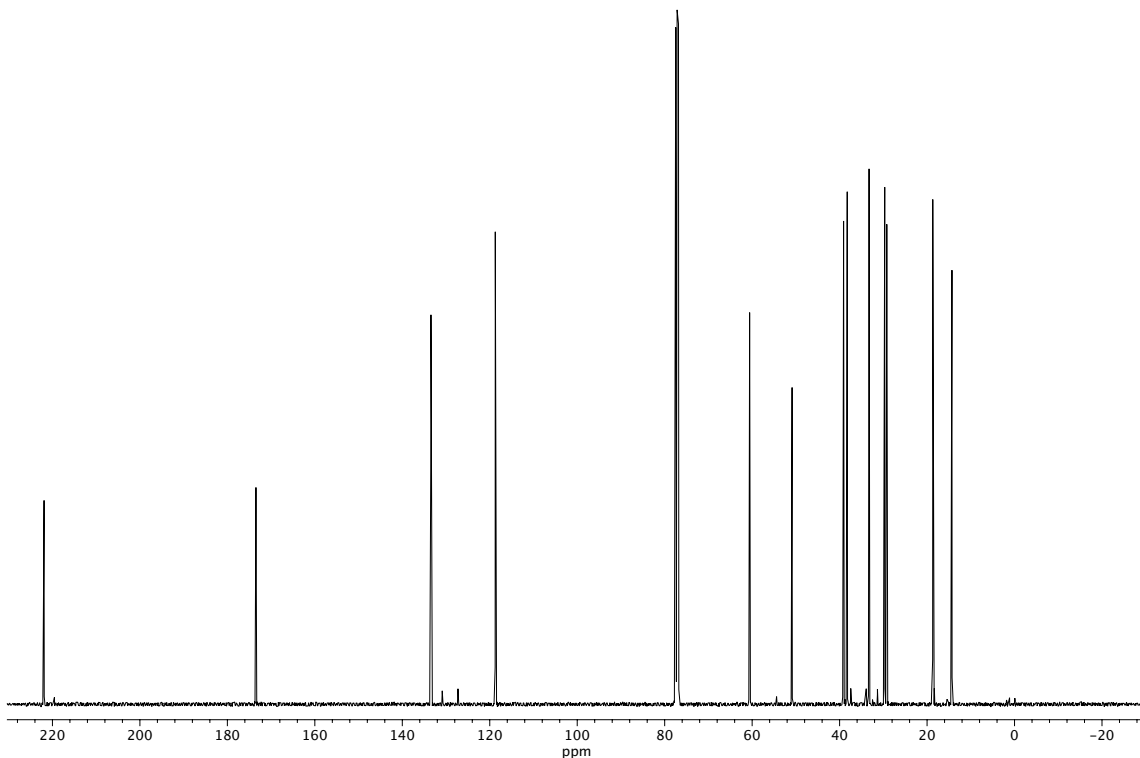


Figure A1.6. ^{13}C NMR (101 MHz, CDCl_3) of compound 332.

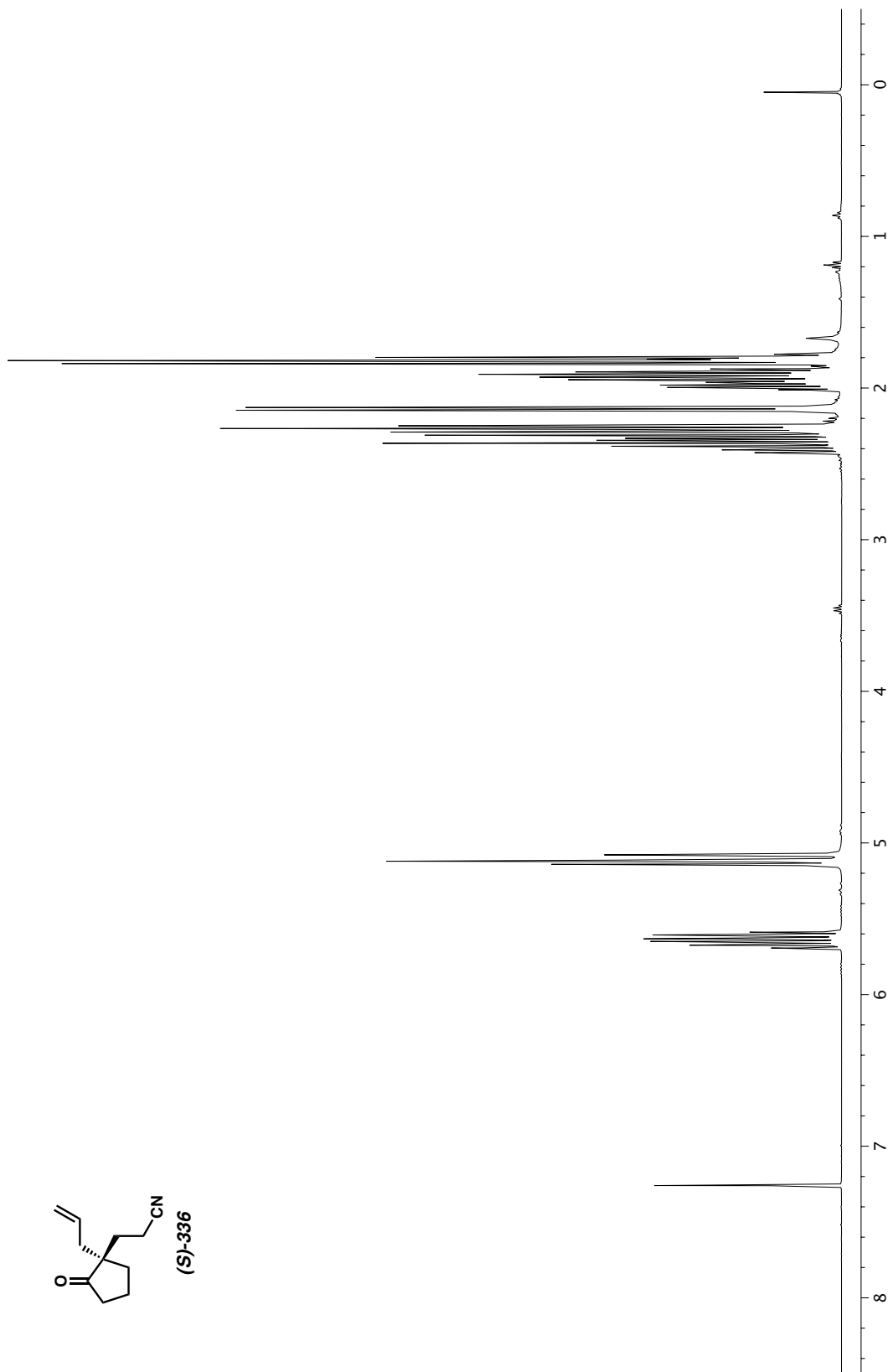
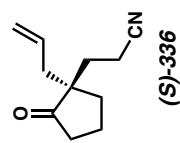


Figure A1.7. ^1H NMR (400 MHz, CDCl_3) of compound 336.

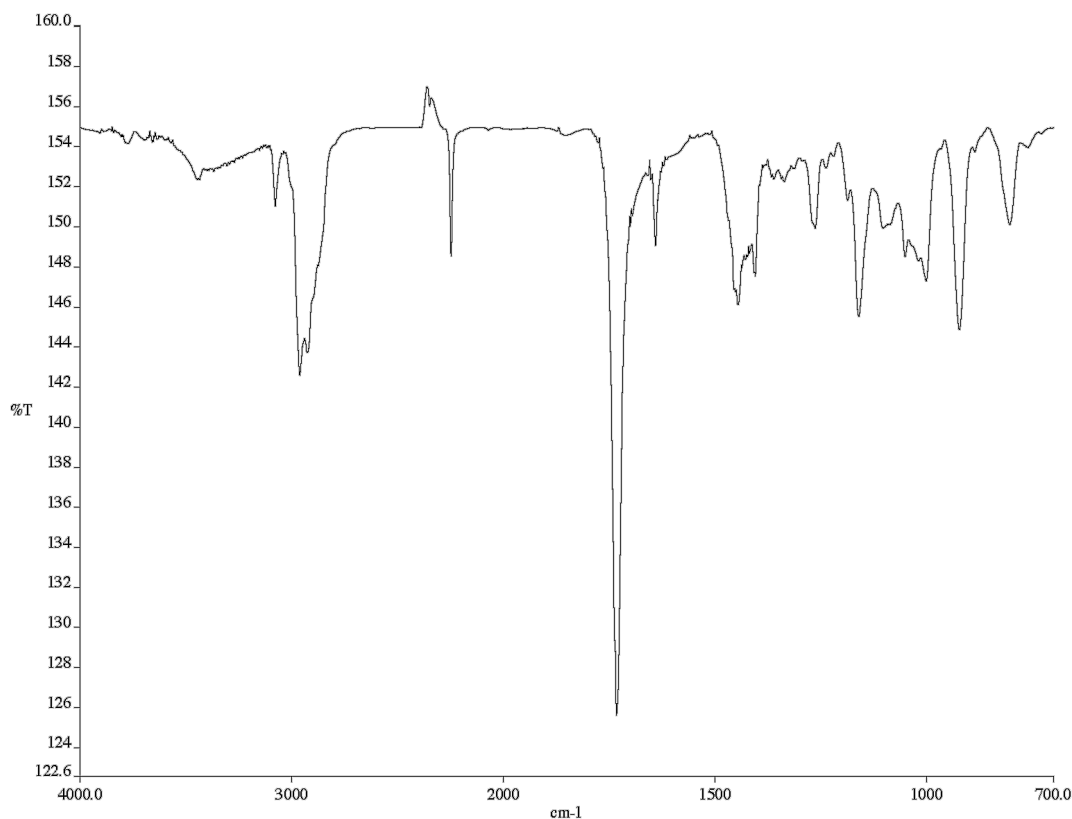


Figure A1.8. Infrared spectrum (Thin Film, NaCl) of compound 336.

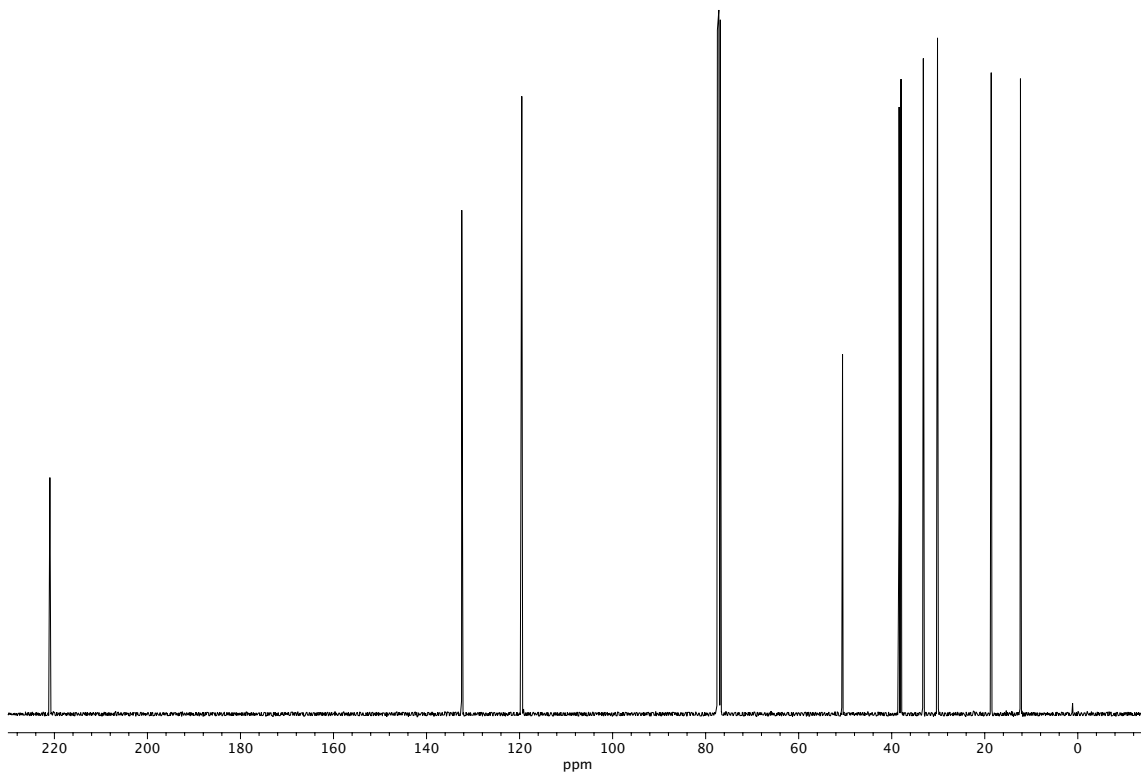
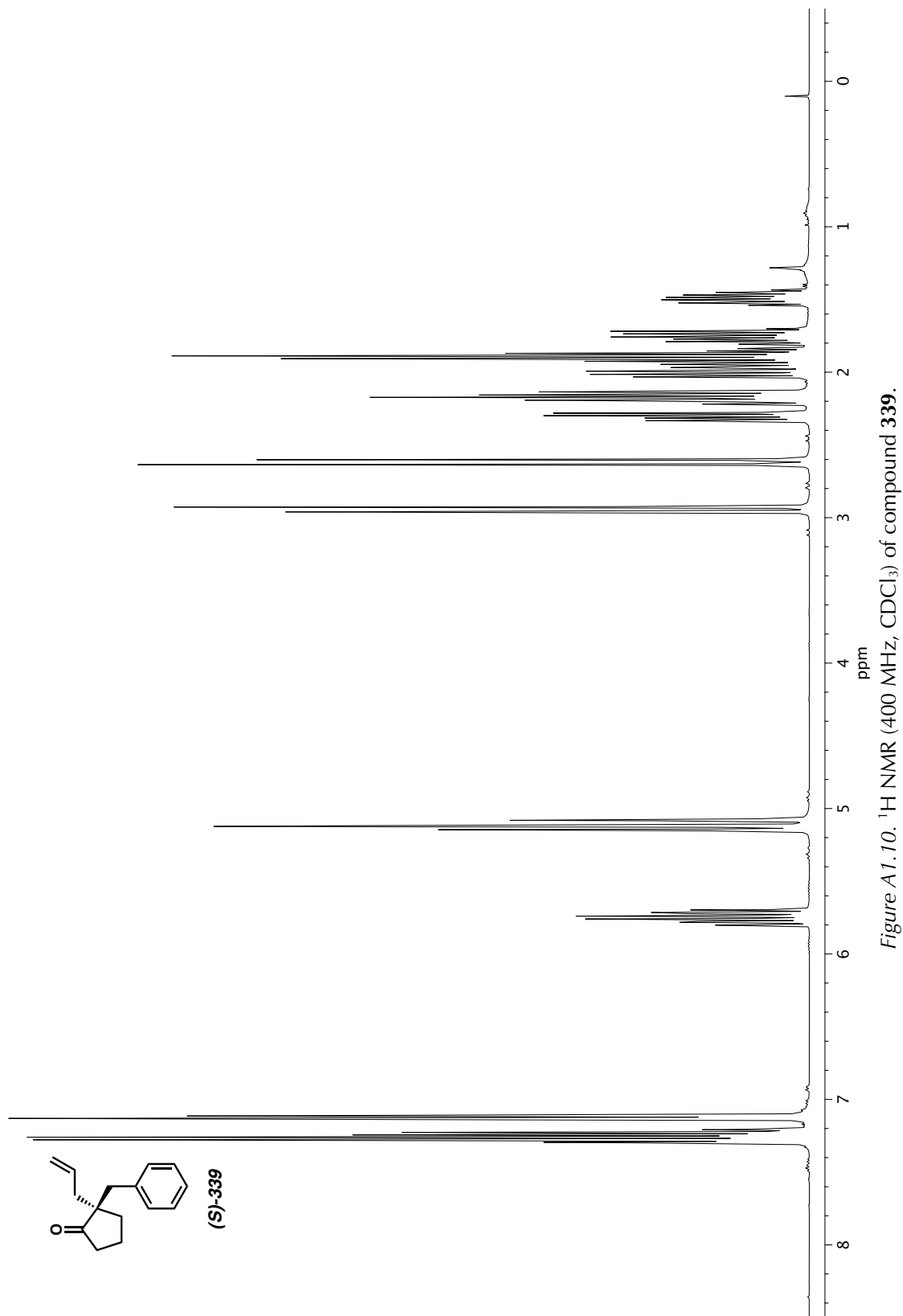


Figure A1.9. ^{13}C NMR (101 MHz, CDCl_3) of compound 336.



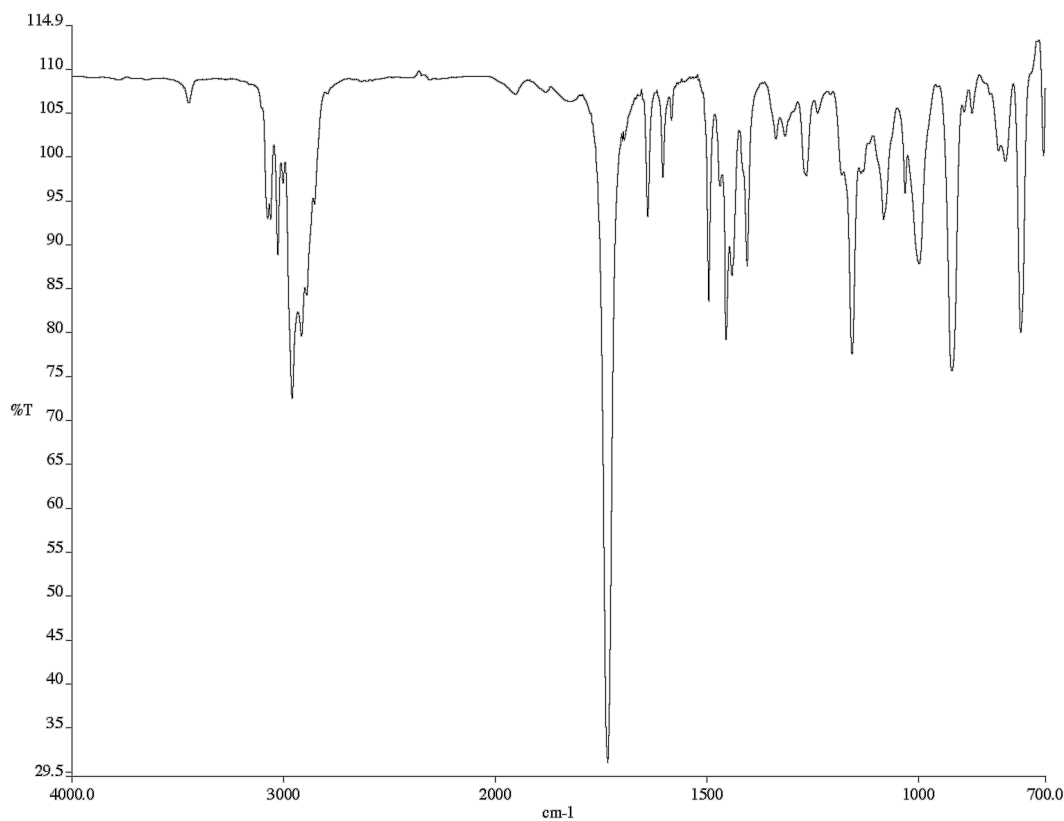


Figure A1. 11. Infrared spectrum (Thin Film, NaCl) of compound 339.

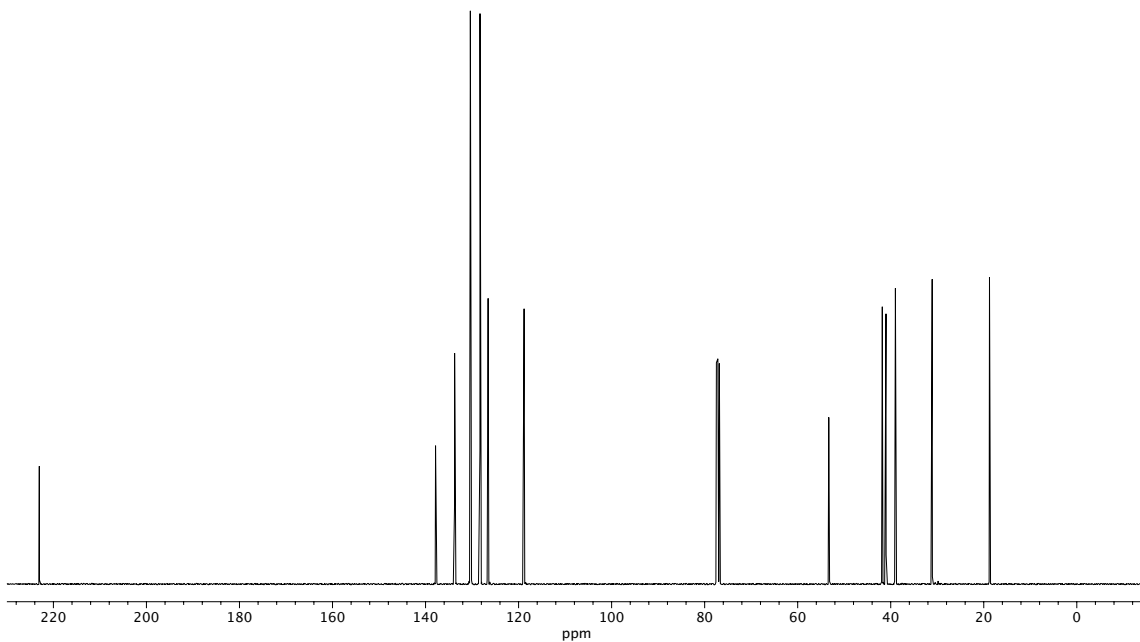


Figure A1. 12. ^{13}C NMR (101 MHz, CDCl_3) of compound 339.

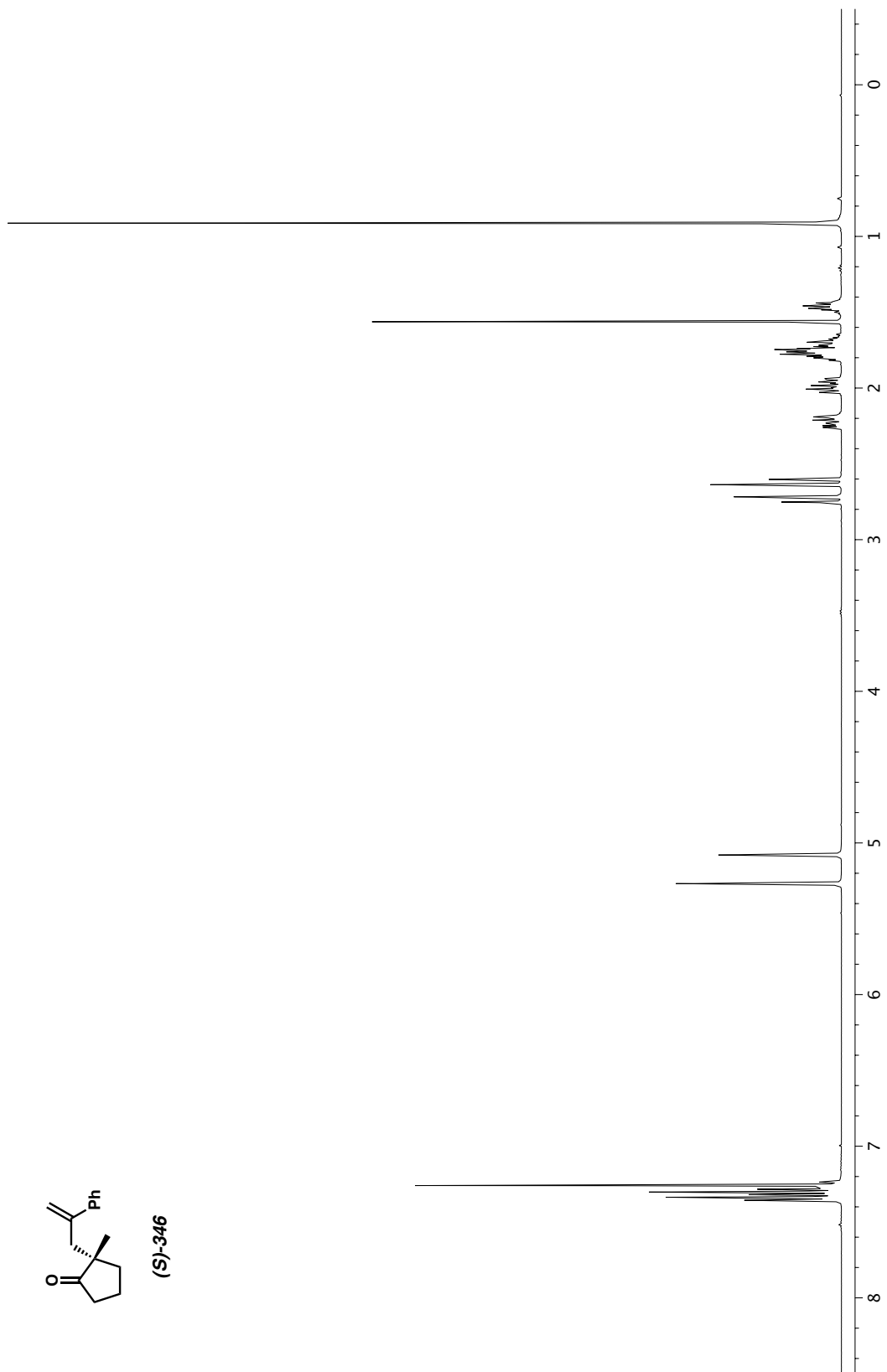
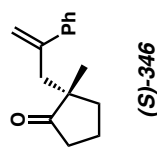


Figure A1.13. ^1H NMR (400 MHz, CDCl_3) of compound 346.

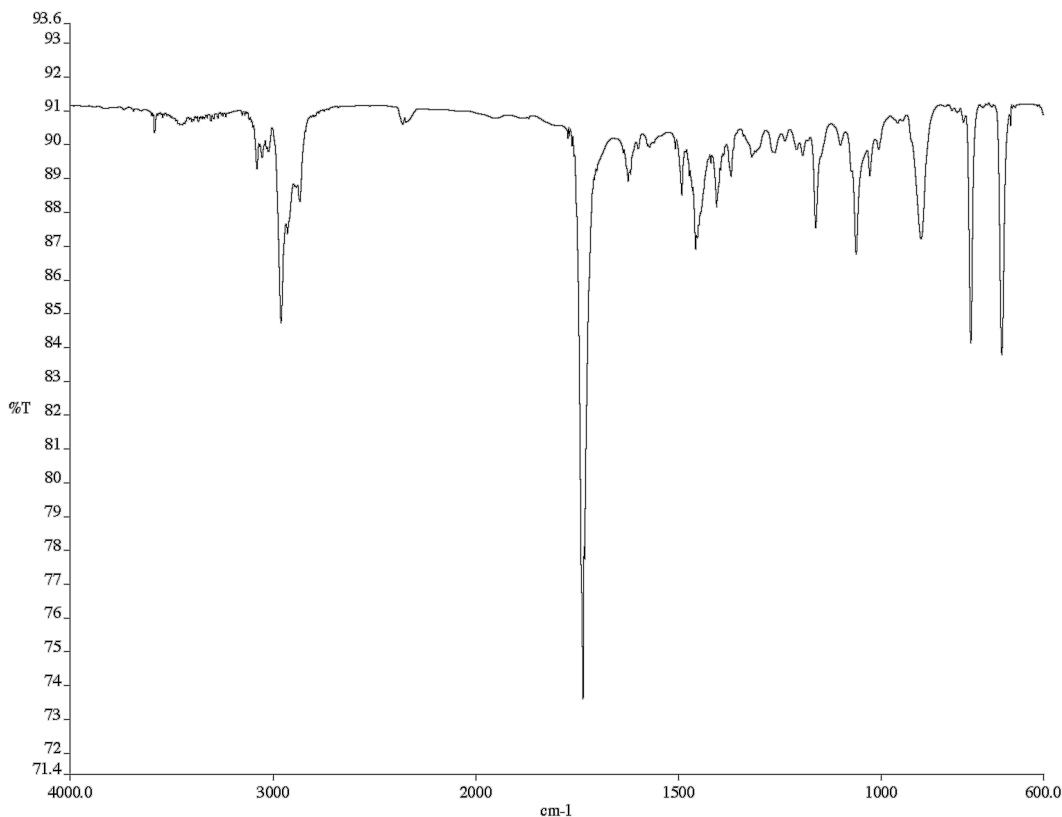


Figure A1. 14. Infrared spectrum (Thin Film, NaCl) of compound 346.

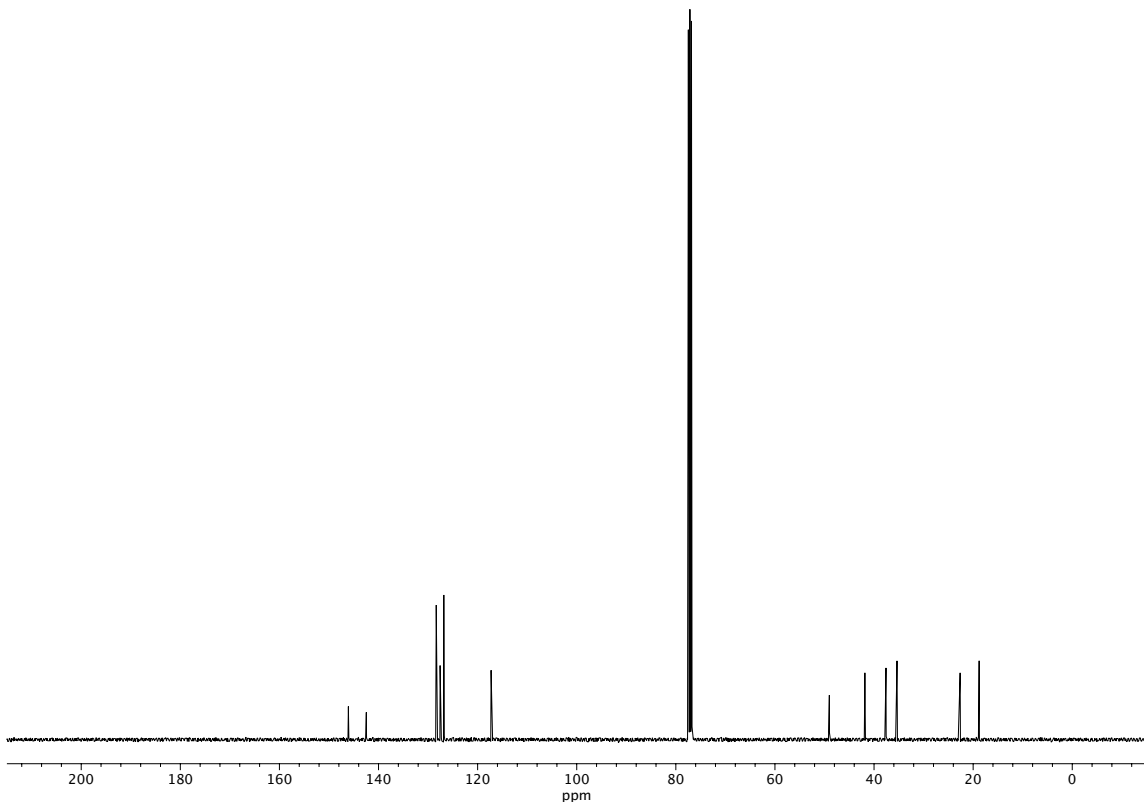


Figure A1.15. ^{13}C NMR (101 MHz, CDCl_3) of compound 346.

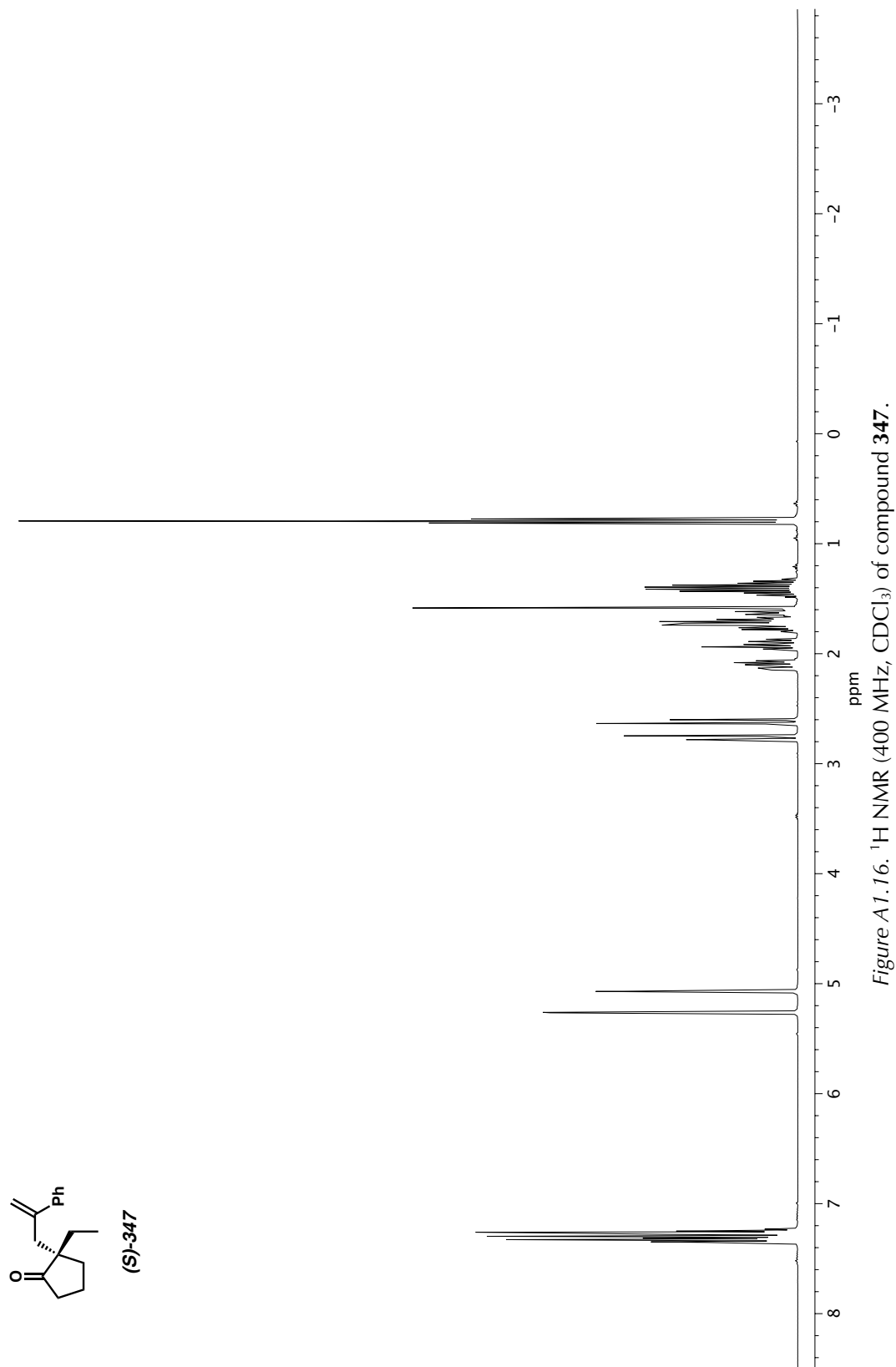


Figure A1.16. ^1H NMR (400 MHz, CDCl_3) of compound 347.

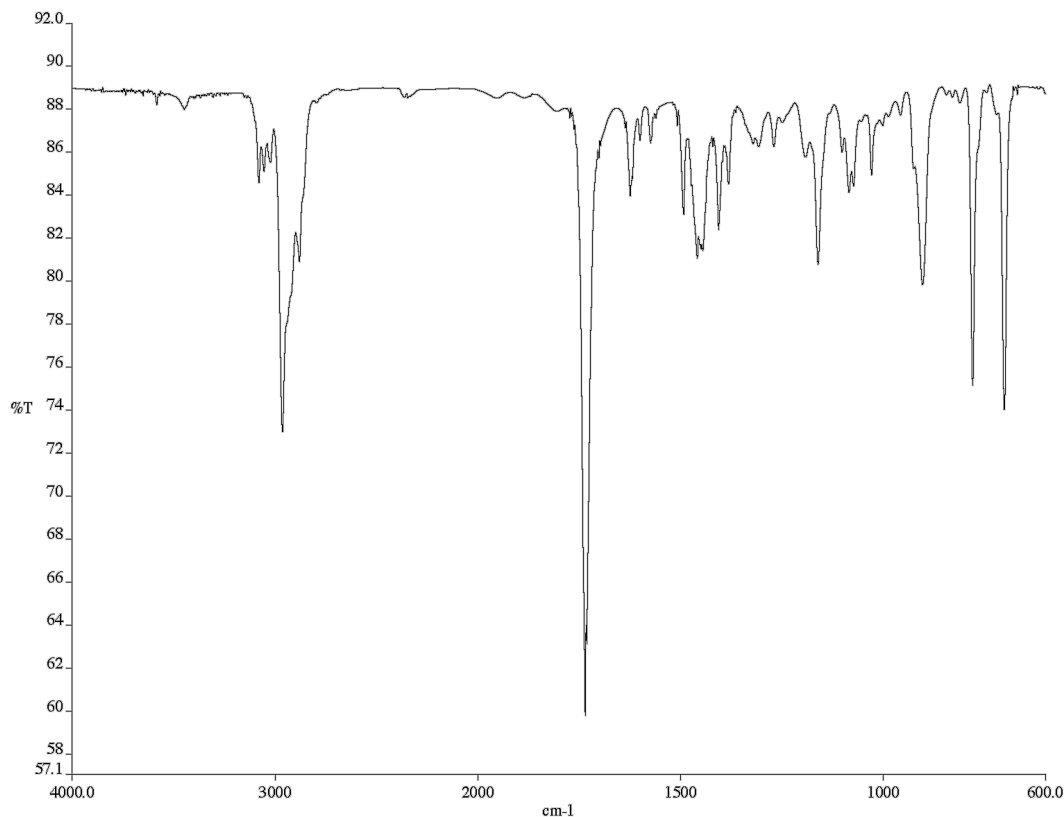


Figure A1.17. Infrared spectrum (Thin Film, NaCl) of compound 347.

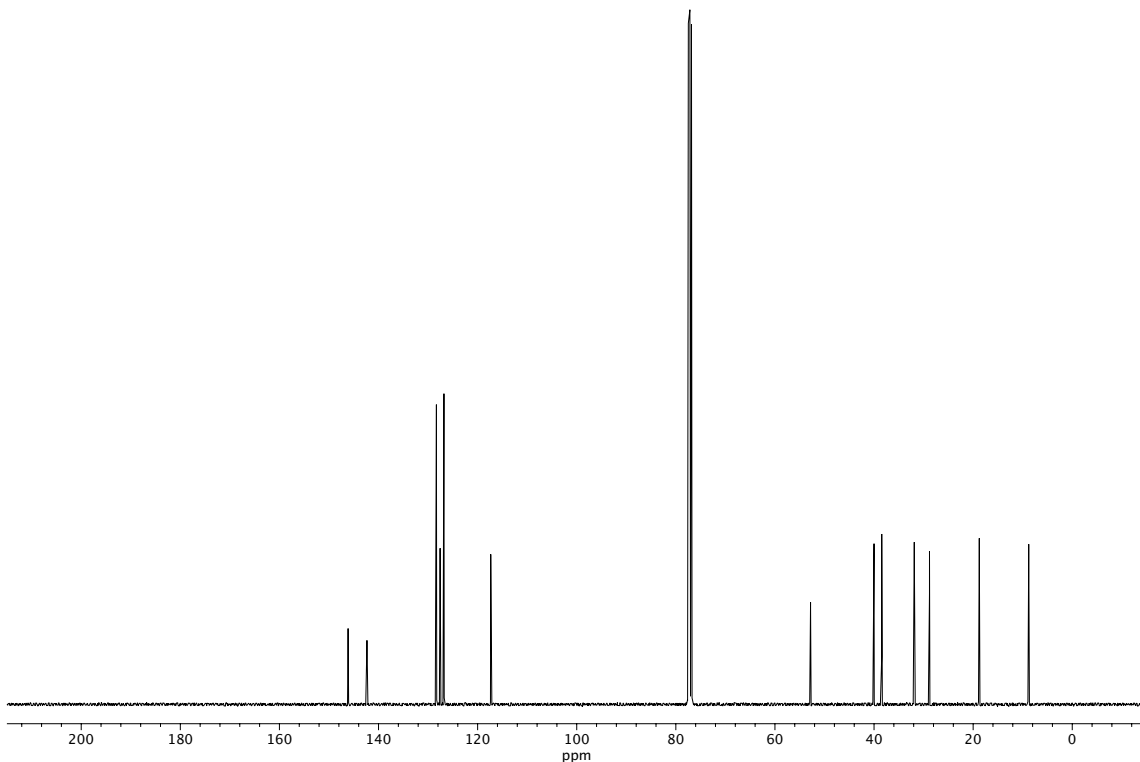


Figure A1.18. ^{13}C NMR (101 MHz, CDCl_3) of compound 347.

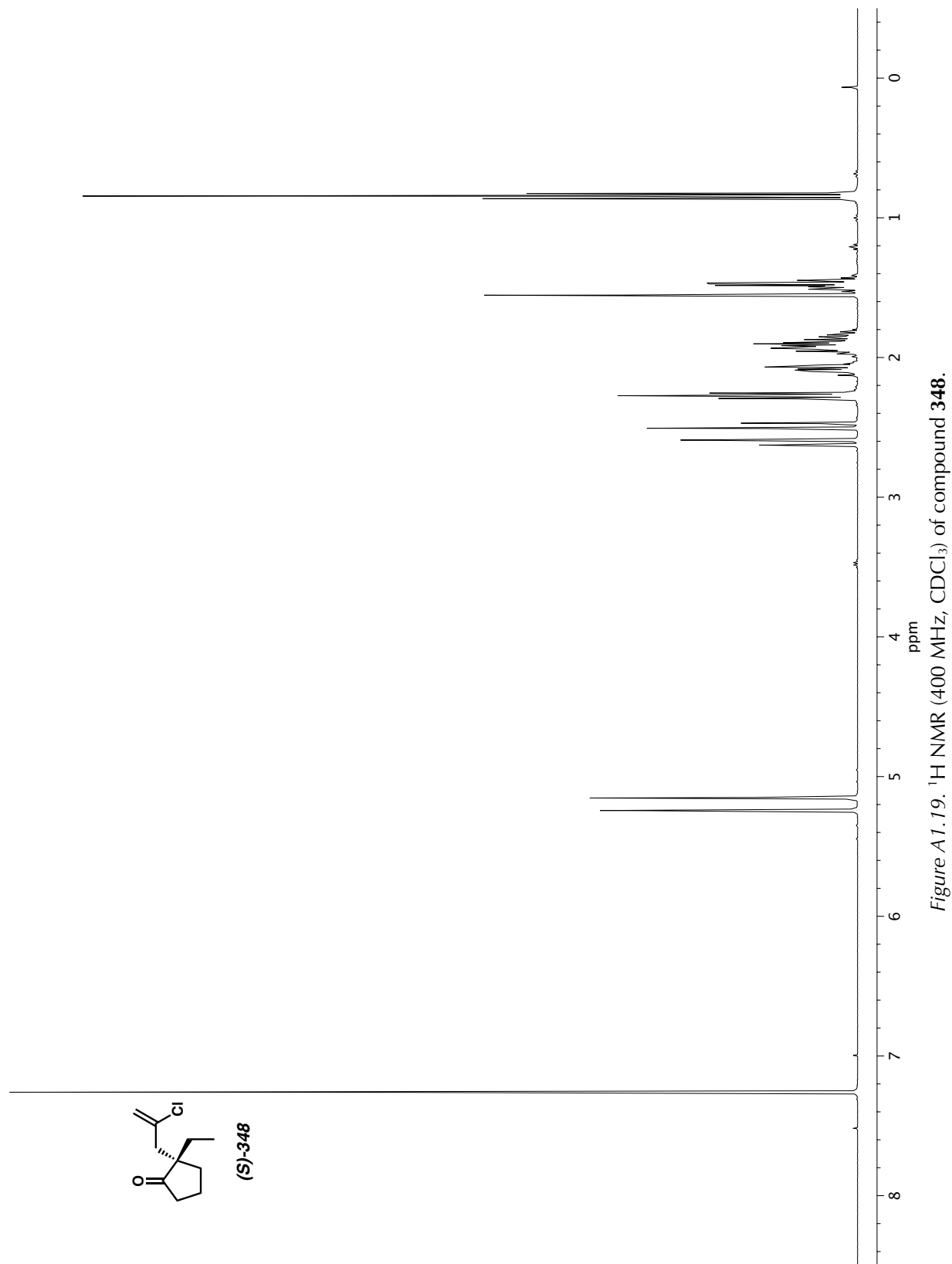


Figure A1.19. ^1H NMR (400 MHz, CDCl_3) of compound 348.

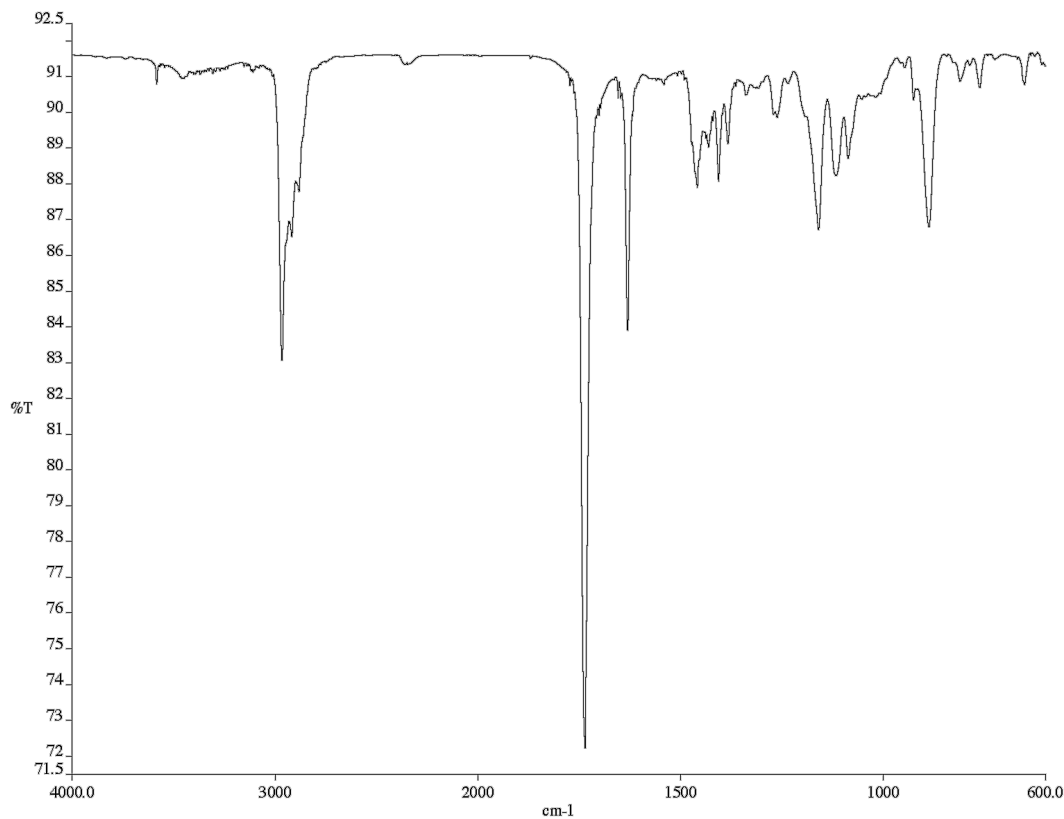


Figure A1.20. Infrared spectrum (Thin Film, NaCl) of compound 348.

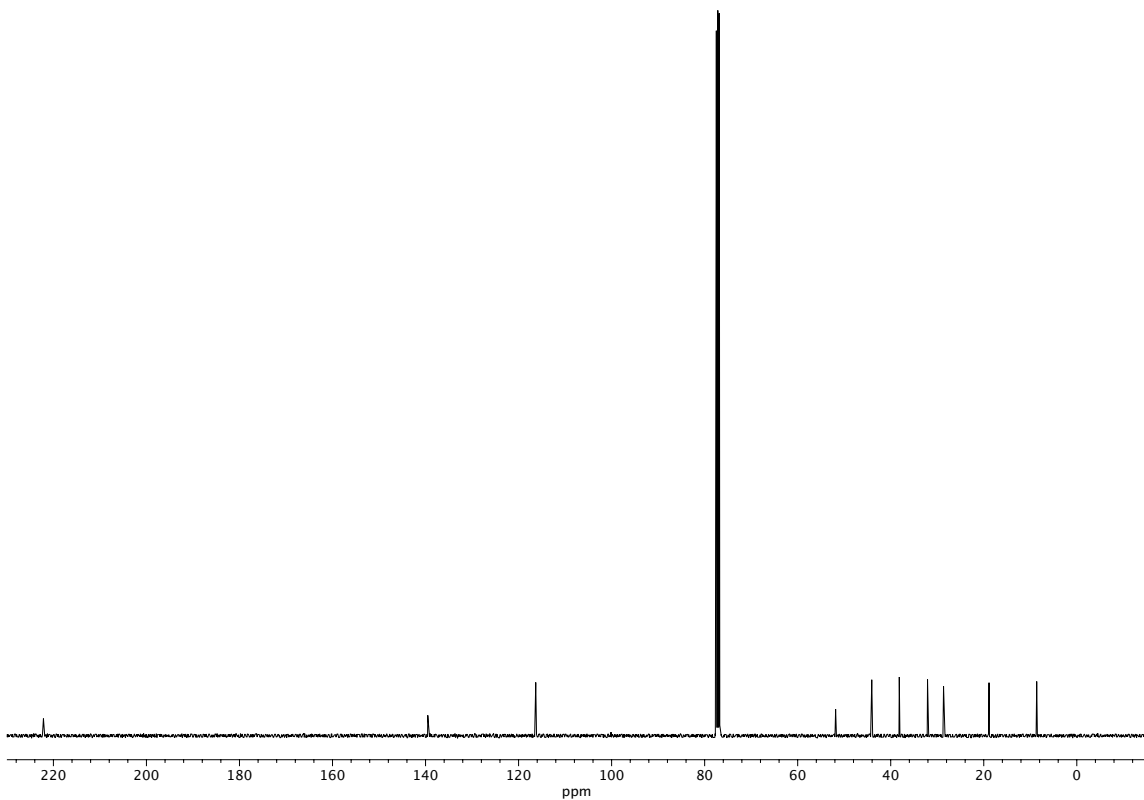


Figure A1.21. ^{13}C NMR (101 MHz, CDCl_3) of compound 348.

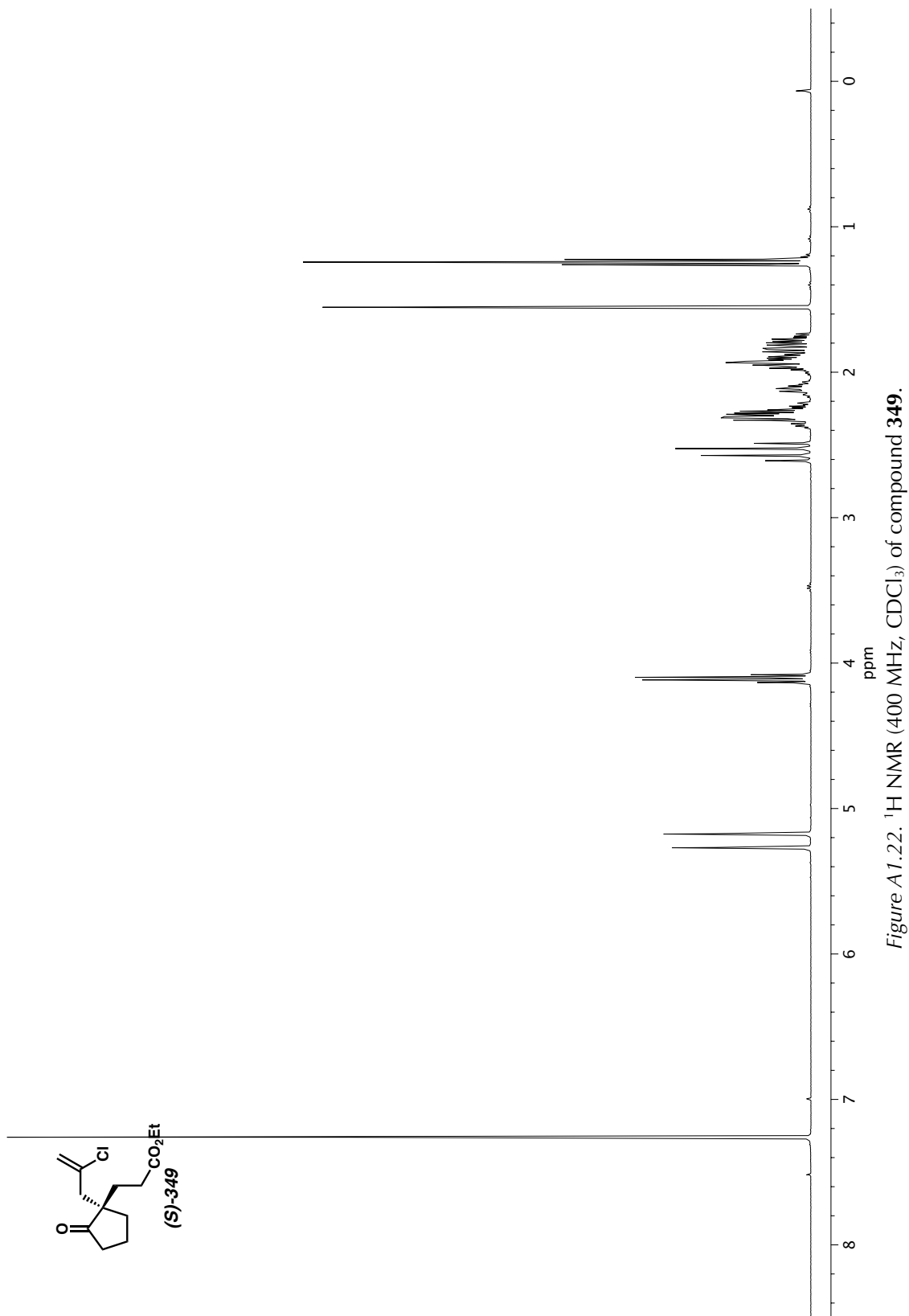


Figure A1.22. ^1H NMR (400 MHz, CDCl_3) of compound 349.

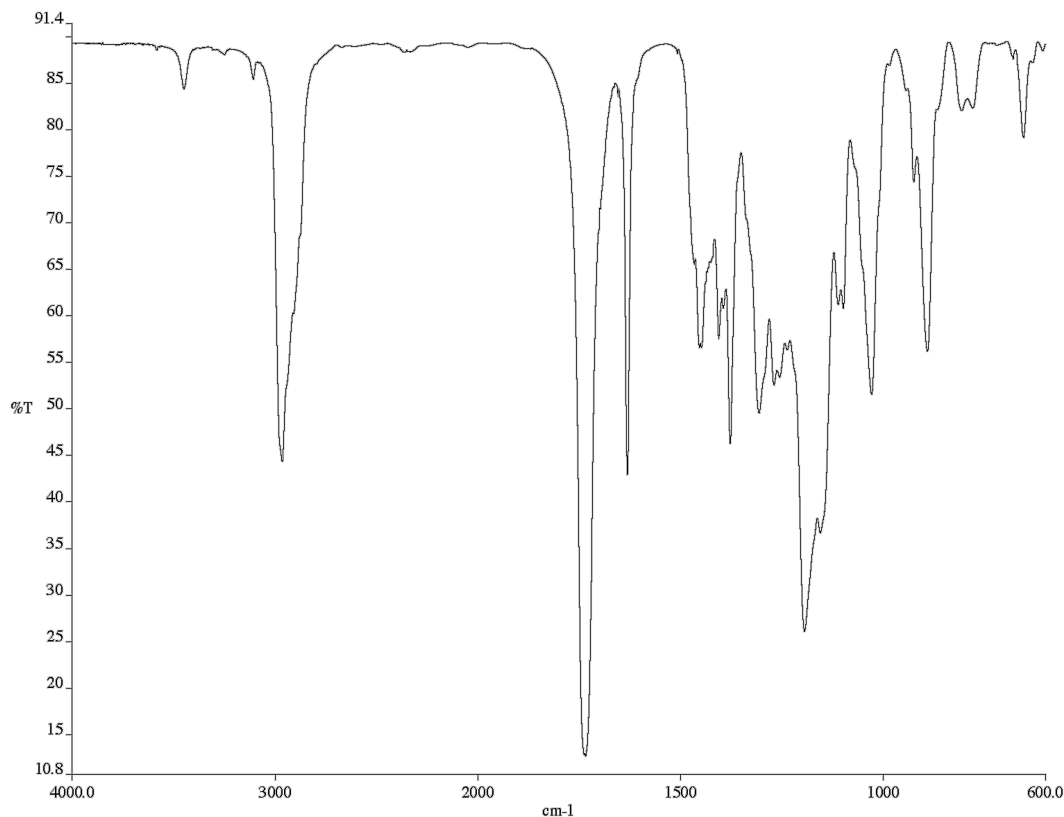


Figure A1.23. Infrared spectrum (Thin Film, NaCl) of compound 349.

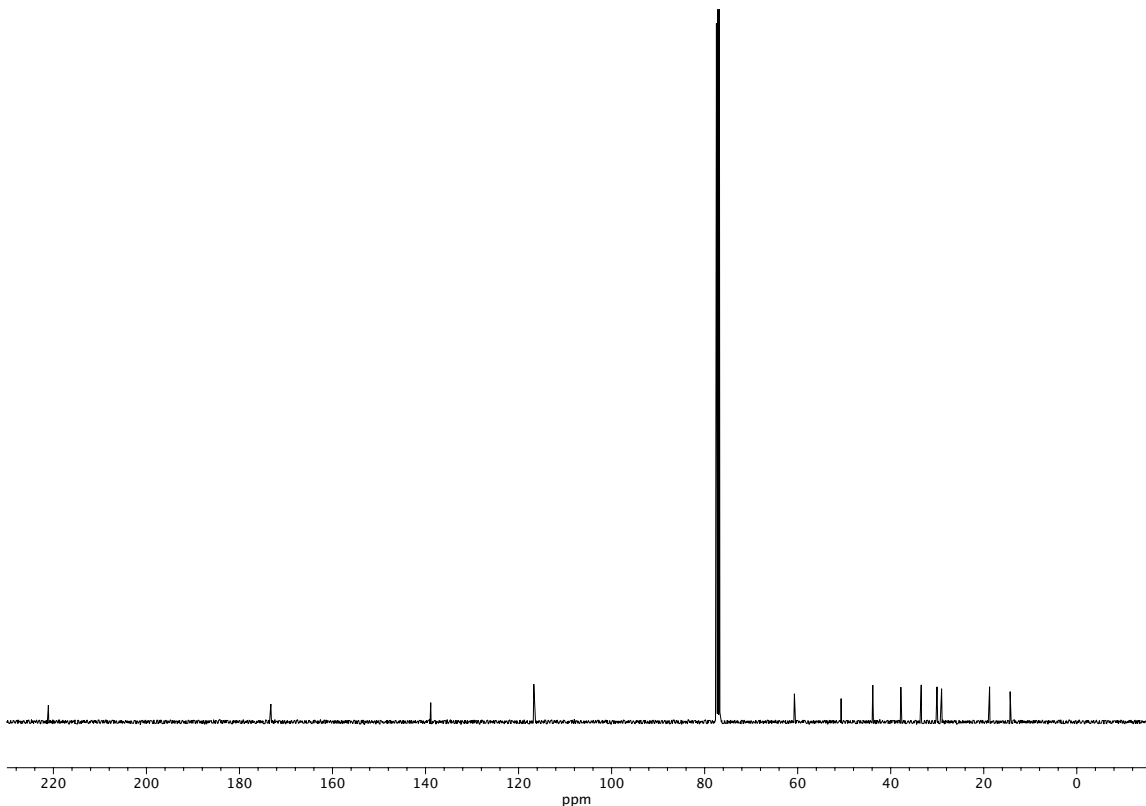
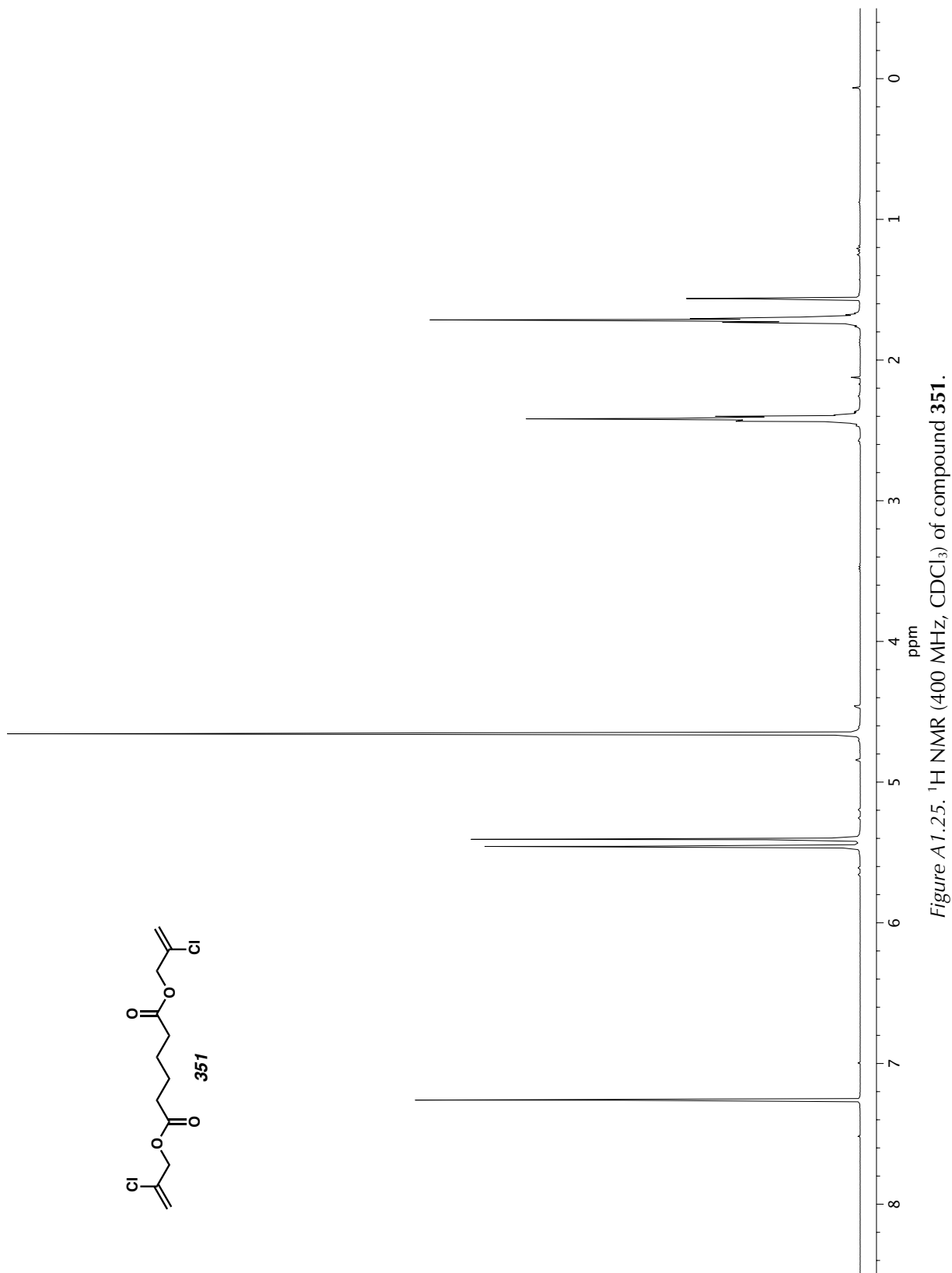


Figure A1.24. ^{13}C NMR (101 MHz, CDCl_3) of compound 349.



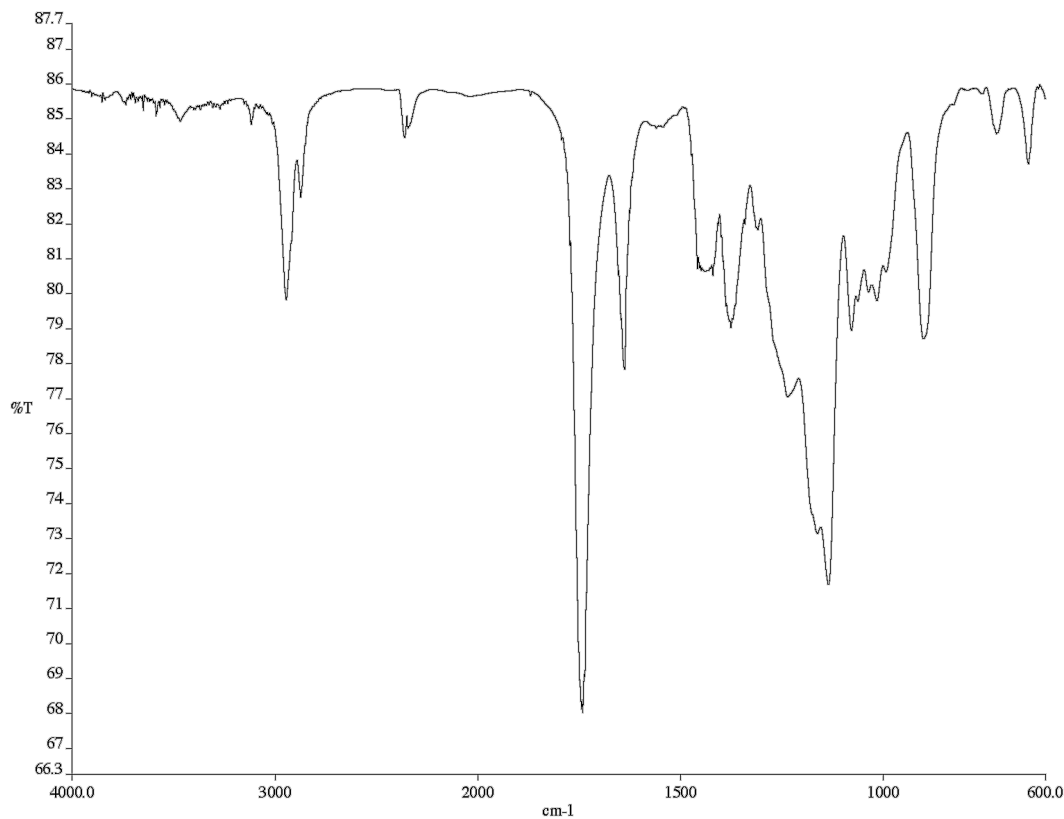


Figure A1.26. Infrared spectrum (Thin Film, NaCl) of compound 351.

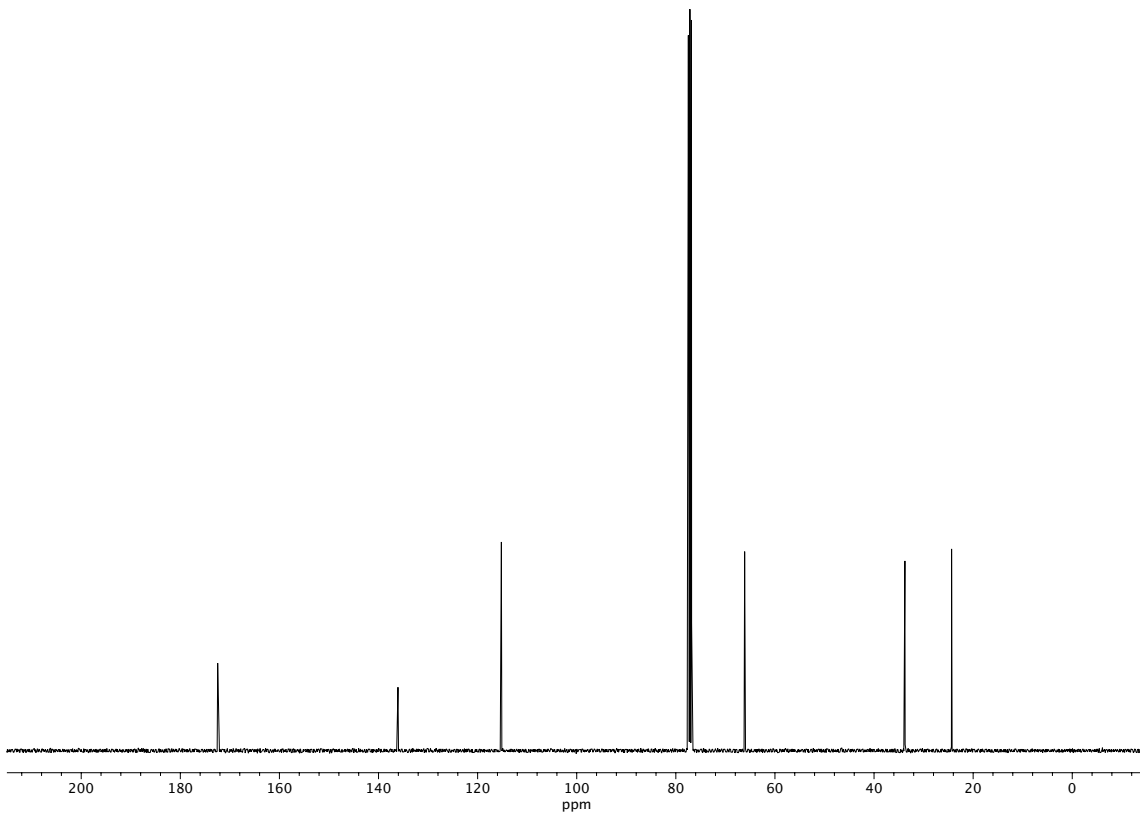


Figure A1.27. ¹³C NMR (101 MHz, CDCl₃) of compound 351.

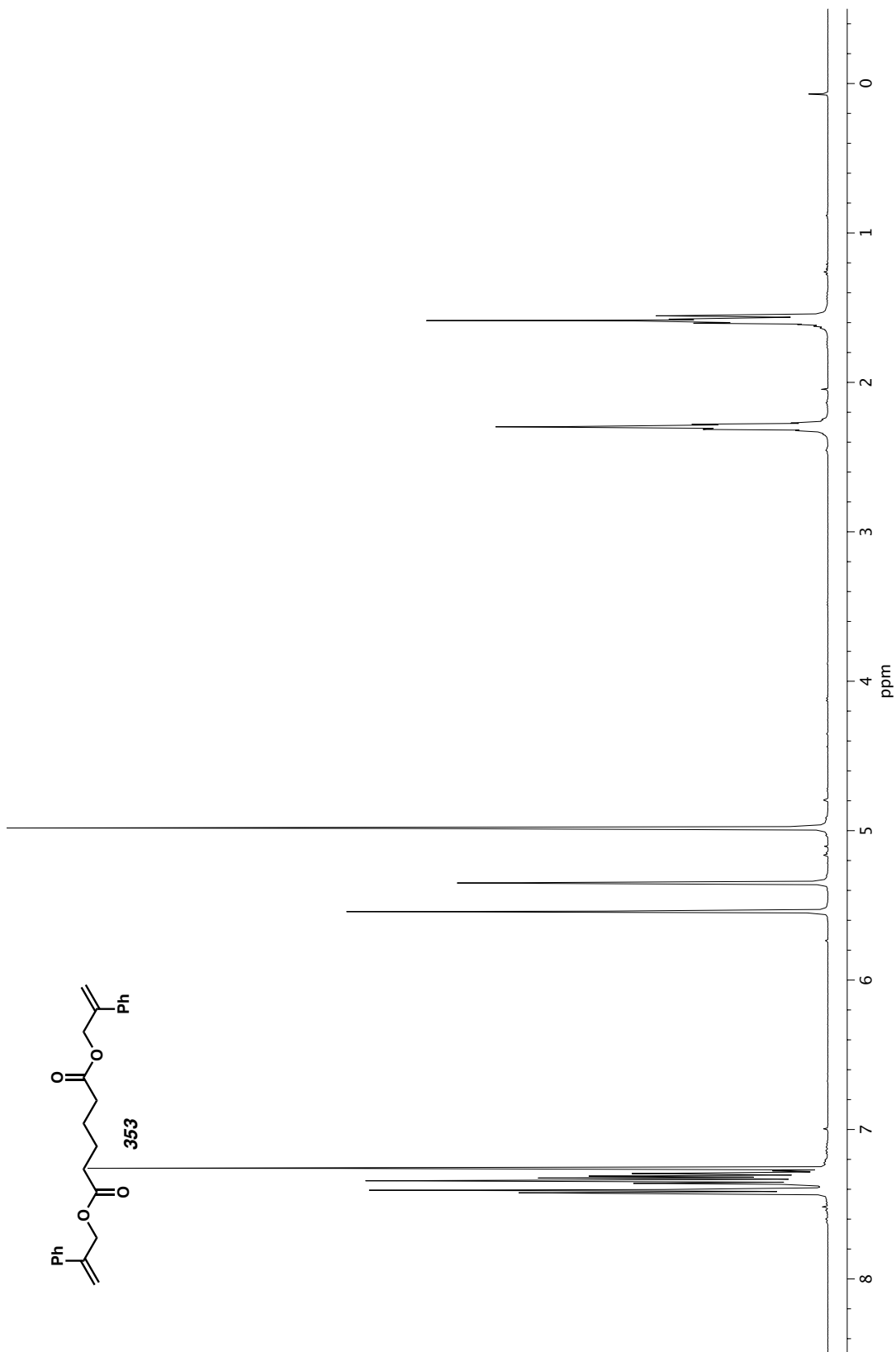


Figure A1.28. ^1H NMR (400 MHz, CDCl_3) of compound 353.

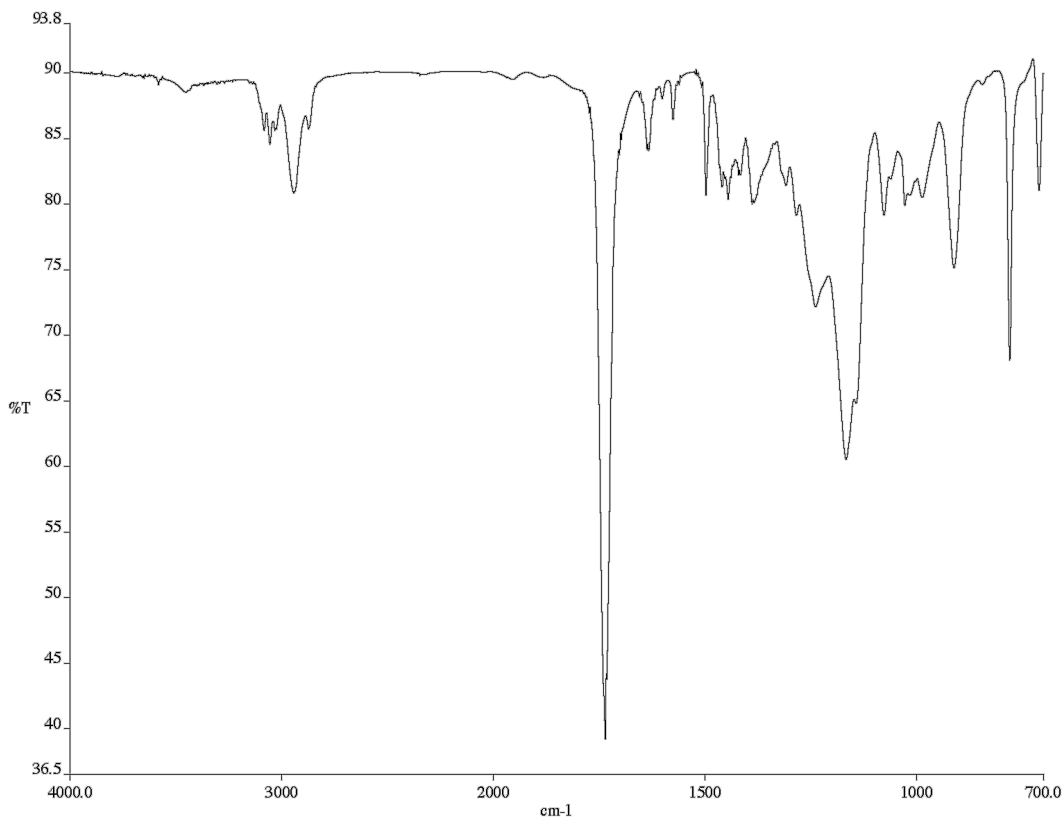


Figure A1.29. Infrared spectrum (Thin Film, NaCl) of compound 353.

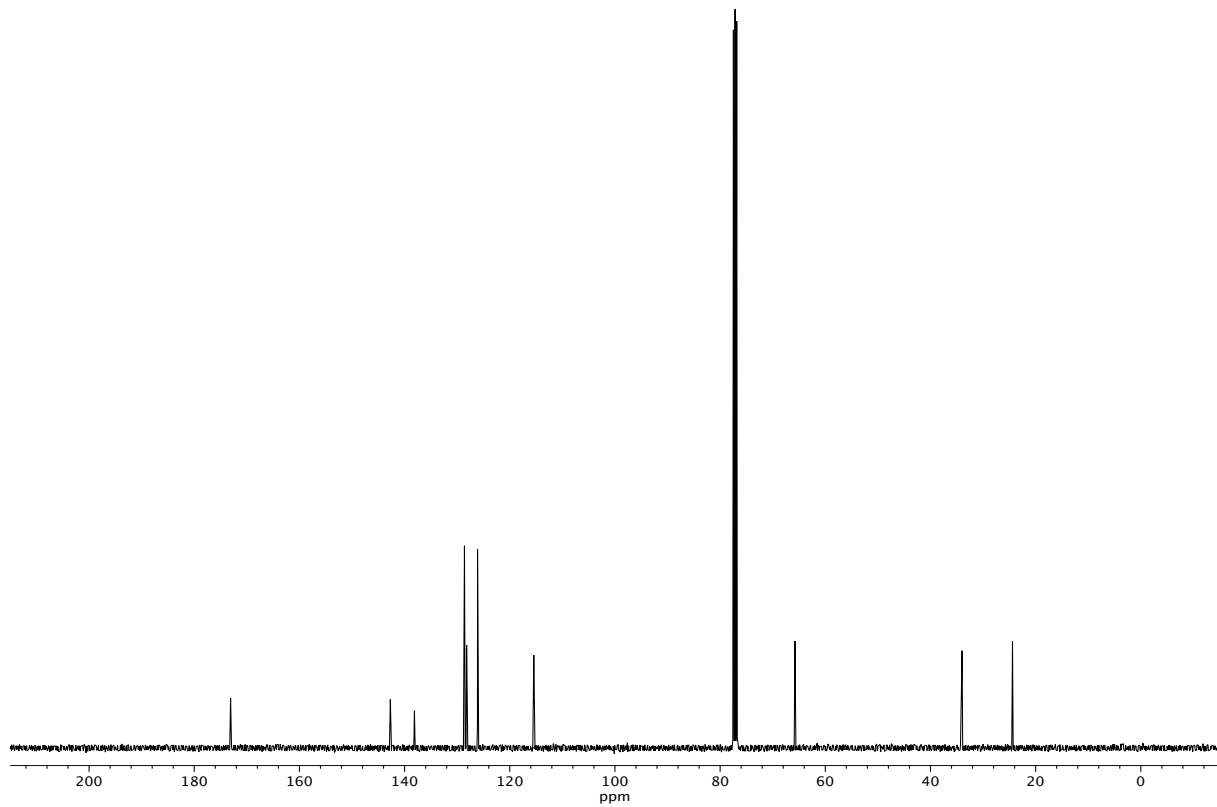
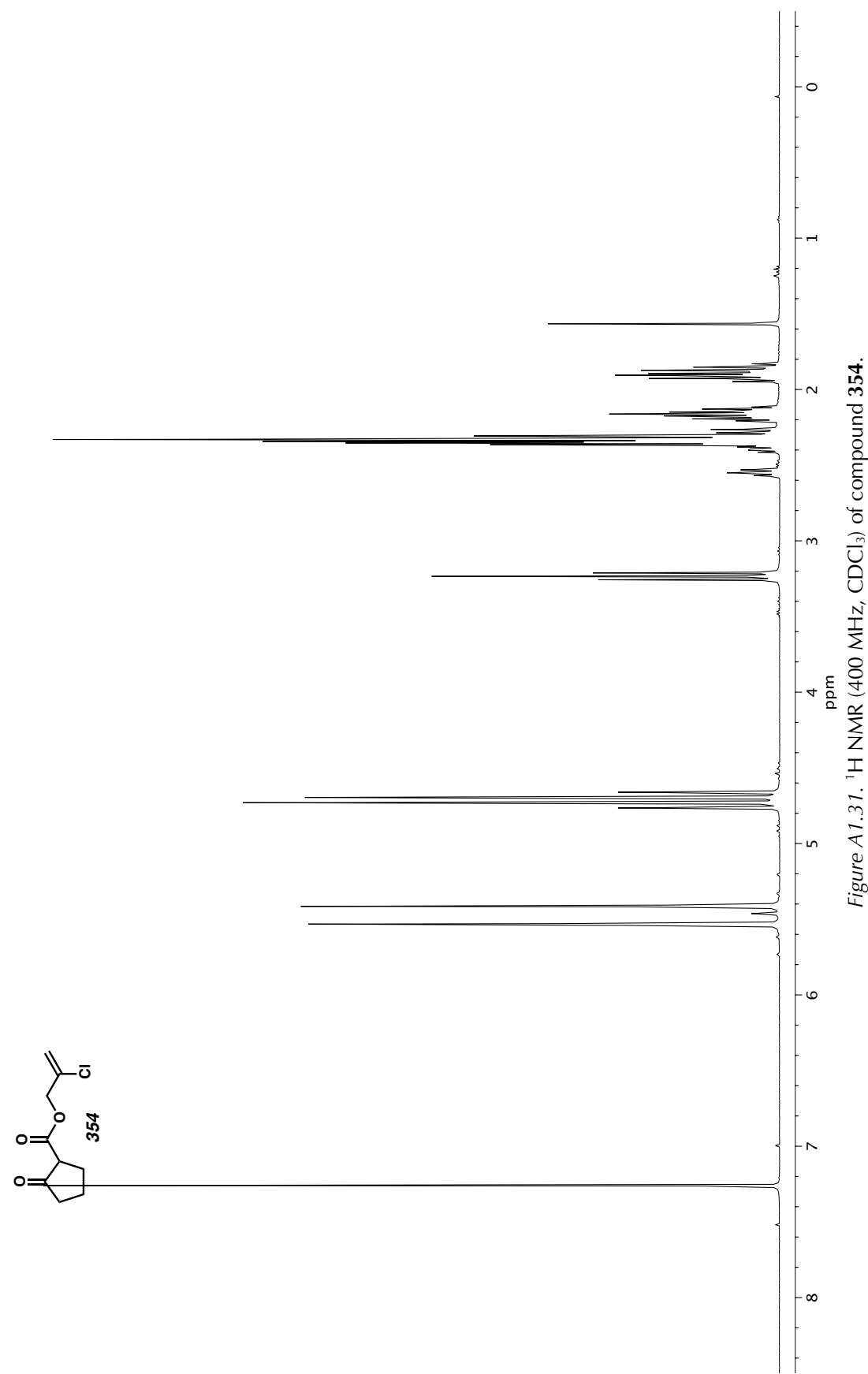


Figure A1.30. ^{13}C NMR (101 MHz, CDCl_3) of compound 353.



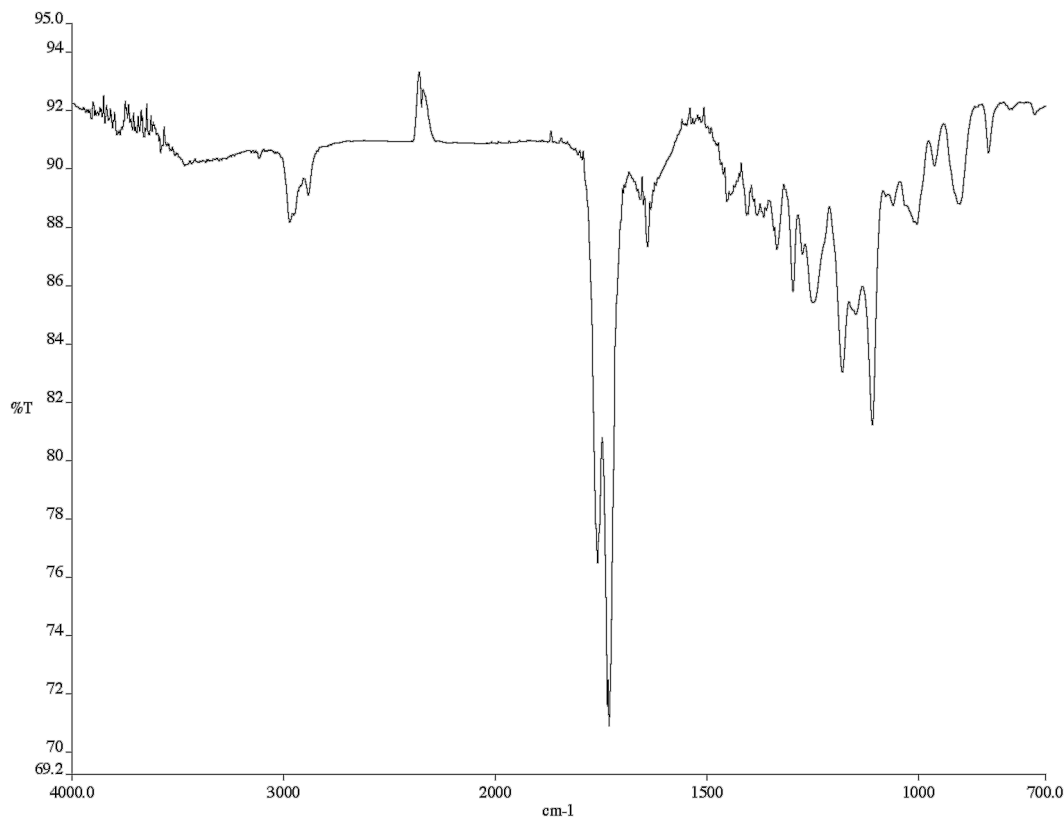


Figure A1.32. Infrared spectrum (Thin Film, NaCl) of compound 354.

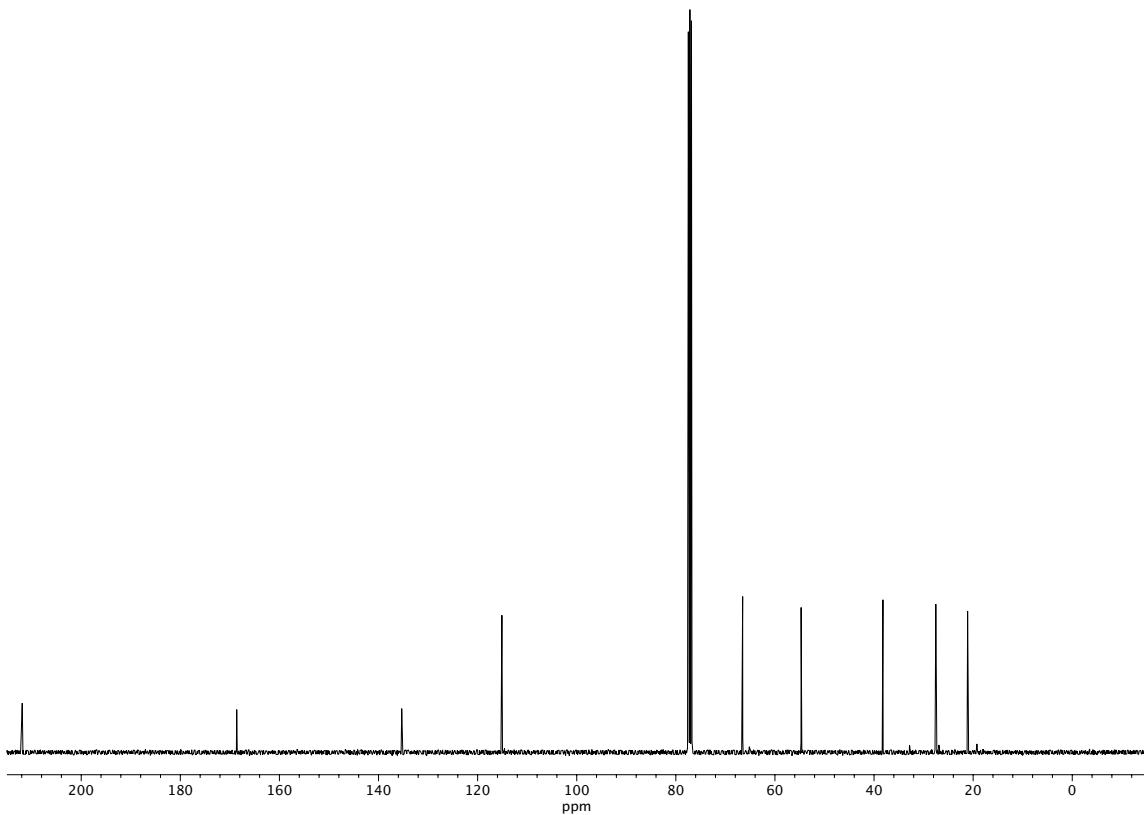
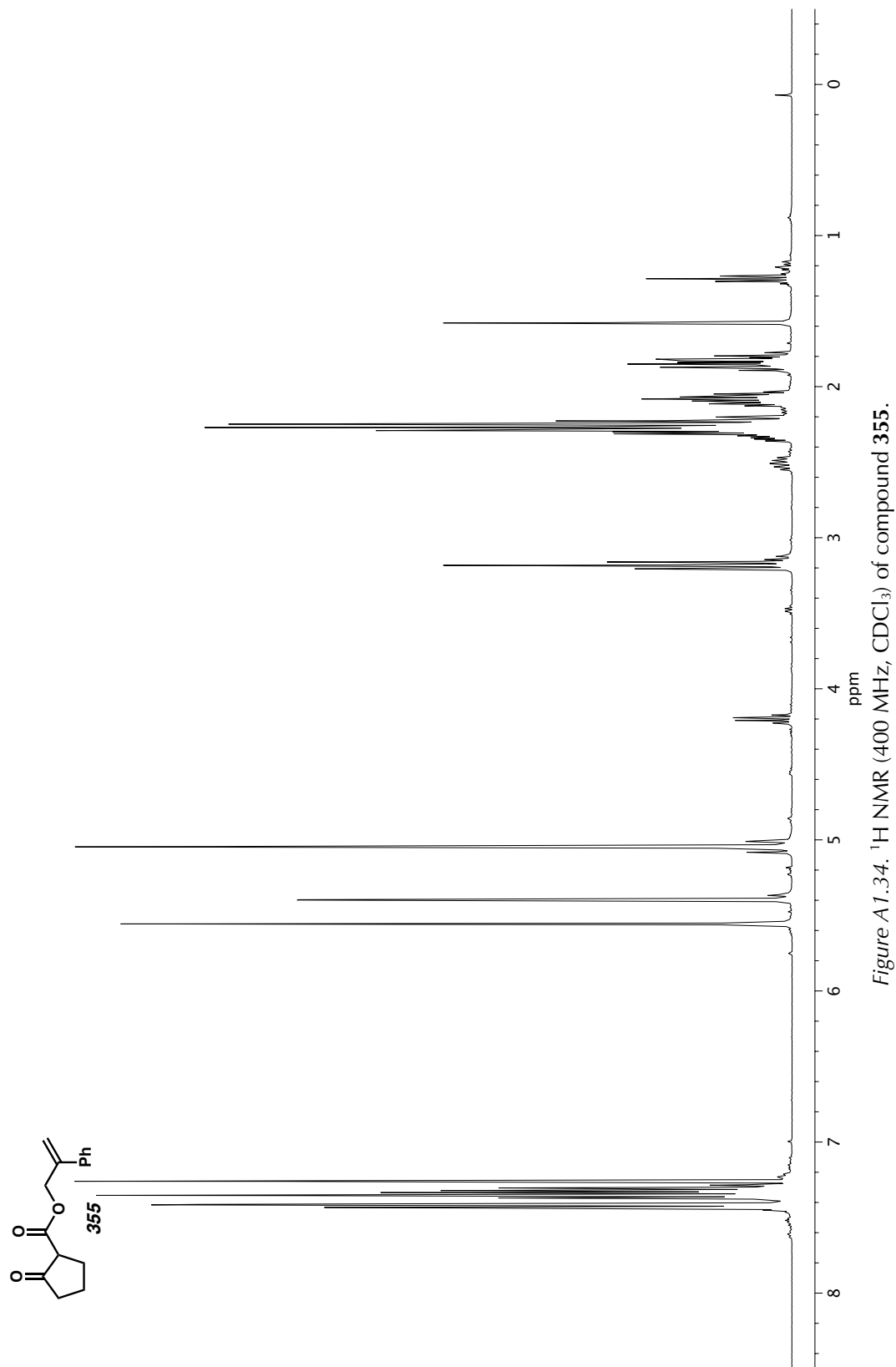


Figure A1.33. ^{13}C NMR (101 MHz, CDCl_3) of compound 354.



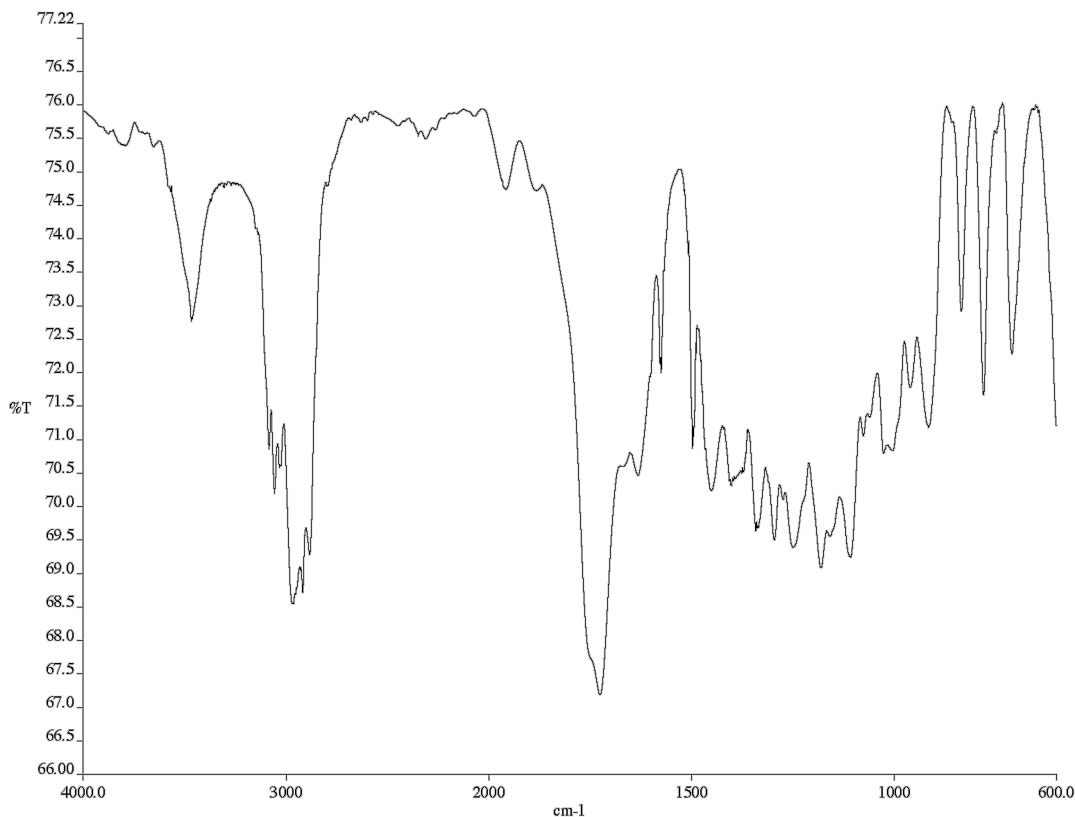


Figure A1.35. Infrared spectrum (Thin Film, NaCl) of compound 355.

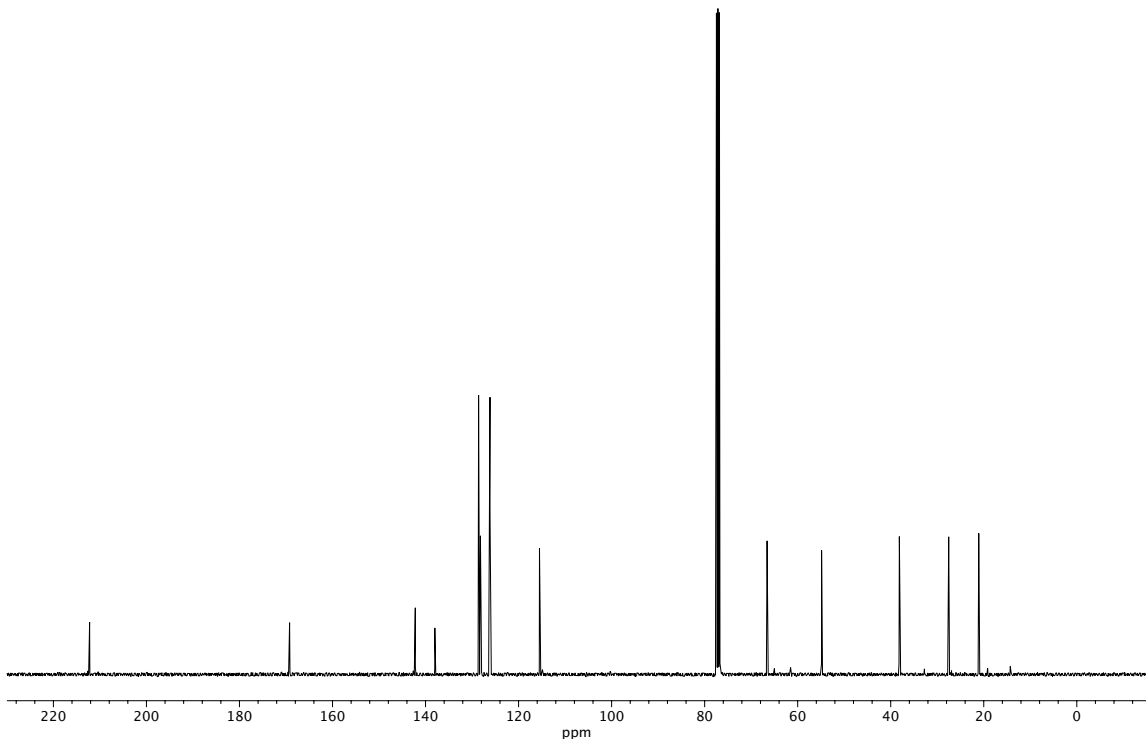


Figure A1.36. ¹³C NMR (101 MHz, CDCl₃) of compound 355.

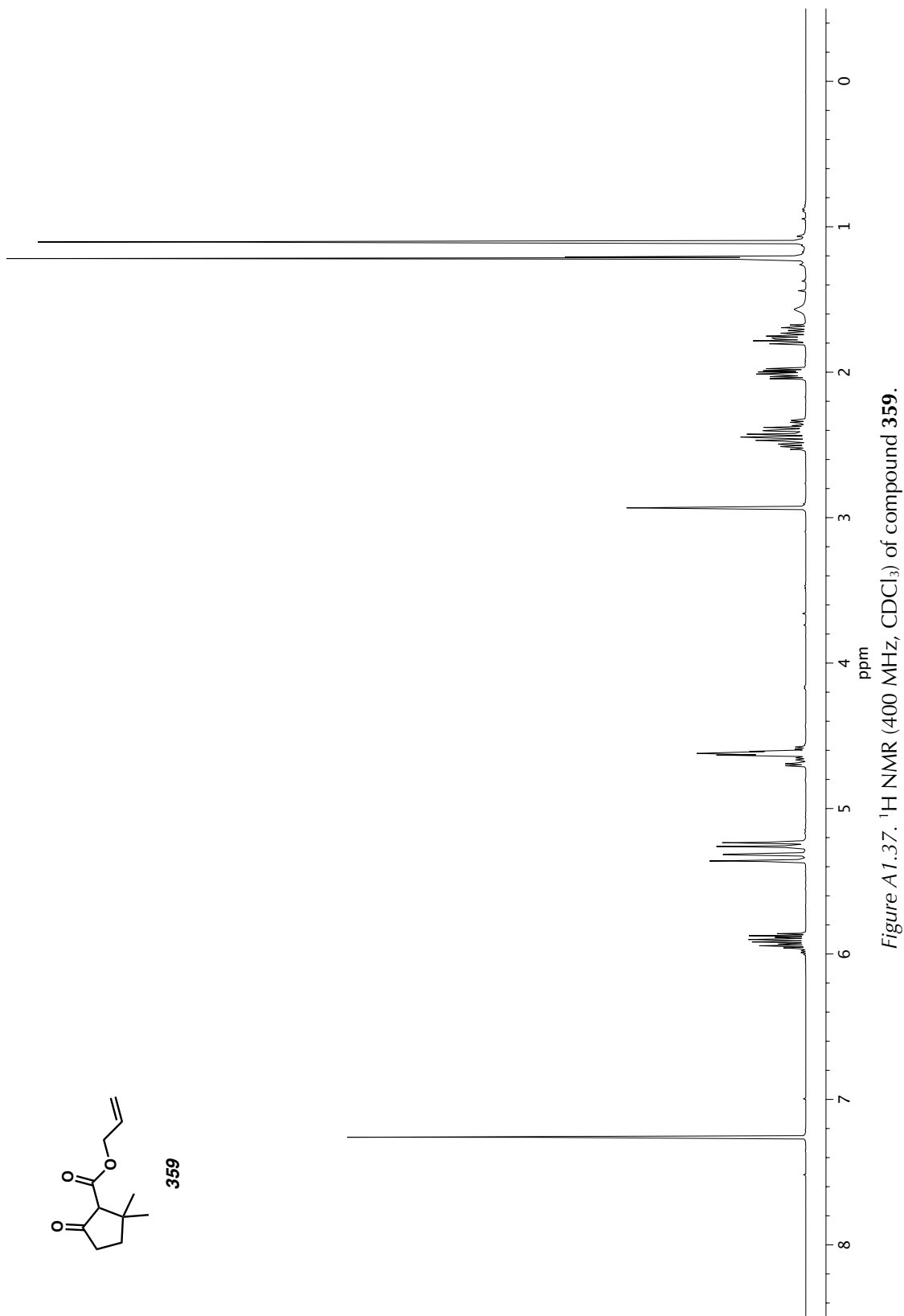
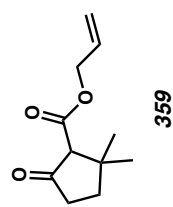


Figure A1.37. ^1H NMR (400 MHz, CDCl_3) of compound 359.

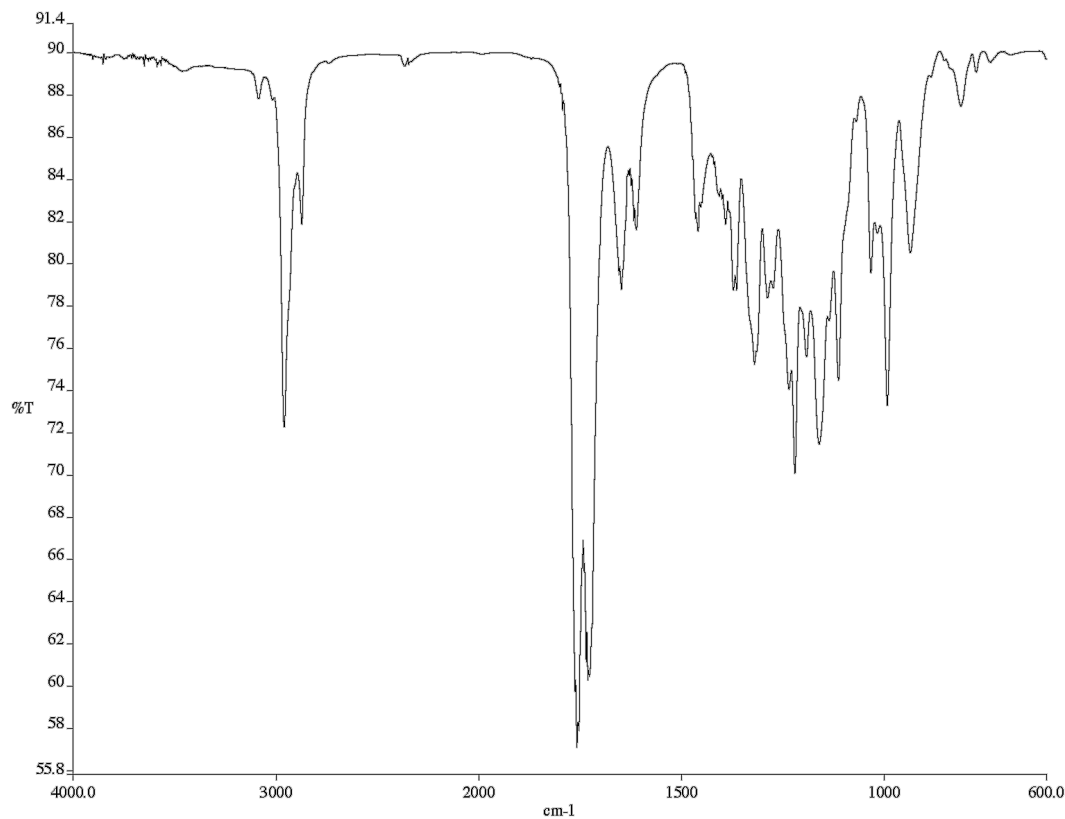


Figure A1.38. Infrared spectrum (Thin Film, NaCl) of compound 359.

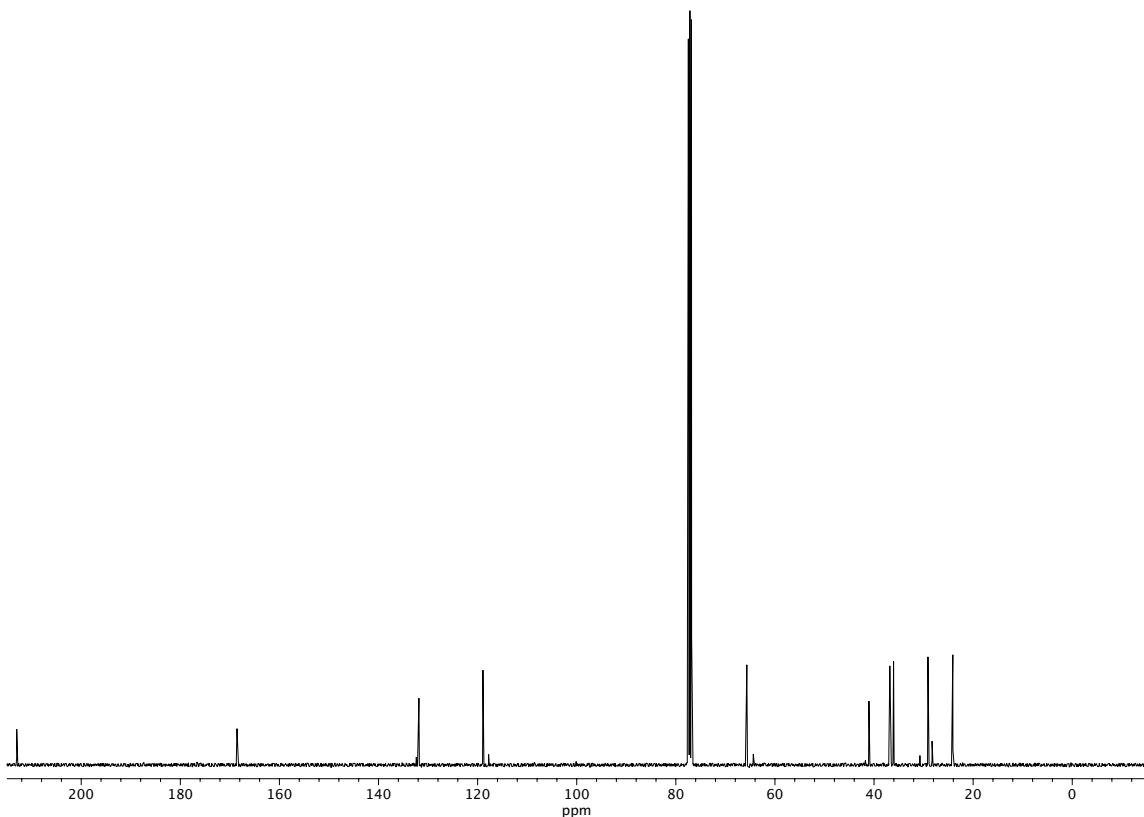


Figure A1.39. ^{13}C NMR (101 MHz, CDCl_3) of compound 359.

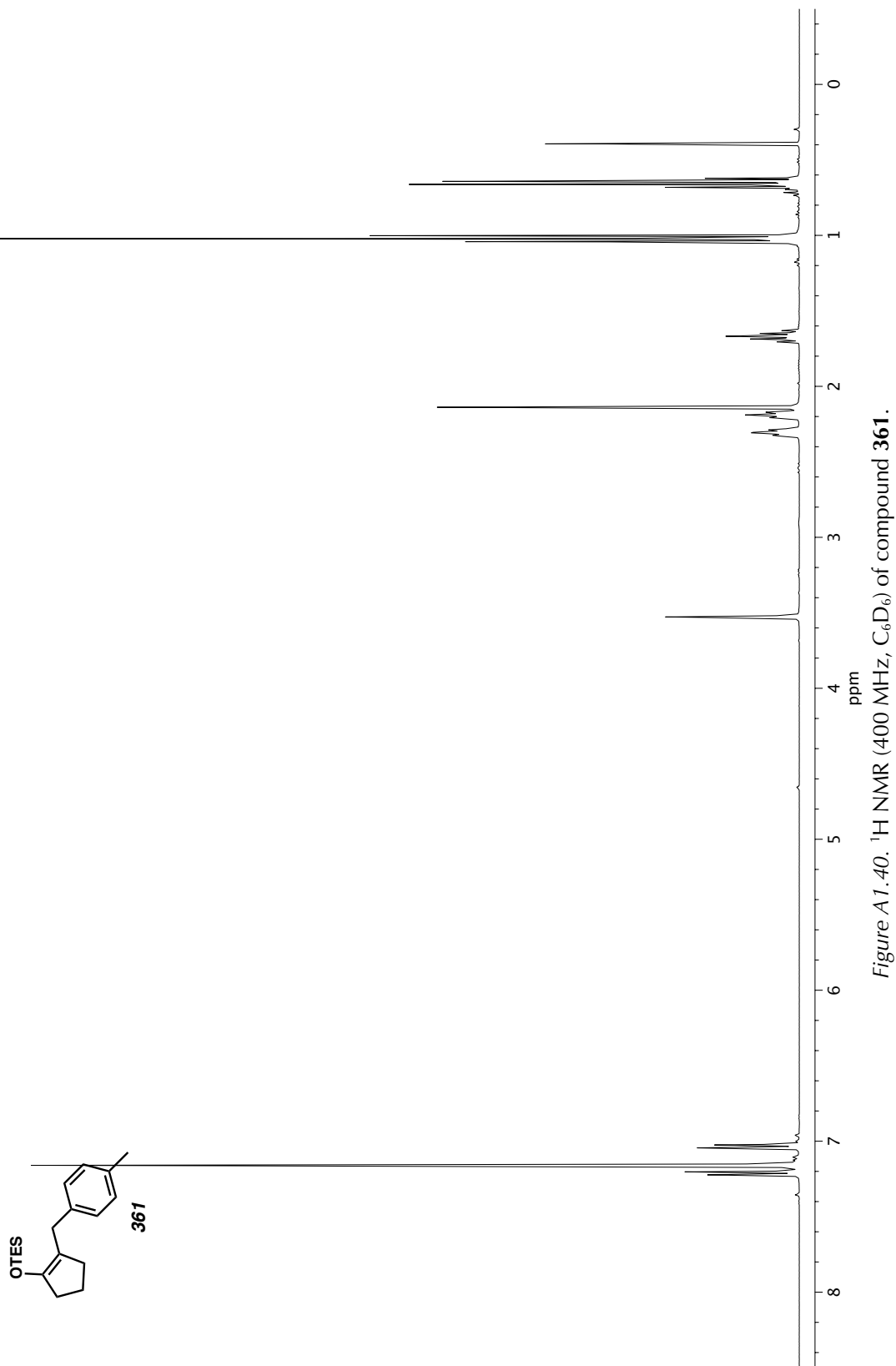


Figure A 1.40. ^1H NMR (400 MHz, C_6D_6) of compound 361.

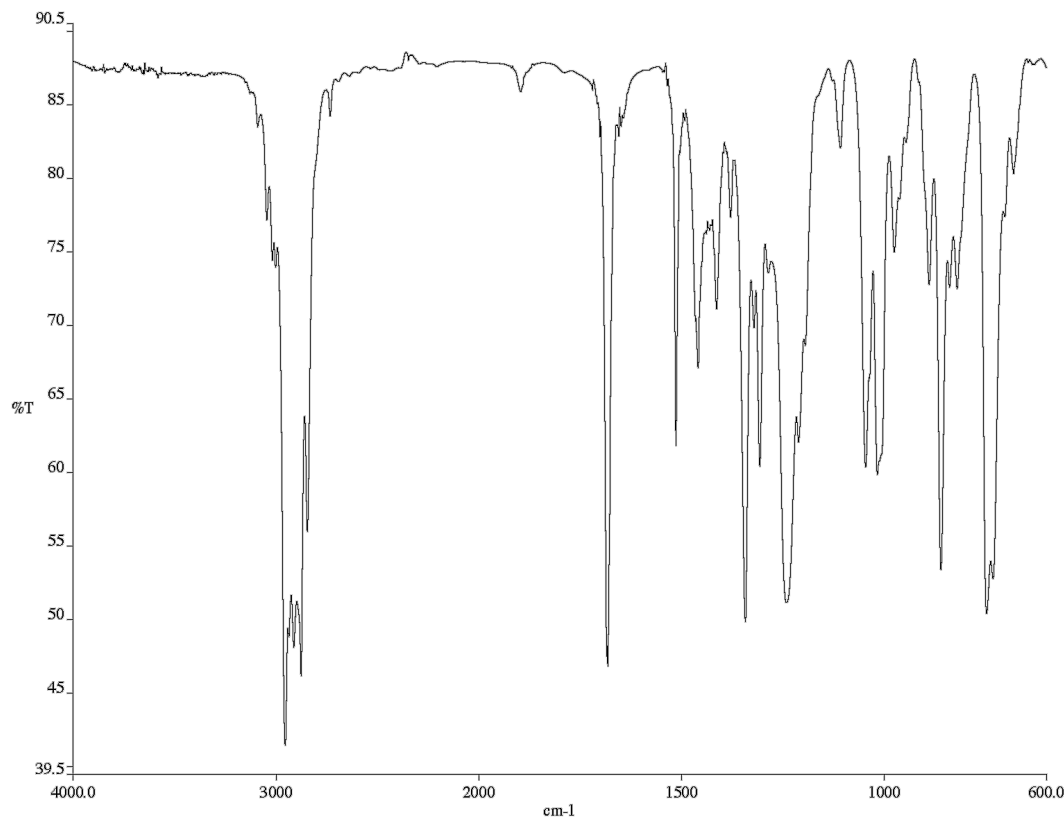


Figure A1.41. Infrared spectrum (Thin Film, NaCl) of compound **361**.

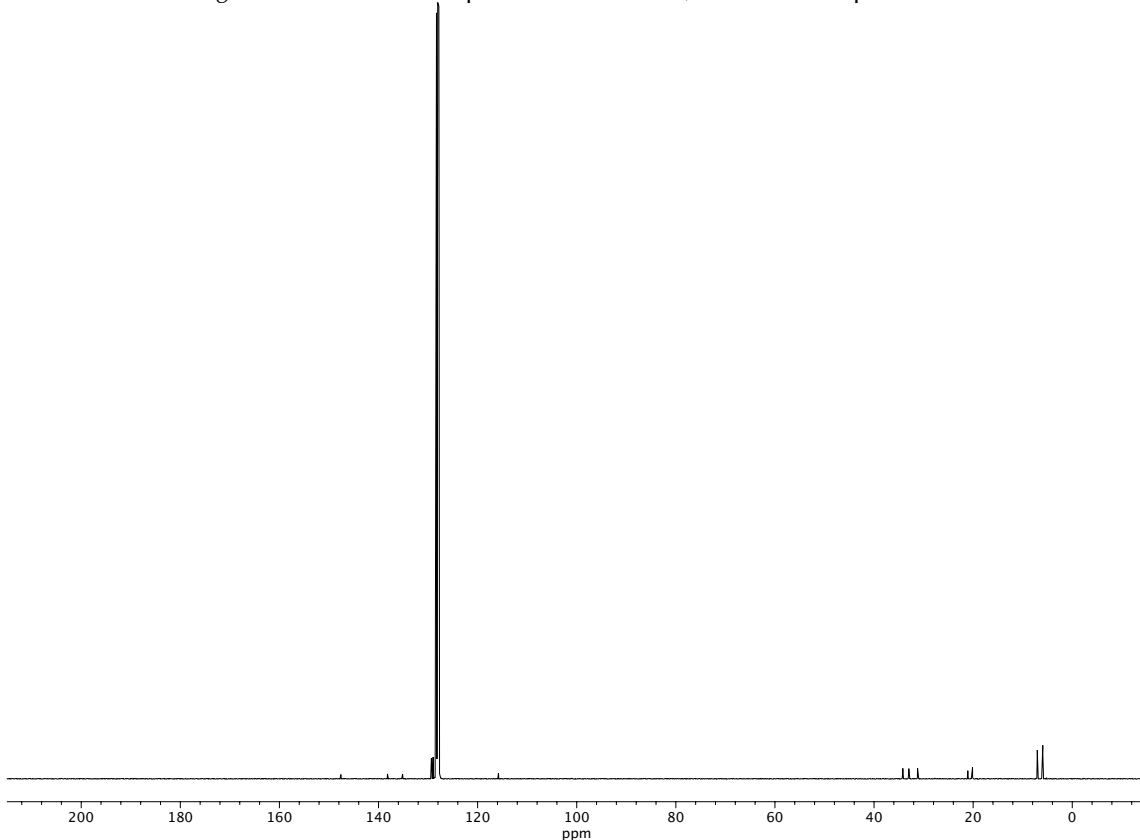


Figure A1.42. ^{13}C NMR (101 MHz, C_6D_6) of compound **361**.

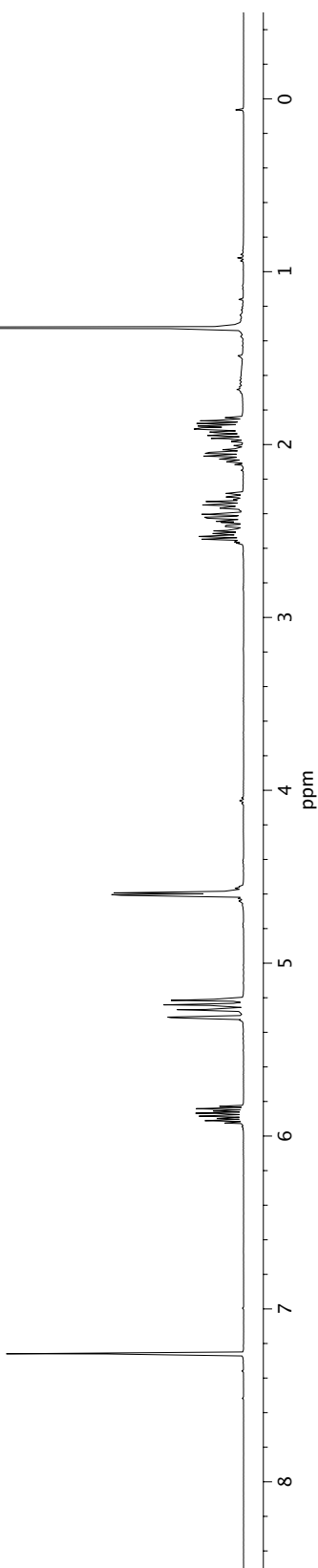
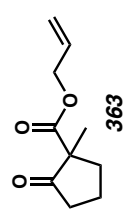


Figure A1.43. ^1H NMR (400 MHz, CDCl_3) of compound 363.

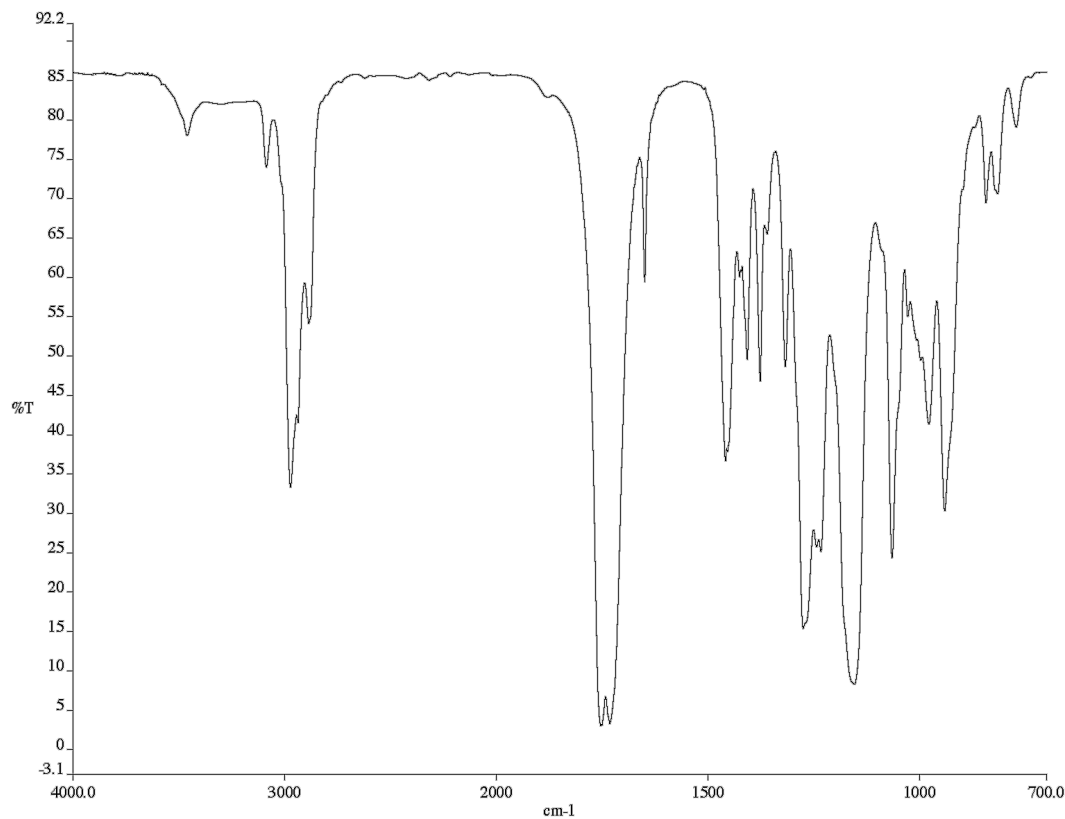


Figure A1. 44. Infrared spectrum (Thin Film, NaCl) of compound 363.

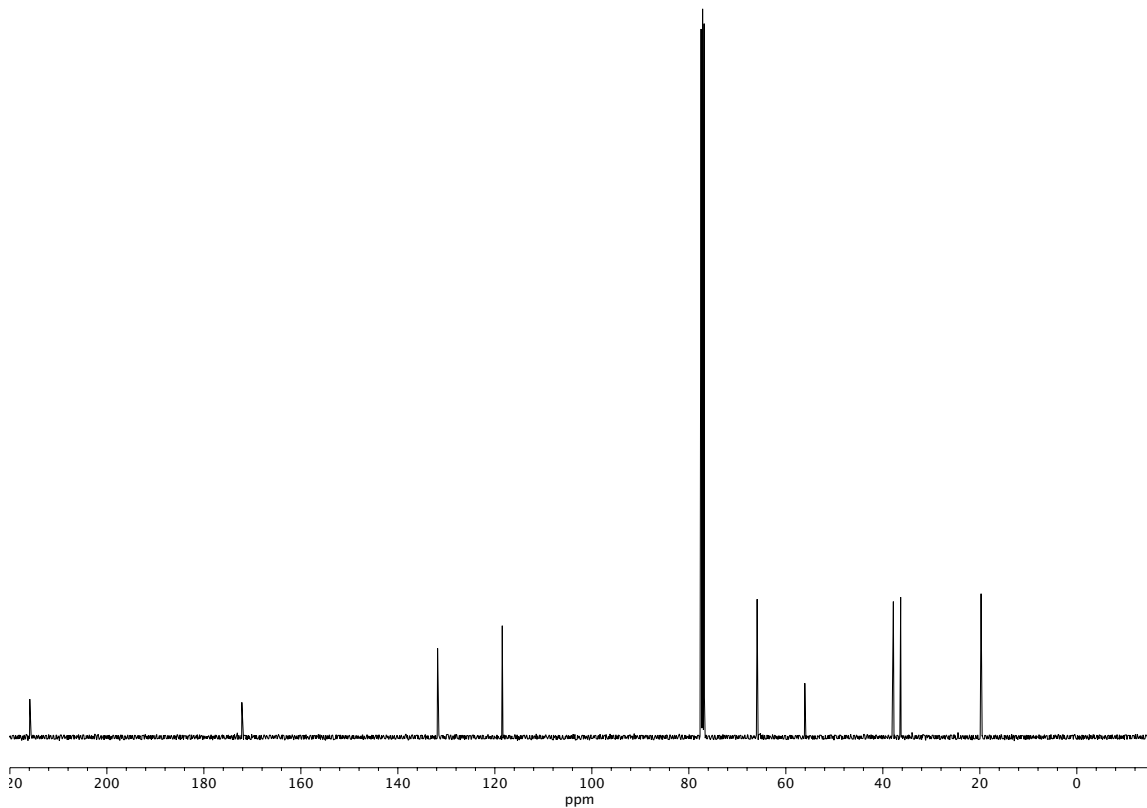


Figure A1. 45. ^{13}C NMR (101 MHz, CDCl_3) of compound 363.

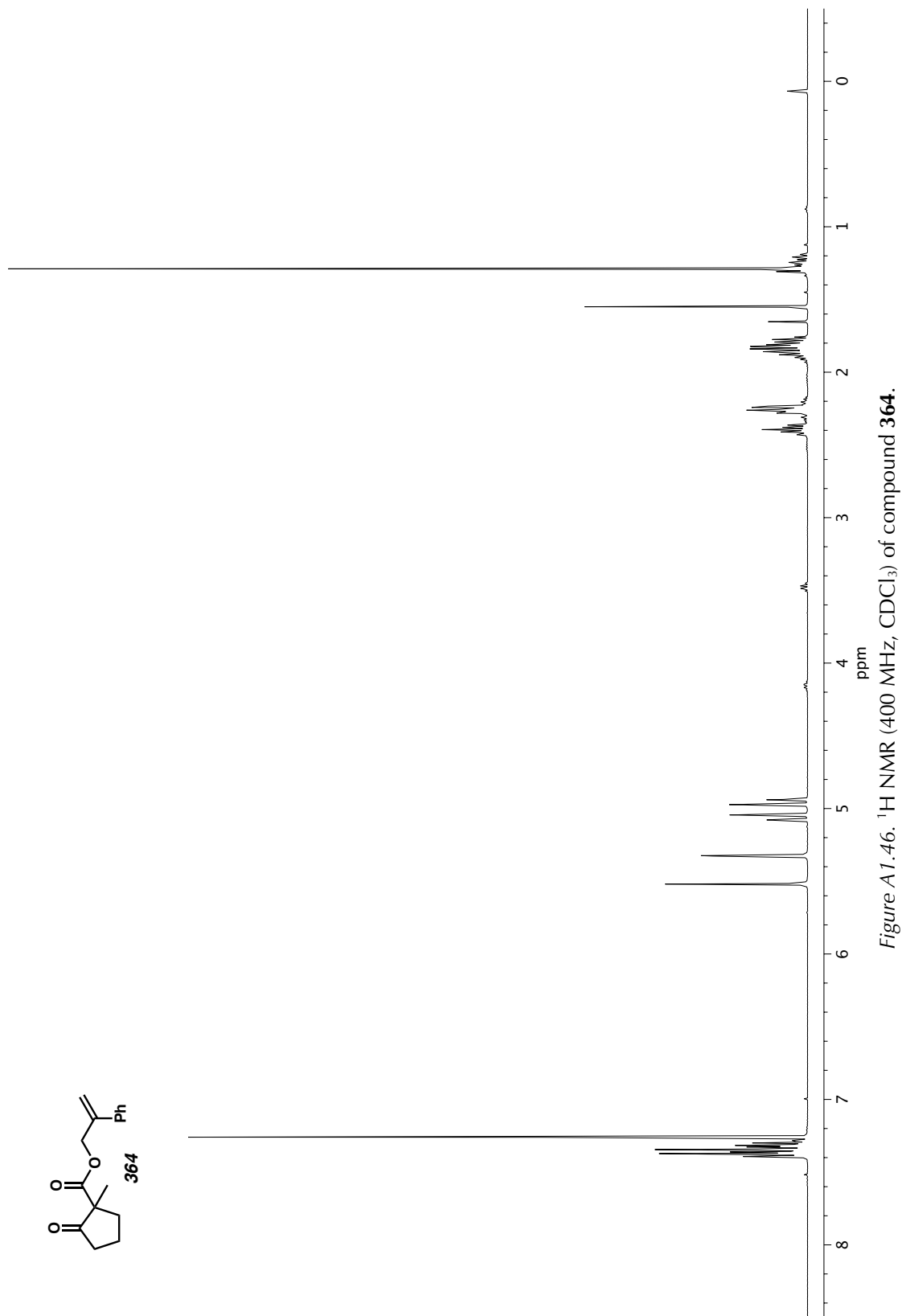
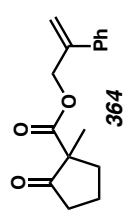


Figure A1.46. ^1H NMR (400 MHz, CDCl_3) of compound 364.

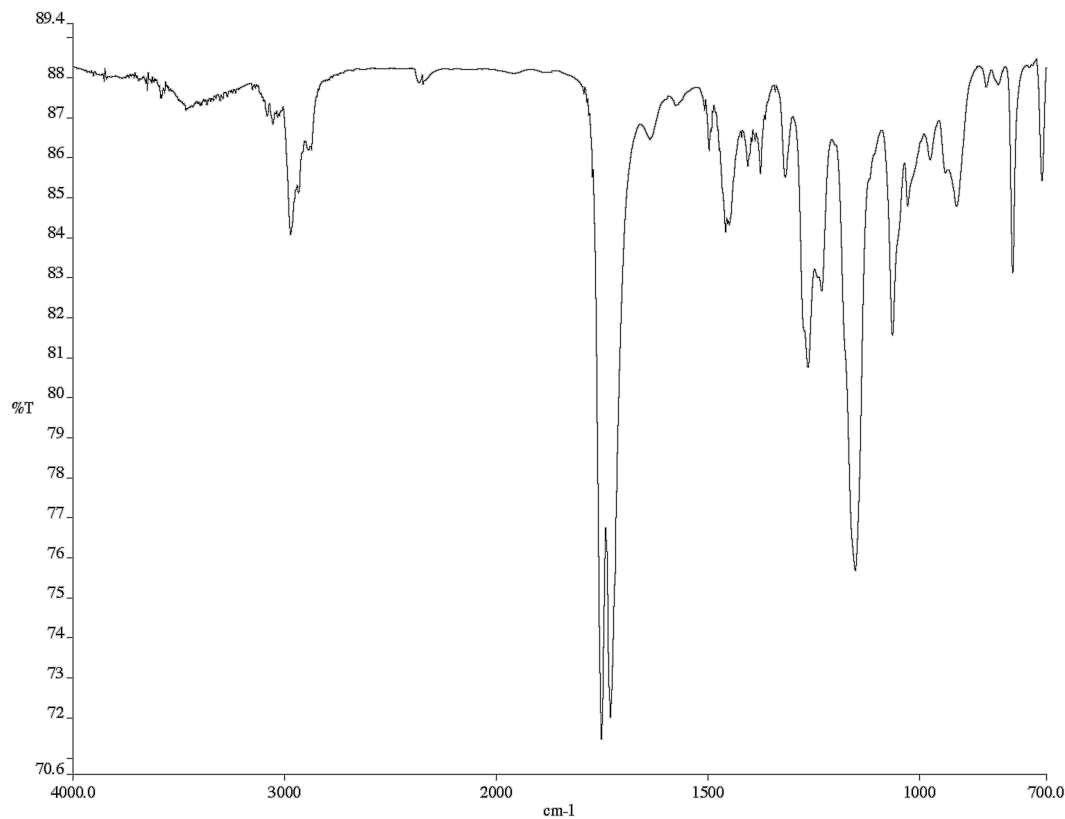


Figure A1.47. Infrared spectrum (Thin Film, NaCl) of compound 364.

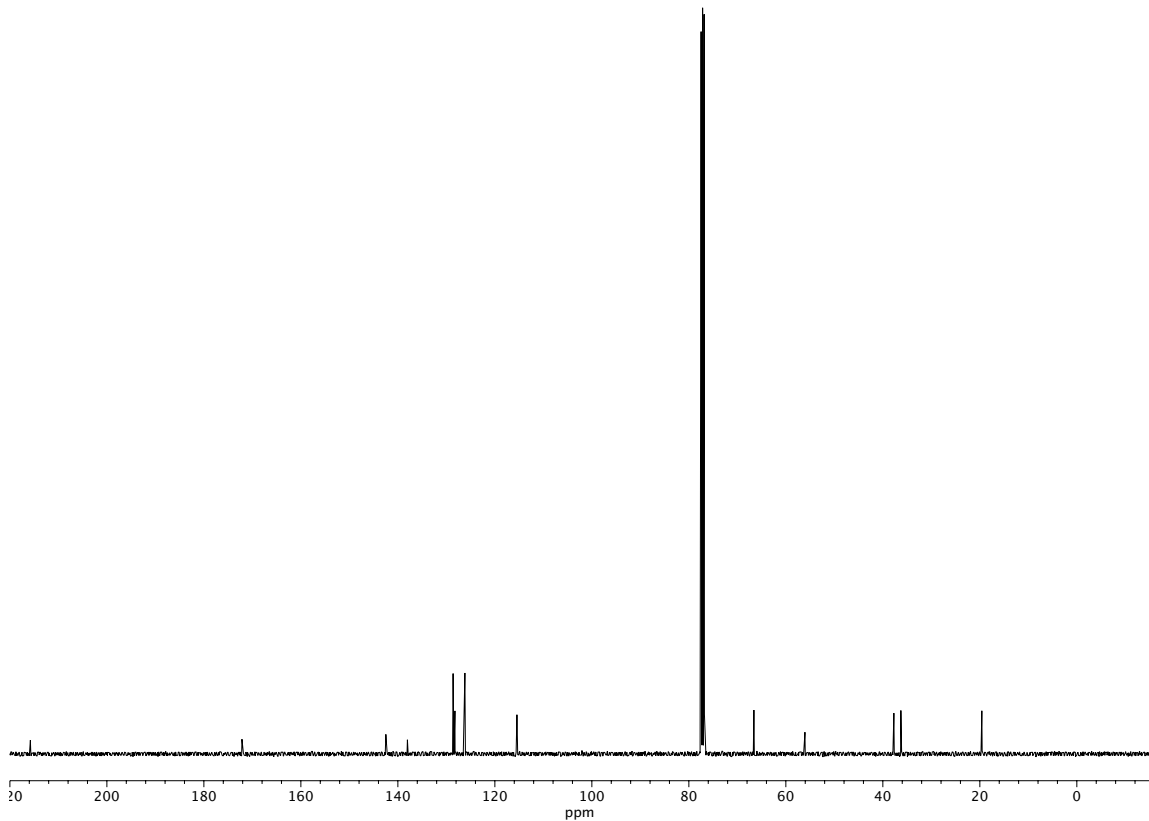
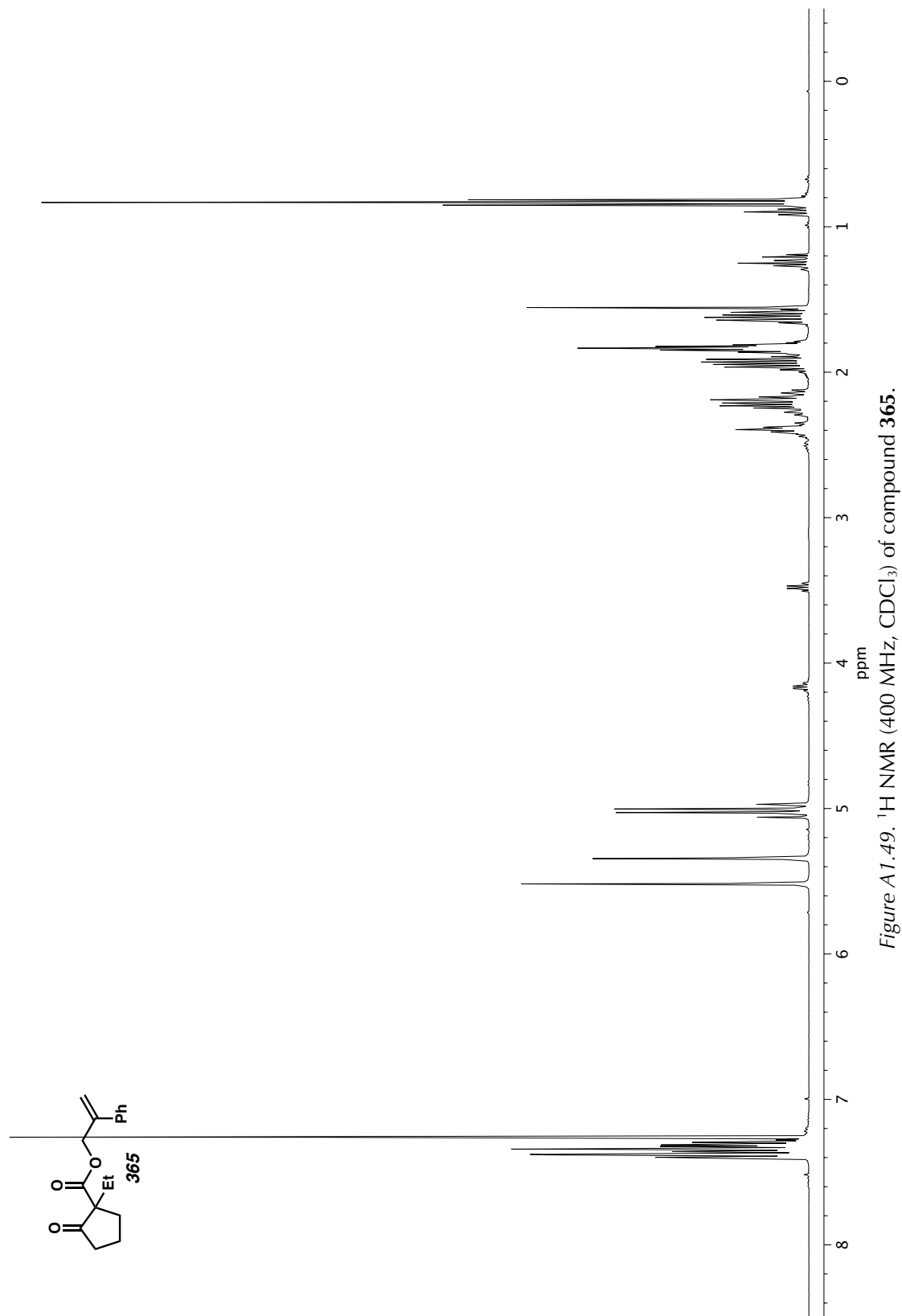


Figure A1.48. ^{13}C NMR (101 MHz, CDCl_3) of compound 364.



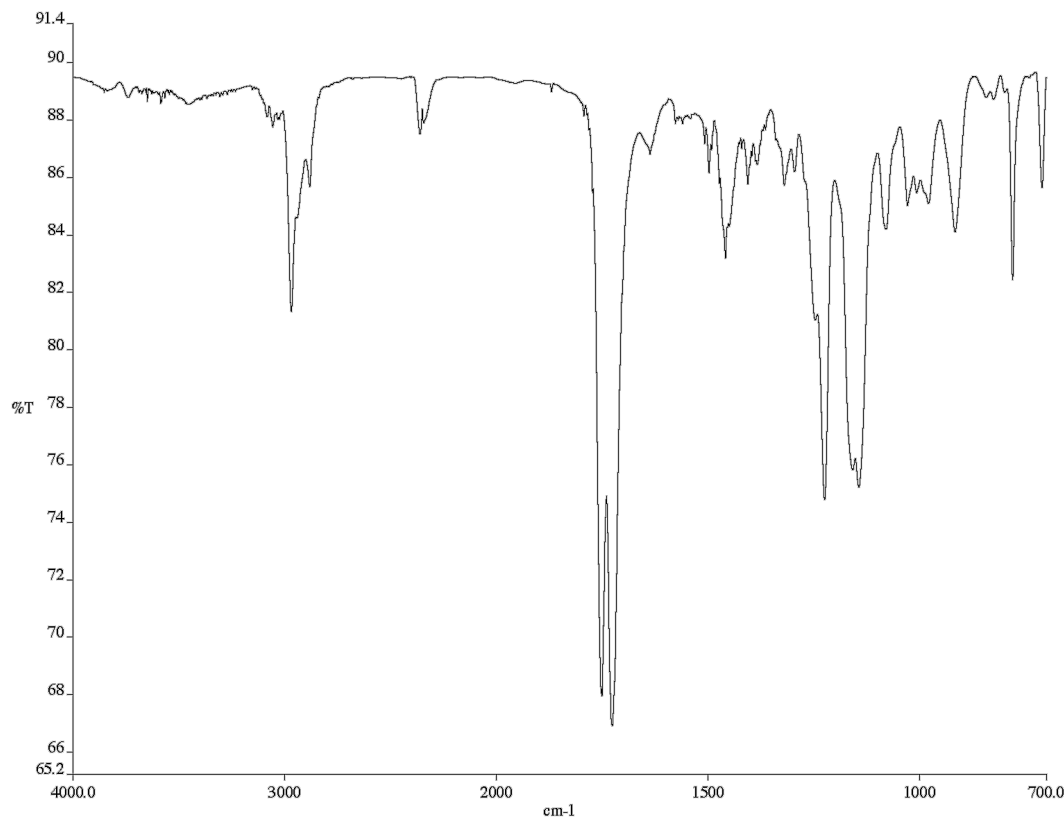


Figure A1.50. Infrared spectrum (Thin Film, NaCl) of compound 365.

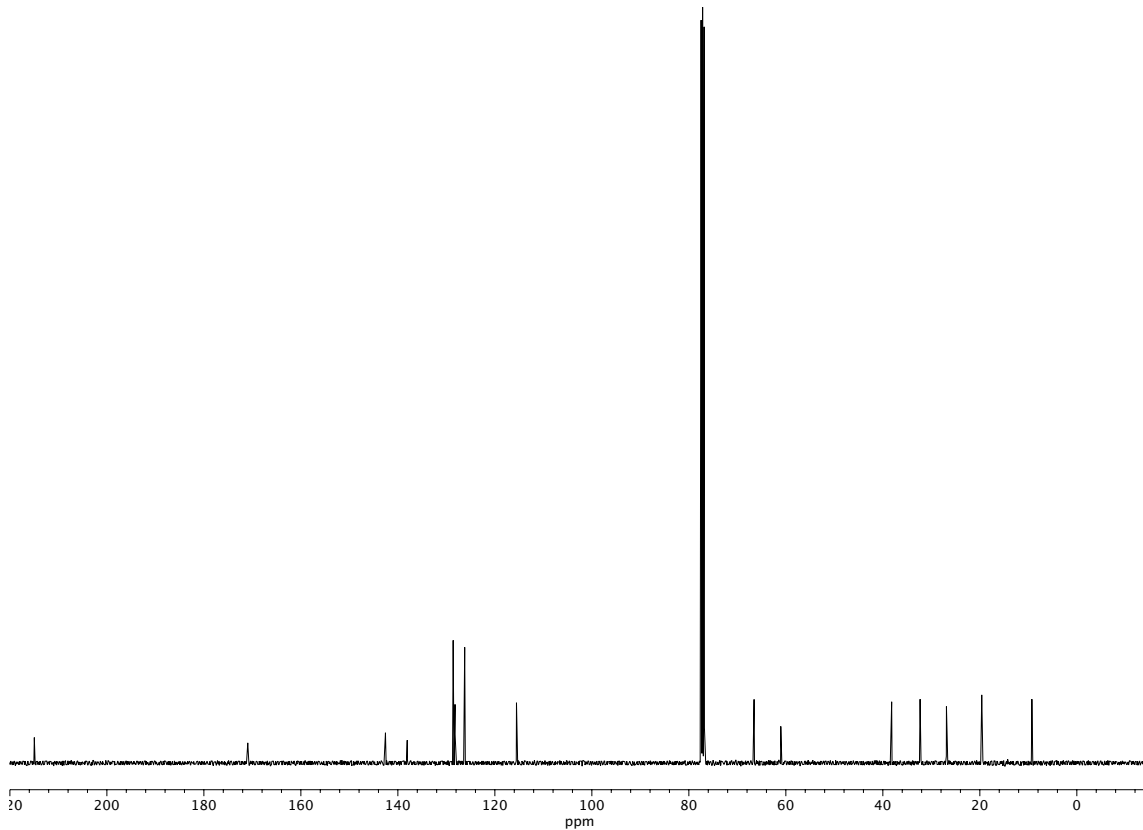


Figure A1.51. ¹³C NMR (101 MHz, CDCl₃) of compound 365.

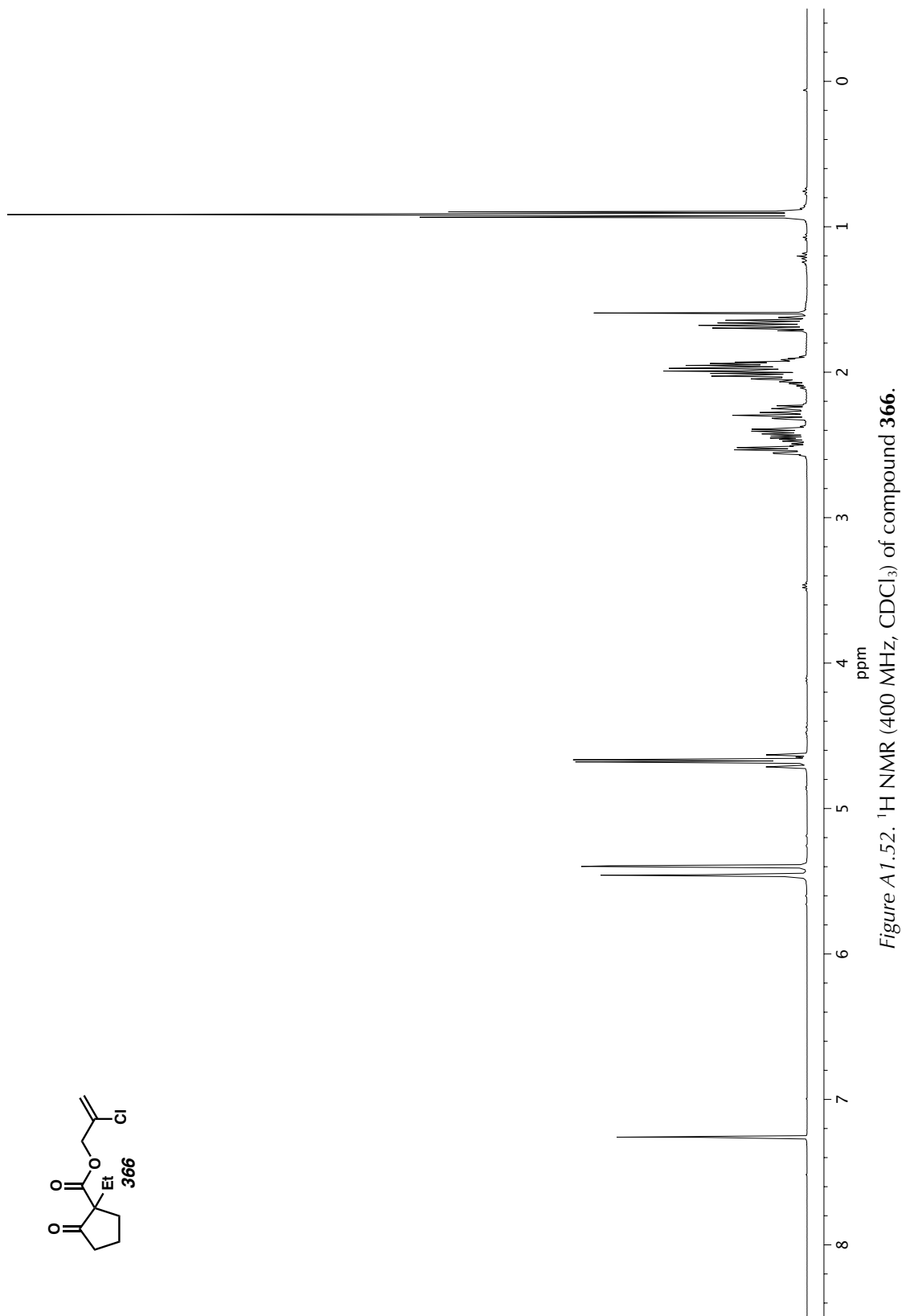


Figure A1.52. ^1H NMR (400 MHz, CDCl_3) of compound 366.

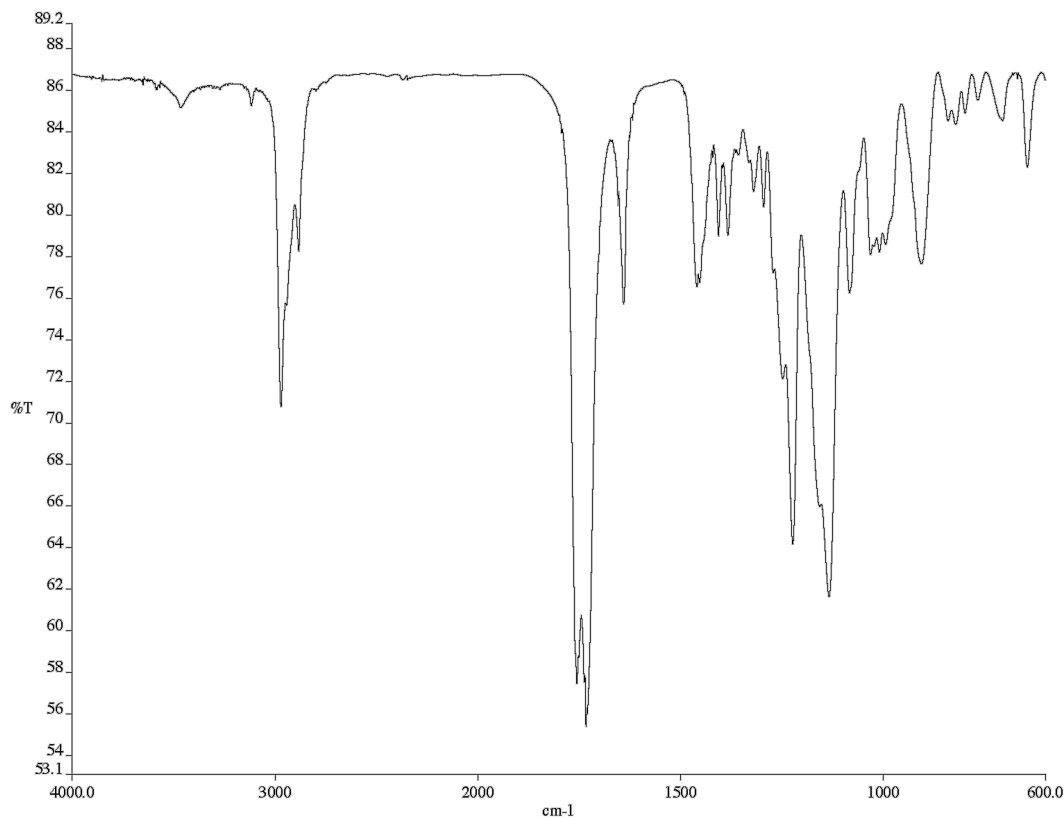


Figure A1.53. Infrared spectrum (Thin Film, NaCl) of compound 366.

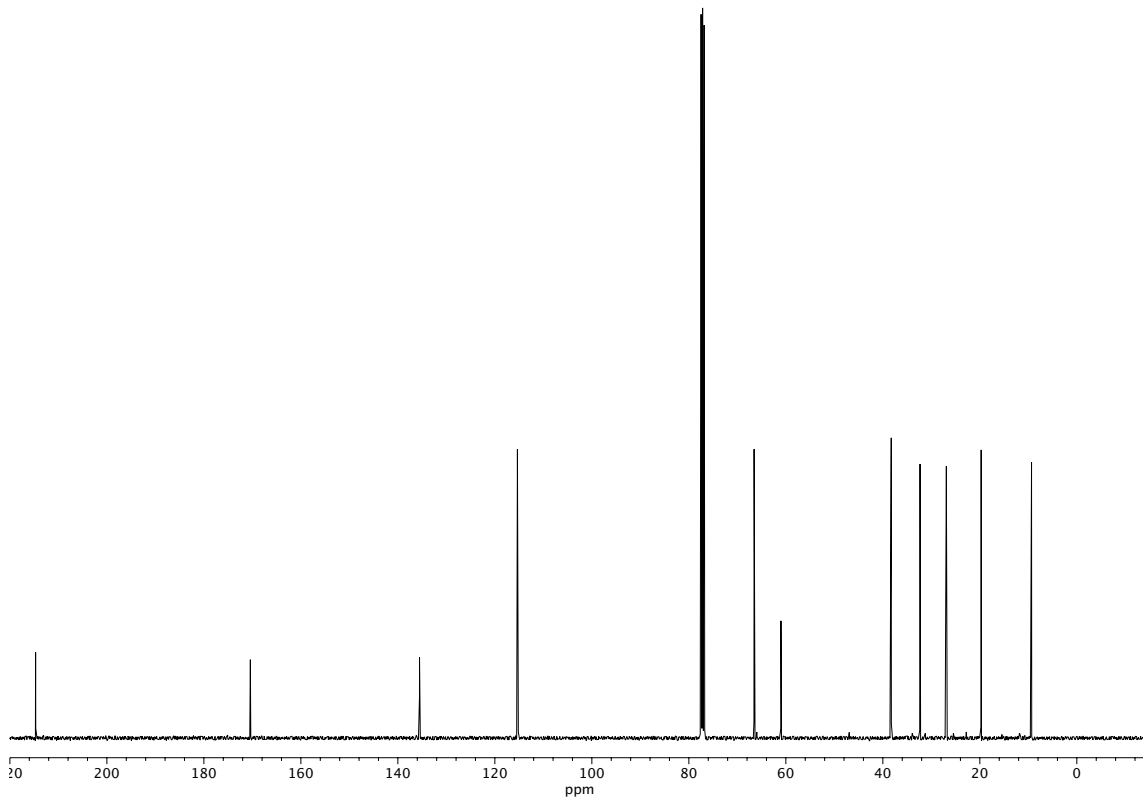


Figure A1.54. ^{13}C NMR (101 MHz, CDCl_3) of compound 366.

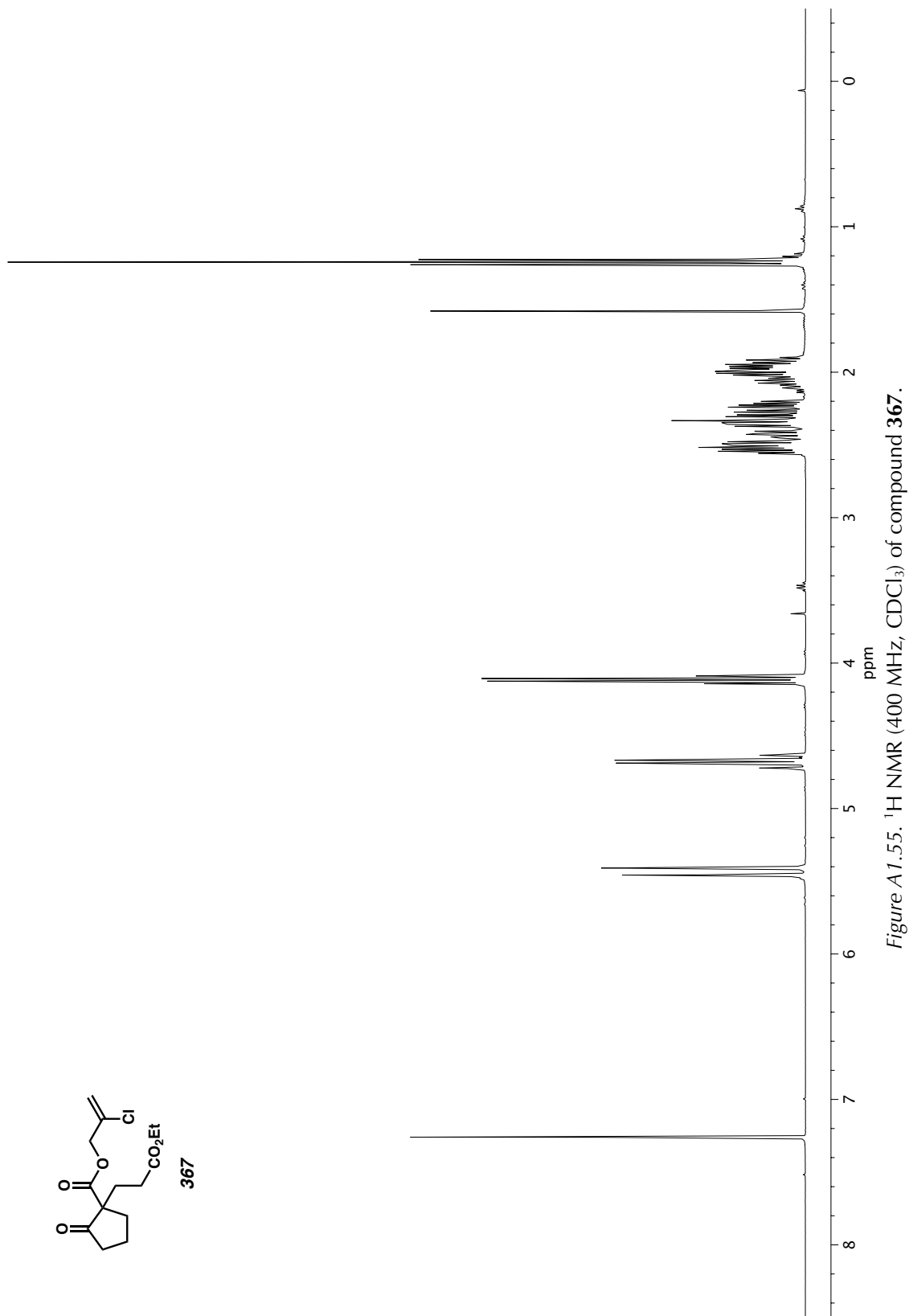
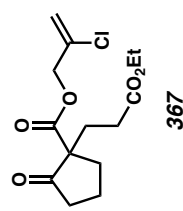


Figure A1.55. ¹H NMR (400 MHz, CDCl₃) of compound 367.

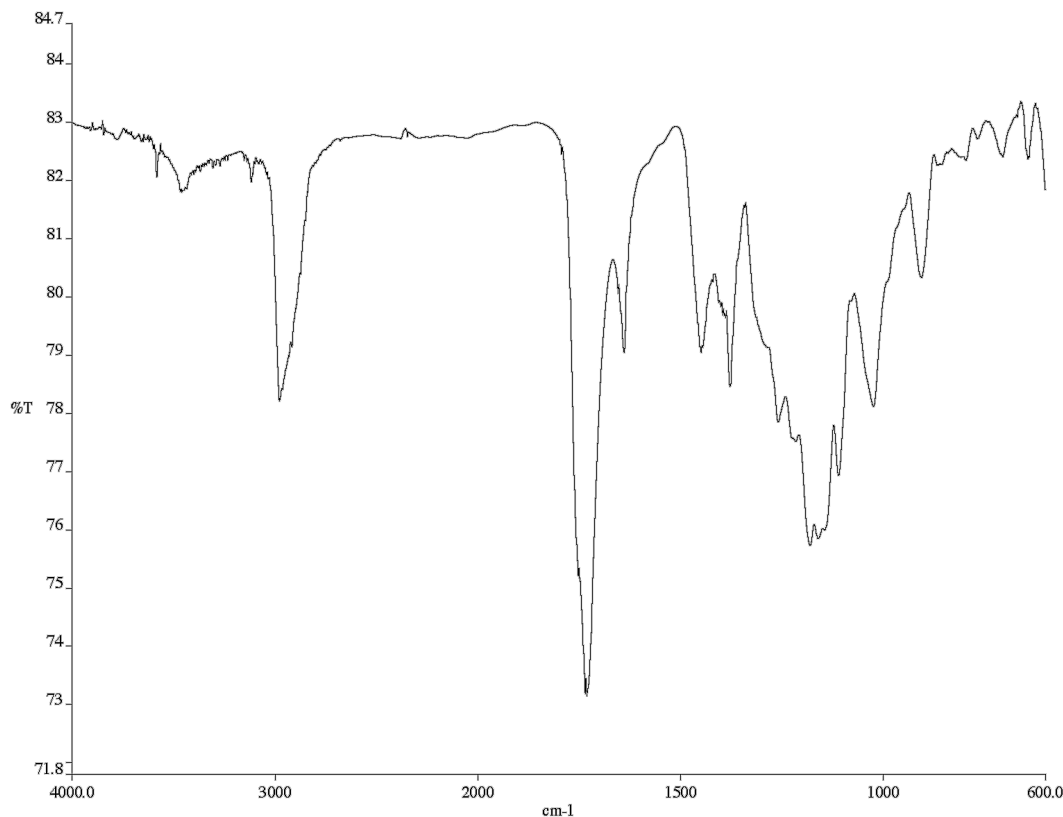


Figure A1.56. Infrared spectrum (Thin Film, NaCl) of compound 367.

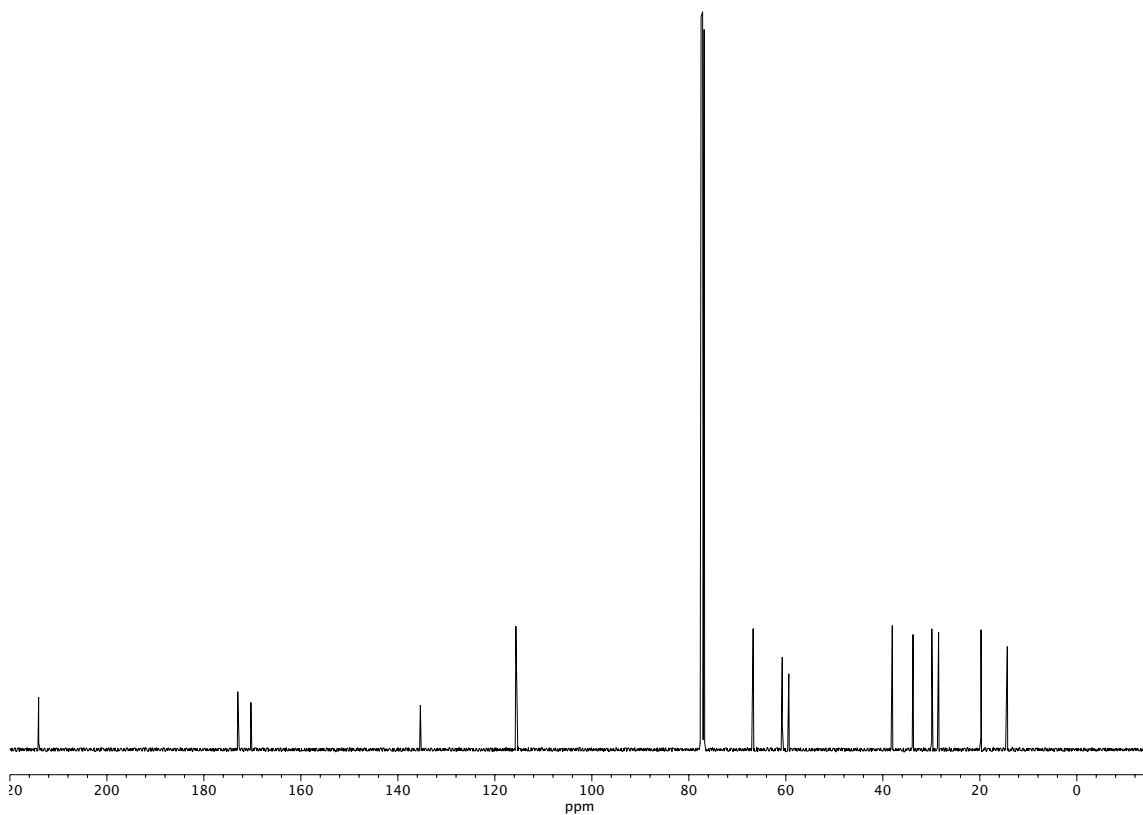


Figure A1.57. ^{13}C NMR (101 MHz, CDCl_3) of compound 367.

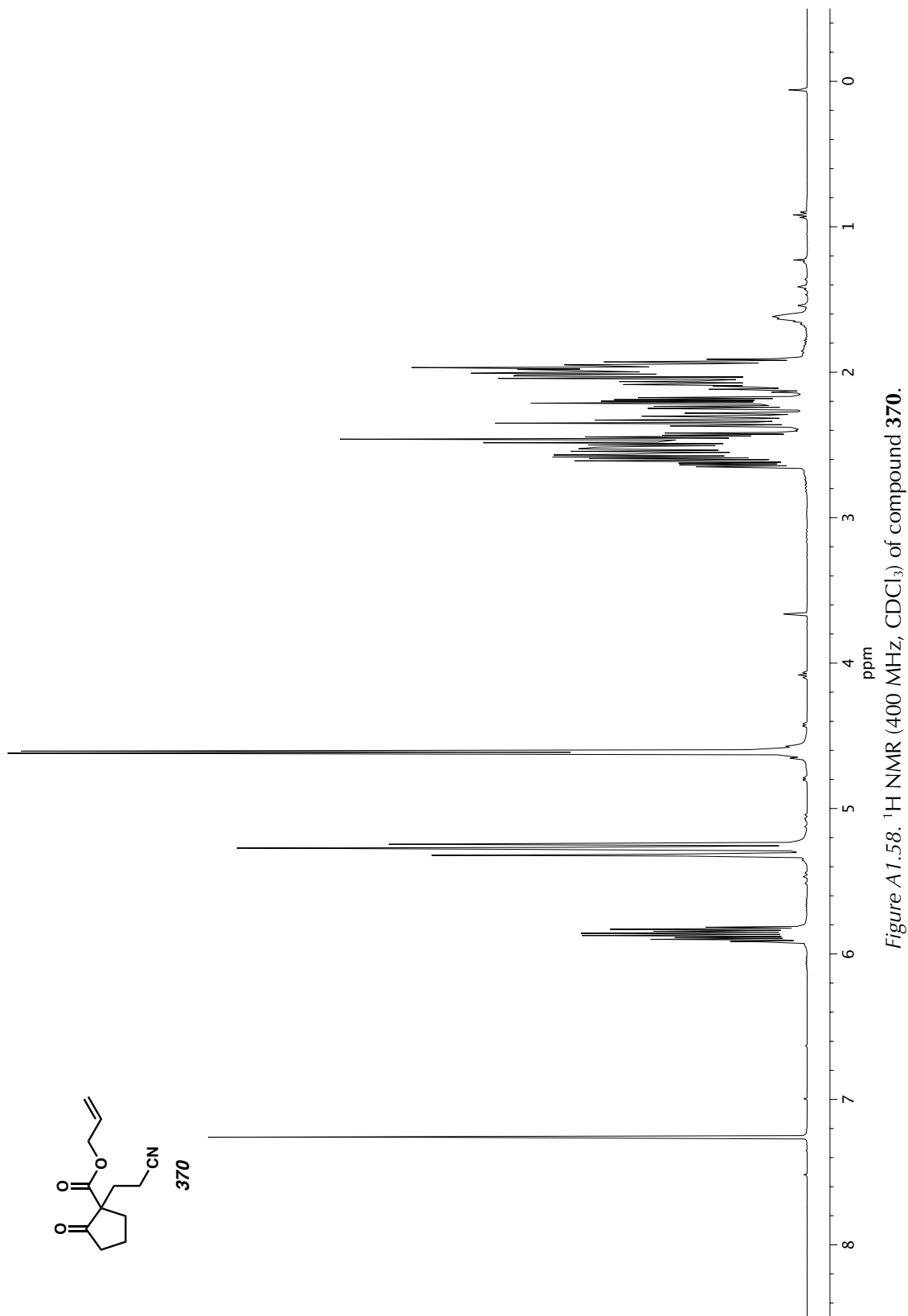


Figure A1.58. ^1H NMR (400 MHz, CDCl_3) of compound 370.

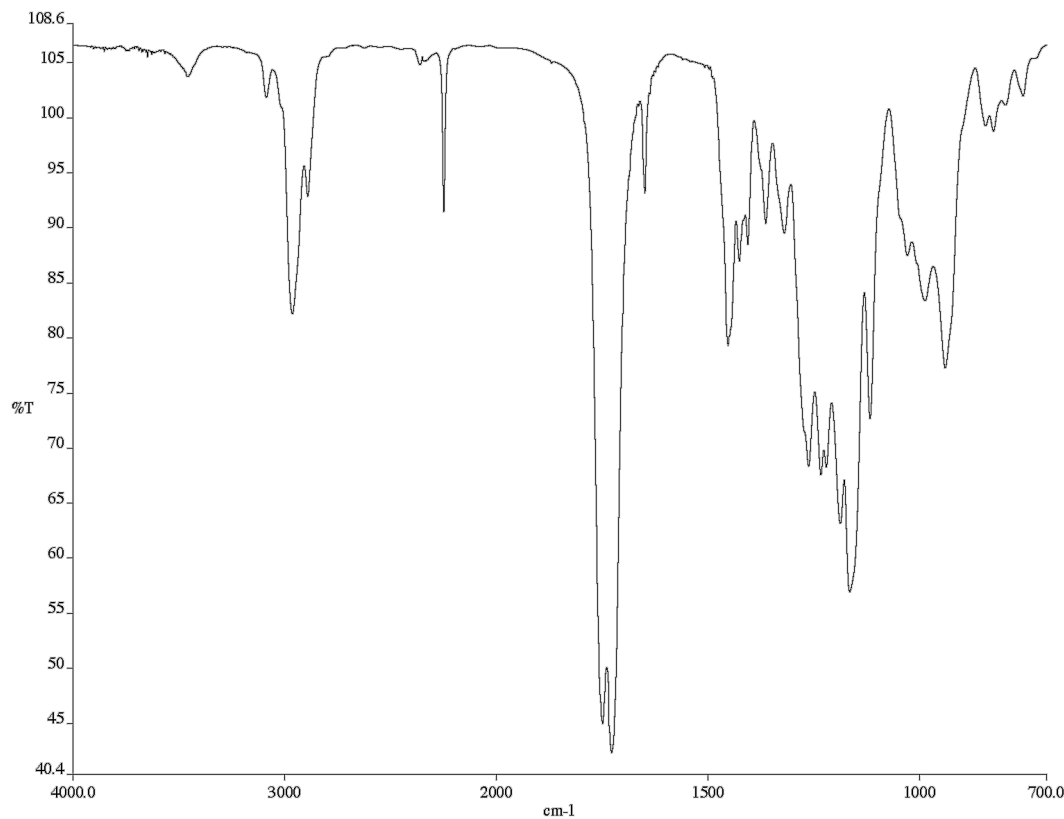


Figure A1.59. Infrared spectrum (Thin Film, NaCl) of compound **370**.

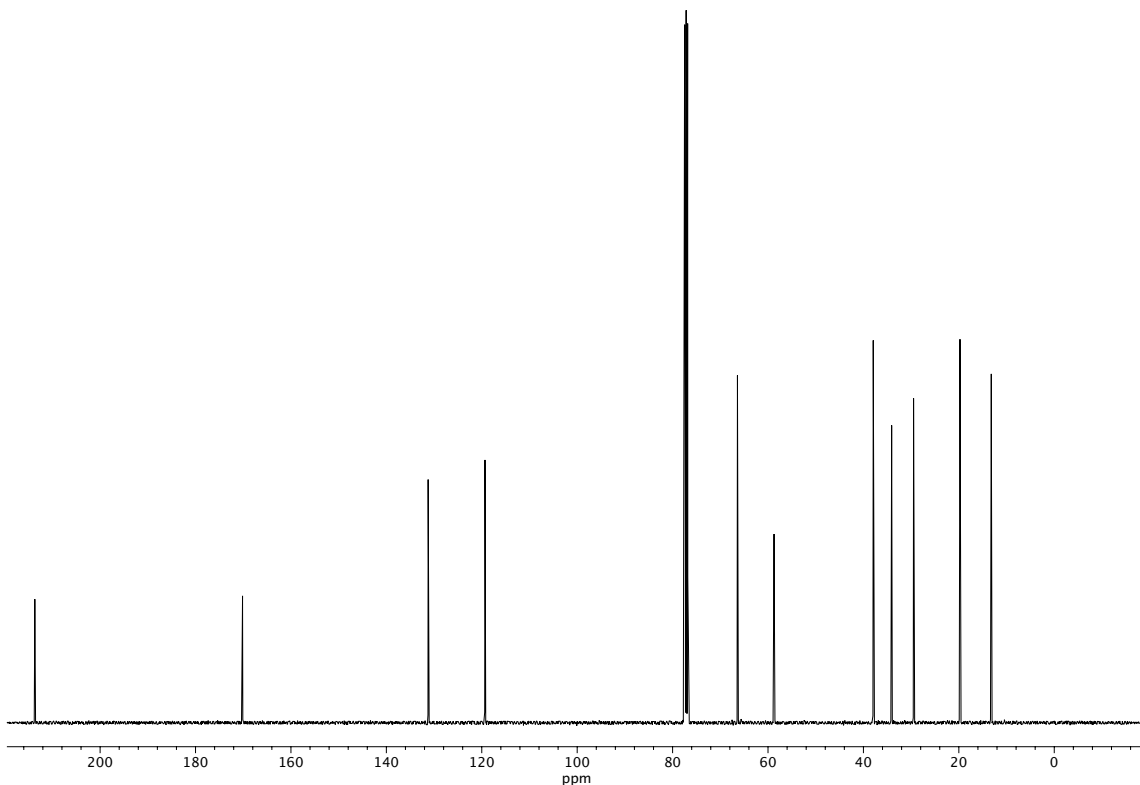
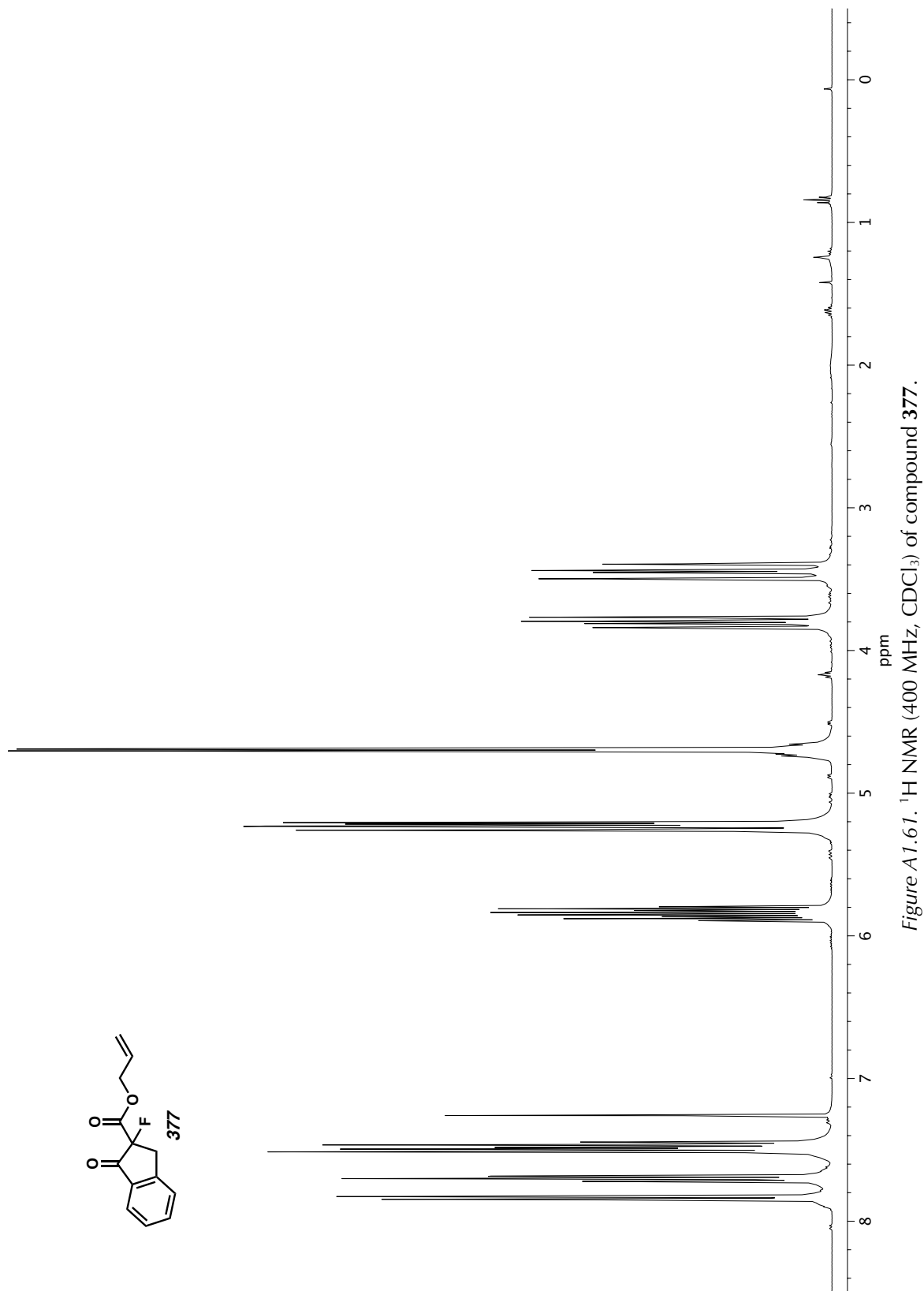


Figure A1.60. ^{13}C NMR (101 MHz, CDCl_3) of compound **370**.



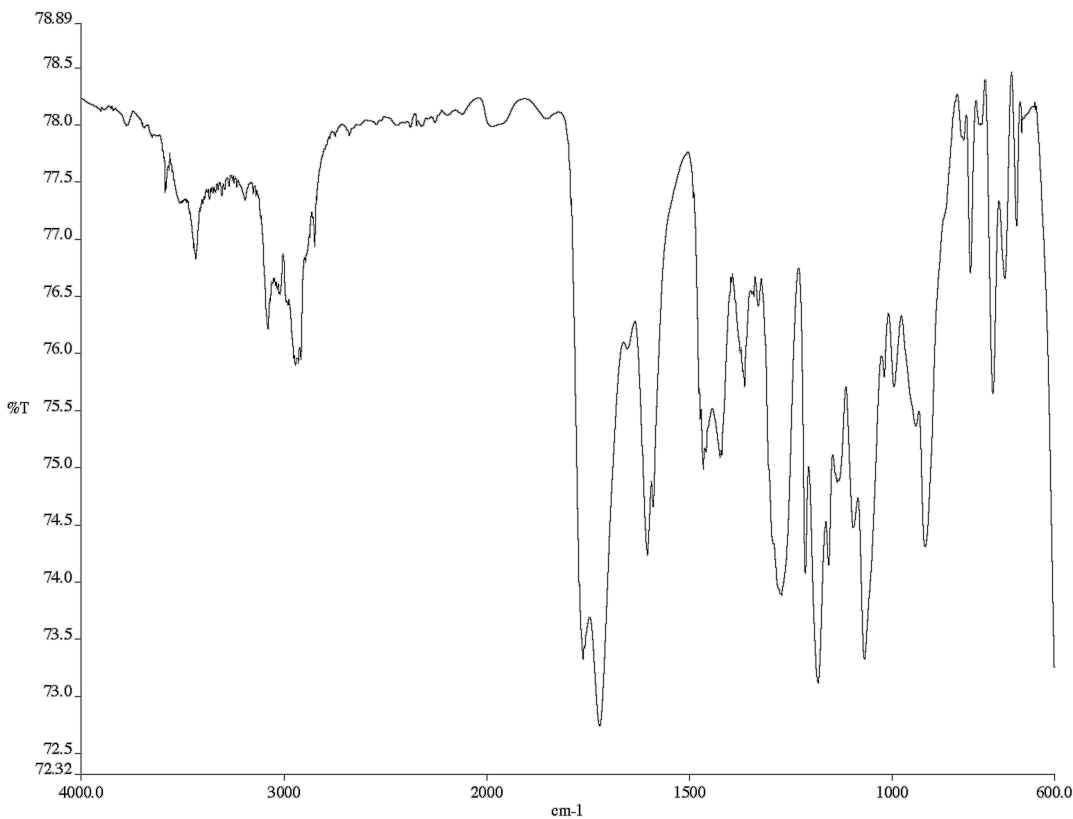


Figure A1.62. Infrared spectrum (Thin Film, NaCl) of compound 377.

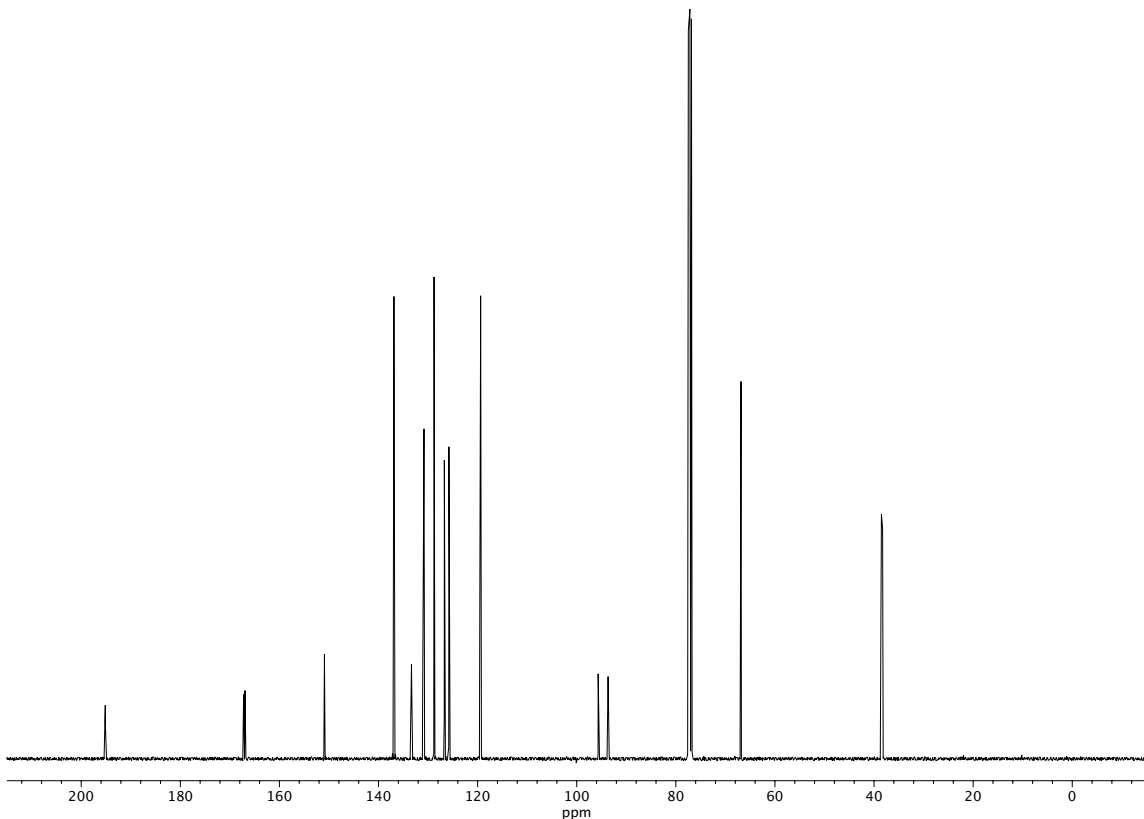


Figure A1.63. ^{13}C NMR (101 MHz, CDCl_3) of compound 377.

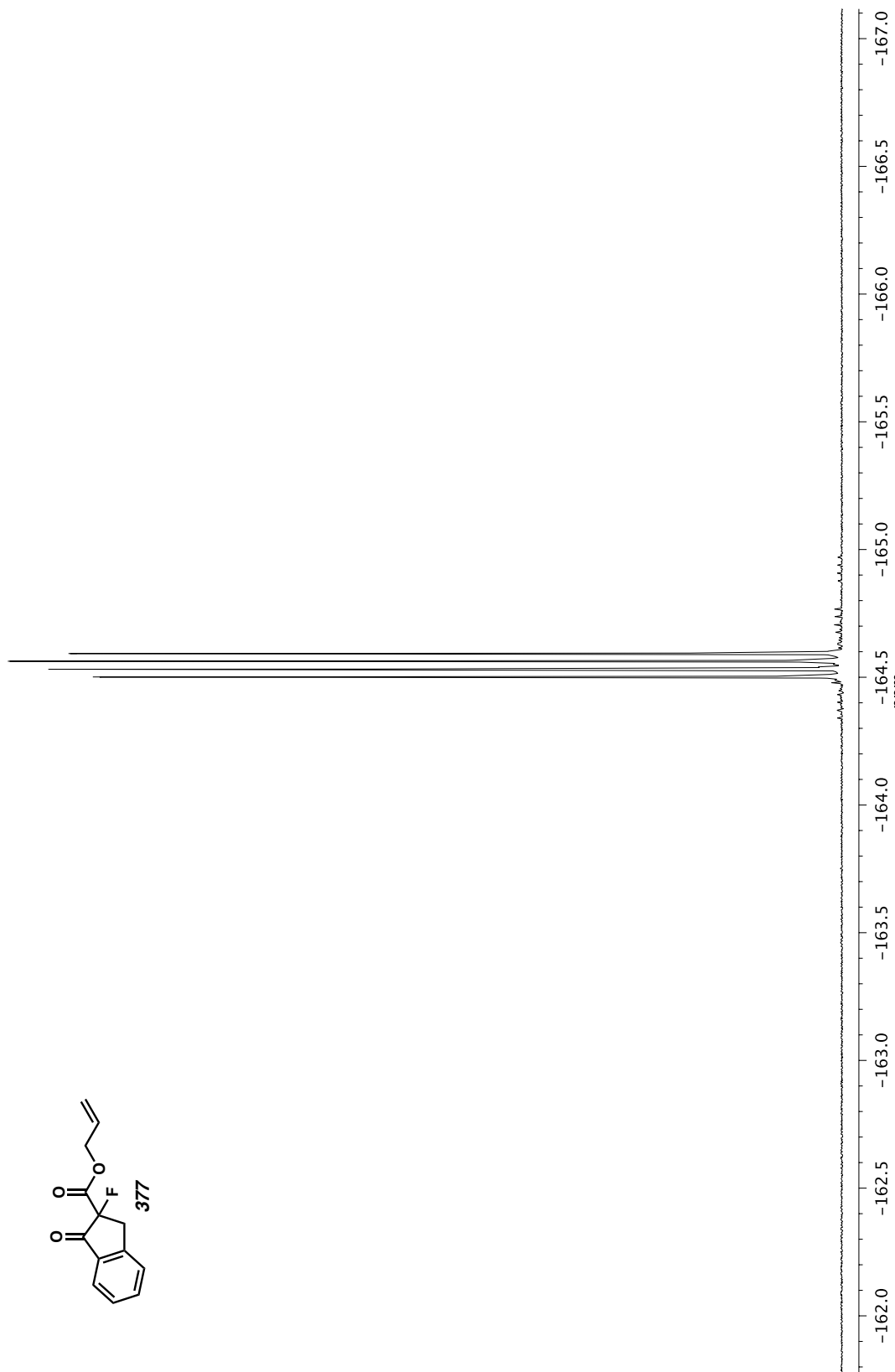


Figure A1.64. ^{19}F NMR (470 MHz, CDCl_3) of compound 377.

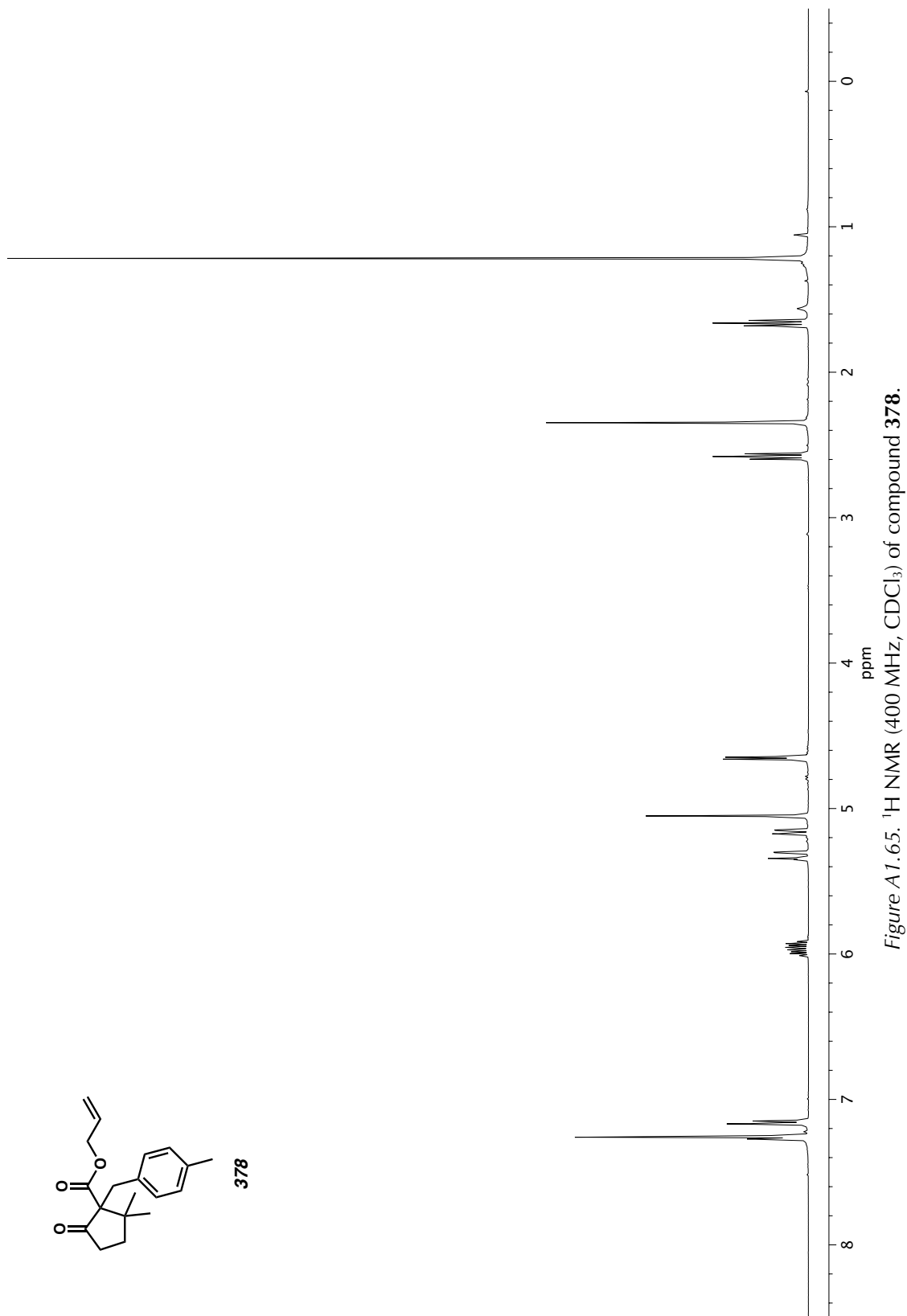
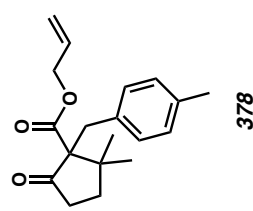


Figure A1.65. ^1H NMR (400 MHz, CDCl_3) of compound 378.

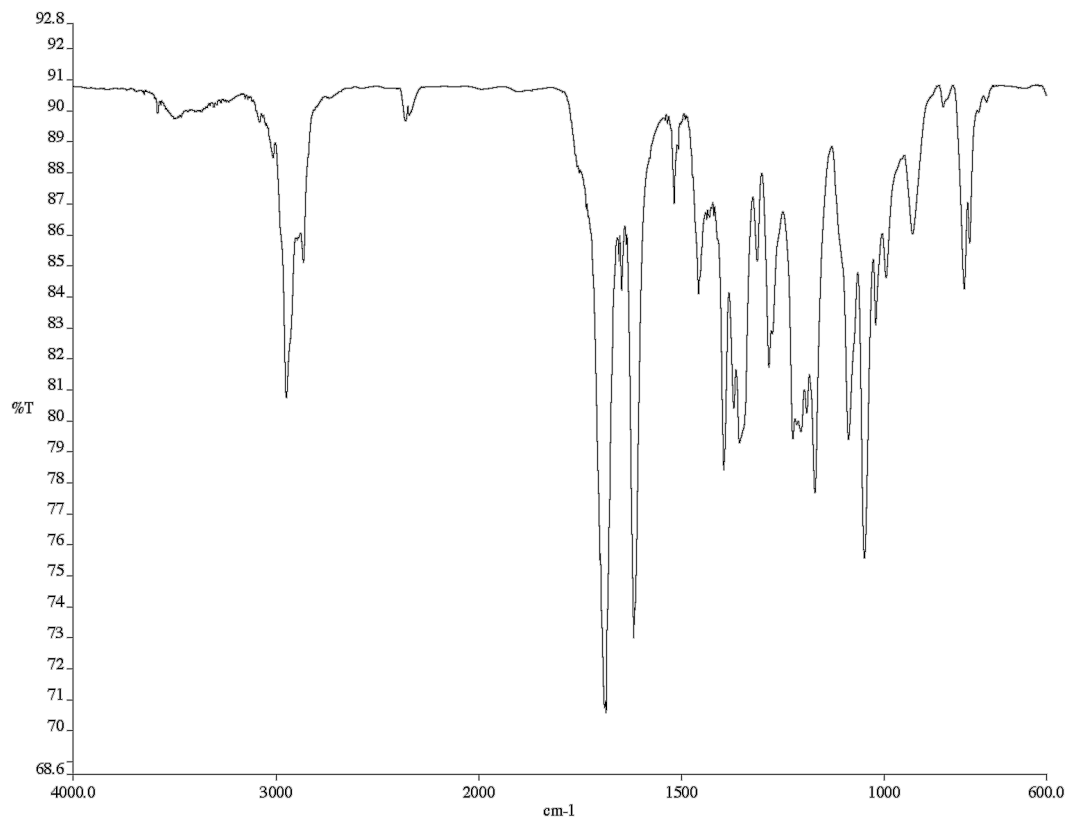


Figure A1.66. Infrared spectrum (Thin Film, NaCl) of compound 378.

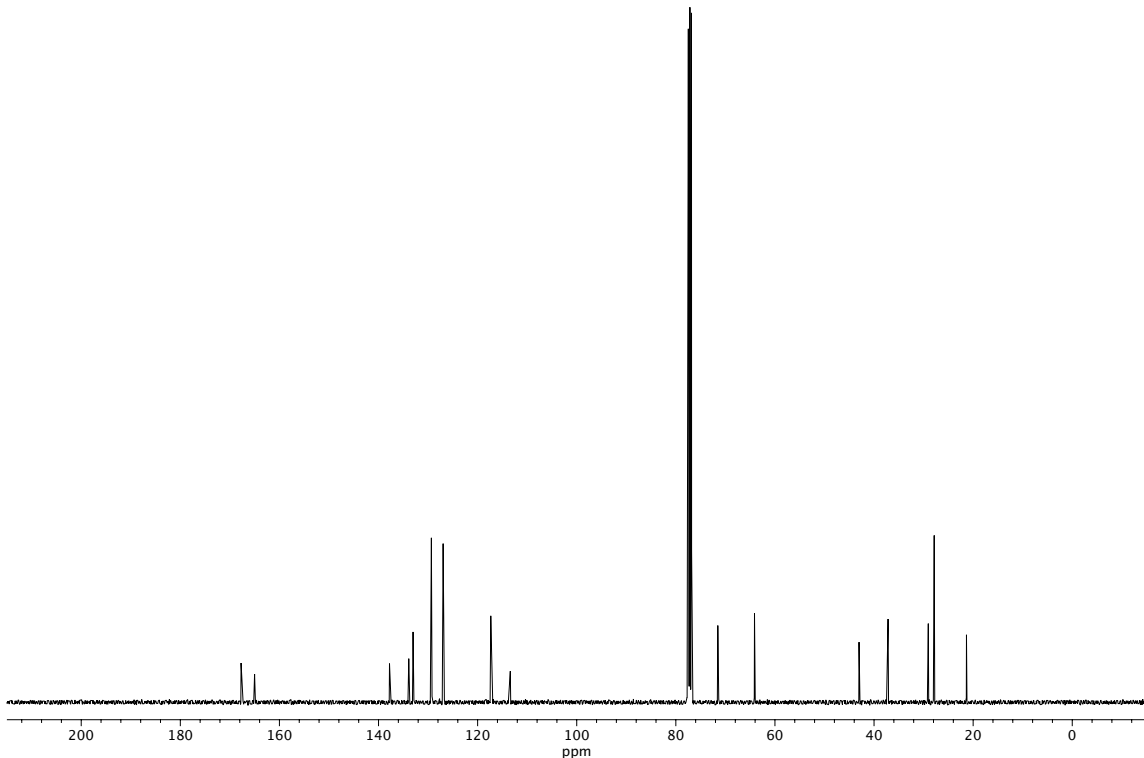
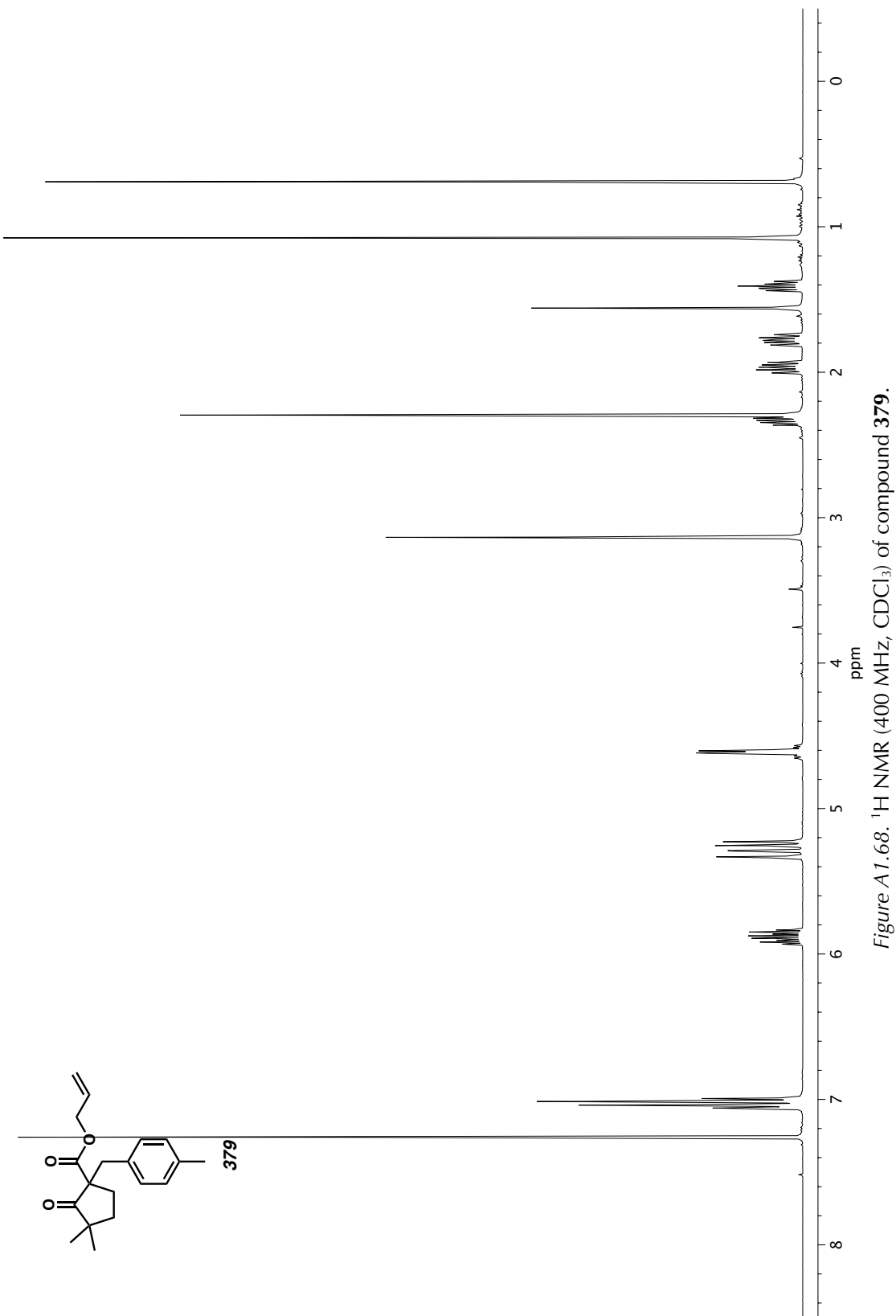


Figure A1.67. ^{13}C NMR (101 MHz, CDCl_3) of compound 378.



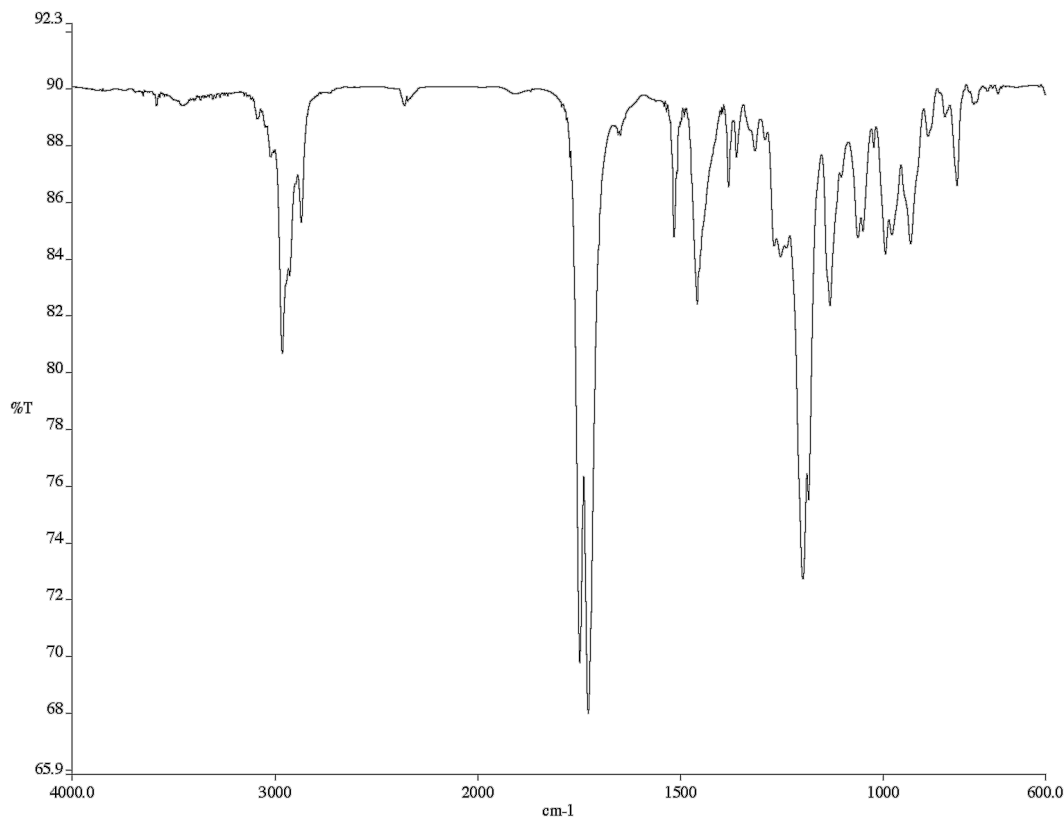


Figure A1.69. Infrared spectrum (Thin Film, NaCl) of compound 379.

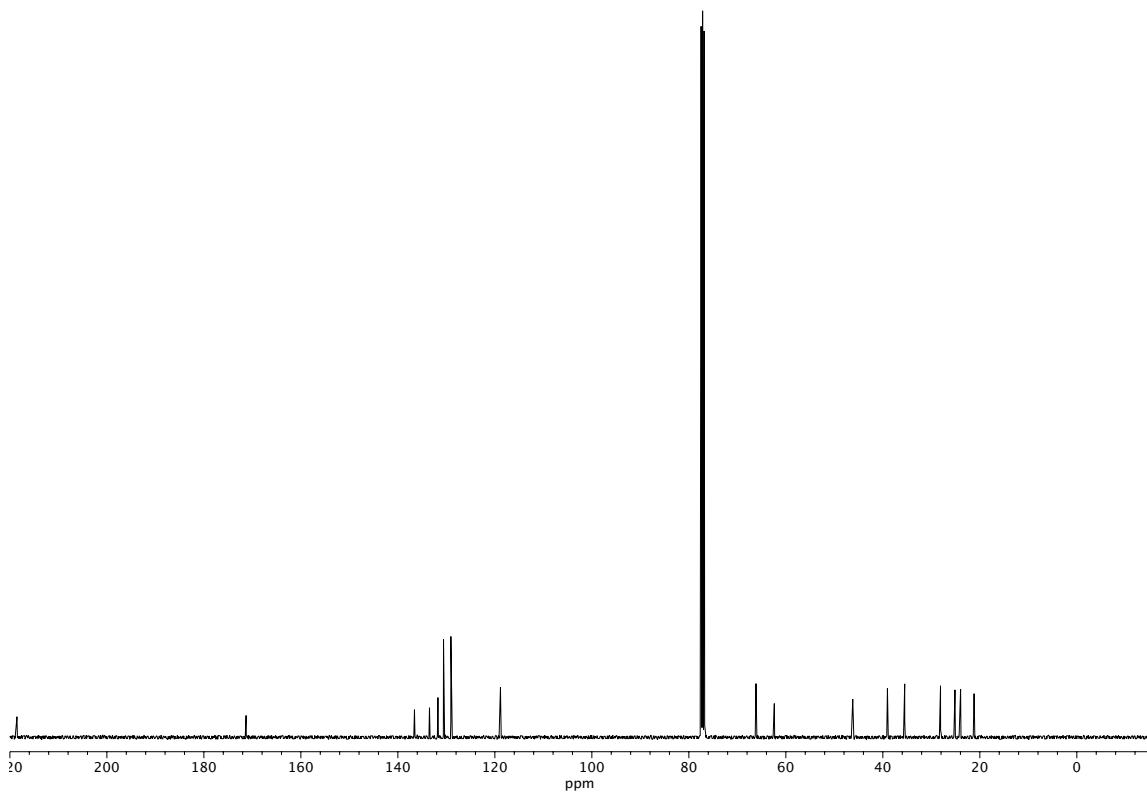


Figure A1.70. ^{13}C NMR (101 MHz, CDCl_3) of compound 379.

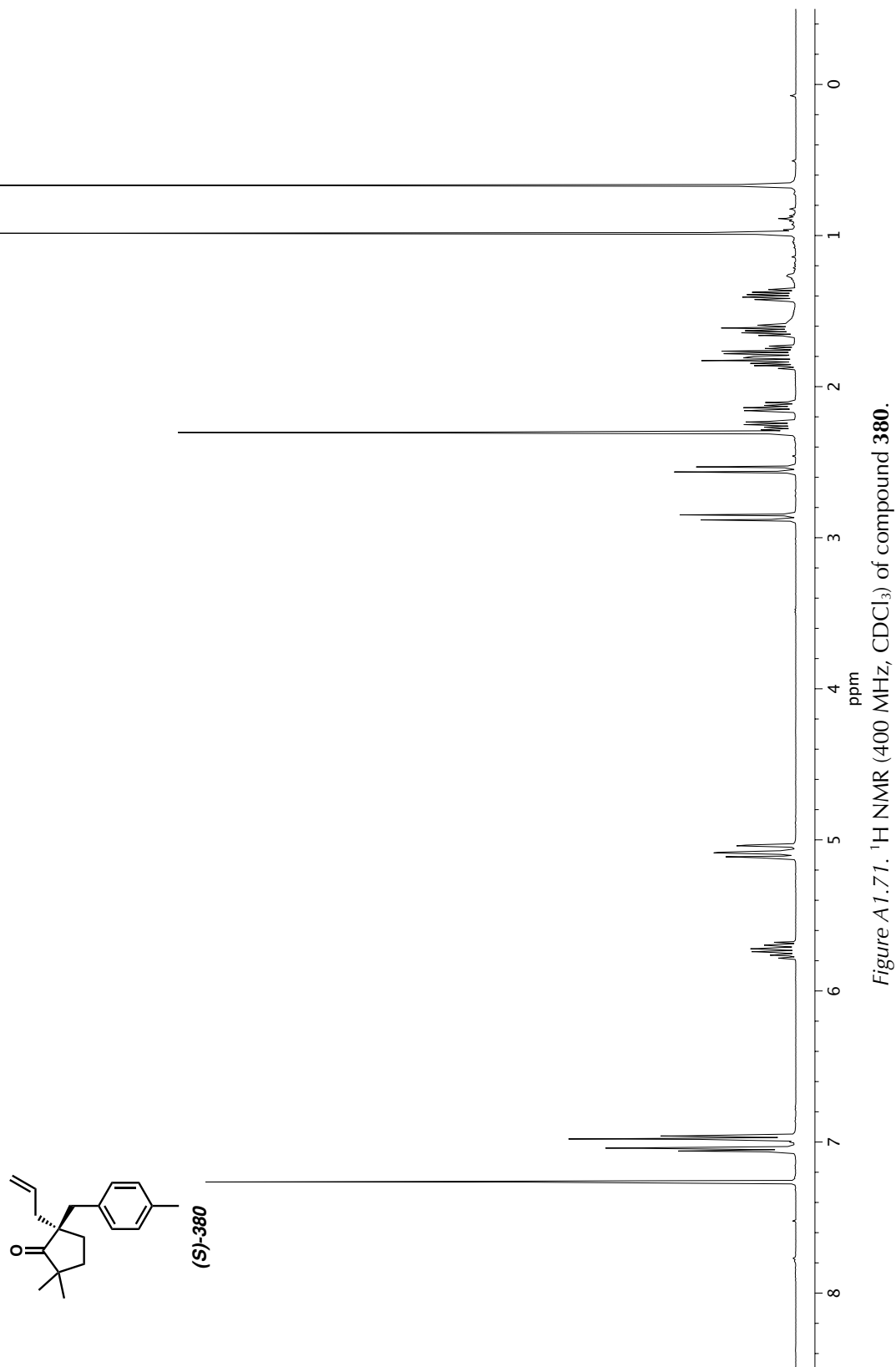


Figure A1.7.1. ^1H NMR (400 MHz, CDCl_3) of compound 380.

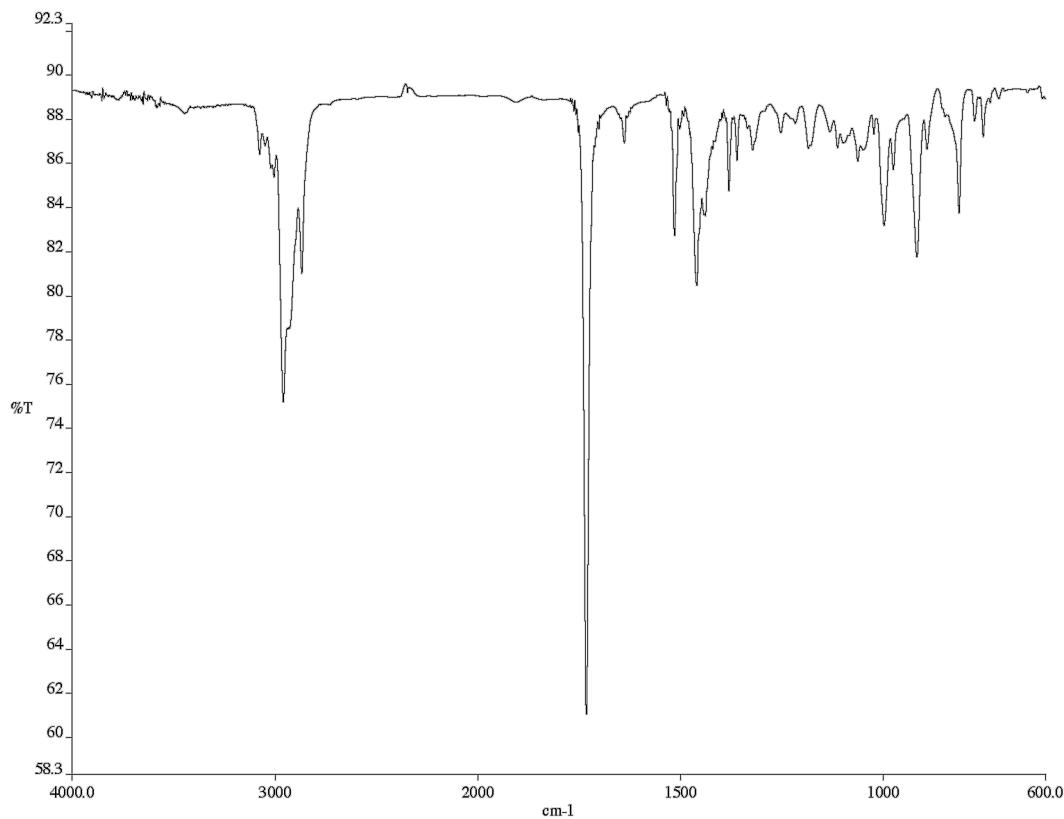


Figure A1.72. Infrared spectrum (Thin Film, NaCl) of compound **380**.

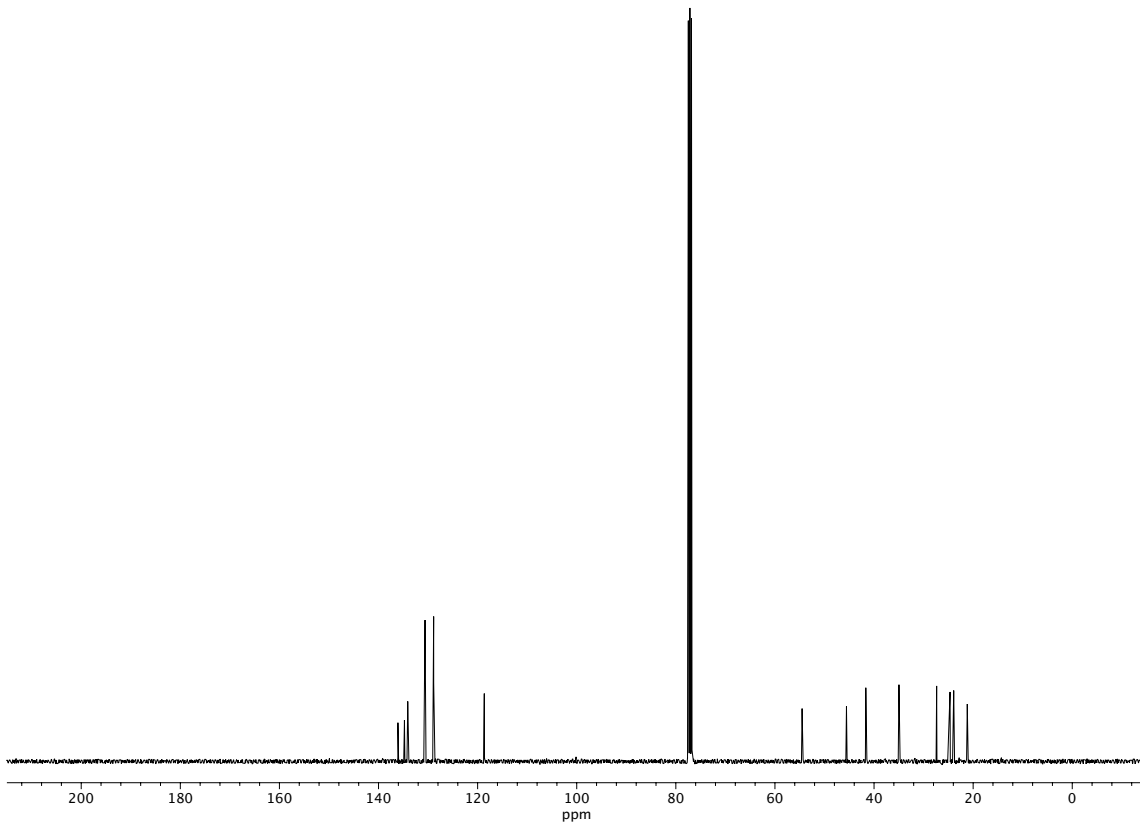


Figure A1.73. ^{13}C NMR (101 MHz, CDCl_3) of compound **380**.

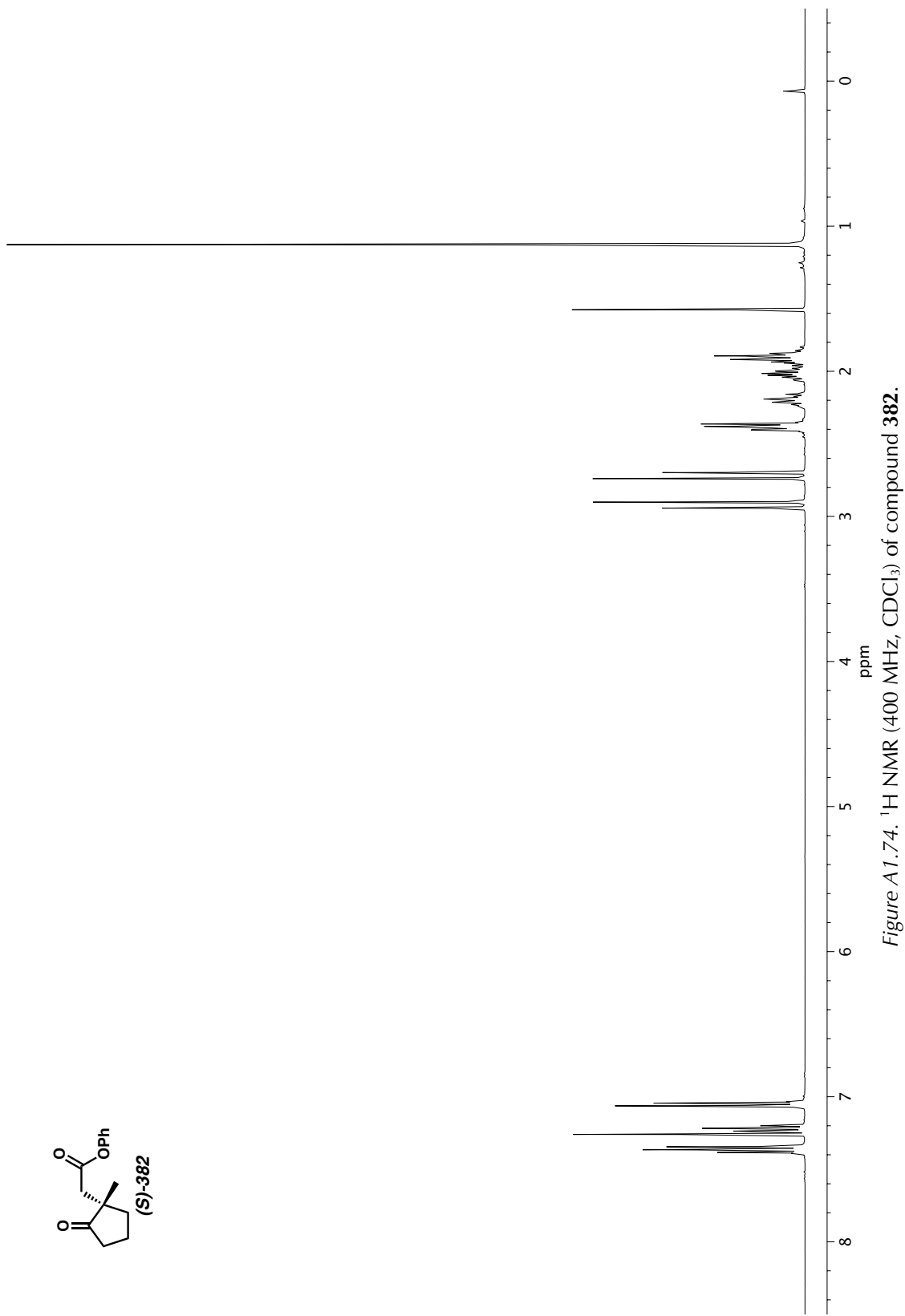
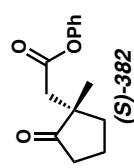


Figure A1.74. ^1H NMR (400 MHz, CDCl_3) of compound 382.

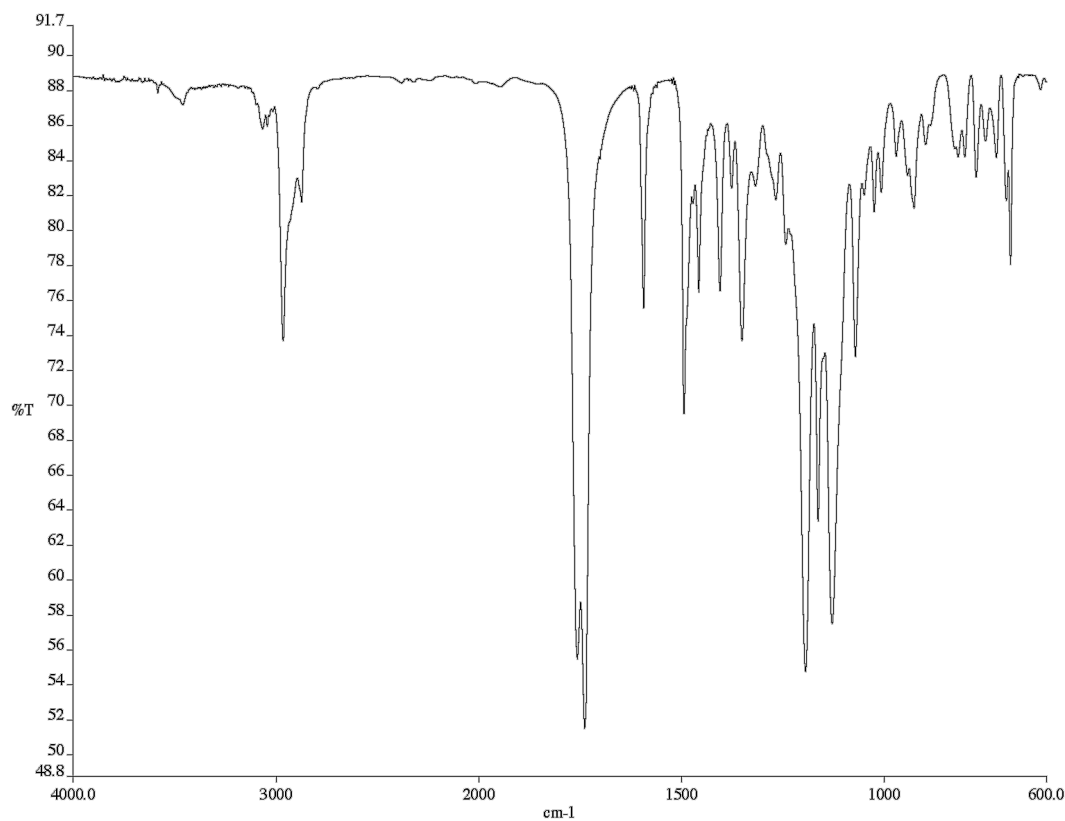


Figure A1.75. Infrared spectrum (Thin Film, NaCl) of compound 382.

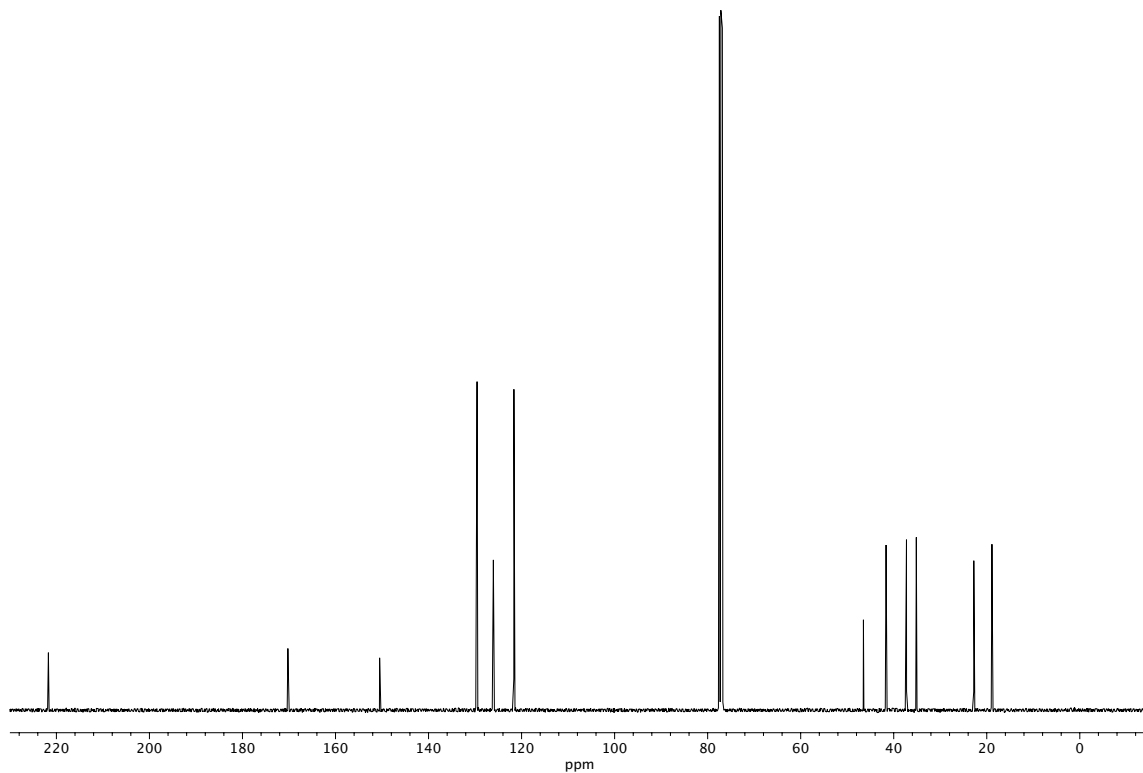


Figure A1.76. ¹³C NMR (101 MHz, CDCl₃) of compound 382.

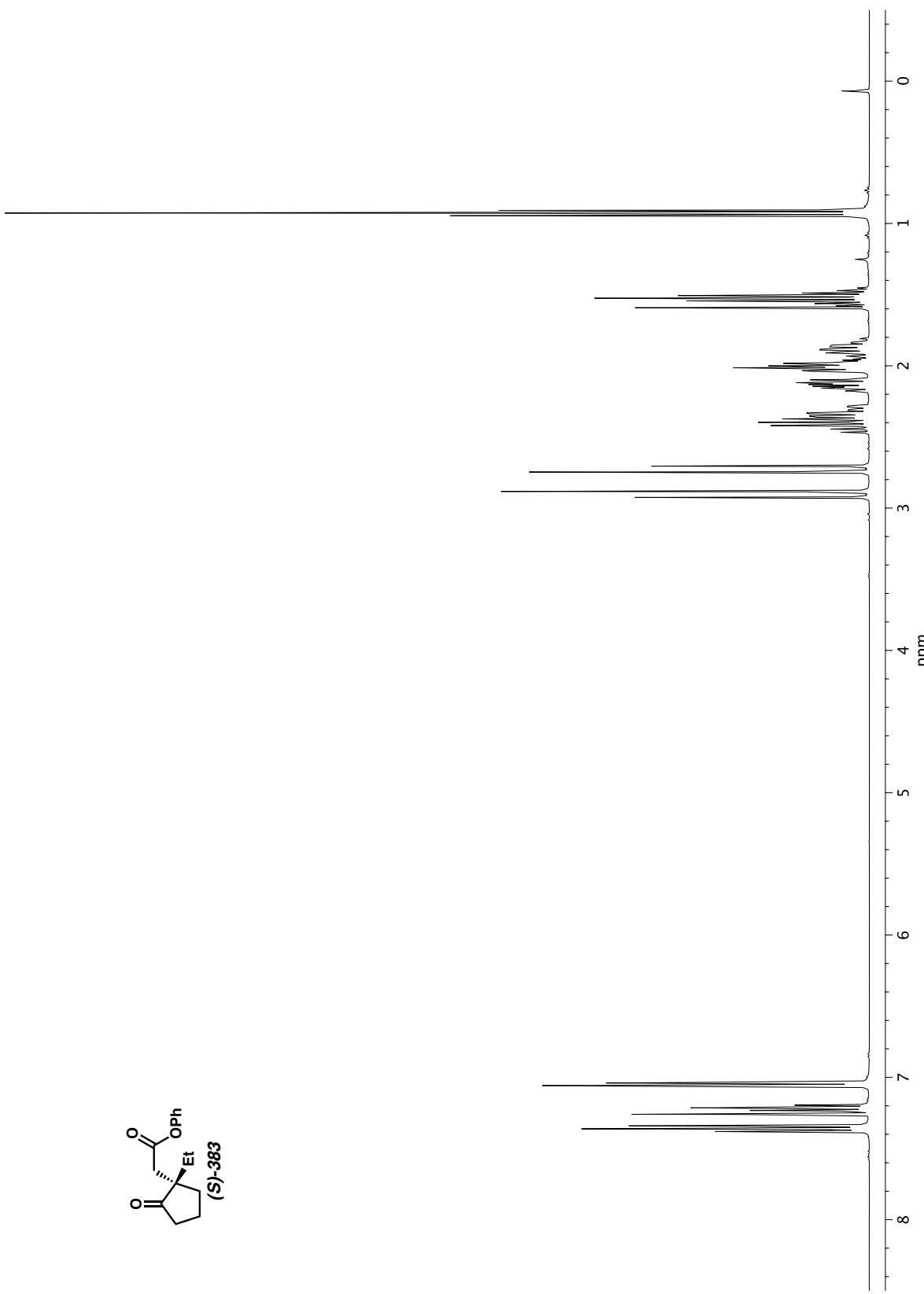
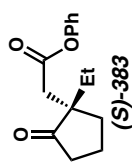


Figure A1.77. ^1H NMR (400 MHz, CDCl_3) of compound 383.

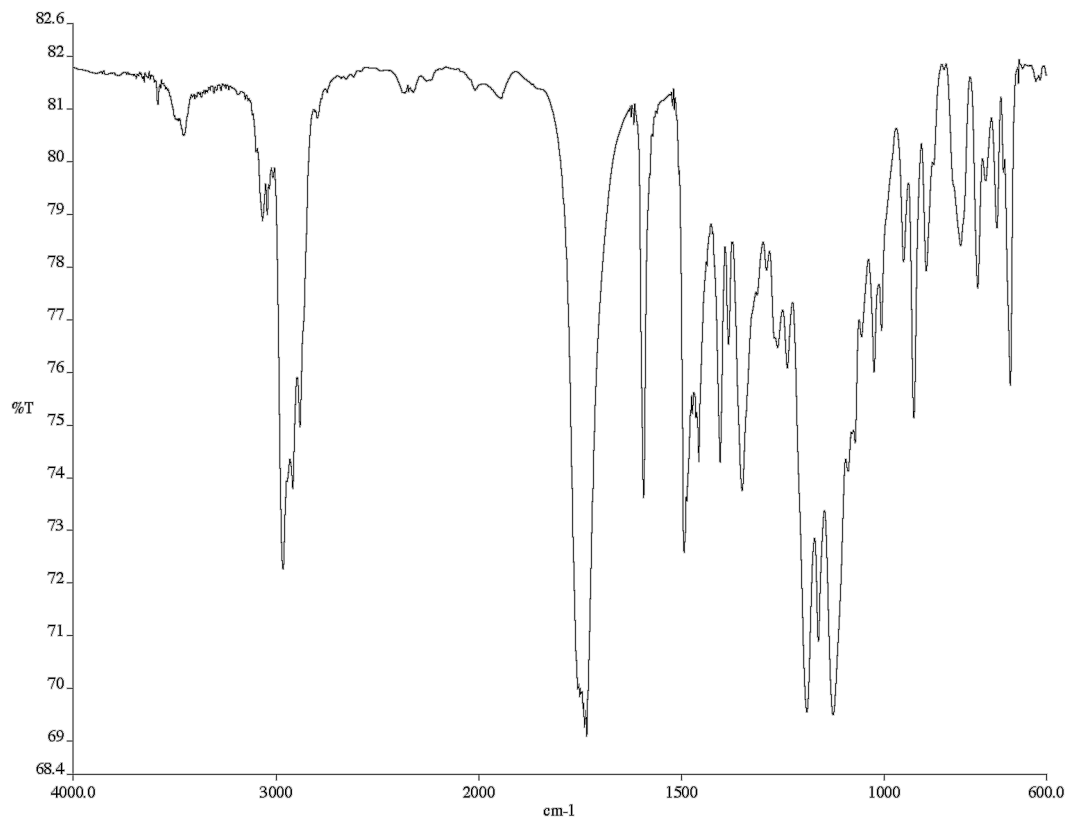


Figure A1.78. Infrared spectrum (Thin Film, NaCl) of compound 383.

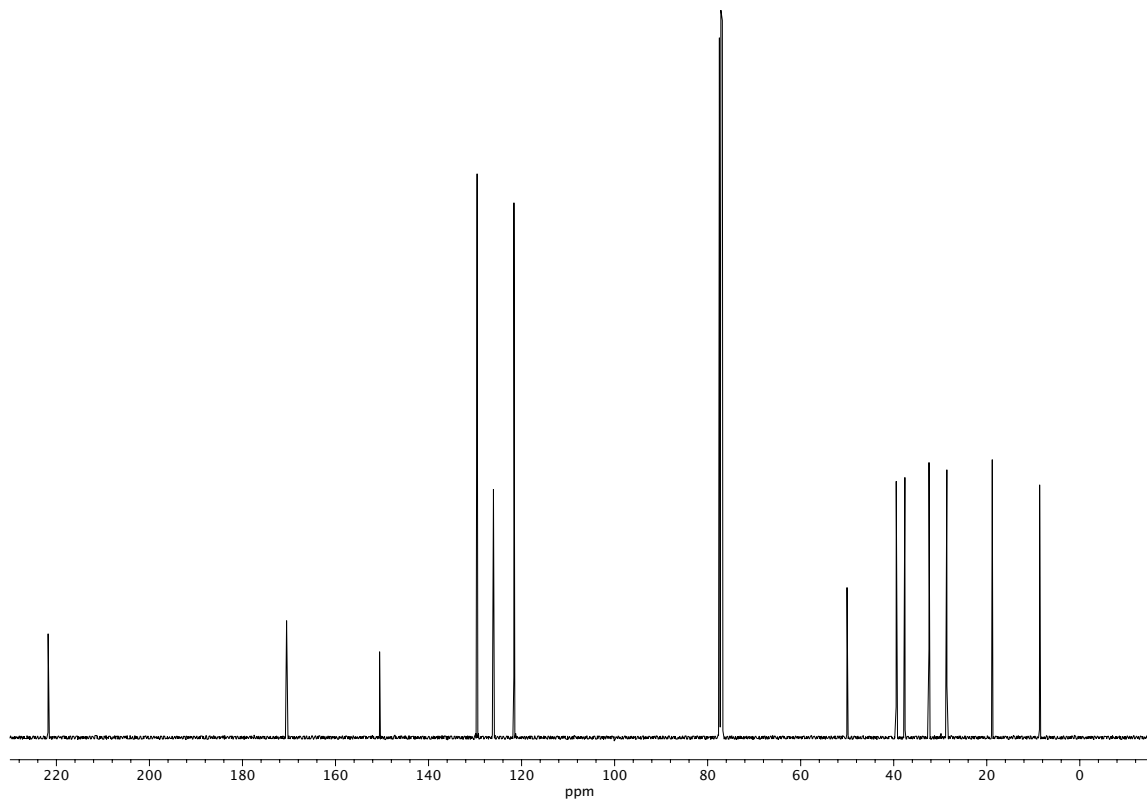


Figure A1.79. ^{13}C NMR (101 MHz, CDCl_3) of compound 383.

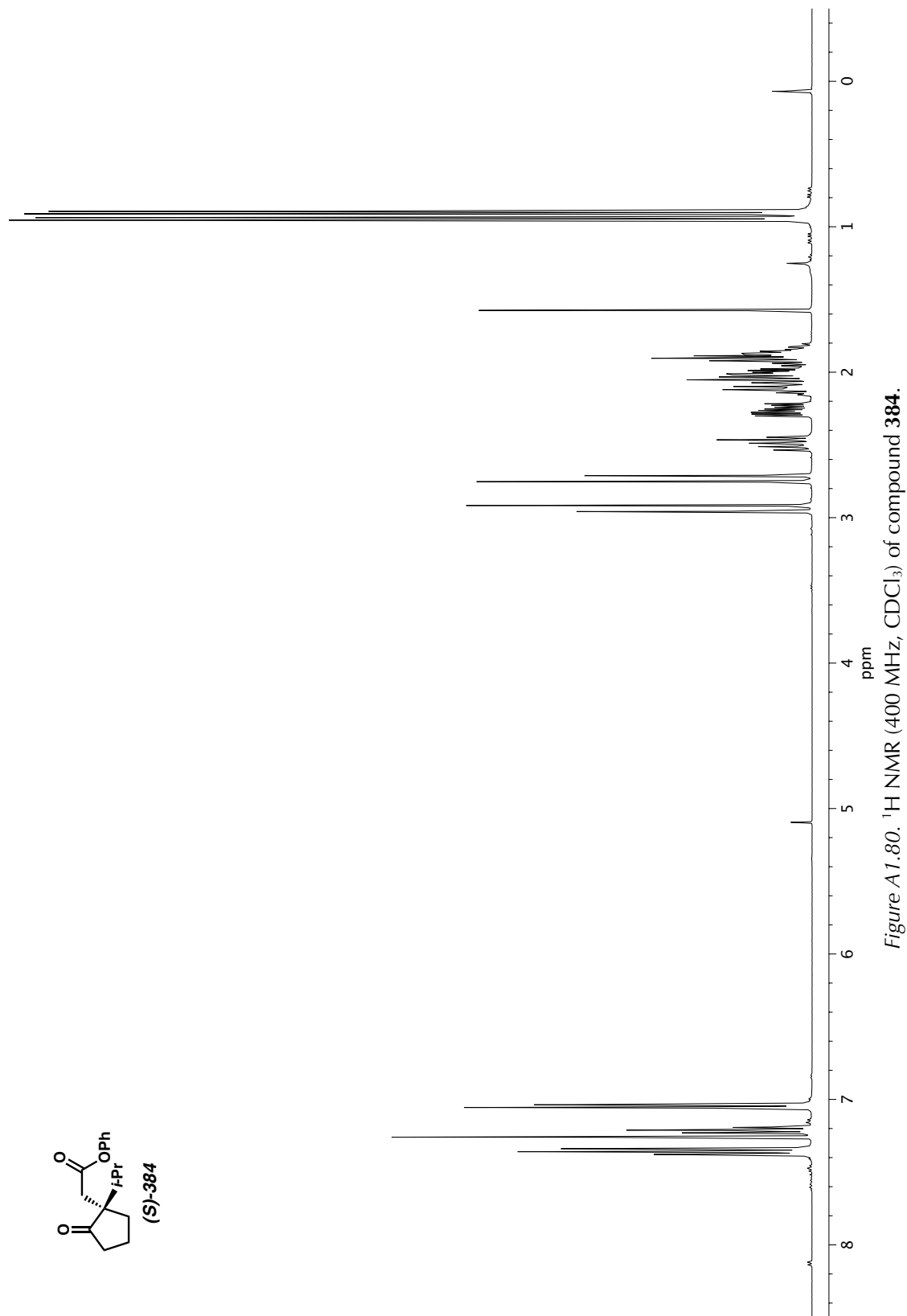
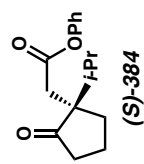


Figure A1.80. ^1H NMR (400 MHz, CDCl_3) of compound 384.

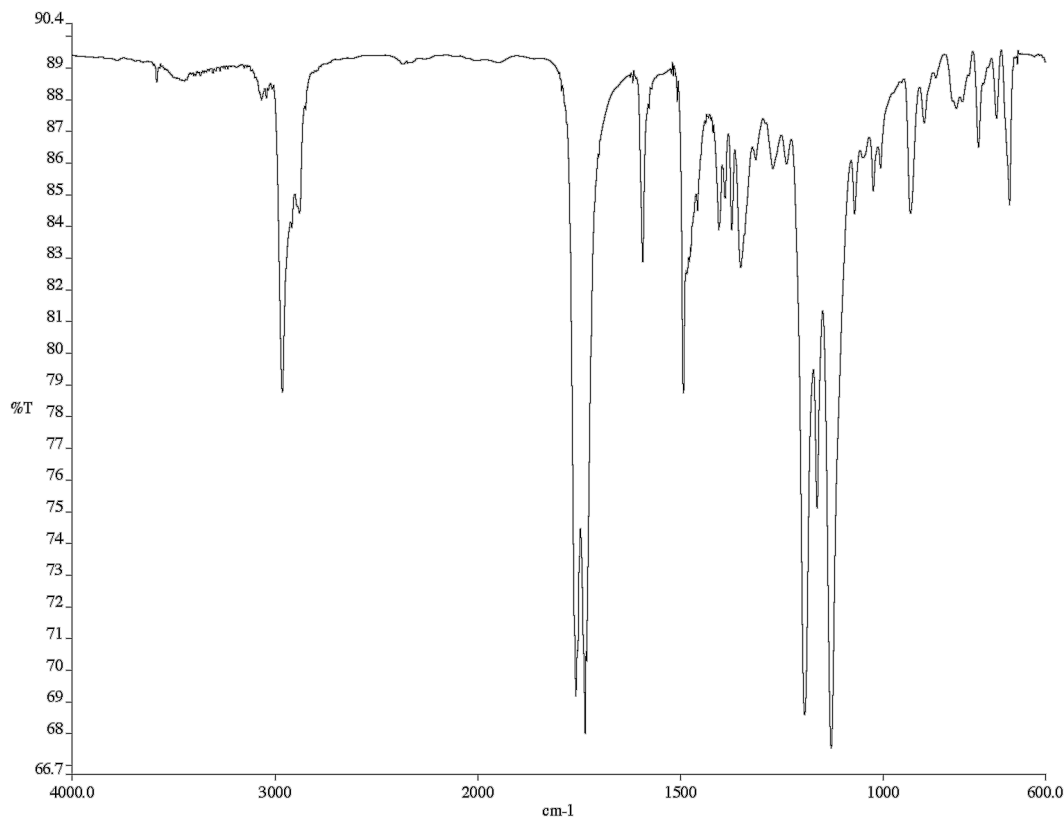


Figure A1.81. Infrared spectrum (Thin Film, NaCl) of compound 384.

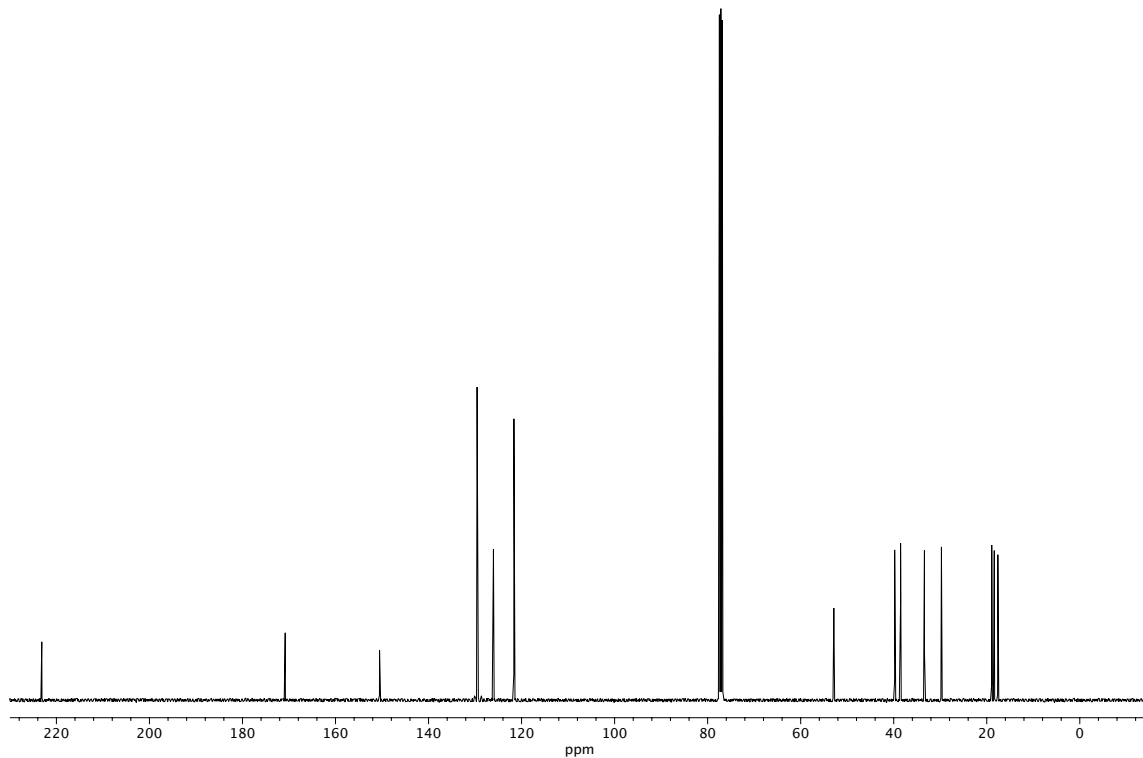


Figure A1.82. ¹³C NMR (101 MHz, CDCl₃) of compound 384.

CHAPTER 3

Enantioselective Total Synthesis of Nigelladine A

Via Late-Stage C–H Oxidation Enabled by an

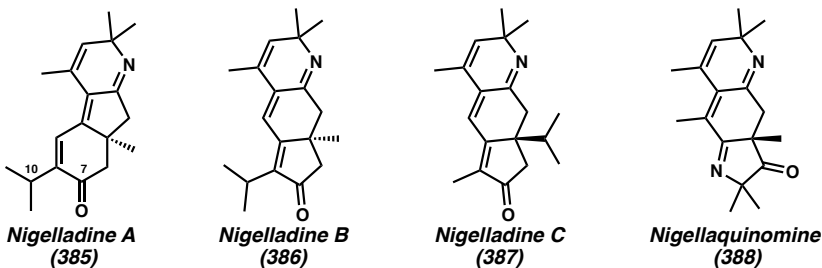
Engineered P450 Enzyme[†]

3.1 INTRODUCTION

The field of organic synthetic chemistry has benefited greatly from the many recent advances in selective C–H functionalization.¹ Indeed, chemical oxidations of C–H bonds are some of the most important transformations in synthetic chemistry because they allow for direct access to oxidized intermediates, without the need for synthetic handles or functional group interconversions. Despite recent advances, there remain significant limitations regarding the regioselectivity of non-directed C–H oxidation reactions. We envisioned that the recently isolated norditerpenoid alkaloids nigelladines A–C (**385–387**) and pyrroloquinoline alkaloid nigellaquinomine (**388**) (Figure 3.1.1)² would present a challenging test bed to evaluate the viability of late-stage C–H oxidation methods.

[†] This research was performed in collaboration with David K. Romney, an postdoctoral scholar of the Arnold group. Additionally, this research has been published and adapted with permission Loskot, S. A.; Romney, D. K.; Arnold, F. A.; Stoltz, B. M. *J. Am. Chem. Soc.* **2017**, *139*, 10196–10199.

Figure 3.1.1. Structures of Nigelladines A–C and Nigellaquinomine



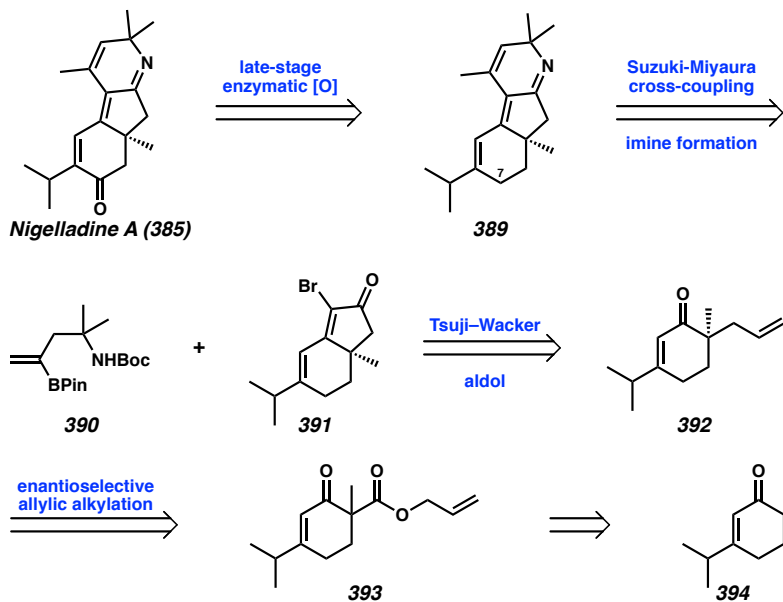
With respect to nigelladine A, we believed that late-stage installation of the C7 ketone would offer significant flexibility in how we chose to construct the highly conjugated core of alkaloid **385**. However, despite the abundance of chemical allylic oxidation conditions, there are relatively few examples of selective oxidation at a 2° carbon (e.g., C7) in the presence of a non-bridging 3° carbon (e.g., C10),³ since oxidation generally occurs at the position where hydrogen abstraction is most favorable.⁴ On the other hand, enzymes are well known to catalyze oxidation reactions with regioselectivity that defies conventional trends of chemical reactivity. Despite this, enzymatic methods are often overlooked in total synthesis efforts due to a typically narrow substrate scope deriving from their exceptional specificity. Fortunately, recent progress in the field of directed evolution has greatly increased the viability of biocatalysis in total synthesis by increasing the reactivity and selectivity of enzymes for non-native transformations.^{5,6} Biocatalytic C–H oxidations with engineered enzymes thus present an alternative approach that can circumvent the limitations of traditional chemical oxidations. Nonetheless, even though there have been examples of the use of engineered enzymes for the functionalization of complex molecules,⁷ their application in total syntheses is still very limited. Herein we describe the first enantioselective total synthesis of tricyclic alkaloid **385**, enabled by the

selective late-stage allylic oxidation of unsaturated imine **389** *via* an engineered P450 enzyme.

3.2 RETROSYNTHETIC ANALYSIS

Retrosynthetically, we surmised that selective late-stage allylic oxidation of **389** at C7 would be essential to the synthesis of enone **385** (Scheme 3.2.1). Imine **389** could be generated by the cross-coupling of vinyl boronic ester **390** and bromide dienone **391**. Vinyl bromide **391** was envisioned to arise via annulation of enone **392**, with the quaternary stereocenter constructed by an asymmetric allylic alkylation reaction from β -ketoester **393**.⁸ With this retrosynthetic analysis, we recognized that the strategically planned C–H oxidation would be particularly challenging due to issues of site selectivity. Imine **389** contains three different allylic carbon centers that could be susceptible to oxidation, a 1°, 2°, and 3°, in addition to a relatively acidic α –carbon adjacent to the imine. Together, the natural product combined with our strategic analysis unveiled a challenging problem for selective C–H functionalization that would need to be addressed in a successful synthesis.

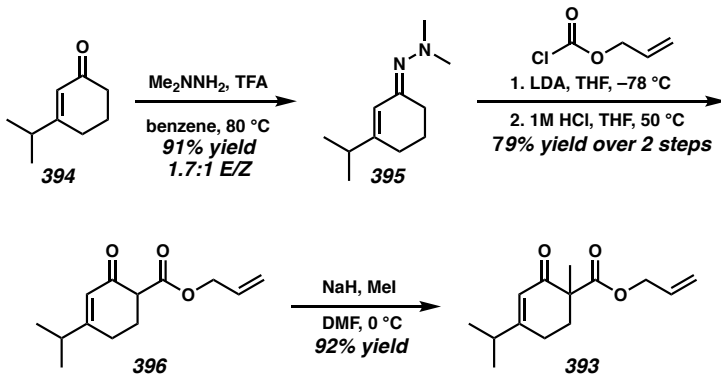
Scheme 3.2.1. Retrosynthetic Analysis of Nigelladine A



3.3 SYNTHESIS OF CROSS-COUPLING FRAGMENTS

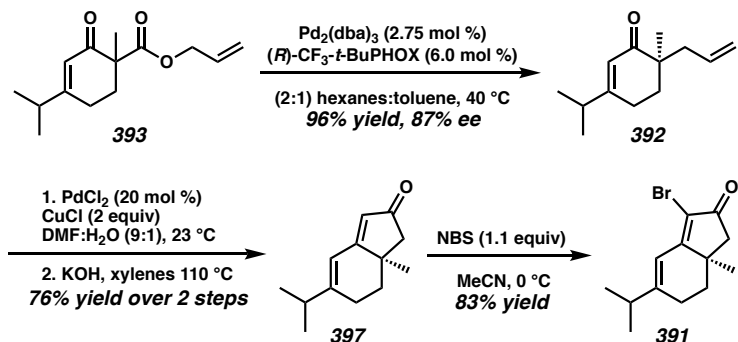
In the forward direction, known enone **394** can be synthesized in excellent yield through a Stork-Danheiser transposition from 1,3-cyclohexanedione.^{9,10} Unfortunately, attempts to directly acylate the α -carbon of **394** resulted in low yields due to competing self-aldol additions. To avoid these issues, we chose to increase the reactivity and steric environment of the enolate by synthesizing the 1,1-dimethyl hydrazone **395**.¹¹ Hydrazone **395** was readily acylated then hydrolyzed, and the resulting β -ketoester **396** was subsequently methylated, providing our desired asymmetric allylic alkylation substrate (**393**) in good yield (Scheme 3.3.1).

Scheme 3.3.1. Synthesis of Asymmetric Allylic Alkylation Precursor



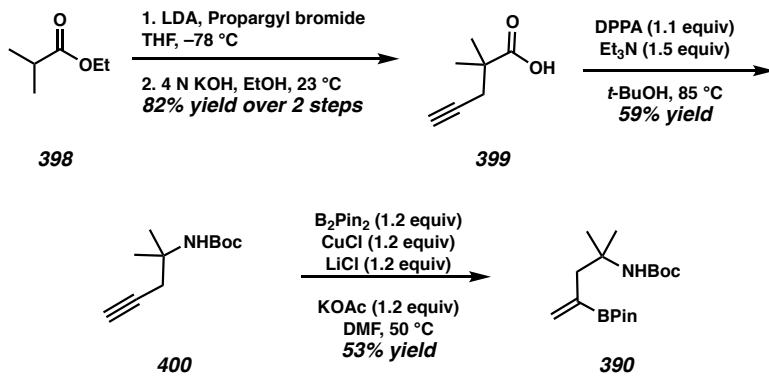
With β -ketoester **393** in hand, we evaluated a variety of reaction parameters for the key quaternary stereocenter-forming asymmetric allylic alkylation and determined that the use of $(CF_3)_3-t\text{-Bu-PHOX}$ (**168**)¹² in 2:1 hexanes–toluene with $Pd_2(dba)_3$ was optimal, generating desired enone **392** in 96% yield and 87% ee. Standard Tsuji–Wacker oxidation of enone **392** using $PdCl_2$ and $CuCl$ under an atmosphere of oxygen generated the desired ketone,¹³ which subsequently underwent an aldol condensation to provide dienone **397** in good yield (76% yield over 2 steps).¹⁴ Enone **397** was then selectively mono-brominated to form vinyl bromide **391**, the desired electrophilic cross-coupling fragment, in 83% yield on gram scale (Scheme 3.3.2).¹⁵

Scheme 3.3.2. Synthesis of Electrophilic Cross-Coupling Fragment



The nucleophilic cross-coupling fragment, Vinyl boronic ester **390**, was readily prepared in three steps from commercially available ethyl isobutyrate (**398**, scheme 3.3.3). Propargylation of ethyl isobutyrate followed by concomitant saponification yielded known acid **399**. Curtius rearrangement of acid **399** followed by a Markovnikov hydroboration of the resultant alkyne **400** generated the desired nucleophilic cross-coupling fragment **390** in three steps.

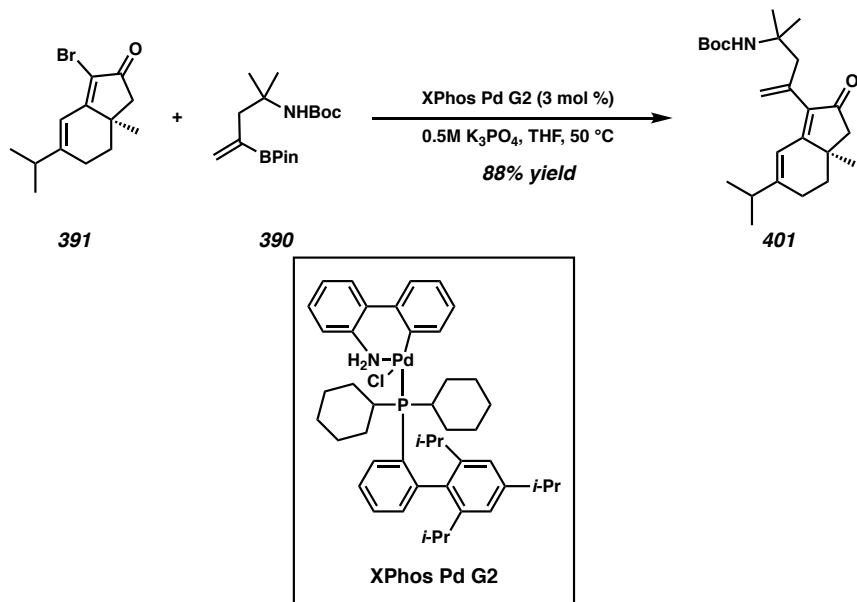
Scheme 3.3.3. Synthesis of the Nucleophilic Cross-Coupling Fragment



3.4 CROSS-COUPLING AND ELABORATION TO THE CARBOCYCLIC CORE

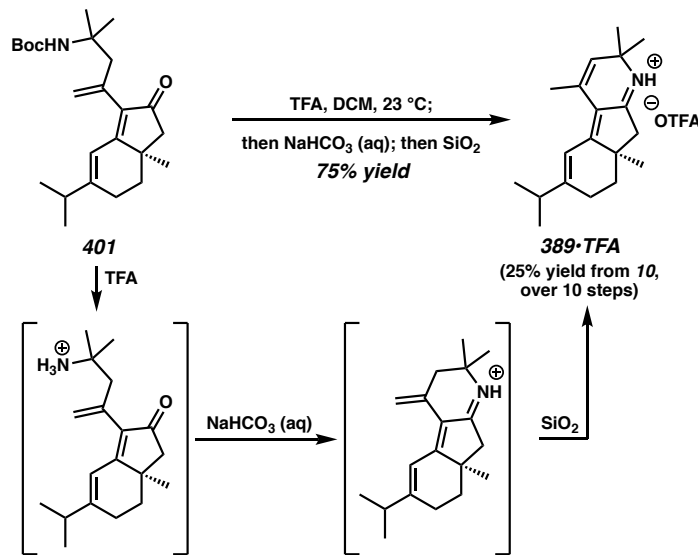
The cross coupling of **390** and **391** was next evaluated for optimal reaction conditions. Ultimately, we found that Buchwald's 2nd generation precatalyst with XPhos (XPhos Pd G2)¹⁶ allowed for the union of **390** and **391** in 88% yield using only a slight excess (1.1 equiv) of **390** (Scheme 3.4.1). Furthermore, triene **401** provided crystals suitable for X-ray diffraction and allowed us to ascertain absolute stereochemistry.¹⁷

Scheme 3.4.1. Cross-Coupling of Dienone **391** and Vinyl Boronic Ester **390**



With triene **401** in hand, we turned our attention to the synthesis of the heterocyclic portion of the alkaloid and the final stages of the synthesis. Toward that end, triene **401** was treated with trifluoroacetic acid (TFA) in CH_2Cl_2 to deprotect the amine, which spontaneously cyclized to form the requisite imine upon quenching with aqueous sodium bicarbonate (Scheme 3.4.2). Fortunately, upon removal of the aqueous layer, treatment with silica gel promoted isomerization of the exocyclic olefin into the ring, which, after purification, afforded the TFA salt of **389** in 75% yield (25% over 10 steps from enone **394**).¹⁸

Scheme 3.4.2. Synthesis of the Tricyclic Core of Nigelladine A



3.5 CHEMICAL OXIDATION OF DESOXY-NIGELLADINE A

With only an allylic oxidation separating tricycle **389** from nigelladine A (**385**), we initiated a broad exploration of oxidation methods for installing an oxidation handle at the desired C7 position. Unfortunately, the required site-selective C–H oxidation of **389** or the intermediate enone **397** proved intractable for traditional synthetic methods (Table 3.5.1). While numerous conditions were probed on both substrates,^{19,20} only a limited few effected oxidation at the desired position. These reactions also exhibited poor selectivity, generating an inseparable mixture of mono-oxidation products, along with over-oxidized byproducts that constituted the majority of the product mixture. We thus turned our attention to enzymes as a potential means to achieve the desired oxidation.

Table 3.5.1. Attempted Chemical Oxidations^a

Substrate **Conditions** **HPLC Yield of Oxygenation Products (%)^{b,c,d}**

		SM	C1	C7	C10	Polyoxygenation
389	SeO ₂ , DCM, 40 °C	21	79 (57) ^e	—	—	—
397	SeO ₂ , DCM, 40 °C	5	26 (22)	—	—	15
389	Pd/C (10 wt%), TBHP, 0 °C	7	—	3	44	46
397	Pd/C (10 wt%), TBHP, 0 °C ^f	46	—	2	42	4
389	Cr(V) (1 equiv), MnO ₂ CF ₃ C ₆ H ₅ , 15-crown-5, 80 °C	55	3	35 ^g	—	6
389	Rh ₂ (esp) ₂ , T-HYDRO, 23 °C	2	8	21(10)	—	34
397	Rh ₂ (esp) ₂ , T-HYDRO, 23 °C	—	—	15	16	43

^a See section 3.8 for reaction conditions and description of the product distribution. ^b Approximated by separating the products on UHPLC-MS and comparing ion count of the various oxidation products. ^c Remaining percent balance were unidentified side products. ^d Numbers given in parenthesis indicate isolated yields of the oxidized product. ^e Protection of 389 as an *N*-acyl enamide results in oxidation at C-14. ^f Shortened reaction time used to observe inherent regioselectivity without over oxidation. ^g Oxidation at C-5 occurred.

3.6

ENZYMATIC OXIDATION OF DESOXY-NIGELLADINE A

The cytochrome P450 enzyme from *Bacillus megaterium* (P450_{BM3}) is a workhorse of protein engineering studies because it is soluble and self-contained, exhibits one of the fastest reaction rates of any P450-catalyzed hydroxylation (17,000 min⁻¹ for arachidonic acid),^{5a} and possesses good stability (*t*_{1/2} = 68 min at 50 °C).²¹ Since the substrate scope of the wild-type protein is mostly limited to long-chain fatty acids, many engineering efforts have focused on expanding the substrate scope of P450_{BM3} to accept larger and more complex substrates. To this end, various approaches have been applied to develop biocatalysts derived from P450_{BM3} that perform regioselective C–H oxygenation of complex molecules for which the wild-type enzyme exhibits minimal activity.^{6c,22}

However, these approaches involved extensive screening endeavors, often requiring high-throughput screening and limiting them to substrates that were readily available.

For biocatalysis to be a viable strategy for the late-stage of a total synthesis, it is desirable to identify a synthetically useful catalyst with minimal screening. Thus, we elected to screen a focused library of variants that had been previously engineered to accept large substrates,²² but had otherwise never encountered substrate **389**. To compare the catalysts, we chose to allow the reactions to proceed to only low conversion and compare the ratio of desired to undesired oxidation products (Table 3.6.1). Encouragingly, wild-type P450_{BM3} exhibited some selectivity for C7, although oxidation of the isopropyl C–H bond was favored 1.2:1 (Table 3.6.1, entry 1). We then probed a small selection of engineered variants that all derive from the same parent (12 mutations from P450_{BM3}). These enzymes were previously evolved for regioselective oxidation of methoxymethyl-protected glycosides, but are distinct in that different combinations of active-site residues have been mutated to alanine. The variant **2A1**, in which leucine residues 75, 181, and 437 are mutated to alanine, exhibited a worse selectivity compared to wild-type, favoring the isopropyl oxidation product, as well as an unidentified oxidation product (Table 3.6.1, entry 2). The two other variants, however, exhibited a reversal in selectivity, favoring oxidation at the desired position in excess of 2:1 (Table 3.6.1, entries 3–4). The best variant proved to be **8C7**, which is identical to **2A1**, but lacks the L437A mutation. This variant favors oxidation at the desired position in a 2.8:1 ratio (Table 3.6.1, entry 4).

Table 3.6.1. Screening of Focused Library for Allylic Oxidation

Entry	Catalyst ^a	Active-Site Ala Substitutions	Desired/Undesired ^b
1	P450 _{BM3}	–	0.86
2	2A1	L75A, L181A, L437A	0.37
3	4H5	L75A, L177A, L181A	2.1
4	8C7	L75A, L181A	2.8

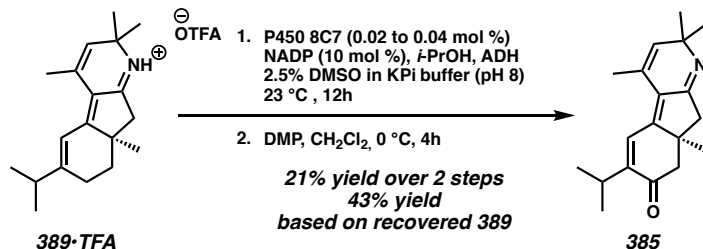
^a See section 3.8 for full list of mutations. ^b Approximated by separating the products on UHPLC-MS and comparing ion count of C-7 oxidation product to all other monooxygenation products (*m/z* = 286). See section 3.8 for more details.

Since enzyme active sites are well known to bind substrate enantiomers differently, we wished to test if the stereochemistry of **389** would affect the activity or selectivity of **8C7**. Using the Pd-catalyzed alkylation, we obtained both enantiomers of **389**, which were then enriched to enantiopurity by chiral preparative HPLC. Each enantiomer was then subjected to oxidation by catalyst **8C7**. Interestingly, at both short (15 min) and long (12 h) reaction times, the enantiomers gave nearly identical results, although the *R* enantiomer exhibited a slightly higher initial rate by a factor of 1.3.

Having achieved the desired regioselectivity, we then needed to improve the yield. Furthermore, we wished to supplant the stoichiometric use of NADPH, which is required if oxygen is used as the terminal oxidant. Fortunately, we could use NADPH in catalytic amounts by regenerating it *in situ* with an alcohol dehydrogenase (ADH) and isopropanol as the terminal reductant.²³ With these new conditions, we conducted the oxidation on a 160 mg scale, followed by subjecting the crude product mixture to oxidation with Dess-Martin periodinane, thus affording the natural product in 21% yield over both steps (43% yield based on recovered **389**, Scheme 3.6.1). The recovered starting material (**389**) was

competent in the same two-step procedure with no loss in efficiency (26% yield).²⁴ Under these conditions, we observed up to 1700 turnovers to the C7 mono-oxygenation product.

Scheme 3.6.1. Completion of the Synthesis of Nigelladine A



3.7 CONCLUSION

In summary, we have completed the first total synthesis of nigelladine A in an expedient 12 steps and 5% overall yield (11% yield based on recovered **389**). The asymmetric allylic alkylation allowed for the construction of the quaternary center in high yield and enantioselectivity. Expedient identification of engineered enzymes allowed for a site-selective 2° allylic oxidation without the need for extensive generational screening or reaction optimization. These results demonstrate that enzymatic transformations are capable of defying standard chemical limitations and should be included in the repertoire of reactions that are traditionally considered for the late stages of total syntheses.

3.8 EXPERIMENTAL METHODS AND ANALYTICAL DATA

3.8.1 MATERIALS AND METHODS

Unless stated otherwise, reactions were performed at ambient temperature (23 °C) in flame-dried or oven-dried glassware under an argon or nitrogen atmosphere using dry, deoxygenated solvents (distilled or passed over a column of activated alumina).²⁵ Commercially obtained reagents were used as received with the exception of anhydrous cerium trichloride (CeCl₃)¹⁰ dipalladium tris(dibenzylideneacetone) (Pd₂(dba)₃), palladium

(II) chloride (PdCl_2), anhydrous copper (I) chloride (CuCl), bis(pinacolato)diboron (B_2Pin_2), anhydrous lithium chloride (LiCl), and anhydrous potassium acetate (KOAc), which were stored in a nitrogen-filled glovebox. Triethylamine (Et_3N) and Diisopropylethylamine ($i\text{-Pr}_2\text{NH}$) were distilled over potassium hydride prior to use, while allyl chloroformate was freshly distilled prior to use. N-bromosuccinimide was recrystallized prior to use.²⁶ (*S*)-(CF₃)₃-*t*-BuPHOX,¹² (*R*)-(CF₃)₃-*t*-BuPHOX,¹² and Dess–Martin periodinane²⁷ were prepared by known methods. Reactions requiring external heat were modulated to the specified temperatures using an IKAmag temperature controller. Reaction progress was monitored by thin-layer chromatography (TLC), which was performed using E. Merck silica gel 60 F254 precoated glass plated (0.25 mm) and visualized by UV fluorescence quenching, potassium permanganate, *p*-anisaldehyde, or iodine staining. Silicycle SiliaFlash® P60 Academic Silica gel (particle size 40-63 nm) was used for column chromatography. ¹H and ¹³C NMR spectra were recorded on a Varian Inova 500 (500 MHz and 126 MHz, respectively), Varian Mercury 300 spectrometer (300 MHz and 75 MHz, respectively), Varian 600 MHz Spectrometer (600 MHz), and a Bruker AV III HD spectrometer equipped with a Prodigy liquid nitrogen temperature cryoprobe (400 MHz and 101 MHz, respectively) and are reported in terms of chemical shift relative to CHCl₃ (δ 7.26 and δ 77.16, respectively) and CH₃OH (δ 3.31 and δ 39.00 respectively). Data for ¹H NMR are reported as follows: chemical shift (δ ppm) (multiplicity, coupling constant (Hz), integration). Multiplicities are reported as follows: s = singlet, d = doublet, t = triplet, q = quartet, p = pentet, sext = sextet, sept = septet, m = multiplet, and br s = broad singlet. Infrared (IR) spectra were recorded on a Perkin Elmer Paragon 1000 spectrometer using thin films deposited on NaCl plates and are reported in frequency of

absorption (cm^{-1}). Optical rotations were measured with a Jasco P-2000 polarimeter operating on the sodium D-line (589 nm), using a 100-mm path-length cell and are reported as: $[\alpha]_D^T$ (concentration in g/100 mL, solvent). Analytical SFC was performed with a Mettler SFC supercritical CO_2 analytical chromatography system utilizing CHIRALCEL OB-H and CHIRALPAK IC columns (4.6 mm x 25 cm) obtained from Daicel Chemical Industries, Ltd. with visualization at 254, 230, and 210 nm. High resolution mass spectra were obtained from the Caltech Mass Spectral Facility using a JEOL JMS-600H High Resolution Mass Spectrometer in fast atom bombardment (FAB+) ionization mode or a Agilent 6200 Series TOF with an Agilent G1978A Multimode source in electrospray ionization (ESI+), atmospheric pressure chemical ionization (APCI+), or mixed (ESI/APCI) ionization mode.

3.8.2 PROTOCOLS FOR PROTEIN EXPRESSION AND LYSIS

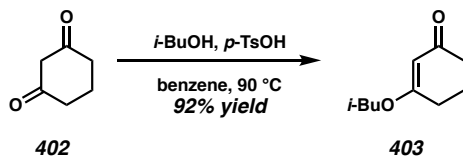
The genes for wild-type $\text{P450}_{\text{BM}3}$ and the variants were previously cloned into the pCWori vector, which was used to transform *Escherichia coli* DH5 α .²¹ In addition to the mutations listed in Table 3.6.1, all variants had the following mutations: V78A F87V P142S T175I A184V S226R H236Q E252G A290V L353V I366V E442K.

For protein expression, a culture (typically 5 mL) of lysogeny broth with 100 $\mu\text{g}/\text{mL}$ of ampicillin (LB_{amp}) was inoculated with a glycerol stock of *E. coli* DH5 α containing the desired plasmid. This culture was shaken at 37 °C and 230 rpm. After 12 hours, the culture was used to inoculate an expression culture (1:100 v/v) of Terrific Broth containing 100 $\mu\text{g}/\text{mL}$ of ampicillin (TB_{amp}) plus 0.1% by volume of trace metal mix (aqueous solution of 50 mM FeCl_3 , 20 mM CaCl_2 , 10 mM MnSO_4 , 10 mM ZnSO_4 , 2 mM CoSO_4 , 2 mM CuCl_2 ,

2 mM NiCl₂, 2 mM Na₂MoO₄, 2 mM H₃BO₃). The expression culture was shaken at 37 °C and 230 rpm. After ~3 hours, the OD₆₀₀ was 0.6–0.8, whereupon the culture was chilled in ice for 30 minutes, then induced with the addition of aminolevulinic acid (1 mM final concentration) and isopropyl β-D-thiogalactopyranoside (0.5 mM final concentration). The culture was then shaken at 230 rpm and 20 °C. After 16–20 hours, the culture was subjected to centrifugation at 5,000×g and 4 °C for 10 minutes. The supernatant was discarded, and then the cell pellet was stored at –30 °C until further use.

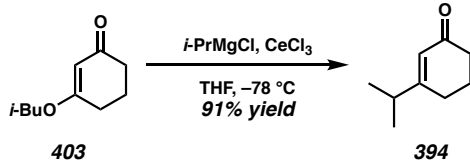
For lysis, the cell pellet was thawed, and then suspended in 4 mL/mg of potassium phosphate buffer (100 mM, pH 8) that contained 1 mg/mL of hen egg white lysozyme and 0.1 mg/mL of bovine pancreas DNase I. The suspension was shaken at 37 °C and 230 rpm (19 mm radius). After 1 hour, the culture was cooled on ice, then subjected to centrifugation at 15,000×g and 4 °C for 10 min. The supernatant was used directly in the biocatalytic transformation. To determine protein concentration, 900 μL of fivefold-diluted lysate was treated with a spatula tip of dithionite, then exposed to an atmosphere of carbon monoxide (CO) for 30 minutes. The absorbance of the CO-bound lysate at 450 nm minus the absorbance at 490 nm was converted to protein concentration using the extinction coefficient ε = 91 mM^{–1}cm^{–1}.

3.8.3 EXPERIMENTAL PROCEDURES



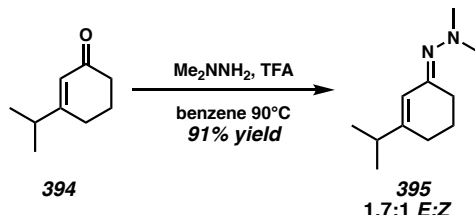
3-isobutoxycyclohex-2-en-1-one (403):²⁸ 1,3-cyclohexadione (**402**, 22.4 g, 200 mmol, 1.0 equiv), *i*-butyl alcohol (55 mL, 600 mmol, 3 equiv), and *p*-TsOH (190 mg, 1.0 mmol,

0.005 equiv) were added to a flask and diluted in benzene (123 mL, 1.6 M). The flask was then fitted with a Dean–Stark trap filled with additional benzene. The reaction flask was heated to reflux with stirring for 8 h, at which time the starting material had been completely consumed (determined by TLC analysis, 8:1 hexanes:EtOAc). The reaction mixture was cooled to ambient temperature (ca. 23 °C) and Et₃N (0.7 mL, 5 mmol, 0.025 equiv) was added. The crude reaction mixture was then concentrated in vacuo and distilled by short path distillation (Pressure 1.0 torr, neck temperature 118 °C, bath temperature 150 °C) to provide vinylogous ester **403** (32.6 g, 97% yield) as a clear colorless oil; R_f = 0.5 (8:1 hexanes:EtOAc); ¹H NMR (300 MHz, CDCl₃) δ 5.34 (s, 1H), 3.59 (d, J = 6.5 Hz, 2H), 2.41 (t, J = 6.3 Hz, 2H), 2.34 (dd, J = 7.2, 6.0 Hz, 2H), 2.10–1.91 (m, 3H), 0.97 (dd, J = 6.7, 0.7 Hz, 6H). All other characterization matches literature values.²⁹



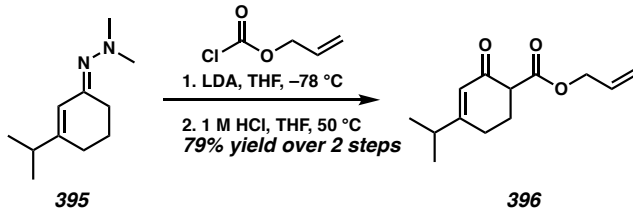
3-isopropylcyclohex-2-en-1-one (394): In a nitrogen-filled glovebox, CeCl₃ (49 g, 200 mmol, 1.5 equiv) was added to a round bottom flask with a magnetic stir bar. The flask was sealed with a rubber septum and removed from the glovebox. The flask was heated at 140 °C under vacuum (ca. 1 Torr) with stirring for 8 h. CeCl₃ was allowed to cool to ambient temperature (23 °C) and the flask was refilled with Ar. The CeCl₃ was then cooled to 0 °C (H₂O:ice bath) and diluted with THF (444 mL, 0.3 M) with vigorous stirred for 3 h. The reaction flask was then cooled to –78 °C (dry ice:acetone bath) whereupon ester **403** (22.4 g, 133 mmol, 1 equiv) was added. After 1 h at –78 °C, *i*-PrMgCl (2.0 M in THF, 100 mL, 1.5 equiv) was added dropwise via cannula and allowed to stir for 1 h, at which time

the starting material had been completely consumed (determined by TLC, 8:1 hexanes:Et₂O). The reaction was then quenched with 1 M HCl (300 mL) and allowed to warm to ambient temperature. The product was extracted from the biphasic mixture with Et₂O (3 × 200 mL), and then the combined organic layers were washed with brine, dried over MgSO₄, and concentrated in vacuo. The crude product can be purified by either flash chromatography (SiO₂, 4:1 hexanes:Et₂O) or by Kugelrohr distillation (pressure 1.0 Torr, 115 °C) to provide enone **394** (16.8 g, 91% yield) as a pale yellow oil, which solidifies to a white solid upon cooling to –20 °C; R_f = 0.29 (4:1 hexanes:Et₂O); ¹H NMR (500 MHz, C₆D₆) δ 5.95 (q, J = 1.4 Hz, 1H), 2.17–2.10 (m, 2H), 1.88 (pd, J = 6.8, 1.0 Hz, 1H), 1.66–1.60 (m, 2H), 1.47–1.38 (m, 2H), 0.74 (d, J = 6.9 Hz, 6H). All other characterization matches literature values.³⁰



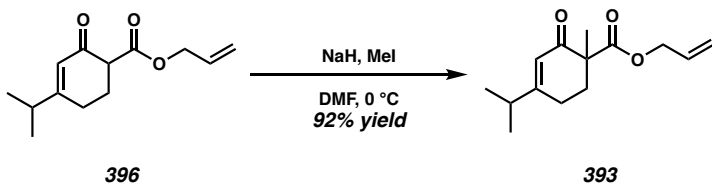
2-(3-isopropylcyclohex-2-en-1-ylidene)-1,1-dimethylhydrazine (395): Hydrazone condensation was adapted from the literature.³¹ Enone **394** (8.2g, 59.0 mmol, 1 equiv), *N,N*-dimethylhydrazine (9 mL, 118 mmol, 2 equiv), TFA (0.1 mL), and benzene (120 mL, 0.4 M) were added to a round-bottom flask. The flask was fitted with a Dean-Stark trap filled with additional benzene. The reaction flask was heated to reflux with stirring for 8 h, at which time the starting material had been completely consumed (determined by TLC analysis, 1:1 hexanes:EtOAc). The crude reaction mixture was then cooled to ambient temperature and concentrated in vacuo. The crude product can be purified by either flash

chromatography (SiO_2 , 1:1 hexanes:EtOAc) or short path distillation (pressure 1 Torr, neck temperature 130 °C, bath temperature 160 °C) to generate hydrazone **395** (9.7 g, 91% yield, 1.7:1 E:Z ratio) as a yellow oil; R_f = 0.5 (E); 0.26 (Z) (1:1 hexanes:EtOAc); ^1H NMR (400 MHz, CDCl_3) (E) δ 6.00 (q, J = 1.4 Hz, 1H), 2.59 (dd, J = 7.5, 5.8 Hz, 2H), 2.52 (s, 6H), 2.33 (sept, J = 6.9 Hz, 1H), 2.20–2.16 (m, 2H), 1.79 (dtd, J = 7.5, 6.4, 5.6 Hz, 2H), 1.08 (d, J = 6.9 Hz, 6H), (Z) δ 6.54 (q, J = 1.5 Hz, 1H), 2.49 (s, 6H), 2.43–2.33 (m, 3H), 2.21–2.17 (m, 2H), 1.85–1.78 (m, 2H), 1.08 (d, J = 6.9 Hz, 6H); ^{13}C NMR (101 MHz, CDCl_3) (E) δ 164.9, 157.3, 121.1, 47.4, 35.6, 27.7, 26.2, 22.5, 21.0, (Z) δ 162.5, 160.2, 113.6, 47.9, 36.0, 31.9, 27.7, 22.9, 21.1; IR thin film, NaCl) 2960, 2857, 2816, 2771, 1634, 1589, 1466, 1436, 1383, 1362, 1327, 1304, 1267, 1251, 1222, 1200, 1154, 1142, 1089, 1022, 980, 969, 890, 790 cm^{-1} ; HRMS (ES/APCI) m/z calc'd $\text{C}_{11}\text{H}_{21}\text{N}_2$ [M+H] $^+$: 181.1699, found: 181.1705.

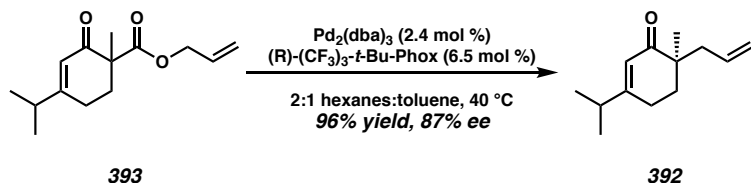


Allyl 4-isopropyl-2-oxocyclohex-3-ene-1-carboxylate (396): A flame-dried round bottom flask was charged with diisopropylamine ($i\text{-Pr}_2\text{NH}$, 9.58 mL, 68.4 mmol, 1.5 equiv) in THF (61 mL, 1.1 M) and cooled to 0 °C. A solution of $n\text{-BuLi}$ in hexanes (2.3 M, 29.7 mL, 68.4 mmol, 1.5 equiv) was added dropwise and the resulting solution was allowed to stir for 0.5 h at 0 °C. Hydrazone **395** (8.22 g, 45.6 mmol, 1 equiv) was added dropwise to the LDA solution, which was then stirred for 1 h at 0 °C. The reaction mixture was cannulated to a separate flame dried flask containing allyl chloroformate (7.3 mL, 68.4 mL,

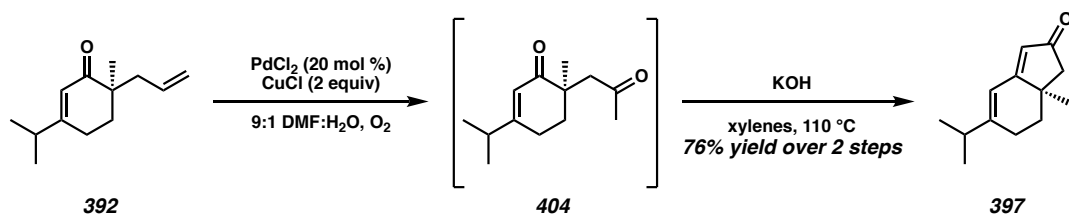
1.5 equiv) in THF (320 mL, 0.2 M) at -78°C . The solution was stirred for 1 h, at which time the starting material had been completely consumed (determined by TLC analysis, 4:1 hexanes:EtOAc). The solution was quenched at -78°C with aqueous NH₄Cl (200 mL) and allowed to warm to ambient temperature. The product was extracted from the biphasic solution with Et₂O (3×150 mL), and the combined organic layers were washed with brine, dried over MgSO₄ and concentrated in vacuo. The crude compound was diluted with THF (230 mL, 0.2 M) and 1 M HCl (91.2 mL, 91.2 mmol, 2.0 equiv) and heated to 50°C for 12 h, at which time the starting material had been completely consumed (determined by TLC analysis, 4:1 pentane:Et₂O). The product was extracted with Et₂O (3×100 mL) and the combined organic layers were washed with brine, dried over MgSO₄, and concentrated in vacuo. The crude product was purified by flash chromatography (SiO₂, 9:1 hexanes:EtOAc) to yield β -Ketoester **396** (7.96 g, 79% yield) as a pale yellow oil; R_f = 0.2 (4:1 pentane:Et₂O); ¹H NMR (500 MHz, CDCl₃) δ 5.98–5.85 (m, 2H), 5.32 (dd, *J* = 17.2, 1.6 Hz, 1H), 5.22 (dd, *J* = 10.5, 1.3 Hz, 1H), 4.71–4.58 (m, 2H), 3.42–3.32 (m, 1H), 2.50–2.29 (m, 4H), 2.24–2.17 (m, 1H), 1.09 (dd, *J* = 6.8, 0.9 Hz, 6H); ¹³C NMR (126 MHz, CDCl₃) δ 194.3, 172.2, 170.1, 131.9, 123.0, 118.5, 65.8, 53.2, 35.8, 26.3, 26.0, 20.8, 20.6; IR thin film, NaCl) 2965, 2940, 2875, 1741, 1650, 1624, 1457, 1425, 1375, 1364, 1307, 1275, 1216, 1166, 1151, 1050, 1027, 989, 884, 767 cm⁻¹; HRMS (ES/APCI) m/z calc'd C₁₃H₁₉O₃ [M+H]⁺: 223.1329, found: 223.1329.



Allyl 4-isopropyl-1-methyl-2-oxocyclohex-3-ene-1-carboxylate (393): NaH (60% dispersion, 3.3 g, 81.9 mmol, 1.4 equiv) was added to DMF (31.5 mL, 2.6 M) at 0 °C. The solution was then charged with β-Ketoester **396** (13 g, 58.4 mmol, 1.0 equiv) in a solution of DMF (25 mL, 2.3 M) and allowed to stir for 1 h at 0 °C. MeI (12.7 mL, 204.4 mmol, 3.5 equiv) was added, followed by additional DMF (20 mL). The reaction was allowed to stir for 1.5 h, at which time the starting material had been completely consumed (determined by TLC analysis, 9:1 hexanes:EtOAc). The reaction was then quenched with water and the product was extracted with Et₂O (40 mL × 3). The combined organic layers were washed with brine (3 × 50 mL), dried over Na₂SO₄, filtered, and concentrated in vacuo. The crude product was purified by flash chromatography (SiO₂, 9:1 hexanes:EtOAc) to generate β-Ketoester **393** (12.7 g, 92% yield) as a pale yellow oil; R_f = 0.30 (9:1 hexanes:EtOAc); ¹H NMR (500 MHz, CDCl₃) δ 5.92 (dt, J = 2.1, 1.1 Hz, 1H), 5.86 (ddt, J = 17.2, 10.5, 5.5 Hz, 1H), 5.28 (dq, J = 17.2, 1.6 Hz, 1H), 5.20 (dq, J = 10.5, 1.3 Hz, 1H), 4.64 (ddt, J = 13.4, 5.6, 1.5 Hz, 1H), 4.56 (ddt, J = 13.4, 5.5, 1.5 Hz, 1H), 2.53–2.37 (m, 3H), 2.33–2.26 (m, 1H), 1.87 (ddd, J = 13.0, 8.4, 5.0 Hz, 1H), 1.39 (s, 3H), 1.09 (d, J = 6.9 Hz, 6H); ¹³C NMR (126 MHz, CDCl₃) δ 197.4, 172.7, 170.7, 131.9, 122.8, 118.3, 65.7, 52.9, 35.7, 33.6, 25.3, 20.9, 20.7, 20.5; IR thin film, NaCl) 2965, 2935, 2875, 1731, 16678, 1626, 1456, 1425, 1375, 1302, 1248, 1217, 1170, 1105, 987, 26, 882, 771, 749 cm⁻¹; HRMS (ES/APCI) m/z calc'd C₁₄H₂₁O₃ [M+H]⁺: 237.1485, found: 237.1482.



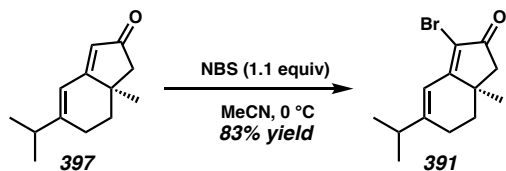
(R)-6-allyl-3-isopropyl-6-methylcyclohex-2-en-1-one (392): In a nitrogen filled glovebox, $\text{Pd}_2(\text{dba})_3$ (725 mg, 0.79 mmol, 0.024 equiv) and (R) - $(\text{CF}_3)_3$ -*t*-Bu-PHOX (1.3 g, 2.2 mmol, 0.065 equiv) were added to a flask. The flask was sealed and removed from the glovebox. The catalyst and ligand were then diluted with a 2:1 hexanes:toluene (1 L, 0.033M) and allowed to stir for 40 minutes at 40 °C. β -Ketoester **393** (8.0 g, 33.9 mmol, 1.0 equiv) was then added in one portion. After 62 h, the consumption of starting material was complete (as determined by TLC analysis, 9:1 hexanes:EtOAc). The crude solution was directly purified by column chromatography (SiO_2 , 100% hexanes then 12:1 hexanes:Et₂O) to furnish enone **392** (6.25 g, 96% yield, 87% ee) as a pale yellow oil; R_f = 0.46 (9:1 hexanes:EtOAc); ¹H NMR (500 MHz, CDCl_3) δ 5.79 (q, J = 1.4 Hz, 1H), 5.73 (ddt, J = 16.8, 10.3, 7.4 Hz, 1H), 5.09–5.01 (m, 2H), 2.43–2.35 (m, 1H), 2.35–2.29 (m, 3H), 2.16 (ddt, J = 13.7, 7.7, 1.2 Hz, 1H), 1.90 (ddd, J = 13.6, 6.9, 5.6 Hz, 1H), 1.71 (ddd, J = 13.6, 6.6, 5.4 Hz, 1H), 1.09 (d, J = 6.8 Hz, 6H), 1.05 (s, 3H); ¹³C NMR (126 MHz, CDCl_3) δ 204.3, 169.8, 134.4, 122.4, 118.0, 43.7, 41.3, 35.6, 33.4, 24.8, 21.9, 20.9, 20.9; IR thin film, NaCl) 2964, 2929, 2873, 1663, 1627, 461, 1428, 1373, 1323, 1274, 1213, 1126, 1107, 999, 912, 881, 613 cm⁻¹; HRMS (ES/APCI) m/z calc'd $\text{C}_{13}\text{H}_{21}\text{O}$ [M+H]⁺: 193.1587, found: 193.1582; (R): $[\alpha]_D^{25}$ +3.15° (*c* 1.215, CDCl_3 , 87% ee); (S): $[\alpha]_D^{25}$ -1.34° (*c* 0.675, CDCl_3 , 87% ee); SFC (OB-H (4 x 25 cm), 1% *i*-PrOH) (*R*) retention time: 1.93 min, (*S*) retention time: 2.30 min.



(R)-5-isopropyl-7a-methyl-1,6,7,7a-tetrahydro-2*H*-inden-2-one (397): A flask containing enone **392** (1.0 g, 5.2 mmol, 1.0 equiv) in 9:1 DMF:H₂O (52 mL, 0.1 M) was charged with PdCl₂ (0.18 g, 1 mmol, 0.2 equiv) and CuCl₂ (1.0 g, 10.4 mmol, 2.0 equiv). The reaction was evacuated/backfilled (vacuum/O₂) and allowed to stir for 14 h, at which time the consumption of starting material was complete (as determined by TLC analysis, 8:2 hexanes:EtOAc). The reaction was then diluted with H₂O and brine and the product was extracted with EtOAc (3 × 50 mL). The combined organic layers were washed with brine (3 × 100 mL), dried over Na₂SO₄, filtered, and concentrated in vacuo. The crude product was purified by flash chromatography (SiO₂, 9:1 hexanes:EtOAc to 8:2 hexanes:EtOAc) to generate ketone **404** (1.02 g, 7:1 ketone:aldehyde) as a pale yellow oil which was carried on to the next reaction without further purification.

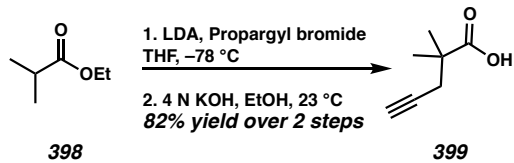
Enone **404** (1.0 g, 4.8 mmol, 1.0 equiv) was dissolved in xylenes (53 mL) in a flask fitted with a Dean–Stark trap and a reflux condenser. Freshly powdered KOH (300 mg, 5.3 mmol, 1.1 equiv) was added in one portion. The reaction was allowed to stir for 14 h at 110 °C, at which time the consumption of starting material was complete (as determined by TLC analysis, 4:1 hexanes:EtOAc). The crude solution was directly purified by flash chromatography (SiO₂, 100% hexanes then 9:1 hexanes:EtOAc) to furnish enone **397** (674 mg, 76% yield over 2 steps) as a yellow oil; R_f = 0.24 (4:1 hexanes:EtOAc); ¹H NMR (400 MHz, CDCl₃) δ 6.36 (d, J = 2.4 Hz, 1H), 5.69 (s, 1H), 2.46–2.28 (m, 4H), 2.20 (d, J = 17.4

Hz, 1H), 1.92 (ddd, $J = 12.9, 5.3, 1.7$ Hz, 1H), 1.71–1.62 (m, 1H), 1.15 (s, 3H), 1.11 (dd, $J = 6.9, 0.9$ Hz, 6H); ^{13}C NMR (101 MHz, CDCl_3) δ 208.1, 179.2, 159.3, 122.7, 116.4, 51.7, 40.4, 35.9, 34.2, 25.8, 25.6, 21.5, 21.1; IR thin film, NaCl) 2962, 2927, 2872, 1698, 1622, 1581, 1464, 1414, 1375, 1329, 1288, 1266, 1247, 1179, 1143, 898 882 cm^{-1} ; HRMS (ES/APCI) m/z calc'd $\text{C}_{13}\text{H}_{19}\text{O} [\text{M}+\text{H}]^+$: 191.1430, found: 191.1440; (R): $[\alpha]_D^{25} -435.36^\circ$ (c 0.93, CDCl_3 , 87% ee); (S): $[\alpha]_D^{25} +302.67^\circ$ (c 0.59, CDCl_3 , 87% ee).

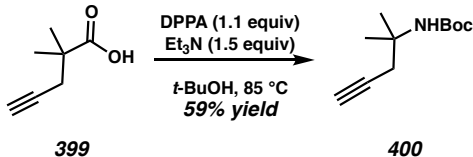


(R)-3-bromo-5-isopropyl-7a-methyl-1,6,7,7a-tetrahydro-2*H*-inden-2-one (391): A flask covered in aluminum foil with enone **397** (100 mg, 0.53 mmol, 1.0 equiv) diluted with MeCN (16 mL, 0.03 M) and cooled to 0 °C. NBS (104 mg, 0.58 mmol, 1.1 equiv) dissolved in MeCN (1.6 mL, 0.3 M) was added dropwise to the reaction over 4 h via syringe pump. After complete addition of NBS, the reaction was allowed to stir for 1 h at 0 °C, at which time complete consumption of starting material was observed (determined by TLC analysis, 4:1 hexanes:EtOAc). The reaction was concentrated in vacuo and purified directly by flash chromatography (9:1 hexanes:EtOAc) to yield vinyl bromide **391** (118 mg, 83% yield) as a yellow oil; $R_f = 0.36$ (4:1 hexanes:EtOAc); ^1H NMR (400 MHz, CDCl_3) δ 6.43 (dq, $J = 2.5, 0.9$ Hz, 1H), 2.53–2.23 (m, 5H), 1.92 (ddd, $J = 13.1, 5.1, 2.0$ Hz, 1H), 1.64 (ddd, $J = 13.0, 11.1, 6.1$ Hz, 1H), 1.17 (s, 3H), 1.15 (d, $J = 6.9$ Hz, 6H); ^{13}C NMR (101 MHz, CDCl_3) δ 199.8, 173.6, 162.2, 115.4, 114.8, 49.6, 40.7, 36.2, 34.2, 26.2, 25.7, 21.5, 21.1; IR thin film, NaCl) 2963, 2928, 2872, 1712, 1614, 1579, 1458, 1421, 1374, 1314, 1259, 1245, 1211, 1175, 955, 881 cm^{-1} ; HRMS (ES/APCI) m/z calc'd $\text{C}_{13}\text{H}_{18}\text{OBr} [\text{M}+\text{H}]^+$:

269.0536, found: 269.0547; (R): $[\alpha]_D^{25} -311.57^\circ$ (*c* 0.875, CDCl₃, 87% ee); (S): $[\alpha]_D^{25} +329.26^\circ$ (*c* 1.245, CDCl₃, 87% ee).

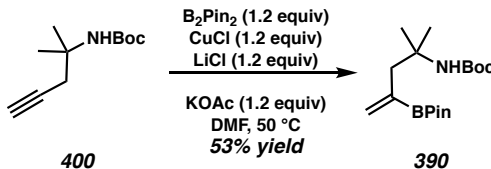


2,2-dimethylpent-4-ynoic acid (399): Acid 399 was formed using known literature procedures³² as a pale orange amorphous solid; ¹H NMR (400 MHz, CDCl₃) δ 11.52 (bs, 1H), 2.47 (d, *J* = 2.7 Hz, 2H), 2.04 (t, *J* = 2.7 Hz, 1H), 1.32 (s, 6H). All other characterization data match known literature values.³²



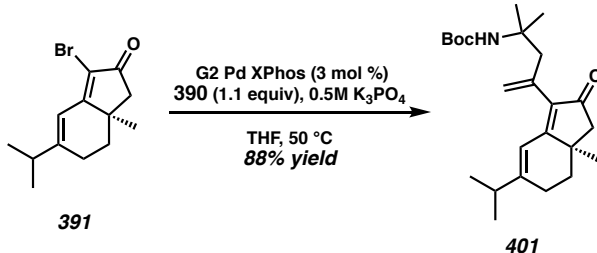
tert-butyl (2-methylpent-4-yn-2-yl)carbamate (400): A flask containing alkyne 399 (3.5 g, 28 mmol, 1.0 equiv) in anhydrous *t*-BuOH (100 mL, 0.28 M) was charged with Et₃N (5.9 mL, 42 mmol, 1.5 equiv) and diphenyl phosphoryl azide (DPPA, 6.7 mL, 30.8 mmol, 1.1 equiv). The reaction was heated to reflux and allowed to stir for 24 h. The reaction was then concentrated in vacuo, dissolved in EtOAc (100 mL), and washed sequentially with 5% citric acid and saturated NaHCO₃. The organic layer was then dried over Na₂SO₄, filtered, and concentrated in vacuo. The crude product was purified by flash chromatography (SiO₂, 5% EtOAc in hexanes) to generate alkyne 400 (3.3 g, 59% yield) as a white amorphous solid; R_f = 0.35 (12:1 hexanes:EtOAc); ¹H NMR (400 MHz, CDCl₃) δ 4.59 (bs, 1H), 2.59 (d, *J* = 2.7 Hz, 2H), 2.00 (t, *J* = 2.7 Hz, 1H), 1.43 (s, 9H), 1.35 (s, 6H); ¹³C NMR (101 MHz, CDCl₃) δ 154.7, 81.3, 79.2, 70.5, 51.9, 30.6, 28.6, 26.9; IR thin

film, NaCl) 3361, 3310, 2977, 2932, 1718, 1501, 1457, 1390, 1367, 1290, 1247, 1170, 1079, 865 cm⁻¹; HRMS (FAB+) m/z calc'd C₁₁H₂₀NO₂ [M+H]⁺: 198.1494, found: 198.1482.



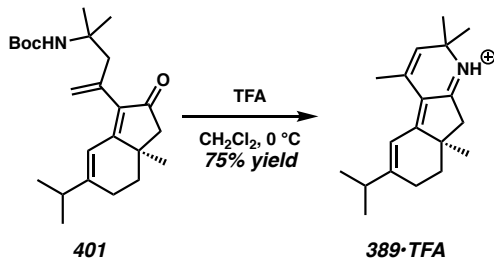
tert-butyl (2-methyl-4-(4,4,5,5-tetramethyl-1,3,2-dioxaborolan-2-yl)pent-4-en-2-yl)carbamate (390): Hydroboration of **400** was adapted from a known procedure.³³ In a nitrogen-filled glovebox, CuCl (420 mg, 4.3 mmol, 1.2 equiv) and LiCl (175 mg, 4.3 mmol, 1.2 equiv) were distributed evenly between seven 1-dram vials (60 mg and 25 mg per vial respectively). DMF (0.85 mL, 0.6 M) was added to each vial and the resulting suspensions were stirred vigorously for 1 h. Each vial was then charged sequentially with KOAc (60 mg, 0.61 mmol, 1.2 equiv), B₂PiN₂ (154 mg, 0.61 mmol, 1.2 equiv), and alkyne **400** (100 mg, 0.51 mmol, 1.0 equiv) dissolved in DMF (0.2 mL). The reactions were heated to 50 °C and stirred for 24 h. The vials were combined and diluted with saturated aqueous solution of NH₄Cl (40 mL) and EtOAc (50 mL). The product was extracted from the biphasic solution with EtOAc (3 × 50 mL) and the combined organic layers were washed with brine (3 × 100 mL), dried over MgSO₄, filtered, and concentrated in vacuo. The crude solution was purified by flash chromatography (SiO₂, 5% Et₂O in hexanes) to generate vinyl boronic ester **390** (610 mg, 53% yield) as a white amorphous solid; R_f = 0.33 (12:1 hexanes:EtOAc); ¹H NMR (400 MHz, CDCl₃) δ 5.98 (d, J = 3.6 Hz, 1H), 5.65 (d, J = 3.6 Hz, 1H), 5.40 (bs, 1H), 2.33 (d, J = 1.0 Hz, 2H), 1.41 (s, 9H), 1.28 (s, 18H); ¹³C NMR (101 MHz, CDCl₃) δ 134.8, 84.1, 78.3, 52.8, 51.0, 47.7, 29.9, 28.7, 26.7, 24.8; IR thin film,

NaCl) 3396, 2976, 2930, 1719, 1517, 1447, 1365, 1305, 1269, 1252, 1165, 1142, 1064, 960, 951, 861, 733 cm⁻¹; HRMS (ES/APCI) m/z calc'd C₁₇H₃₃¹¹BO₄N [M+H]⁺: 326.2497, found: 326.2507.



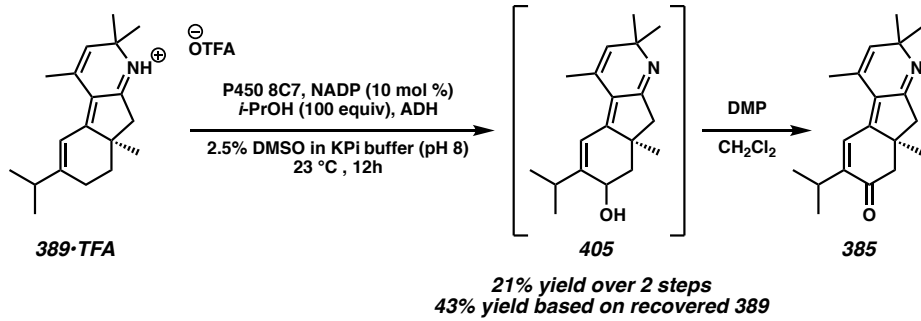
tert-butyl (R)-(4-(5-isopropyl-7a-methyl-2-oxo-2,6,7,7a-tetrahydro-1*H*-inden-3-yl)-2-methylpent-4-en-2-yl)carbamate (401): A flask was charged with vinyl bromide **391** (300 mg, 1.11 mmol, 1.0 equiv), vinyl boronic acid **390** (387 mg, 1.22 mmol, 1.1 equiv), 0.5 M K₃PO₄ in degassed H₂O (4.4 mL, 0.25 M), and THF (2.2 mL, 0.5 M). Buchwald's 2nd generation precatalyst XPhos (26 mg, 0.03 mmol, 0.03 equiv) was added to the reaction with an overpressure of Ar. The reaction was allowed to stir for 16 h at 60 °C, at which time complete consumption of starting material was observed (determined by TLC analysis, 9:1 hexanes:EtOAc). The product was extracted with Et₂O (3 x 10 mL) and the combined organic layers were washed with brine, dried with MgSO₄, filtered, and concentrated in vacuo. The crude product was purified by flash chromatography (SiO₂ 9:1 hexanes:EtOAc) to furnish enone **401** (377 mg, 88% yield) as a white crystalline solid; R_f = 0.17 (9:1 hexanes:EtOAc); mp: 97.7 – 98.5 °C; ¹H NMR (400 MHz, CDCl₃) δ 6.49 (d, *J* = 2.5 Hz, 1H), 5.24 (d, *J* = 2.3 Hz, 1H), 5.00 (d, *J* = 2.4 Hz, 1H), 4.49 (s, 1H), 2.79 (d, *J* = 13.6 Hz, 1H), 2.66 (d, *J* = 13.5 Hz, 1H), 2.49–2.24 (m, 4H), 2.20 (d, *J* = 17.4 Hz, 1H), 1.93 (ddd, *J* = 12.9, 5.4, 1.6 Hz, 1H), 1.62 (dt, *J* = 12.5, 6.2 Hz, 1H), 1.41 (s, 9H), 1.22 (s, 3H), 1.20 (s, 3H), 1.13 (s, 3H), 1.13 (d, *J* = 0.9 Hz, 3H), 1.11 (d, *J* = 0.9 Hz, 3H); ¹³C NMR (101

MHz, CDCl₃) δ 206.2, 171.3, 159.1, 137.9, 135.2, 121.0, 115.5, 78.5, 52.7, 51.4, 45.7, 38.4, 36.0, 34.1, 28.5, 27.5, 25.5, 25.1, 21.6, 21.0; IR thin film, NaCl) cm⁻¹; HRMS (ES/APCI) m/z calc'd C₂₄H₃₈NO₃ [M+H]⁺: 388.2846, found: 388.2864; (R): [α]_D²⁵ -256.26° (c 0.45, CDCl₃, 87% ee); (S): [α]_D²⁵ +265.13° (c 0.27, CDCl₃, 87% ee); SFC (IC, 30% IPA) (R) retention time: 6.385, (S) retention time: 5.691. The ee of **401** can be increased to 99% through preparative HPLC (IC, 20 x 250 μm, 30% IPA in hexanes, (R) retention time: 18.2 min, (S) retention time: 16.6 min); (R): [α]_D²⁵ -297.74° (c 0.51, CHCl₃, 99% ee); (S): [α]_D²⁵ +294.25° (c 0.44, CHCl₃, 99% ee).



(R)-6-isopropyl-2,2,4,8a-tetramethyl-7,8,8a,9-tetrahydro-2*H*-indeno[2,1-*b*]pyridine (389): TFA (0.34 mL, 0.4 M) was added to enone **401** (53 mg, 0.14 mmol) in CH₂Cl₂ (1.4 mL, 0.1 M) at 0 °C. The reaction was allowed to warm to ambient temperature and stirred for an additional 1 h, at which time complete consumption of starting material was observed (determined by TLC analysis (4:1 hexanes:EtOAc)). The reaction was quenched with saturated aqueous NaHCO₃ until the solution was neutralized and allowed to stir for 1 h, at which time complete cyclization occurred (determined through LC-MS analysis, m/z = 270.1 [M+H]⁺). The product was extracted from the biphasic mixture with CH₂Cl₂ (3 × 30 mL), dried over Na₂SO₄, and filtered. SiO₂ was added and the suspension was stirred for 1 h. The solution was concentrated and purified by flash chromatography (SiO₂, 0–10% methanol in EtOAc) to generate imine **389**•TFA as a tan amorphous solid. **389**•TFA

can be deprotonated by washing a 10% aqueous solution of potassium carbonate to afford **389** (28 mg, 75% yield) as a viscous yellow oil; $R_f = 0.25$ (8% methanol in EtOAc); ^1H NMR (400 MHz, CDCl_3) δ 6.56 (d, $J = 2.4$ Hz, 1H), 5.56 (d, $J = 1.5$ Hz, 1H), 2.51 – 2.27 (m, 4H), 2.24 – 2.15 (m, 1H), 2.02 (d, $J = 1.5$ Hz, 3H), 1.88 (ddd, $J = 12.7, 5.6, 1.7$ Hz, 1H), 1.59 (td, $J = 12.3, 5.8$ Hz, 1H), 1.24 (d, $J = 4.1$ Hz, 6H), 1.08 (d, $J = 6.8$ Hz, 6H), 1.06 (s, 3H); ^{13}C NMR (101 MHz, CDCl_3) δ 171.1, 152.2, 150.5, 135.6, 125.0, 119.3, 115.1, 58.4, 45.9, 39.3, 34.9, 33.6, 30.3, 30.1, 27.4, 24.1, 24.0, 20.6, 20.2, 20.1; IR thin film, NaCl) 2962, 2922, 2177, 1660, 1615, 1456, 1407, 1374, 1286, 1261, 1154, 1048, 873, 842, 811, 732 cm^{-1} ; HRMS (ES/APCI) m/z calc'd $\text{C}_{19}\text{H}_{28}\text{N}$ [M+H] $^+$: 270.2216, found: 270.2228; (R): $[\alpha]_D^{25} -223.18$ (c 0.3, CHCl₃, 87% ee); (S): $[\alpha]_D^{25} +250.16^\circ$ (c 0.28, CDCl₃, 87% ee); (R): $[\alpha]_D^{25} -340.60^\circ$ (c 0.6, CHCl₃, 99% ee); (S): $[\alpha]_D^{25} +391.68^\circ$ (c 1.39, CHCl₃, 99% ee).



Nigelladine A (385): Lysate containing the enzyme “8C7” was prepared from a 500-mL TB_{amp} expression culture as described above. The concentration of 8C7 was determined to be 8.5 μM .

A 1-L Erlenmeyer flask was charged with **5**•trifluoroacetate (160 mg, 417 μmol), followed by NADP disodium salt (33 mg, 41.7 μmol). The solids were dissolved in 10 mL

of DMSO and 400 mL of potassium phosphate buffer (100 mM, pH 8). Next, isopropanol (3.2 mL) and lysate (21 mL) were added. Finally, alcohol dehydrogenase (recombinant from *E. coli*, 49641 Sigma) was added. The reaction was shaken at ambient temperature and 100 rpm (19 mm radius). After 12 hours, the reaction volume was reduced *in vacuo* to ~100 mL, then the products were extracted with ethyl acetate (250 mL plus 2×100 mL). An emulsion formed on the third extraction, so the mixture was subjected to centrifugation (5,000×*g*, 20 °C, 2 minutes) in order to separate the layers. The combined organic extracts were dried over sodium sulfate, filtered, and then concentrated *in vacuo*. The crude reaction was subjected to column chromatography (SiO₂, 0–15% methanol in ethyl acetate) yielding free imine **389** (57 mg, 0.21 mmol, 51% recovery) and an inseparable mixture of diastereomers and constitutional isomers of oxidation products, which were carried on to the next reaction without further purification.

Crude alcohol **405** (55.4 mg, 0.19 mmol, 1.0 equiv) was dissolved in wet CH₂Cl₂ (4 mL, 0.05M). DMP (98.7 mg, 0.23 mmol, 1.2 equiv) was added in one portion and allowed to stir at ambient temperature. After 3 hours, the reaction was quenched with saturated aqueous Na₂S₂O₃ and the product was extracted with CH₂Cl₂ (3 × 15 mL). The organic layers were combined and washed with a saturated aqueous solution of K₂CO₃ dried over Na₂SO₄ and concentrated *in vacuo*. The crude product was purified by column chromatography (SiO₂, 0–16% methanol in ethyl acetate) to generate nigelladine A (**385**) (25 mg, 21% yield) as an orange oil; R_f = 0.54 (8% methanol in ethyl acetate); ¹H NMR (400 MHz, C₆D₆) δ 7.22 (d, *J* = 1.0 Hz, 1H), 5.63 (q, *J* = 1.4 Hz, 1H), 3.16 (pd, *J* = 6.8, 1.1 Hz, 1H), 2.47 (d, *J* = 15.4 Hz, 1H), 2.42 (d, *J* = 16.9 Hz, 1H), 2.27 (d, *J* = 16.9 Hz, 1H), 2.09 (dd, *J* = 15.4, 0.9 Hz, 1H), 1.77 (d, *J* = 1.4 Hz, 3H), 1.40 (s, 3H), 1.35 (s, 3H), 1.06

(d, $J = 6.9$ Hz, 3H), 1.03 (d, $J = 6.9$ Hz, 3H), 0.93 (s, 3H); ^{13}C NMR (101 MHz, C_6D_6) δ 196.1, 170.2, 147.2, 147.0, 141.9, 130.6, 126.0, 125.1, 61.2, 51.7, 46.5, 43.6, 31.1, 30.8, 27.5, 26.8, 22.1, 21.7, 21.0; IR thin film, NaCl) 2962, 2926, 2872, 1670, 1618, 1458, 1375, 1303, 1230, 1147, 1045, 920, 840 cm^{-1} ; HRMS (ES/APCI) m/z calc'd $\text{C}_{19}\text{H}_{26}\text{NO} [\text{M}+\text{H}]^+$: 284.2009, found: 284.2021; (*R*): $[\alpha]_D^{25} -200.3$ (*c* 0.10, MeOH).

3.8.4 ENZYMATIC SCREENS AND ENANTIOMER SCREEN

Initial screen of enzymes:

Lysates containing the desired enzymes were prepared from 5-mL expression cultures according to the procedure described above.

A 2-mL vial was charged with 5•trifluoroacetate as a solution in DMSO (5 μL , 280 mM). Potassium phosphate buffer (100 mM, pH 8, 35 μL) was added, followed by lysate (80 μL). The reactions were initiated by the addition of NADPH (80 μL , 50 mM aqueous solution) and shaken at ambient temperature and 450 rpm (Labnet Orbit P4 shaker). After 1 hour, the reactions were diluted with 1:1 CH₃CN/H₂O (800 μL), and subjected to centrifugation at 20,000 $\times g$ and 4 °C (10 minutes). The supernatant was analyzed by LCMS (ESI, positive mode) with a C-18 column (1.8 μm , 2.1 \times 50 mm). The compounds were eluted with water (0.1% acetic acid by volume) and acetonitrile at a gradient of 5% to 95% acetonitrile over 4 minutes. Selectivity was approximated by extracting m/z = 286 from the total ion count, and comparing the integration of the desired product (1.6 min) to the isopropyl oxidation product (1.3 min) and an additional product (1.8 min).

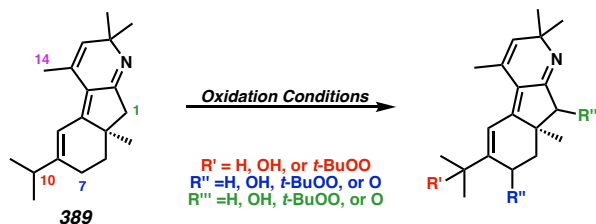
Comparison of enantiomers:

Lysates containing the desired enzymes were prepared from 5-mL expression cultures according to the procedure described above. Reactions were conducted in duplicate.

A 2-mL vial was charged with 5•trifluoroacetate as a solution in DMSO (10 µL, 200 mM). Potassium phosphate buffer (100 mM, pH 8, 290 µL) was added, followed by lysate (20 µL). Finally, the reactions were initiated by the addition of NADPH (80 µL, 50 mM aqueous solution) and shaken at ambient temperature and 500 rpm (Labnet Orbit P4 shaker). After 15 minutes, the reactions were diluted fivefold with 1:1 CH₃CN/H₂O, and subjected to centrifugation at 20,000×g and 4 °C (10 minutes). The supernatant was analyzed by LCMS using the method described above. Selectivity was approximated by extracting m/z from 269.5 to 286.5, so as to include residual starting material and all mono-oxygenation products. The desired product peak partially overlapped with a trace oxidation byproduct formed during preparation of the starting material, therefore the % integration of the peak at 1.4 minutes was subtracted by the % integration of the corresponding peak in the unreacted starting material. This gave % integrations of the desired product of 2.763% and 3.144% for the *S* enantiomer, and 3.828% and 4.069% for the *R* enantiomer. The *k*_{rel} was approximated as the ratio of the average % integration for each enantiomer.

3.8.5 CHEMICAL OXIDATION TABLES

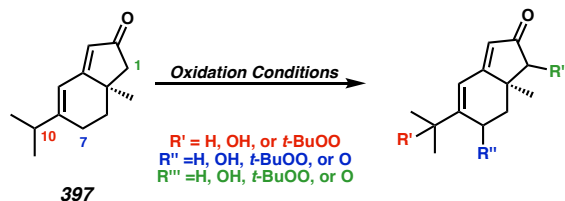
Table 3.8.5.1. Oxidations of Imine 389



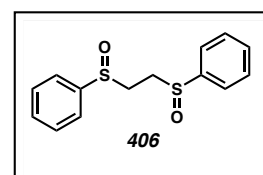
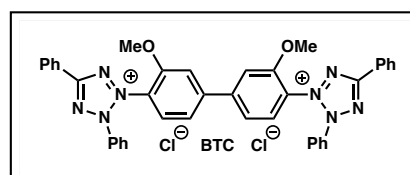
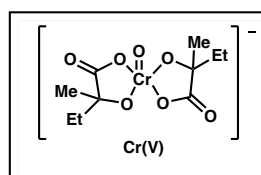
Entry	Conditions	SM M/z= (270)	HPLC Yield of Oxygenation Products (%) ^{a,b,c}											
			C1 (284)	C7		C10		Polyoxygenation						
				(286)	(284)	(286)	(358)	(302)	(300)	(298)	(314)	(374)	(316)	(390)
1	SeO ₂ , DCM, 40 °C	21	79 (57) ^d	–	–	–	–	–	–	–	–	–	–	
2	SeO ₂ (anhydrous), dioxane, 80 °C	–	–	–	–	–	–	–	–	60 (24)	12	–	5	
3	Pd/C (10 wt%), TBHP, 0 °C	3	–	–	3	–	44	–	–	4	–	35	–	
4	Cr(V) (5 equiv), MnO ₂ , CF ₃ C ₆ H ₅ , 15-crown-5, 80 °C	–	–	–	5	–	–	6	–	55	10	–	19	
5	Cr(V) (1 equiv), MnO ₂ , CF ₃ C ₆ H ₅ , 15-crown-5, 80 °C	55	3	–	35 ^e	–	–	2	1	3	–	–	–	
6	Rh ₂ (esp) ₂ , T-HYDRO, 23 °C	2	8	–	21 (10)	–	–	4	–	–	–	–	4	
7	CrO ₃ , 3,5-dimethylpyrazole, ^f DCE, 80 °C	–	–	–	–	–	–	–	–	–	–	–	–	
8	8C7 P450 oxidation	47	–	32	–	11	–	–	1	–	–	–	–	

^a Approximated by separating the products on UHPLC-MS and comparing ion counts of the various oxidation products. ^b Remaining percent balance remaining were unidentified side products. ^c Numbers given in parenthesis indicate isolated yields of the oxidized product. ^d Protection of 389 as an N-acyl enamide results in oxidation at C-14. ^e Observed C-7 olefin isomerization yielding oxidation at C-5. ^f No reaction was observed.

Table 3.8.5.2. Oxidations of Enone 397



Entry	Conditions	SM M/z= (191)	HPLC Yield of Oxygenation Products (%) ^{a,b,c}						Polyoxygenation			
			C1 (205)	C7 (205) (207)	C10 (279) (207)	(223)	(295)	(367)	(221)	(238)		
1	SeO_2 , DCM, 40 °C	5	26 (22)	–	–	–	–	–	–	–	15	–
2	Pd/C (10 wt%), TBHP, 0 °C ^d	46	–	2	–	40 (23)	2	3	1	–	–	–
3	$\text{Rh}_2(\text{esp})_2$, T-HYDRO, 23 °C	–	–	10	5	14	2	9	9	15	10	–
4	Cr(V) (5 equiv), MnO_2 , $\text{CF}_3\text{C}_6\text{H}_5$, 15-crown-5, 80 °C	58	2	7	–	–	15	–	–	–	4	–
5	Cr(V) (1 equiv), MnO_2 , $\text{CF}_3\text{C}_6\text{H}_5$, 15-crown-5, 80 °C	84	–	4	–	–	5	–	–	–	–	1
6	PIFA, TBHP, Cs_2CO_3 , O_2 , 4 Å mol sieves, EtOAc , –78 to –15 °C	76	–	–	–	24 ^e	–	–	–	–	–	–
7	$\text{Cl}_4\text{-NHPI}$, LiClO_4 , acetone TBHP, pyridine, e [–]	68	–	–	–	5	–	4	–	–	–	–
8	PCC, NaOAc benzene, celite, 80 °C	79	9	4	–	–	–	–	–	–	–	–
9	CrO_3 , 3,5-dimethylpyrazole, ^f DCE, 80 °C	–	–	–	–	–	–	–	–	–	–	–
10	Pd(OAc)_2 , 406, AcOH, ^f dioxane, air	–	–	–	–	–	–	–	–	–	–	–
11	Pd(OAc)_2 , oxone, ^g AcOH, 95 °C	–	–	–	–	–	–	–	–	–	–	–
12	BTC, KOH, EtOH, 80 °C ^g	–	–	–	–	–	–	–	–	–	–	–
13	$\text{Pd(OH)}_2/\text{C}$ (10 wt%), ^f trityl peroxide, 0 °C CH_2Cl_2	–	–	–	–	–	–	–	–	–	–	–



^a Approximated by separating the products on UHPLC-MS and comparing ion count of the various oxidation products. ^b Remaining percent balance were unidentified side products. ^c Numbers given in parentheses indicate isolated yields of the oxidized product. ^d Shortened reaction time used to observe inherent regioselectivity without over oxidation. ^e Site-selectivity determined by analogy from Table 3.8.5.1 entry 3. ^f No reaction observed. ^g Decomposition was observed.

3.8.6 COMPARISON OF NATURAL AND SYNTHETIC NIGELLADINE A

Table 3.8.6.1. Comparison of Synthetic and Natural Nigelladine A³⁴

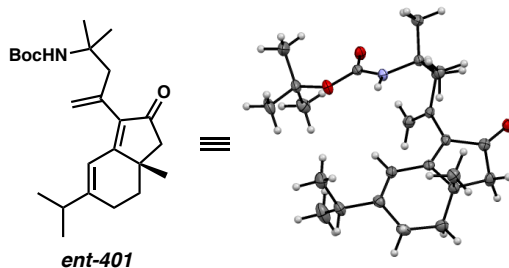
Synthetic mono-deuterated, DCl salt of Nigelladine A (385)	Isolated Nigelladine A ^{2a}
¹ H NMR (400 MHz, methanol- <i>d</i> ₄)	¹ H NMR (600 MHz, methanol- <i>d</i> ₄)
7.64 (br, 1H)	7.64 (br, 1H)
5.97 (q, <i>J</i> = 1.5 Hz, 1H)	5.97 (q, <i>J</i> = 1.2 Hz, 1H)
3.05 (pd, <i>J</i> = 6.8, 1.1 Hz, 1H)	3.05 (pd, <i>J</i> = 6.9, 0.8 Hz, 1H)
2.99 (s, 1H)	3.01 (s, 1H)
2.84 (s, 2H)	2.84 (s, 2H)
2.25 (d, <i>J</i> = 1.5 Hz, 3H)	2.25 (d, <i>J</i> = 1.2 Hz, 3H)
1.55 (s, 3H)	1.55 (s, 3H)
1.53 (s, 3H)	1.54 (s, 3H)
1.17 (d, <i>J</i> = 6.8 Hz, 3H)	1.17 (d, <i>J</i> = 6.9 Hz, 3H)
1.14 (d, <i>J</i> = 6.9 Hz, 3H)	1.14 (d, <i>J</i> = 7.2 Hz, 3H)
¹³ C NMR (101 MHz, Methanol- <i>d</i> ₄)	¹³ C NMR (150 MHz, Methanol- <i>d</i> ₄)
197.5	197.6
184.3	184.3
165.8	165.8
154.6	154.7
136.2	136.4
130.1	130.1
126.6	126.7
125.9	126.0
61.3	61.5
51.4	51.6
49.7	49.6
44.0	44.2
29.3	29.5
29.0	29.2
29.0	29.1
27.7	27.8
22.0	22.1
21.5	21.6
20.5	20.6
<i>Optical Rotation</i>	<i>Optical Rotation</i>
[α] _D ²⁶ = -200.3 (<i>c</i> 0.10, MeOH)	[α] _D ²⁰ = -53 (<i>c</i> 0.10, MeOH)

3.8.8 NOTES & REFERENCES

1. For recent reviews on direct C–H functionalization see: (a) Lyons, T. W.; Sanford, M. S. *Chem. Rev.* **2010**, *110*, 1147–1169. (b) Wencel-Delord, J.; Dröge, T. *Chem. Soc. Rev.* **2011**, *40*, 4740–4761. (c) Engle, K. M.; Mei, T.-S.; Wasa, M.; Yu, J.-Q. *Acc. Chem. Res.* **2012**, *45*, 788–802. (d) Wendlandt, A. E.; Suess, A. M.; Stahl, S. S. *Angew. Chem., Int. Ed. Engl.* **2011**, *50*, 11062–11087. (e) Gutekunst, W. R.; Baran, P. S. *Chem. Soc. Rev.* **2011**, *40*, 1976–1991. (f) Yamaguchi, J.; Yamaguchi, A. D.; Itami, K. *Angew. Chem. Int. Ed. Engl.* **2012**, *51*, 8960–9009. (g) Davies, H. M. L.; Manning, J. R. *Nature* **2008**, *451*, 417–424
2. (a) Chen, Q. B.; Xin, X. L.; Yang, Y.; Lee, S. S.; Aisa, H. A. *J. Nat. Prod.* **2014**, *77*, 807–812. (b) Zhang, S.; Zhang, Z. Y. *Drug Discovery Today* **2007**, 373–381.
3. Nakamura, A.; Nakada, M. *Synthesis* **2013**, *45*, 1421–1451.
4. Weidmann, V.; Maison, W. *Synthesis* **2013**, *45*, 2201–2221.
5. For reviews of biocatalysis and directed evolution see: (a) Arnold, F. H. *Acc. Chem. Res.* **1998**, *31*, 125–131. (b) Reetz, M. T. *Angew. Chem., Int. Ed. Engl.* **2001**, *40*, 284–310. (c) Turner N. J. *Nat. Chem. Biol.* **2009**, *5*, 567–573. (d) Wohlgemuth, R. *Curr. Opin. Biotechnol.* **2010**, *21*, 713–724. (e) Reetz, M. T. *J. Am. Chem. Soc.* **2013**, *135*, 12480–12496. (f) Nestl, B. M.; Hammer, S. C.; Nebel, B. A.; Hauer, B. *Angew. Chem., Int. Ed. Engl.* **2014**, *53*, 3070–3095. (g) Denard, C. A.; Ren, H.; Zhao, H. *Curr. Opin. Chem. Biol.* **2015**, *25*, 55–64.
6. (a) Jung, S. T.; Lauchli, R.; Arnold, F. H. *Curr. Opin. Biotechnol.* **2011**, *22*, 809–817. (b) Whitehouse, C. J.; Bell, S. G.; Wong, L. L. *Chem. Soc. Rev.* **2012**, *41*,

-
- 1218–1260. (c) Janocha, S.; Schmitz, D.; Bernhardt, R.
Adv. Biochem. Eng./Biotechnol. **2015**, *148*, 215–250. (d) Roiban, G.-D.; Reetz, M.
T. Chem. Commun. **2015**, *51*, 2208–2224.
7. (a) Hoffmeister, D.; Yang, J.; Liu, L.; Thorson, J. S. *Proc. Natl. Acad. Sci. U. S. A.* **2003**, *100*, 13184–13189. (b) Whitehouse, C. J. C.; Bell, S. G.; Tufton, H. G.; Kenny, R. J. P.; Ogilvie, L. C. I.; Wong, L. L. *Chem. Commun.* **2008**, 966–968. (c) Zhang, K.; Shafer, B. M.; Demars, M. D., II; Stern, H. A.; Fasan, R. *J. Am. Chem. Soc.* **2012**, *134*, 18695–18704. (d) Abreu, M.; Alvaro-Benito, M.; Sanz-Aparicio, J.; Plou, F. J.; Fernandez-Lobato, M.; Alcalde, M. *Adv. Synth. Catal.* **2013**, *355*, 1698–1702.
8. Behenna, D. C.; Mohr, J. T.; Sherden, N. H.; Marinescu, S. C.; Harned, A. M.; Tani, K.; Seto, M.; Ma, S.; Novak, Z.; Krout, M. R.; McFadden, R. M.; Roizen, J. L.; Enquist, J. A., Jr.; White, D. E.; Levine, S. R.; Petrova, K.V.; Iwashita, A.; Virgil, S. C.; Stoltz, B. M. *Chem. – Eur. J.* **2011**, *17*, 14199–14223.
9. Stork, G.; Danheiser, R. L. *J. Org. Chem.* **1973**, *38*, 1775–1776.
10. Dimitrov, V.; Kostova, K.; Genov, M. *Tetrahedron Lett.* **1996**, *37*, 6787–6790.
11. Corey, E. J.; Enders, D. *Tetrahedron Lett.* **1976**, *17*, 3–6.
12. McDougal, N. T.; Streuff, J.; Mukherjee, H.; Virgil, S. C.; Stoltz, B. M. *Tetrahedron Lett.* **2010**, *51*, 5550–5554.
13. Mehta, G.; Shinde, H. M. *J. Org. Chem.* **2012**, *77*, 8056–8070.
14. Day, J. J.; McFadden, R. M.; Virgil, S. C.; Kolding, H.; Alleva, J. L.; Stoltz, B. M. *Angew. Chem., Int. Ed. Engl.* **2011**, *50*, 6814–6818.

15. Zhu, J.; Germain, A. R.; Porco, J. A. Jr. *Angew. Chem., Int. Ed. Engl.* **2004**, *43*, 1239–1243.
16. Bruno, N. C.; Tudge, M. T.; Buchwald, S. L. *Chem. Sci.* **2013**, *4*, 916–920.
17. Crystals grown for X-ray crystallography were synthesized in the enantiomeric series using (*S*)-CF₃-*t*-Bu-PHOX for the asymmetric allylic alkylation of **393**.



18. The TFA salt of **389** can be deprotonated to the free imine by an aqueous wash with 10% potassium carbonate.
19. See Appendix 4 for full list of conditions and results.
20. (a) Salmond, W. G.; Barta, M. A.; Havens, J. L. *J. Org. Chem.* **1978**, *43*, 2057–2059. (b) Chen, M. S.; Prabagaran, N.; Labenz, N. A.; White, C. M. *J. Am. Chem. Soc.* **2005**, *127*, 6970–6971. (c) Yu, J.-Q.; Corey, E. J. *Org. Lett.* **2002**, *4*, 2727–2730. (d) Xing, X.; O’Connor, N. R.; Stoltz, B. M. *Angew. Chem., Int. Ed. Engl.* **2015**, *54*, 11186–11190. (e) Sparling, B. A.; Moebius, D. C.; Shair, M. D. *J. Am. Chem. Soc.* **2013**, *135*, 644–647. (f) Schmuff, N. R.; Trost, B. M. *J. Org. Chem.* **1983**, *48*, 1404–1412. (g) Zhao, Y.; Yeung, Y.-Y. *Org. Lett.* **2010**, *12*, 2128–2131. (h) Wang, Y.; Kuang, Y.; Wang, Y. *Chem. Commun.* **2015**, *51*, 5852–5855. (i) Wilde, N. C.; Isomura, M.; Mendoza, A.; Baran, P. S. *J. Am. Chem. Soc.* **2014**, *136*, 4909–4912. (j) Young, W. B.; Masters, J. J.; Danishefsky, S. *J. Am. Chem. Soc.*

- 1995, 117, 5228–5234. (k) Jasiczak, J. *J. Chem. Soc., Perkin Trans. I* **1988**, 2687–2692. (l) Horn, E. J.; Rosen, B. R.; Chen, Y.; Tang, J.; Chen, K.; Eastgate, M. D.; Baran, P. S. *Nature* **2016**, 533, 77–81. (m) Allen, J. G.; Danishefsky, S. J. *J. Am. Chem. Soc.* **2001**, 123, 351–352. (n) Quinn, R. K.; Könst, Z. A.; Michalak, S. E.; Schmidt, Y.; Szklarski, A. R.; Flores, A. R.; Nam, S.; Horne, D. A.; Vanderwal, C. D.; Alexanian, E. *J. Am. Chem. Soc.* **2016**, 138, 696–702.
21. Lewis, J. C.; Mantovani, S. M.; Fu, Y.; Snow, C. D.; Komor, R. S. Wong, C.-H.; Arnold, F. H. *ChemBioChem* **2010**, 11, 2502–2505.
22. (a) Rentmeister, A.; Arnold, F. H.; Fasan, R. *Nat. Chem. Biol.* **2009**, 5, 26–28. (b) Lewis, J. C.; Bastian, S.; Bennett, C. S.; Fu, Y.; Mitsuda, Y.; Chen, M. M.; Greenberg, W. A.; Wong, C.-H.; Arnold, F. H. *Proc. Natl. Acad. Sci. U. S. A.* **2009**, 106, 16550–16555. (c) Kille, S.; Zilly, F. E.; Acevedo, J. P.; Reetz, M. T. *Nat. Chem.* **2011**, 3, 738–743.
23. Wolberg, M.; Hummel, W.; Wandrey, C.; Müller, M. *Angew. Chem., Int. Ed. Engl.* **2000**, 39, 4306–4308.
24. The TFA salt of **389** was used to avoid deleterious aerobic oxidation of **389**. Both the TFA salt and the free base of **389** were competent substrates and reacted identically for the enzymatic oxidation.
25. Pangborn, A. M.; Giardello, M. A.; Grubbs, R. H.; Rosen, R. K.; Timmers, F. J. *Organometallics* **1996**, 15, 1518–1520.
26. Dauben, H. J.; McCoy, L. L. *J. Am. Chem. Soc.* **1959**, 81, 4863–4873.
27. Ireland, R. E.; Liu, L. *J. Org. Chem.* **1993**, 58, 2899–2899.

28. Liu, Y.; Liniger, M.; McFadden, R. M.; Roizen, J. L.; Malette, J.; Reeves, C. M.; Behenna, D. C.; Seto, M.; Kim, J.; Mohr, J. T. *Beilstein J. Org. Chem.* **2014**, *10*, 2501–2512.
29. Gulias, M.; Rodriguez, J. R.; Castedo, L.; Mascarenas, J. L. *Org. Lett.* **2003**, *5*, 1975–1977.
30. Martin, N. J. A.; List, B. *J. Am. Chem. Soc.* **2006**, *128*, 12268–13369.
31. Mino, T.; Masuda, S.; Nishio, M; Yamashita, M. *J. Org. Chem.* **1997**, *62*, 2633–2635.
32. Doering, W. V. E.; Yamashita, Y. *J. Am. Chem. Soc.* **1983**, *105*, 5368–5372.
33. Takahashi, K.; Ishiyama, T.; Miyaura, N. *J. Organomet. Chem.* **2001**, *47*–53.
34. Nigelladine A **385** was repurified by preparative HPLC prior to optical rotation and therefore we believe that nigelladine A is either possibly isolated as a scalemic mixture or the isolation chemists isolated a mixture of protonated and free imine.

APPENDIX 2

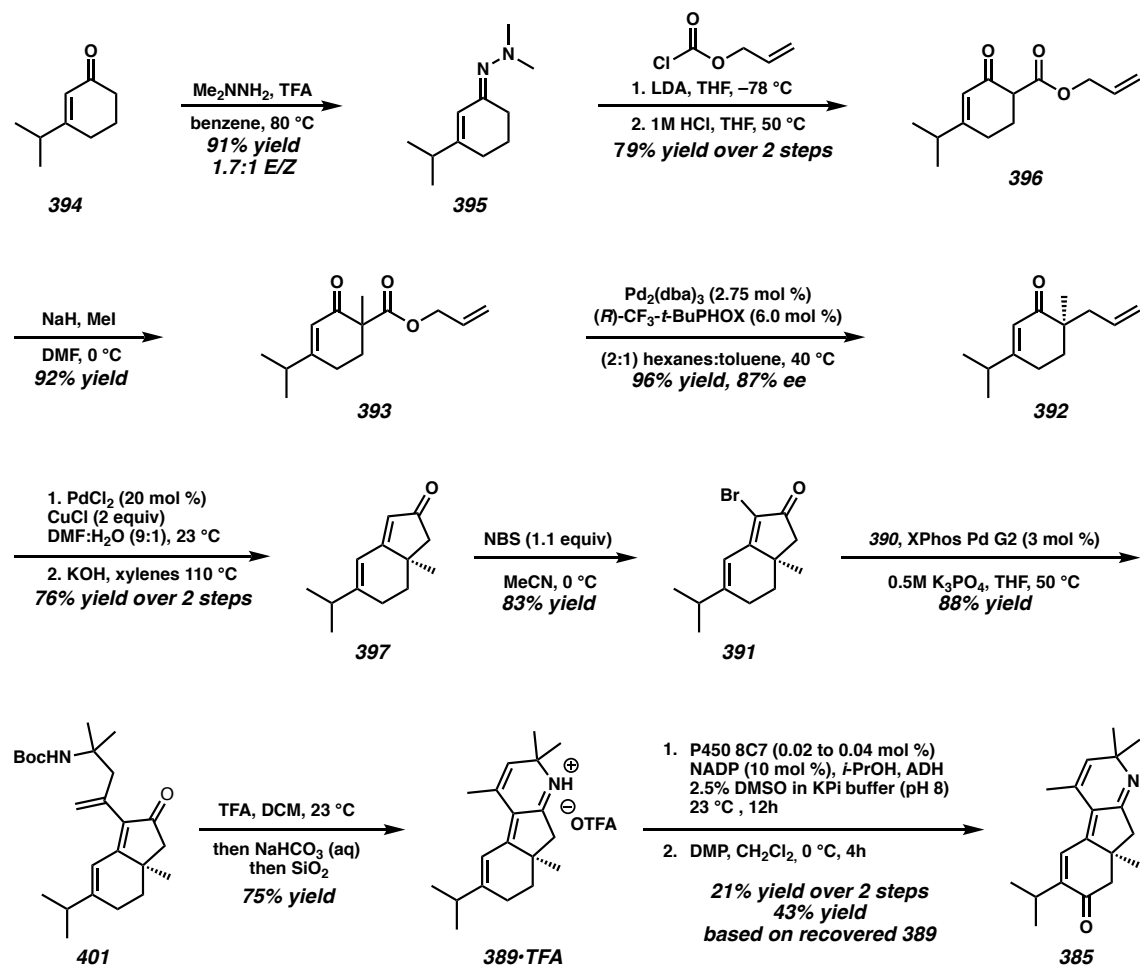
Synthetic Summary of Chapter 3:

Enantioselective Total Synthesis of Nigelladine A

Via Late-Stage C–H Oxidation Enabled by an

Engineered P450 Enzyme

Scheme A2.1. Synthetic Summary for Construction of Nigelladine A 385



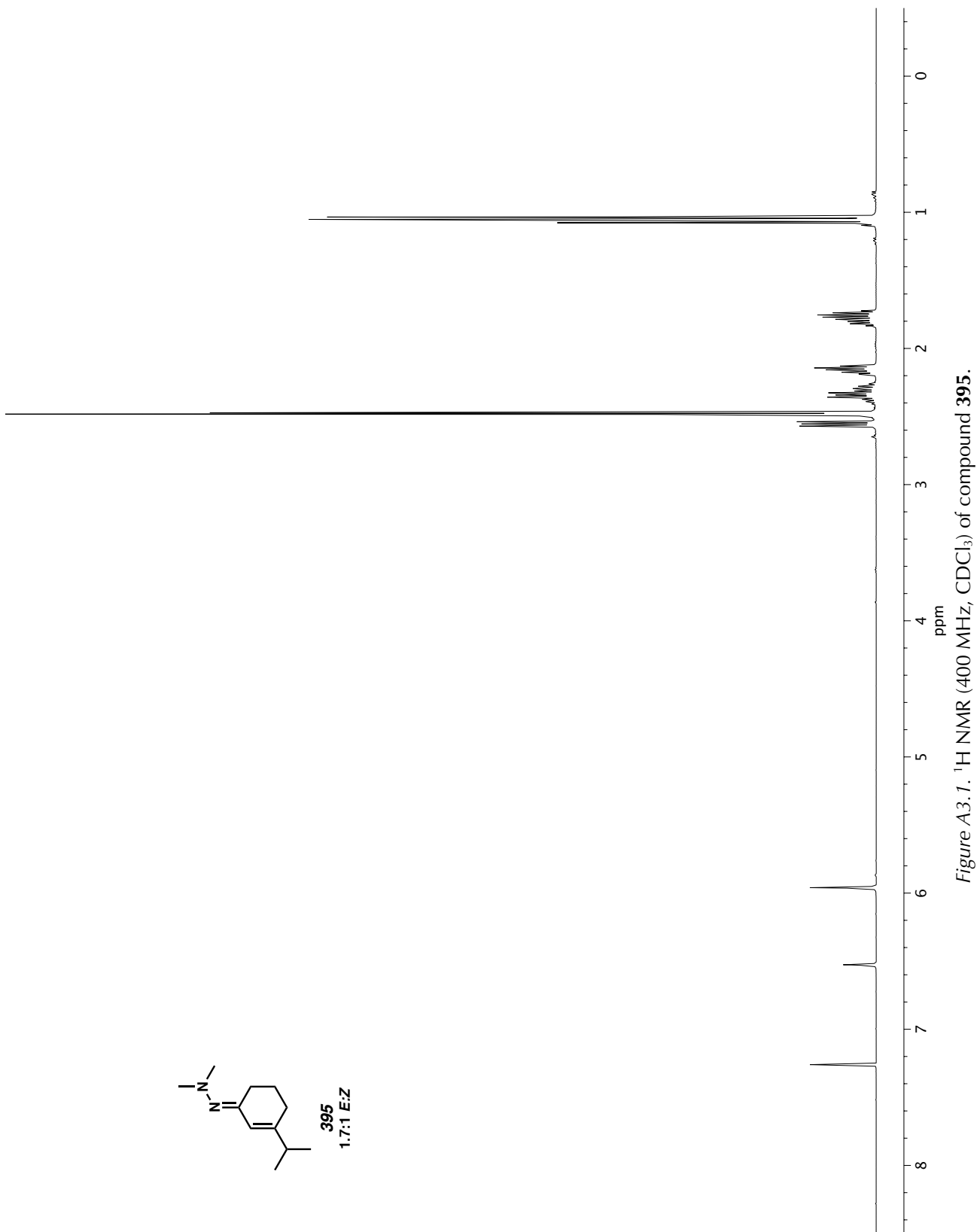
APPENDIX 3

Spectra Relevant to Chapter 3:

Enantioselective Total Synthesis of Nigelladine A

Via Late-Stage C–H Oxidation Enabled by an

Engineered P450 Enzyme



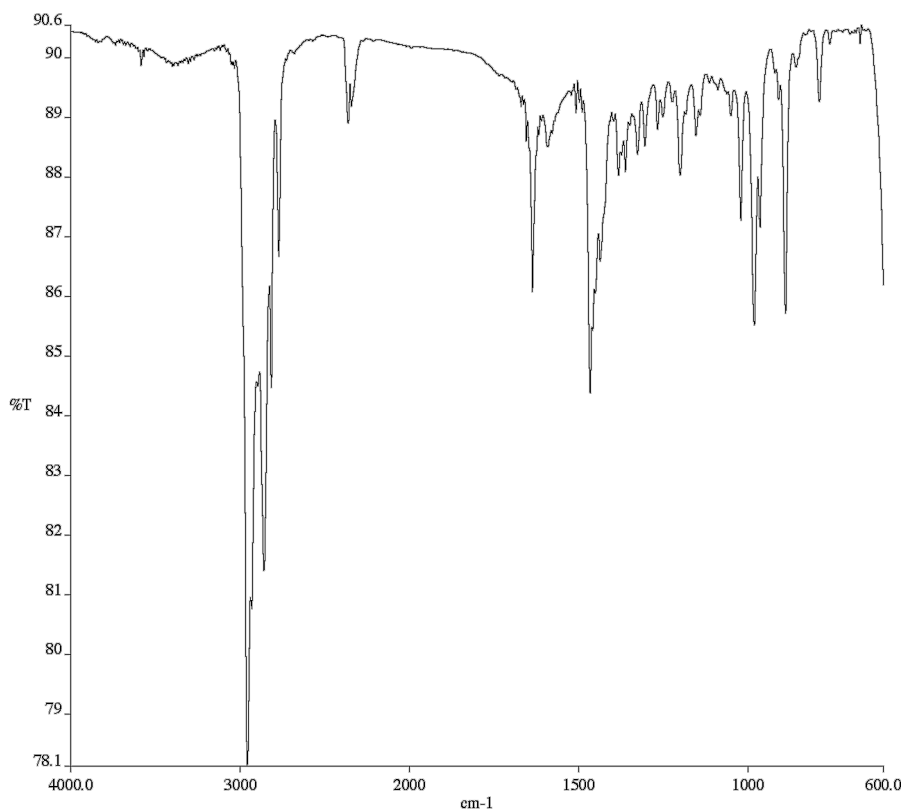


Figure A3.2. Infrared spectrum (Thin Film, NaCl) of compound 395.

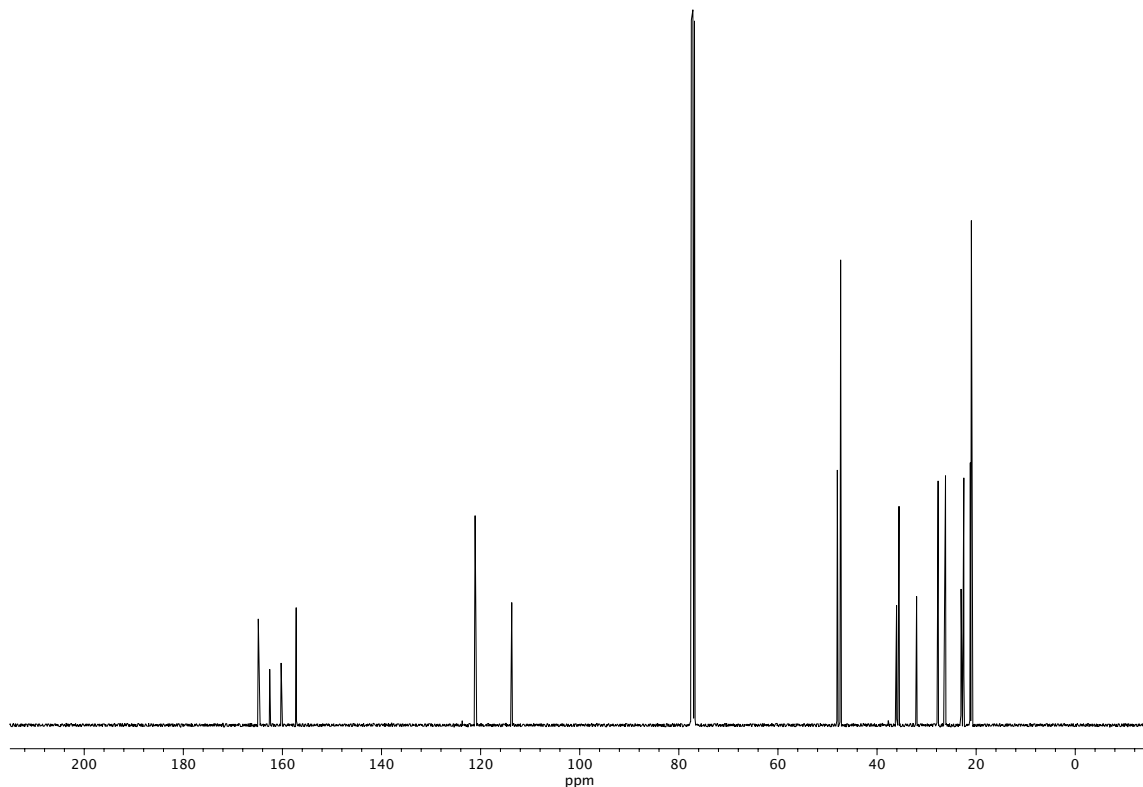


Figure A3.3. ^{13}C NMR (101 MHz, CDCl_3) of compound 395.

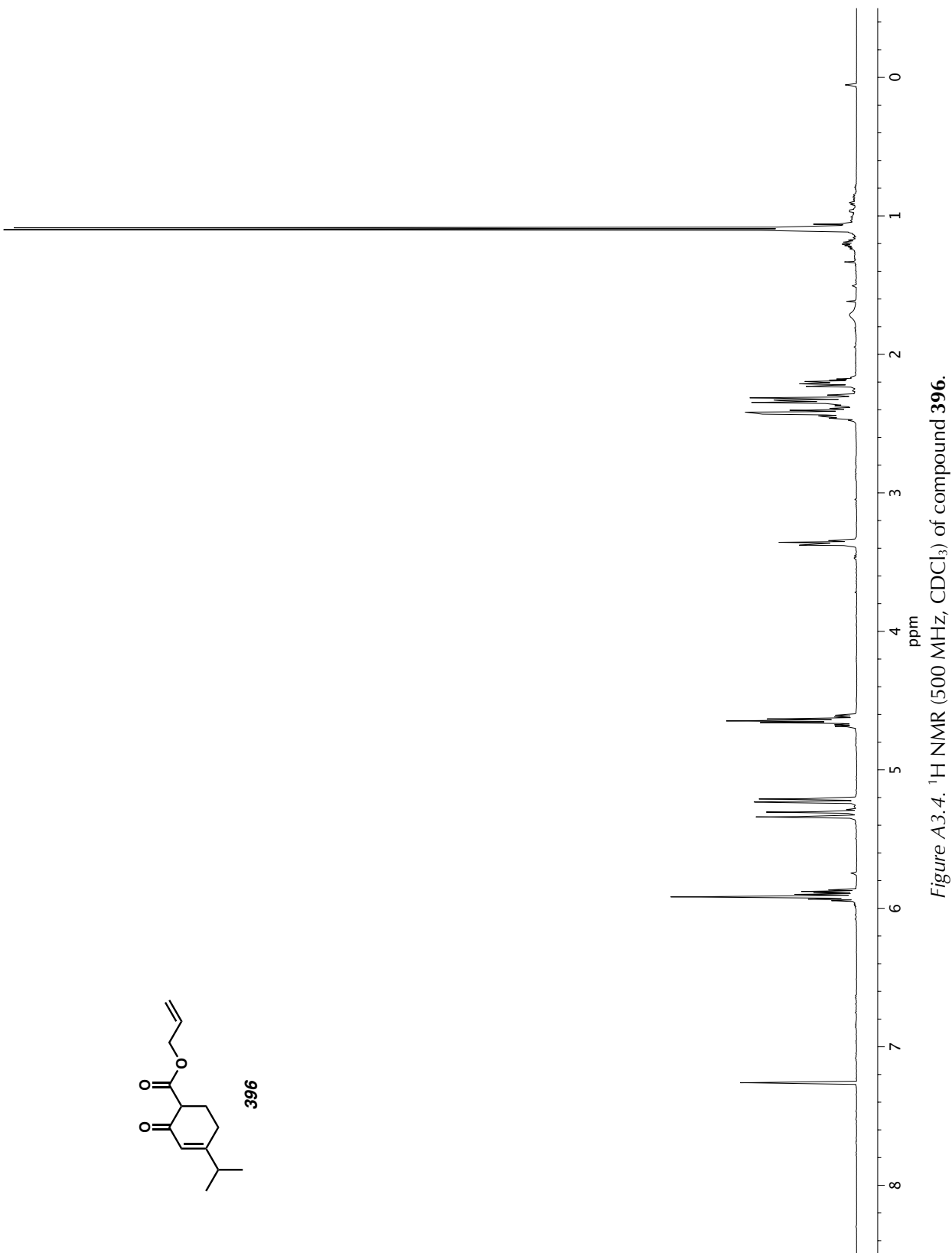


Figure A3.4. ^1H NMR (500 MHz, CDCl_3) of compound 396.

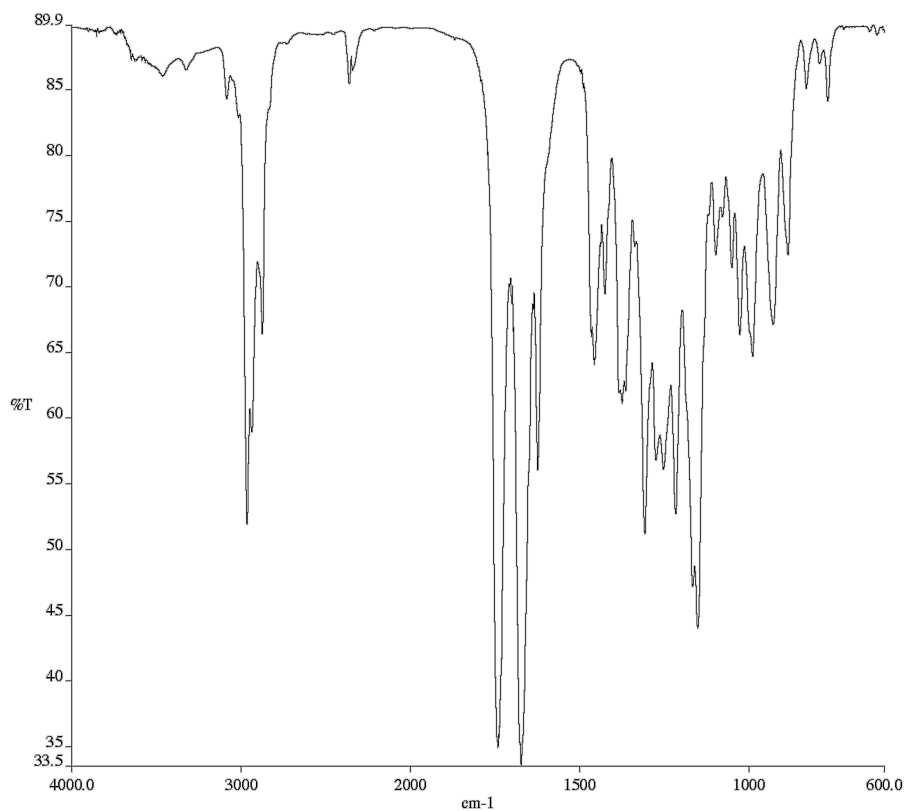


Figure A3.5. Infrared spectrum (Thin Film, NaCl) of compound **396**.

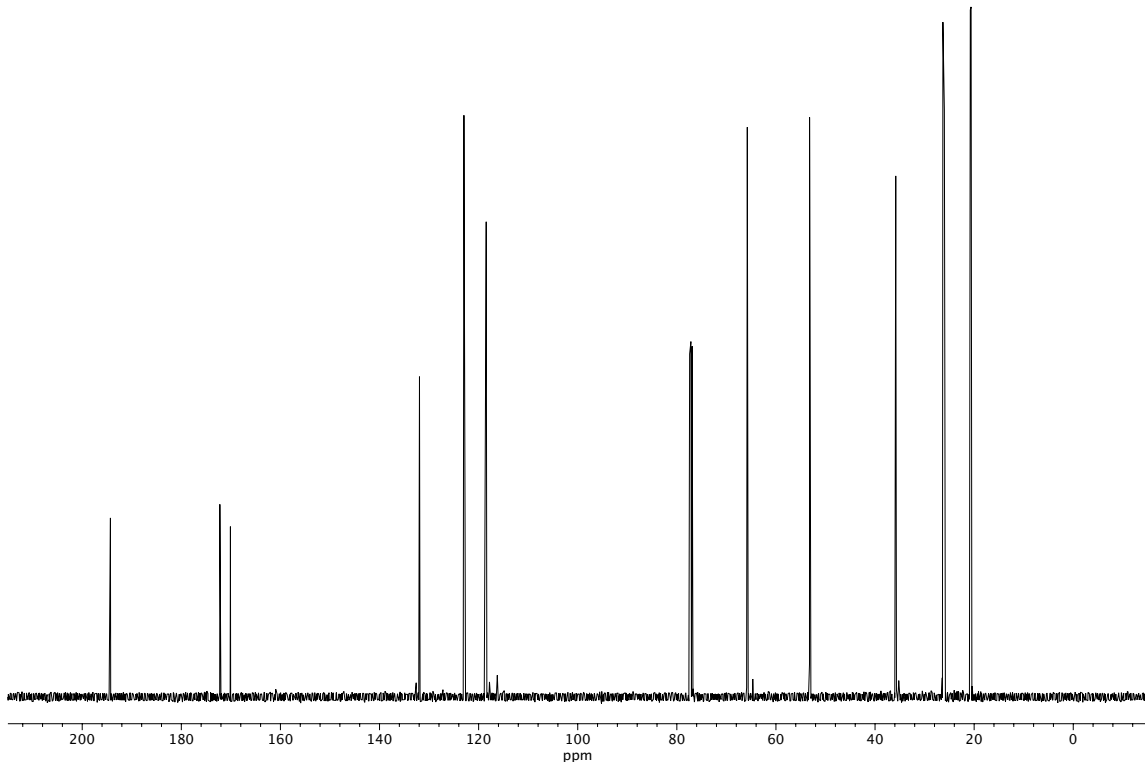
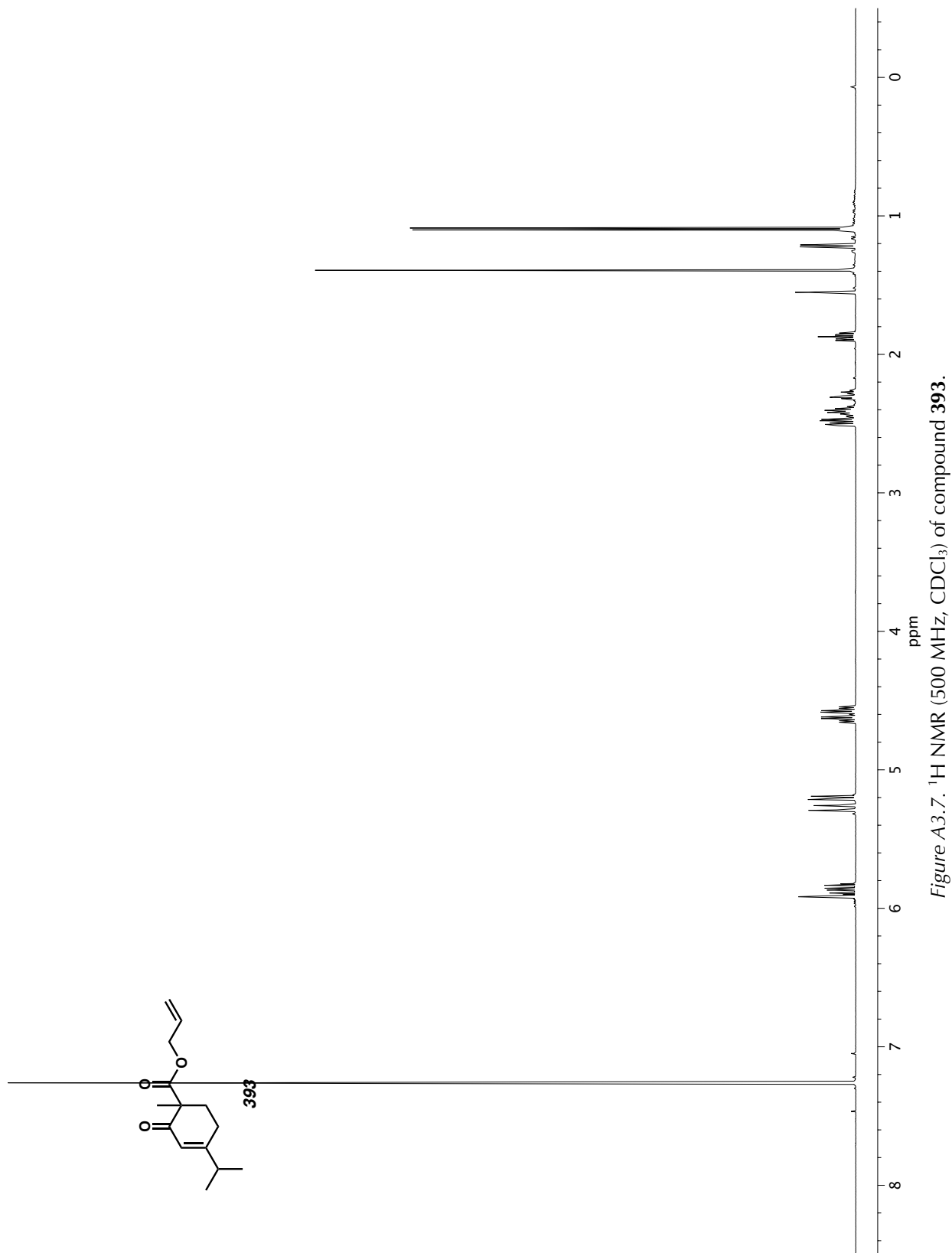


Figure A3.6. ^{13}C NMR (126 MHz, CDCl_3) of compound **396**.



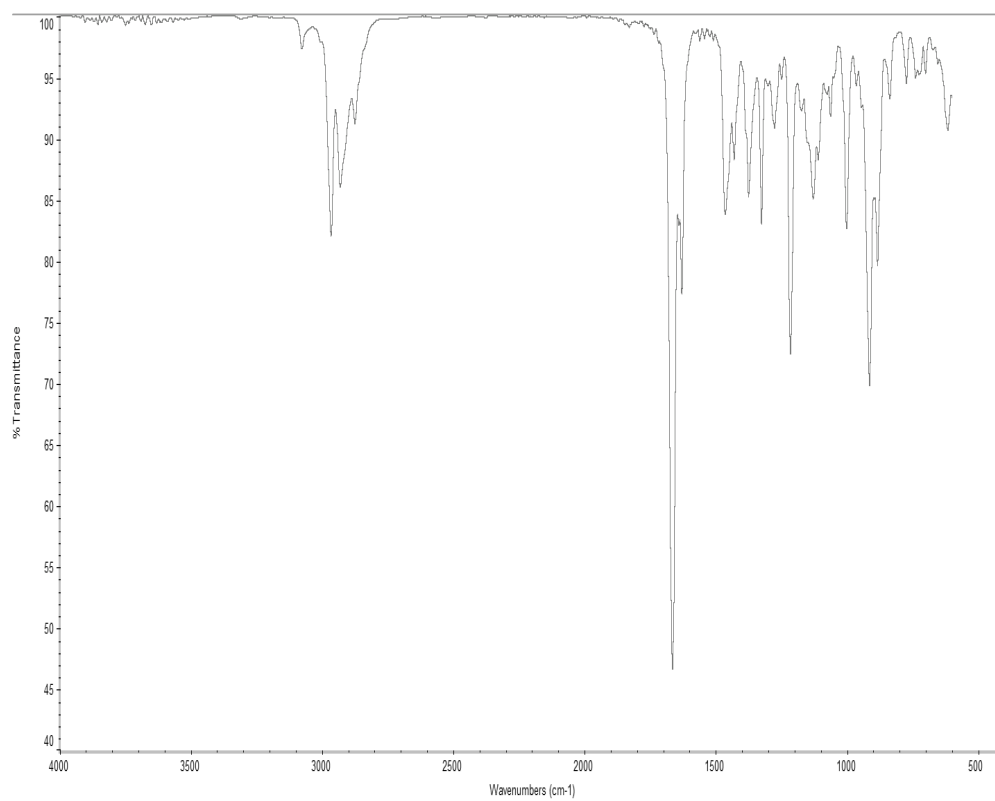


Figure A3.8. Infrared spectrum (Thin Film, NaCl) of compound **393**.

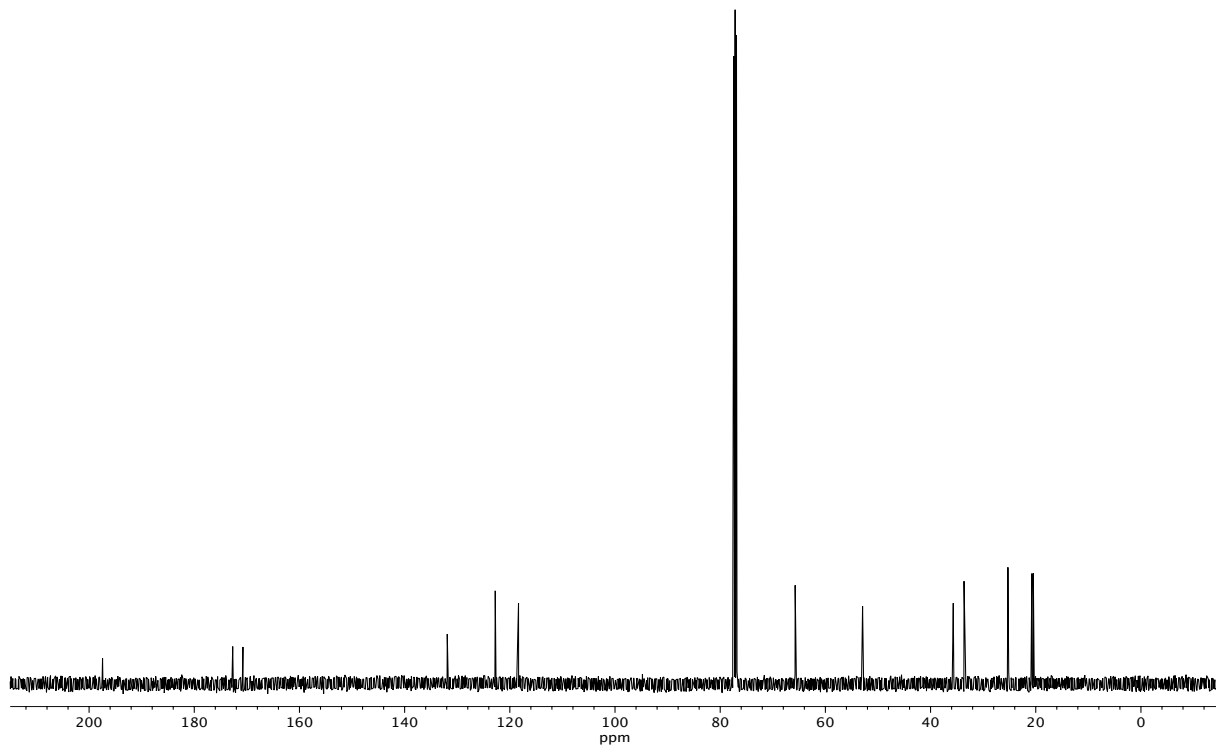


Figure A3.9. ¹³C NMR (126 MHz, CDCl₃) of compound **393**.

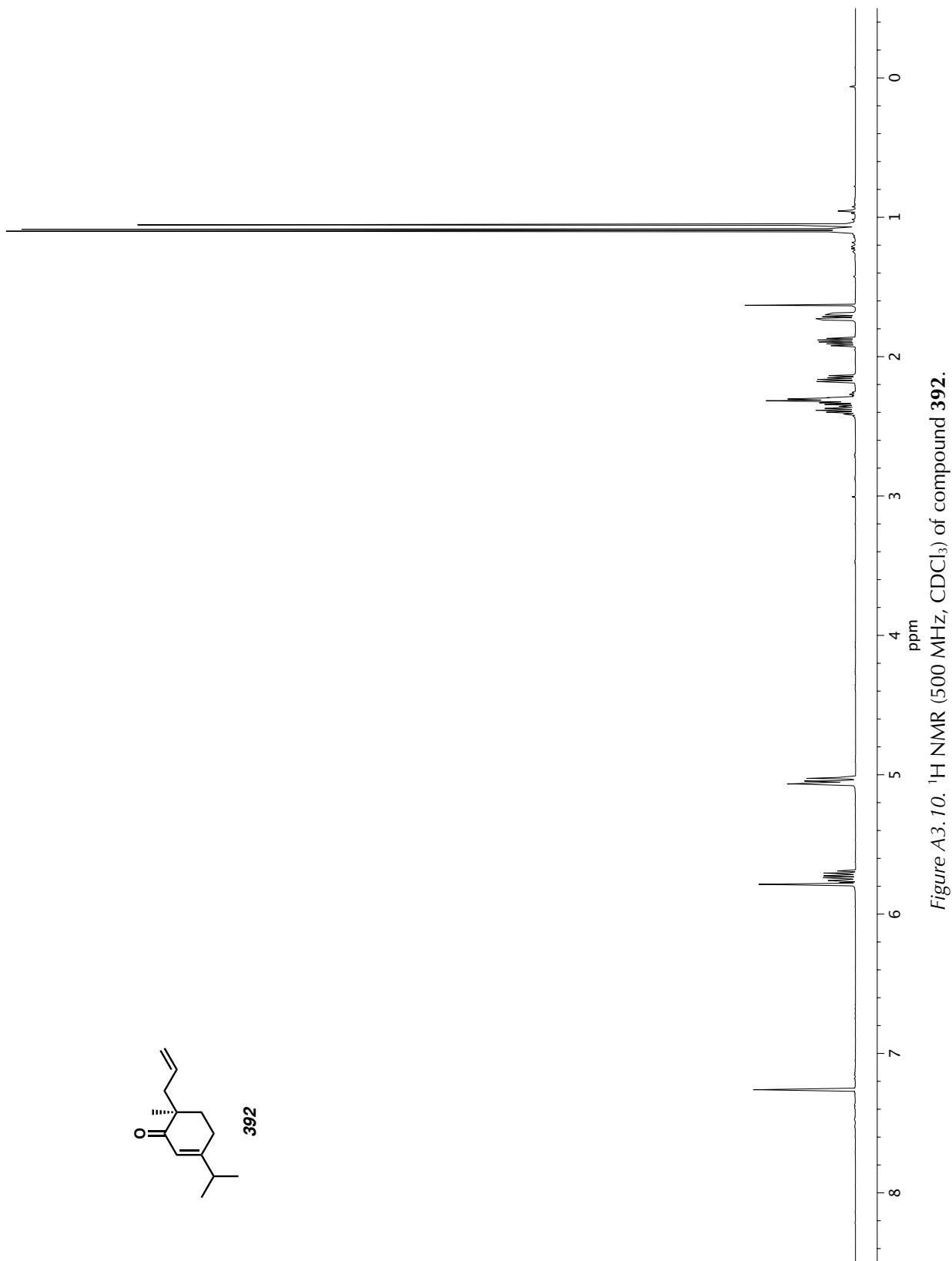


Figure A3.10. ^1H NMR (500 MHz, CDCl_3) of compound 392.

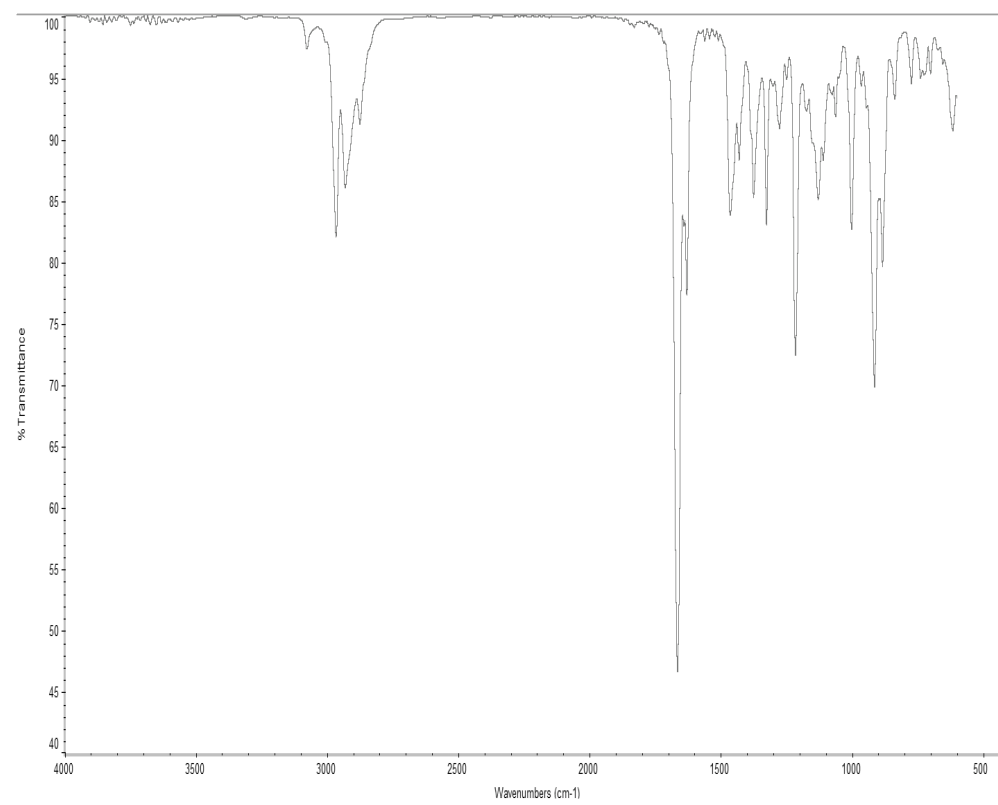


Figure A3.11. Infrared spectrum (Thin Film, NaCl) of compound 392.

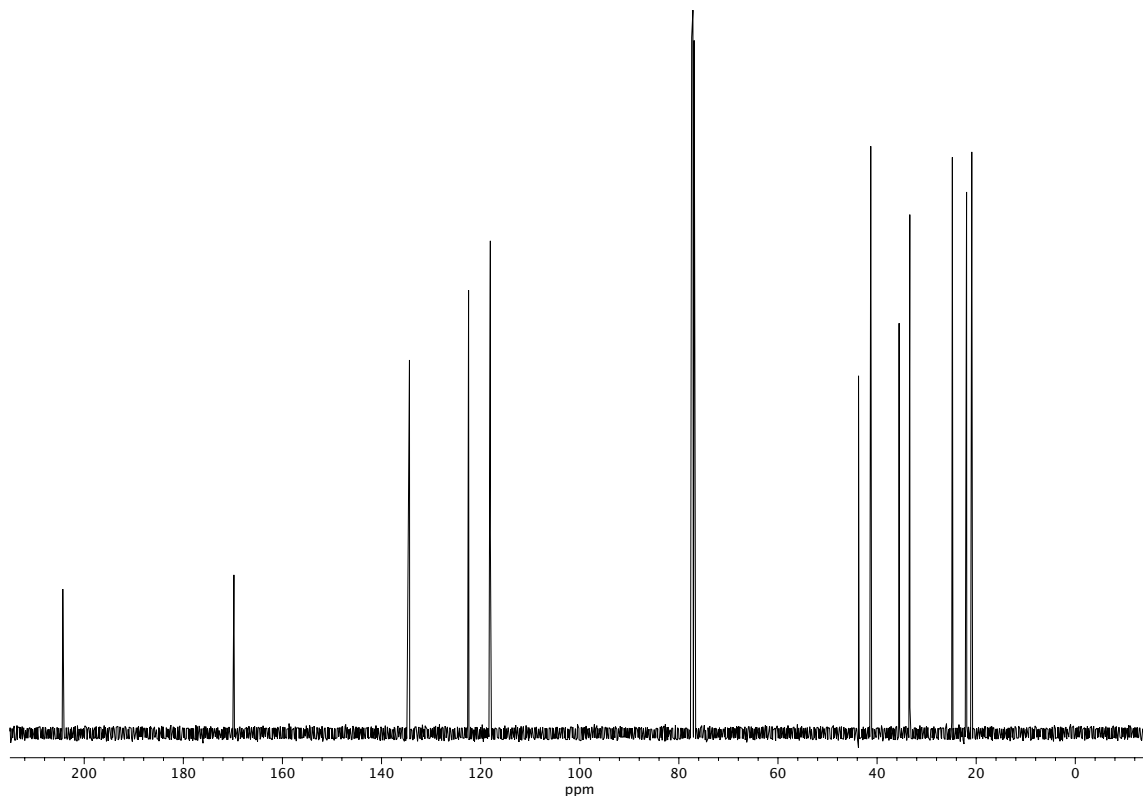


Figure A3.12. ¹³C NMR (126 MHz, CDCl₃) of compound 392.

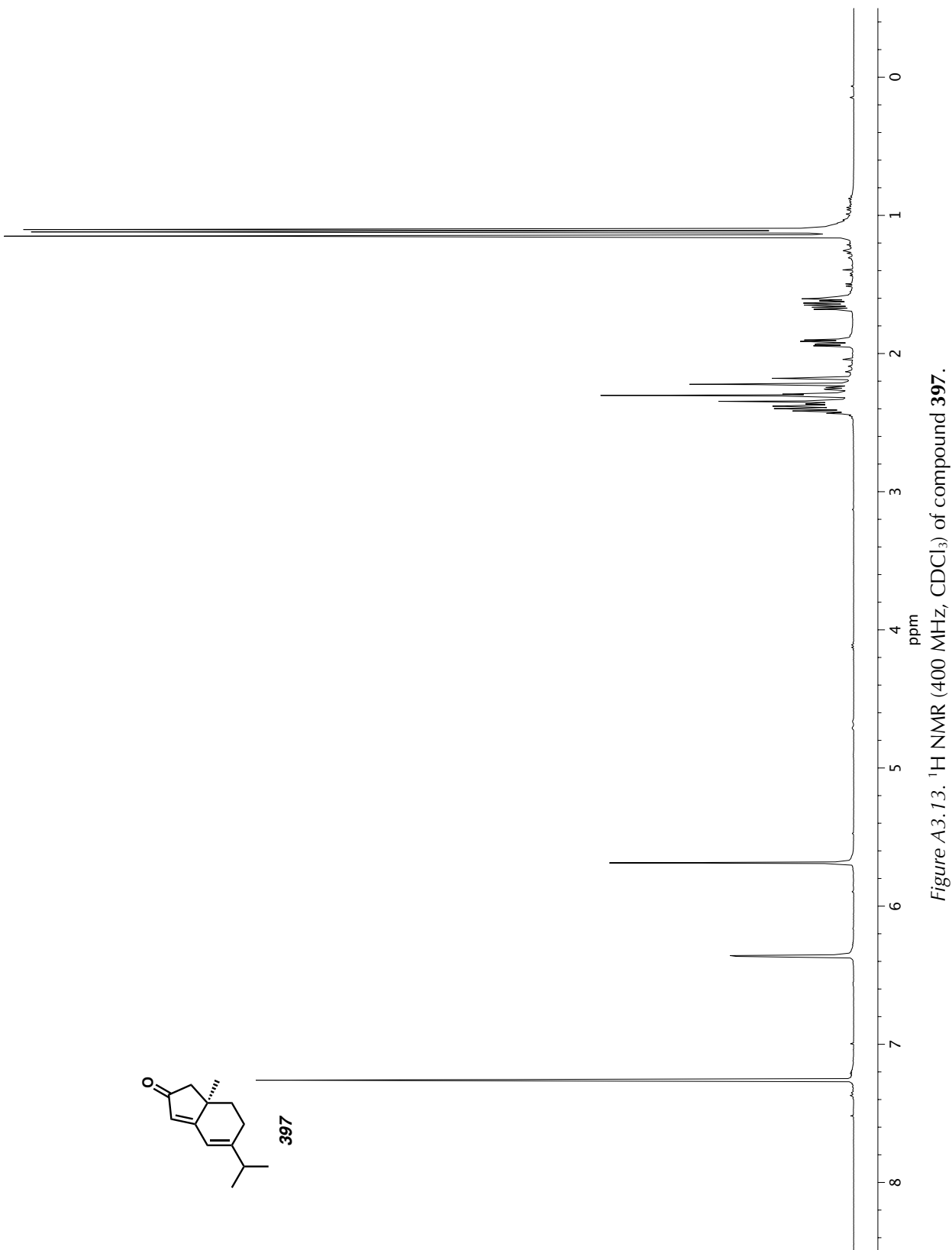


Figure A3.13. ^1H NMR (400 MHz, CDCl_3) of compound 397.

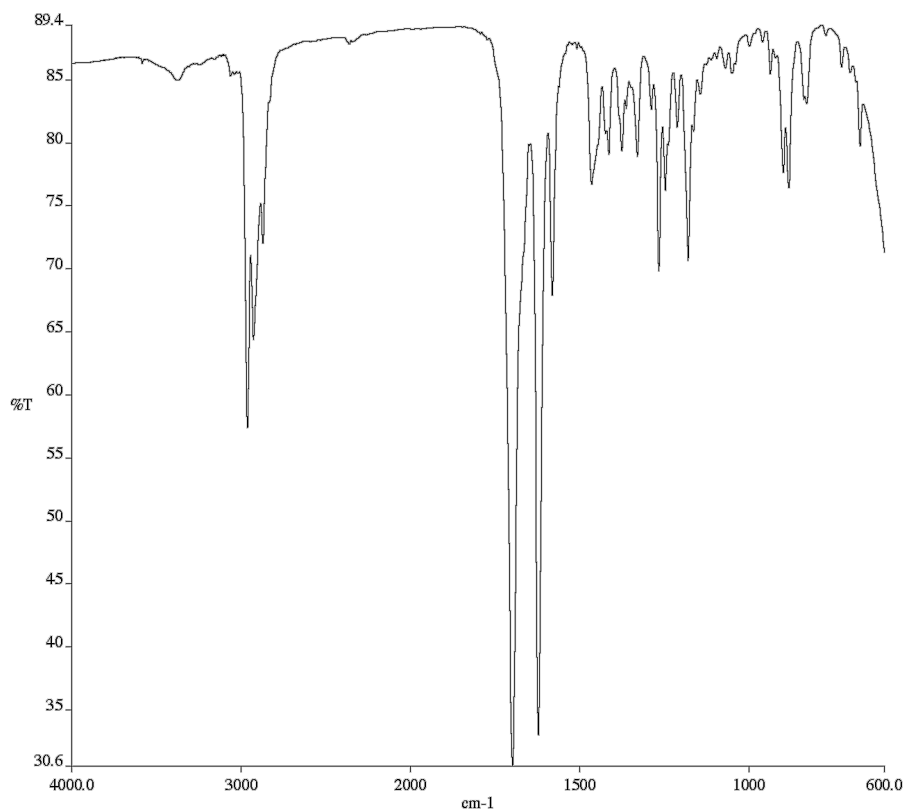


Figure A3.14. Infrared spectrum (Thin Film, NaCl) of compound 397.

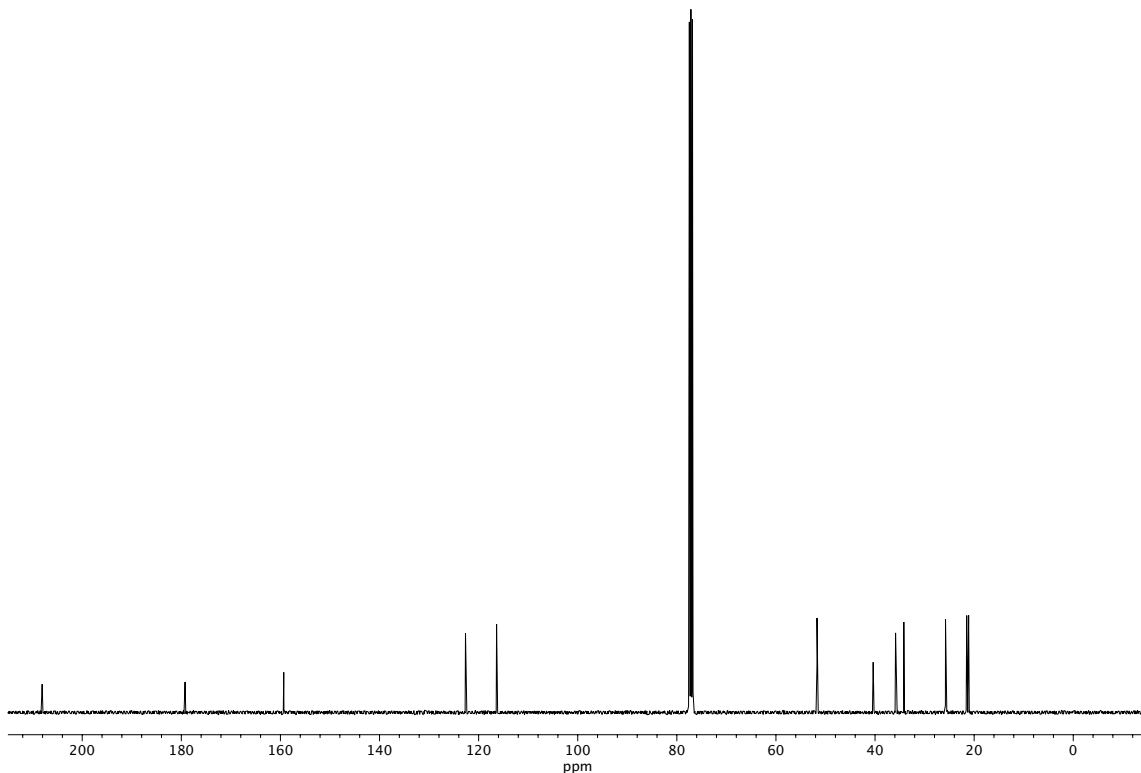


Figure A3.15. ^{13}C NMR (101 MHz, CDCl_3) of compound 397.

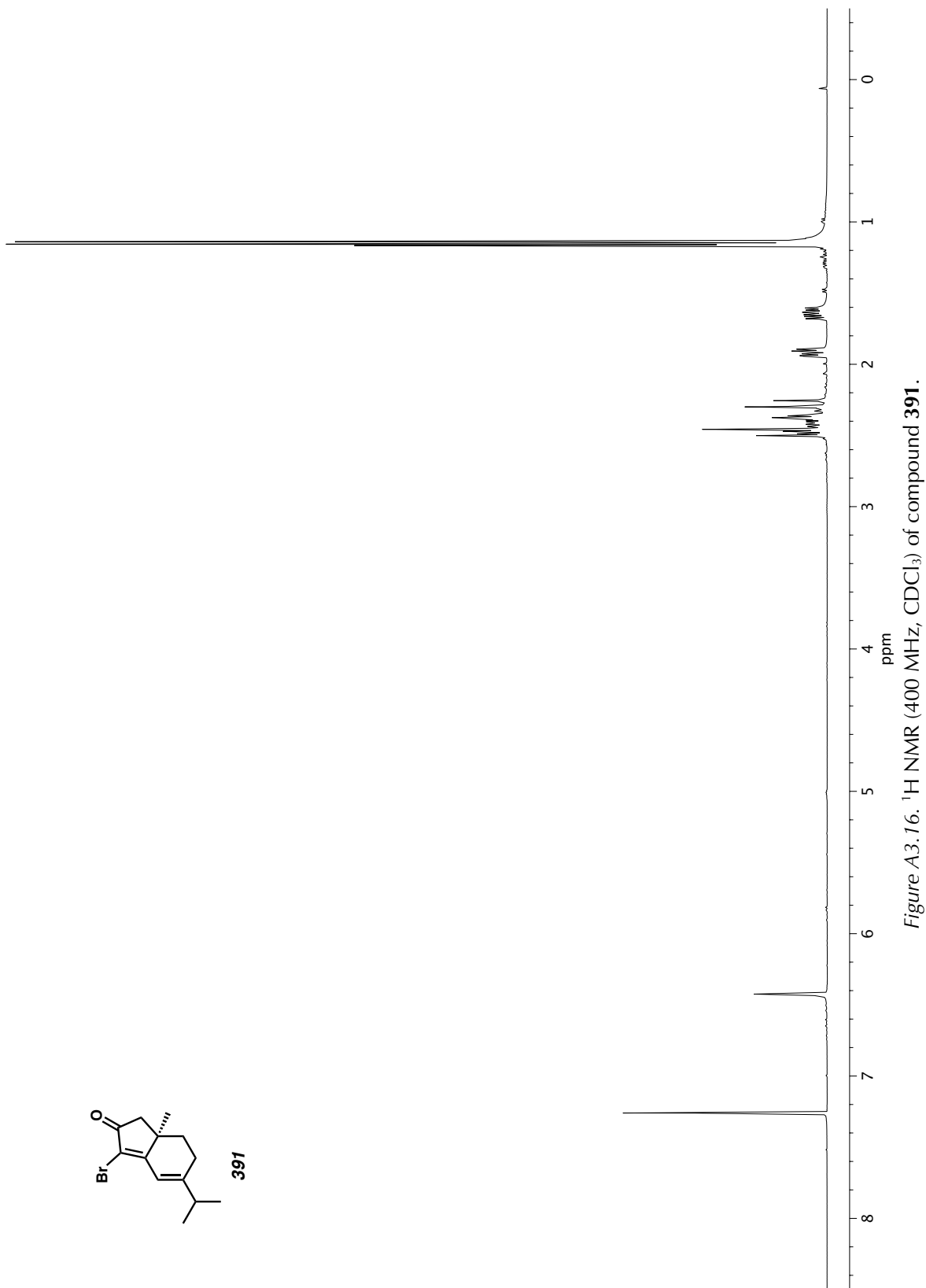


Figure A3.16. ^1H NMR (400 MHz, CDCl_3) of compound 391.

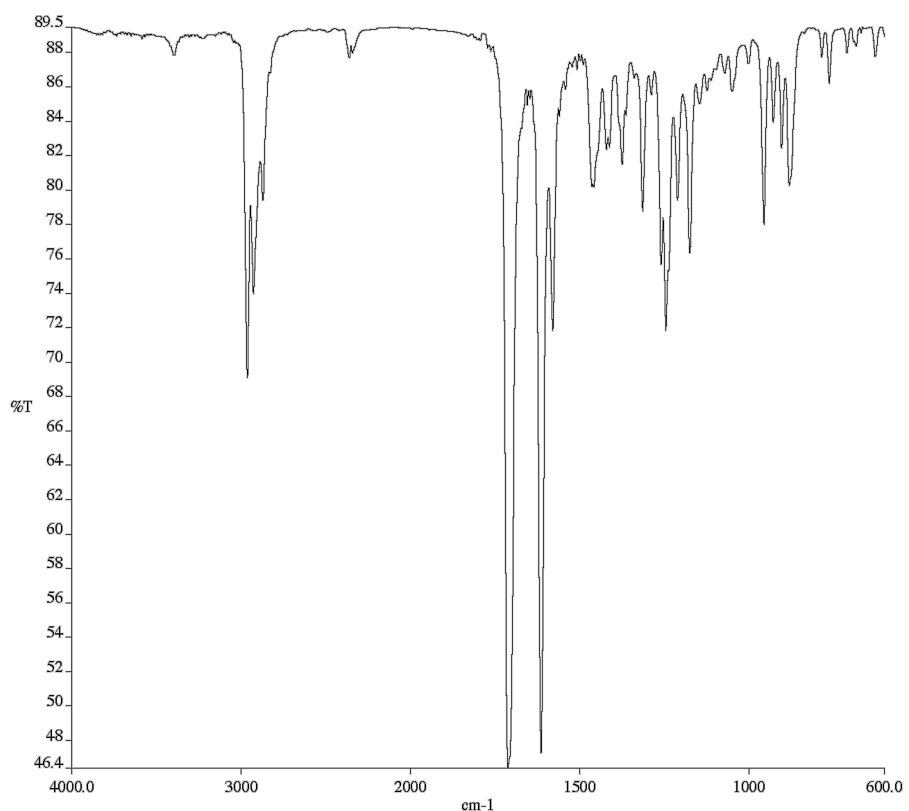


Figure A3.17. Infrared spectrum (Thin Film, NaCl) of compound **391**.

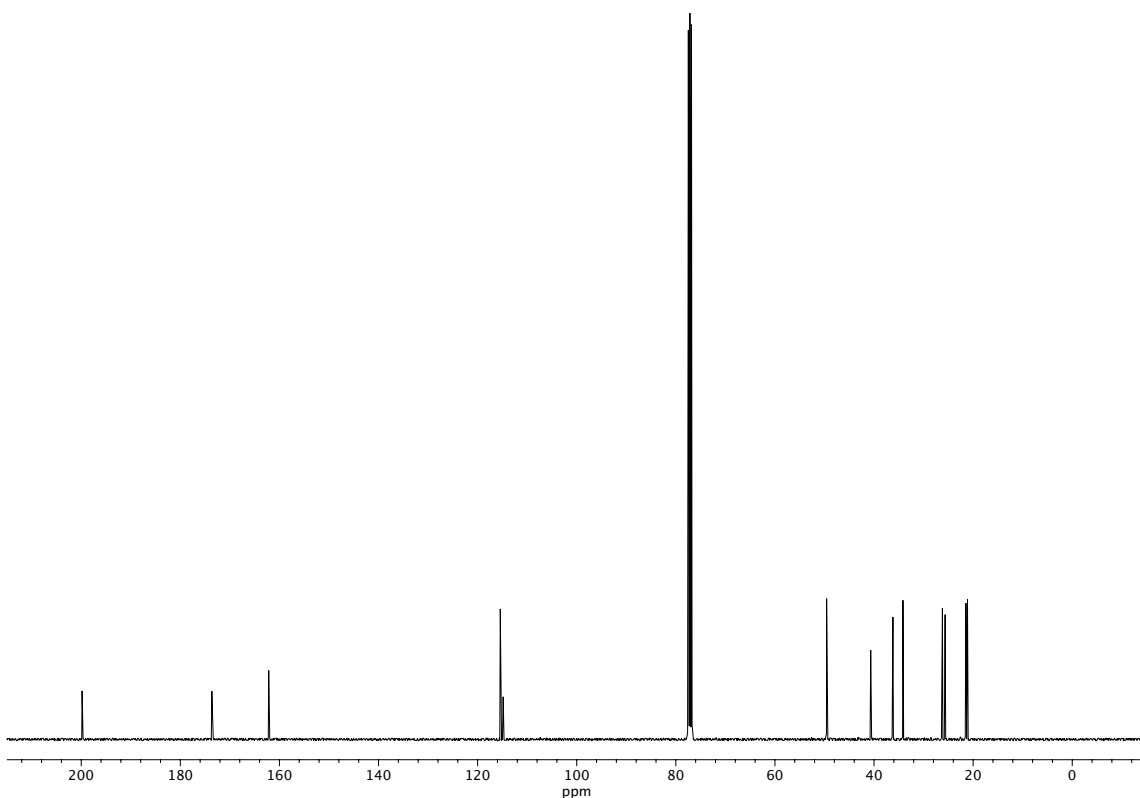


Figure A3.18. ^{13}C NMR (101 MHz, CDCl_3) of compound **391**.

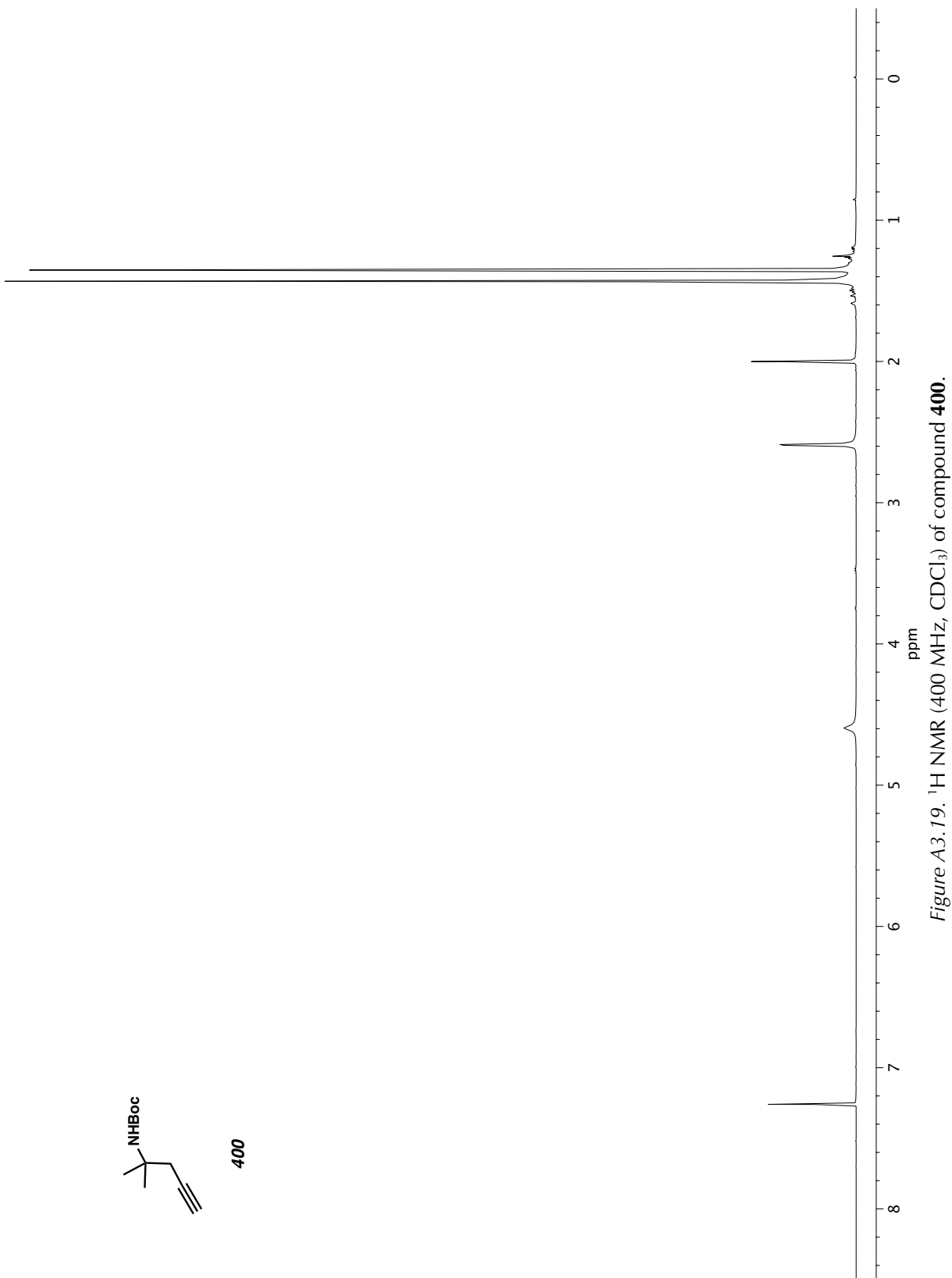


Figure A3.19. ^1H NMR (400 MHz, CDCl_3) of compound 400.

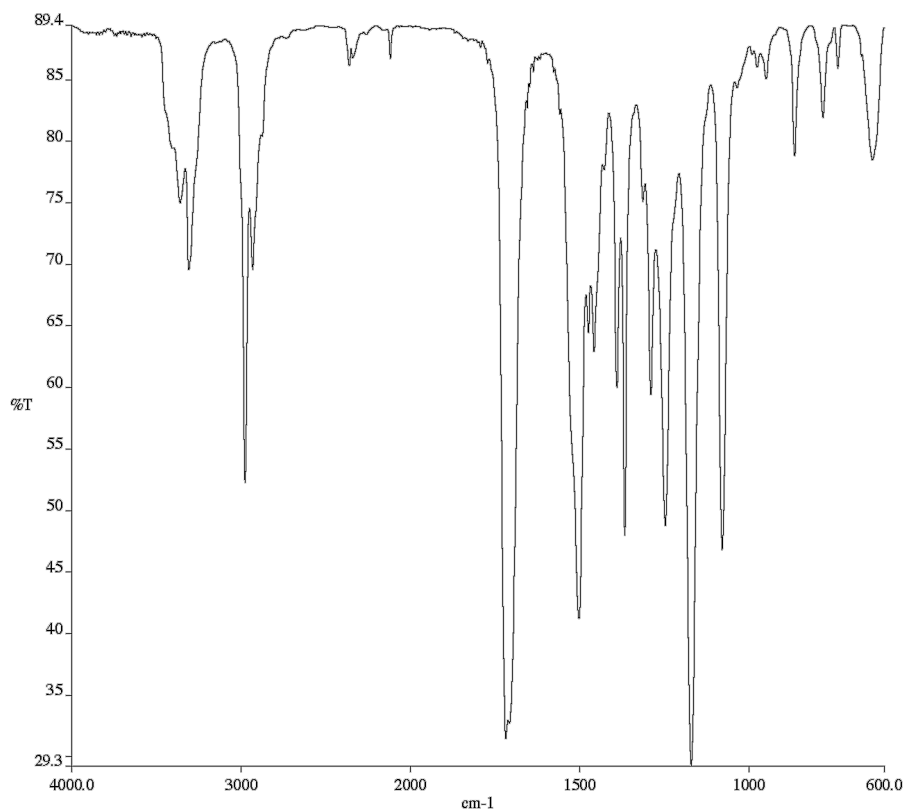


Figure A3.20. Infrared spectrum (Thin Film, NaCl) of compound **400**.

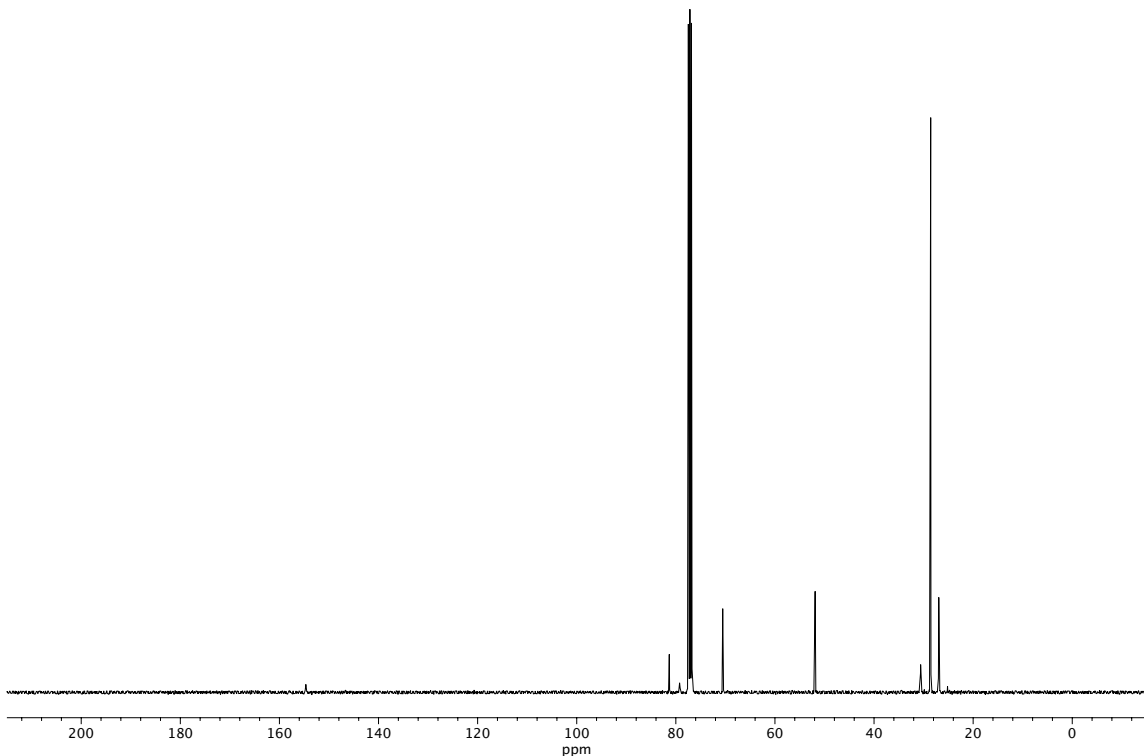


Figure A3.21. ¹³C NMR (101 MHz, CDCl₃) of compound **400**.

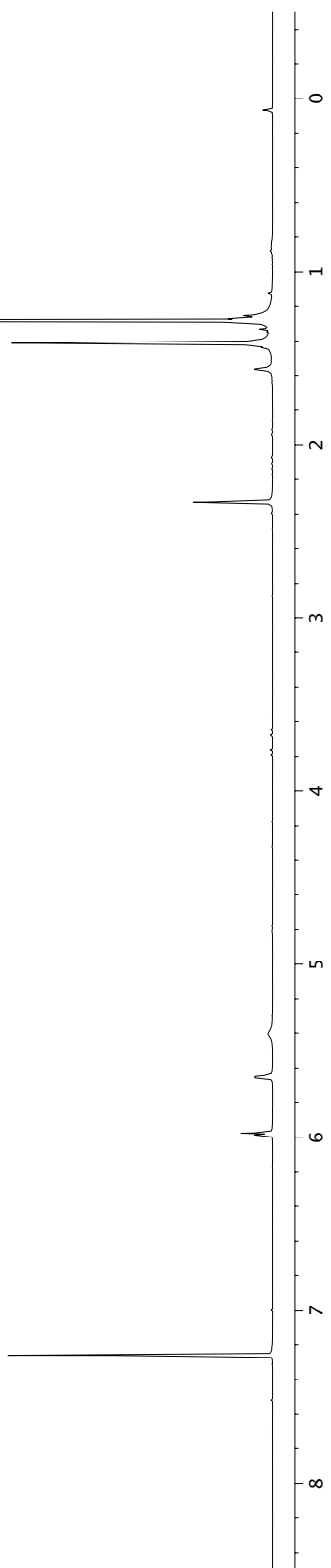
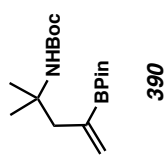


Figure A3.22. ^1H NMR (400 MHz, CDCl_3) of compound **390**.

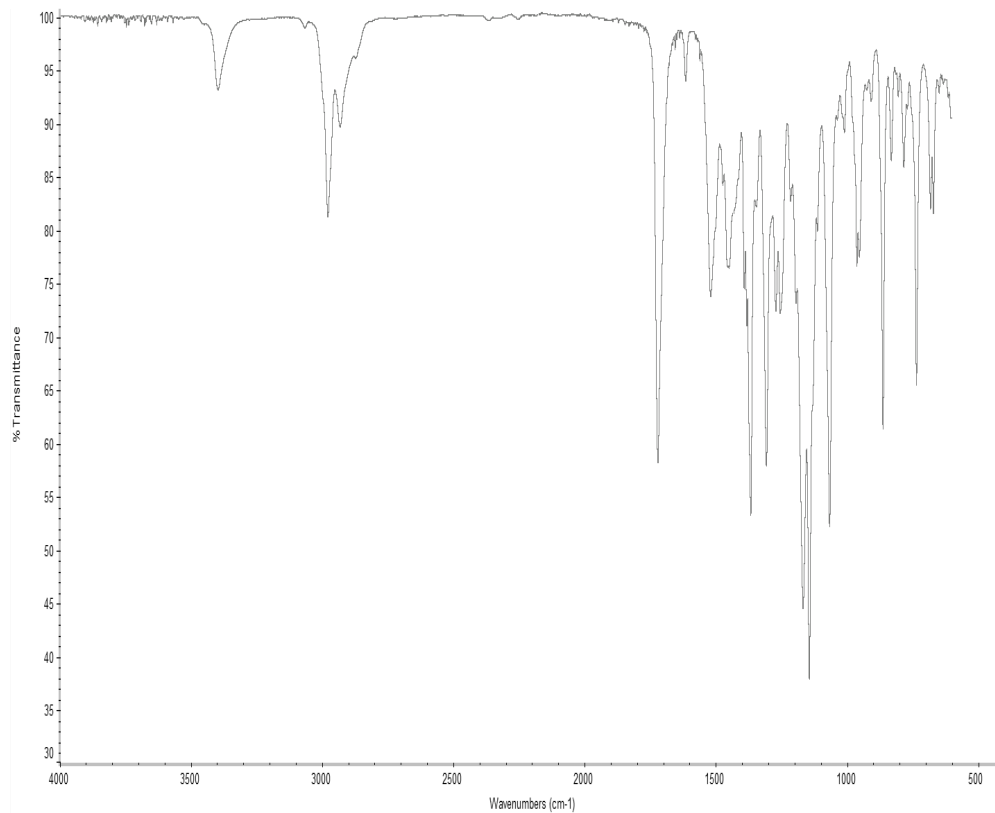


Figure A3.23. Infrared spectrum (Thin Film, NaCl) of compound **390**.

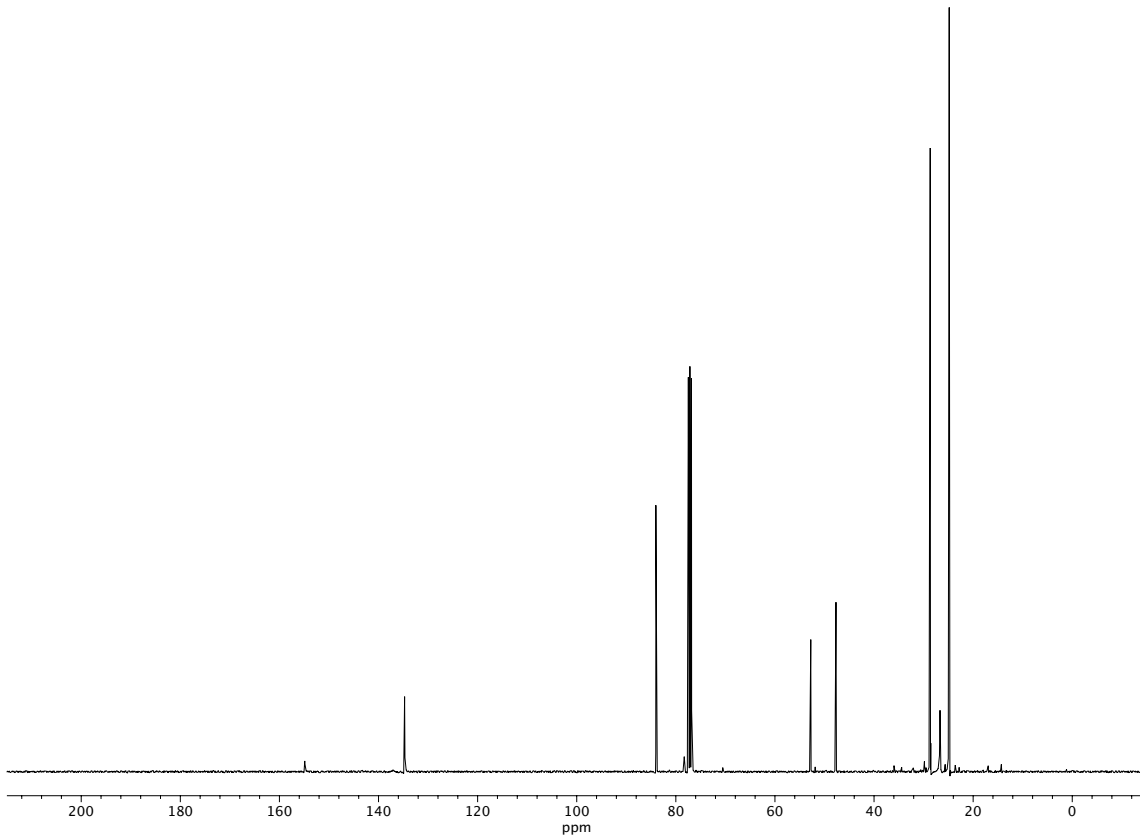


Figure A3.24. ^{13}C NMR (101 MHz, CDCl_3) of compound **390**.

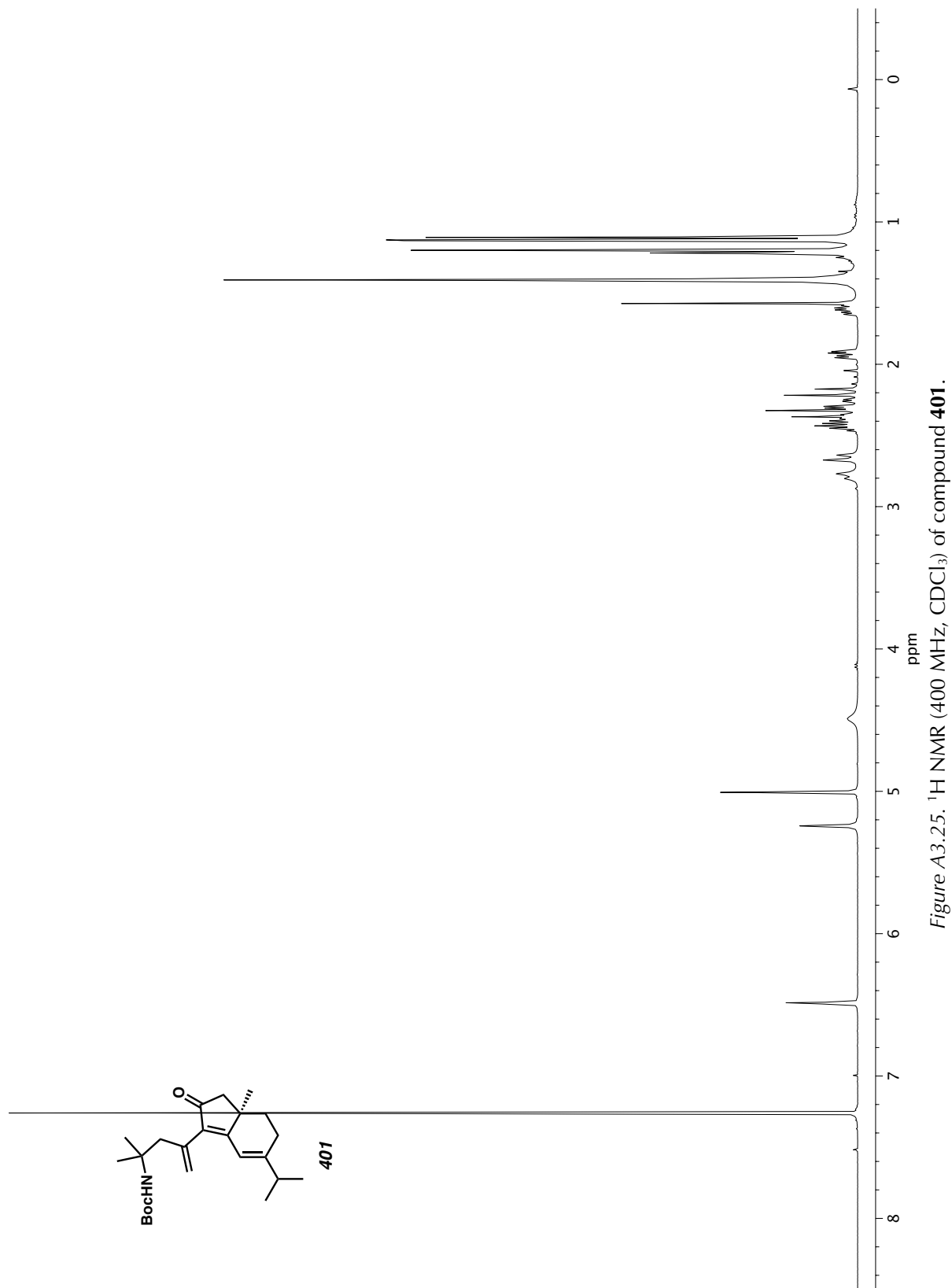


Figure A3.25. ^1H NMR (400 MHz, CDCl_3) of compound 401.

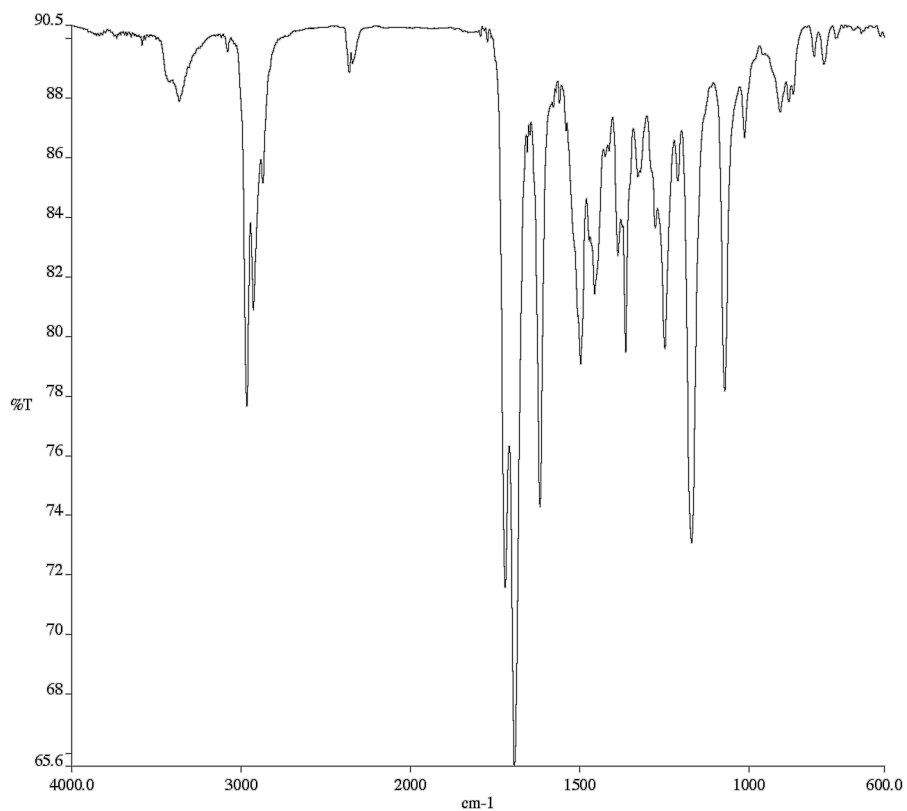


Figure A3.26. Infrared spectrum (Thin Film, NaCl) of compound **401**.

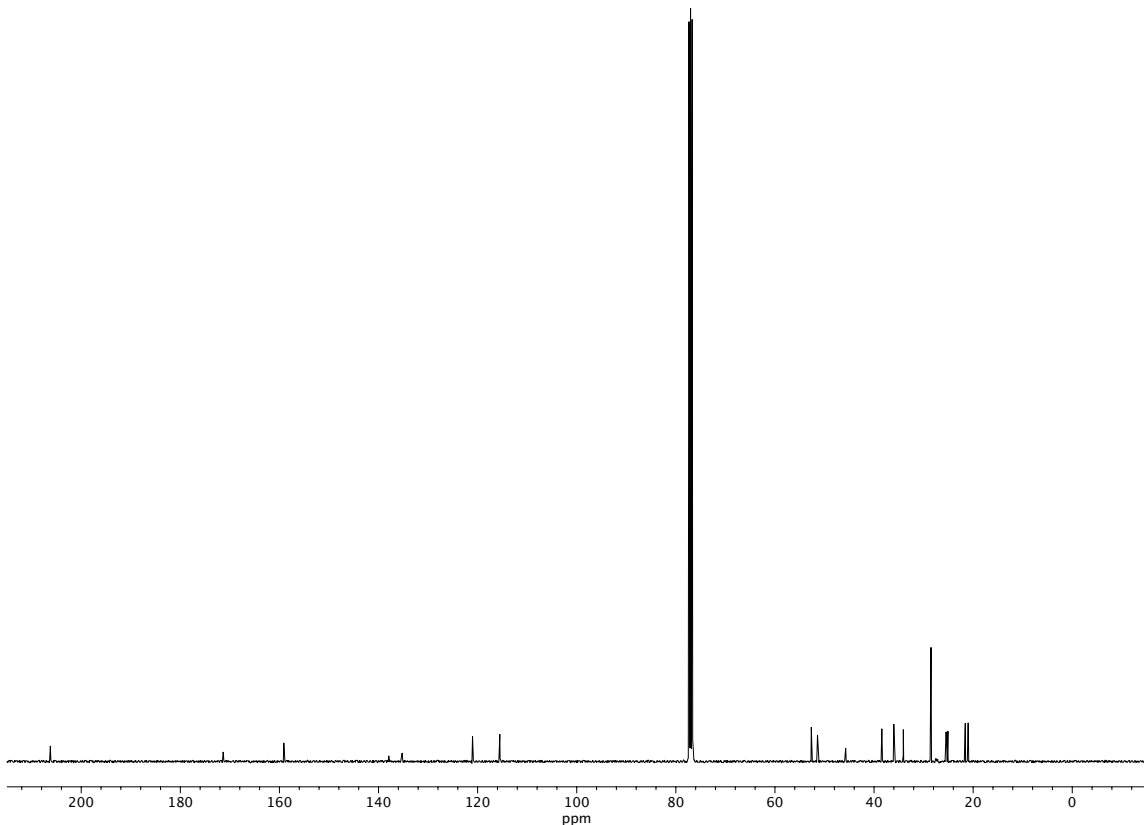


Figure A3.27. ^{13}C NMR (101 MHz, CDCl_3) of compound **401**.

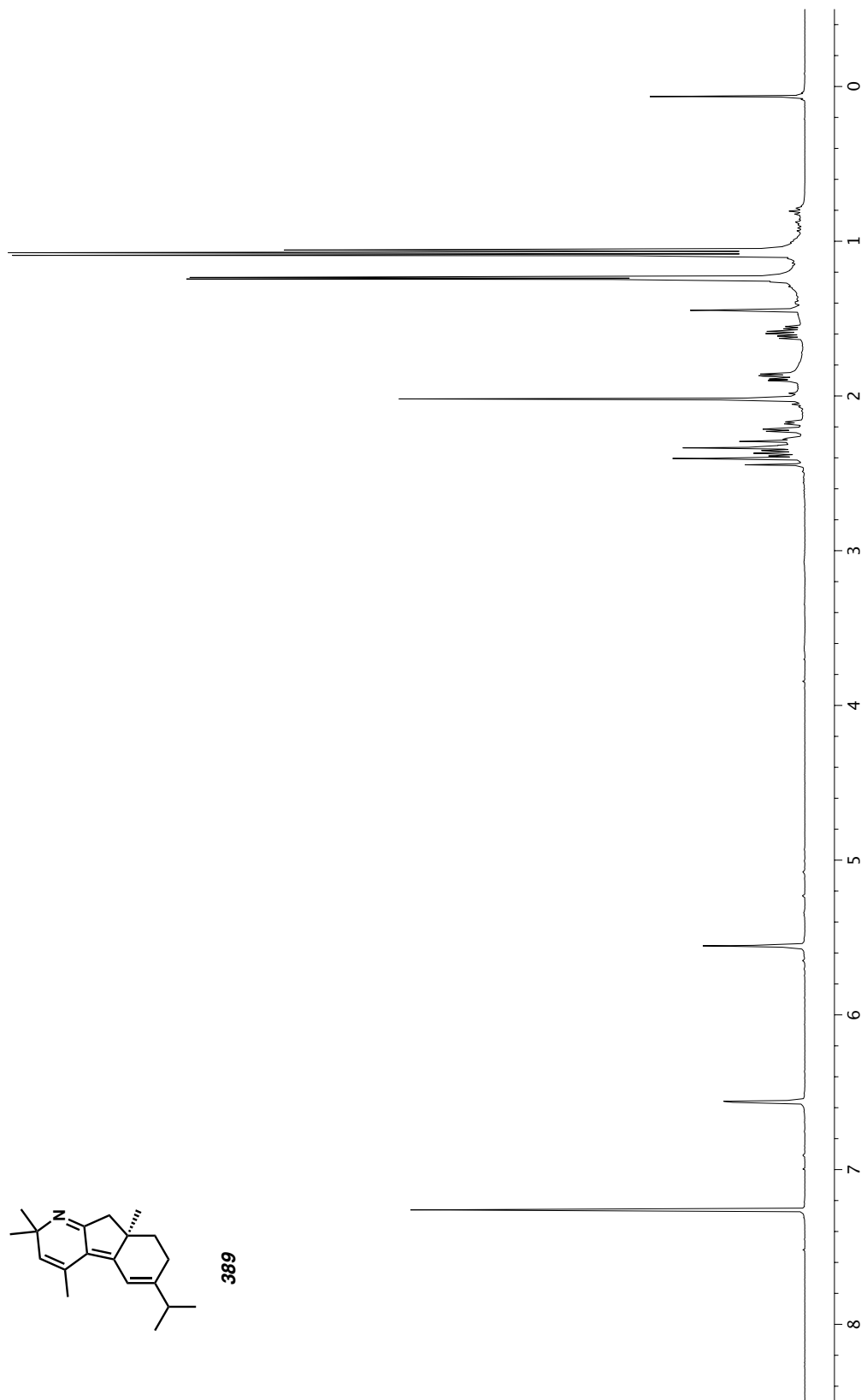


Figure A3.28. ^1H NMR (400 MHz, CDCl_3) of compound 389.

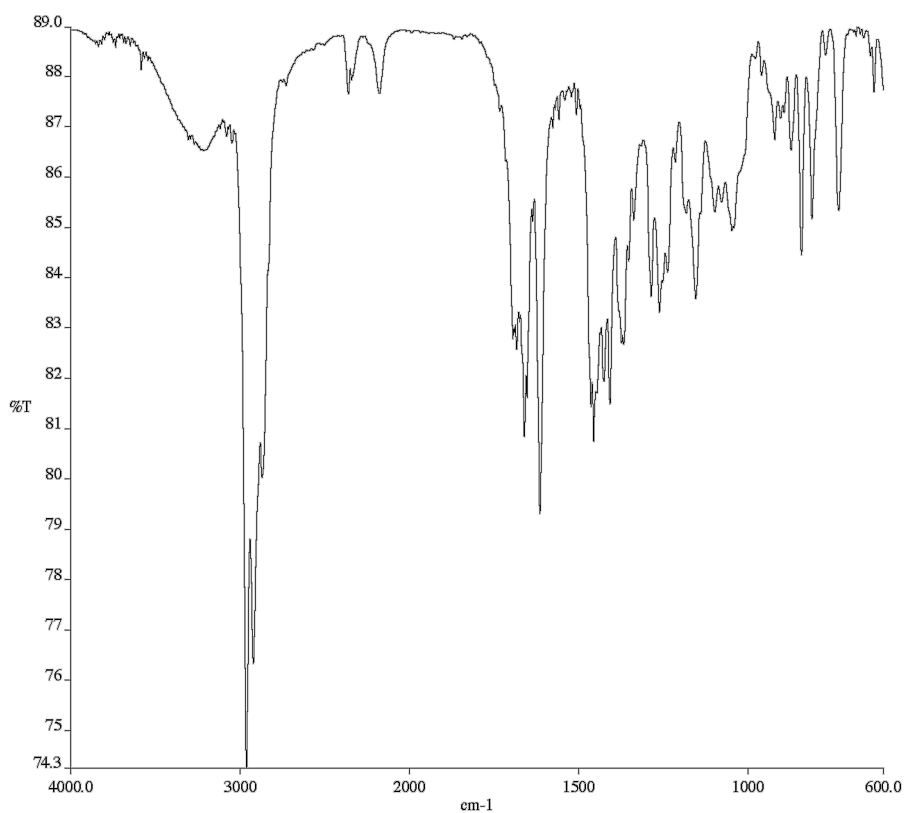


Figure A3.29. Infrared spectrum (Thin Film, NaCl) of compound **389**.

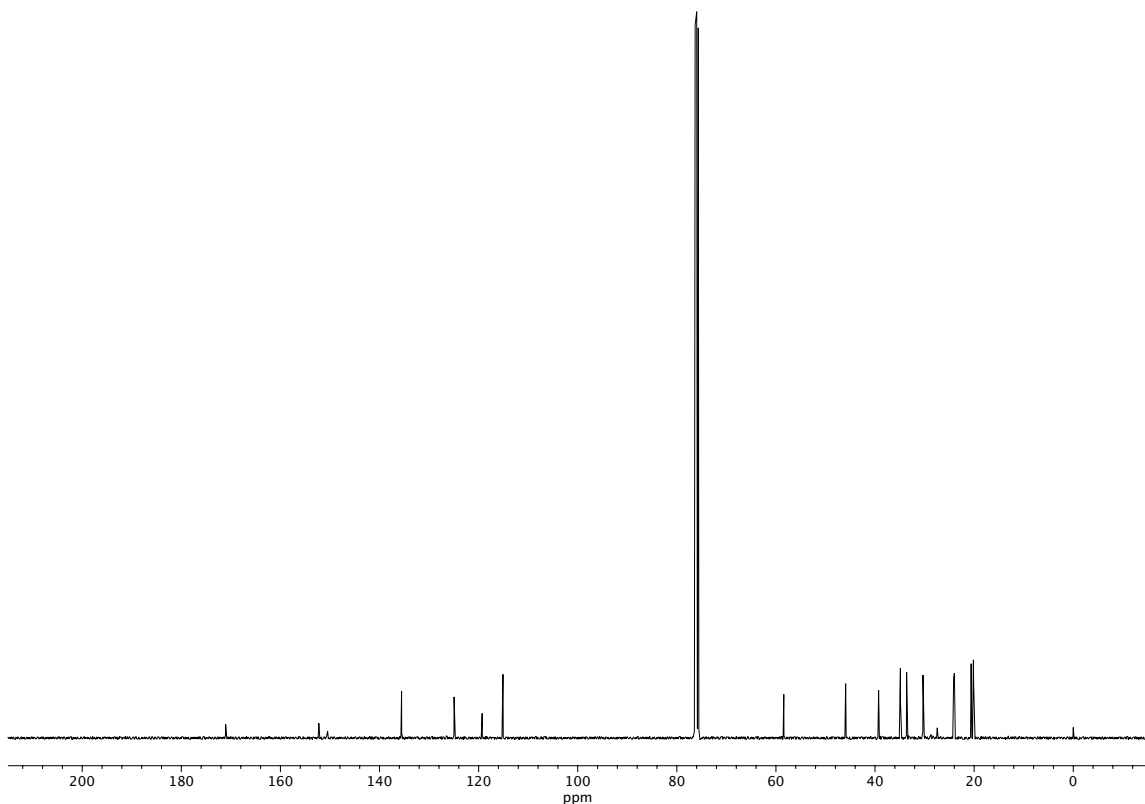
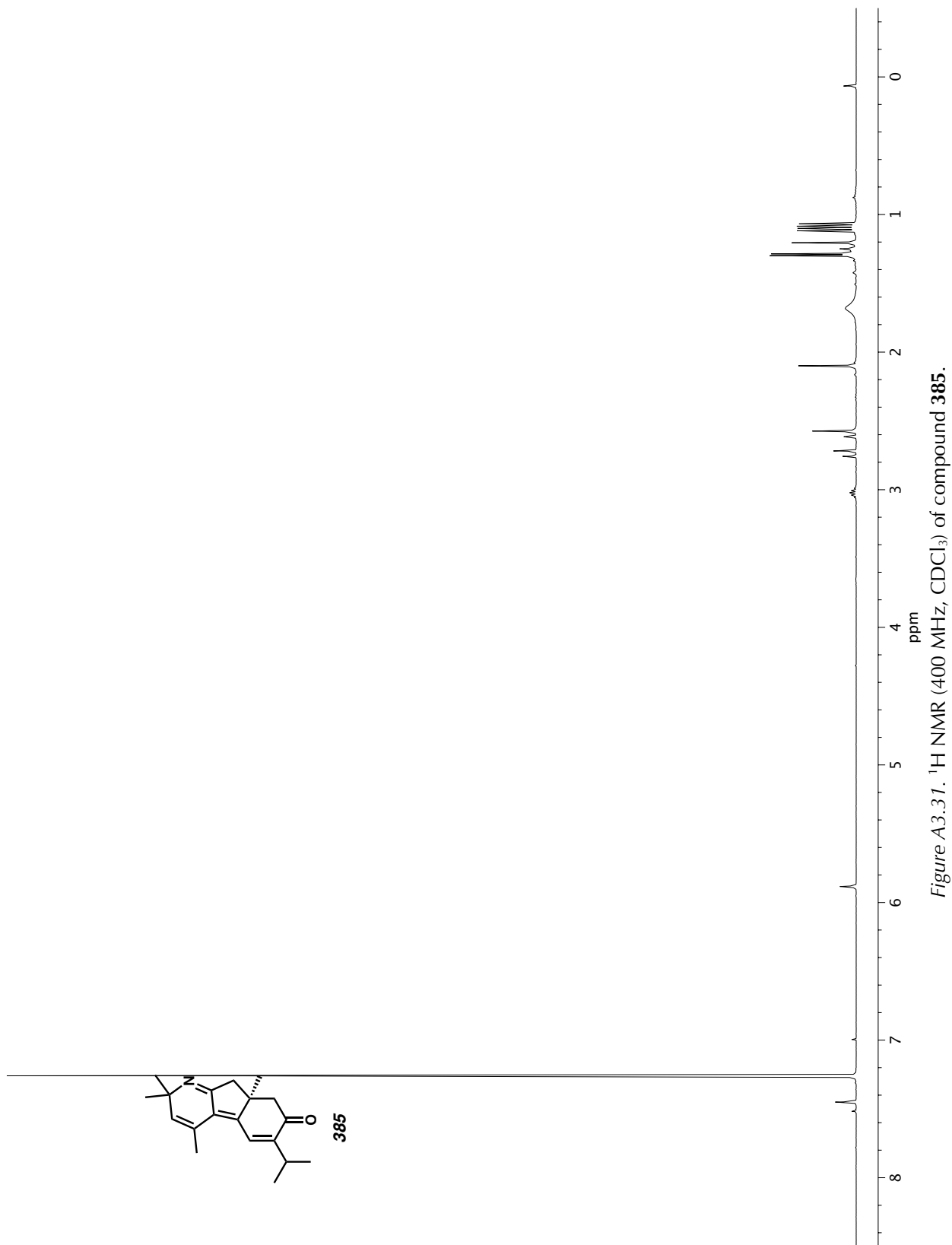


Figure A3.30. ^{13}C NMR (101 MHz, CDCl_3) of compound **389**.



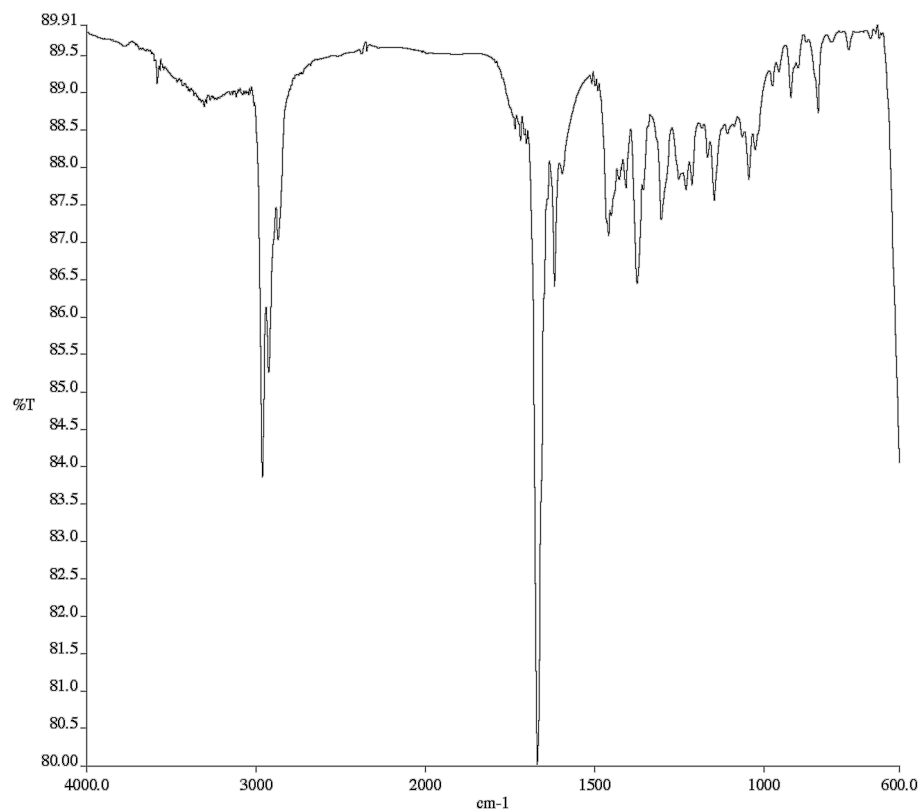


Figure A3.32. Infrared spectrum (Thin Film, NaCl) of compound **385**.

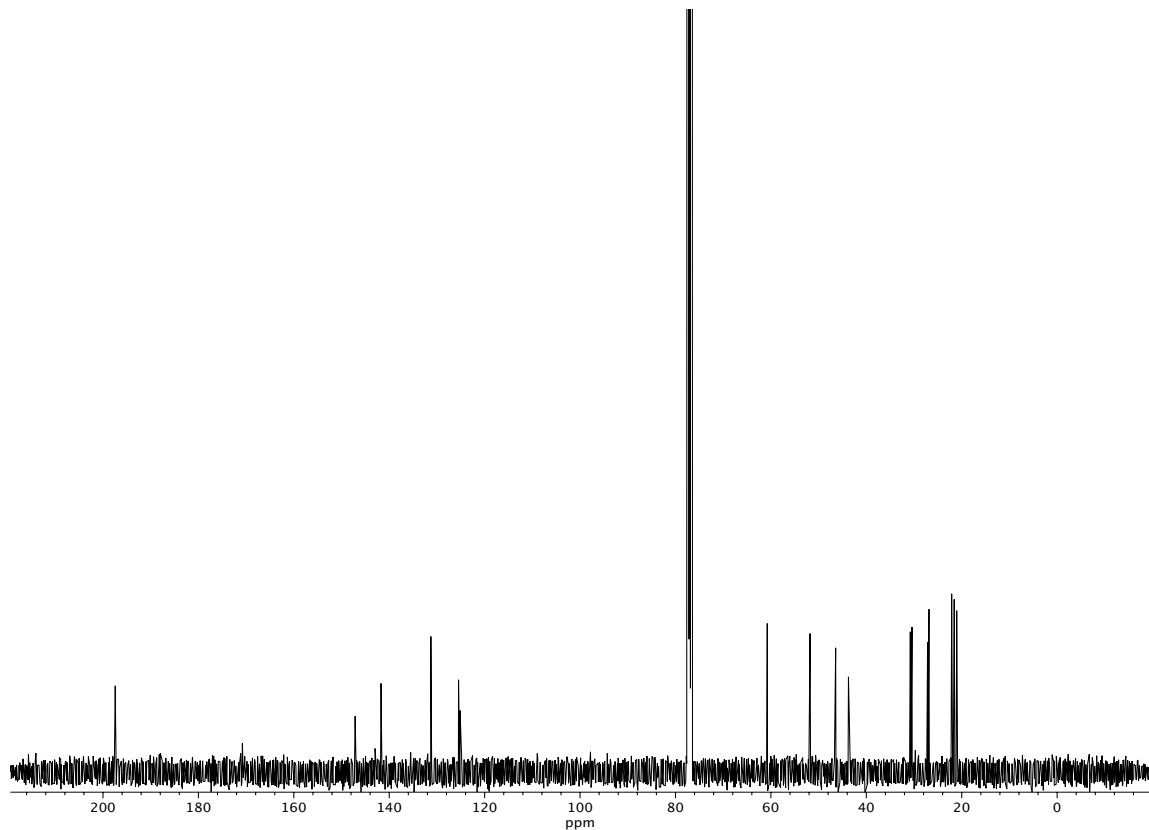


Figure A3.33. ^{13}C NMR (101 MHz, CDCl_3) of compound **385**.

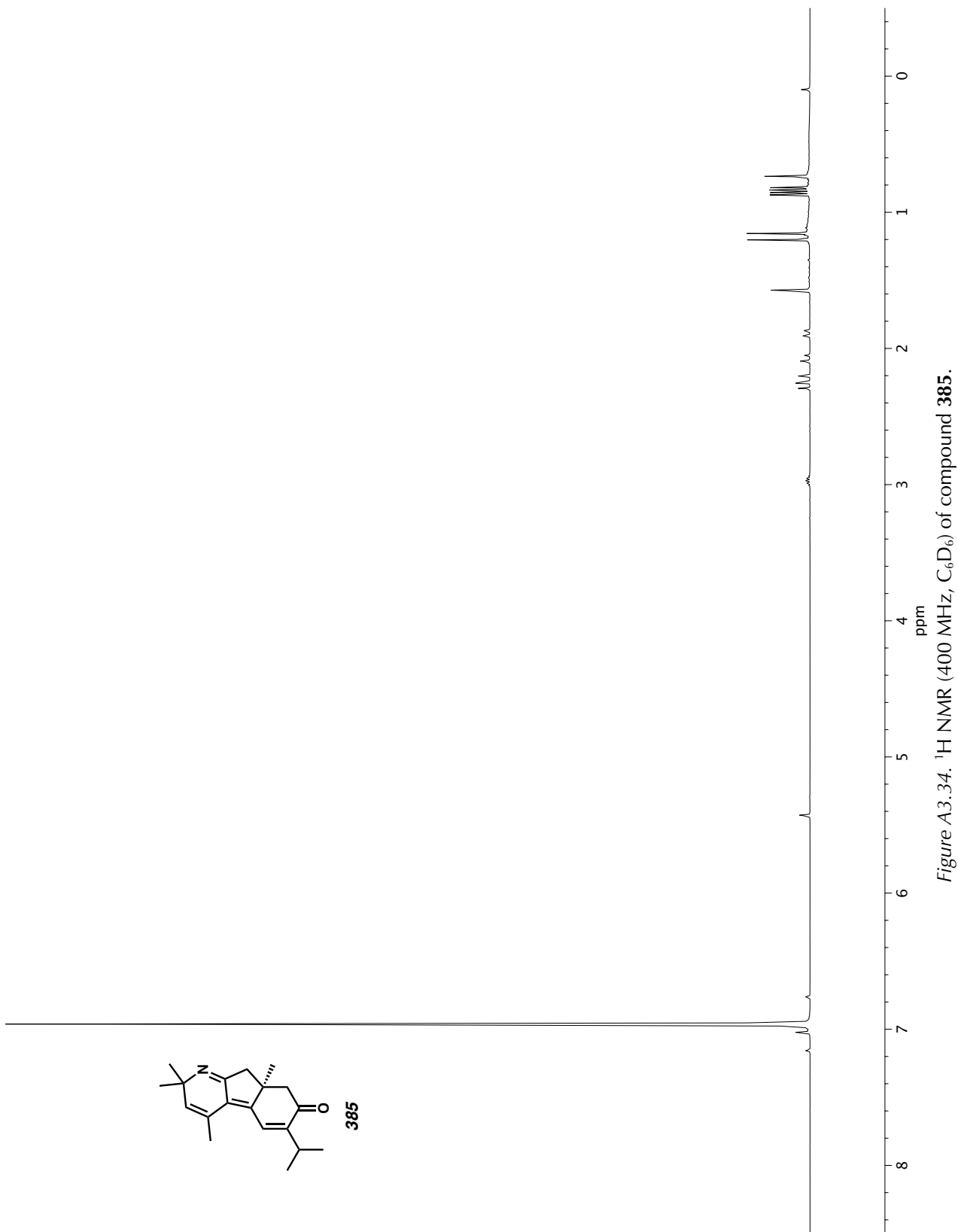


Figure A3.34. ^1H NMR (400 MHz, C_6D_6) of compound 385.

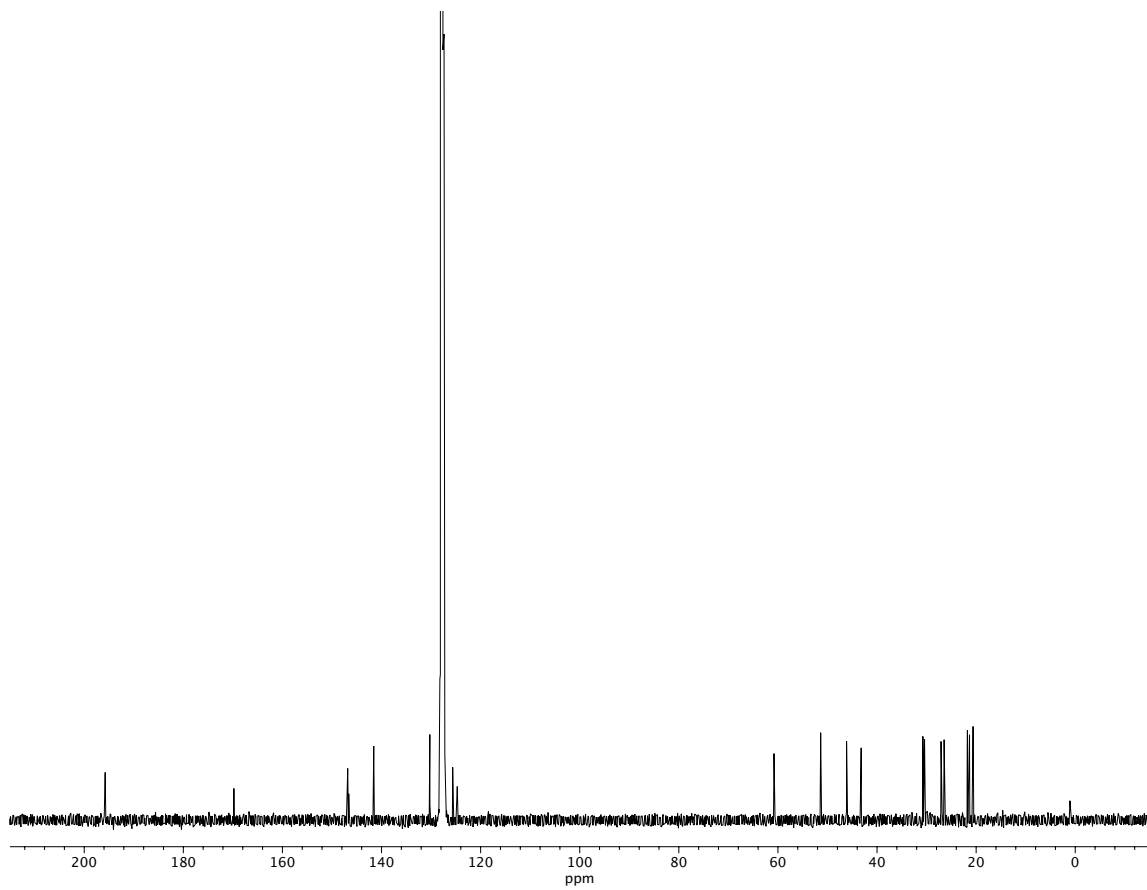


Figure A3.35. ^{13}C NMR (101 MHz, C_6D_6) of compound **385**.

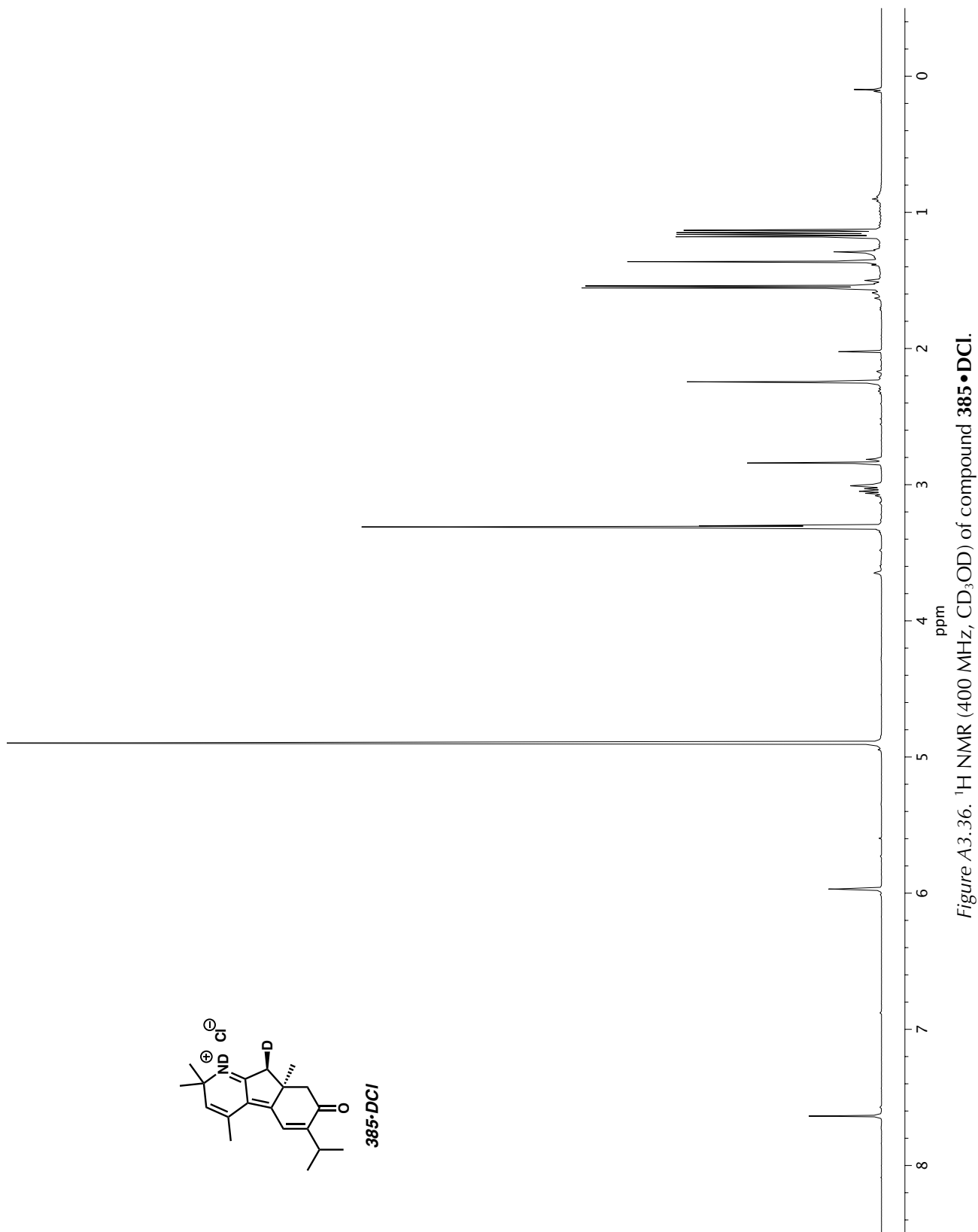


Figure A3.36. ^1H NMR (400 MHz, CD_3OD) of compound $385 \bullet \text{DCl}$.

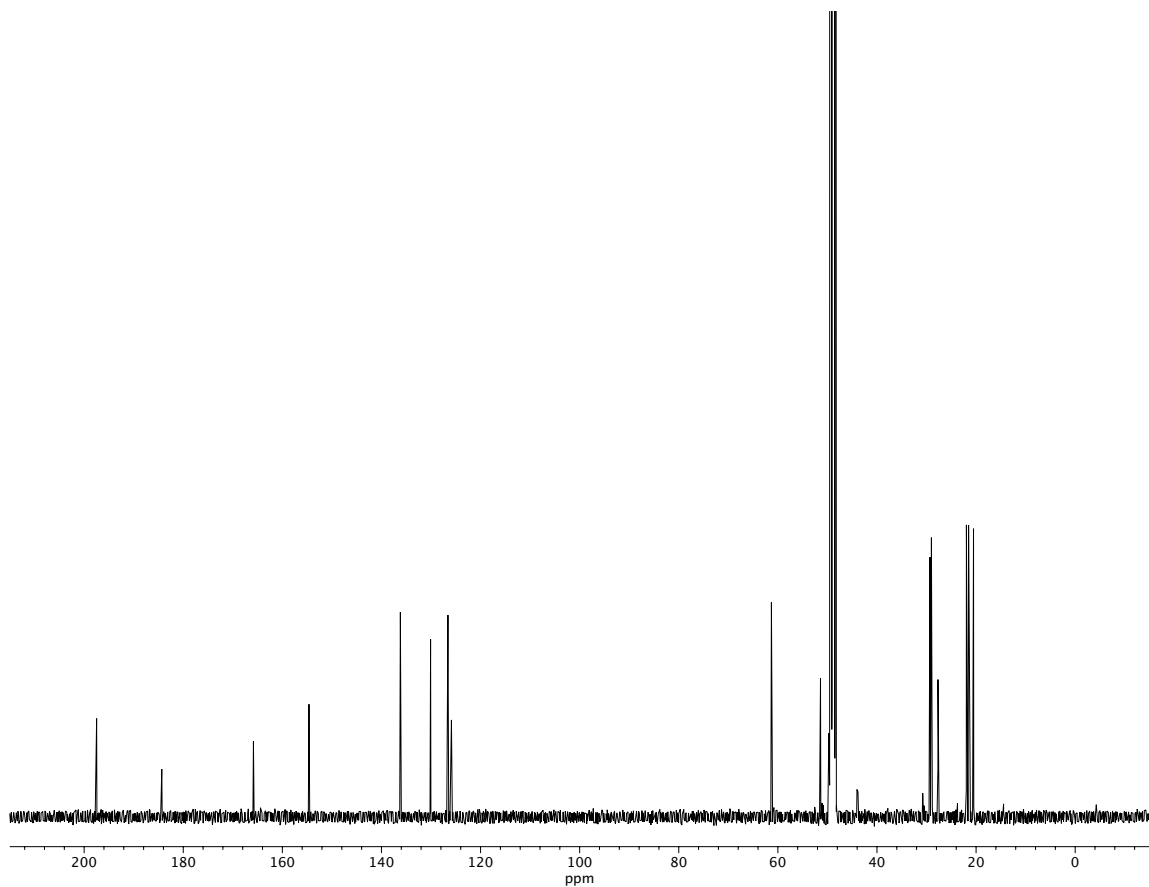


Figure A3.37. ¹³C NMR (101 MHz, CD₃OD) of compound **385•DCl**.

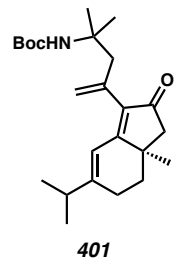
APPENDIX 4

X-Ray Crystallography Reports Relevant to Chapter 3:

Enantioselective Total Synthesis of Nigelladine A

Via Late-Stage C–H Oxidation Enabled by an

Engineered P450 Enzyme

A4.1 X-RAY CRYSTAL STRUCTURE ANALYSIS OF TRIENE **401**Contents*Table A4.1.1. Experimental Details**Table A4.1.2. Crystal Data**Table A4.1.3. Atomic Coordinates**Table A4.1.4. Full Bond Distances and Angles**Table A4.1.5. Anisotropic Displacement Parameters**Table A4.1.6. Hydrogen Atomic Coordinates**Table A4.1.7. Torsion Angles**Table A4.1.8. Hydrogen Bond Distances and Angle*

*Figure A4.1.1. X-Ray Crystal Structure of Triene **401***

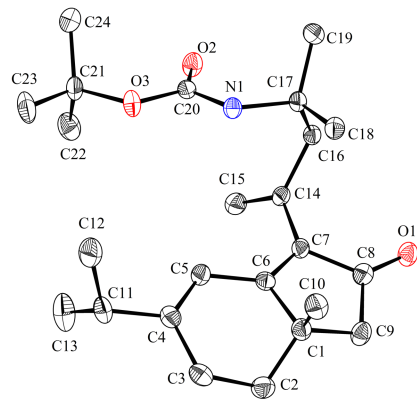


*Table A4.1.1. Experimental Details for X-Ray Structure Determination of Triene **401***

Low-temperature diffraction data (ϕ -and ω -scans) were collected on a Bruker AXS KAPPA APEX II diffractometer coupled to a APEX II CCD detector with graphite monochromated Mo $K\alpha$ radiation ($\lambda = 0.71073 \text{ \AA}$) for the structure of triene **401**. The structure was solved by direct methods using SHELXS¹ and refined against F^2 on all data by full-matrix least squares with SHELXL-2014² using established refinement techniques.³ All non-hydrogen atoms were refined anisotropically. All hydrogen atoms were included into the model at geometrically calculated positions and refined using a riding model. The isotropic displacement parameters of all hydrogen atoms were fixed to 1.2 times the U value of the atoms they are linked to (1.5 times for methyl groups).

Table A4.1.2. Crystal Data and Structure Refinement for Triene **401**

Empirical formula	C ₂₄ H ₃₇ N O ₃	
Formula weight	387.54	
Temperature	100 K	
Wavelength	1.54178 Å	
Crystal system	Triclinic	
Space group	P1	
Unit cell dimensions	a = 9.6892(11) Å	a = 89.402(8)°
	b = 10.0478(9) Å	b = 77.360(8)°
	c = 11.9882(11) Å	g = 89.745(8)°
Volume	1138.76(19) Å ³	
Z	2	
Density (calculated)	1.130 Mg/m ³	
Absorption coefficient	0.574 mm ⁻¹	
F(000)	424	
Crystal size	0.31 x 0.15 x 0.15 mm ³	
Theta range for data collection	3.779 to 79.188°.	
Index ranges	-12<=h<=12, -12<=k<=12, -15<=l<=15	
Reflections collected	44144	
Independent reflections	9136 [R(int) = 0.0587]	
Completeness to theta = 67.000°	99.6 %	
Absorption correction	Semi-empirical from equivalents	
Max. and min. transmission	0.9470 and 0.8656	
Refinement method	Full-matrix least-squares on F ²	
Data / restraints / parameters	9136 / 3 / 521	
Goodness-of-fit on F ²	1.062	
Final R indices [I>2sigma(I)]	R1 = 0.0497, wR2 = 0.1066	
R indices (all data)	R1 = 0.0568, wR2 = 0.1114	
Absolute structure parameter	0.08(8)	
Extinction coefficient	n/a	
Largest diff. peak and hole	0.318 and -0.238 e.Å ⁻³	

*Table A4.1.3. Atomic Coordinates ($x \cdot 10^4$) and Equivalent Isotropic Displacement Parameters ($\text{\AA}^2 \times 10^3$) for Triene **401**. $U(\text{eq})$ is Defined as One Third of the Trace of the Orthogonalized U^{ij} Tensor.*

	x	y	z	$U(\text{eq})$
O(1)	6427(3)	5529(2)	4290(2)	25(1)
O(2)	1594(2)	3334(2)	8236(2)	24(1)
O(3)	2950(3)	2423(2)	9381(2)	24(1)
N(1)	3663(3)	4279(3)	8426(2)	19(1)
C(1)	8553(4)	3624(3)	5846(3)	22(1)
C(2)	9499(4)	2396(4)	5692(3)	27(1)
C(3)	9318(4)	1614(3)	6823(3)	26(1)
C(4)	7794(4)	1450(3)	7447(3)	23(1)
C(5)	6748(4)	2160(3)	7164(3)	21(1)
C(6)	7031(4)	3176(3)	6278(3)	19(1)
C(7)	6109(3)	3839(3)	5775(3)	19(1)
C(8)	6912(4)	4726(3)	4874(3)	21(1)
C(9)	8471(4)	4390(3)	4741(3)	25(1)
C(10)	8980(4)	4589(4)	6705(3)	28(1)
C(11)	7516(4)	404(3)	8396(3)	28(1)
C(12)	6811(5)	994(4)	9543(3)	40(1)
C(13)	6667(5)	-743(4)	8076(4)	45(1)
C(14)	4548(3)	3702(3)	6030(2)	18(1)
C(15)	3982(4)	2511(3)	5934(3)	24(1)
C(16)	3632(3)	4898(3)	6411(3)	18(1)
C(17)	3666(3)	5403(3)	7625(3)	19(1)
C(18)	5001(4)	6206(3)	7619(3)	22(1)
C(19)	2376(4)	6285(3)	8055(3)	24(1)
C(20)	2632(3)	3355(3)	8639(3)	19(1)
C(21)	1988(4)	1295(3)	9736(3)	26(1)
C(22)	1986(4)	410(3)	8715(3)	31(1)
C(23)	2671(5)	576(4)	10590(3)	37(1)

Table A4.1.3 Cont'd

C(24)	514(5)	1766(4)	10308(4)	47(1)
O(1B)	6314(3)	4207(2)	-587(2)	25(1)
O(2B)	1567(2)	6339(2)	3346(2)	23(1)
O(3B)	3051(2)	7332(2)	4333(2)	21(1)
N(1B)	3720(3)	5462(3)	3414(2)	20(1)
C(1B)	8278(3)	6485(3)	780(3)	21(1)
C(2B)	8972(4)	6488(4)	1797(3)	27(1)
C(3B)	8775(4)	7833(4)	2410(3)	30(1)
C(4B)	7286(4)	8363(3)	2592(3)	23(1)
C(5B)	6354(4)	7851(3)	2047(3)	21(1)
C(6B)	6729(3)	6804(3)	1209(3)	19(1)
C(7B)	5858(3)	6011(3)	769(3)	19(1)
C(8B)	6728(4)	5017(3)	34(3)	22(1)
C(9B)	8233(4)	5137(4)	190(3)	27(1)
C(10B)	8957(4)	7542(4)	-132(3)	29(1)
C(11B)	6859(4)	9458(3)	3462(3)	26(1)
C(12B)	7716(4)	10730(4)	3123(4)	38(1)
C(13B)	6903(5)	8998(5)	4671(3)	39(1)
C(14B)	4297(3)	6029(3)	1009(3)	19(1)
C(15B)	3619(4)	7141(3)	826(3)	24(1)
C(16B)	3495(3)	4785(3)	1467(3)	21(1)
C(17B)	3681(4)	4317(3)	2662(3)	21(1)
C(18B)	5065(4)	3555(3)	2590(3)	24(1)
C(19B)	2448(4)	3397(3)	3194(3)	27(1)
C(20B)	2677(3)	6368(3)	3662(3)	19(1)
C(21B)	2079(4)	8434(3)	4721(3)	22(1)
C(22B)	2867(4)	9229(3)	5458(3)	28(1)
C(23B)	1886(4)	9273(4)	3704(3)	33(1)
C(24B)	690(4)	7918(4)	5439(3)	29(1)

Table A4.1.4. Bond Lengths [\AA] and angles [$^\circ$] for Triene **401**

O(1)-C(8)	1.221(4)
O(2)-C(20)	1.208(4)
O(3)-C(20)	1.365(4)
O(3)-C(21)	1.470(4)
N(1)-H(1)	0.8800
N(1)-C(17)	1.475(4)
N(1)-C(20)	1.348(4)
C(1)-C(2)	1.522(5)
C(1)-C(6)	1.520(5)
C(1)-C(9)	1.542(4)
C(1)-C(10)	1.543(5)
C(2)-H(2A)	0.9900
C(2)-H(2B)	0.9900
C(2)-C(3)	1.537(5)
C(3)-H(3A)	0.9900
C(3)-H(3B)	0.9900
C(3)-C(4)	1.510(5)
C(4)-C(5)	1.337(5)
C(4)-C(11)	1.522(4)
C(5)-H(5)	0.9500
C(5)-C(6)	1.450(4)
C(6)-C(7)	1.351(4)
C(7)-C(8)	1.478(4)
C(7)-C(14)	1.484(4)
C(8)-C(9)	1.520(5)

Table A4.1.4. cont'd

C(9)-H(9A)	0.9900
C(9)-H(9B)	0.9900
C(10)-H(10A)	0.9800
C(10)-H(10B)	0.9800
C(10)-H(10C)	0.9800
C(11)-H(11)	1.0000
C(11)-C(12)	1.520(6)
C(11)-C(13)	1.520(5)
C(12)-H(12A)	0.9800
C(12)-H(12B)	0.9800
C(12)-H(12C)	0.9800
C(13)-H(13A)	0.9800
C(13)-H(13B)	0.9800
C(13)-H(13C)	0.9800
C(14)-C(15)	1.335(4)
C(14)-C(16)	1.505(4)
C(15)-H(15A)	0.9500
C(15)-H(15B)	0.9500
C(16)-H(16A)	0.9900
C(16)-H(16B)	0.9900
C(16)-C(17)	1.554(4)
C(17)-C(18)	1.526(4)
C(17)-C(19)	1.526(5)
C(18)-H(18A)	0.9800
C(18)-H(18B)	0.9800
C(18)-H(18C)	0.9800

Table A4.1.4. cont'd

C(19)-H(19A)	0.9800
C(19)-H(19B)	0.9800
C(19)-H(19C)	0.9800
C(21)-C(22)	1.520(5)
C(21)-C(23)	1.512(5)
C(21)-C(24)	1.519(6)
C(22)-H(22A)	0.9800
C(22)-H(22B)	0.9800
C(22)-H(22C)	0.9800
C(23)-H(23A)	0.9800
C(23)-H(23B)	0.9800
C(23)-H(23C)	0.9800
C(24)-H(24A)	0.9800
C(24)-H(24B)	0.9800
C(24)-H(24C)	0.9800
O(1B)-C(8B)	1.234(4)
O(2B)-C(20B)	1.217(4)
O(3B)-C(20B)	1.365(4)
O(3B)-C(21B)	1.463(4)
N(1B)-H(1B)	0.8800
N(1B)-C(17B)	1.474(4)
N(1B)-C(20B)	1.343(4)
C(1B)-C(2B)	1.516(5)
C(1B)-C(6B)	1.510(5)
C(1B)-C(9B)	1.539(5)
C(1B)-C(10B)	1.557(4)

Table A4.1.4. cont'd

C(2B)-H(2BA)	0.9900
C(2B)-H(2BB)	0.9900
C(2B)-C(3B)	1.536(5)
C(3B)-H(3BA)	0.9900
C(3B)-H(3BB)	0.9900
C(3B)-C(4B)	1.507(5)
C(4B)-C(5B)	1.333(5)
C(4B)-C(11B)	1.516(5)
C(5B)-H(5B)	0.9500
C(5B)-C(6B)	1.451(4)
C(6B)-C(7B)	1.355(4)
C(7B)-C(8B)	1.473(5)
C(7B)-C(14B)	1.477(4)
C(8B)-C(9B)	1.515(5)
C(9B)-H(9BA)	0.9900
C(9B)-H(9BB)	0.9900
C(10B)-H(10D)	0.9800
C(10B)-H(10E)	0.9800
C(10B)-H(10F)	0.9800
C(11B)-H(11B)	1.0000
C(11B)-C(12B)	1.529(5)
C(11B)-C(13B)	1.526(5)
C(12B)-H(12D)	0.9800
C(12B)-H(12E)	0.9800
C(12B)-H(12F)	0.9800
C(13B)-H(13D)	0.9800

Table A4.1.4. cont'd

C(13B)-H(13E)	0.9800
C(13B)-H(13F)	0.9800
C(14B)-C(15B)	1.334(5)
C(14B)-C(16B)	1.509(4)
C(15B)-H(15C)	0.9500
C(15B)-H(15D)	0.9500
C(16B)-H(16C)	0.9900
C(16B)-H(16D)	0.9900
C(16B)-C(17B)	1.551(4)
C(17B)-C(18B)	1.528(5)
C(17B)-C(19B)	1.534(4)
C(18B)-H(18D)	0.9800
C(18B)-H(18E)	0.9800
C(18B)-H(18F)	0.9800
C(19B)-H(19D)	0.9800
C(19B)-H(19E)	0.9800
C(19B)-H(19F)	0.9800
C(21B)-C(22B)	1.523(4)
C(21B)-C(23B)	1.520(5)
C(21B)-C(24B)	1.520(5)
C(22B)-H(22D)	0.9800
C(22B)-H(22E)	0.9800
C(22B)-H(22F)	0.9800
C(23B)-H(23D)	0.9800
C(23B)-H(23E)	0.9800
C(23B)-H(23F)	0.9800

Table A4.1.4. cont'd

C(24B)-H(24D)	0.9800
C(24B)-H(24E)	0.9800
C(24B)-H(24F)	0.9800
C(20)-O(3)-C(21)	119.5(3)
C(17)-N(1)-H(1)	118.6
C(20)-N(1)-H(1)	118.6
C(20)-N(1)-C(17)	122.9(3)
C(2)-C(1)-C(9)	115.8(3)
C(2)-C(1)-C(10)	110.7(3)
C(6)-C(1)-C(2)	108.4(3)
C(6)-C(1)-C(9)	102.1(3)
C(6)-C(1)-C(10)	110.1(3)
C(9)-C(1)-C(10)	109.4(3)
C(1)-C(2)-H(2A)	109.6
C(1)-C(2)-H(2B)	109.6
C(1)-C(2)-C(3)	110.5(3)
H(2A)-C(2)-H(2B)	108.1
C(3)-C(2)-H(2A)	109.6
C(3)-C(2)-H(2B)	109.6
C(2)-C(3)-H(3A)	108.8
C(2)-C(3)-H(3B)	108.8
H(3A)-C(3)-H(3B)	107.7
C(4)-C(3)-C(2)	113.7(3)
C(4)-C(3)-H(3A)	108.8
C(4)-C(3)-H(3B)	108.8

Table A4.1.4. cont'd

C(3)-C(4)-C(11)	116.0(3)
C(5)-C(4)-C(3)	122.1(3)
C(5)-C(4)-C(11)	121.9(3)
C(4)-C(5)-H(5)	119.3
C(4)-C(5)-C(6)	121.4(3)
C(6)-C(5)-H(5)	119.3
C(5)-C(6)-C(1)	118.0(3)
C(7)-C(6)-C(1)	113.0(3)
C(7)-C(6)-C(5)	128.9(3)
C(6)-C(7)-C(8)	108.8(3)
C(6)-C(7)-C(14)	127.2(3)
C(8)-C(7)-C(14)	123.9(3)
O(1)-C(8)-C(7)	127.0(3)
O(1)-C(8)-C(9)	125.5(3)
C(7)-C(8)-C(9)	107.3(3)
C(1)-C(9)-H(9A)	110.8
C(1)-C(9)-H(9B)	110.8
C(8)-C(9)-C(1)	104.7(3)
C(8)-C(9)-H(9A)	110.8
C(8)-C(9)-H(9B)	110.8
H(9A)-C(9)-H(9B)	108.9
C(1)-C(10)-H(10A)	109.5
C(1)-C(10)-H(10B)	109.5
C(1)-C(10)-H(10C)	109.5
H(10A)-C(10)-H(10B)	109.5
H(10A)-C(10)-H(10C)	109.5

Table A4.1.4. cont'd

H(10B)-C(10)-H(10C)	109.5
C(4)-C(11)-H(11)	107.4
C(12)-C(11)-C(4)	112.1(3)
C(12)-C(11)-H(11)	107.4
C(13)-C(11)-C(4)	110.5(3)
C(13)-C(11)-H(11)	107.4
C(13)-C(11)-C(12)	111.8(4)
C(11)-C(12)-H(12A)	109.5
C(11)-C(12)-H(12B)	109.5
C(11)-C(12)-H(12C)	109.5
H(12A)-C(12)-H(12B)	109.5
H(12A)-C(12)-H(12C)	109.5
H(12B)-C(12)-H(12C)	109.5
C(11)-C(13)-H(13A)	109.5
C(11)-C(13)-H(13B)	109.5
C(11)-C(13)-H(13C)	109.5
H(13A)-C(13)-H(13B)	109.5
H(13A)-C(13)-H(13C)	109.5
H(13B)-C(13)-H(13C)	109.5
C(7)-C(14)-C(16)	119.6(3)
C(15)-C(14)-C(7)	119.2(3)
C(15)-C(14)-C(16)	121.2(3)
C(14)-C(15)-H(15A)	120.0
C(14)-C(15)-H(15B)	120.0
H(15A)-C(15)-H(15B)	120.0
C(14)-C(16)-H(16A)	108.5

Table A4.1.4. cont'd

C(14)-C(16)-H(16B)	108.5
C(14)-C(16)-C(17)	114.9(3)
H(16A)-C(16)-H(16B)	107.5
C(17)-C(16)-H(16A)	108.5
C(17)-C(16)-H(16B)	108.5
N(1)-C(17)-C(16)	110.9(2)
N(1)-C(17)-C(18)	106.7(2)
N(1)-C(17)-C(19)	109.6(3)
C(18)-C(17)-C(16)	111.5(3)
C(18)-C(17)-C(19)	108.8(3)
C(19)-C(17)-C(16)	109.1(3)
C(17)-C(18)-H(18A)	109.5
C(17)-C(18)-H(18B)	109.5
C(17)-C(18)-H(18C)	109.5
H(18A)-C(18)-H(18B)	109.5
H(18A)-C(18)-H(18C)	109.5
H(18B)-C(18)-H(18C)	109.5
C(17)-C(19)-H(19A)	109.5
C(17)-C(19)-H(19B)	109.5
C(17)-C(19)-H(19C)	109.5
H(19A)-C(19)-H(19B)	109.5
H(19A)-C(19)-H(19C)	109.5
H(19B)-C(19)-H(19C)	109.5
O(2)-C(20)-O(3)	124.8(3)
O(2)-C(20)-N(1)	126.1(3)
N(1)-C(20)-O(3)	109.1(3)

Table A4.1.4. cont'd

O(3)-C(21)-C(22)	109.7(3)
O(3)-C(21)-C(23)	102.3(3)
O(3)-C(21)-C(24)	111.4(3)
C(23)-C(21)-C(22)	110.2(3)
C(23)-C(21)-C(24)	110.4(3)
C(24)-C(21)-C(22)	112.4(4)
C(21)-C(22)-H(22A)	109.5
C(21)-C(22)-H(22B)	109.5
C(21)-C(22)-H(22C)	109.5
H(22A)-C(22)-H(22B)	109.5
H(22A)-C(22)-H(22C)	109.5
H(22B)-C(22)-H(22C)	109.5
C(21)-C(23)-H(23A)	109.5
C(21)-C(23)-H(23B)	109.5
C(21)-C(23)-H(23C)	109.5
H(23A)-C(23)-H(23B)	109.5
H(23A)-C(23)-H(23C)	109.5
H(23B)-C(23)-H(23C)	109.5
C(21)-C(24)-H(24A)	109.5
C(21)-C(24)-H(24B)	109.5
C(21)-C(24)-H(24C)	109.5
H(24A)-C(24)-H(24B)	109.5
H(24A)-C(24)-H(24C)	109.5
H(24B)-C(24)-H(24C)	109.5
C(20B)-O(3B)-C(21B)	119.7(2)
C(17B)-N(1B)-H(1B)	118.3

Table A4.1.4. cont'd

C(20B)-N(1B)-H(1B)	118.3
C(20B)-N(1B)-C(17B)	123.3(3)
C(2B)-C(1B)-C(9B)	116.2(3)
C(2B)-C(1B)-C(10B)	111.3(3)
C(6B)-C(1B)-C(2B)	107.8(3)
C(6B)-C(1B)-C(9B)	102.6(3)
C(6B)-C(1B)-C(10B)	109.4(3)
C(9B)-C(1B)-C(10B)	109.1(3)
C(1B)-C(2B)-H(2BA)	109.3
C(1B)-C(2B)-H(2BB)	109.3
C(1B)-C(2B)-C(3B)	111.4(3)
H(2BA)-C(2B)-H(2BB)	108.0
C(3B)-C(2B)-H(2BA)	109.3
C(3B)-C(2B)-H(2BB)	109.3
C(2B)-C(3B)-H(3BA)	108.9
C(2B)-C(3B)-H(3BB)	108.9
H(3BA)-C(3B)-H(3BB)	107.7
C(4B)-C(3B)-C(2B)	113.2(3)
C(4B)-C(3B)-H(3BA)	108.9
C(4B)-C(3B)-H(3BB)	108.9
C(3B)-C(4B)-C(11B)	117.7(3)
C(5B)-C(4B)-C(3B)	121.4(3)
C(5B)-C(4B)-C(11B)	120.9(3)
C(4B)-C(5B)-H(5B)	118.9
C(4B)-C(5B)-C(6B)	122.2(3)
C(6B)-C(5B)-H(5B)	118.9

Table A4.1.4. cont'd

C(5B)-C(6B)-C(1B)	118.1(3)
C(7B)-C(6B)-C(1B)	113.5(3)
C(7B)-C(6B)-C(5B)	128.4(3)
C(6B)-C(7B)-C(8B)	108.4(3)
C(6B)-C(7B)-C(14B)	128.1(3)
C(8B)-C(7B)-C(14B)	123.4(3)
O(1B)-C(8B)-C(7B)	126.6(3)
O(1B)-C(8B)-C(9B)	125.4(3)
C(7B)-C(8B)-C(9B)	107.9(3)
C(1B)-C(9B)-H(9BA)	110.8
C(1B)-C(9B)-H(9BB)	110.8
C(8B)-C(9B)-C(1B)	104.9(3)
C(8B)-C(9B)-H(9BA)	110.8
C(8B)-C(9B)-H(9BB)	110.8
H(9BA)-C(9B)-H(9BB)	108.8
C(1B)-C(10B)-H(10D)	109.5
C(1B)-C(10B)-H(10E)	109.5
C(1B)-C(10B)-H(10F)	109.5
H(10D)-C(10B)-H(10E)	109.5
H(10D)-C(10B)-H(10F)	109.5
H(10E)-C(10B)-H(10F)	109.5
C(4B)-C(11B)-H(11B)	106.7
C(4B)-C(11B)-C(12B)	112.2(3)
C(4B)-C(11B)-C(13B)	112.2(3)
C(12B)-C(11B)-H(11B)	106.7
C(13B)-C(11B)-H(11B)	106.7

Table A4.1.4. cont'd

C(13B)-C(11B)-C(12B)	111.8(3)
C(11B)-C(12B)-H(12D)	109.5
C(11B)-C(12B)-H(12E)	109.5
C(11B)-C(12B)-H(12F)	109.5
H(12D)-C(12B)-H(12E)	109.5
H(12D)-C(12B)-H(12F)	109.5
H(12E)-C(12B)-H(12F)	109.5
C(11B)-C(13B)-H(13D)	109.5
C(11B)-C(13B)-H(13E)	109.5
C(11B)-C(13B)-H(13F)	109.5
H(13D)-C(13B)-H(13E)	109.5
H(13D)-C(13B)-H(13F)	109.5
H(13E)-C(13B)-H(13F)	109.5
C(7B)-C(14B)-C(16B)	119.1(3)
C(15B)-C(14B)-C(7B)	119.8(3)
C(15B)-C(14B)-C(16B)	121.1(3)
C(14B)-C(15B)-H(15C)	120.0
C(14B)-C(15B)-H(15D)	120.0
H(15C)-C(15B)-H(15D)	120.0
C(14B)-C(16B)-H(16C)	108.5
C(14B)-C(16B)-H(16D)	108.5
C(14B)-C(16B)-C(17B)	115.1(2)
H(16C)-C(16B)-H(16D)	107.5
C(17B)-C(16B)-H(16C)	108.5
C(17B)-C(16B)-H(16D)	108.5
N(1B)-C(17B)-C(16B)	111.0(3)

Table A4.1.4. cont'd

N(1B)-C(17B)-C(18B)	106.7(3)
N(1B)-C(17B)-C(19B)	110.0(3)
C(18B)-C(17B)-C(16B)	111.8(3)
C(18B)-C(17B)-C(19B)	108.5(3)
C(19B)-C(17B)-C(16B)	108.8(3)
C(17B)-C(18B)-H(18D)	109.5
C(17B)-C(18B)-H(18E)	109.5
C(17B)-C(18B)-H(18F)	109.5
H(18D)-C(18B)-H(18E)	109.5
H(18D)-C(18B)-H(18F)	109.5
H(18E)-C(18B)-H(18F)	109.5
C(17B)-C(19B)-H(19D)	109.5
C(17B)-C(19B)-H(19E)	109.5
C(17B)-C(19B)-H(19F)	109.5
H(19D)-C(19B)-H(19E)	109.5
H(19D)-C(19B)-H(19F)	109.5
H(19E)-C(19B)-H(19F)	109.5
O(2B)-C(20B)-O(3B)	124.9(3)
O(2B)-C(20B)-N(1B)	125.7(3)
N(1B)-C(20B)-O(3B)	109.4(3)
O(3B)-C(21B)-C(22B)	102.6(3)
O(3B)-C(21B)-C(23B)	110.0(3)
O(3B)-C(21B)-C(24B)	110.6(3)
C(23B)-C(21B)-C(22B)	109.9(3)
C(24B)-C(21B)-C(22B)	110.3(3)
C(24B)-C(21B)-C(23B)	113.0(3)

Table A4.1.4. cont'd

C(21B)-C(22B)-H(22D)	109.5
C(21B)-C(22B)-H(22E)	109.5
C(21B)-C(22B)-H(22F)	109.5
H(22D)-C(22B)-H(22E)	109.5
H(22D)-C(22B)-H(22F)	109.5
H(22E)-C(22B)-H(22F)	109.5
C(21B)-C(23B)-H(23D)	109.5
C(21B)-C(23B)-H(23E)	109.5
C(21B)-C(23B)-H(23F)	109.5
H(23D)-C(23B)-H(23E)	109.5
H(23D)-C(23B)-H(23F)	109.5
H(23E)-C(23B)-H(23F)	109.5
C(21B)-C(24B)-H(24D)	109.5
C(21B)-C(24B)-H(24E)	109.5
C(21B)-C(24B)-H(24F)	109.5
H(24D)-C(24B)-H(24E)	109.5
H(24D)-C(24B)-H(24F)	109.5
H(24E)-C(24B)-H(24F)	109.5

Symmetry transformations used to generate equivalent atoms:

*Table A4.1.5. Anisotropic Displacement Parameters ($\text{\AA}^2 \times 10^3$) for Triene **401**. The Anisotropic Displacement Factor Exponent Takes the Form: $-2p^2[h^2a^{*2}U^{11} + \dots + 2hka^{*}b^{*}U^{12}]$.*

	U ¹¹	U ²²	U ³³	U ²³	U ¹³	U ¹²
O(1)	24(1)	28(1)	23(1)	8(1)	-7(1)	-1(1)
O(2)	21(1)	26(1)	26(1)	6(1)	-8(1)	-4(1)
O(3)	32(1)	18(1)	23(1)	6(1)	-12(1)	-4(1)
N(1)	21(1)	19(1)	17(1)	2(1)	-6(1)	-1(1)
C(1)	22(2)	22(2)	24(2)	3(1)	-6(1)	-1(1)
C(2)	23(2)	29(2)	27(2)	0(1)	-4(1)	2(2)
C(3)	26(2)	25(2)	31(2)	-1(1)	-10(2)	5(1)
C(4)	27(2)	20(2)	23(2)	-1(1)	-7(1)	1(1)
C(5)	23(2)	21(2)	19(2)	2(1)	-4(1)	-1(1)
C(6)	22(2)	16(1)	17(1)	-3(1)	-2(1)	1(1)
C(7)	24(2)	14(1)	17(1)	0(1)	-1(1)	-1(1)
C(8)	23(2)	21(2)	20(2)	-1(1)	-5(1)	-3(1)
C(9)	20(2)	28(2)	27(2)	6(1)	-6(1)	-5(1)
C(10)	28(2)	27(2)	32(2)	1(2)	-10(2)	-3(2)
C(11)	34(2)	21(2)	31(2)	8(1)	-11(2)	0(2)
C(12)	50(3)	38(2)	30(2)	11(2)	-7(2)	4(2)
C(13)	55(3)	31(2)	54(3)	16(2)	-27(2)	-14(2)
C(14)	20(2)	20(1)	14(1)	2(1)	-2(1)	-1(1)
C(15)	23(2)	24(2)	25(2)	0(1)	-4(1)	-2(1)
C(16)	18(2)	18(1)	19(1)	3(1)	-4(1)	0(1)
C(17)	21(2)	17(1)	18(1)	2(1)	-4(1)	0(1)
C(18)	26(2)	20(2)	20(2)	0(1)	-5(1)	-2(1)
C(19)	26(2)	22(2)	24(2)	0(1)	-3(1)	4(1)
C(20)	21(2)	17(1)	17(1)	0(1)	-2(1)	2(1)
C(21)	33(2)	17(2)	26(2)	6(1)	-1(2)	-2(1)
C(22)	33(2)	21(2)	42(2)	0(2)	-13(2)	-5(2)
C(23)	57(3)	20(2)	34(2)	9(2)	-12(2)	-1(2)

Table A4.1.5. cont'd

C(24)	43(3)	35(2)	50(3)	18(2)	16(2)	8(2)
O(1B)	27(1)	24(1)	24(1)	-6(1)	-6(1)	4(1)
O(2B)	20(1)	27(1)	24(1)	-6(1)	-7(1)	2(1)
O(3B)	22(1)	20(1)	23(1)	-6(1)	-8(1)	4(1)
N(1B)	21(1)	21(1)	19(1)	-5(1)	-5(1)	2(1)
C(1B)	19(2)	23(2)	19(2)	1(1)	-1(1)	0(1)
C(2B)	22(2)	31(2)	28(2)	0(1)	-7(1)	2(2)
C(3B)	26(2)	36(2)	32(2)	-6(2)	-12(2)	0(2)
C(4B)	25(2)	22(2)	22(2)	1(1)	-5(1)	-1(1)
C(5B)	21(2)	20(2)	20(2)	1(1)	-1(1)	-1(1)
C(6B)	21(2)	19(2)	16(1)	3(1)	-2(1)	-2(1)
C(7B)	23(2)	19(1)	16(1)	2(1)	-3(1)	1(1)
C(8B)	26(2)	19(2)	19(2)	2(1)	-4(1)	2(1)
C(9B)	24(2)	27(2)	31(2)	-7(1)	-6(1)	6(2)
C(10B)	26(2)	28(2)	31(2)	6(2)	2(2)	2(2)
C(11B)	27(2)	25(2)	27(2)	-5(1)	-8(1)	-1(2)
C(12B)	34(2)	33(2)	45(2)	-10(2)	-3(2)	-2(2)
C(13B)	45(3)	45(2)	30(2)	-7(2)	-10(2)	11(2)
C(14B)	21(2)	20(2)	15(1)	-3(1)	-4(1)	-1(1)
C(15B)	25(2)	23(2)	25(2)	2(1)	-6(1)	0(1)
C(16B)	20(2)	23(2)	19(2)	-5(1)	-3(1)	-1(1)
C(17B)	24(2)	20(2)	18(2)	-4(1)	-3(1)	0(1)
C(18B)	31(2)	19(2)	21(2)	1(1)	-4(1)	4(1)
C(19B)	29(2)	23(2)	25(2)	1(1)	1(1)	-5(2)
C(20B)	20(2)	20(2)	16(1)	-2(1)	-2(1)	0(1)
C(21B)	25(2)	16(1)	26(2)	-2(1)	-5(1)	-1(1)
C(22B)	27(2)	22(2)	32(2)	-9(1)	-2(2)	-4(1)
C(23B)	34(2)	23(2)	43(2)	6(2)	-13(2)	2(2)
C(24B)	26(2)	28(2)	31(2)	-9(2)	0(2)	-4(2)

*Table A4.1.6. Hydrogen Coordinates ($\times 10^4$) and Isotropic Displacement Parameters ($\text{\AA}^2 \times 10^3$) for Triene **401**.*

	x	y	z	U(eq)
H(1)	4366	4207	8780	22
H(2A)	10499	2670	5430	32
H(2B)	9253	1819	5100	32
H(3A)	9749	721	6664	32
H(3B)	9838	2079	7328	32
H(5)	5799	1993	7553	25
H(9A)	9048	5210	4663	30
H(9B)	8810	3830	4061	30
H(10A)	8415	5405	6742	43
H(10B)	9985	4809	6455	43
H(10C)	8810	4167	7463	43
H(11)	8453	39	8472	34
H(12A)	7392	1723	9724	60
H(12B)	6712	304	10138	60
H(12C)	5873	1337	9504	60
H(13A)	5734	-419	8004	67
H(13B)	6551	-1434	8672	67
H(13C)	7167	-1115	7346	67
H(15A)	4578	1765	5703	29
H(15B)	2983	2410	6095	29
H(16A)	2643	4676	6392	22
H(16B)	3935	5632	5855	22
H(18A)	4964	6554	8386	33
H(18B)	5063	6949	7074	33
H(18C)	5833	5631	7394	33
H(19A)	1512	5767	8092	36
H(19B)	2392	7042	7531	36
H(19C)	2396	6611	8819	36

Table A4.1.6. cont'd

H(22A)	1610	910	8140	47
H(22B)	1391	-370	8965	47
H(22C)	2954	120	8383	47
H(23A)	3615	266	10207	55
H(23B)	2089	-189	10912	55
H(23C)	2753	1185	11206	55
H(24A)	576	2379	10925	71
H(24B)	-67	998	10624	71
H(24C)	83	2225	9743	71
H(1B)	4464	5557	3715	24
H(2BA)	9994	6299	1534	32
H(2BB)	8554	5774	2340	32
H(3BA)	9033	7732	3161	36
H(3BB)	9429	8489	1953	36
H(5B)	5412	8182	2213	25
H(9BA)	8914	5122	-557	33
H(9BB)	8462	4400	674	33
H(10D)	8543	7468	-805	44
H(10E)	9979	7390	-355	44
H(10F)	8774	8435	190	44
H(11B)	5851	9685	3469	31
H(12D)	8713	10555	3115	57
H(12E)	7359	11429	3676	57
H(12F)	7623	11020	2359	57
H(13D)	6310	8206	4871	59
H(13E)	6548	9711	5211	59
H(13F)	7880	8782	4707	59
H(15C)	4140	7918	543	29
H(15D)	2615	7157	980	29
H(16C)	3803	4057	918	25
H(16D)	2476	4943	1507	25
H(18D)	5865	4149	2300	36
H(18E)	5101	2802	2071	36

Table A4.1.6. cont'd

H(18F)	5116	3225	3352	36
H(19D)	2575	3069	3938	40
H(19E)	2426	2642	2688	40
H(19F)	1556	3892	3296	40
H(22D)	3045	8663	6083	41
H(22E)	2293	9998	5777	41
H(22F)	3769	9539	4990	41
H(23D)	2813	9553	3259	49
H(23E)	1315	10060	3976	49
H(23F)	1405	8746	3220	49
H(24D)	188	7418	4952	44
H(24E)	105	8670	5780	44
H(24F)	881	7332	6046	44

Table A4.1.7. Torsion Angles [$^{\circ}$] for Triene **401**.

O(1)-C(8)-C(9)-C(1)	165.9(3)
C(1)-C(2)-C(3)-C(4)	44.6(4)
C(1)-C(6)-C(7)-C(8)	4.9(4)
C(1)-C(6)-C(7)-C(14)	-176.8(3)
C(2)-C(1)-C(6)-C(5)	43.1(4)
C(2)-C(1)-C(6)-C(7)	-138.5(3)
C(2)-C(1)-C(9)-C(8)	137.0(3)
C(2)-C(3)-C(4)-C(5)	-13.6(5)
C(2)-C(3)-C(4)-C(11)	164.9(3)
C(3)-C(4)-C(5)-C(6)	-3.1(5)
C(3)-C(4)-C(11)-C(12)	121.6(4)
C(3)-C(4)-C(11)-C(13)	-113.0(4)
C(4)-C(5)-C(6)-C(1)	-12.6(5)
C(4)-C(5)-C(6)-C(7)	169.3(3)
C(5)-C(4)-C(11)-C(12)	-59.8(5)
C(5)-C(4)-C(11)-C(13)	65.6(5)
C(5)-C(6)-C(7)-C(8)	-176.9(3)
C(5)-C(6)-C(7)-C(14)	1.4(5)
C(6)-C(1)-C(2)-C(3)	-57.7(4)
C(6)-C(1)-C(9)-C(8)	19.6(3)
C(6)-C(7)-C(8)-O(1)	-175.4(3)
C(6)-C(7)-C(8)-C(9)	8.6(3)
C(6)-C(7)-C(14)-C(15)	-58.0(5)
C(6)-C(7)-C(14)-C(16)	121.0(3)
C(7)-C(8)-C(9)-C(1)	-18.0(3)
C(7)-C(14)-C(16)-C(17)	-69.5(3)
C(8)-C(7)-C(14)-C(15)	120.0(3)
C(8)-C(7)-C(14)-C(16)	-60.9(4)
C(9)-C(1)-C(2)-C(3)	-171.6(3)
C(9)-C(1)-C(6)-C(5)	165.8(3)
C(9)-C(1)-C(6)-C(7)	-15.8(4)
C(10)-C(1)-C(2)-C(3)	63.1(4)

Table A4.1.7. cont'd

C(10)-C(1)-C(6)-C(5)	-78.1(4)
C(10)-C(1)-C(6)-C(7)	100.3(3)
C(10)-C(1)-C(9)-C(8)	-97.0(3)
C(11)-C(4)-C(5)-C(6)	178.4(3)
C(14)-C(7)-C(8)-O(1)	6.2(5)
C(14)-C(7)-C(8)-C(9)	-169.8(3)
C(14)-C(16)-C(17)-N(1)	-40.6(4)
C(14)-C(16)-C(17)-C(18)	78.2(3)
C(14)-C(16)-C(17)-C(19)	-161.5(3)
C(15)-C(14)-C(16)-C(17)	109.5(3)
C(17)-N(1)-C(20)-O(2)	-1.4(5)
C(17)-N(1)-C(20)-O(3)	177.9(3)
C(20)-O(3)-C(21)-C(22)	66.4(4)
C(20)-O(3)-C(21)-C(23)	-176.6(3)
C(20)-O(3)-C(21)-C(24)	-58.7(4)
C(20)-N(1)-C(17)-C(16)	-58.1(4)
C(20)-N(1)-C(17)-C(18)	-179.7(3)
C(20)-N(1)-C(17)-C(19)	62.6(4)
C(21)-O(3)-C(20)-O(2)	0.1(5)
C(21)-O(3)-C(20)-N(1)	-179.2(3)
O(1B)-C(8B)-C(9B)-C(1B)	165.9(3)
C(1B)-C(2B)-C(3B)-C(4B)	45.3(4)
C(1B)-C(6B)-C(7B)-C(8B)	2.9(4)
C(1B)-C(6B)-C(7B)-C(14B)	179.1(3)
C(2B)-C(1B)-C(6B)-C(5B)	42.3(4)
C(2B)-C(1B)-C(6B)-C(7B)	-135.5(3)
C(2B)-C(1B)-C(9B)-C(8B)	133.4(3)
C(2B)-C(3B)-C(4B)-C(5B)	-13.9(5)
C(2B)-C(3B)-C(4B)-C(11B)	163.2(3)
C(3B)-C(4B)-C(5B)-C(6B)	-3.1(5)
C(3B)-C(4B)-C(11B)-C(12B)	63.3(4)
C(3B)-C(4B)-C(11B)-C(13B)	-63.5(4)
C(4B)-C(5B)-C(6B)-C(1B)	-12.2(5)
C(4B)-C(5B)-C(6B)-C(7B)	165.2(3)

Table A4.1.7. cont'd

C(5B)-C(4B)-C(11B)-C(12B)	-119.5(4)
C(5B)-C(4B)-C(11B)-C(13B)	113.7(4)
C(5B)-C(6B)-C(7B)-C(8B)	-174.6(3)
C(5B)-C(6B)-C(7B)-C(14B)	1.6(5)
C(6B)-C(1B)-C(2B)-C(3B)	-57.8(4)
C(6B)-C(1B)-C(9B)-C(8B)	16.0(3)
C(6B)-C(7B)-C(8B)-O(1B)	-173.1(3)
C(6B)-C(7B)-C(8B)-C(9B)	8.2(3)
C(6B)-C(7B)-C(14B)-C(15B)	57.4(5)
C(6B)-C(7B)-C(14B)-C(16B)	-122.1(3)
C(7B)-C(8B)-C(9B)-C(1B)	-15.4(3)
C(7B)-C(14B)-C(16B)-C(17B)	63.7(4)
C(8B)-C(7B)-C(14B)-C(15B)	-126.9(3)
C(8B)-C(7B)-C(14B)-C(16B)	53.6(4)
C(9B)-C(1B)-C(2B)-C(3B)	-172.3(3)
C(9B)-C(1B)-C(6B)-C(5B)	165.5(3)
C(9B)-C(1B)-C(6B)-C(7B)	-12.3(4)
C(10B)-C(1B)-C(2B)-C(3B)	62.1(4)
C(10B)-C(1B)-C(6B)-C(5B)	-78.8(4)
C(10B)-C(1B)-C(6B)-C(7B)	103.4(3)
C(10B)-C(1B)-C(9B)-C(8B)	-99.9(3)
C(11B)-C(4B)-C(5B)-C(6B)	179.9(3)
C(14B)-C(7B)-C(8B)-O(1B)	10.4(5)
C(14B)-C(7B)-C(8B)-C(9B)	-168.3(3)
C(14B)-C(16B)-C(17B)-N(1B)	38.7(4)
C(14B)-C(16B)-C(17B)-C(18B)	-80.3(3)
C(14B)-C(16B)-C(17B)-C(19B)	159.9(3)
C(15B)-C(14B)-C(16B)-C(17B)	-115.8(3)
C(17B)-N(1B)-C(20B)-O(2B)	3.0(5)
C(17B)-N(1B)-C(20B)-O(3B)	-177.3(3)
C(20B)-O(3B)-C(21B)-C(22B)	178.2(3)
C(20B)-O(3B)-C(21B)-C(23B)	-64.9(3)
C(20B)-O(3B)-C(21B)-C(24B)	60.5(4)
C(20B)-N(1B)-C(17B)-C(16B)	57.1(4)

Table A4.1.7. cont'd

C(20B)-N(1B)-C(17B)-C(18B)	179.1(3)
C(20B)-N(1B)-C(17B)-C(19B)	-63.4(4)
C(21B)-O(3B)-C(20B)-O(2B)	-0.1(4)
C(21B)-O(3B)-C(20B)-N(1B)	-179.8(2)

Symmetry transformations used to generate equivalent atoms:

Table A4.1.8. Hydrogen Bonds for Triene **401** [\AA and $^\circ$].

D-H...A	d(D-H)	d(H...A)	d(D...A)	\angle (DHA)
N(1)-H(1)...O(1B)#1	0.88	2.18	3.054(4)	170.5
N(1B)-H(1B)...O(1)	0.88	2.16	3.032(4)	171.0

Symmetry transformations used to generate equivalent atoms:

#1 x,y,z+1

A4.2 NOTES AND REFERENCES

1. Sheldrick, G. M. *Acta Cryst.* **1990**, A46, 467–473.
2. Sheldrick, G. M. *Acta Cryst.* **2008**, A64, 112–122.
3. Müller, P. *Crystallography Reviews* **2009**, 15, 57–83.

CHAPTER 4

Progress Toward the Total Synthesis

of Scabrolide A[†]

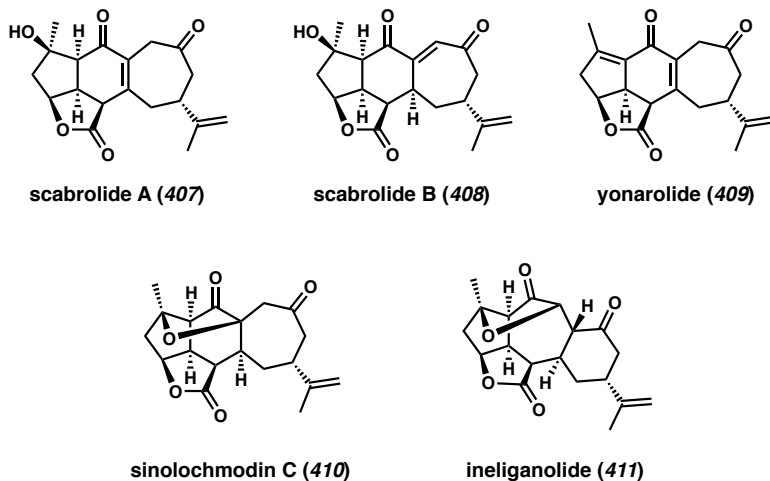
4.1 INTRODUCTION

Throughout history, natural products have played an integral role in the development of new medicines.¹ These products have been used to treat a number of different ailments including cancer, pain, and infectious bacteria.² Despite the numerous medical advances attributed to natural products, there remains a need for new and more effective therapies for the treatment of diseases. The norcembranoid class of natural products is a vast family of highly oxygenated diterpenoids, some of which display biological activity including antileukemic and anti-inflammatory activity of IL-6.³ While the polycyclic norcembranoids have been known since 1975,⁴ there has only been one reported de novo synthesis of any norcembranoid diterpenoid, Pavidolide B, by Yang and coworkers.⁵ The lack of completed total syntheses of this family of natural products is a testament to the inherent synthetic challenges that are associated with their highly congested structures. Some examples of the polycyclic norcembranoids are scabrolide A (**407**), scabrolide B (**408**), yonarolide (**409**), sinolochmodin C (**410**), and ineleganolide

[†] This research was performed in collaboration with Dr. Beau Pritchett, Chris Reimann, and Nick Hafeman

(**411**) (Figure 4.1.1). All except ineleganolide consist of a [5,5,6,7]-tetracyclic core containing a high degree of oxygenation and 4–7 stereocenters. We are drawn to the unique scaffold of these norcembranoid diterpenoids and sought to design a convergent synthesis of late-stage intermediate **412** which would allow for divergent access to a number of the norcembranoid diterpenoids including **407**, **408**, **409**, and **410**.

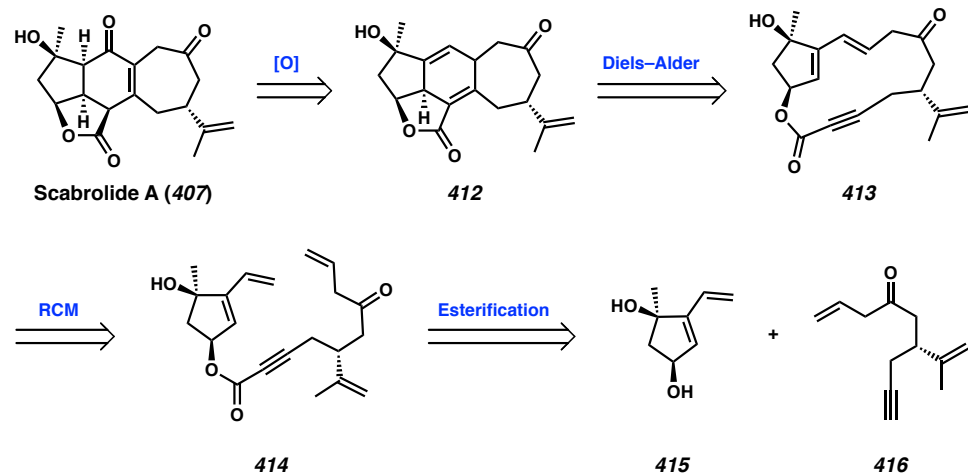
Figure 4.1.1. Select Examples of Polycyclic Furanobutenolide-Derived Norcembranoid Diterpenes



4.2 RETROSYNTHETIC ANALYSIS; TRANSANNULAR DIELS–ALDER

From a retrosynthetic perspective, we believed that construction of scabrolide A (**407**), can be achieved through the oxidation and olefin isomerization of 1,6-hexadiene **412** (Scheme 4.2.1). The central cyclohexadiene ring in **412** may be generated from an intramolecular Diels–Alder reaction of macrocycle **413** in order to form the core carbon skeleton. Ring-closing metathesis (RCM) of tetraene **414** would allow access to requisite macrocycle **413**. Finally, tetraene **414** can be convergently synthesized from the coupling of alkyne **416** and cyclopentene diol **415**.

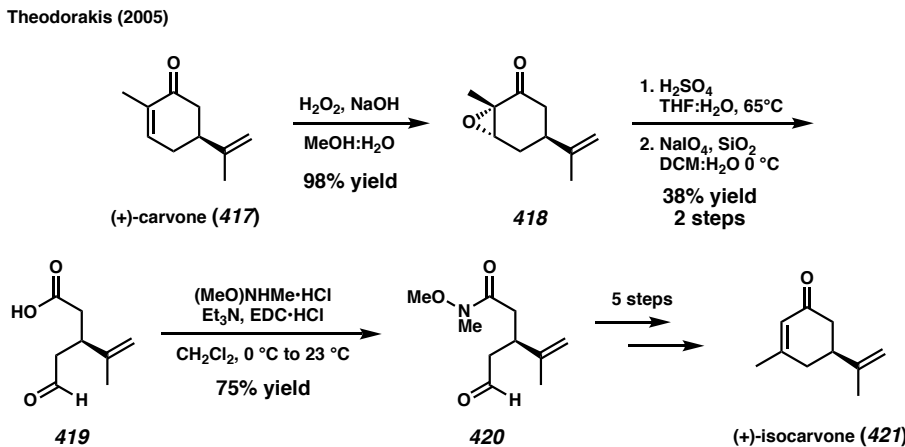
Scheme 4.2.1. Retrosynthetic Analysis of Scabrolide A via Transannular Diels–Alder



4.3 SYNTHESIS OF CONVERGENT COUPLING FRAGMENTS

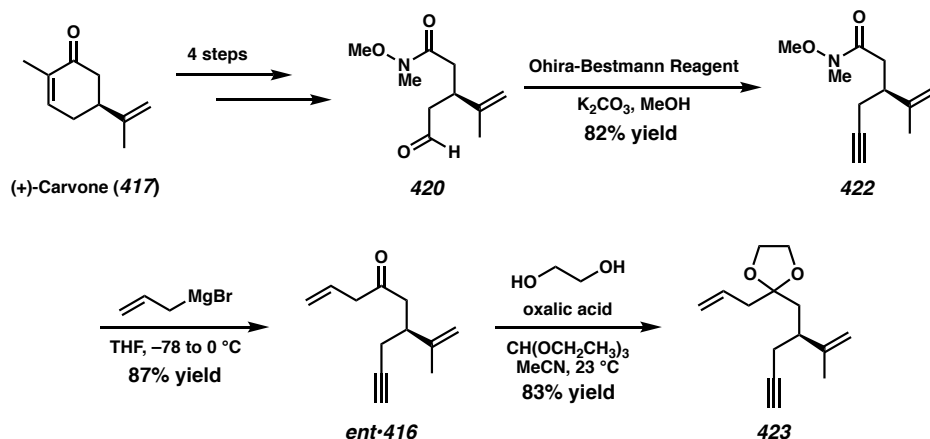
In 2005, Theodorakis and coworkers reported the synthesis of isocarvone (421) from carvone (417).⁶ Starting from (+)-carvone (417), they were able to perform a nucleophilic epoxidation with hydrogen peroxide to generate epoxy ketone 418 (Scheme 4.3.1). Epoxide 418 is then hydrolyzed followed by oxidative cleavage with NaIO₄ to afford acid 419 in a modest yield. Amidation of acid 419 with methoxy methylamine generates Weinreb amide 420 can be progressed to isocarvone in 5 further steps.

Scheme 4.3.1. Synthesis of Isocarvone From Carvone



By utilizing Theodorakis' key Weinreb amide intermediate (**420**), we can expediently synthesize alkyne **ent•416** with the isopropenyl stereocenter set (Scheme 4.3.2). Treatment of aldehyde **420** with the Ohira–Bestmann reagent furnishes alkyne **422**,⁷ which upon addition of allyl magnesium bromide affords our desired ketone **ent•416** in a 71% yield over 2 steps. Unfortunately, protection of the ketone moiety is necessary to couple **ent•416** with diol **415**, in order to avoid competing enolate formation and subsequent olefin isomerization during the carboxylation. Gratifyingly, treatment of ketone **ent•416** with ethylene glycol and anhydrous oxalic acid in triethylorthoformate and acetonitrile affords 1,3-dioxolane **423** in 83% yield and without any observable olefin isomerization.⁸

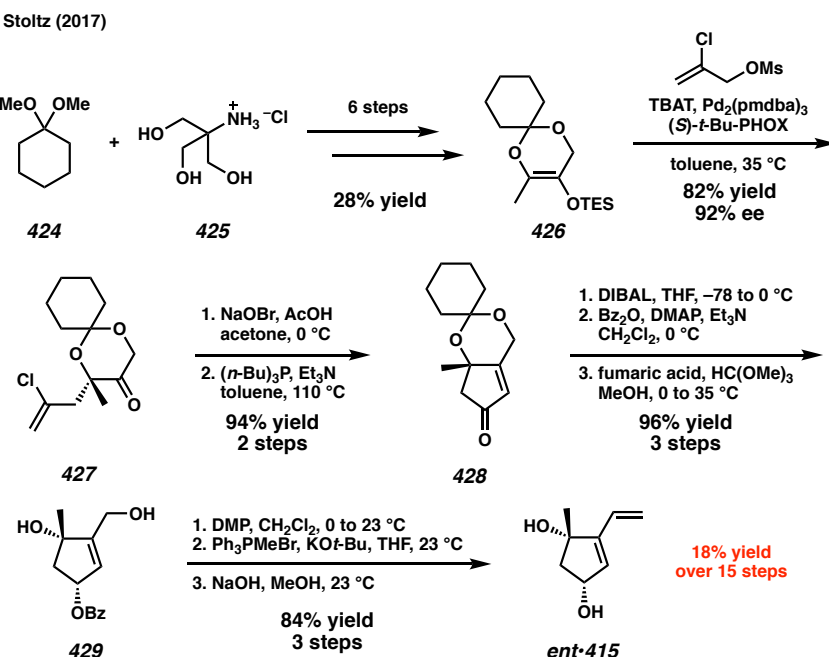
Scheme 4.3.2. Synthesis of Alkyne **423** from Carvone



Fortunately in 2017, our lab reported the utility of the key cyclopentene diol **ent•415** in a convergent synthesis of ineleganoloids.⁹ The first generation enantioselective synthesis of diol **ent•415** starts from dimethyl ketal **424** and TRIS•HCl (**425**) through a 6 step sequence (28% yield) to generate silyl enol ether **426** (Scheme 4.3.3). Silyl enol ether **426** then undergoes an asymmetric allylic alkylation, setting the tertiary stereocenter of **427** in 92% ee. The 2-chloroallyl moiety is then oxidized to the α -bromo ketone followed

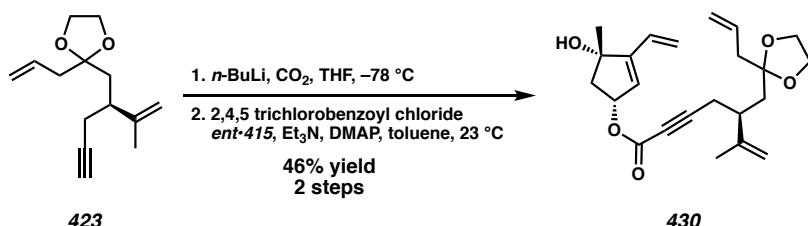
by an aldol condensation to afford enone **428**. Ketone **428** is then subjected to a 1,2 reduction, benzoyl protection, and acetonide cleavage to provide triol **429**, in an excellent yield over three steps. DMP oxidation of the primary alcohol, followed by Wittig olefination and benzoyl deprotection affords the desired diol **ent•415** in a 15 step sequence and 18% overall yield.

*Scheme 4.3.3. 1st Generation Synthesis of Cyclopentene Diol **ent•415***

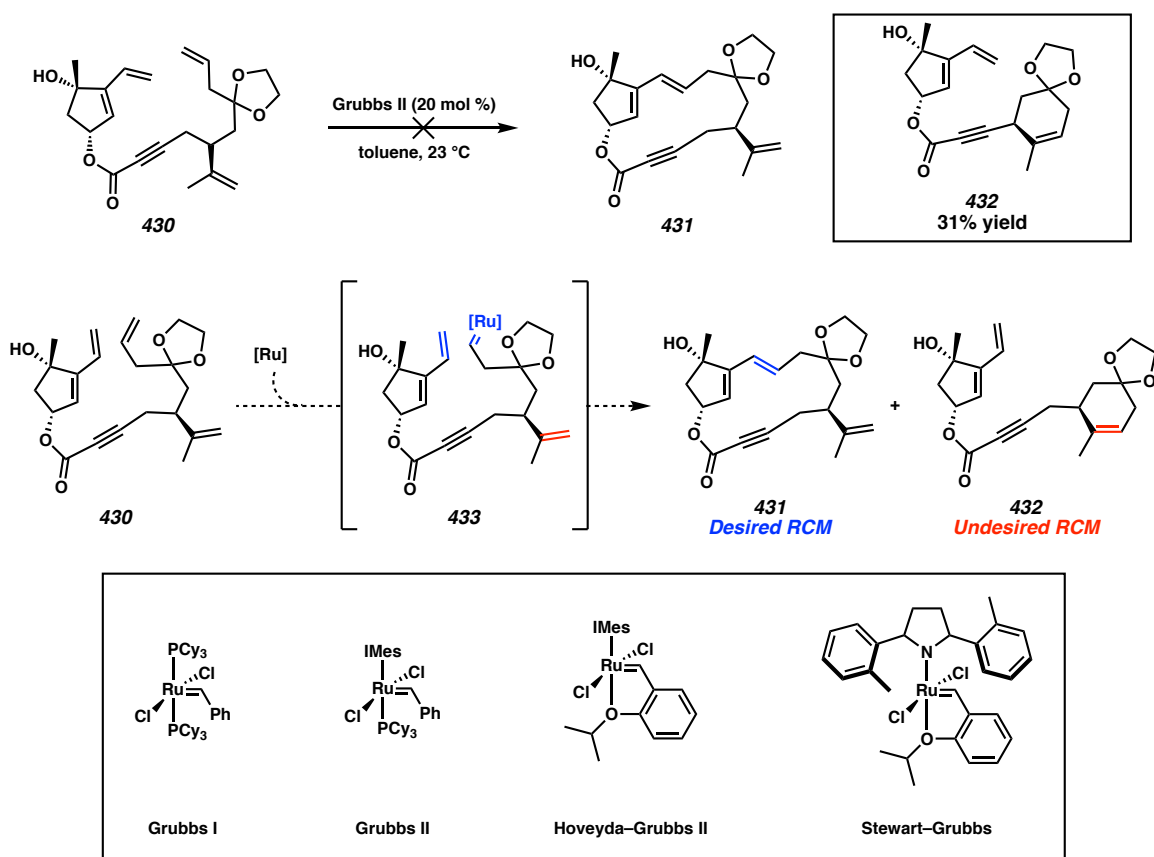


4.4 FRAGMENT COUPLING AND RING CLOSING METATHESIS

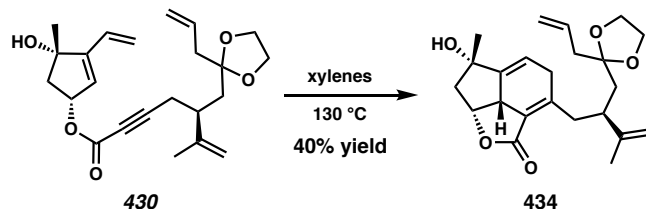
Having successfully synthesized both fragments **ent•415** and **423**, we turned our attention to investigating the coupling of these two compounds to form macrocycle **430**. Carboxylation of alkyne **423** was performed followed by Yamaguchi esterification with diol **ent•415** to afford our desired RCM substrate, ester **430** (Scheme 4.4.1).¹⁰

Scheme 4.4.1. Convergent Coupling of RCM Precursor **430**

We anticipated that the RCM of tetraene **430** would be challenging due to the presence of 3 terminal olefins, a diene, and an ynoate moiety. We Subjected tetraene **430** to a variety of RCM catalysts (e.g. Grubbs I, Grubbs II, Hoveyda-Grubbs II, and Stewart-Grubbs), solvent, and temperatures, but unfortunately no desired RCM was observed (i.e. **431**, Scheme 4.4.2). Instead, cyclohexenone **432** is observed as the sole product. We suspect this selectivity problem arises from the fact that the catalyst preferentially inserts into the most accessible olefin, as is common with Ru-based catalysts.¹¹ Although both the diene and allyl moieties possess mono-substituted olefins, the vinyl diene is electronically deactivated through conjugation. Therefore, the allyl group is the preferred initial site of metathesis in order to form Ru carbenoid **433**. Carbenoid **433** then undergoes olefin metathesis with the undesired *isopropenyl* fragment to form cyclohexene **432**. Due to these factors, we presumed that controlling the site selectivity for the initial insertion of the Ru catalyst will be crucial to the success to the RCM. Relay ring-closing metathesis (RRCM) offers an appealing solution to this challenge. Initially disclosed by Hoye and coworkers,¹² RRCM has been shown to overcome inherent selectivity bias as well as to allow traditionally inert olefins such as dienes to react smoothly under standard RCM conditions. Unfortunately, any attempt to direct Rh insertion into the diene moiety preferentially failed, and we observed either no reaction or the removal of the relay handle.

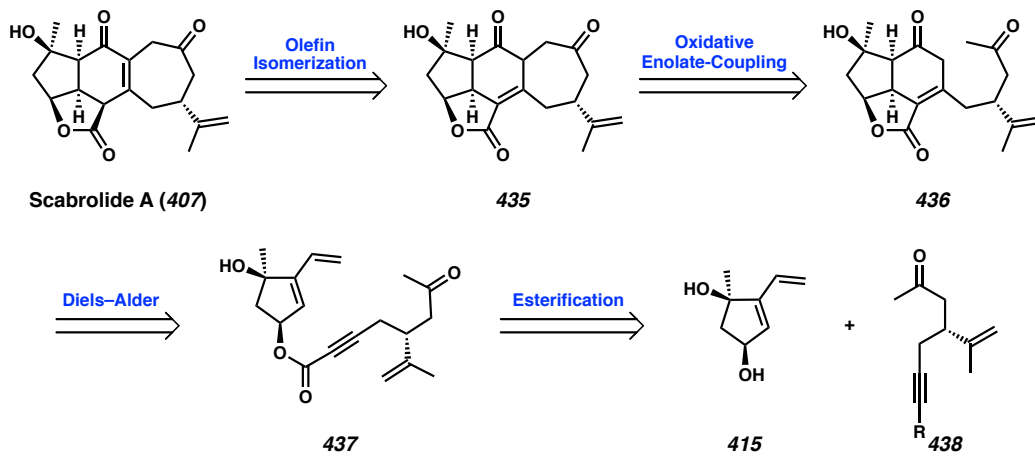
Scheme 4.4.2. Ring-Closing Metathesis of Ester **430**

Even though we have yet to successfully perform the desired RCM to generate macrocycle **431**, obtaining these late-stage intermediates allowed us to test whether an intramolecular Diels–Alder reaction would be able to generate the central cyclohexane ring of the norcembranoid diterpenes. Indeed, heating ester **430** at 130 °C in xylenes furnished the desired intramolecular Diels–Alder product **434** in an unoptimized 40% yield (Scheme 4.4.3).

Scheme 4.4.3. Intramolecular Diels–Alder of Ester **430**

4.5 RETROSYNTHETIC ANALYSIS; OXIDATIVE ENOLATE COUPLING

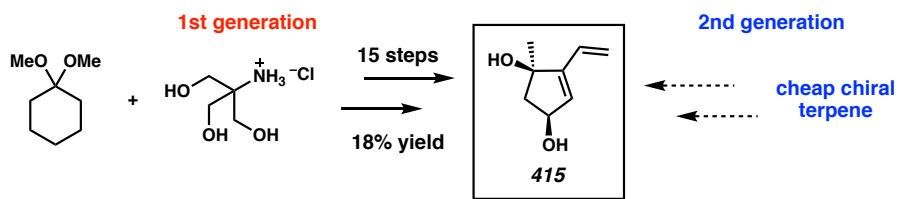
The potential challenges associated with the late stage RCM have incentivized the formulation an alternative retrosynthetic analysis. Thus, scabrolide A (**407**), can arise from the olefin isomerization of **435**, which itself may be generated from an intramolecular oxidative enolate coupling of **436** (Scheme 4.5.1). Tricycle **436** may arise from the oxidation of the intramolecular Diels–Alder reaction of diene **437**, which will be formed from the convergent esterification of the previous diol fragment **415** and methyl ketone **438**.

Scheme 4.5.1. 2nd Generation Retrosynthetic Analysis of Scabrolide A

At this time we also were interested in developing a second generation synthesis of diol **415**. The first generation route hinged upon the previously developed asymmetric allylic alkylation in the Stoltz lab to obtain the desired diol in a high 92% ee but required

15 steps and afforded an 18% overall yield of the desired product (Scheme 4.5.2). We believed that by taking advantage of readily available chiral terpenes, we would be able to not only decrease the number of synthetic steps and increase the yield, but also obtain the diol product enantiopure.

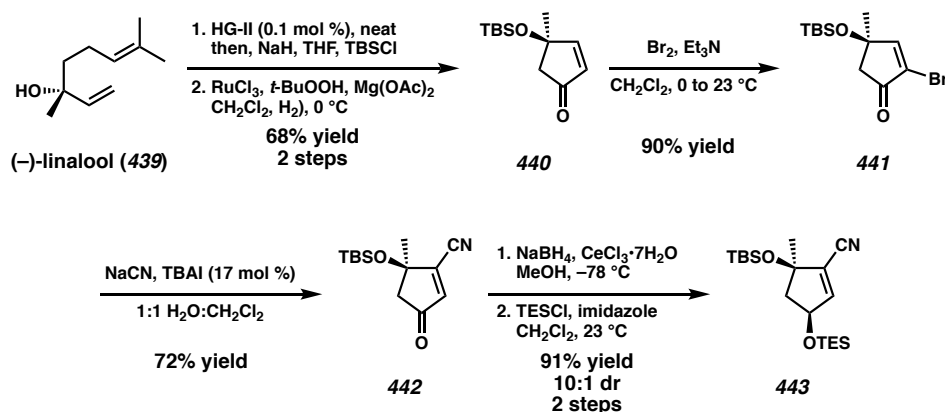
Scheme 4.5.2. Development of Modified Synthesis of Diol 415



4.6 SECOND GENERATION SYNTHESIS OF THE CYCLOPENTENE DIOL FRAGMENT

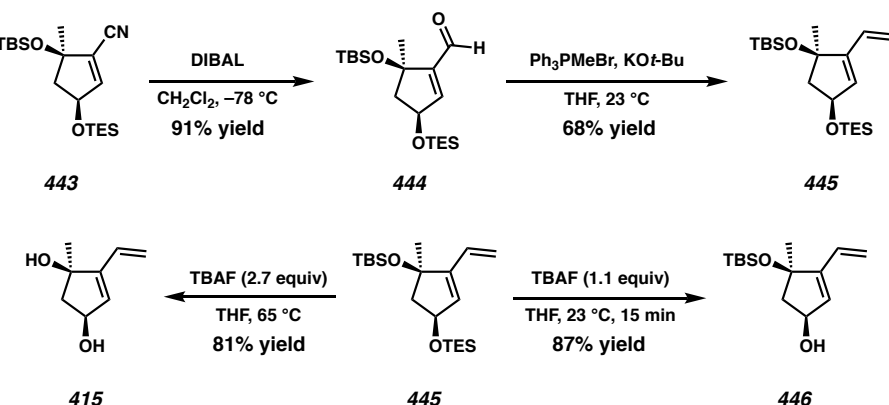
In 2016, Maimone and coworkers disclosed the enantioselective synthesis of ophiobolin N, and showed that commercially available (–)-linalool can afford cyclopentenone **440** in a two-step sequence.¹³ Linalool (**339**) first undergoes an RCM with Hoveyda–Grubbs II and TBS protection of the tertiary alcohol followed by a RuCl₃-catalyzed allylic oxidation generates the desired enone **440** (Scheme 4.6.1). We believed enone **440** would allow rapid access to our desired diol **415**. α -Bromonation generates α -bromo enone **441**, allowing for tandem phase-transfer mediated sodium cyanide conjugate addition and halide elimination to afford vinylogous ketonitrile **442**.¹⁴ Unfortunately we observed low yields and diastereoselectivity upon double reduction of the nitrile and ketone moieties in **442**. Instead using a Luche reduction at low temperatures performs a diastereoselective reduction of the enone to the *syn*-diol, which can subsequently be TES-protected, generating diol **443**.

Scheme 4.6.1. Terpene-Derived Synthesis Toward Diol 415



After initial reduction and protection of enone 442, a reduction of nitrile 443 with DIBAL, affords enal 444 in excellent yield (Scheme 4.6.2). Enal 444 then undergoes a Wittig olefination to yield bis-protected diol 445. Due to the judicious choice of protecting groups, we next selectively deprotected the secondary alcohol in the presence of the tertiary to afford diene 446. Treating diol 445 with harsh deprotection conditions such as an excess of TBAF in refluxing THF, we can obtain the same cyclopentene diol 415 fragment as the first generation route. This second generation synthesis not only decreased the number of steps required from 15 to 9 but also increased the overall yield to 30%.

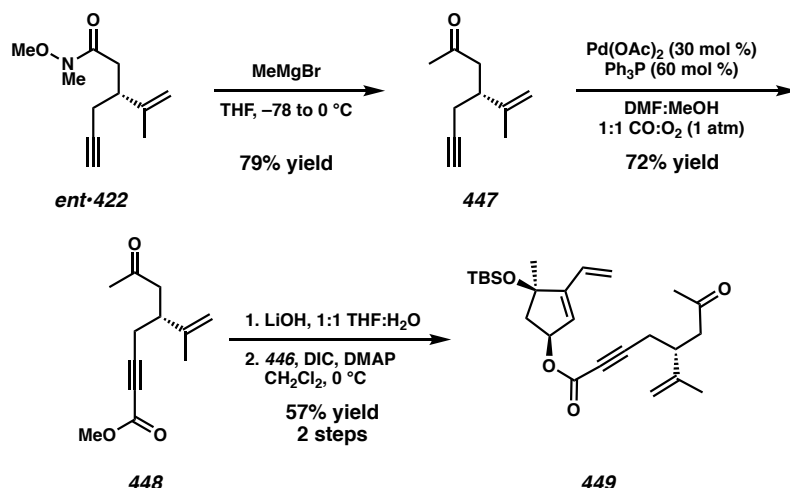
Scheme 4.6.2. Synthesis of Cyclopentene Diol 415



4.7 ALKyne SYNTHESIS AND FRAGMENT COUPLING

Alkyne **ent•422** was synthesized in 5 steps from (–)-carvone following previously described methods (Scheme 4.7.1). The Weinreb amide moiety was then monomethylated with methyl magnesium bromide to afford ketone **447**, which then undergoes a palladium-catalyzed oxidative carbonylation using one atmosphere of a 1:1 mixture of CO:O₂ in a methanol:DMF solution, affording methyl ester **448**.¹⁵ Saponification of ester **448** followed by Steglich esterification with DIC yields the Diels–Alder precursor **449**.

Scheme 4.7.1. Synthesis of Methyl Ketone Diels–Alder Precursor

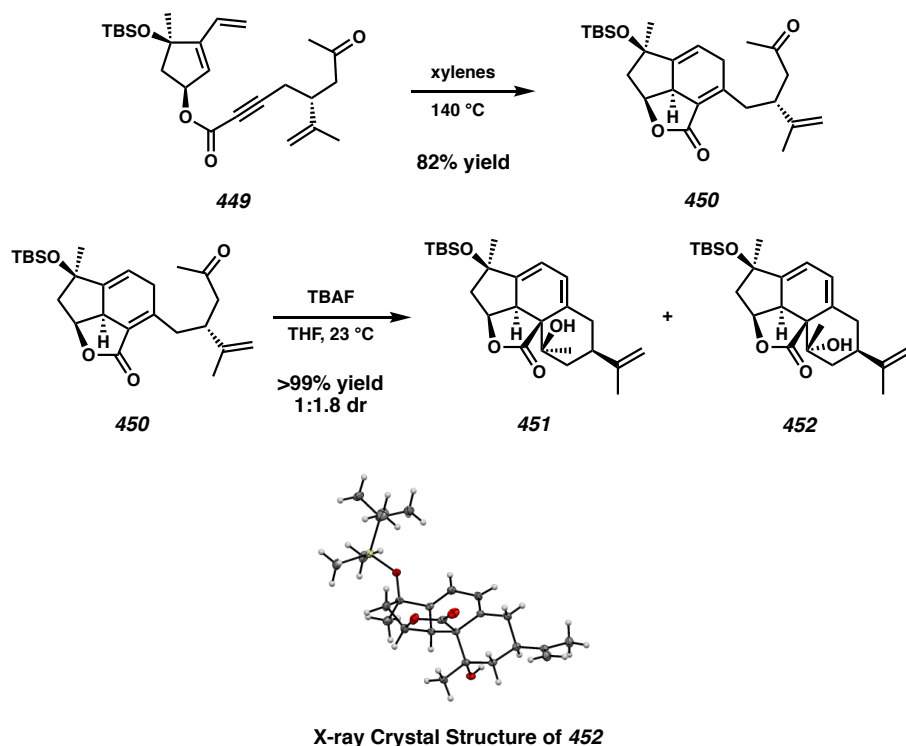


4.8 INTRAMOLECULAR DIELS–ALDER REACTION AND LATE-STAGE FUNCTIONALIZATION

Similar to tetraene **430**, heating triene **449** to 140 °C in rigorously degassed xylenes produces the desired Diels–Alder products as a single diastereomer (**450**) in excellent yield (75%, Scheme 4.8.1). Having synthesized 3 of the 4 rings of the carbocyclic core of scabrolide A, we intended to deprotect the tertiary alcohol of **450** in order to set the stage for a directed oxidation of the 1,4-cyclohexadiene moiety. Unfortunately, after subjecting tricycle **450** to TBAF, we observed spontaneous and quantitative conversion to tetracycle

451 and **452** as a mixture of diastereomers. Tricycle **450** and analogous compounds appear to be extremely sensitive to base, treatment with milder bases such as triethylamine at 0 °C still result in quantitative aldol reaction. Any attempt to functionalize, protect, or anneal the final ring onto tricycle **450** again resulted in the deleterious aldol product.

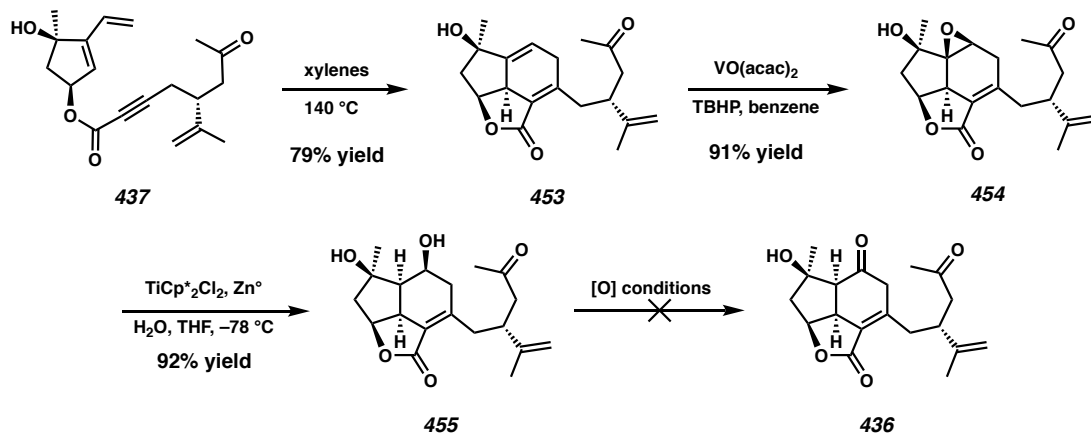
Scheme 4.8.1. Unexpected Aldol Condensation of Tricycle **450**



In order to avoid the problematic aldol reaction, double deprotection of the cyclopentene diol fragment is required prior to the requisite coupling and Diels–Alder reaction. Ester **437** successfully undergoes the Diels–Alder reaction at 140 °C in xylenes to afford tricycle **453** (Scheme 4.8.2). The free alcohol is now able to participate in a directed epoxidation utilizing vanadyl acetylacetone to generate the *syn*-epoxy alcohol **454** in an excellent 91% yield. Epoxide **454** can be selectively reduced to the 1,3 diol employing in situ-generated titanocene(III) chloride.^{9,16} With 1,3-diol **455** in hand, we

investigated possible oxidation conditions to obtain oxidative enolate coupling precursor **436**. Unfortunately we have yet to determine optimal conditions to effect the desired transformation. Basic oxidation conditions such as the Swern oxidation¹⁷ again resulted in an undesired aldol product. Neutral oxidations, such as the Ley oxidation¹⁸ and Stahl oxidation,¹⁹ afforded recovered starting material due to the large steric encumbrance posed by the caged tricyclic core. Moreover, acidic oxidation primarily resulted in decomposition. Ultimately we were unable to obtain sufficient quantities of enone **436** to investigate the oxidative enolate coupling, necessitating the development of a new retrosynthetic analysis.

*Scheme 4.8.2. Selective Oxidation of Deprotected Tricycle **437***

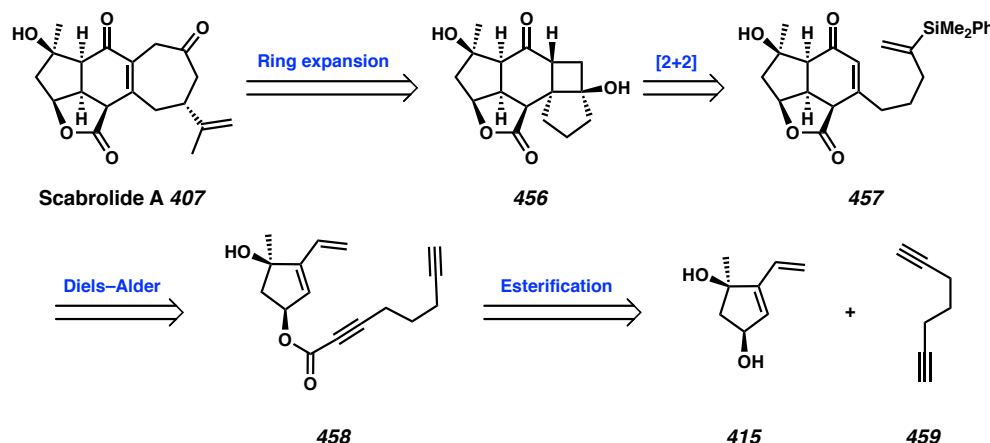


4.9 THIRD GENERATION RETROSYNTHETIC ANALYSIS; RING EXPANSION

Learning from our previous synthetic routes, direct construction of the 7-membered ring would likely require the avoidance of ketone functionalities on the carvone fragment in order to prevent the problematic aldol reaction. Retrosynthetically, we believed that using the inherent energy in a strained small membered ring would facilitate the synthesis of the cycloheptanone ring.²⁰ We believed this could be achieved by the ring fission of

cyclobutanol **456**, which itself can be formed through a photocatalytic [2+2] cycloaddition of enone **457** (Scheme 4.9.1). Tricycle **457** again can be synthesized through the redox manipulation of the Diels–Alder adduct of ester **458**. Finally, ester **458** can be convergently synthesized from diol **415** and diyne **459**.

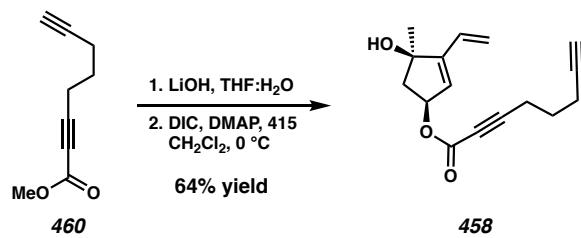
Scheme 4.9.1. 3rd Generation Retrosynthetic Analysis Utilizing Energy of a Strained Cyclobutane Ring



4.10 SYNTHESIS OF [2+2] PRECURSOR

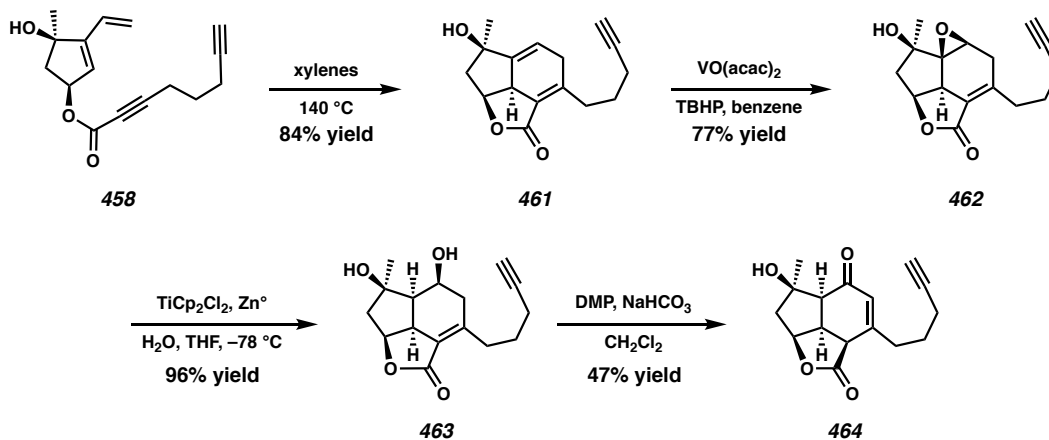
In order to provide more facile access to late stage material, a model system was constructed. Employing 1,6-heptadiyne as the starting material instead of carvone, we could rapidly access ester **460** in a single known step instead of 6 steps (Scheme 4.10.1).²¹ Ester **460** then undergoes saponification and Steglich esterification with diol **415** to afford the Diels–Alder precursor **458** efficiently and in excellent yield.

*Scheme 4.10.1. Convergent Esterification of Diol **415** and Ester **460***



Cyclization of ester **458** was again performed in xylenes at 140 °C to furnish the desired tricycle **461** (Scheme 4.10.2). By utilizing the double deprotected diol **415** instead of **446**, we can perform a directed epoxidation utilizing vanadyl acetylacetonate and TBHP to afford the *syn*-epoxy alcohol **462**. Epoxide **462** can be selectively opened using in situ-generated titanocene(III) chloride to form the *syn*-1,3 diol **463**, which upon treatment with DMP is oxidized to afford enone **464**, a moiety that strongly absorbs UV light at 350 nm.

*Scheme 4.10.2. Diels–Alder and Oxidation of Model System **458***

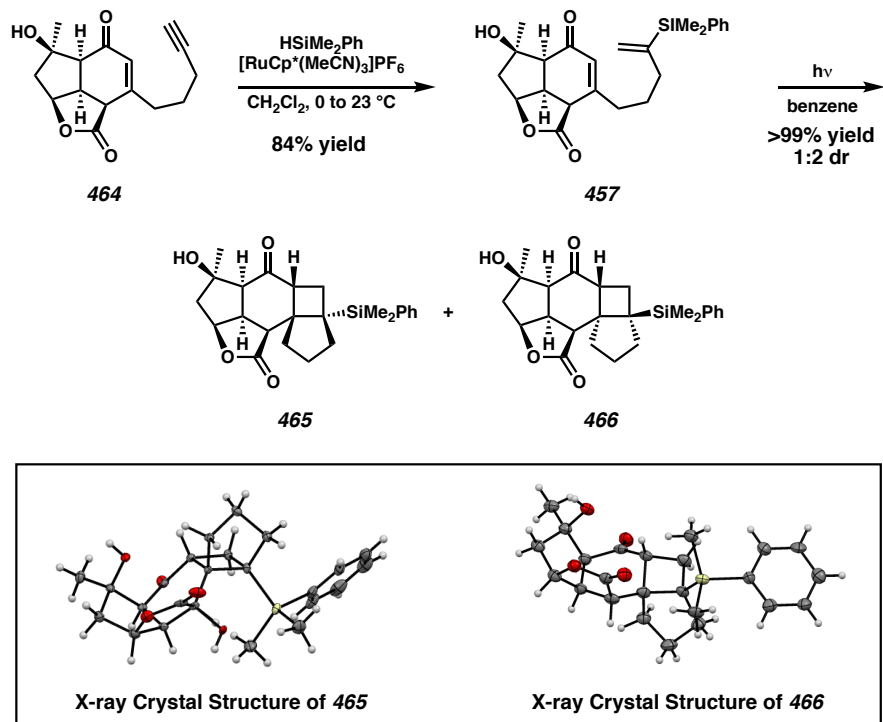


4.11

[2+2] PHOTOCYCLOADDITION AND RING EXPANSION

The successful installation of the enone moiety of tricycle **464** allowed us to perform the Markovnikov hydrosilylation using $\text{RuCp}^*(\text{MeCN})_3\text{PF}_6$ and dimethylphenylsilane (Scheme 4.11.1).²² While other hydrosilanes are competent in the hydrosilylation reaction,²³ the presence of an aryl group was paramount to the success of the subsequent Tamao–Fleming oxidation. [2+2] cyclization of enone **457**, affords a 2:1 mixture of diastereomers **465** and **466** in quantitative yield. The structures of **465** and **466** have both been confirmed by single crystal X-ray diffraction.

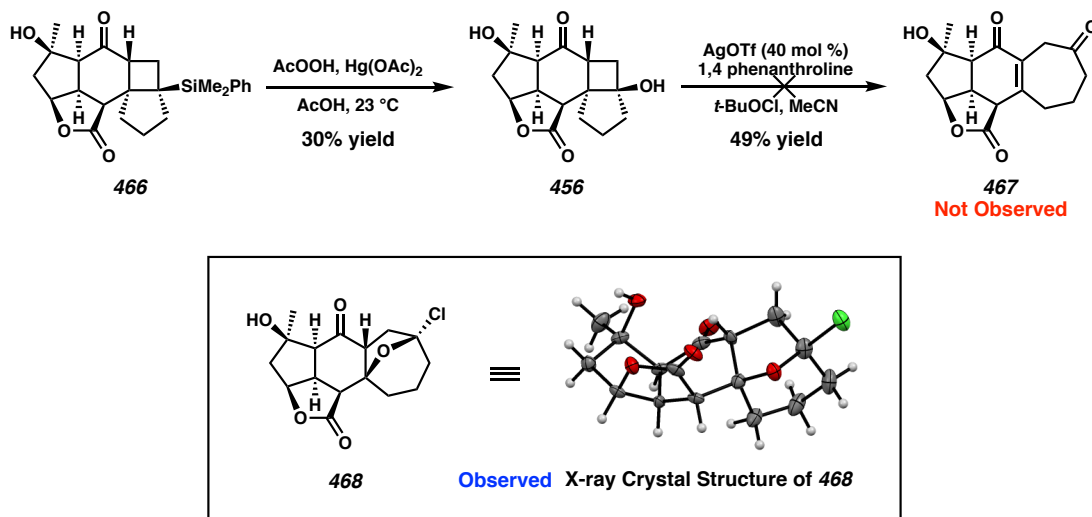
Scheme 4.11.1. [2+2] Cyclization of Enone 457



Oxidation of **466** using conditions developed by Fleming, using $\text{Hg}(\text{OAc})_2$ in peracetic acid generated the desired cyclobutanol **456** in moderate yield (30%, Scheme 4.11.2).²⁴ Interestingly only diastereomer **466** reacted under these oxidation conditions, while **465** required harsher conditions.²⁵ Finally, having synthesized cyclobutanol **456**, we focused our attention on the strain-release-driven ring expansion. Multiple attempts to form the hypoiodite of **456** in-situ followed by homolytic cleavage by thermal or photochemical means, resulted in either no reaction or decomposition.²⁶ Fortunately in 2016, Xhang and coworkers reported the AgOTf -catalyzed β -scission of cyclic alcohols to the corresponding chloroketone.²⁷ Subjecting cyclobutanol **456** to these reaction conditions (Scheme 4.11.2), we hoped to obtain the tetracyclic core of scabrolide A **467**, but unfortunately these conditions also failed to afford the expected product. Fortunately, concentration of this product in CDCl_3 provided a crystalline solid, from which we were able to obtain an X-ray

crystal structure. From this data we determined that the product of this reaction was actually furan **468**. Similar to expected tetracycle **467**, furan **468** possesses the key seven membered ring, thus completing the carbocyclic skeleton of scabrolide A.

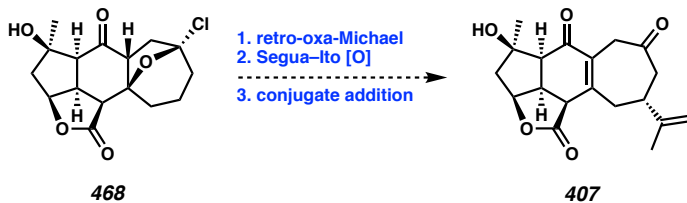
*Scheme 4.11.2. Ring Expansion of Cyclobutanol **466***



4.12 FUTURE DIRECTIONS

Having achieved the successful synthesis of the carbocyclic skeleton of scabrolide A through the use of the ring expansion of a four-membered ring on model system **458**, we can now focus on the late-stage functionalization to complete the total synthesis. Currently we envision furan **468** to undergo a retro-oxa-Michael reaction to afford cycloheptenone followed by selective enolization, Segusa–Ito oxidation, and diastereoselective conjugate addition of *isopropenyl* organometallic to complete the synthesis of scabrolide A (Scheme 4.12.1). If derivatization of model system **458** fails it may be possible to synthesize the carvone fragment with the *isopropenyl* fragment already installed. Early introduction of the *isopropenyl* stereocenter removes the need for late-stage functionalize of tetracycle **468** and only requires a retro-oxa-Michael reaction to complete the synthesis.

Scheme. 4.12.1. Future Directions Toward the Completion of Scabrolide A



4.13 CONCLUSION

We have reported significant progress toward the total synthesis of scabrolide A. A key ring expansion of a strained small ring allowed for the synthesis of the [5,5,6,7] tetracyclic core in an expedient 16 steps (longest linear) from known enone **440** and in an overall yield of 1.1 %. Current endeavors include early introduction of the *isopropenyl* fragment by adapting the carvone route yet again. Moreover we are also investigating the oxidation of furan **468** to allow for a diastereoselective conjugate addition of *isopropenyl* organometallic reagent, thus completing the synthesis of scabrolide A.

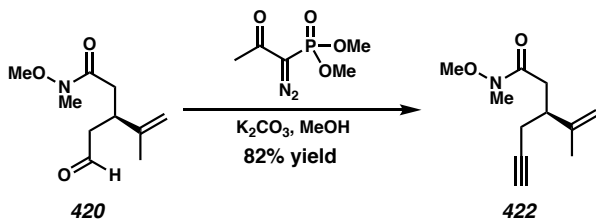
4.14 EXPERIMENTAL METHODS AND ANALYTICAL DATA

4.14.1 MATERIALS AND METHODS

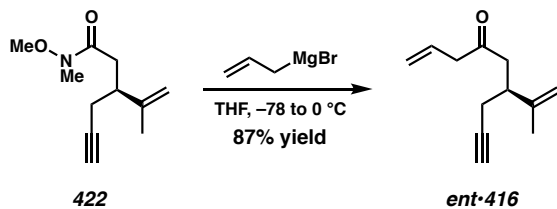
Unless stated otherwise, reactions were performed at ambient temperature (23 °C) in flame-dried or oven-dried glassware under an argon or nitrogen atmosphere using dry, deoxygenated solvents (distilled or passed over a column of activated alumina).²⁸ Commercially obtained reagents were used as received with the exception of [RuCp*(MeCN)₃]PF₆ and Ph₃PMeBr which were stored in a nitrogen-filled glovebox. Triethylamine (Et₃N) was distilled over potassium hydride prior to use. Dess–Martin periodinane²⁹ were prepared by known methods. Reactions requiring external heat were modulated to the specified temperatures using an IKAmag temperature controller. Reaction progress was monitored by thin-layer chromatography (TLC), which was performed using

E. Merck silica gel 60 F254 precoated glass plated (0.25 mm) and visualized by UV fluorescence quenching, potassium permanganate, *p*-anisaldehyde, or iodine staining. Silicycle SiliaFlash® P60 Academic Silica gel (particle size 40-63 nm) was used for column chromatography. ¹H and ¹³C NMR spectra were recorded on a Varian Inova 500 (500 MHz and 126 MHz, respectively), Varian Mercury 300 spectrometer (300 MHz and 75 MHz, respectively), Varian 600 MHz Spectrometer (600 MHz), and a Bruker AV III HD spectrometer equipped with a Prodigy liquid nitrogen temperature cryoprobe (400 MHz and 101 MHz, respectively) and are reported in terms of chemical shift relative to CHCl₃ (δ 7.26 and δ 77.16, respectively) and C₆H₆ (δ 7.16 and δ 128.4 respectively). Data for ¹H NMR are reported as follows: chemical shift (δ ppm) (multiplicity, coupling constant (Hz), integration). Multiplicities are reported as follows: s = singlet, d = doublet, t = triplet, q = quartet, p = pentet, sext = sextet, sept = septet, m = multiplet, and br s = broad singlet. Infrared (IR) spectra were recorded on a Perkin Elmer Paragon 1000 spectrometer using thin films deposited on NaCl plates and are reported in frequency of absorption (cm⁻¹). Optical rotations were measured with a Jasco P-2000 polarimeter operating on the sodium D-line (589 nm), using a 100-mm path-length cell and are reported as: [α]_D^T (concentration in g/100 mL, solvent). High resolution mass spectra were obtained from the Caltech Mass Spectral Facility using a JEOL JMS-600H High Resolution Mass Spectrometer in fast atom bombardment (FAB+) ionization mode or a Agilent 6200 Series TOF with an Agilent G1978A Multimode source in electrospray ionization (ESI+), atmospheric pressure chemical ionization (APCI+), or mixed (ESI/APCI) ionization mode.

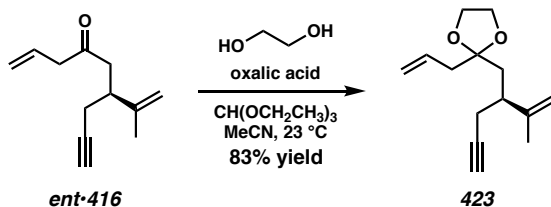
4.14.2 EXPERIMENTAL PROCEDURES



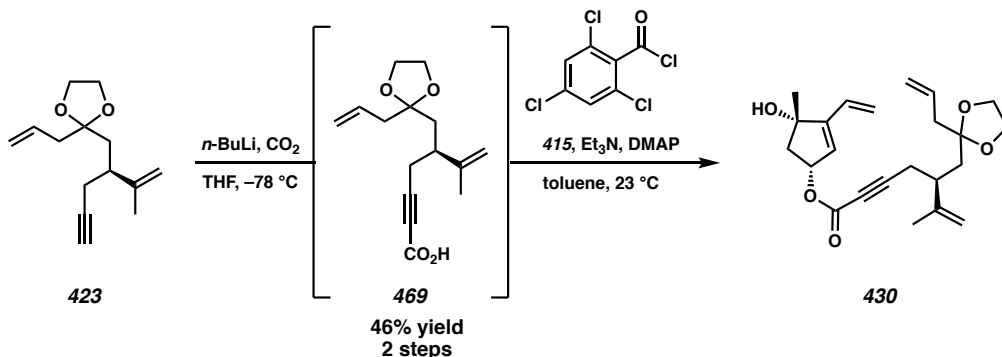
(S)-N-methoxy-N-methyl-3-(prop-1-en-2-yl)hex-5-ynamide (422): In a round-bottom flask, known aldehyde **420** (6.27 g, 31.5 mmol, 1.0 equiv) and K_2CO_3 (8.7 g, 62.9 mmol, 2.0 equiv) was diluted with dry methanol (52.5 mL, 0.6 M) and cooled to 0 °C (ice/water bath). Neat Ohira–Bestmann reagent (7.25 g, 37.8 mmol, 1.2 equiv) was added dropwise via syringe and the resultant solution was allowed to stir for 12 h and warm to ambient temperature (23 °C). Upon complete consumption of starting material (determined by TLC analysis, 9:1 $\text{CH}_2\text{Cl}_2:\text{EtOAc}$), the reaction was diluted with Et_2O and washed with a saturated solution of NaHCO_3 . The organic layer was dried over Na_2SO_4 , filtered, and concentrated in vacuo. The crude product was purified by flash chromatography (SiO_2 , 9:1 $\text{CH}_2\text{Cl}_2:\text{EtOAc}$) to generate alkyne **422** (5.0 g, 82% yield) as a pale yellow oil; $R_f = 0.71$ (9:1 $\text{CH}_2\text{Cl}_2:\text{EtOAc}$); ^1H NMR (500 MHz, CDCl_3) δ 4.85 (p, $J = 1.5$ Hz, 1H), 4.82 (dp, $J = 1.7, 0.9$ Hz, 1H), 3.70 (s, 3H), 3.17 (s, 3H), 2.92–2.82 (m, 1H), 2.76–2.60 (m, 2H), 2.38 (ddd, $J = 6.4, 3.5, 2.7$ Hz, 2H), 1.99 (t, $J = 2.7$ Hz, 1H), 1.77 (dd, $J = 1.6, 0.8$ Hz, 3H); ^{13}C NMR (126 MHz, CDCl_3) δ 173.0, 146.2, 111.6, 82.4, 69.9, 61.3, 40.8, 34.8, 32.2, 23.0, 20.7; IR (thin film, NaCl) 3293, 3250, 3076, 2967, 2938, 2820, 2116, 1661, 1430, 1384, 1334, 1175, 1175, 1108, 1002, 936, 894 cm^{-1} ; HRMS (ES/APCI) m/z calc'd $\text{C}_{11}\text{H}_{18}\text{O}_2\text{N}$ [M+H]⁺: 196.1332, found: 196.1336.



(S)-6-(prop-1-en-2-yl)non-1-en-8-yn-4-one *ent*•416: In a flame dried round bottom flask, amide **422** (50 mg, 0.26 mmol, 1.0 equiv) was dissolved in THF (0.8 mL, 0.3 M) and cooled to $-78\text{ }^{\circ}\text{C}$. Allyl magnesium bromide (0.52 mL, 0.52 mmol, 1.0 M, 2.0 equiv) was added dropwise to the reaction solution. The reaction was allowed to stir for 15 min at $-78\text{ }^{\circ}\text{C}$ and then warmed to $0\text{ }^{\circ}\text{C}$ and stirred for 16 h. Upon complete consumption of starting material (determined by TLC analysis, 9:1 hexanes:Et₂O), the reaction was quenched with a saturated solution of NH₄Cl and the product was extracted from the biphasic mixture with Et₂O (3 x 10 mL). The combined organic layers were washed with brine, dried over MgSO₄, filtered, and concentrated in vacuo. The crude product was purified by flash chromatography (SiO₂, 9:1 hexanes:Et₂O) to generate alkyne **ent**•416 (39 mg, 87% yield) as a pale yellow oil; ¹H NMR (500 MHz, CDCl₃) δ 5.91 (ddt, *J* = 17.2, 10.2, 7.0 Hz, 1H), 5.18 (dq, *J* = 10.2, 1.3 Hz, 1H), 5.14 (dq, *J* = 17.1, 1.5 Hz, 1H), 4.82 (p, *J* = 1.5 Hz, 1H), 4.78 (dt, *J* = 1.5, 0.8 Hz, 1H), 3.18 (dt, *J* = 6.9, 1.4 Hz, 2H), 2.86–2.77 (m, 1H), 2.74 (dd, *J* = 16.7, 6.6 Hz, 1H), 2.62 (dd, *J* = 16.7, 7.4 Hz, 1H), 2.32 (ddd, *J* = 14.5, 6.5, 2.7 Hz, 2H), 1.99 (t, *J* = 2.7 Hz, 1H), 1.73 (dd, *J* = 1.5, 0.8 Hz, 3H); ¹³C NMR (126 MHz, CDCl₃) δ 207.3, 145.9, 130.52, 119.1, 111.8, 82.2, 70.3, 48.2, 45.1, 40.2, 23.0, 20.7; IR (thin film, NaCl) 3297, 3078, 2969, 2917, 2117, 1715, 1646, 1430, 1376, 993, 920, 895 cm⁻¹; HRMS (ESI) m/z calc'd C₁₂H₁₆O [M⁺]: 176.1201, found: 176.1191. $[\alpha]_D^{25} - 24.90$ (*c* 3.7, CDCl₃).



(S)-2-allyl-2-(2-(prop-1-en-2-yl)pent-4-yn-1-yl)-1,3-dioxolane (423): Dried oxalic acid (109 mg, 1.2 mmol, 8.5 equiv) was dissolved in a solution of ethylene glycol (0.27 mL, 4.69 mmol, 33 equiv), triethyl orthoformate (0.14 mL, 0.85 mmol, 6 equiv), and MeCN (1.95 mL, 0.073 M). After complete dissolution of the oxalic acid, ketone **ent•416** (25 mg, 0.14 mmol, 1 equiv) was added. The reaction was sealed and allowed to stir at ambient temperature (23 °C) for 36 h. Upon complete consumption of starting material (as determined by TLC analysis, 4:1 hexanes: Et₂O), the reaction was diluted with H₂O and the product was extracted with Et₂O (3 x 5 mL). The combined organic layers were washed with brine, dried with MgSO₄, filtered, and concentrated in vacuo. The crude product was purified by flash chromatography (SiO₂, 4:1 hexanes:Et₂O) to afford dioxolane **423** (26 mg, 83% yield) as a pale yellow oil (R_f = 0.68, 4:1 hexanes:EtOAc); ¹H NMR (400 MHz, CDCl₃) δ = 5.81 (ddt, J = 16.9, 10.5, 7.2 Hz, 1H), 5.12 (ddt, J = 8.2, 2.2, 1.3 Hz, 1H), 5.08 (t, J = 1.3 Hz, 1H), 4.79 (q, J = 1.3 Hz, 2H), 3.94 (q, J = 1.3 Hz, 4H), 2.52 (dq, J = 8.2, 6.3 Hz, 1H), 2.43–2.34 (m, 3H), 2.26 (ddd, J = 16.7, 8.1, 2.7 Hz, 1H), 1.97 (t, J = 2.6 Hz, 1H), 1.83 (d, J = 6.5 Hz, 2H), 1.70 (t, J = 1.2 Hz, 3H); ¹³C NMR (101 MHz, CDCl₃) δ = 147.5, 133.3, 118.4, 111.4, 110.8, 83.3, 69.4, 65.0, 65.0, 42.5, 41.3, 39.2, 24.1, 19.2; IR (thin film, NaCl) 3302, 3075, 2949, 2888, 2117, 1643, 1433, 1374, 1311, 1124, 1100, 996, 918, 890, 862, 837, 635 cm⁻¹; HRMS (FAB⁺) m/z calc'd C₁₄H₂₁O₂ [M+H]⁺: 221.1536, found: 221.1531; $[\alpha]_{23}^D$ = -2.45 (c = 0.79, CHCl₃).

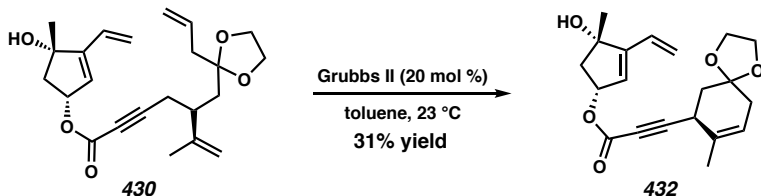


(1*R*,4*S*)-4-hydroxy-4-methyl-3-vinylcyclopent-2-en-1-yl (*S*)-5-((2-allyl-1,3-dioxolan-2-yl)methyl)-6-methylhept-6-en-2-yneate (430):

Dioxolane **423** (95 mg, 0.43 mmol, 1 equiv) was dissolved in THF (4.3 mL, 0.1 M) and cooled –78 °C. The solution was allowed to stir for 5 min followed by the addition powdered dry ice (0.56 g, 1.3 g/mmol of **423**). After 10 min, the reaction was quenched with a saturated solution of NH₄Cl and was allowed to warm to ambient temperature (23°C). The solution was acidified with a 5% solution of citric acid (5 mL) and the product was extracted with EtOAc (5 x 15 mL). The combined organic layers were dried over MgSO₄, filtered, and concentrated in vacuo. The crude product **469** (103 mg, 93%) was used crude in the following reaction.

To a solution of acid **469** (58 mg, 0.22 mmol, 1.1 equiv) in THF (2 mL, 0.1 M), Et₃N (92 µL, 0.66 mmol, 3.3 equiv) and 2,4,6-trichlorobenzoyl chloride (34 µL, 0.22 mmol, 1.1 equiv) was added. The reaction was allowed to stir for 1 h followed by the addition of a THF solution (2 mL, 0.1 M) of diol **415** (28 mg, 0.2 M, 1 equiv) and DMAP (24 mg, 0.2 mmol, 1 equiv). The reaction was allowed to stir at ambient temperature (23 °C) until complete. Upon complete consumption of diol **415** (as determined by TLC analysis, 4:1 hexanes:EtOAc) the reaction was directly purified by column chromatography (SiO₂, 100% hexanes then 1:1 hexanes:EtOAc) to afford ester **430** (43 mg, 50%) as a yellow oil (*R*_f = 0.22); ¹H NMR (400 MHz, CDCl₃) δ 6.31 (dd, *J* = 17.8,

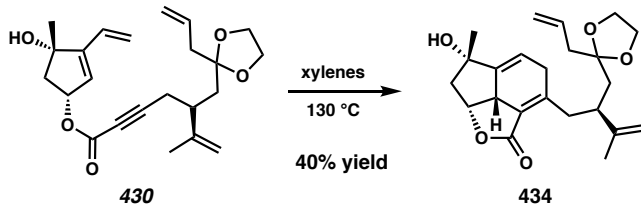
11.3 Hz, 1H), 5.87–5.73 (m, 3H), 5.53 (ddd, $J = 7.1, 4.5, 2.3$ Hz, 1H), 5.32 (dd, $J = 11.3, 1.6$ Hz, 1H), 5.16–5.10 (m, 1H), 5.08 (t, $J = 1.3$ Hz, 1H), 4.80 (d, $J = 1.2$ Hz, 2H), 3.94 (s, 4H), 2.65–2.53 (m, 3H), 2.45–2.39 (m, 1H), 2.36 (dq, $J = 6.1, 1.2$ Hz, 2H), 2.08–2.01 (m, 1H), 1.92 (s, 1H), 1.85 (dd, $J = 14.7, 6.1$ Hz, 1H), 1.77 (dd, $J = 14.7, 6.2$ Hz, 1H), 1.69 (t, $J = 1.2$ Hz, 3H), 1.43 (s, 3H); ^{13}C NMR (101 MHz, CDCl_3) δ 153.6, 151.7, 146.6, 133.2, 129.0, 126.2, 119.5, 118.6, 112.1, 110.7, 88.9, 81.0, 77.0, 74.2, 65.1, 65.0, 49.0, 42.5, 40.6, 39.4, 26.7, 24.2, 19.4; IR (thin film, NaCl) 3369, 2956, 2918, 2847, 2232, 1705, 1633, 1460, 1418, 1372, 1258, 1063, 801 cm^{-1} ; HRMS (FAB $^+$) m/z calc'd $\text{C}_{23}\text{H}_{31}\text{O}_5$ [M+H] $^+$: 387.2171, found: 387.2158; $[\alpha]_{25}^D = +26.7$ ($c = 0.045$, CHCl_3).



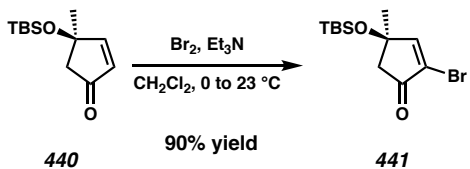
(1*R*,4*S*)-4-hydroxy-4-methyl-3-vinylcyclopent-2-en-1-yl 3-((*S*)-8-methyl-1,4-

dioxaspiro[4.5]dec-8-en-7-yl)propiolate (432): To a stirred, Ar sparged solution of ester **430** (6 mg, 0.016 mmol, 1.0 equiv) in toluene (1 mL, 0.016 M) had Grubbs II (2.6 mg, 3.1 μmol , 0.2 equiv) added in one portion. The reaction was allowed to stir for 2 h followed by direct purification of column chromatography (SiO_2 , 100% hexanes to 4:1 hexanes:EtOAc) to afford ester **432** (1.7 mg, 31 %) as a pale yellow oil ($R_f = 0.17$); ^1H NMR (400 MHz, CDCl_3) δ 6.26 (ddt, $J = 17.8, 11.3, 0.7$ Hz, 1H), 5.76 (d, $J = 2.4$ Hz, 1H), 5.75–5.68 (m, 1H), 5.52–5.45 (m, 1H), 5.35 (ddt, $J = 4.6, 3.2, 1.5$ Hz, 1H), 5.27 (dd, $J = 11.3, 1.6$ Hz, 1H), 3.94–3.87 (m, 4H), 2.58 (dd, $J = 14.3, 7.3$ Hz, 1H), 2.50 (d, $J = 1.9$ Hz, 3H), 2.26–2.11 (m, 2H), 2.00 (dd, $J = 14.2, 4.4$ Hz, 1H), 1.90–1.76 (m, 2H), 1.64 (q, $J = 2.0$ Hz, 3H), 1.38 (s, 3H); ^{13}C NMR (101 MHz, CDCl_3) δ 153.6, 151.8, 133.9, 128.9, 126.1,

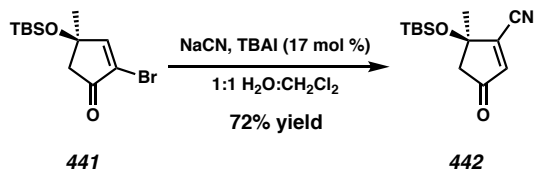
121.8, 119.6, 108.0, 88.5, 81.1, 77.1, 74.4, 64.7, 64.5, 49.0, 38.1, 36.2, 36.1, 26.8, 22.6, 21.1; IR (thin film, NaCl) 3447, 2926, 2233, 1734, 1701, 1559, 1540, 1420, 1372, 1248, 1122, 1072, 988, 948, 874, 810, 753, 731; HRMS (ESI) m/z calc'd C₂₁H₂₇O₅ [M+H]⁺: 358.1853, found: 358.1833; [α]_D²³ + 125.4 (c 0.75, CHCl₃).



(2a1*R*,6*S*,7a*R*)-3-((*S*)-2-((2-allyl-1,3-dioxolan-2-yl)methyl)-3-methylbut-3-en-1-yl)-6-hydroxy-6-methyl-4,6,7,7a-tetrahydroindeno[1,7-*bc*]furan-2(2a1*H*)-one (434): Ester **430** (5.3 mg, 13.7 μmol, 1 equiv) was dissolved xylenes (0.5 mL), sparged with Ar, sealed, and heated to 130 °C for 1 h. Upon complete consumption of starting material (as determined by TLC analysis, 1:1 hexanes: EtOAc), the reaction was loaded directly flash column (SiO₂, 100% hexanes to 1:1 hexanes:EtOAc) to afford tricycle **434** (2.1 mg, 40% yield) as an amorphous solid; ¹H NMR (400 MHz, CDCl₃) δ 5.91–5.72 (m, 2H), 5.16–5.03 (m, 2H), 4.96 (ddd, *J* = 9.1, 8.0, 7.0 Hz, 1H), 4.64 (dq, *J* = 2.9, 1.5 Hz, 1H), 4.57 (dd, *J* = 2.3, 1.0 Hz, 1H), 4.01–3.86 (m, 4H), 3.30 (t, *J* = 9.7 Hz, 1H), 3.10–2.90 (m, 2H), 2.75–2.59 (m, 3H), 2.50 (ddd, *J* = 12.7, 7.0, 0.9 Hz, 1H), 2.39 (dq, *J* = 7.2, 1.5 Hz, 2H), 1.90 (dd, *J* = 14.8, 7.9 Hz, 1H), 1.72–1.64 (m, 4H), 1.64–1.60 (m, 1H), 1.40 (d, *J* = 1.0 Hz, 3H); ¹³C NMR (101 MHz, CDCl₃) δ 168.3, 156.7, 152.0, 148.6, 133.5, 124.9, 118.4, 116.6, 111.3, 110.9, 80.0, 75.2, 65.1, 65.0, 49.8, 45.7, 42.5, 41.9, 39.4, 36.8, 35.3, 26.6, 18.3; IR (thin film, NaCl) 3458, 2924, 1749, 1642, 1432, 1210, 1093, 1044, 823 cm⁻¹; HRMS (FAB⁺) m/z calc'd C₂₃H₃₁O₅ [M+H]⁺: 387.2171, found: 387.2188; [α]_D²³ + 37.5 (c 0.12, CHCl₃).

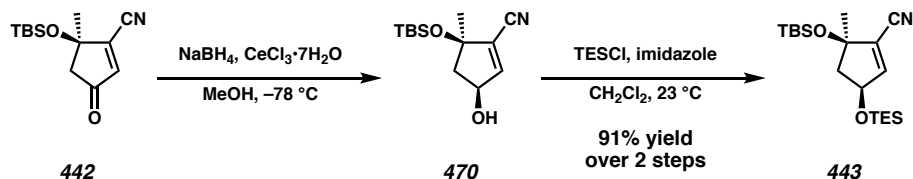


(R)-2-bromo-4-((tert-butyldimethylsilyl)oxy)-4-methylcyclopent-2-en-1-one (441): In a flame dried round-bottom flask, Enone **440** (2.76g, 12.2 mmol, 1.0 equiv) dissolved in CH_2Cl_2 (122 mL, 0.1 M) was cooled to 0 °C (ice: water bath). Br_2 (0.687 mL, 13.4 mmol, 1.1 equiv) was added dropwise over 10 min and the resultant solution stirred for 30 min. Upon complete consumption of starting material (as determined by TLC analysis, 9:1 hexanes:EtOAc), Et_3N (2.5 mL, 18.3 mmol, 1.5 equiv) was added and allowed to stir for 1 h at ambient temperature (23 °C). The reaction was diluted with a saturated solution of $\text{Na}_2\text{S}_2\text{O}_3$ and the product was extracted with EtOAc (3 x 100 mL). The combined organic layers were washed with brine, dried over MgSO_4 , filtered, and concentrated in vacuo. The crude product was purified by column chromatography (SiO_2 , 9:1 hexanes:EtOAc) to afford enone **441** (3.3 g, 90% yield) as a colorless oil ($R_f = 0.45$); ^1H NMR (400 MHz, CDCl_3) δ = 7.51 (s, 1H), 2.64 (d, J = 3.6 Hz, 2H), 1.51 (s, 3H), 0.85 (d, J = 0.5 Hz, 9H), 0.09 (s, 3H), 0.08 (s, 3H); ^{13}C NMR (101 MHz, CDCl_3) δ = 198.9, 165.0, 125.4, 50.4, 29.2, 25.7, 18.0, -2.3, -2.4; IR (thin film, NaCl) 2956, 2930, 2888, 2858, 1733, 1593, 1472, 1463, 1374, 1292, 1254, 1205, 1106, 1081, 1018, 922, 837, 776 cm^{-1} ; HRMS (ESI) m/z calc'd $\text{C}_{12}\text{H}_{22}\text{BrO}_2\text{Si} [\text{M}+\text{H}]^+$: 305.0567, found: 305.0567; $[\alpha]_D^{23} + 2.3$ (c 0.21, CHCl_3).



(R)-5-((tert-butyldimethylsilyl)oxy)-5-methyl-3-oxocyclopent-1-ene-1-carbonitrile (442):

In a round-bottom flask, NaCN (2.3 g, 47 mmol, 2.2 equiv) and TBAI (1.1 g, 3.6 mmol, 0.17 equiv) is dissolved in H₂O (66 mL, 0.32 M). Upon complete dissolution, a solution of enone **441** (6.5 g, 21.3 mmol, 1 equiv) in CH₂Cl₂ (107 mL, 0.2 M) was added and the biphasic mixture was stirred vigorously for 16 h. Upon completion of starting material (as determined by TLC analysis, 9:1 hexanes:EtOAc), the reaction was allowed to stand until complete separation of the biphasic mixture occurred. The organic layer was separated and the aqueous layer was extracted with EtOAc (5 x 100 mL). The combined organic layers were washed with brine, dried over MgSO₄, filtered, and concentrated in vacuo. The crude product was purified by column chromatography (SiO₂, 9:1 hexanes:EtOAc) to afford enone **442** (3.8 g, 72% yield) as a pale yellow oil (*R*_f = 0.43); ¹H NMR (400 MHz, CDCl₃) δ = 6.56 (s, 1H), 2.65 (d, *J* = 3.7 Hz, 2H), 1.64 (s, 3H), 0.88 (s, 9H), 0.17 (s, 3H), 0.13 (s, 3H); ¹³C NMR (101 MHz, CDCl₃) δ = 203.0, 149.6, 139.6, 113.3, 78.8, 51.1, 28.1, 25.6, 18.1, -2.4, -2.7; IR (thin film, NaCl) 3449, 3087, 2957, 2932, 2888, 2859, 2231, 2736, 1606, 1473, 1378, 1290, 1254, 1217, 1170, 1093, 1006, 838, 778, 673 cm⁻¹; HRMS (FAB+) m/z calc'd C₁₃H₂₂O₂NSi [M+H]⁺: 252.1420, found: 252.1416; [α]_D²³ – 34.6 (c 0.34, CHCl₃).

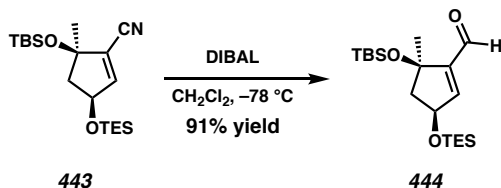


(3*S*,5*R*)-5-((*tert*-butyldimethylsilyl)oxy)-3-hydroxy-5-methylcyclopent-1-ene-1-carbonitrile (470):

In a round bottom flask, enone **442** (9.4 g, 37.3 mmol, 1 equiv) was dissolved in methanol (373 mL, 0.1 M). The solution was stirred for 5 min followed by the addition of $\text{CeCl}_3 \cdot 7\text{H}_2\text{O}$ (13.2 g, 41 mmol, 1.1 equiv). Once the reaction is homogeneous, the solution is cooled to -78°C and allowed to stir for 1 h. NaBH_4 (1.4 g, 37.3 mmol, 1 equiv) was added slowly in portions to the reaction and was allowed to stir until completion (as determined by TLC analysis 4:1 hexanes:EtOAc). Upon complete consumption of starting material, the reaction was quenched with a saturated solution of NH_4Cl (300 mL) and the biphasic mixture was allowed to warm to room temperature. The biphasic mixture was extracted with 2:1 Et_2O :hexanes (3 x 300 mL) and the combined organic layers were dried over Na_2SO_4 , filtered, and concentrated in vacuo. The crude product was assumed to have quantitative conversion and was used directly into the next reaction without further purification. Alcohol **470** could be purified by column chromatography (SiO_2 , 9:1 hexanes:EtOAc) to afford pure alcohol **470** as a white amorphous powder; $R_f = 0.74$ (4:1 hexanes:EtOAc); ^1H NMR (400 MHz, CDCl_3) δ = 6.40 (d, $J = 2.1$ Hz, 1H), 4.60 (dd, $J = 8.1, 7.1, 5.2, 2.2$ Hz, 1H), 2.34 (dd, $J = 13.3, 6.9$ Hz, 1H), 1.80 (dd, $J = 13.2, 5.2$ Hz, 1H), 1.65 (d, $J = 8.2$ Hz, 1H), 1.29 (d, $J = 0.6$ Hz, 3H), 0.72 (s, 9H), 0.00 (s, 3H), -0.01 (s, 3H); ^{13}C NMR (101 MHz, CDCl_3) δ 146.6, 127.2, 114.7, 83.0, 74.2, 50.8, 27.8, 25.7, 18.0, -2.2, -2.4; IR (thin film, NaCl) 3429, 2956, 2930, 2887, 2858, 2229, 1472, 1255, 1176, 1126,

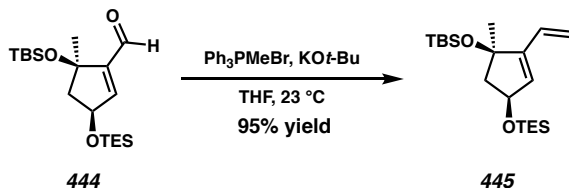
1082, 1031, 868, 838, 777, 668 cm⁻¹; HRMS (ESI) m/z calc'd C₁₃H₂₇N₂O₂Si [M+NH₄]⁺: 271.1836; found: 271.1842; [α]_D²³ – 53.0 (c 0.28, CHCl₃).

(3*S*,5*R*)-5-((tert-butyldimethylsilyl)oxy)-5-methyl-3-((triethylsilyl)oxy)cyclopent-1-ene-1-carbonitrile (443): Crude alcohol **470** (37.3 mmol, 1 equiv) was dissolved in CH₂Cl₂ (266 mL, 0.14 M). Once the solution is homogeneous Imidazole (7.6 g, 111.9 mmol, 3 equiv) and TESCl (7.1 mL, 55.9 mL, 1.5 equiv) was added. The reaction was allowed to stir until completion at 23 °C. Upon complete consumption of starting material (as determined by TLC analysis, 9:1 hexanes:EtOAc), the reaction was quenched with H₂O (200 mL) and the biphasic mixture was extracted with Et₂O (3 x 400 mL). The combined organic layers were washed with brine, dried over MgSO₄, filtered, and concentrated in vacuo. The resultant crude product was the purified by column chromatography (SiO₂, 9:1 hexanes:EtOAc) to afford nitrile **443** (12.5 g, 91% yield, 11:1 dr) as a pale yellow oil (R_f = 0.5); ¹H NMR (400 MHz, CDCl₃) δ = 6.41 (d, J = 2.0 Hz, 1H), 4.72 (ddd, J = 7.0, 6.2, 2.0 Hz, 1H), 2.49 (dd, J = 12.8, 7.0 Hz, 1H), 1.98 (ddd, J = 12.8, 6.3, 0.8 Hz, 1H), 1.40 (d, J = 0.8 Hz, 3H), 0.96 (t, J = 7.9 Hz, 9H), 0.89 (s, 9H), 0.61 (q, J = 7.8 Hz, 6H), 0.14 (s, 3H), 0.13 (s, 3H); ¹³C NMR (101 MHz, CDCl₃) δ = 147.3, 126.1, 114.9, 82.4, 73.8, 51.5, 28.7, 25.8, 18.1, 6.8, 4.8, -2.2, -2.6; IR (thin film, NaCl) 2957, 2879, 2858, 2224, 1463, 1414, 1360, 1308, 1254, 1198, 1177, 1132, 1099, 1047, 1006, 893, 869, 837, 809, 777 cm⁻¹; HRMS (ESI) m/z calc'd C₁₉H₃₈NO₂Si₂ [M+H]⁺: 268.2436; found: 368.2449; [α]_D²³ – 52.0 (c 0.40, CHCl₃).



(3*S*,5*R*)-5-((*tert*-butyldimethylsilyl)oxy)-5-methyl-3-((triethylsilyl)oxy)cyclopent-1-ene-1-carbaldehyde (444):

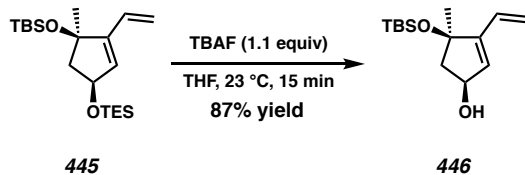
Nitrile **443** (250 mg, 0.68 mmol, 1 equiv) was added to CH_2Cl_2 (6.8 mL, 0.1M) and cooled to -78°C . DIBAL (1.36 mL, 1 M in DCM, 2 equiv) was added dropwise and allowed to stir for 1 h at -78°C . Upon complete consumption of starting material (as determined by TLC analysis, 19:1 hexanes:Et₂O) the reaction was quenched with EtOAc (0.5 mL), diluted with Et₂O and warmed to room temperature. A 50% solution of Rochelle's salt (10 mL) was added and the biphasic mixture was allowed to stir for 0.5 h. If the biphasic mixture does not separate completely, another portion of Rochelle's salt is added and stirred for another 0.5 h. The biphasic mixture is separated and the aqueous layer is extracted with Et₂O (3 x 10 mL). The combined organic layers are dried over MgSO₄, filtered, and concentrated in vacuo. The resultant crude product was purified by column chromatography (SiO₂, 19:1 hexanes:Et₂O) to afford enal **444** (252 mg, 91% yield, 17:1 dr) as a pale yellow oil ($R_f = 0.46$); ¹H NMR (400 MHz, CDCl₃) δ = 9.77 (s, 1H), 6.53 (d, $J = 1.8$ Hz, 1H), 4.70 (td, $J = 6.9, 1.9$ Hz, 1H), 2.49 (dd, $J = 12.7, 7.1$ Hz, 1H), 2.08 (dd, $J = 12.6, 6.6$ Hz, 1H), 1.45 (s, 3H), 0.97 (t, $J = 7.9$ Hz, 9H), 0.84 (d, $J = 0.9$ Hz, 9H), 0.63 (q, $J = 7.9$ Hz, 6H), 0.11 (s, 3H), 0.07 (s, 3H); ¹³C NMR (101 MHz, CDCl₃) δ = 189.7, 149.8, 147.8, 80.6, 72.9, 53.9, 28.6, 25.8, 18.1, 6.9, 4.9, -2.2, -2.4; IR (thin film, NaCl) 2956, 2936, 2879, 2857, 2805, 2708, 1698, 1627, 1472, 1462, 1414, 1359, 1253, 1203, 1172, 1103, 1058, 975, 897, 837, 806, 775, 746, 671; HRMS (FAB+) m/z calc'd C₁₉H₃₇O₃Si₂ [M+H-H₂]⁺: 369.2250, found: 369.2262; $[\alpha]_D^{23} = -117.2$ (*c* 0.20, CHCl₃).



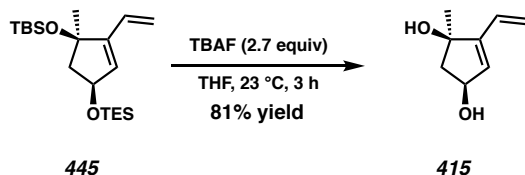
***tert*-butyldimethyl(((1*R*,4*S*)-1-methyl-4-((triethylsilyl)oxy)-2-vinylcyclopent-2-en-1-yloxy)silane (445):**

To a round-bottom flask in an N₂-filled glovebox were charged Ph₃PMeBr (1.7 g, 4.86 mmol, 3.00 equiv) and KOt-Bu (490 mg, 4.37 mmol, 2.70 equiv) as solids followed by THF (162 mL, 0.01 M). The bright yellow reaction mixture was then sealed with a rubber septum, removed from the glovebox, and placed under an argon atmosphere with stirring. After 2 h, a solution of aldehyde **444** in THF (3.00 mL) was added dropwise, causing the reaction mixture to become dark orange-brown. After the consumption of starting material was complete (as determined by TLC analysis, 19:1 hexanes:EtOAc). The reaction was poured onto a mixture of H₂O (90 mL) and Et₂O (30 mL). The organics were separated and the aqueous layer was extracted with Et₂O (3 x 30 mL). The combined organic layers were washed with brine (30 mL), dried over MgSO₄, filtered, and concentrated in vacuo. The crude dark brown residue was purified by column chromatography (SiO₂, 19:1 hexanes:Et₂O) to afford diene **445** (567 mg, 95% yield) as a colorless oil (*R*_f = 0.80); ¹H NMR (400 MHz, CDCl₃) δ = 6.24 (dd, *J* = 17.3, 11.2 Hz, 1H), 5.68 (dd, *J* = 18.2, 2.0 Hz, 1H), 5.62 (d, *J* = 1.9 Hz, 1H), 5.18 (ddt, *J* = 11.3, 2.2, 0.6 Hz, 1H), 4.60 (dddd, *J* = 6.7, 6.0, 2.0, 0.9 Hz, 1H), 2.43 (dd, *J* = 12.2, 6.8 Hz, 1H), 2.00 (ddd, *J* = 12.1, 6.6, 0.9 Hz, 1H), 1.34 (d, *J* = 0.9 Hz, 3H), 0.97 (t, *J* = 7.9 Hz, 9H), 0.86 (s, 9H), 0.61 (q, *J* = 7.9 Hz, 6H), 0.11 (s, 3H), 0.08 (s, 3H); ¹³C NMR (101 MHz, CDCl₃) δ = 149.4, 130.0, 129.9, 117.4, 82.1, 73.2, 53.5, 29.0, 26.0, 18.2, 7.0, 5.0, -2.0, -2.5; IR (thin film, NaCl) 2956, 2935, 2877, 2857, 1591, 1462, 1414, 1359, 1252, 1171, 1126, 1079, 1055,

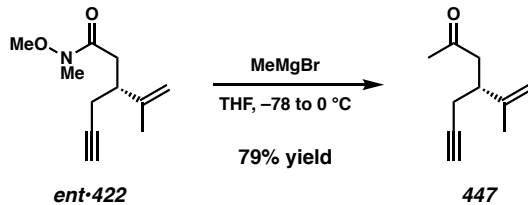
1018, 1004, 855, 836, 774, 744 cm^{-1} ; HRMS (FAB+) m/z calc'd C₂₀H₄₄NO₂Si [M+NH₄]⁺: 386.2905, found: 386.2889; $[\alpha]_D^{23} - 3.87$ (*c* 0.35, CHCl₃).



(1*S*,4*R*)-4-((tert-butyldimethylsilyl)oxy)-4-methyl-3-vinylcyclopent-2-en-1-ol (446): A solution of Diene **445** (195 mg, 0.53 mmol, 1 equiv) in THF (7.6 mL, 0.07 M) had a THF solution of TBAF (0.58 mL, 0.58 mmol, 1 M, 1.1 equiv). The reaction was allowed to stir for 15 min at which time total consumption of starting material occur (as determined by TLC analysis, 3:1 hexanes:Et₂O). The reaction was diluted with water (10 mL) and the aqueous layer was extracted with Et₂O (3 x 10 mL). The combined organic layers were washed with brine, dried over MgSO₄, filtered, and concentrated in vacuo. The crude product was purified by column chromatography (SiO₂, 3:1 hexanes:Et₂O) to afford diene **446** (117 mg, 87%) as a viscous colorless oil which solidifies at -20 °C ($R_f = 0.2$); ¹H NMR (400 MHz, CDCl₃) δ = 6.32–6.22 (m, 1H), 5.75–5.67 (m, 2H), 5.25–5.19 (m, 1H), 4.64–4.55 (m, 1H), 2.53 (dd, *J* = 12.7, 6.9 Hz, 1H), 1.93 (ddd, *J* = 12.7, 6.0, 0.8 Hz, 1H), 1.59 (s, 1H), 1.36 (d, *J* = 0.9 Hz, 3H), 0.86 (s, 9H), 0.12 (s, 3H), 0.10 (s, 3H); ¹³C NMR (101 MHz, CDCl₃) δ = 150.6, 129.8, 129.1, 118.1, 82.5, 73.5, 53.2, 28.7, 25.9, 18.2, -2.0, -2.4; IR (thin film, NaCl) 3324, 2957, 2929, 2886, 2857, 1590, 1472, 1462, 1370, 1254, 1204, 1170, 1134, 1042, 1017, 835, 774, 679; HRMS (FAB+) m/z calc'd C₁₄H₃₀NO₂Si [M+NH₄]⁺: 272.204, found 272.2027; $[\alpha]_D^{23} + 25.4$ (*c* 0.19, CHCl₃).

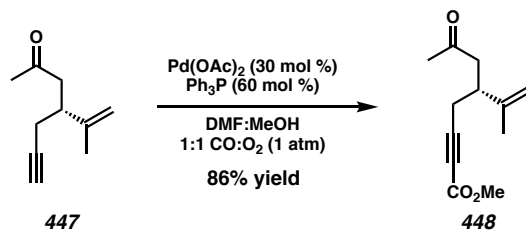


(1*R*,3*S*)-1-methyl-5-vinylcyclopent-4-ene-1,3-diol (415): A solution of Diene **445** (270 mg, 0.57 mmol, 1 equiv) in THF (8.1 mL, 0.07 M) had a THF solution of TBAF (1.25 mL, 1.25 mmol, 1 M, 2.2 equiv). The reaction was allowed to stir for 2 h at 65 °C at which time another solution of TBAF (0.25 mL, 0.25 mmol, 0.5 equiv) was added. Upon total consumption of starting material (as determined by TLC analysis, 3:1 hexanes:Et₂O), the reaction was diluted with water (10 mL) and the aqueous layer was extracted with Et₂O (5 x 25 mL). The combined organic layers were washed with brine, dried over MgSO₄, filtered, and concentrated in vacuo. The crude product was purified by column chromatography (SiO₂, 1:3 hexanes:EtOAc) to afford diene **415** (64 mg, 81%) as a white amorphous solid; ¹H NMR (300 MHz, CDCl₃) δ 6.30 (dd, J = 17.8, 11.3, 1H), 5.82 (d, J = 2.1, 1H), 5.73 (dd, J = 17.9, 1.7, 1H), 5.26 (dd, J = 11.2, 1.7, 1H), 4.65 (dd, J = 11.5, 5.1, 1H), 2.54 (dd, J = 13.6, 6.8, 1H), 1.85 (dd, J = 13.6, 4.8, 2H), 1.68 (d, J = 6.6, 1H), 1.40 (s, 3H). All other characterization data matched known values.⁹



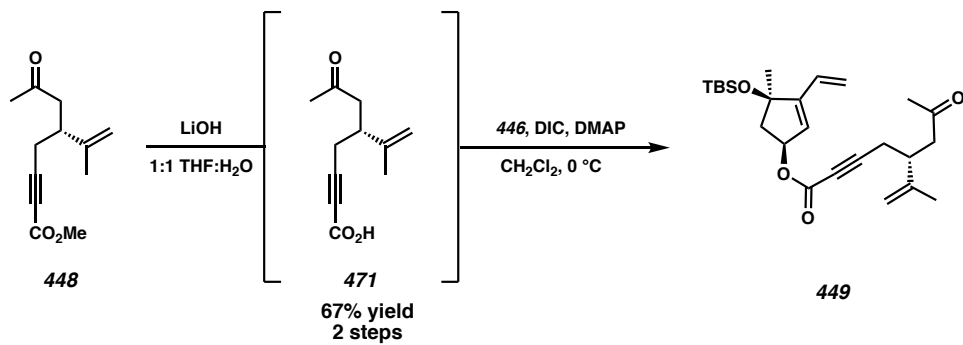
(S)-4-(prop-1-en-2-yl)hept-6-yn-2-one (447): Amide **ent•422** (2.0 g, 10.2 mmol, 1 equiv) in THF (51 mL, 0.2 M) was cooled to –78 °C. A solution of MeMgBr in Et₂O (7.1 mL, 21.5 mmol, 3 M, 2.1 equiv) was added dropwise. The reaction was allowed to stir for 12 h, gradually warming up to ambient temperature (23 °C). Upon complete consumption of

starting material (as determined by TLC analysis, 4:1 hexanes:Et₂O), the reaction was quenched with a saturated solution of NH₄Cl (50 mL), and diluted with Et₂O (25 mL). The organics were separated and the aqueous layer was extracted with Et₂O (3 x 40 mL) and the combined organic layers were washed with brine, dried over MgSO₄, filtered, and concentrated in vacuo. The crude product was purified by column chromatography (SiO₂, 4:1 hexanes, Et₂O) to afford ketone **447** (1.2 g, 79%) as a pale yellow oil (R_f = 0.6); ¹H NMR (400 MHz, CDCl₃) δ = 4.83 (p, J = 1.5 Hz, 1H), 4.78 (dt, J = 1.6, 0.8 Hz, 1H), 2.81 (p, J = 6.7 Hz, 1H), 2.73 (dd, J = 16.5, 6.6 Hz, 1H), 2.59 (dd, J = 16.5, 7.5 Hz, 1H), 2.36 (ddd, J = 16.9, 6.3, 2.7 Hz, 1H), 2.29 (ddd, J = 16.9, 6.6, 2.7 Hz, 1H), 2.15 (s, 3H), 1.99 (t, J = 2.6 Hz, 1H), 1.73 (dd, J = 1.5, 0.8 Hz, 3H); ¹³C NMR (101 MHz, CDCl₃) δ = 207.6, 145.9, 111.9, 82.2, 70.2, 46.5, 40.5, 30.5, 23.1, 20.6; IR (thin film, NaCl) 3294, 3078, 2970, 2918, 2117, 1715, 1648, 1433, 1360, 1233, 1160, 1059, 997, 896, 641; HRMS (ESI) m/z calc'd C₁₀H₁₅O [M+H]⁺: 151.1197, found: 151.1115; $[\alpha]_D^{23}$ + 22.2 (c 0.59, CHCl₃).



methyl (S)-7-oxo-5-(prop-1-en-2-yl)oct-2-yneate (448): Palladium acetate (112 mg, 0.5 mmol, 0.3 equiv) and triphenylphosphine (260 mg, 1.0 mmol, 0.6 equiv) were mixed in dimethylformamide (17 mL, 0.1 M) in a round-bottomed flask under N₂ and allowed to stir for 5 min. Methanol (1.7 mL, 41.5 mmol, 25 equiv) and ketone **447** (250 mg, 1.66 mmol, 1 equiv) were added, followed by attachment of 2 rubber balloons, one filled with oxygen and the other CO, to the flask. The reaction was sparged with both CO and O₂ balloons for

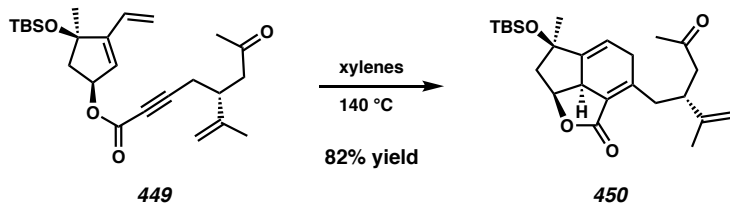
5 min and allowed to stir at ambient temperature (23 °C) for 16 h. Upon complete consumption of starting material (as determined by TLC, 4:1 hexanes:EtOAc), the mixture was diluted with Et₂O and a saturated solution of LiCl and the aqueous layer was extracted with Et₂O. The combined organic layers were dried over MgSO₄, filtered, and concentrated in vacuo. The crude product was purified by column chromatography (SiO₂, 4:1 hexanes:EtOAc) to afford ester **448** (249 mg, 86%) as a colorless oil ($R_f = 0.25$); ¹H NMR (400 MHz, CDCl₃) δ = 4.86 (t, $J = 1.4$ Hz, 1H), 4.81 (q, $J = 0.9$ Hz, 1H), 3.75 (s, 3H), 2.85 (p, $J = 6.7$ Hz, 1H), 2.66 (dd, $J = 9.4, 7.1$ Hz, 2H), 2.48 (dd, $J = 6.5, 4.9$ Hz, 2H), 2.16 (s, 3H), 1.73 (dd, $J = 1.4, 0.8$ Hz, 3H); ¹³C NMR (101 MHz, CDCl₃) δ = 207.0, 154.2, 145.2, 112.5, 87.3, 74.6, 52.8, 46.3, 39.7, 30.6, 23.1, 20.7; IR (thin film, NaCl) 2923, 2236, 1714, 1647, 1434, 1361, 1259, 1158, 1074, 942, 901, 752, 679 cm⁻¹; HRMS (FAB+) m/z calc'd C₁₂H₁₇O₃ [M+H]⁺: 209.1172; found 209.1164; $[\alpha]_D^{23} + 46.5$ (*c* 0.18, CHCl₃).



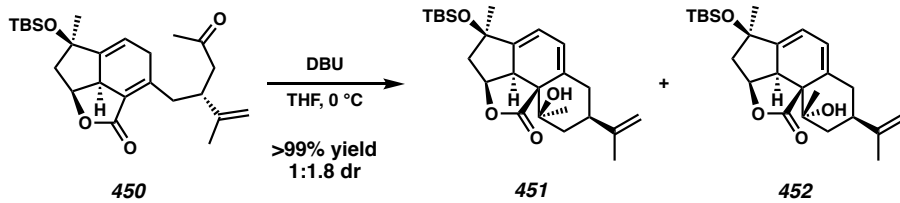
(1*S*,4*R*)-4-((tert-butyldimethylsilyl)oxy)-4-methyl-3-vinylcyclopent-2-en-1-yl (R)-7-oxo-5-(prop-1-en-2-yl)oct-2-ynoate (471): Ester **448** (1.5 g, 5.7 mmol, 1 equiv) in a solution of THF (28 mL, 0.2M), was added to a solution of LiOH (205 mg, 8.6 mmol, 1.5 equiv) in H₂O (28 mL, 0.2M). The reaction was stirred vigorously for 4 h when complete consumption of starting material was observed (as determined by TLC analysis 4:1 hexanes:EtOAc). The reaction was washed with EtOAc (1 X 20 mL) and the aqueous layer

was subsequently acidified to a pH of 1 with 1 N HCl. The acidic aqueous layer was then extracted with EtOAc (5 x 30 mL) and the combined organic layers were washed with brine, dried over MgSO₄, filtered, and concentrated in vacuo. The crude acid **471** (1.3 g, 81%) was used without further purification or characterization.

Diol **446** (10 mg, 0.039 mmol, 1 equiv), acid **471** (15 mg, 0.079 mmol 2 equiv), and DMAP (16 mg, 0.039 mmol, 1 equiv) were added to a solution of CH₂Cl₂ (0.4 mL, 0.1 M) and cooled to 0 °C. DIC (12 µL, 0.079 mmol, 2 equiv) was added dropwise and the reaction was allowed to stir for 2 h. Upon complete consumption of starting material (as determined by TLC analysis, 4:1 hexanes:EtOAc), the reaction was diluted with H₂O (5 mL) and extracted with Et₂O (3 x 5 mL). The combined organic layers were dried over MgSO₄, filtered, and concentrated in vacuo. The crude product was purified by column chromatography (SiO₂, 4:1 hexanes:EtOAc) to afford ester **449** (12 mg, 70%) as a pale yellow oil (*R*_f = 0.4); ¹H NMR (400 MHz, CDCl₃) δ = 6.27 (ddd, *J* = 17.8, 11.2, 0.8 Hz, 1H), 5.75–5.69 (m, 2H), 5.53 (dddd, *J* = 7.3, 5.9, 2.3, 0.8 Hz, 1H), 5.27 (dd, *J* = 11.3, 1.9 Hz, 1H), 4.86–4.83 (m, 1H), 4.83–4.77 (m, 1H), 2.93–2.81 (m, 1H), 2.67 (dd, *J* = 13.2, 7.1 Hz, 2H), 2.63–2.56 (m, 1H), 2.48 (dd, *J* = 7.5, 6.4 Hz, 2H), 2.16 (s, 3H), 2.10 (ddd, *J* = 13.1, 5.9, 0.8 Hz, 1H), 1.73 (dd, *J* = 1.5, 0.8 Hz, 3H), 1.38 (d, *J* = 0.8 Hz, 3H), 0.86 (s, 9H), 0.12 (s, 3H), 0.08 (s, 3H); ¹³C NMR (101 MHz, CDCl₃) δ = 207.1, 153.7, 152.7, 145.2, 129.3, 123.9, 119.0, 112.4, 87.2, 82.3, 74.9, 48.9, 46.3, 39.7, 30.5, 29.2, 25.9, 23.2, 20.7, 18.2, -2.2, -2.6; IR (thin film, NaCl) 2956, 2929, 2856, 2234, 1711, 1649, 1472, 1439, 1359, 1250, 1169, 1069, 1022, 837, 774, 752 cm⁻¹; HRMS (FAB+) m/z calc'd C₂₅H₃₉O₄Si [M+H]⁺: 431.2612; found 431.2629; [α]_D²³ -71.1 (*c* 0.59, CHCl₃).



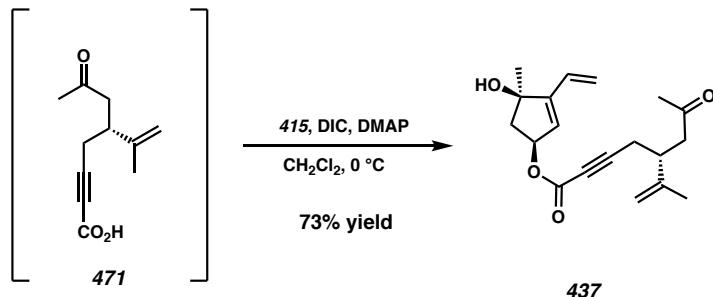
(2a1*S*,6*R*,7a*S*)-6-((*tert*-butyldimethylsilyl)oxy)-6-methyl-3-((*R*)-4-oxo-2-(prop-1-en-2-yl)pentyl)-4,6,7,7a-tetrahydroindeno[1,7-*bc*]furan-2(2a1*H*)-one (450): Ester **449** (65 mg, 0.15 mmol) was transferred to a Schlenk bomb with xylenes (15 mL, 0.01 M). The Schlenk was rigorously degassed by standard freeze-pump-thaw technique and upon reaching ambient temperature (23 °C) the flask was sealed and heat to 140 °C. The reaction was allowed to stir at this temperature of 2 h at which time complete consumption of starting material was observed (as determined by TLC analysis, 4:1 hexanes:EtOAc). The reaction was allowed to cool to room temperature and was directly purified by column chromatography (SiO₂, 100% hexanes then 4:1 hexanes:EtOAc) to furnish tricycle **450** (53 mg, 82%) as a white amorphous solid ($R_f = 0.35$); ¹H NMR (400 MHz, CDCl₃) δ = δ 5.78 (ddd, $J = 6.4, 2.9, 1.9$ Hz, 1H), 4.93 (ddd, $J = 9.0, 8.1, 7.0$ Hz, 1H), 4.68 (p, $J = 1.5$ Hz, 1H), 4.63 (dt, $J = 1.8, 0.8$ Hz, 1H), 3.19 (t, $J = 9.6$ Hz, 1H), 3.13–3.04 (m, 1H), 2.93 (p, $J = 7.1$ Hz, 1H), 2.84 (dddd, $J = 10.7, 7.1, 2.4, 1.3$ Hz, 1H), 2.75 (ddd, $J = 12.7, 7.7, 1.2$ Hz, 1H), 2.66 (ddt, $J = 18.1, 10.1, 1.6$ Hz, 1H), 2.59 (d, $J = 1.4$ Hz, 1H), 2.57 (d, $J = 1.5$ Hz, 1H), 2.42–2.34 (m, 1H), 2.12 (s, 3H), 1.70–1.63 (m, 4H), 1.36 (d, $J = 1.0$ Hz, 3H), 0.86 (s, 9H), 0.10 (s, 3H), 0.03 (s, 3H); ¹³C NMR (101 MHz, CDCl₃) δ = 208.0, 168.7, 156.7, 151.8, 146.4, 125.4, 116.5, 112.3, 81.2, 76.2, 48.8, 47.3, 44.8, 40.9, 35.7, 34.8, 30.8, 28.1, 25.8, 19.5, 18.1, -2.1, -2.3; IR (thin film, NaCl) 2957, 2929, 2857, 1753, 1714, 1645, 1442, 1359, 1327, 1291, 1257, 1209, 1177, 1028, 856, 836, 774, 680 cm⁻¹; HRMS (FAB+) m/z calc'd C₂₅H₃₉O₄Si [M+H]⁺: 431.2612, found: 431.2643; $[\alpha]_D^{23} -64.5$ (c 0.39, CHCl₃).



(2*R*,2*a*1*S*,6*R*,8*R*,8*aS*,10*a**S*)-2-((*tert*-butyldimethylsilyl)oxy)-8-hydroxy-2,8-dimethyl-6-(prop-1-en-2-yl)-1,2,2*a*1,5,6,7,8,10*a*-octahydro-9*H*-benzo[6,7]indeno[1,7-*bc*]furan-9-one (451) and (2*R*,2*a*1*S*,6*R*,8*S*,8*a**S*,10*a**S*)-2-((*tert*-butyldimethylsilyl)oxy)-8-hydroxy-2,8-dimethyl-6-(prop-1-en-2-yl)-1,2,2*a*1,5,6,7,8,10*a*-octahydro-9*H*-benzo[6,7]indeno[1,7-*bc*]furan-9-one (452):** Tricycle XXX (3 mg, 7.2 µmol, 1 equiv) in THF (0.2 mL) had DBU (1.7 µL, 7.2 µmol, 1 equiv). After 5 min, the reaction was concentrated and directly purified by column chromatography (SiO₂, 4:1 hexanes:EtOAc) to afford tetracycle 451 and 452 (1:1.8 dr, 3 mg, >99%) as an amorphous film (*R*_f = 0.48 452 and 0.34 451)

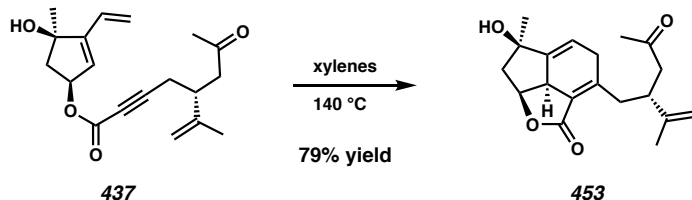
452: ¹H NMR (400 MHz, CDCl₃) δ = 5.99 (dd, *J* = 5.7, 2.5 Hz, 1H), 5.83 (ddd, *J* = 5.8, 2.8, 1.1 Hz, 1H), 4.89 – 4.68 (m, 3H), 3.76–3.69 (m, 1H), 2.88–2.76 (m, 1H), 2.47 (dd, *J* = 13.7, 7.4 Hz, 1H), 2.39–2.27 (m, 2H), 2.27–2.04 (m, 1H), 1.86 (dd, *J* = 13.7, 3.9 Hz, 1H), 1.78 (dd, *J* = 1.5, 0.8 Hz, 3H), 1.71 (dt, *J* = 13.0, 2.6 Hz, 1H), 1.40 (d, *J* = 1.0 Hz, 3H), 1.25 (s, 3H), 0.89 (s, 9H), 0.12 (s, 3H), 0.08 (s, 3H); ¹³C NMR (101 MHz, CDCl₃) δ = 176.6, 148.1, 142.2, 131.1, 123.2, 112.7, 110.2, 80.0, 79.7, 74.4, 56.7, 49.0, 42.0, 40.7, 40.0, 35.7, 29.9, 28.5, 25.9, 24.9, 20.6, 18.2, 14.3, -2.0, -2.2; IR (thin film, NaCl) 3523, 2925, 2856, 2759, 1461, 1372, 1292, 1257, 1153, 1065, 964, 833, 771, 732, 705, 655 cm⁻¹; HRMS (FAB+) m/z calc'd C₂₅H₄₂O₄SiN [M+NH₄]⁺ 448.2878, found: 448.2889; [α]_D²³ +4.12 (*c* 0.235, CHCl₃).

451: ^1H NMR (400 MHz, CDCl_3) δ = 5.86 (dd, J = 5.7, 2.6 Hz, 1H), 5.82 (ddd, J = 5.8, 2.7, 1.0 Hz, 1H), 4.89 (td, J = 7.2, 3.2 Hz, 1H), 4.80 (dq, J = 1.8, 0.9 Hz, 1H), 4.78 (q, J = 1.5 Hz, 1H), 3.47 (d, J = 7.4 Hz, 1H), 2.86–2.73 (m, 1H), 2.48–2.36 (m, 2H), 2.31 (ddd, J = 15.0, 4.4, 1.9 Hz, 1H), 2.20 (tt, J = 12.8, 3.8 Hz, 1H), 1.94 (dd, J = 14.0, 3.1 Hz, 1H), 1.78 (s, 3H), 1.66 (ddd, J = 12.0, 3.4, 1.9 Hz, 1H), 1.39 (d, J = 1.1 Hz, 3H), 1.29 (d, J = 0.8 Hz, 3H), 0.88 (d, J = 1.1 Hz, 9H), 0.12 (s, 3H), 0.08 (s, 3H); ^{13}C NMR (101 MHz, CDCl_3) δ = 177.3, 148.1, 142.1, 132.2, 121.3, 113.4, 110.1, 80.1, 80.0, 76.2, 57.8, 48.7, 42.7, 42.3, 41.3, 35.5, 29.2, 26.7, 25.9, 20.5, 18.2, -2.0, -2.3; IR (thin film, NaCl) 3462, 2956, 2928, 2856, 1739, 1643, 1450, 1375, 1293, 1257, 1163, 1132, 1018, 837, 809, 773 cm^{-1} ; HRMS (FAB+) m/z calc'd $\text{C}_{25}\text{H}_{42}\text{O}_4\text{SiN}$ [M+NH₄]⁺ 448.2878, found: 448.2890; $[\alpha]_D^{23} -33.7$ (*c* 0.1, CHCl_3).



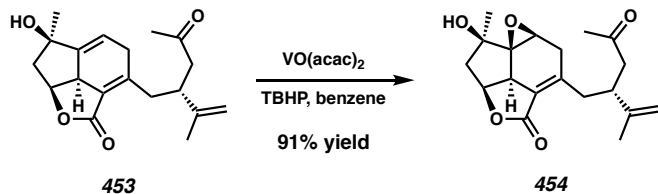
(1*S*,4*R*)-4-hydroxy-4-methyl-3-vinylcyclopent-2-en-1-yl (R)-7-oxo-5-(prop-1-en-2-yl)oct-2-ynoate (437): Diol **415** (18 mg, 0.13 mmol, 1 equiv), acid **471** (56 mg, 0.28 mmol 2.2 equiv), and DMAP (17 mg, 0.17 mmol, 1.1 equiv) were added to a solution of CH_2Cl_2 (1.4 mL, 0.09 M) and cooled to 0 °C. DIC (44 μL , 0.28 mmol, 2.2 equiv) was added dropwise and the reaction was allowed to stir for 1 h. Upon complete consumption of starting material (as determined by TLC analysis, 1:1 hexanes:EtOAc), the reaction was diluted with H_2O (5 mL) and extracted with Et₂O (3 x 5 mL). The combined organic layers

were dried over MgSO₄, filtered, and concentrated in vacuo. The crude product was purified by column chromatography (SiO₂, 1:1 hexanes:EtOAc) to afford ester **437** (30 mg, 73%) as a colorless oil ($R_f = 0.27$); ¹H NMR (400 MHz, CDCl₃) δ = 6.32 (ddt, J = 17.8, 11.3, 0.8 Hz, 1H), 5.85–5.75 (m, 2H), 5.54 (ddd, J = 7.1, 4.7, 2.5 Hz, 1H), 5.33 (dd, J = 11.3, 1.6 Hz, 1H), 4.90–4.82 (m, 1H), 4.80 (q, J = 0.9 Hz, 1H), 2.86 (p, J = 6.6 Hz, 1H), 2.74–2.59 (m, 3H), 2.55–2.41 (m, 2H), 2.16 (s, 3H), 2.06 (dd, J = 14.3, 4.4 Hz, 1H), 1.73 (dd, J = 1.4, 0.8 Hz, 3H), 1.44 (s, 3H); ¹³C NMR (101 MHz, CDCl₃) δ = 207.1, 153.5, 151.9, 145.2, 129.0, 126.1, 119.6, 112.5, 87.5, 81.1, 77.4, 74.8, 48.9, 46.4, 39.7, 30.6, 26.8, 23.2, 20.7; IR (thin film, NaCl) 3462, 2969, 2926, 2233, 1704, 1422, 1249, 1163, 1071, 944, 751; HRMS (ESI) m/z calc'd C₁₉H₂₆O₅ [M+H₂O]⁺: 334.1775, found: 334.1785; $[\alpha]_D^{23}$ −65.9 (*c* 0.18, CHCl₃).



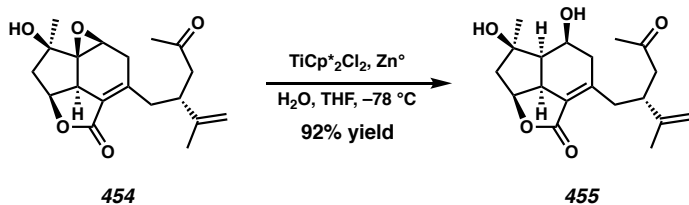
(2a1*S*,6*R*,7a*S*)-6-hydroxy-6-methyl-3-((*R*)-4-oxo-2-(prop-1-en-2-yl)pentyl)-4,6,7,7a-tetrahydroindeno[1,7-bc]furan-2(2a1*H*)-one (453): Ester **437** (100 mg, 0.32 mmol) was transferred to a Schlenk bomb with xylenes (32 mL, 0.01 M). The Schlenk was rigorously degassed by standard freeze-pump-thaw technique and upon reaching ambient temperature (23 °C) the flask was sealed and heat to 140 °C. The reaction was allowed to stir at this temperature of 2 h at which time complete consumption of starting material was observed (as determined by TLC analysis, 1:1 hexanes:EtOAc). The reaction was allowed to cool to room temperature and was directly purified by column chromatography (SiO₂, 100% hexanes then 1:1 hexanes:EtOAc) to furnish tricycle **453** (79 mg, 79%) as a white

amorphous solid ($R_f = 0.27$); ^1H NMR (400 MHz, CDCl_3) $\delta = \delta$ 5.84 (dt, $J = 6.4, 2.3$ Hz, 1H), 5.02–4.91 (m, 1H), 4.75–4.69 (m, 1H), 4.67 (d, $J = 1.9$ Hz, 1H), 3.26 (t, $J = 9.6$ Hz, 1H), 3.12–2.98 (m, 2H), 2.97–2.87 (m, 1H), 2.74 (ddt, $J = 18.2, 10.1, 1.6$ Hz, 1H), 2.59 (dd, $J = 6.7, 4.1$ Hz, 2H), 2.57–2.44 (m, 2H), 2.11 (s, 3H), 1.69 (d, $J = 1.3$ Hz, 3H), 1.64 (dd, $J = 12.8, 8.0$ Hz, 1H), 1.40 (s, 3H); ^{13}C NMR (101 MHz, CDCl_3) $\delta = 207.9, 168.4, 156.5, 151.6, 146.9, 125.2, 116.6, 112.0, 80.0, 75.4, 49.7, 47.2, 45.6, 41.1, 36.2, 35.4, 30.7, 26.7, 19.6$; IR (thin film, NaCl) 3440, 2968, 1746, 1713, 1644, 1442, 1418, 1359, 1289, 1213, 1117, 1042, 1021, 995, 973, 913, 810, 732; HRMS (ESI) m/z calc'd $\text{C}_{19}\text{H}_{25}\text{O}_4$ [M+H] $^+$: 317.1747, found: 317.1733; $[\alpha]_D^{23} -99.1$ (c 0.375, CHCl_3).



(1aR,1aS,2R,3aS,7aS)-2-hydroxy-2-methyl-6-((R)-4-oxo-2-(prop-1-en-2-yl)pentyl)-1a1,2,3,3a,7,7a-hexahydro-5H-oxireno[2',3':3a,4]indeno[1,7-bc]furan-5-one (454): To a pale yellow stirred solution of diene **453** (80 mg, 0.25 mmol, 1.0 equiv) in a round-bottom flask in benzene (8.4 mL, 0.044M) and CH_2Cl_2 (0.2 mL, 1 M) was added $\text{VO}(\text{acac})_2$ (6.7 mg, 0.025 mmol, 0.1 equiv). After 15 minutes, to this dark green solution was added *t*-butyl hydroperoxide (TBHP, 76 μL , 0.38 mmol, 1.5 equiv) as a 5 M solution in decane dropwise causing the reaction to immediately become deep ruby red. After 1 hour, the reaction had lost all red color and became pale yellow, and complete consumption of starting material was observed (as determined by TLC analysis, 1:1 hexanes:EtOAc). The crude reaction was directly purified by column chromatography (SiO_2 , 100% hexanes then 1:1 hexanes:EtOAc) to furnish epoxide **454** (76.3 mg, 91%) as a white amorphous solid.

($R_f = 0.11$); ^1H NMR (400 MHz, C_6D_6) δ 4.83 (q, $J = 0.9$ Hz, 1H), 4.75 (t, $J = 1.6$ Hz, 1H), 4.08 (ddd, $J = 8.5, 7.4, 6.3$ Hz, 1H), 3.38–3.31 (m, 1H), 3.05 (d, $J = 3.4$ Hz, 1H), 2.90 (dq, $J = 9.3, 6.3$ Hz, 1H), 2.41 (dd, $J = 17.0, 6.8$ Hz, 3H), 2.29–2.20 (m, 3H), 2.11 (ddd, $J = 12.7, 5.4, 1.9$ Hz, 1H), 2.05 (dd, $J = 13.5, 7.5$ Hz, 1H), 1.86 (dd, $J = 16.7, 2.4$ Hz, 1H), 1.82–1.74 (m, 1H), 1.70 (s, 3H), 1.63 (t, $J = 1.2$ Hz, 3H), 0.99 (s, 3H); ^{13}C NMR (101 MHz, C_6D_6) δ = 206.0, 168.9, 149.6, 147.7, 120.8, 111.5, 76.3, 73.3, 69.5, 51.6, 50.2, 47.0, 44.5, 41.0, 37.6, 36.0, 30.2, 22.4, 20.0; IR (thin film, NaCl) 3469, 2933, 1746, 1711, m1645, 1360, 1294, 1200, 1114, 1029, 967, 792 cm^{-1} ; HRMS (ESI) m/z calc'd $\text{C}_{19}\text{H}_{25}\text{O}_5$ [M+H] $^+$: 333.1697, found: 333.1703; $[\alpha]_D^{23} -88.9$ (c 0.375, CHCl_3).

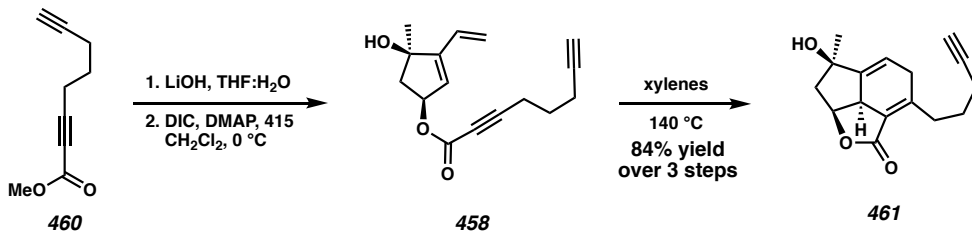


(2a1*S*,5*S*,5a*R*,6*R*,7a*S*)-5,6-dihydroxy-6-methyl-3-((*R*)-4-oxo-2-(prop-1-en-2-yl)pentyl)-4,5,5a,6,7,7a-hexahydroindeno[1,7-*bc*]furan-2(2a1*H*)-one (455):

Preparation of a 0.50 M Stock Solution: of Titanocene Monochloride (Cp_2TiCl): Into a thoroughly flame-dried Schlenk tube under an overpressure of argon was charged with zinc(0) dust (647 mg, 9.90 mmol, 3.00 equiv) and titanocene dichloride (Cp_2TiCl_2 , 822 mg, 3.30 mmol, 1.00 equiv). The flask was then evacuated and back filled with argon (3 x 5 minute cycles). To the reaction vessel was then added THF (6.6 mL). After 1.5 h, the bright red reaction mixture had become dark green and stirring was halted. After 30 minutes, the supernatant was used as a 0.50 M stock solution of Cp_2TiCl .

A stirred solution of epoxide **454** (15 mg, 0.045 mmol, 1.0 equiv) in THF (1.5 mL, 0.03 M). The homogeneous reaction mixture was then cooled to -78 °C followed by the

addition of H₂O (62 µL, 3.46 mmol, 76.9 equiv). After stirring for 5 minutes, Cp₂TiCl (0.87 mmol, 0.50 M in THF, 19.2 equiv) was added dropwise. After 2 h, was allowed to warm to ambient temperature (23 °C). After an additional 12 h, the complete consumption of starting material was observed (as determined by TLC 3:1 EtOAc:hexanes). The reaction was quenched by the addition of saturated NaH₂PO₄ (1.0 mL) and brine (1.0 mL), sparged with compressed air for 5 minutes, and allowed to stir for an additional 15 minutes. The reaction mixture was then filtered through a Celite® plug, washing with H₂O and EtOAc. The biphasic mixture was separated and the aqueous layer was extracted with EtOAc (3 X 3 mL). The combined organic layers were dried over MgSO₄, filtered, and concentrated in vacuo. The crude product was purified by column chromatography (SiO₂, 3:1 EtOAc:hexanes), furnishing diol **455** (14 mg, 92% yield) as a white amorphous solid (*R*_f= 0.22); ¹H NMR (400 MHz, CDCl₃) δ = 4.90 (ddd, *J* = 8.2, 6.6, 4.1 Hz, 1H), 4.80 (dt, *J* = 1.7, 0.8 Hz, 1H), 4.76 (p, *J* = 1.5 Hz, 1H), 4.69 (dt, *J* = 7.8, 3.2 Hz, 1H), 3.35–3.25 (m, 1H), 3.05 (ddd, *J* = 9.9, 8.0, 2.0 Hz, 1H), 2.94 (dq, *J* = 9.2, 6.5 Hz, 1H), 2.67–2.49 (m, 3H), 2.41–2.29 (m, 2H), 2.14–1.98 (m, 6H), 1.75 (dd, *J* = 1.5, 0.8 Hz, 3H), 1.43 (s, 3H); ¹³C NMR (101 MHz, CDCl₃) δ = 208.3, 169.7, 151.7, 147.8, 124.9, 111.5, 81.7, 79.2, 68.5, 49.6, 48.5, 47.2, 44.4, 41.3, 40.6, 37.7, 30.8, 28.8, 20.1; IR (thin film, NaCl) 3384, 2966, 1738, 1666, 1420, 1359, 1304, 1222, 1200, 1145, 1105, 1040, 1020, 910, 733 cm⁻¹; HRMS (ESI) m/z calc'd C₁₉H₂₇O₅ [M+H]⁺: 335.1853, found: 335.1844; [α]_D²³ -15.4 (c 0.205, CHCl₃).

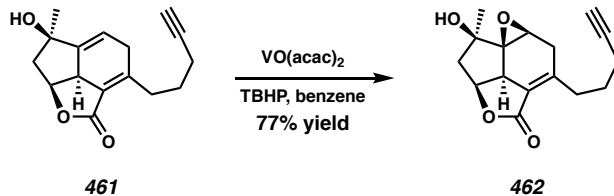


(2a1*S*,6*R*,7a*S*)-6-hydroxy-6-methyl-3-(pent-4-yn-1-yl)-4,6,7,7a-tetrahydroindeno[1,7-*bc*]furan-2(2a1*H*)-one (461): Ester **460** was saponified under the same conditions

reported above for ester **448**. A stirred solution of Diol **415** (250 mg, 1.8 mmol, 1 equiv), octa-2,7-diynoic acid (435 mg, 3.2 mmol, 1.8 equiv), and DMAP (21.8 mg, 0.18 mmol, 0.1 equiv) in CH_2Cl_2 (18 mL, 0.1 M) and THF (10 mL, 0.18 M) was cooled to 0 °C. DIC (0.50 mL, 3.2 mmol, 1.8 equiv) was added dropwise via syringe and the resultant solution was allowed to stir for 2 h. Upon complete consumption of starting material (as determined by TLC analysis, 4:1 hexanes:EtOAc), the reaction was diluted with H_2O (20 mL) and extracted with Et₂O (3 x 20 mL). The combined organic layers were dried over MgSO₄, filtered, and concentrated in vacuo. The crude product was purified by column chromatography (SiO₂, 4:1 hexanes:EtOAc) to afford a mixture of triphenylphosphine oxide and ester **458** which is used directly in the next reaction. Ester **458** can be further purified by another column of the same eluent to obtain pure ester **458** ($R_f = 0.22$); ¹H NMR (400 MHz, CDCl₃) δ = 6.32 (ddt, J = 17.8, 11.3, 0.8 Hz, 1H), 5.82 (dd, J = 2.3, 0.8 Hz, 1H), 5.81–5.75 (m, 1H), 5.55 (dd, J = 7.4, 4.4, 2.3, 0.7 Hz, 1H), 5.33 (dd, J = 11.3, 1.5 Hz, 1H), 2.64 (dd, J = 14.3, 7.3 Hz, 1H), 2.48 (t, J = 7.1 Hz, 2H), 2.32 (td, J = 6.9, 2.7 Hz, 2H), 2.06 (dd, J = 14.3, 4.4 Hz, 1H), 1.98 (t, J = 2.6 Hz, 1H), 1.80 (p, J = 7.0 Hz, 2H), 1.44 (s, 3H); ¹³C NMR (101 MHz, CDCl₃) δ = 153.5, 151.9, 128.9, 126.0, 119.6, 88.7, 82.8, 81.1, 77.1, 73.7, 69.6, 48.9, 26.8, 26.5, 17.8, 17.7; IR (thin film, NaCl) 3295,

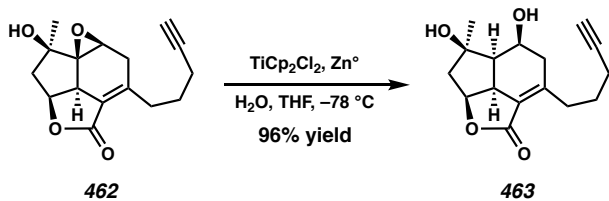
2972, 2236, 1703, 1432, 1252, 1073, 990, 950, 872, 752, 641 cm⁻¹; HRMS (ESI) m/z calc'd C₁₆H₂₂NO₃ [M+NH₄]⁺: 276.1595, found: 276.15811; [α]_D²³ –155.1 (c 0.57, CHCl₃).

Crude ester **458** (460 mg, 1.78 mmol) was transferred to a Schlenk bomb with xylenes (178 mL, 0.01 M). The Schlenk was the rigorously degassed by standard freeze-pump-thaw technique and upon reaching ambient temperature (23 °C) the flask was sealed and heat to 140 °C. The reaction was allowed to stir at this temperature of 2 h at which time complete consumption of starting material was observed (as determined by TLC analysis, 1:1 hexanes:EtOAc). The reaction was allowed to cool to room temperature and was directly purified by column chromatography (SiO₂, 100% hexanes then 1:1 hexanes:EtOAc) to furnish tricycle **461** (560 mg, 84% over 3 steps) as a pale yellow solid (R_f = 0.25); ¹H NMR (400 MHz, CDCl₃) δ = 5.85 (ddd, *J* = 6.3, 2.9, 1.9 Hz, 1H), 4.97 (ddd, *J* = 9.0, 7.9, 7.1 Hz, 1H), 3.30 (ttd, *J* = 9.2, 1.9, 1.0 Hz, 1H), 3.11–2.96 (m, 2H), 2.75 (ddt, *J* = 18.4, 10.1, 1.5 Hz, 1H), 2.62–2.54 (m, 1H), 2.51 (ddd, *J* = 12.8, 7.1, 0.8 Hz, 1H), 2.22 (tt, *J* = 7.1, 2.5 Hz, 2H), 1.98 (t, *J* = 2.6 Hz, 1H), 1.78 (td, *J* = 6.6, 5.5, 3.3 Hz, 1H), 1.76–1.63 (m, 3H), 1.41 (d, *J* = 1.1 Hz, 3H); ¹³C NMR (101 MHz, CDCl₃) δ = 168.2, 157.1, 152.1, 124.4, 116.4, 84.0, 80.0, 75.4, 69.1, 49.7, 45.5, 35.2, 31.0, 27.2, 26.8, 18.4; IR (thin film, NaCl) 3425, 3288, 2971, 1738, 1643, 1439, 1326, 1288, 1256, 1218, 1194, 1117, 1041, 996, 967, 817, 742, 638 cm⁻¹; HRMS (ESI) m/z calc'd C₁₆H₁₉O₃ [M+H]⁺: 259.1329, found: 259.1323; [α]_D²³ –120.3 (c 0.635, CHCl₃).



(1a*R*,1a*S*,2*R*,3a*S*,7a*S*)-2-hydroxy-2-methyl-6-(pent-4-yn-1-yl)-1a1,2,3,3a,7,7a-hexahydro-5*H*-oxireno[2',3':3a,4]indeno[1,7-*bc*]furan-5-one (462):

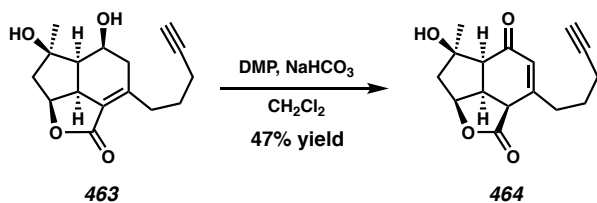
To a pale yellow stirred solution of diene **461** (376 mg, 1.5 mmol, 1.0 equiv) in a round-bottom flask in benzene (49 mL, 0.03M) was added VO(acac)₂ (29 mg, 0.11 mmol, 0.075 equiv). After 15 minutes, to this dark green solution was added *t*-butyl hydroperoxide (TBHP, 0.58 mL, 2.9 mmol, 2.0 equiv) as a 5 M solution in decane dropwise causing the reaction to immediately become deep ruby red. After 2 hours, the reaction had lost all red color and become pale yellow and complete consumption of starting material was observed (as determined by TLC analysis, 3:7 hexanes:EtOAc). The crude reaction was directly purified by column chromatography (SiO₂, 100% hexanes then 3:7 hexanes:EtOAc) to furnish epoxide **462** (307 mg, 77%) as a white amorphous solid (*R*_f = 0.3); ¹H NMR (400 MHz, CDCl₃) δ = 4.83 (ddd, *J* = 8.5, 7.4, 6.3 Hz, 1H), 3.81 (dd, *J* = 3.3, 0.8 Hz, 1H), 3.28 (d, *J* = 8.1 Hz, 1H), 2.88 (dd, *J* = 16.7, 3.4 Hz, 1H), 2.84–2.68 (m, 2H), 2.59 (ddd, *J* = 13.6, 7.4, 0.6 Hz, 1H), 2.55–2.45 (m, 2H), 2.35–2.12 (m, 2H), 2.08–1.99 (m, 1H), 1.98 (t, *J* = 2.6 Hz, 1H), 1.81–1.62 (m, 2H), 1.44 (d, *J* = 1.0 Hz, 3H); ¹³C NMR (101 MHz, CDCl₃) δ = 169.1, 150.9, 119.9, 84.1, 76.6, 73.6, 70.0, 69.0, 51.8, 50.1, 44.8, 35.7, 31.6, 26.9, 22.7, 18.3; IR (thin film, NaCl) 3529, 3270, 2976, 2938, 2116, 1742, 1649, 1454, 1422, 1391, 1348, 1324, 1296, 1268, 1195, 1113, 1093, 1030, 964, 923, 899, 795, 756, 733, 678 cm⁻¹; HRMS (ESI) m/z calc'd C₁₆H₁₉O₄ [M+H]⁺: 275.1278, found: 275.1268; [α]_D²³ –179.9 (*c* 0.39, CHCl₃).



(2a1*S*,5*S*,5a*R*,6*R*,7a*S*)-5,6-dihydroxy-6-methyl-3-(pent-4-yn-1-yl)-4,5,5a,6,7,7a-hexahydroindeno[1,7-*bc*]furan-2(2a1*H*)-one (463):

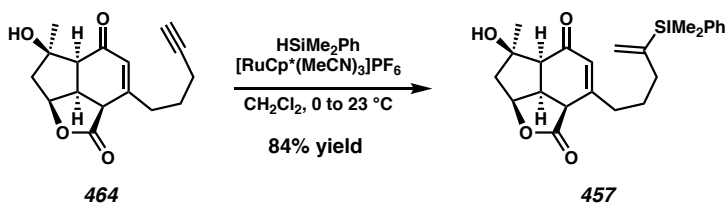
A stirred solution of epoxide **462** (278 mg, 1.01 mmol, 1.0 equiv) in THF (34 mL, 0.03 M). The homogeneous reaction mixture was then cooled to $-78\text{ }^{\circ}\text{C}$ followed by the addition of H_2O (0.9 mL, 50.0 mmol, 50 equiv). After stirring for 5 minutes, Cp_2TiCl (11.1 mmol, 0.50 M in THF, 11 equiv) was added dropwise. After 2 h, was allowed to slowly warm to ambient temperature ($23\text{ }^{\circ}\text{C}$). After an additional 12 h, the complete consumption of starting material was observed (as determined by TLC 3:1 EtOAc:hexanes). The reaction was quenched by the addition of saturated NaH_2PO_4 (20 mL) and brine (10 mL), sparged with compressed air for 5 minutes, and allowed to stir for an additional 15 minutes. The reaction mixture was then filtered through a Celite® plug, washing with H_2O and EtOAc. The biphasic mixture was separated and the aqueous layer was extracted with EtOAc (3 X 50 mL). The combined organic layers were dried over MgSO_4 , filtered, and concentrated in vacuo. The crude product was purified by column chromatography (SiO_2 , 3:1 EtOAc:hexanes), furnishing diol **463** (270 mg, 96% yield) as a viscous colorless oil ($R_f = 0.3$); ^1H NMR (400 MHz, CDCl_3) δ = 4.91 (ddd, $J = 8.1, 6.7, 3.1\text{ Hz}$, 1H), 4.69 (ddd, $J = 8.1, 3.5, 2.8\text{ Hz}$, 1H), 3.43 (s, 2H), 3.08 (ddd, $J = 9.7, 7.9, 2.0\text{ Hz}$, 1H), 2.98–2.88 (m, 1H), 2.70 (dtd, $J = 12.6, 7.4, 1.8\text{ Hz}$, 1H), 2.58 (dd, $J = 14.9, 2.8\text{ Hz}$, 1H), 2.39 (dd, $J = 9.4, 8.0\text{ Hz}$, 1H), 2.23 (qd, $J = 7.2, 2.6\text{ Hz}$, 2H), 2.13 (dd, $J = 14.4, 3.1\text{ Hz}$, 1H), 2.10–2.03 (m, 1H), 1.99 (dd, $J = 14.3, 6.6\text{ Hz}$, 1H), 1.95 (t, $J = 2.6\text{ Hz}$, 1H), 1.72 (p, $J = 7.4\text{ Hz}$, 2H), 1.44 (s, 3H); ^{13}C NMR (101

MHz, CDCl₃) δ = 169.9, 152.5, 124.3, 84.4, 82.0, 79.5, 68.8, 68.3, 49.8, 48.6, 44.6, 41.4, 31.9, 28.6, 26.5, 18.5; IR (thin film) 3302, 2966, 2930, 2251, 1738, 1731, 1668, 1454, 1427, 1358, 1336, 1305, 1278, 1248, 1222, 1198, 1144, 1119, 1104, 1069, 1045, 1018, 989, 926, 912, 874, 853, 768, 737, 650; HRMS (ESI) m/z calc'd C₁₆H₂₁O₄ [M+H]⁺: 277.1434, found: 277.1430; [α]_D²³ -16.0 (c 0.72, CHCl₃).



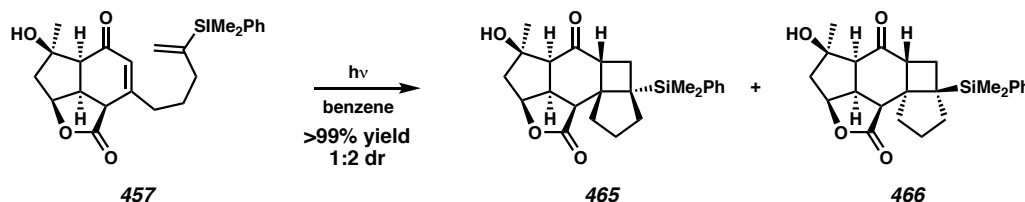
(2a*S*,2a1*S*,5a*S*,6*R*,7a*S*)-6-hydroxy-6-methyl-3-(pent-4-yn-1-yl)-2a,2a1,5a,6,7,7a-hexahydroindeno[1,7-*bc*]furan-2,5-dione (464): Diol **463** (270 mg, 0.98 mmol, 1.0 equiv) in CH₂Cl₂ (27 mL, 0.036 M) was added NaHCO₃ (330 mg, 3.9 mmol, 4 equiv) and DMP (538 mg, 1.3 mmol, 1.3 equiv) at ambient temperature (23 °C) with stirring. The reaction vessel was then sealed and stirred for 3 h. Each subsequent hour, more DMP was added (1 equiv) until complete consumption of starting material (as determined by TLC analysis, 1:3 hexanes:EtOAc). The reaction was then quenched by the addition of saturated Na₂S₂O₃ (30 mL) and saturated NaHCO₃ (20 mL). After stirring for 10 minutes, the reaction mixture was extracted with CH₂Cl₂ (3 x 30 mL). The combined organics were then dried over MgSO₄, filtered, and concentrated in vacuo. The crude product was then purified by column chromatography (SiO₂, 1:3 hexanes:EtOAc) to afford enone **464** (117 mg, 47%) as a colorless viscous oil (*R*_f = 0.6); ¹H NMR (400 MHz, CDCl₃) δ = 6.07 (q, *J* = 1.5 Hz, 1H), 5.12 (dd, *J* = 7.1, 5.4 Hz, 1H), 3.63 (dd, *J* = 10.9, 10.2, 7.1, 0.6 Hz, 1H), 3.51–3.45 (m, 1H), 2.90–2.78 (m, 1H), 2.78–2.66 (m, 1H), 2.53 (d, *J* = 10.2 Hz, 1H), 2.33 (d, *J* = 15.0 Hz, 1H), 2.27 (tdd, *J* = 7.1, 6.1, 2.7 Hz, 2H), 1.99 (t, *J* = 2.6 Hz, 1H), 1.91 (dd, *J* = 15.0,

5.5 Hz, 1H), 1.87–1.74 (m, 2H), 1.51 (s, 3H); ^{13}C NMR (101 MHz, CDCl_3) δ = 196.0, 173.5, 157.6, 127.5, 83.6, 82.8, 82.5, 69.4, 55.2, 47.4, 42.5, 42.2, 34.7, 26.4, 25.6, 18.2; IR (thin film, NaCl) 3442, 3282, 2966, 1757, 1649, 1375, 1289, 1255, 1214, 1179, 1104, 1033, 1017, 993, 938; HRMS (ESI) m/z calc'd $\text{C}_{16}\text{H}_{19}\text{O}_4$ [M+H] $^+$: 275.1278, found: 275.1269; $[\alpha]_D^{23} -195$ (c 0.32, CHCl_3).



(2a*S*,2a1*S*,5a*S*,6*R*,7a*S*)-3-(4-(dimethylphenylsilyl)pent-4-en-1-yl)-6-hydroxy-6-methyl-2a,2a1,5a,6,7,7a-hexahydroindeno[1,7-*bc*]furan-2,5-dione (457): Alkyne **464** (28 mg, 0.1 mmol, 1 equiv) and dimethylphenylsilane (18 μL , 0.12 mmol, 1.2 equiv) was dissolved in CH_2Cl_2 (0.5 mL, 0.2 M) and sparged with Ar for 5 min. A stock solution of $[\text{RuCp}^*(\text{MeCN})_3]\text{PF}_6$ (0.5 mg, 1mg/mL, 0.01 equiv) prepared in the gloved box and was added to the reaction. The reaction was allowed to stir for 15 min, at which time complete consumption of starting material was observed (as determined by TLC analysis, 1:3 hexanes:EtOAc). The solution was then concentrated and directly purified by column chromatography (SiO_2 , 1:3 hexanes:EtOAc) to afford vinyl silane **457** (19 mg, 64%) as a colorless amorphous solid ($R_f = 0.55$); ^1H NMR (400 MHz, CDCl_3) δ = 7.60–7.48 (m, 2H), 7.44–7.30 (m, 3H), 5.94 (q, $J = 1.4$ Hz, 1H), 5.70 (dt, $J = 2.9, 1.5$ Hz, 1H), 5.46 (dt, $J = 2.7, 1.0$ Hz, 1H), 5.07 (dd, $J = 7.2, 5.4$ Hz, 1H), 3.48 (dd, $J = 10.9, 10.2, 7.1, 0.6$ Hz, 1H), 3.16 (dd, $J = 11.1, 1.5$ Hz, 1H), 2.66–2.50 (m, 2H), 2.48 (d, $J = 10.2$ Hz, 1H), 2.30 (d, $J = 15.0$ Hz, 1H), 2.24–2.08 (m, 2H), 1.89 (dd, $J = 15.0, 5.5$ Hz, 1H), 1.67–1.51 (m, 2H), 1.49 (s, 3H), 0.37 (s, 6H); ^{13}C NMR (101 MHz, CDCl_3) δ = 196.0, 173.4, 158.7, 149.7,

138.4, 134.1, 129.1, 128.0, 127.3, 126.7, 82.7, 82.4, 55.2, 47.4, 42.2, 41.9, 35.7, 35.4, 26.5, 26.1, -2.8, -2.9; IR (thin film, NaCl) 3450, 2958, 1759, 1650, 1378, 1290, 1248, 1173, 1107, 992, 818 cm^{-1} ; HRMS (ESI) m/z calc'd $\text{C}_{23}\text{H}_{31}\text{O}_4\text{Si}$ [M+H]⁺: 411.1986, found: 411.1972; $[\alpha]_D^{23} -115.3$ (*c* 0.25, CHCl_3).

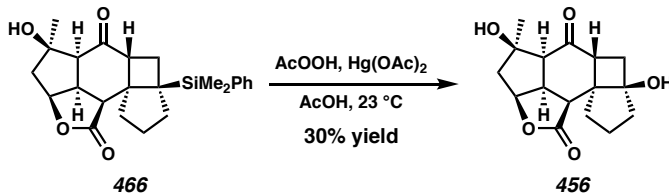


(2a*S*,2a*1S*,4*R*,4a*S*,5a*R*,6a*S*,9a*S*,9b*S*)-6a-(dimethyl(phenyl)silyl)-4-hydroxy-4-methyldodecahydrocyclopenta[2',3']cyclobuta[1',2':5,6]indeno[1,7-*bc*]furan-1,5-dione (465) and (2a*S*,2a*1S*,4*R*,4a*S*,5a*R*,6a*R*,9a*R*,9b*S*)-6a-(dimethyl(phenyl)silyl)-4-hydroxy-4-methyldodecahydrocyclopenta[2',3']cyclobuta[1',2':5,6]indeno[1,7-*bc*]furan-1,5-dione (466): Enone 457 (19 mg, 0.0465 mmol, 1 equiv) in a 20 mL vial was dissolved in benzene (4.65 mL, 0.01 M) and was sparged with Ar for 10 min. The reaction vessel was sealed and irradiated with UVB light. After 2 hours complete consumption of starting material was observed (as determined by TLC analysis, 1:1 hexanes:EtOAc) and was directly purified by column chromatography (SiO_2 , 100% hexanes then 1:1 hexanes:EtOAc) to afford a 2:1 mixture of pentacycle 465 and 466 (19 mg, >99%) as a colorless amorphous solid which crystallizes in benzene ($R_f = 0.85$, 465, and 0.65, 366).

465: ^1H NMR (400 MHz, CDCl_3) δ = 7.66–7.53 (m, 2H), 7.45–7.37 (m, 3H), 4.59 (ddd, J = 6.6, 5.6, 2.0 Hz, 1H), 3.02 (s, 1H), 2.92 (ddd, J = 11.1, 9.8, 6.7 Hz, 1H), 2.74–2.66 (m, 2H), 2.41–2.33 (m, 2H), 2.31–2.21 (m, 1H), 2.17 (s, 1H), 2.13 (dd, J = 14.6, 2.0 Hz, 1H), 2.03–1.82 (m, 4H), 1.81–1.72 (m, 1H), 1.66–1.59 (m, 1H), 1.18 (s, 3H), 0.41 (s, 3H), 0.30 (s, 3H); ^{13}C NMR (101 MHz, CDCl_3) δ = 215.6, 174.9, 138.3, 134.4, 129.9, 128.5, 80.9,

80.9, 55.4, 53.3, 48.4, 45.8, 44.5, 43.4, 39.7, 39.0, 38.7, 29.0, 28.6, 24.5, -2.9, -3.9; IR (thin film, NaCl) 3416, 2957, 1759, 1673, 1359, 1107, 731 cm^{-1} ; HRMS (ESI) m/z calc'd C₂₃H₃₁O₄Si [M+H]⁺: 411.1986, found: 411.1976; $[\alpha]_D^{23} -17.7$ (*c* 0.3, CHCl₃).

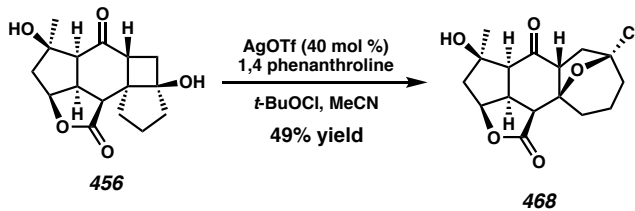
466: ¹H NMR (400 MHz, CDCl₃) δ = 7.57–7.47 (m, 2H), 7.37–7.28 (m, 3H), 4.91 (dd, *J* = 6.1, 4.5 Hz, 1H), 3.60–3.52 (m, 1H), 3.52–3.48 (m, 1H), 2.94 (dd, *J* = 9.0, 0.7 Hz, 1H), 2.56 (d, *J* = 10.6 Hz, 1H), 2.36 (d, *J* = 15.2 Hz, 1H), 2.21–2.14 (m, 2H), 2.08–2.00 (m, 1H), 1.96–1.88 (m, 2H), 1.88–1.76 (m, 1H), 1.73–1.59 (m, 2H), 1.45 (s, 3H), 1.32 (dd, *J* = 11.9, 6.6 Hz, 1H), 0.55 (s, 3H), 0.52 (s, 3H); ¹³C NMR (101 MHz, CDCl₃) δ = 205.7, 174.8, 141.4, 134.2, 128.5, 127.6, 82.1, 81.4, 60.6, 60.1, 51.3, 50.1, 48.6, 47.7, 43.9, 39.9, 37.1, 27.6, 27.1, 24.5, -2.1, -4.7; IR (thin film, NaCl) 3393, 2949, 1769, 1687, 1373, 1242, 1209, 1147, 1104, 1089, 826, 783, 733; HRMS (ESI) m/z calc'd C₂₃H₃₁O₄Si [M+H]⁺: 411.1986, found: 411.1972; $[\alpha]_D^{23} -19.7$ (*c* 0.35, CHCl₃).



(2a*S*,2a*1S*,4*R*,4a*S*,5a*R*,6a*R*,9a*R*,9b*S*)-4,6a-dihydroxy-4-methyldodecahydrocyclopenta[2',3']cyclobuta[1',2':5,6]indeno[1,7-bc]furan-1,5-dione (456):

To a solution of lactone **466** (25 mg, 0.061 mmol) in 35% AcOOH-AcOH (3.05 mL, 0.02 M) at 23 °C was added Hg(OAc)₂ (92 mg, 0.29 mmol, 4.8 equiv), and the clear solution was stirred for 1 h at which time complete consumption of starting material was observed (as determined by TLC analysis, 1:3 hexanes:EtOAc). The reaction mixture was diluted with Et₂O (5 mL), washed sequentially with 10% aq Na₂S₂O₃ (7 mL), H₂O (7 mL), saturated solution of NaHCO₃ (7 mL), and brine (7 mL), dried over MgSO₄, filtered,

and concentrated in vacuo. The crude product was purified by column chromatography (SiO_2 , 1:3 hexanes:EtOAc) to afford diol **456** (6 mg, 30%) as a white amorphous powder ($R_f = 0.20$) ^1H NMR (400 MHz, CDCl_3) δ = 6.16 (s, 1H), 5.13 (dd, $J = 5.9, 4.6$ Hz, 1H), 3.90 (t, $J = 9.5$ Hz, 1H), 3.57–3.43 (m, 1H), 3.21 (dd, $J = 9.0, 0.8$ Hz, 1H), 2.58 (d, $J = 10.6$ Hz, 1H), 2.47–2.34 (m, 2H), 2.07–1.94 (m, 2H), 1.94–1.87 (m, 1H), 1.87–1.78 (m, 1H), 1.78–1.68 (m, 3H), 1.48 (s, 3H), 1.25 (d, $J = 2.5$ Hz, 1H); ^{13}C NMR (101 MHz, CDCl_3) δ = 205.5, 179.1, 88.5, 86.1, 81.5, 60.8, 55.4, 52.3, 49.4, 47.7, 47.1, 38.1, 36.4, 34.5, 27.8, 23.1; IR (thin film, NaCl) 3421, 2972, 2923, 1741, 1686, 1448, 1400, 1377, 1305, 1276, 1211, 1161, 1112, 1088, 1069, 1010, 921, 850, 813, 777, 733, 719; HRMS (ESI) m/z calc'd $\text{C}_{16}\text{H}_{21}\text{O}_5$ [M+H] $^+$: 293.1384, found: 293.1372; $[\alpha]_D^{23} -40.4$ (c 0.13, CHCl_3).



(2a*S*,2a*S*,4*R*,4a*S*,5a*R*,7*R*,10a*R*,10b*S*)-7-chloro-4-hydroxy-4-methyldodecahydro-7,10a-epoxycyclohepta[5,6]indeno[1,7-*bc*]furan-1,5-dione (468): Diol **456** (10 mg, 0.034 mmol, 1 equiv), AgOTf (1.2 mg, 0.012 mmol, 0.4 equiv), and 1,10-phenanthroline (4.8 mg, 0.024 mmol, 0.8 equiv) were placed in a round-bottom flask and dissolved in MeCN (1 mL, 0.034 M) followed by the addition of *t*-BuOCl (7.8 μL , 0.068 mmol, 2 equiv). The reaction mixture was stirred at ambient temperature (23 °C) for 6 h. The reaction was quenched with saturated solution of $\text{Na}_2\text{S}_2\text{O}_3$ and extracted with EtOAc (3 x 5 mL). The combined organic layers were washed with brine, dried over MgSO_4 , filtered, and concentrated in vacuo. The crude product was purified by column chromatography (SiO_2 , 1:3 hexanes:EtOAc) to obtain furan **468** (5.4 mg, 49%) as a white amorphous solid.

which can be crystallized in CHCl₃ (R_f = 0.26); ¹H NMR (400 MHz, CDCl₃) δ = 5.02 (dd, J = 5.9, 4.5 Hz, 1H), 3.79–3.66 (m, 1H), 3.42 (dddd, J = 10.3, 9.5, 5.9, 0.6 Hz, 1H), 3.34 (dd, J = 9.5, 0.7 Hz, 1H), 2.88 (ddd, J = 13.8, 7.4, 0.9 Hz, 1H), 2.71 (d, J = 10.4 Hz, 1H), 2.42 (d, J = 15.4 Hz, 1H), 2.35 (ddd, J = 13.8, 11.6, 1.1 Hz, 1H), 2.29–2.09 (m, 1H), 2.07–1.96 (m, 2H), 1.75–1.64 (m, 3H), 1.49 (s, 3H), 1.46–1.34 (m, 1H); ¹³C NMR (101 MHz, CDCl₃) δ = 202.8, 172.0, 101.8, 85.2, 82.7, 82.3, 60.6, 56.4, 48.6, 47.5, 45.9, 40.1, 36.3, 33.1, 27.6, 18.9; IR (thin film, NaCl) 3472, 2921, 1766, 1713, 1359, 1243, 1214, 1171, 1126, 1093, 1000, 953, 905, 845, 759, 731; HRMS (ESI) m/z calc'd C₁₆H₂₀O₅Cl [M+H]⁺: 327.0994, found: 327.0980; $[\alpha]_D^{23}$ –43.3 (*c* 0.13, CHCl₃).

4.15 NOTES & REFERENCES

1. Newman, D. J.; Cragg, G. M.; Snader, K. M. *Nat Prod. Rep.* **2000**, *17*, 215–234.
2. Dias, D. A.; Urban, S.; Roessner, U. *Metabolites* **2012**, *2*, 303–336.
3. Kamel, H. N.; Slattery, M. *Pharmaceutical Biology* **2005**, *43*, 253–269.
4. Missakian, M. G.; Burreson, B. J.; Scheuer, P. J. *Tetrahedron* **1975**, *31*, 2513–2515.
5. Zhang, P.-P.; Yan, Z.-M.; Li, Y.-H.; Gong, J.-X.; Yang, Z. *J. Am. Chem. Soc.* **2017**, *139*, 13989–13992.
6. González, M. A.; Ghosh, S.; Rivas, F.; Fischer, D.; Theodorakis, E. A. *Tetrahedron Lett.* **2004**, *45*, 5039–5041.
7. Müller, S.; Liepold, B.; Roth, G. J.; Bestmann, H. J. *Synlett* **1996**, 521–522.
8. Anderson, N. H.; Uh, H.-S. *Synth. Commun.* **1973**, *3*, 125–128.
9. Craig, II, R. A.; Roizen, J. L.; Smith, R. C.; Jones, A. C.; Virgil, S. C.; Stoltz, B. M. *Chem. Sci.* **2017**, *8*, 507–514.

-
10. Inanaga, J.; Hirata, K.; Saeki, H.; Katsuki, T.; Yamaguchi, M. *Bull. Chem. Soc. Jpn.* **1979**, *52*, 1989–1993.
 11. (a) Grubbs, R. H. *Tetrahedron* **2004**, *60*, 7117–7140. (b) Gradillas, A.; Pérez-Castells, J. *Angew. Chem. Int. Ed.* **2006**, *45*, 6086–610.
 12. Hoye, T. R.; Jeffrey, C. S.; Tennakoon, M. A.; Wang, J.; Zhao, H. *J. Am. Chem. Soc.* **2004**, *126*, 10210–10211.
 13. Brill, Z. G.; Grover, H. K.; Maimone, T. J. *Science* **2016**, *27*, 1078–1082.
 14. Bauta, W.; Booth, J.; Bos, M. E.; DeLuca, M.; Diorazio, L.; Donohoe, T.; Magnus, N.; Magnus, P.; Mendoza, J.; Pye, P.; Tarrant, J.; Thom, S.; Ujjainwalla, F. *Tetrahedron Lett.* **1995**, *36*, 5327–5330.
 15. Yusuke, I.; Isao, S.; Akio, Y. *Bull Chem. Soc. Jpn.* **2004**, *77*, 2033–2045.
 16. Jiménez, T.; Campaña, A. G.; Bazdi, B.; Paradas, M.; Arráez-Román, D.; Segura-Carretero, A.; Fernández-Gutiérrez, A.; Oltra, J. E.; Robles, R.; Justicia, J.; Cuerva, J. M. *Eur. J. Org. Chem.* **2010**, 4288–4295.
 17. Ireland, R. E.; Norbeck, D. W. *J. Org. Chem.* **1985**, *50*, 2198–2200.
 18. Ley, S. V.; Norman, J.; Griffith, W. P.; Marsden, S. P. *Synthesis* **1994**, 639–666.
 19. Hoover, J. M.; Stahl, S. S. *J. Am. Chem. Soc.* **2011**, *133*, 16901–16910.
 20. Kantorowski, E. J.; Kurth, M. J. *Tetrahedron* **2000**, *56*, 4317–4353
 21. Piers, E.; Wong, T.; Ellis, K. A. *Can. J. Chem.* **1992**, *70*, 2058–2064.
 22. Trost, B. M.; Ball, Z. T. *J. Am. Chem. Soc.* **2001**, *123*, 12726–12727.
 23. Hydrosilylation with triethoxysilane has been performed as well
 24. Stoltz, B. M.; Kano, T.; Corey, E. J. *J. Am. Chem. Soc.* **2000**, *122*, 9044–9045.

-
25. Preliminary results suggest that heat the solution to 60 °C allows for conversion to the desired product.
 26. (a) Hiroshi, S.; Masahito, I.; Kazuhiro, K. *Chem. Lett.* **1987**, *16*, 1527–1530. (b) Renata, H.; Zhou, Q.; Dünstl, G.; Felding, J.; Merchant, R., R.; Yeh, C.-H.; Baran, P. S. *J. Am. Chem. Soc.* **2015**, *137*, 1330–1340. (c) Takasu, K.; Nagao, S.; Ihara, M. *Tetrahedron Lett.* **2005**, *46*, 1005–1008.
 27. Huang, F.-Q., Sun J.-G.; Wang, Y.-W.; Dong, X.; Qi, L.-W.; Zhang, B. *Org. Lett.* **2016**, *18*, 684–687.
 28. Pangborn, A. M.; Giardello, M. A.; Grubbs, R. H.; Rosen, R. K.; Timmers, F. J. *Organometallics* **1996**, *15*, 1518–1520.
 29. Ireland, R. E.; Liu, L. *J. Org. Chem.* **1993**, *58*, 2899–2899.

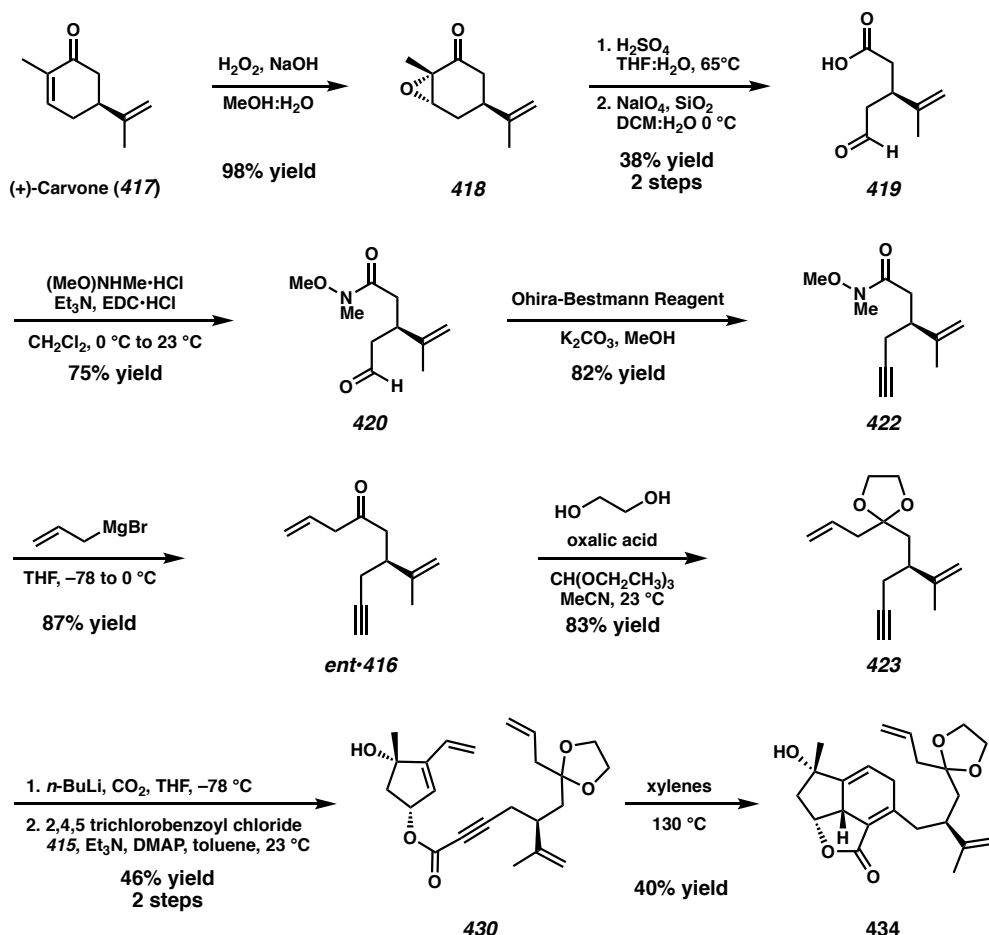
APPENDIX 5

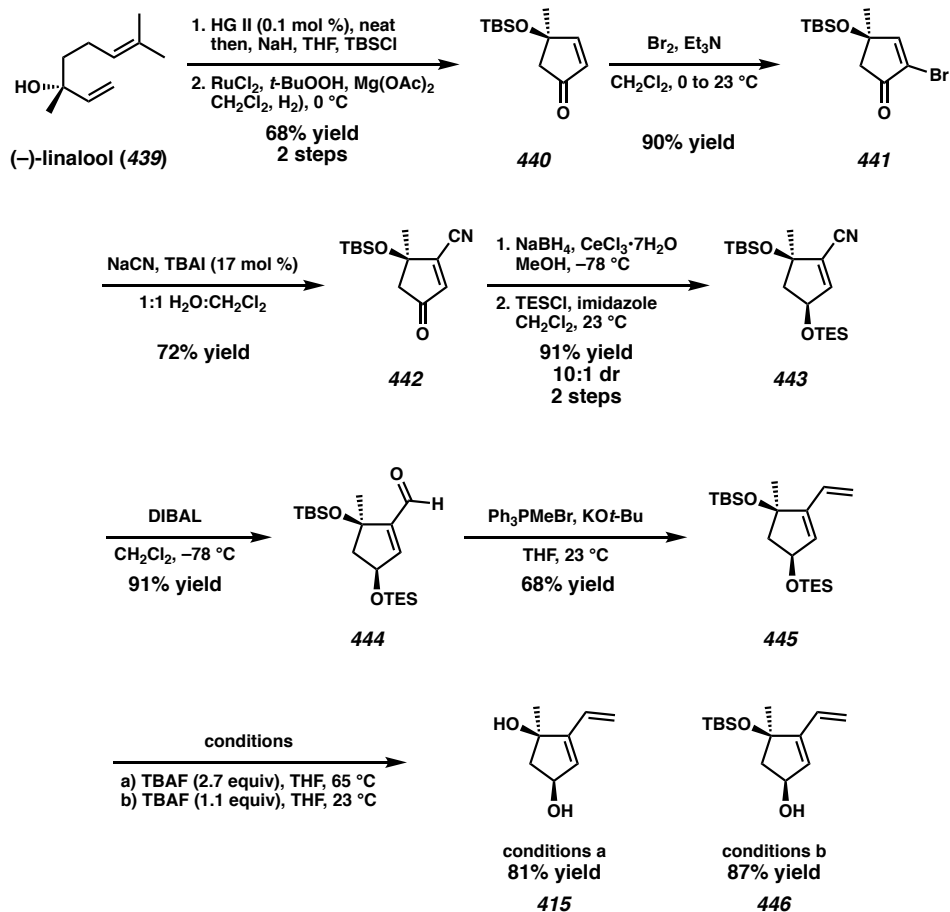
Synthetic Summary of Chapter 4:

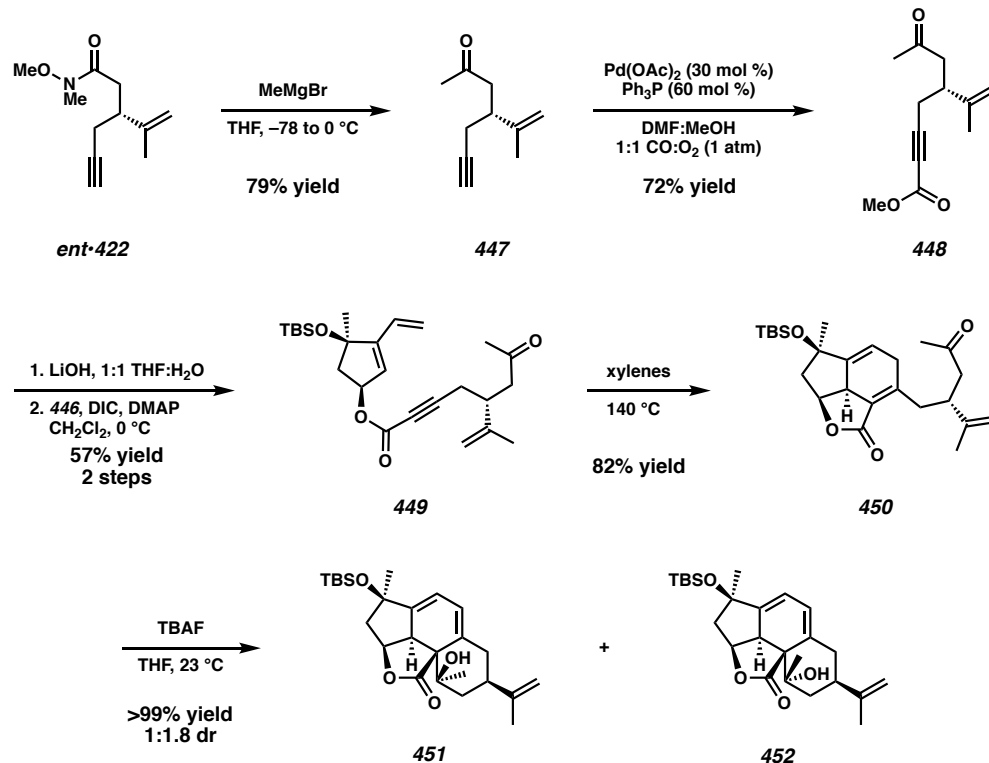
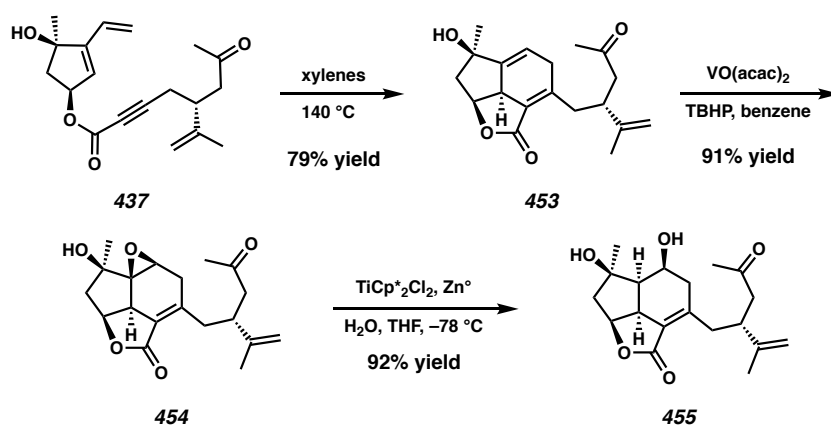
Progress Toward the Total Synthesis

of Scabrolide A

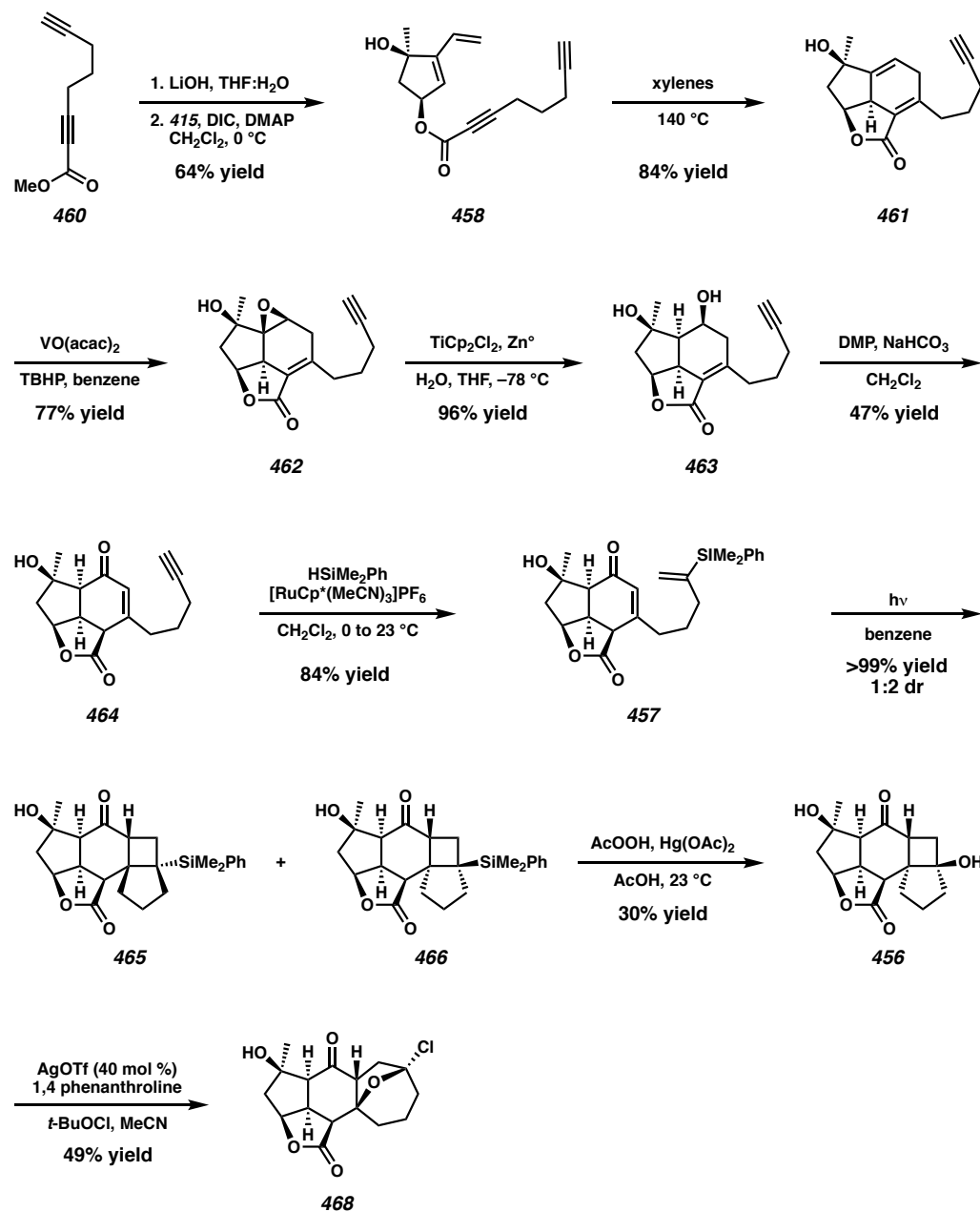
Scheme A5.1. Synthetic Summary for Construction of Tricycle 434



Scheme A5.2. Synthetic Summary for 2nd Generation Synthesis of Diol 415

Scheme A5.3 Synthetic Summary for Undesired Aldol Products **451** and **452**Scheme A5.4 Synthetic Summary for Late-Stage Functionalization of Diels–Alder Adduct **453**

Scheme A5.5 Synthetic Summary for Ring Expansion Model System 458

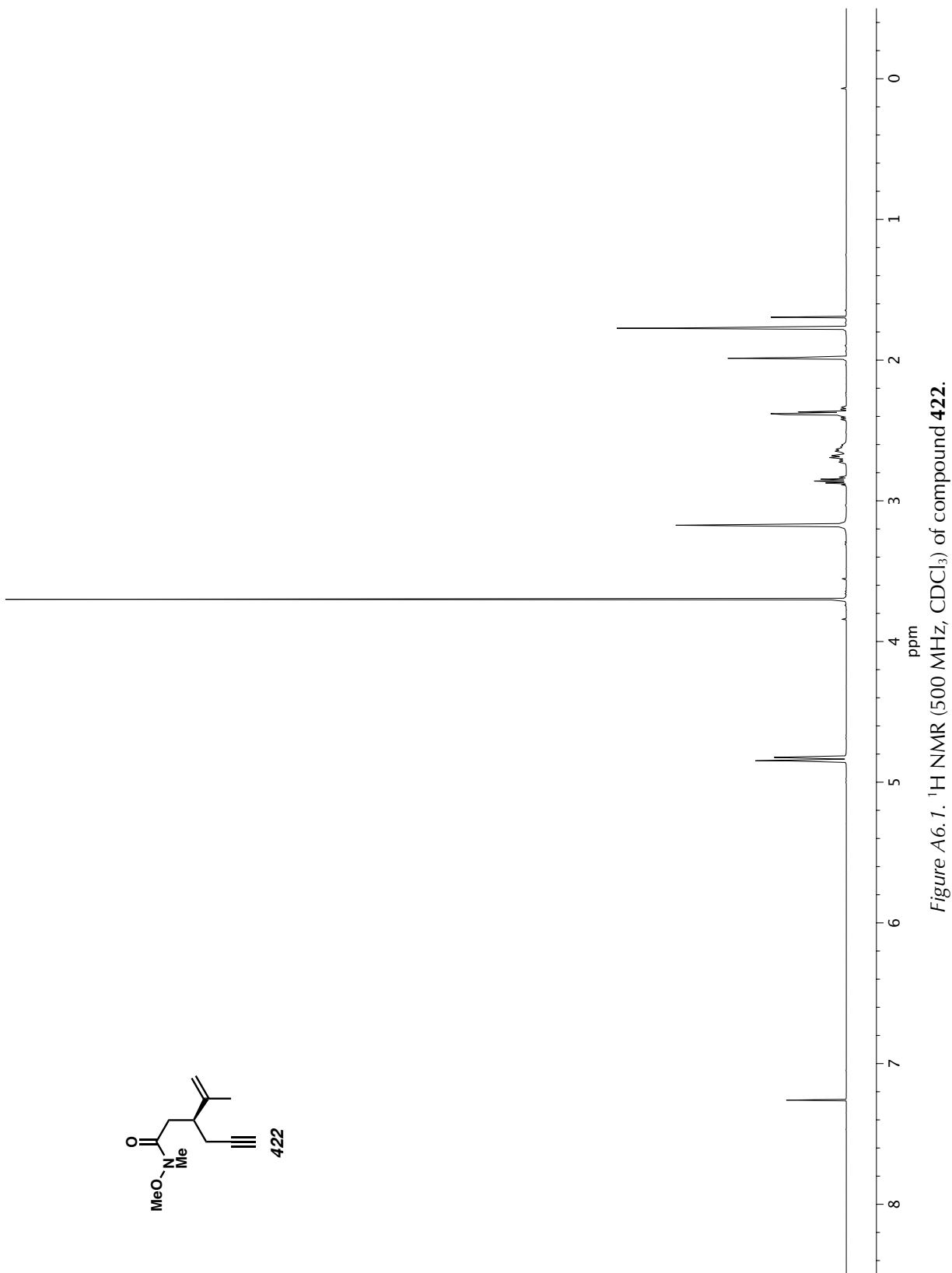


APPENDIX 6

Spectra Relevant to Chapter 4:

Progress Toward the Total Synthesis

of Scabrolide A



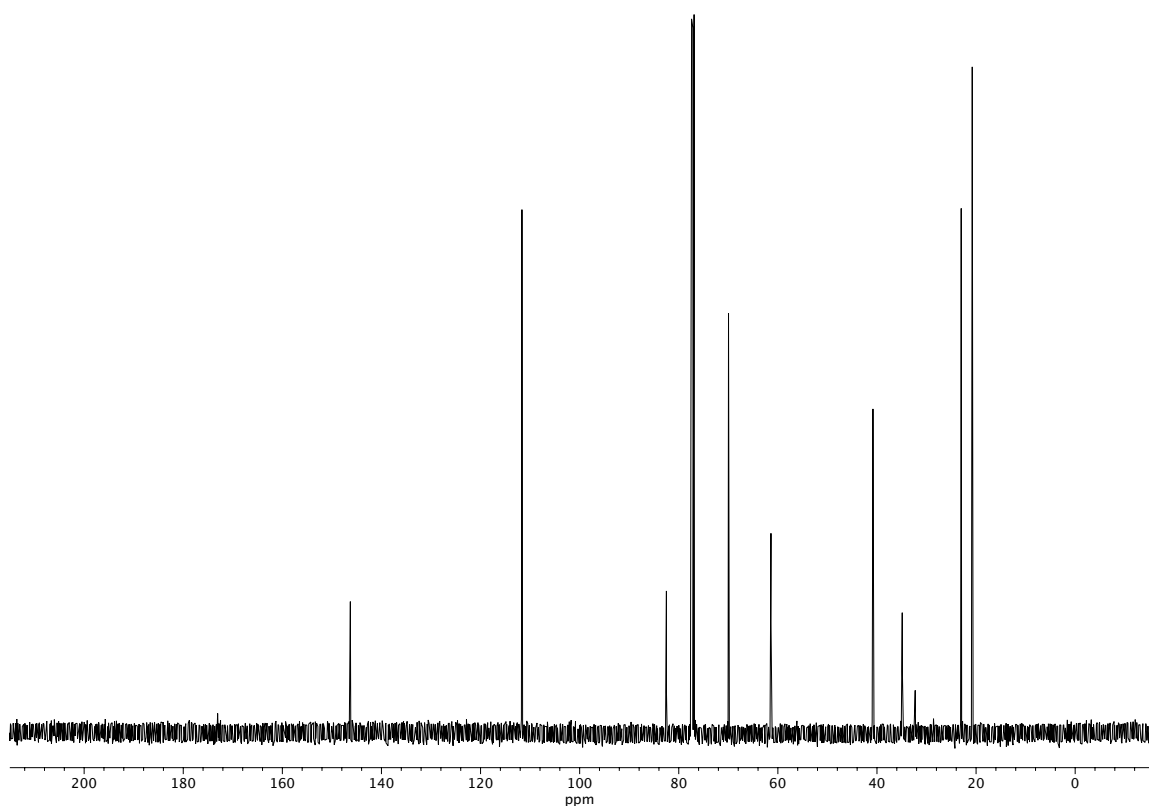


Figure A6.2. ^{13}C NMR (126 MHz, CDCl_3) of compound 422.

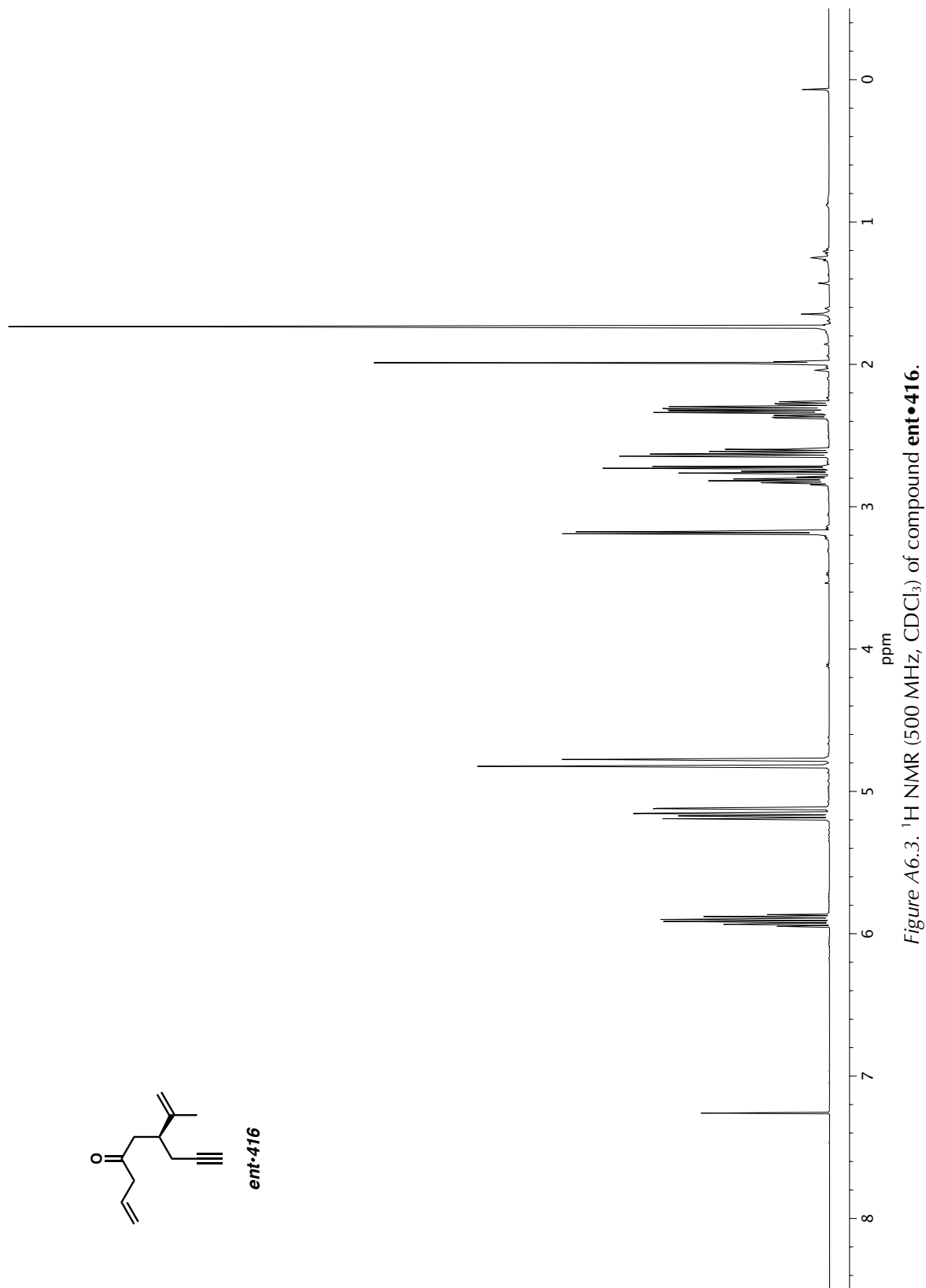


Figure A6.3. ^1H NMR (500 MHz, CDCl_3) of compound **ent•416**.

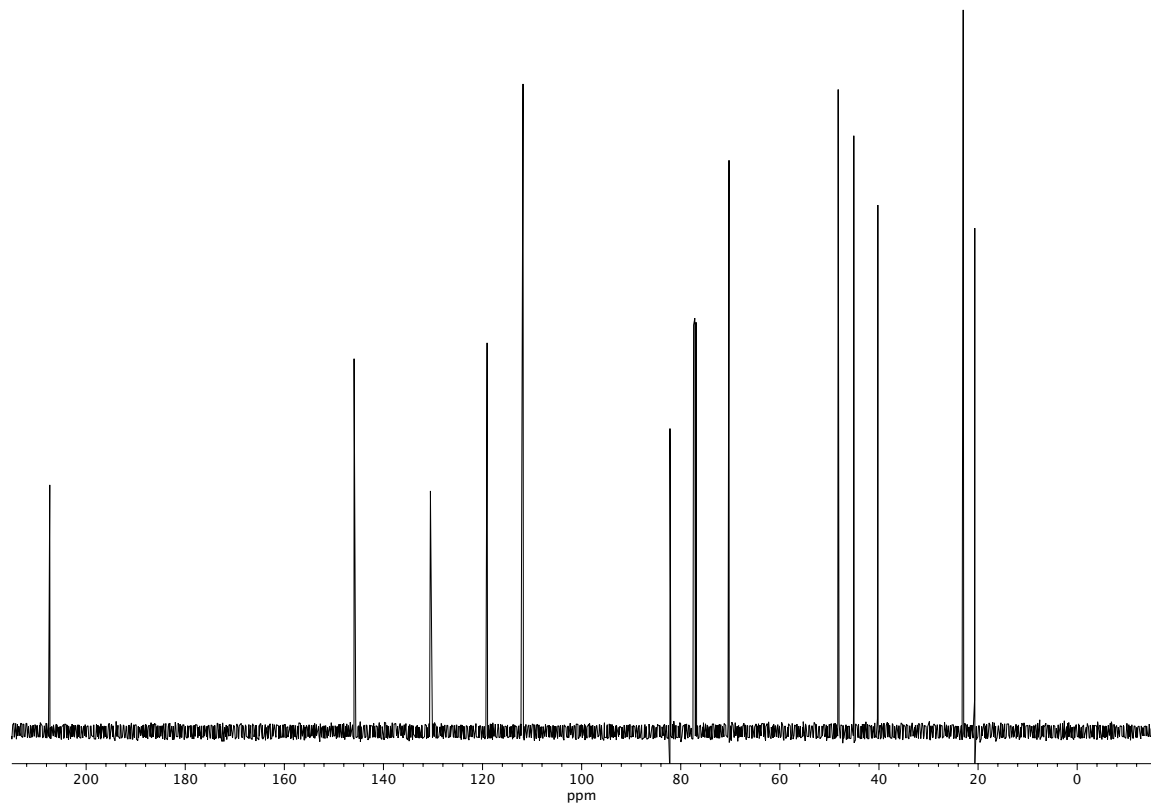


Figure A6.4. ^{13}C NMR (126 MHz, CDCl_3) of compound **ent•416**.

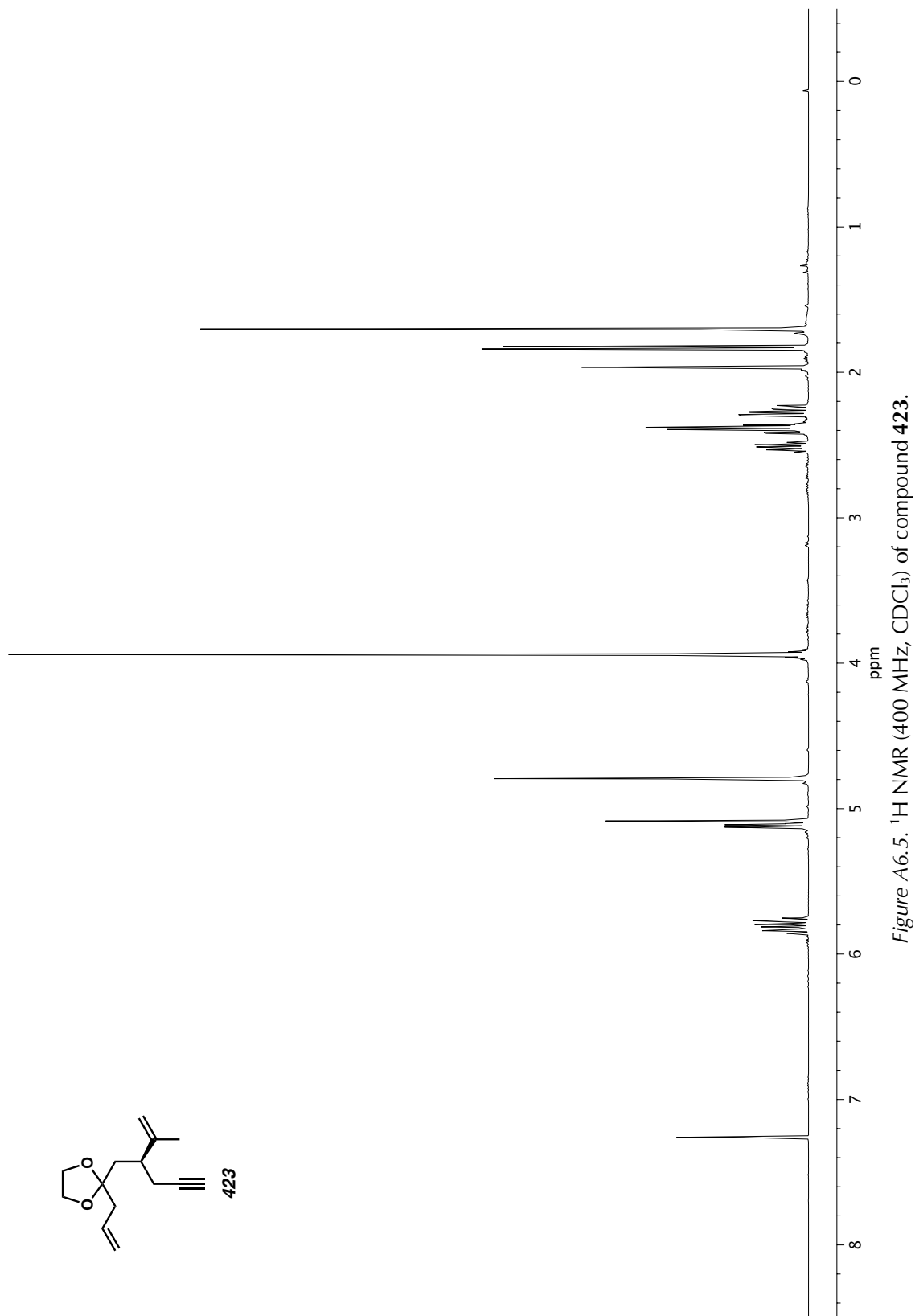


Figure A6.5. ^1H NMR (400 MHz, CDCl_3) of compound 423.

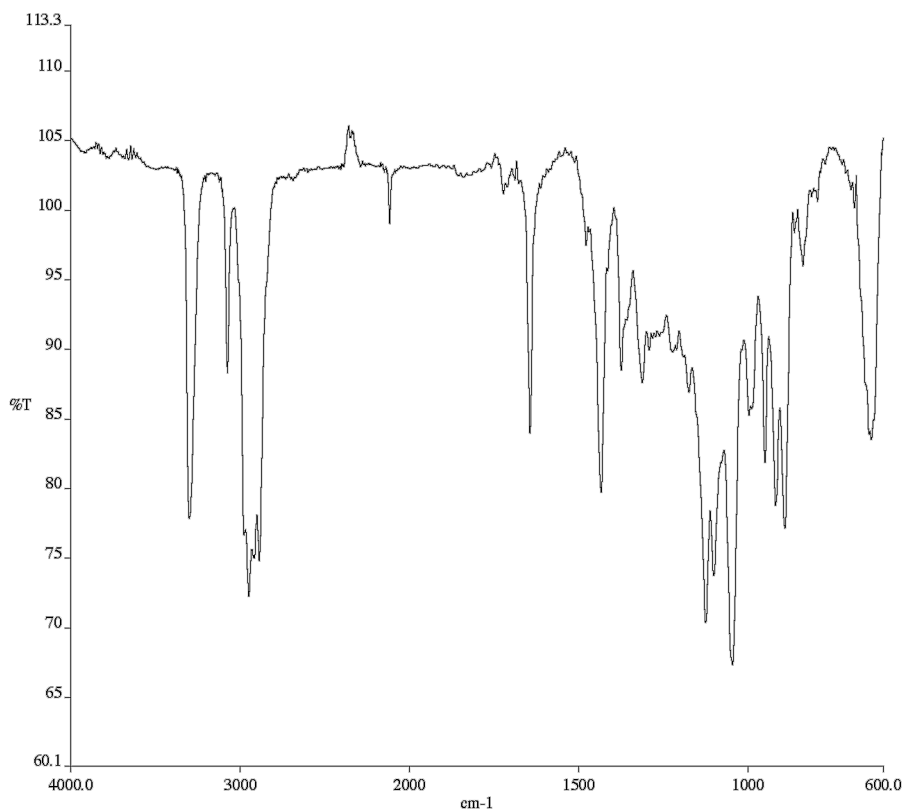


Figure A6.6. Infrared spectrum (Thin Film, NaCl) of compound 423.

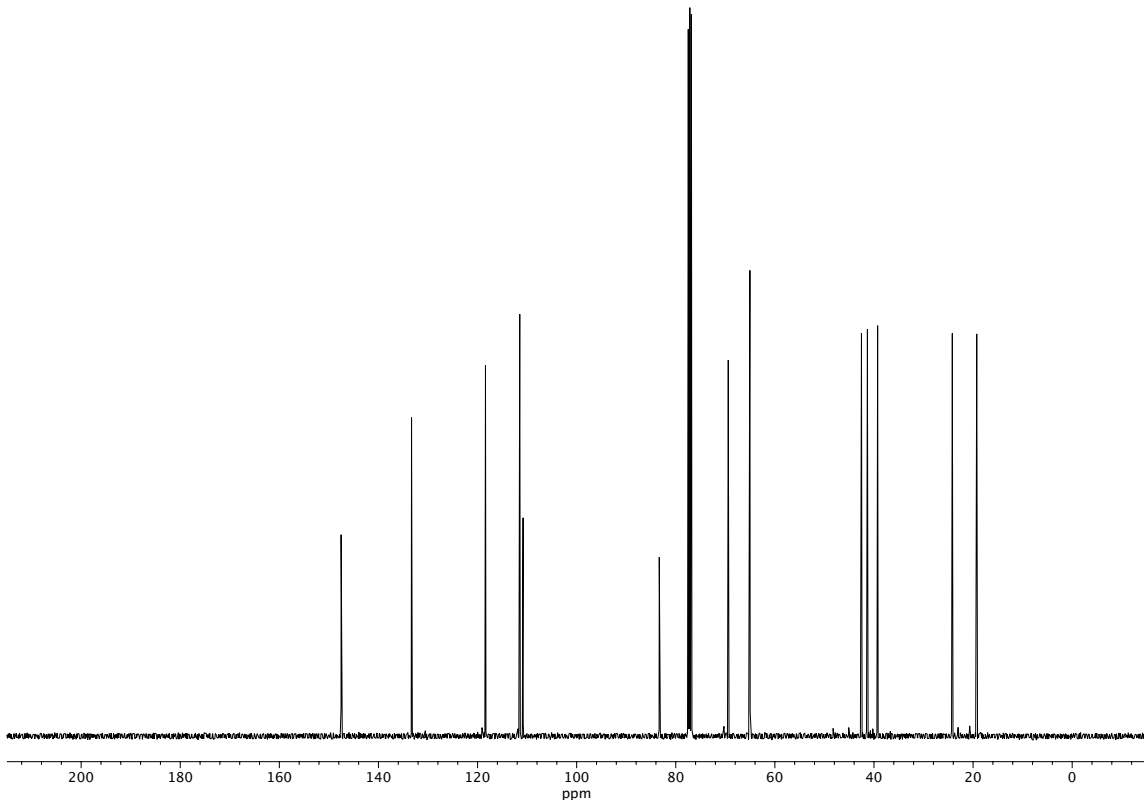
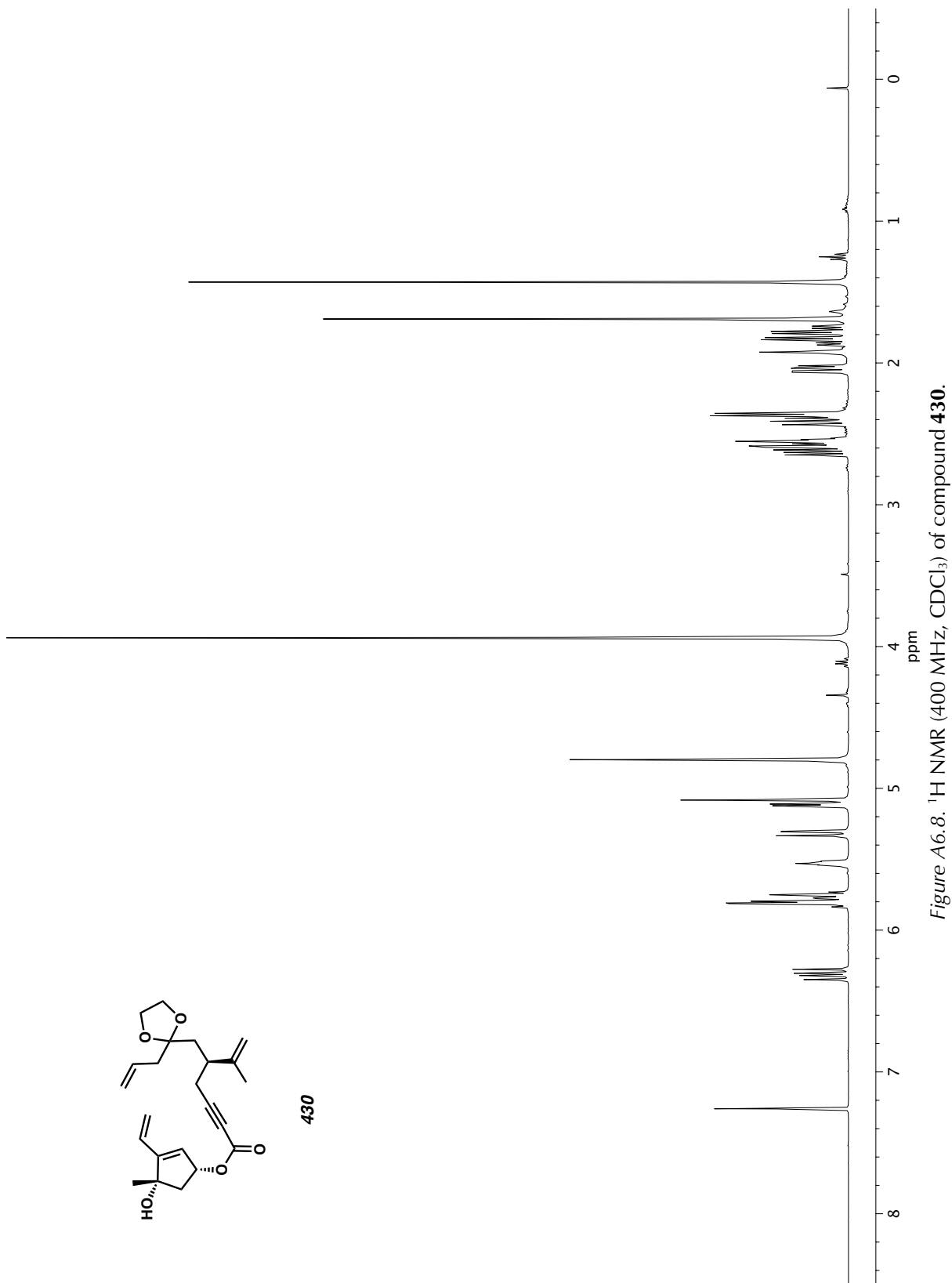


Figure A6.7. ^{13}C NMR (101 MHz, CDCl_3) of compound 423.



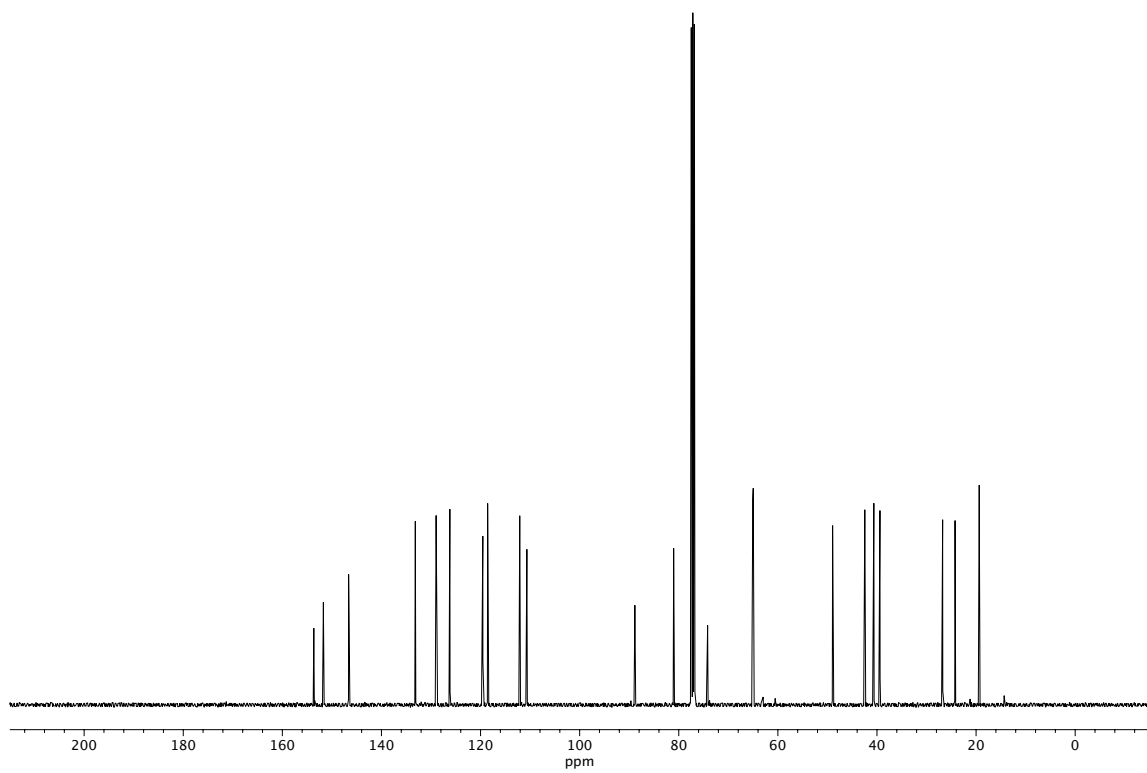


Figure A6.9. ^{13}C NMR (101 MHz, CDCl_3) of compound **430**.

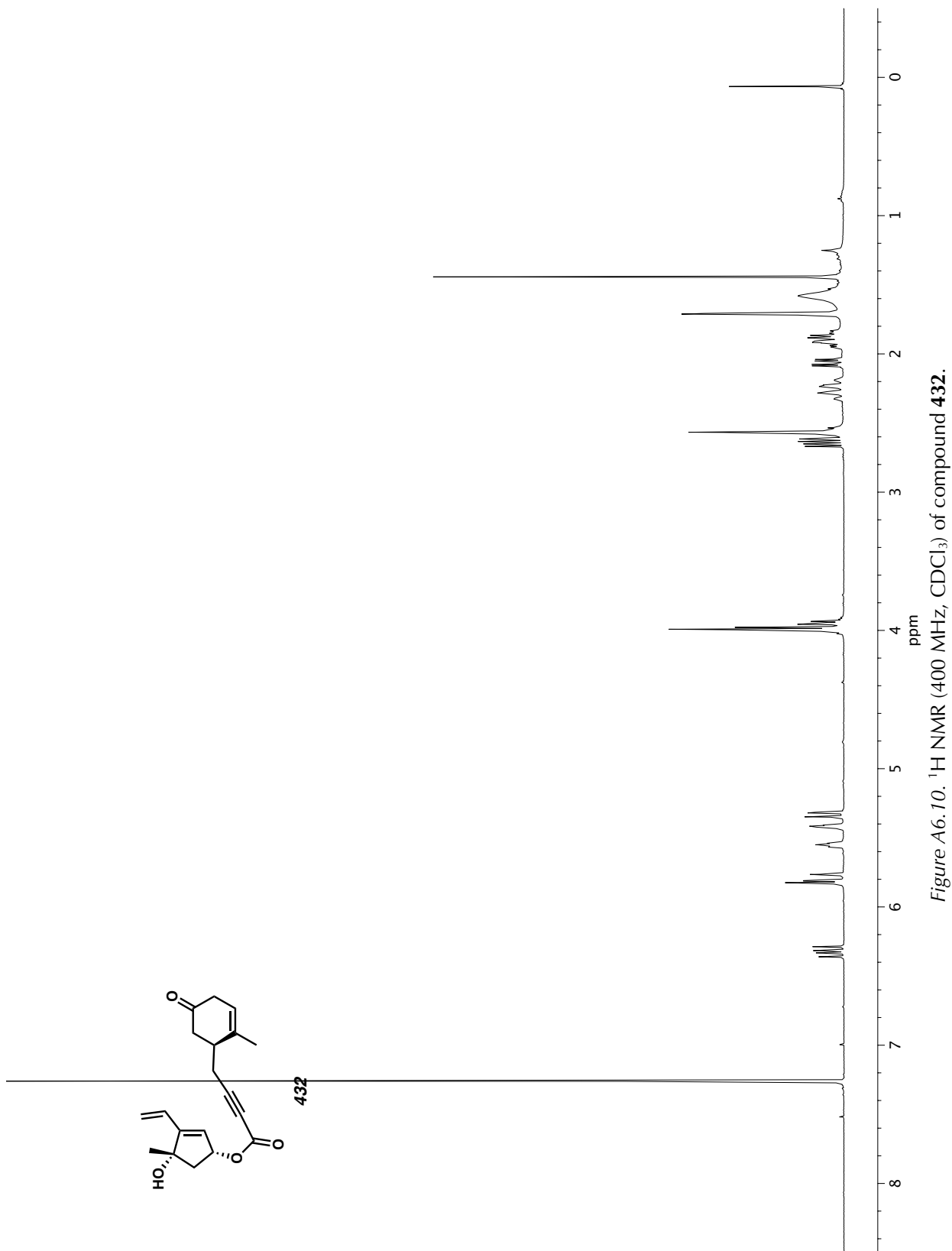


Figure A6.10. ^1H NMR (400 MHz, CDCl_3) of compound 432.

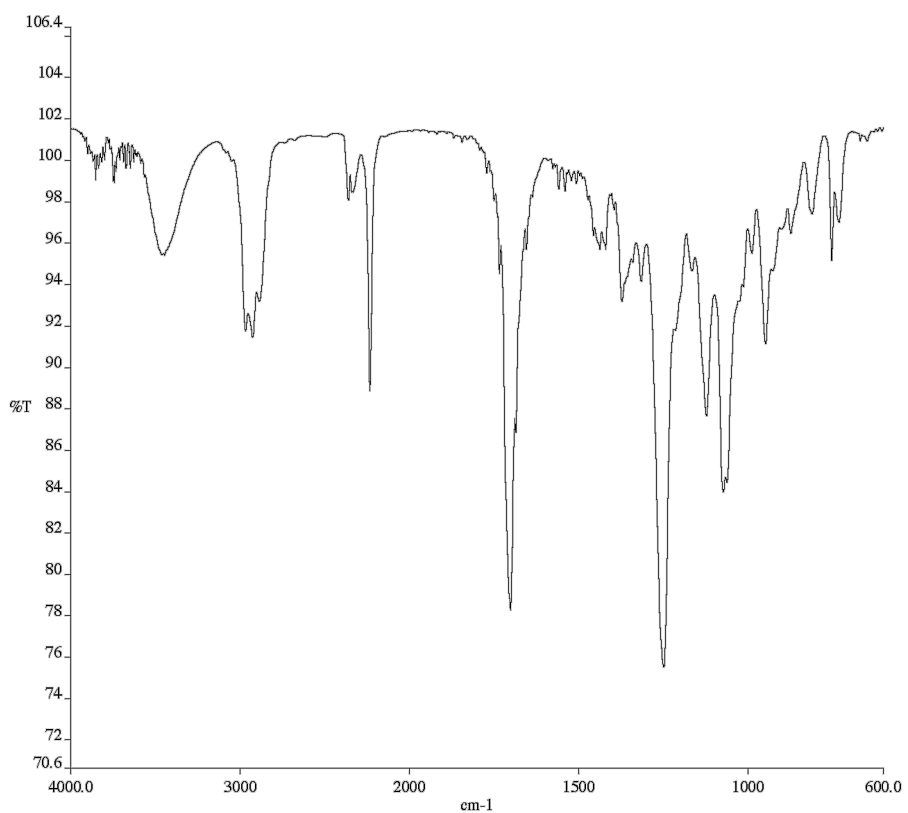


Figure A6.11. Infrared spectrum (Thin Film, NaCl) of compound **432**.

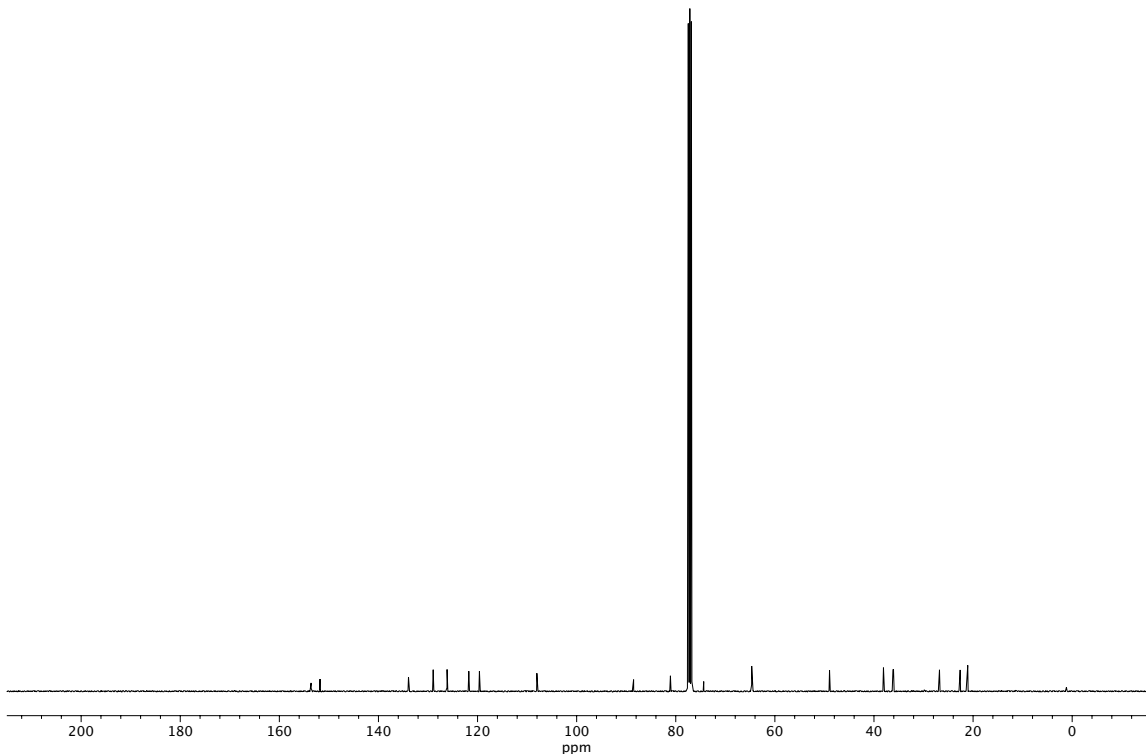


Figure A6.12. ¹³C NMR (101 MHz, CDCl₃) of compound **432**.

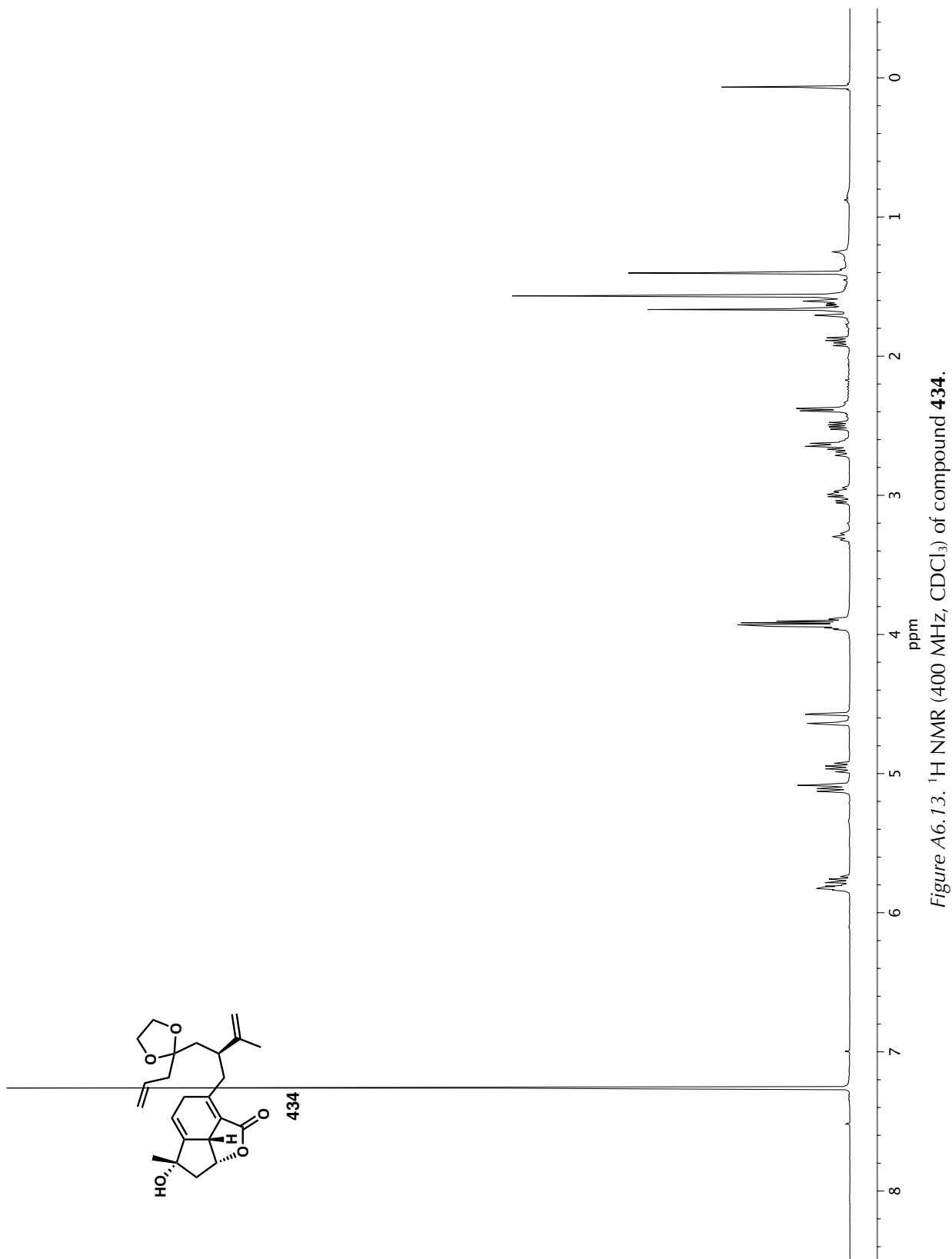


Figure A6.13. ^1H NMR (400 MHz, CDCl_3) of compound 434.

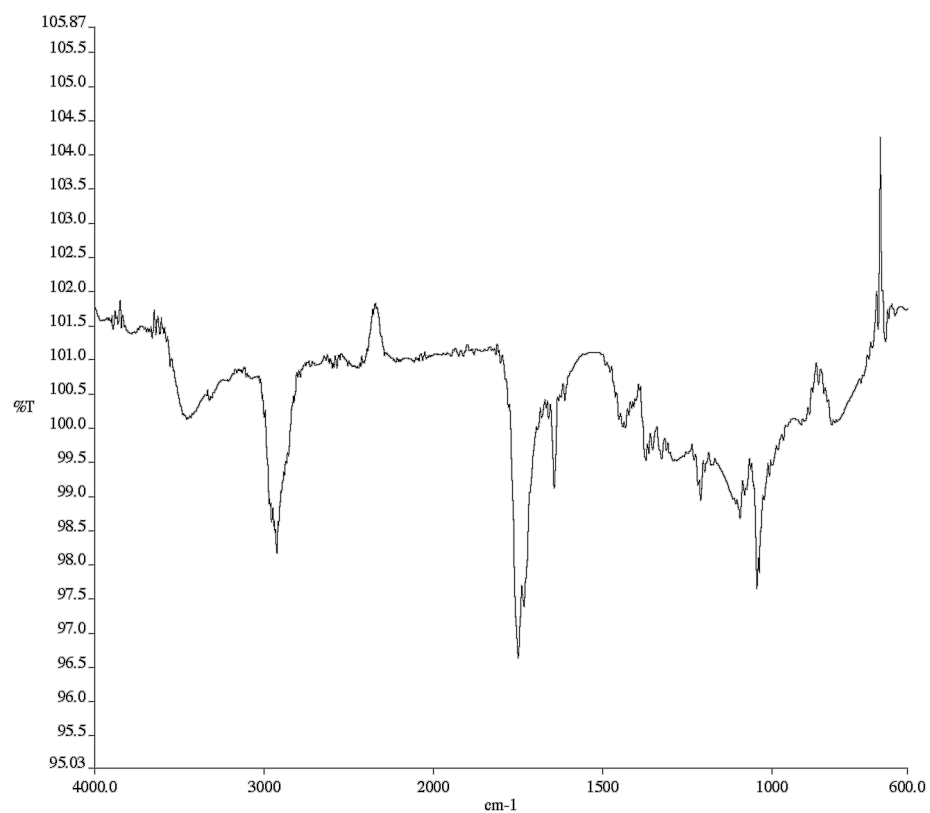


Figure A6.14. Infrared spectrum (Thin Film, NaCl) of compound **434**.

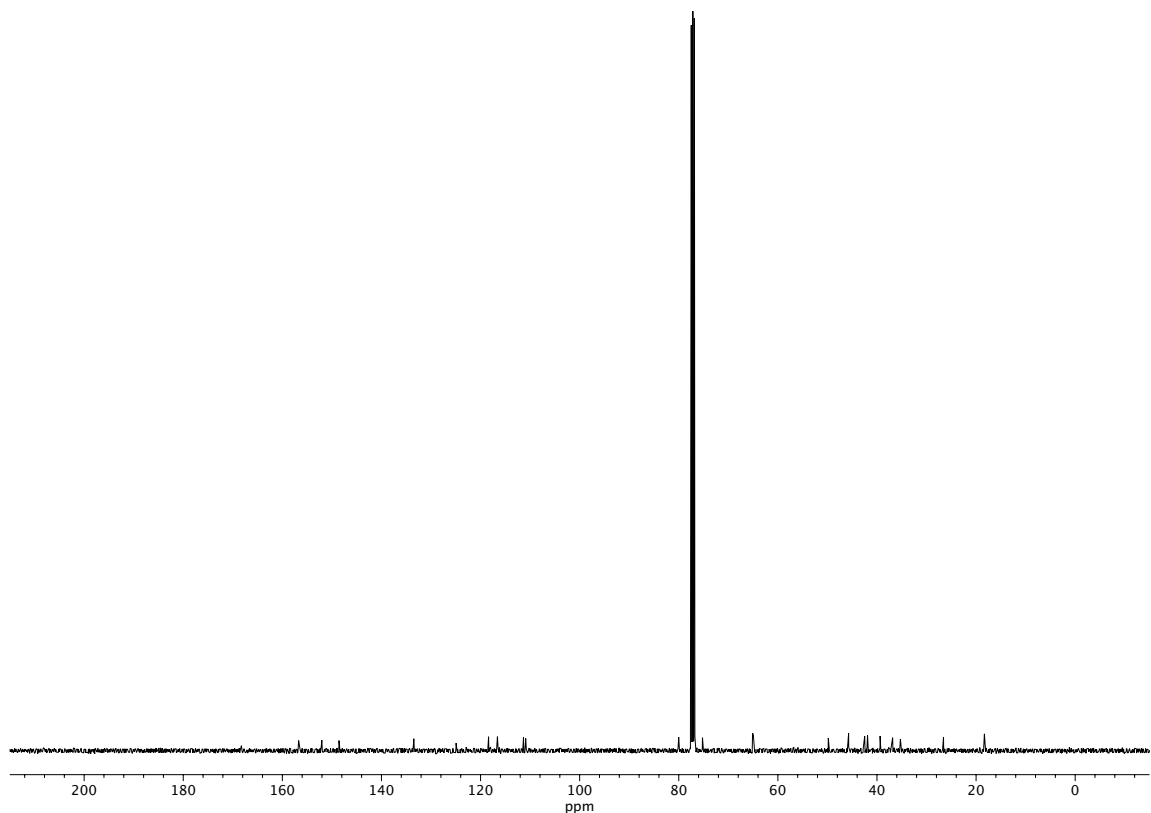


Figure A6.15. ^{13}C NMR (101 MHz, CDCl_3) of compound **434**.

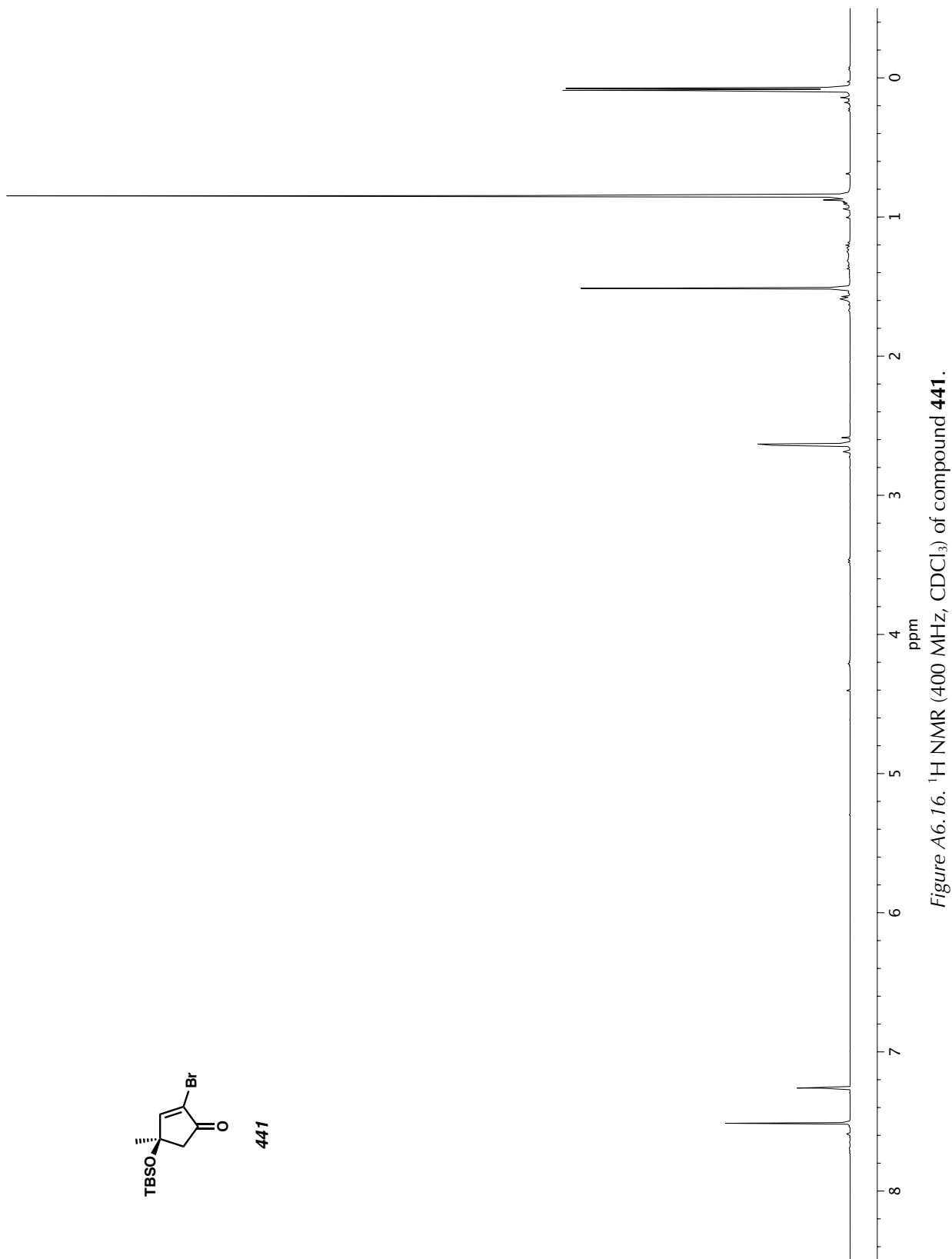


Figure A6.16. ^1H NMR (400 MHz, CDCl_3) of compound 441.

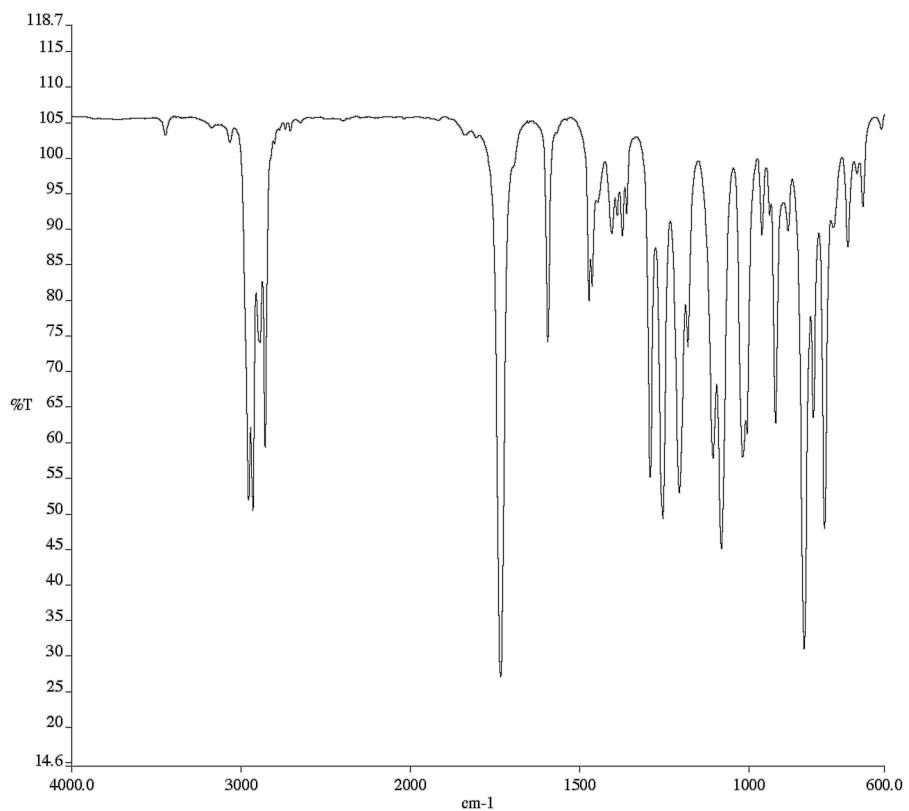


Figure A6.17. Infrared spectrum (Thin Film, NaCl) of compound **441**.

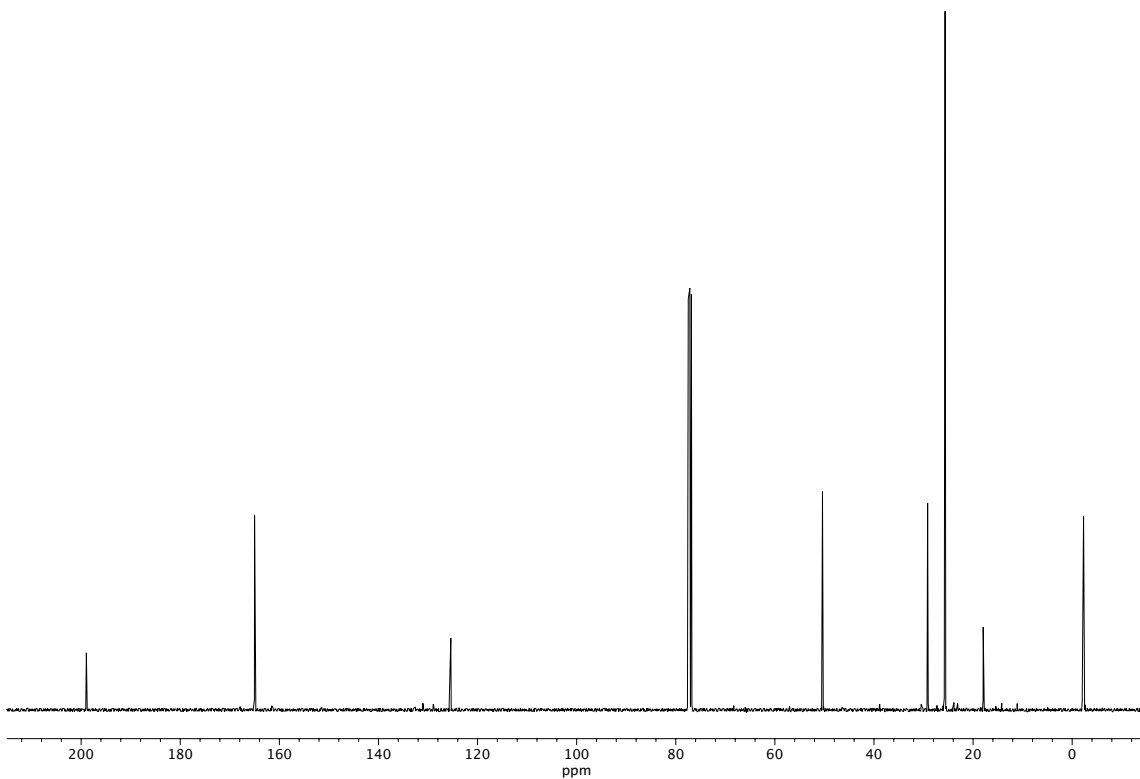


Figure A6.18. ¹³C NMR (101 MHz, CDCl₃) of compound **441**.

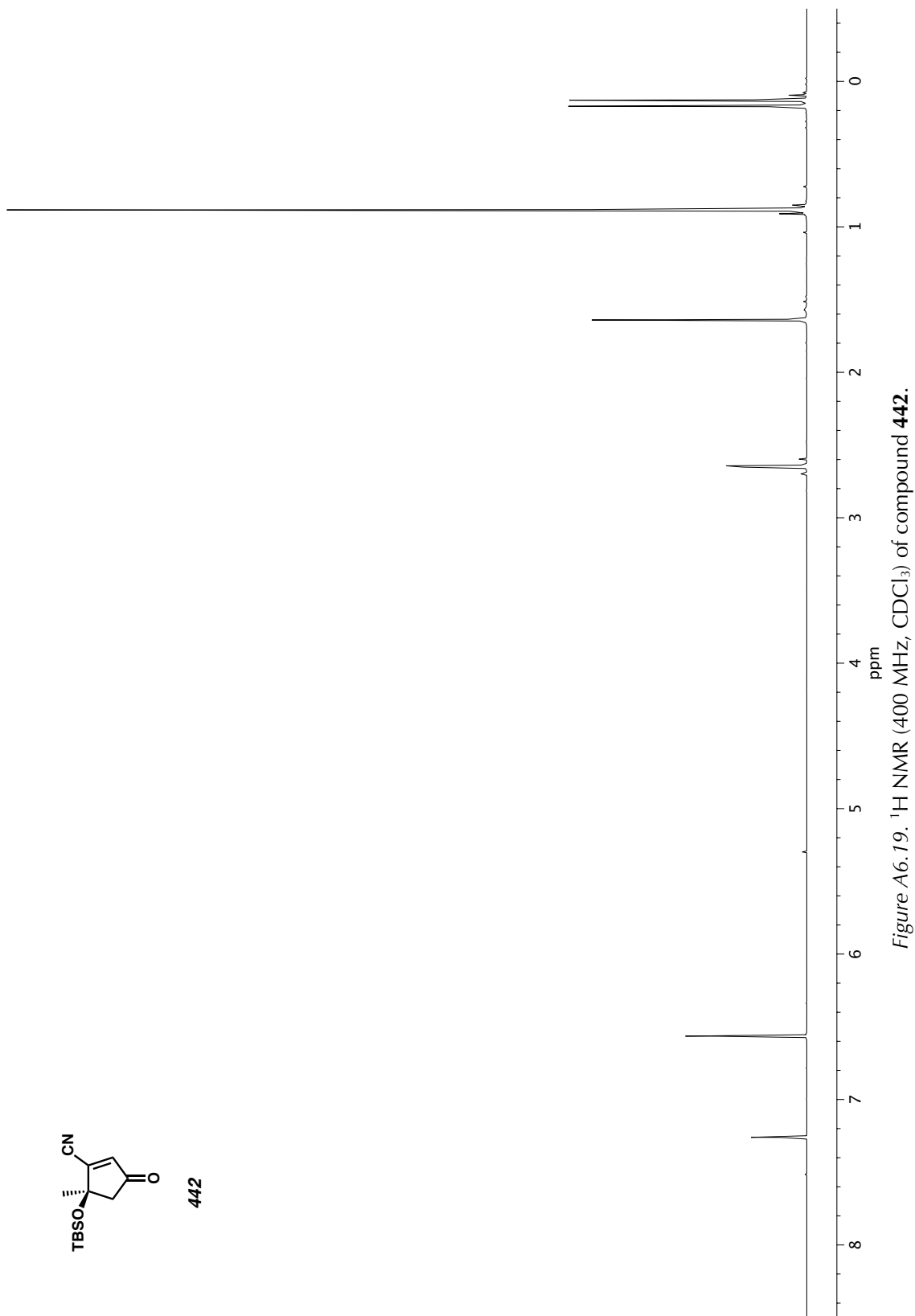


Figure A6.19. ^1H NMR (400 MHz, CDCl_3) of compound 442.

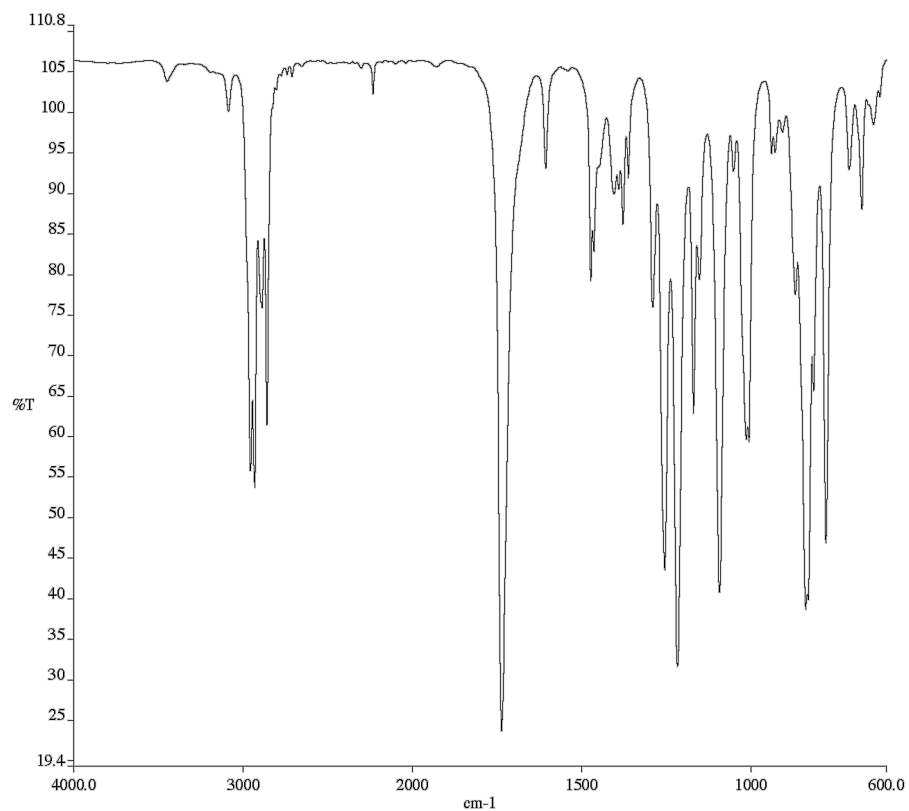


Figure A6.20. Infrared spectrum (Thin Film, NaCl) of compound **442**.

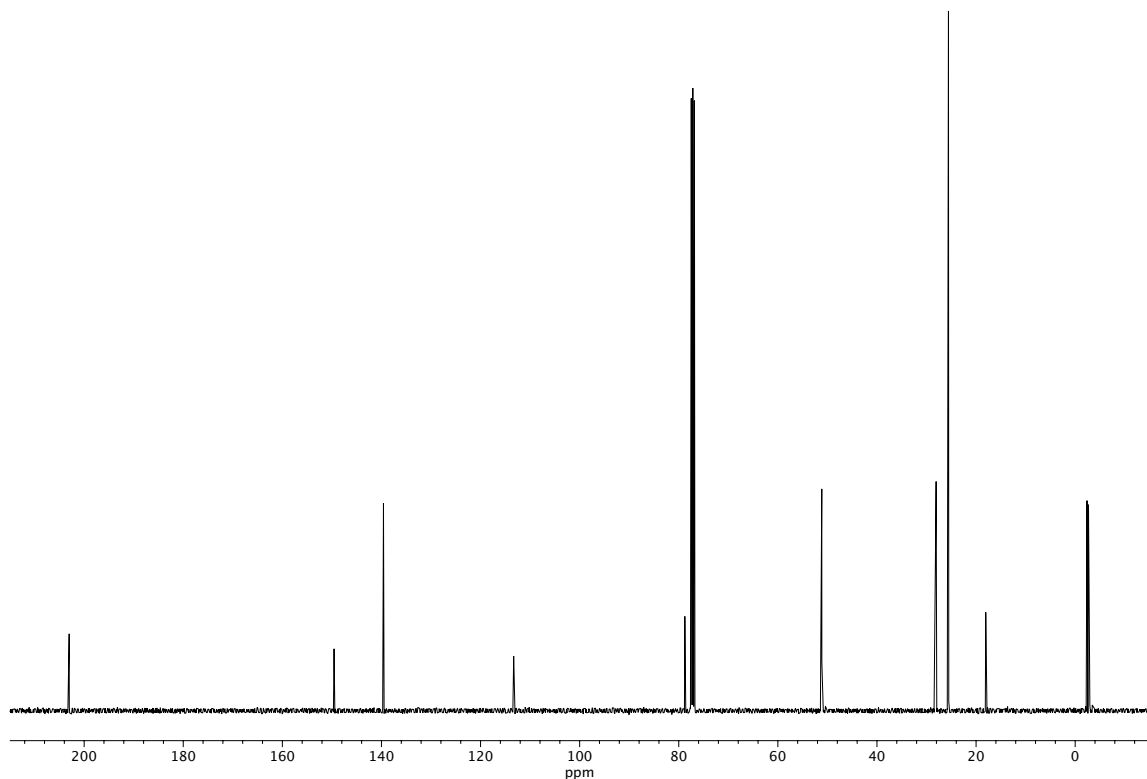


Figure A6.21. ¹³C NMR (101 MHz, CDCl₃) of compound **442**.

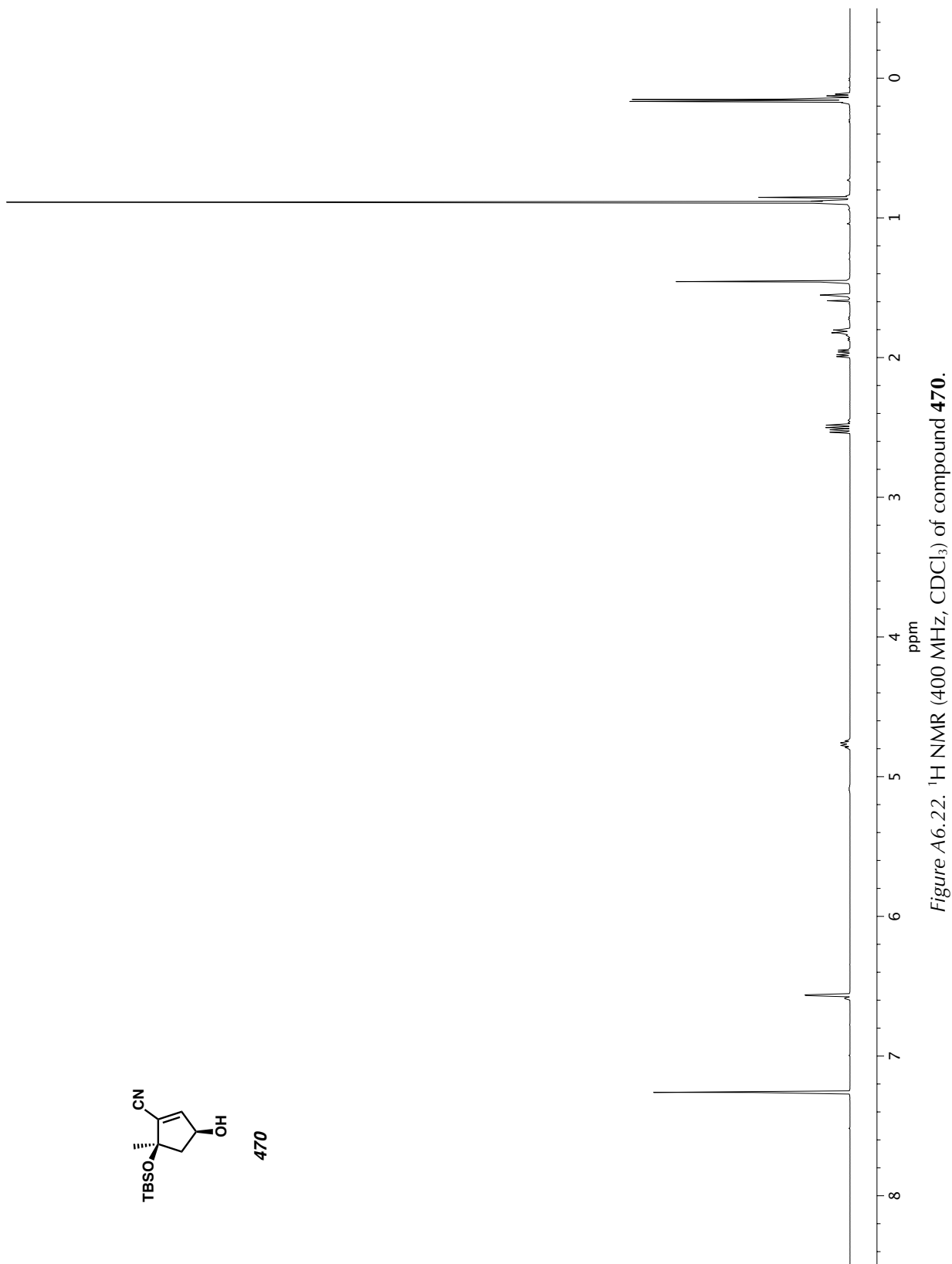


Figure A6.22. ^1H NMR (400 MHz, CDCl_3) of compound 470.

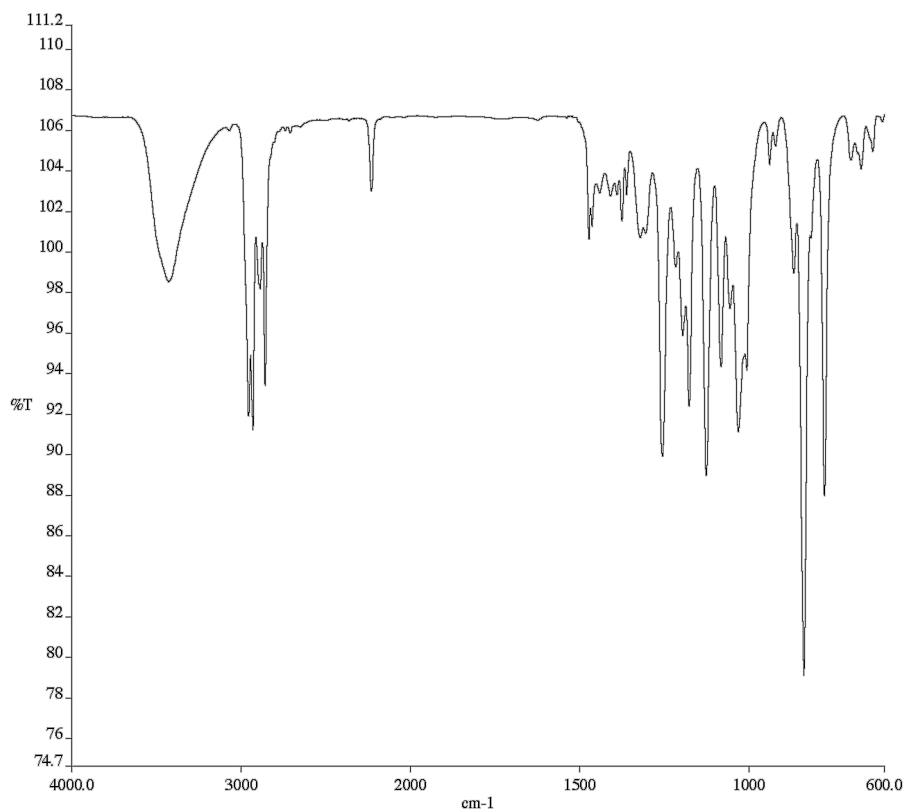


Figure A6.23. Infrared spectrum (Thin Film, NaCl) of compound **470**.

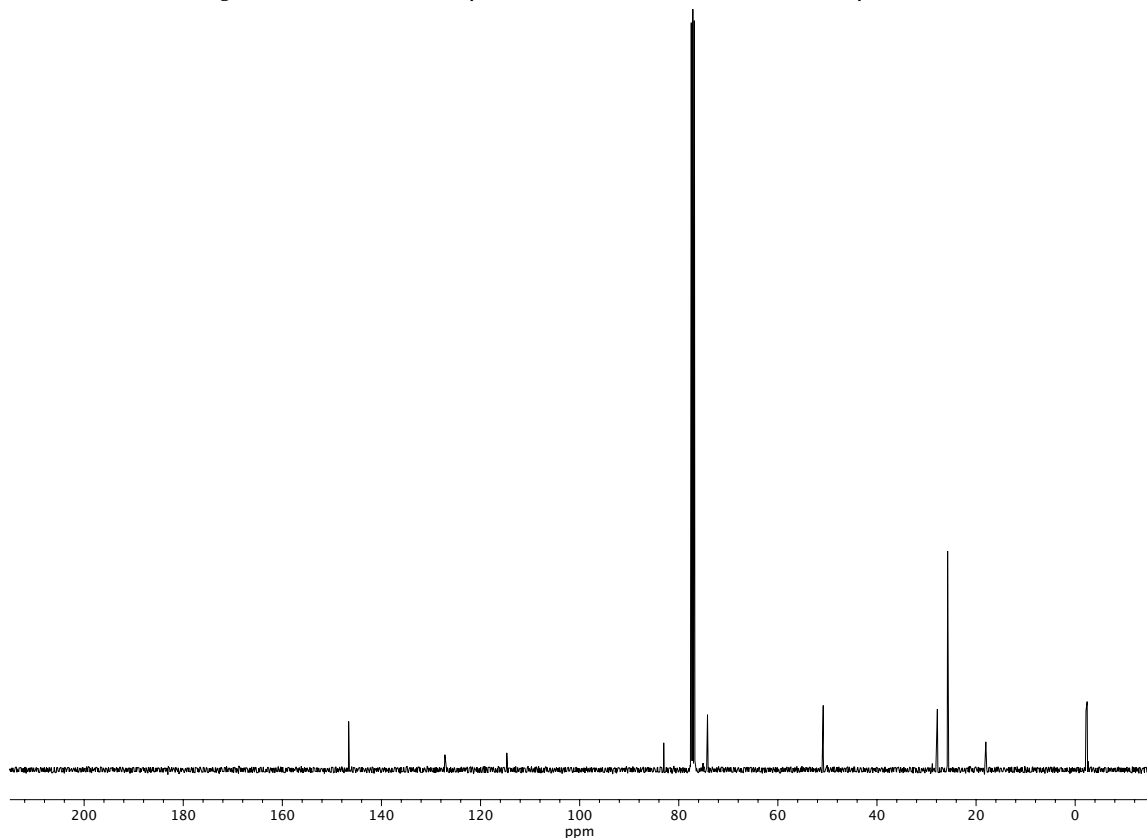
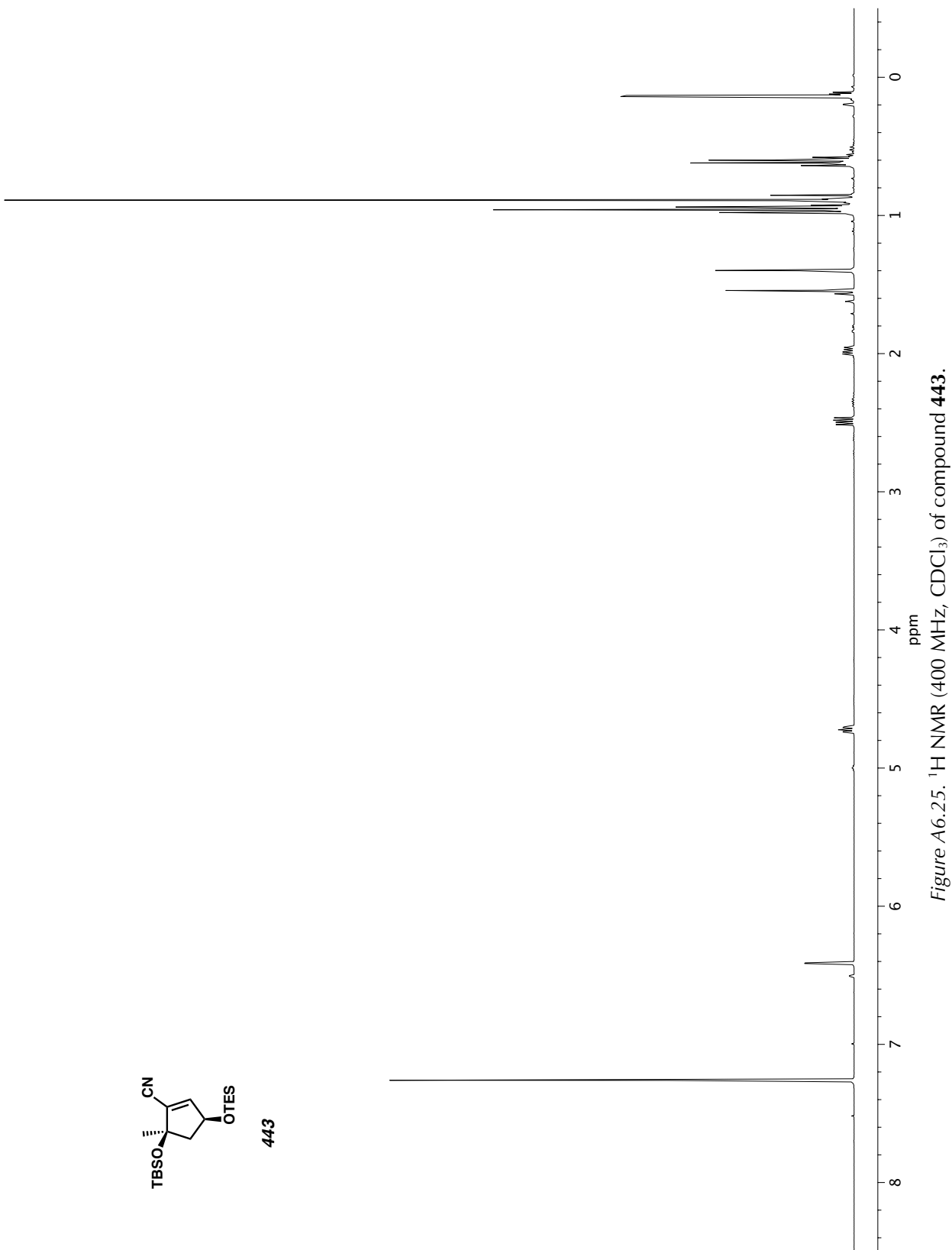


Figure A6.24. ^{13}C NMR (101 MHz, CDCl_3) of compound **470**.



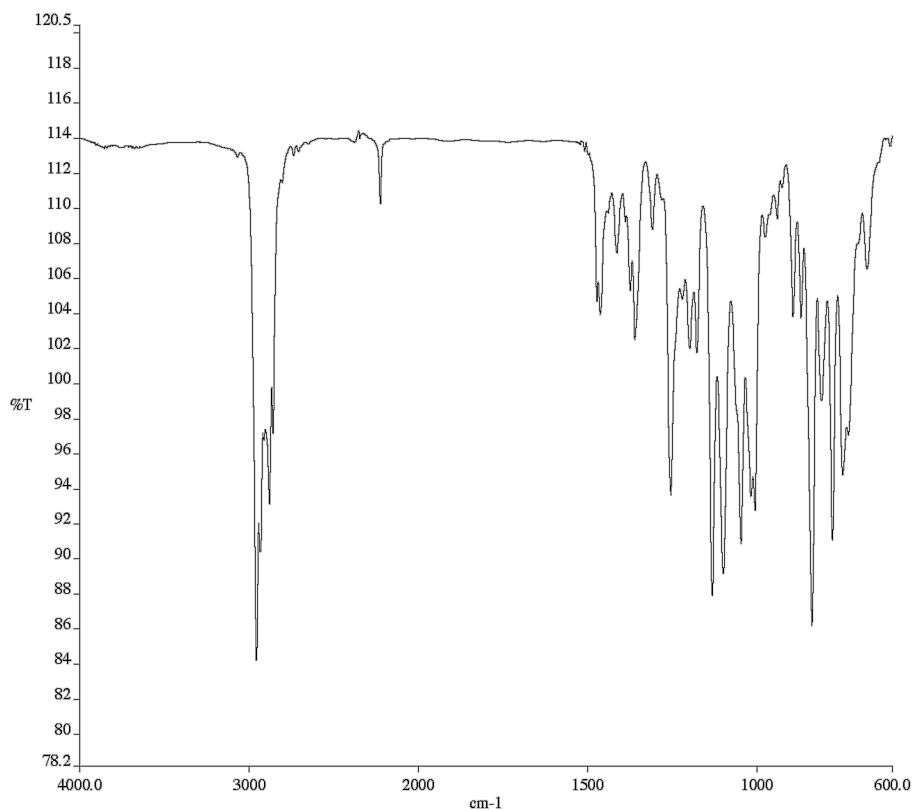


Figure A6.26. Infrared spectrum (Thin Film, NaCl) of compound **443**.

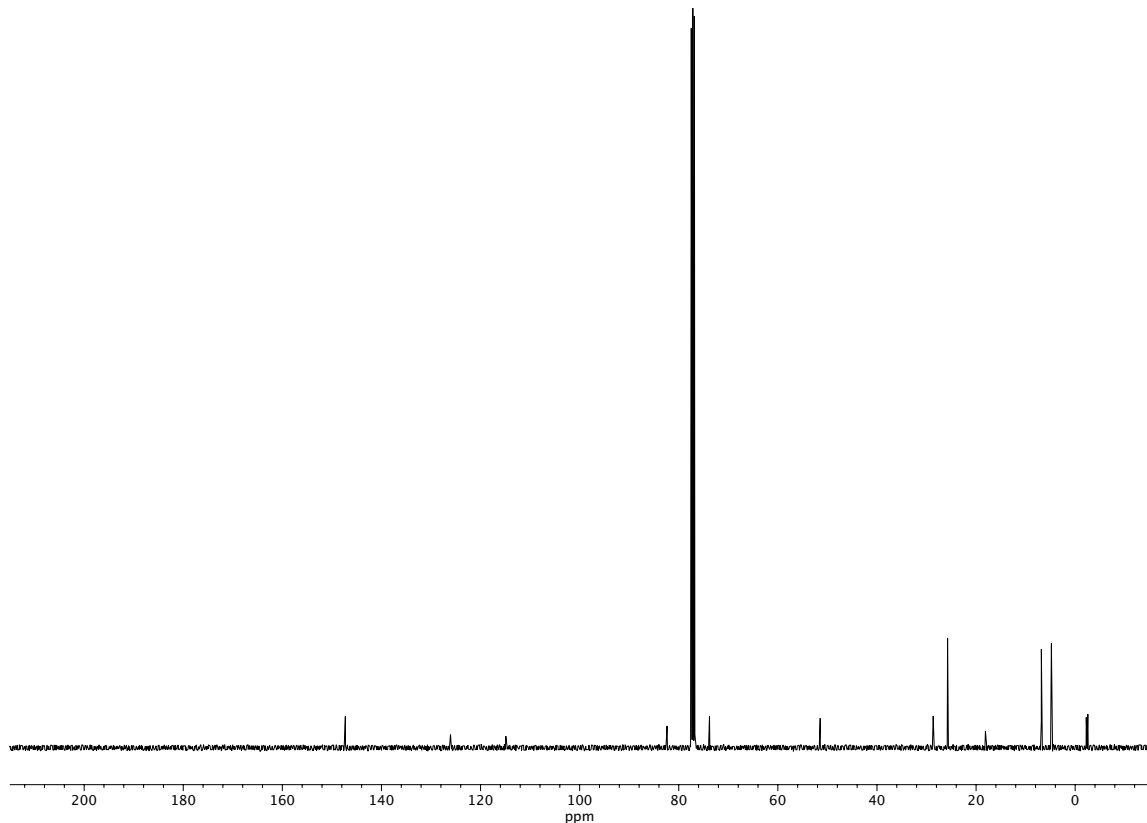


Figure A6.27. ^{13}C NMR (101 MHz, CDCl_3) of compound **443**.

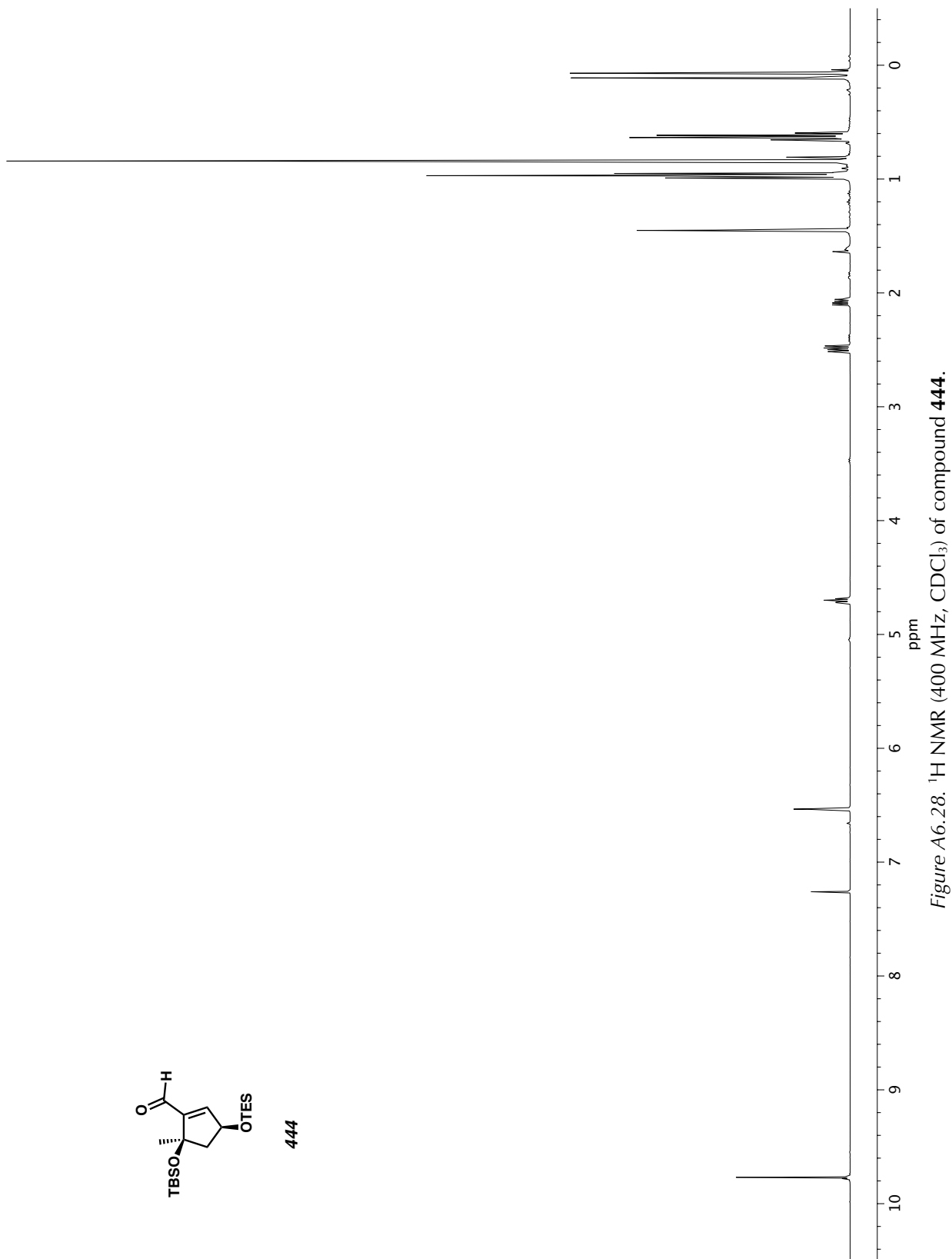


Figure A6.28. ^1H NMR (400 MHz, CDCl_3) of compound 444.

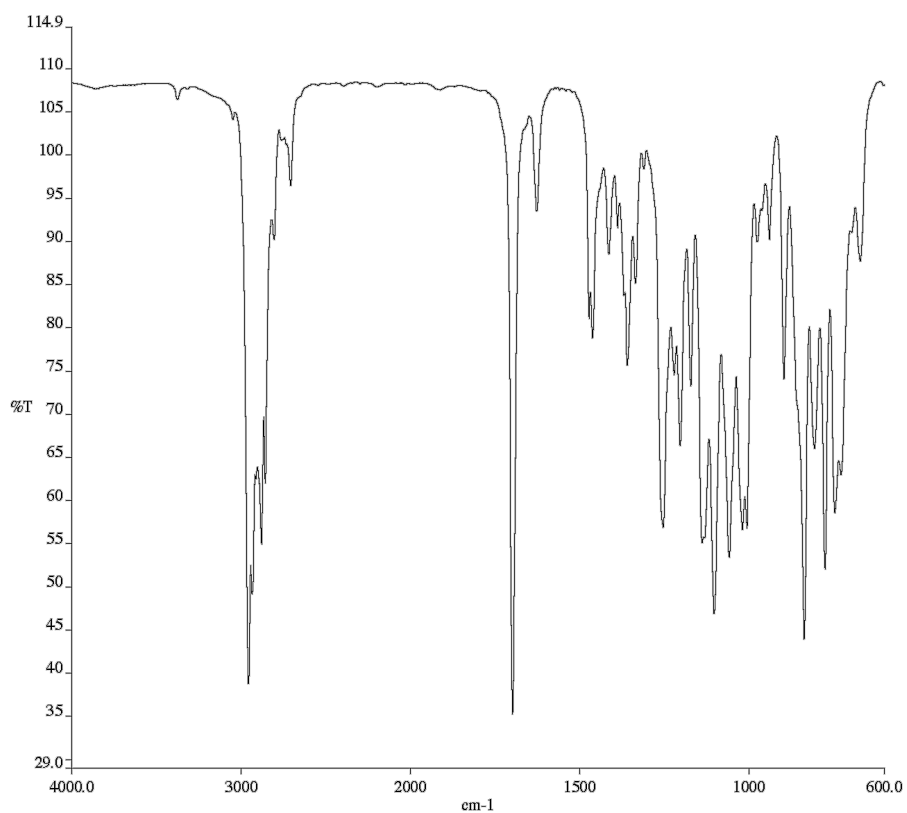


Figure A6.29. Infrared spectrum (Thin Film, NaCl) of compound **444**.

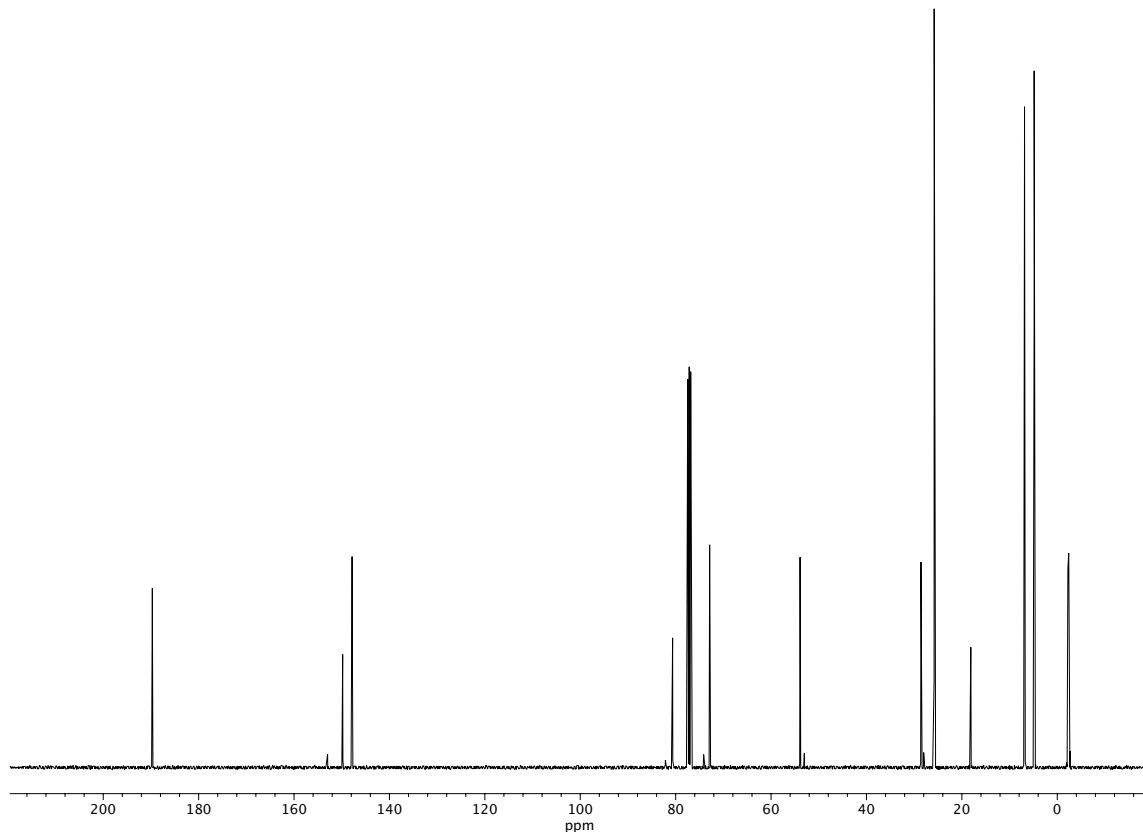


Figure A6.30. ¹³C NMR (101 MHz, CDCl₃) of compound **444**.

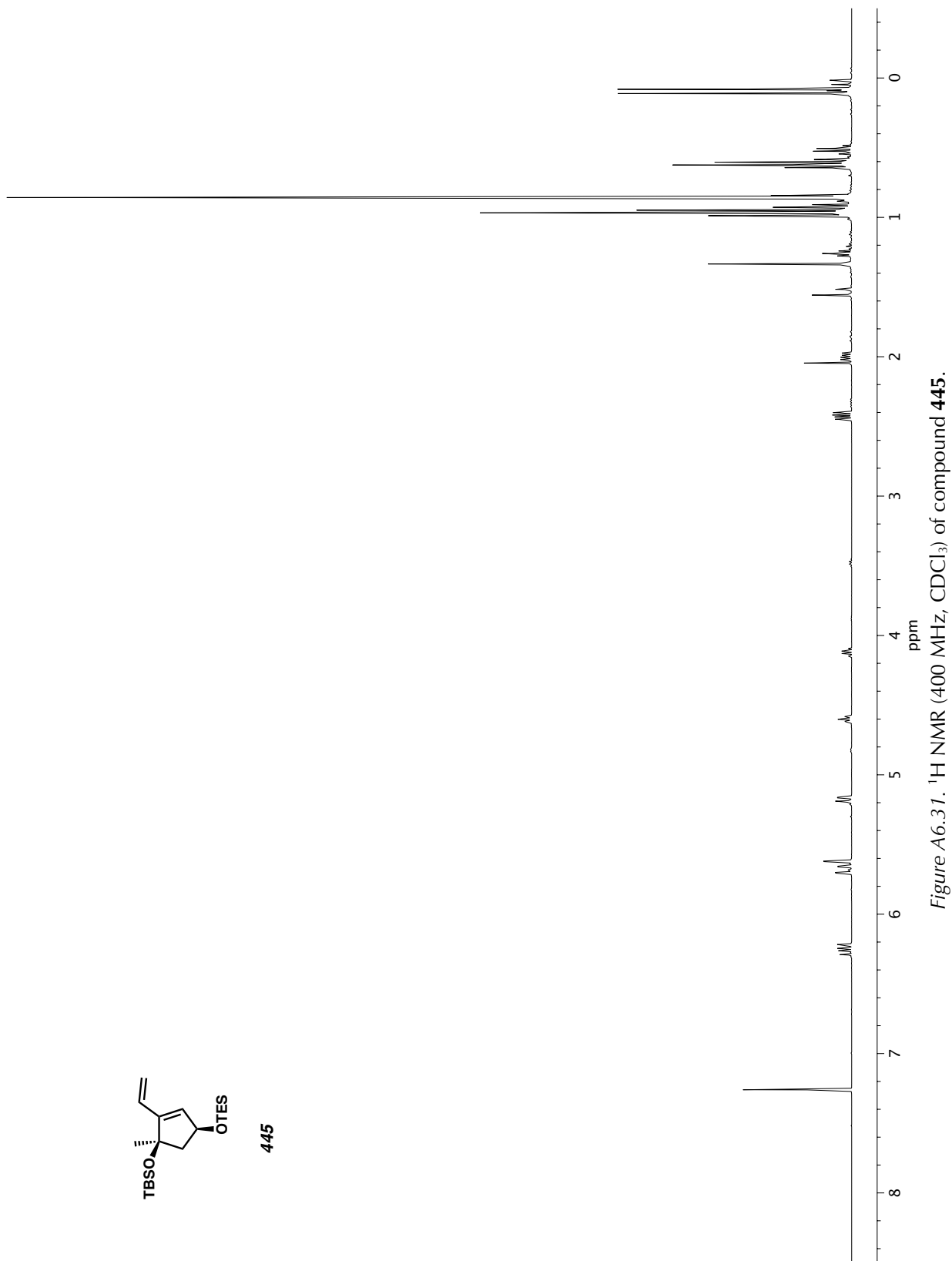


Figure A6.31. ^1H NMR (400 MHz, CDCl_3) of compound 445.

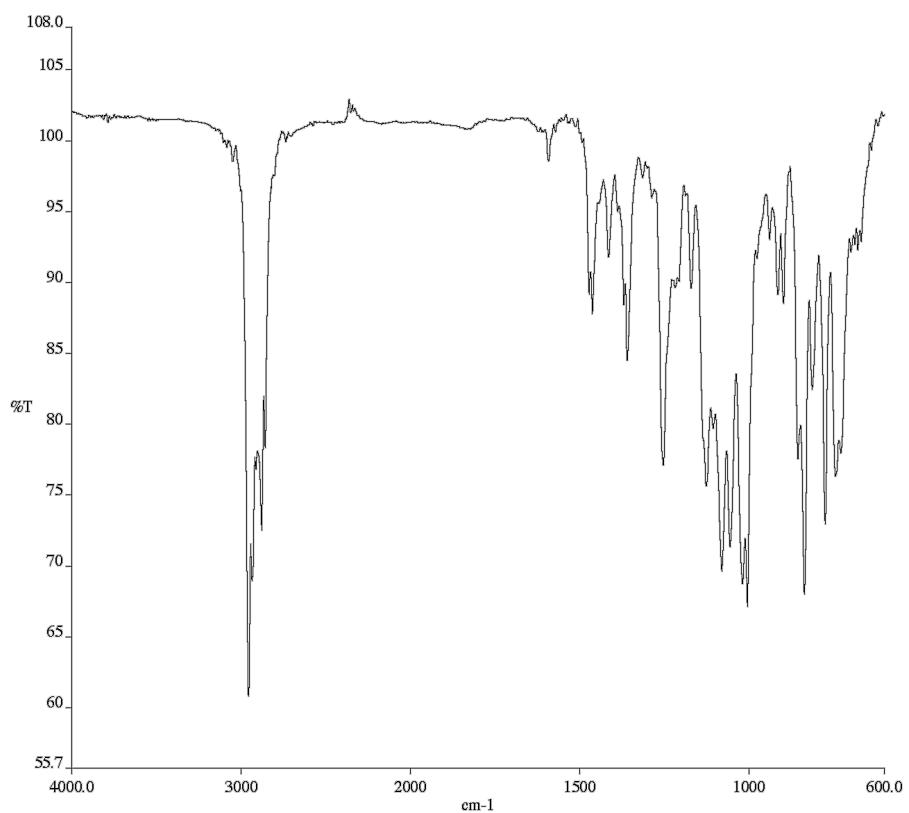


Figure A6.32. Infrared spectrum (Thin Film, NaCl) of compound **445**.

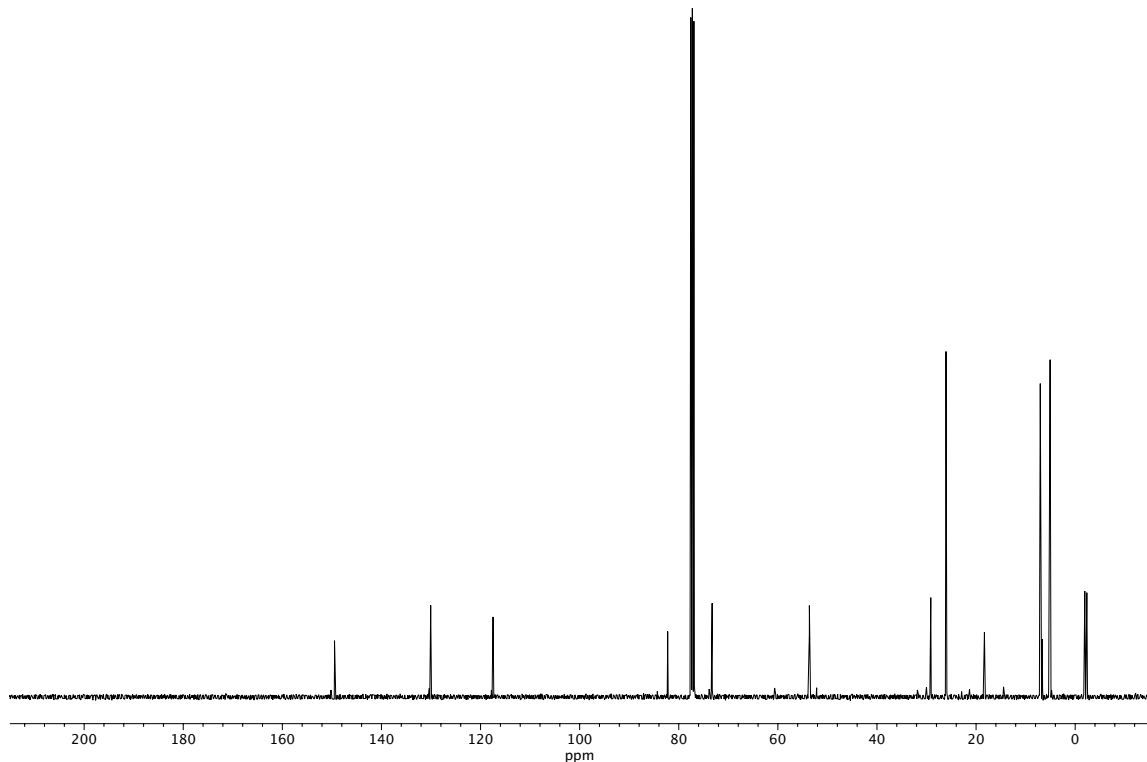


Figure A6.33. ^{13}C NMR (101 MHz, CDCl_3) of compound **445**.

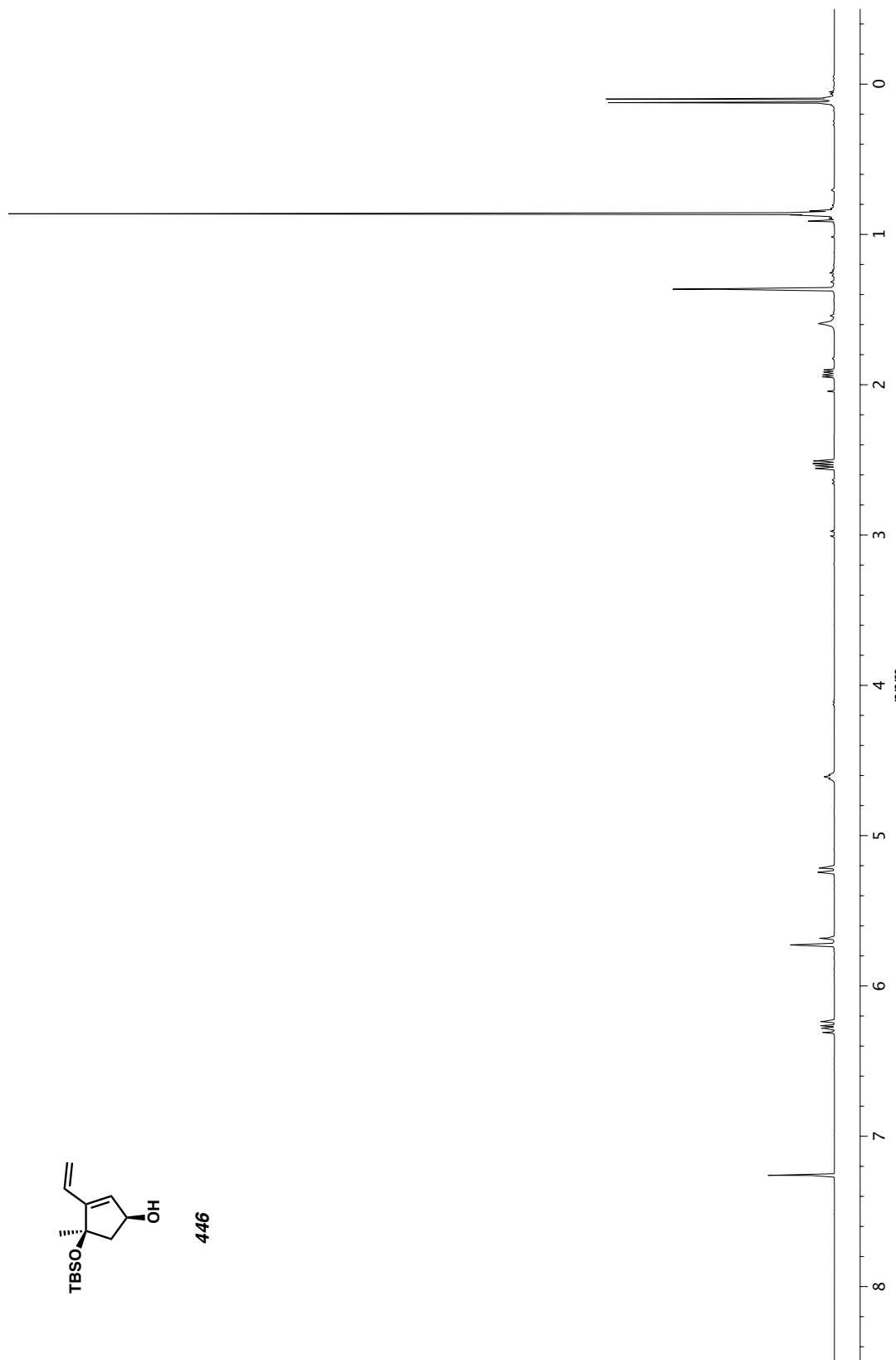
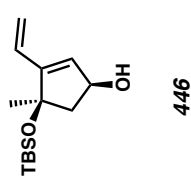


Figure A6.34. ^1H NMR (400 MHz, CDCl_3) of compound 446.

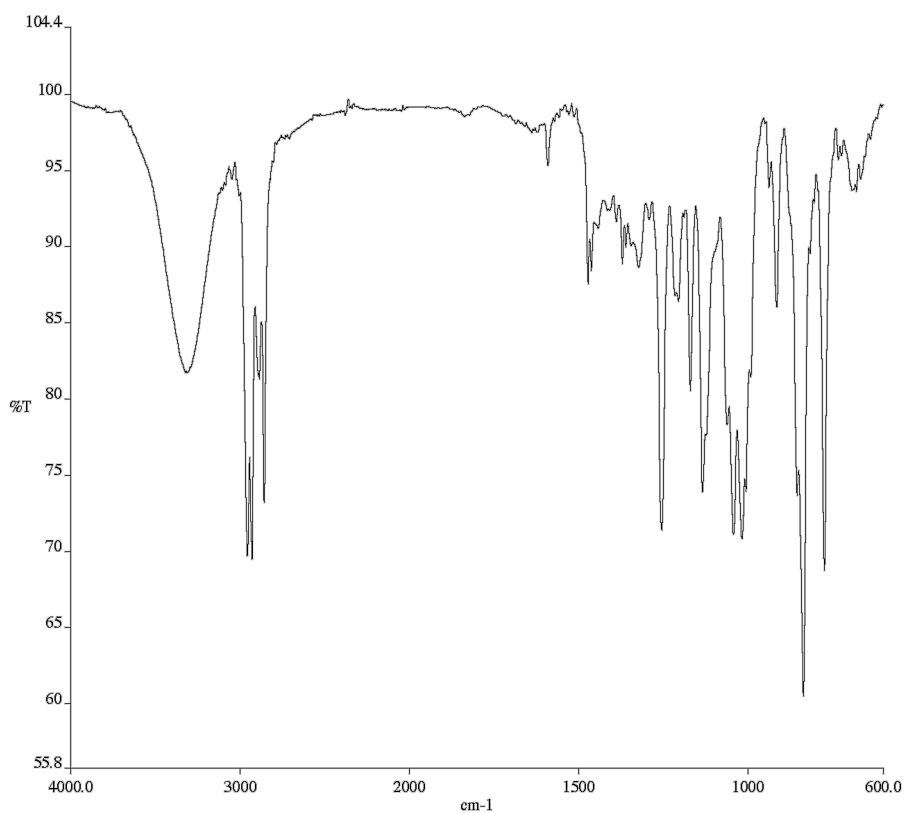


Figure A6.35. Infrared spectrum (Thin Film, NaCl) of compound **446**.

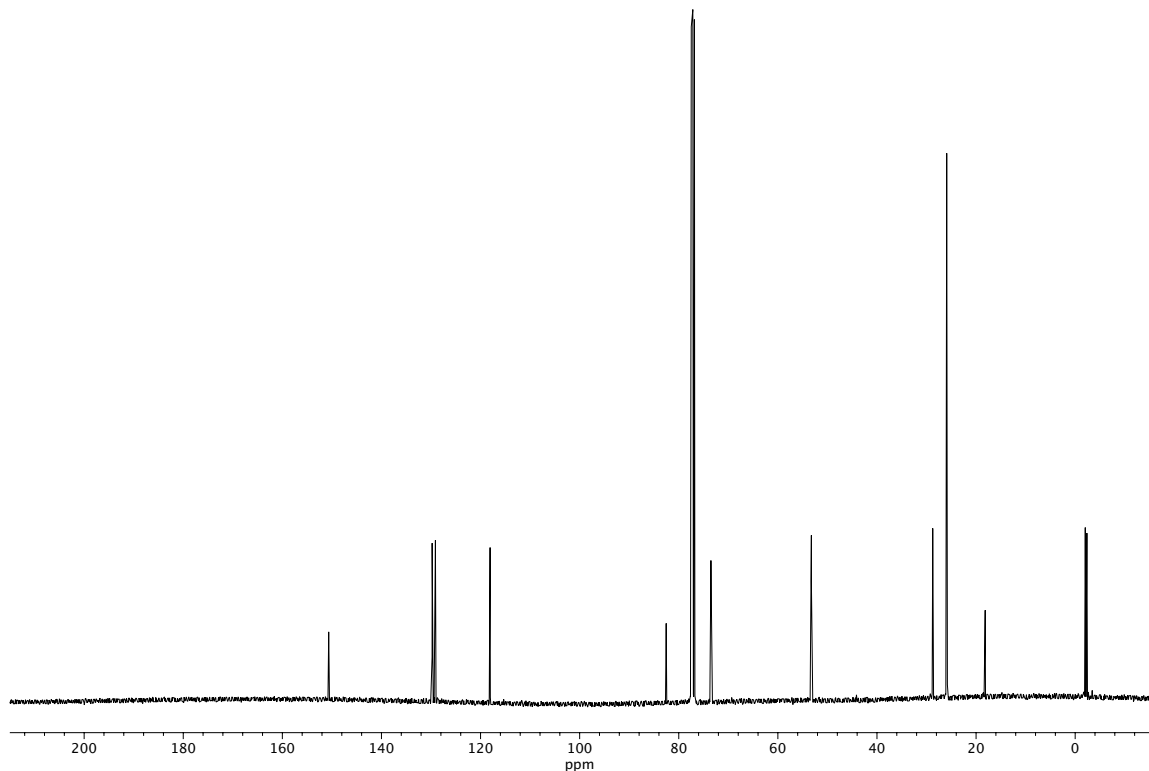
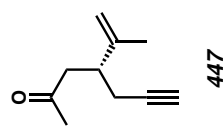


Figure A6.36. ^{13}C NMR (101 MHz, CDCl_3) of compound **446**.



447

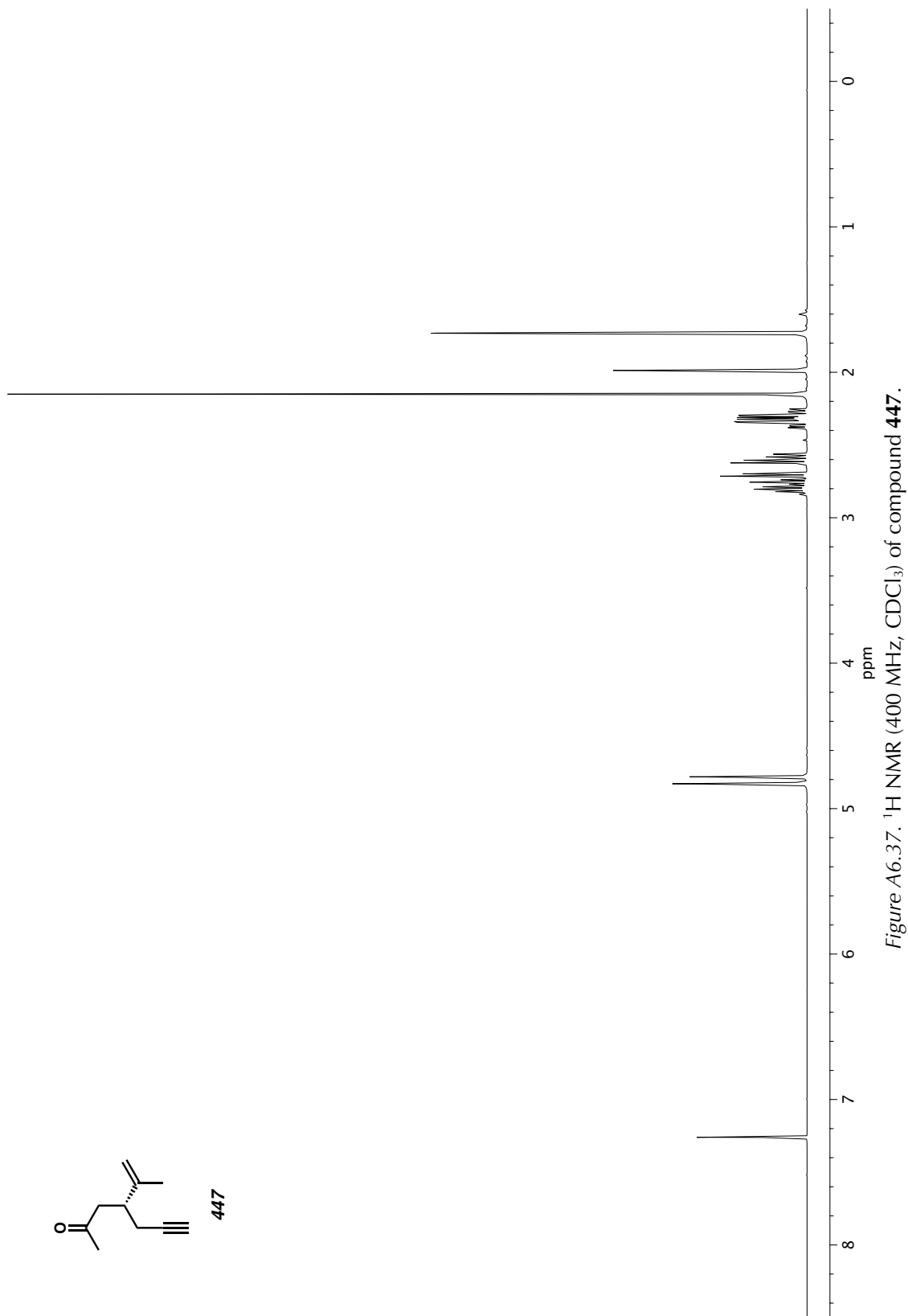


Figure A6.37. ^1H NMR (400 MHz, CDCl_3) of compound 447.

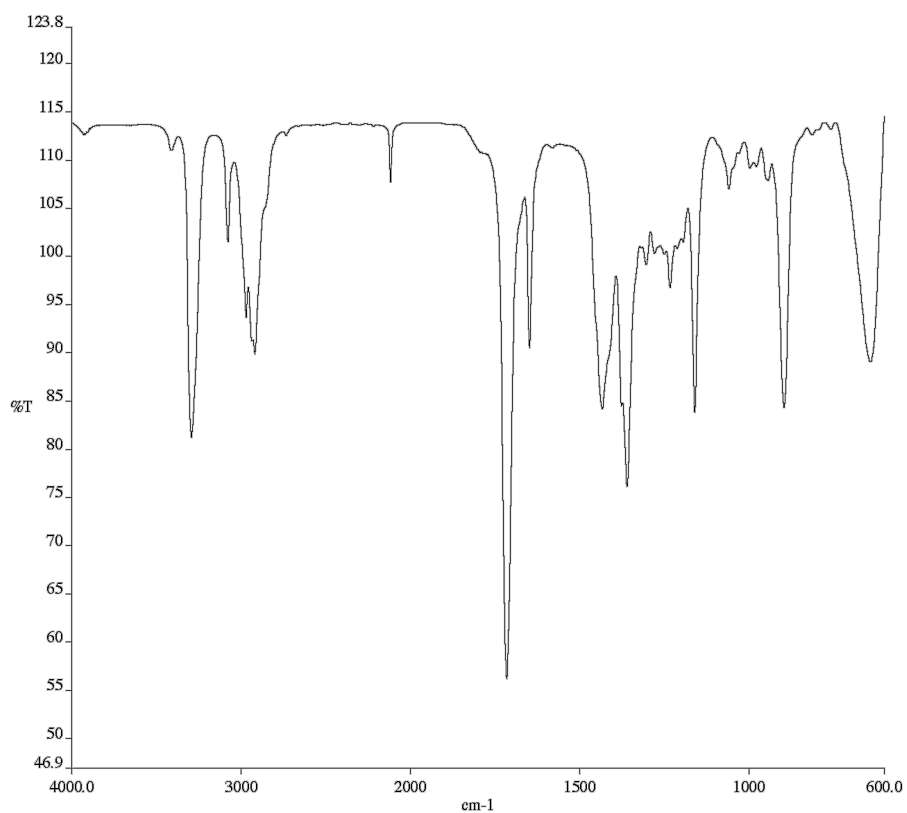


Figure A6.38. Infrared spectrum (Thin Film, NaCl) of compound **447**.

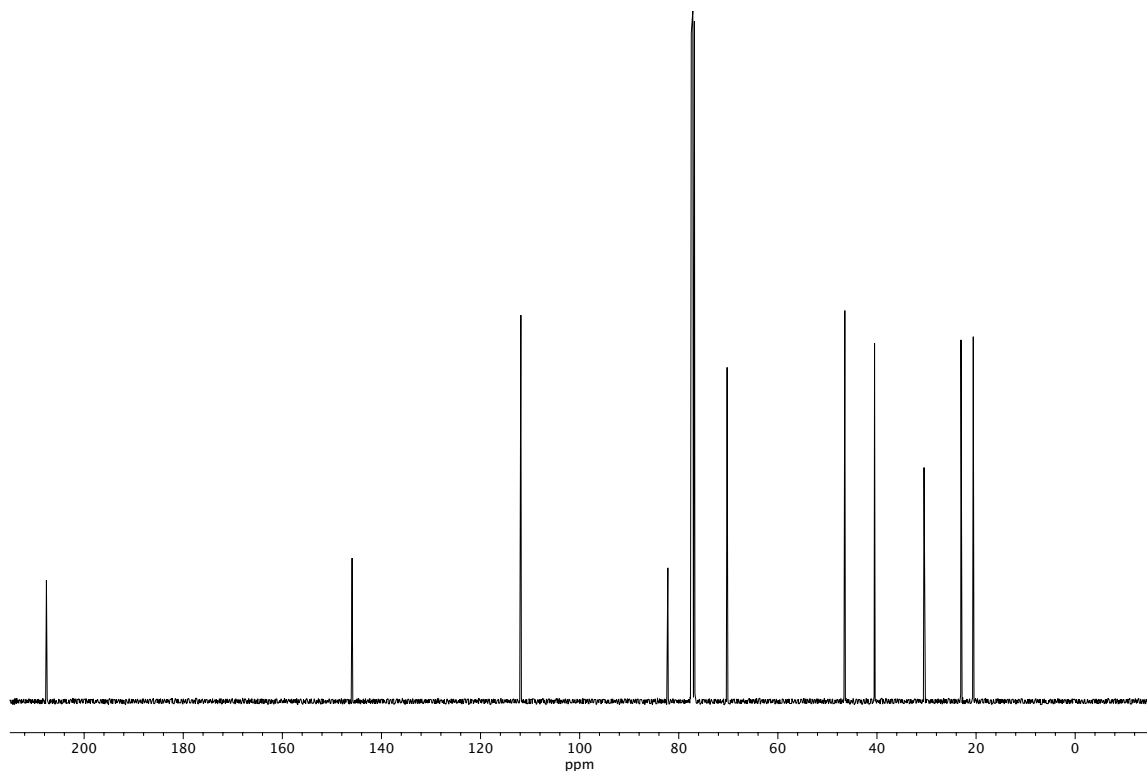


Figure A6.39. ^{13}C NMR (101 MHz, CDCl_3) of compound **447**.

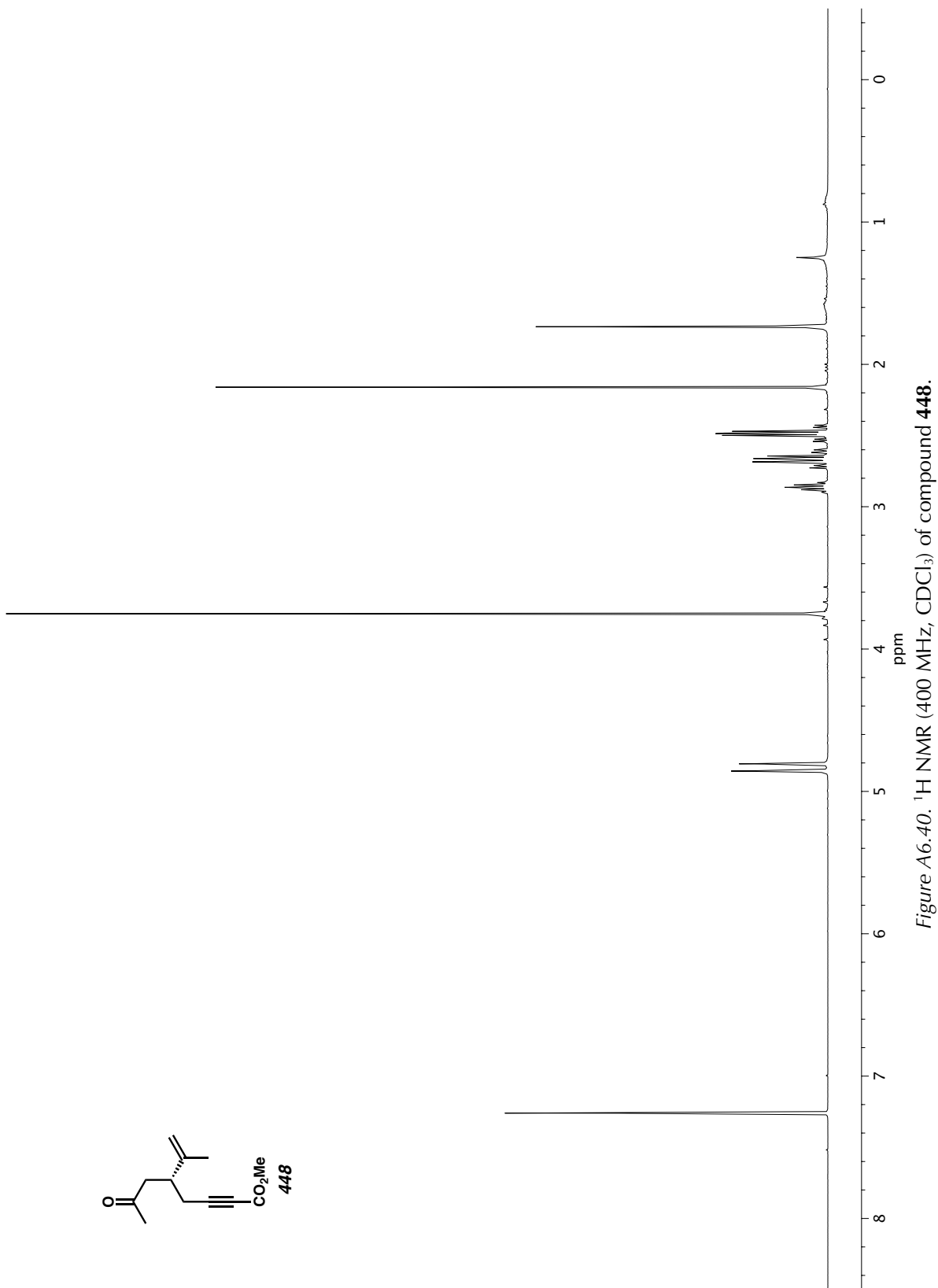


Figure A6.40. ^1H NMR (400 MHz, CDCl_3) of compound 448.

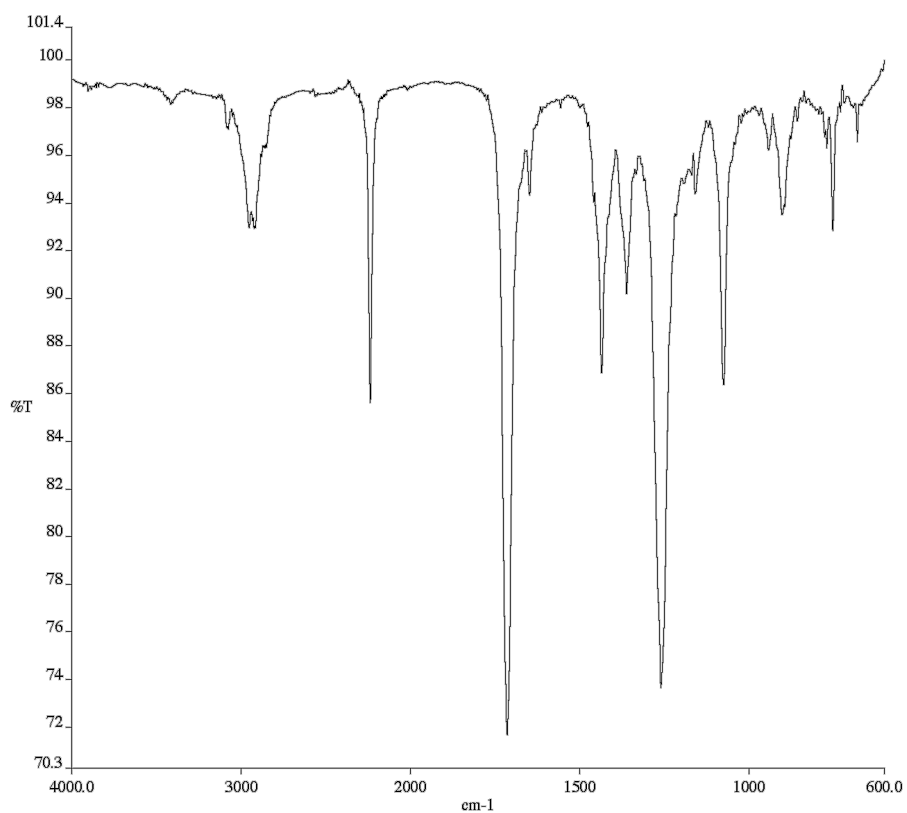


Figure A6.41. Infrared spectrum (Thin Film, NaCl) of compound **448**.

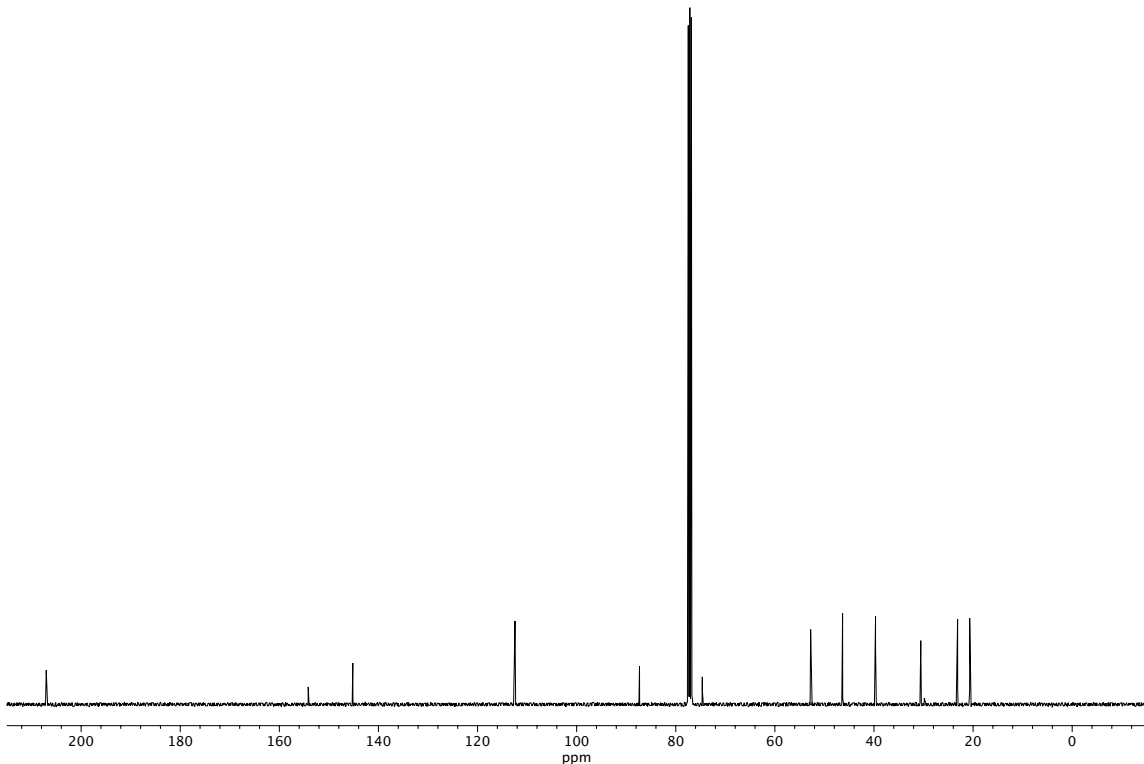
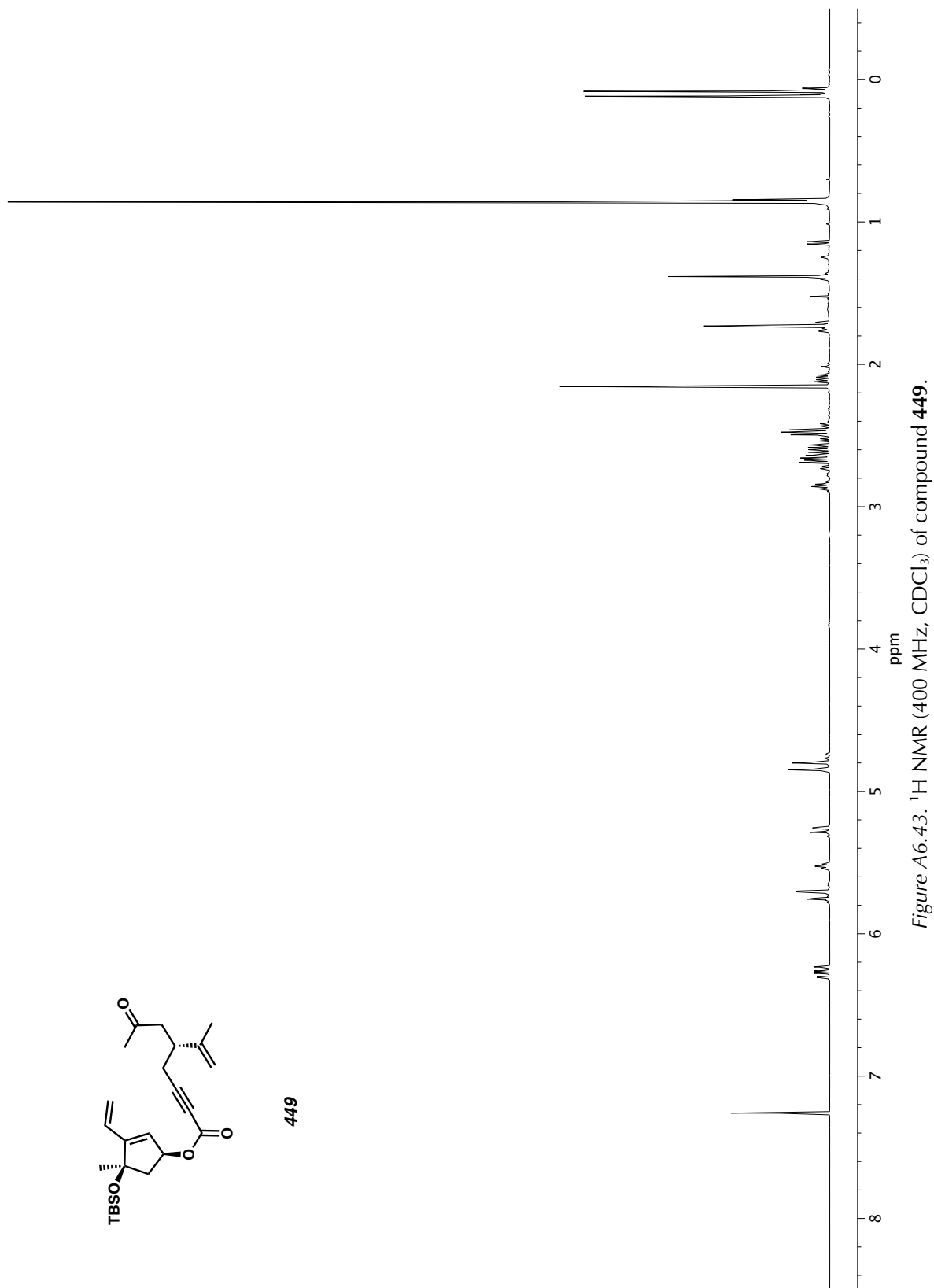


Figure A6.42. ^{13}C NMR (101 MHz, CDCl_3) of compound **448**.



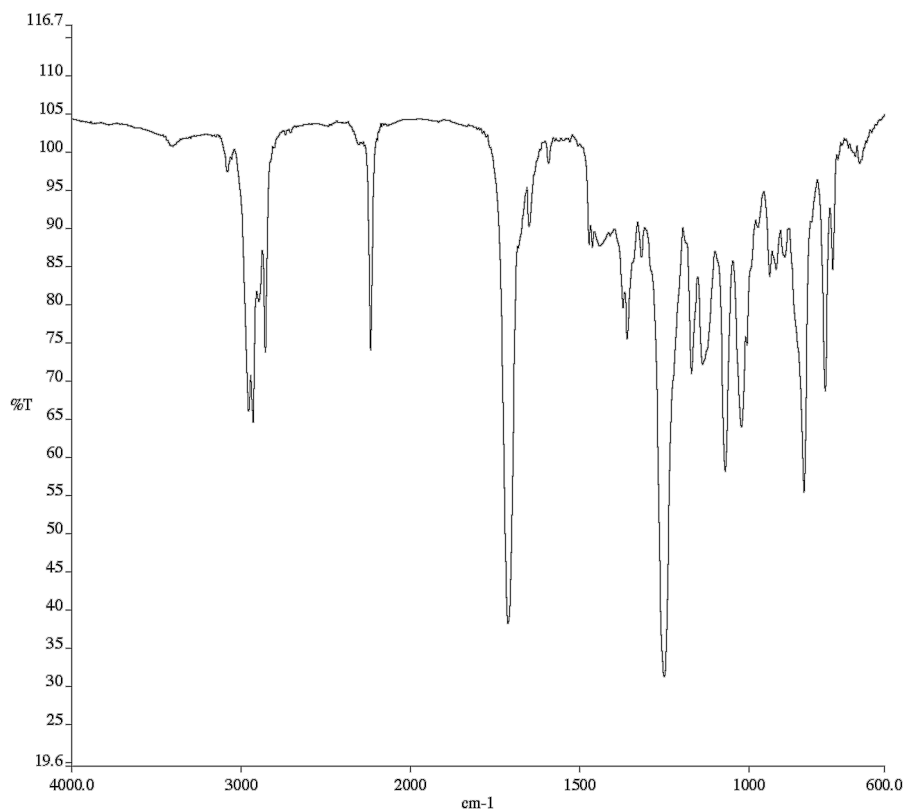


Figure A6.44. Infrared spectrum (Thin Film, NaCl) of compound **449**.

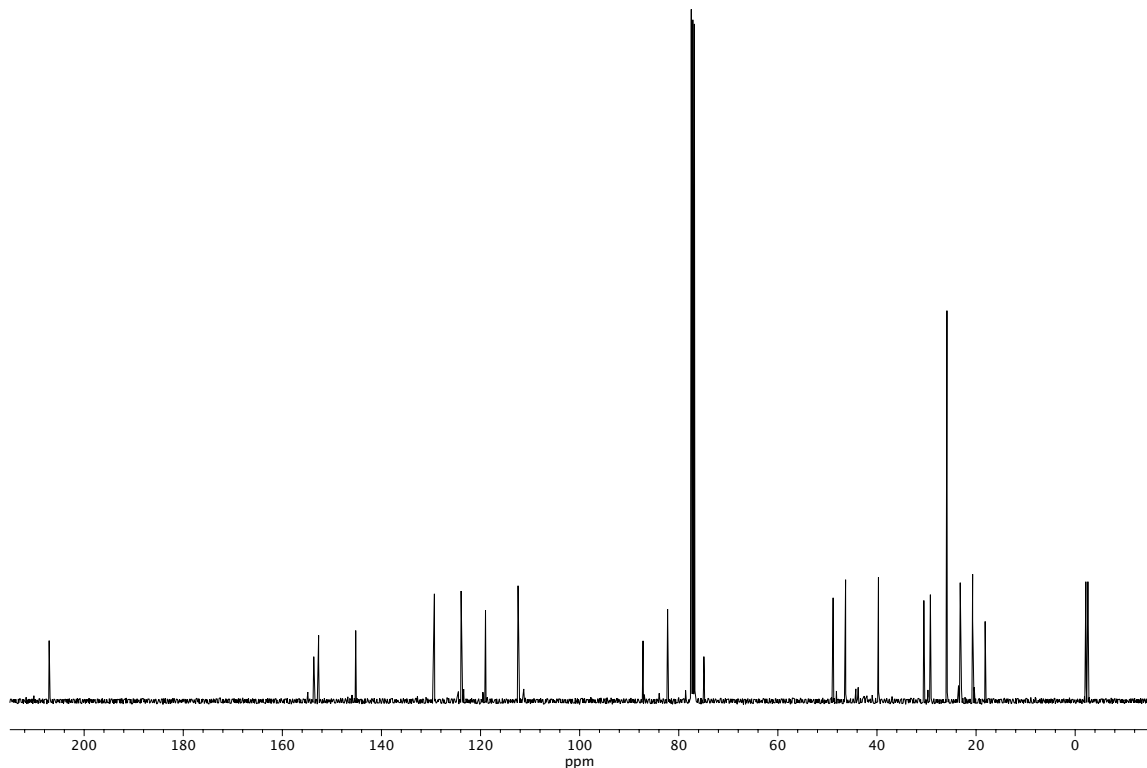


Figure A6.45. ^{13}C NMR (101 MHz, CDCl_3) of compound **449**.

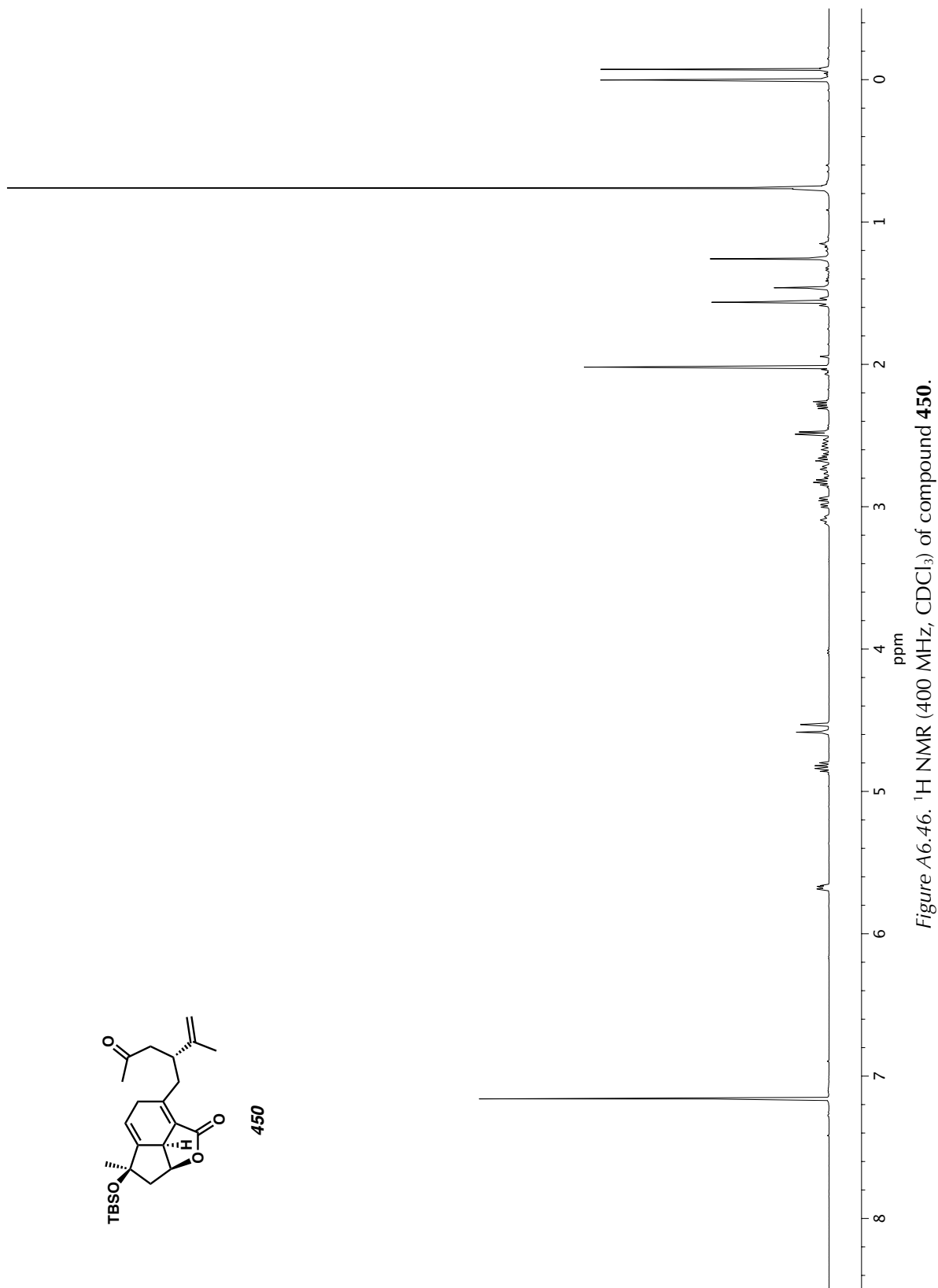


Figure A6.46. ^1H NMR (400 MHz, CDCl_3) of compound 450.

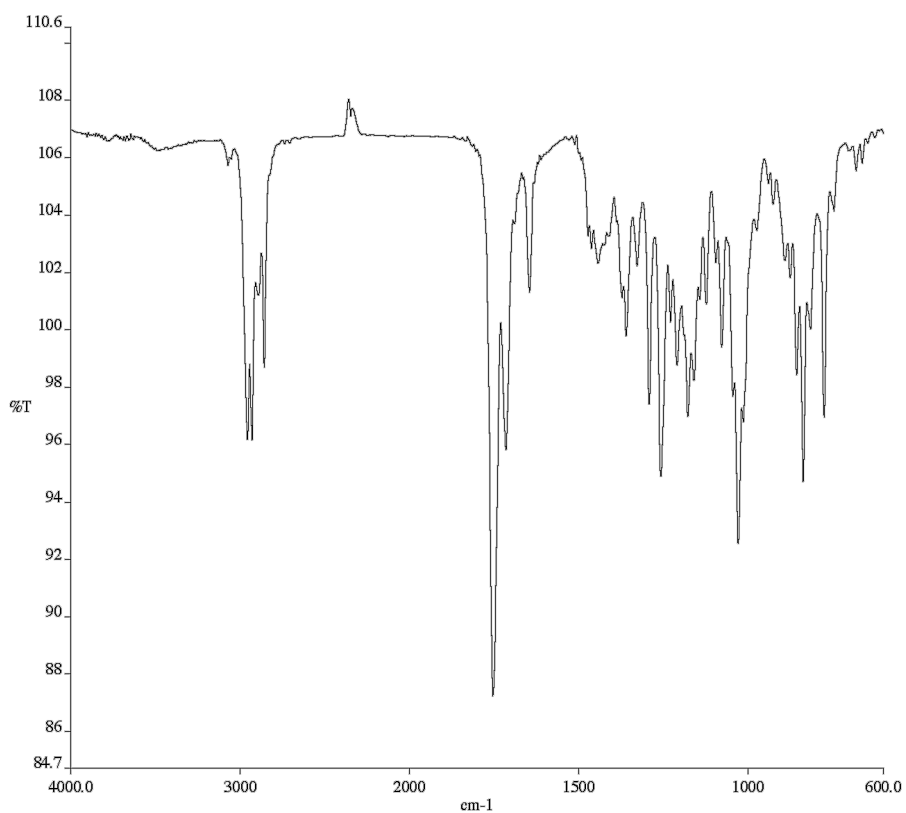


Figure A6.47. Infrared spectrum (Thin Film, NaCl) of compound **450**.

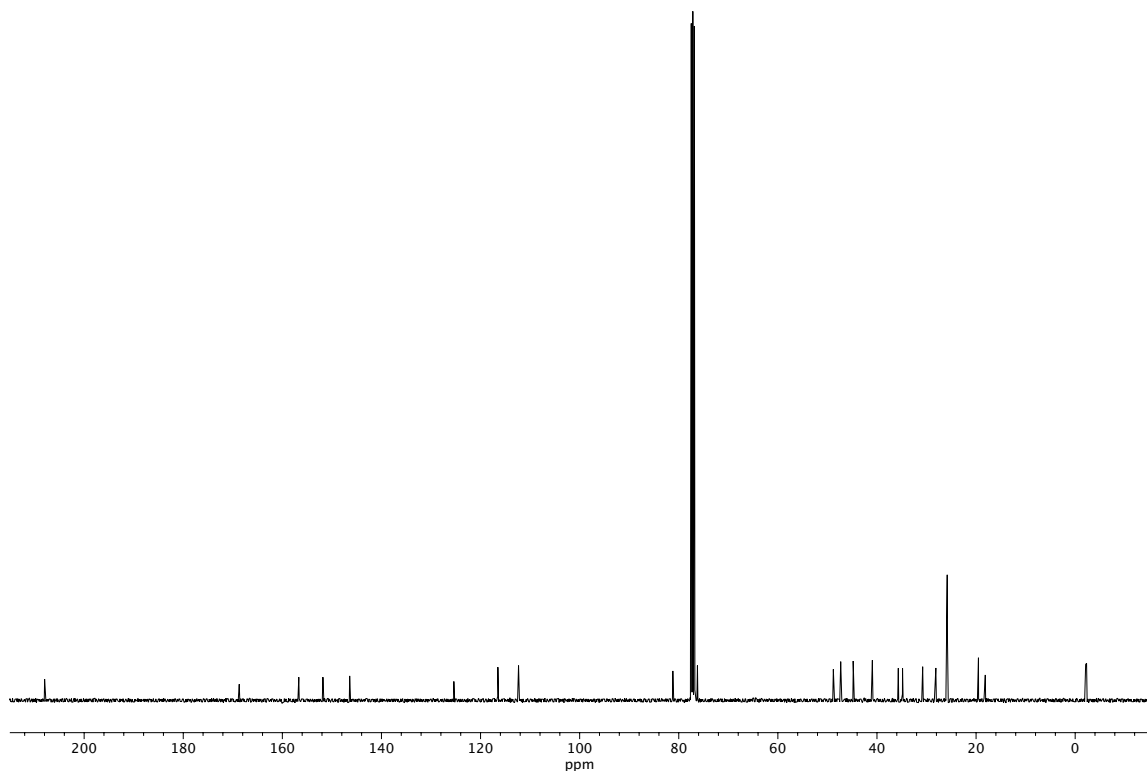


Figure A6.48. ^{13}C NMR (101 MHz, CDCl_3) of compound **450**.

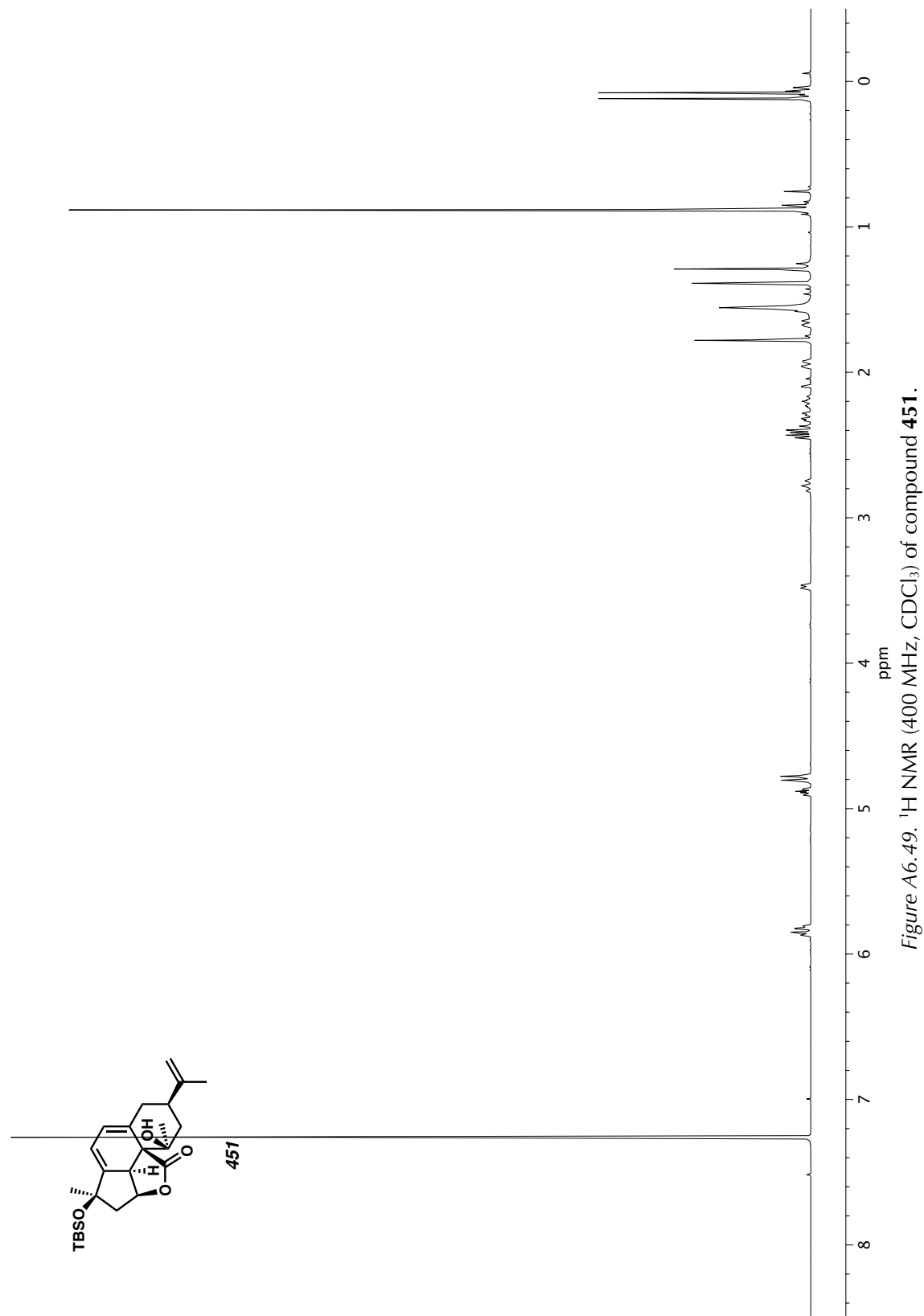


Figure A6.49. ^1H NMR (400 MHz, CDCl_3) of compound 451.

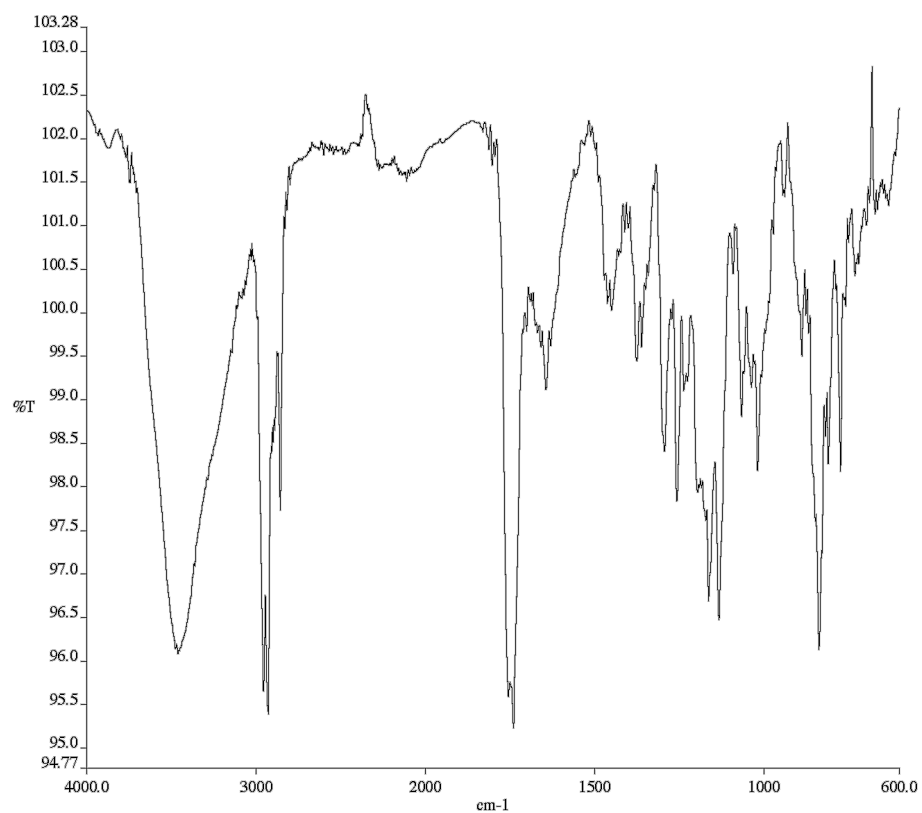


Figure A6.50. Infrared spectrum (Thin Film, NaCl) of compound **451**.

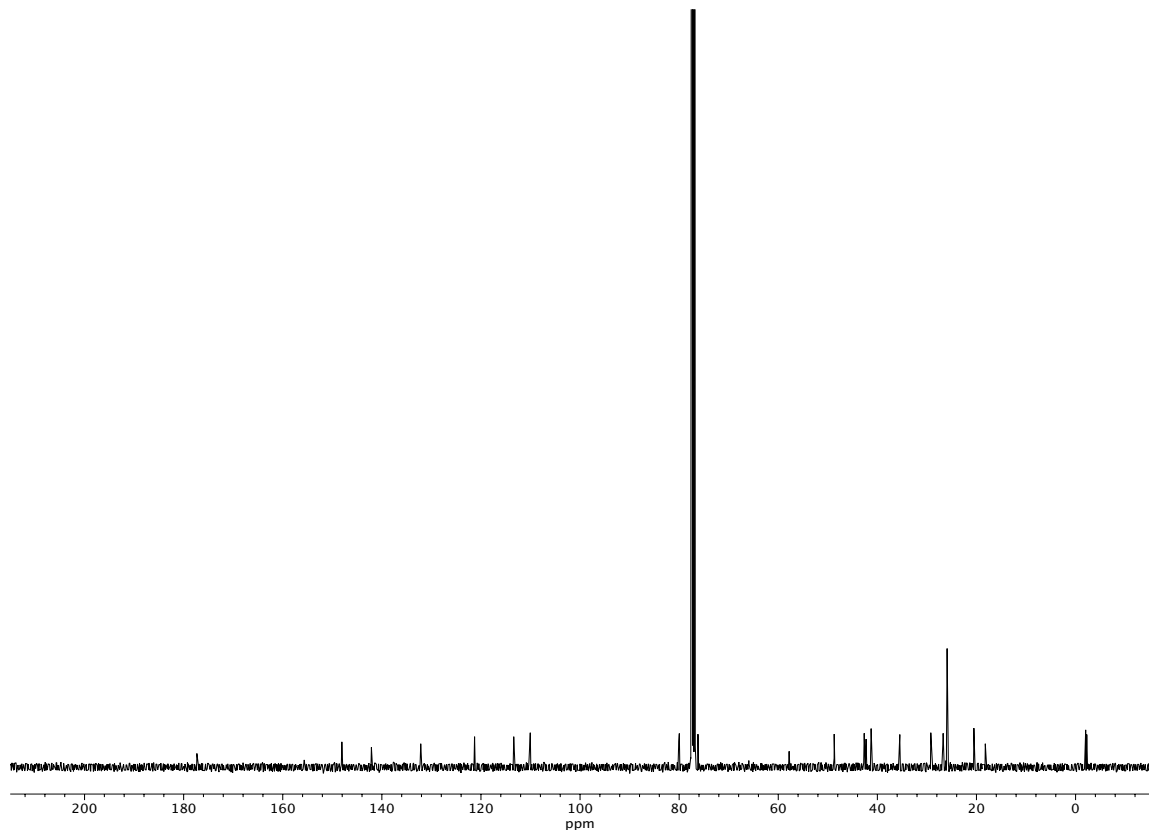


Figure A6.51. ^{13}C NMR (101 MHz, CDCl_3) of compound **451**.

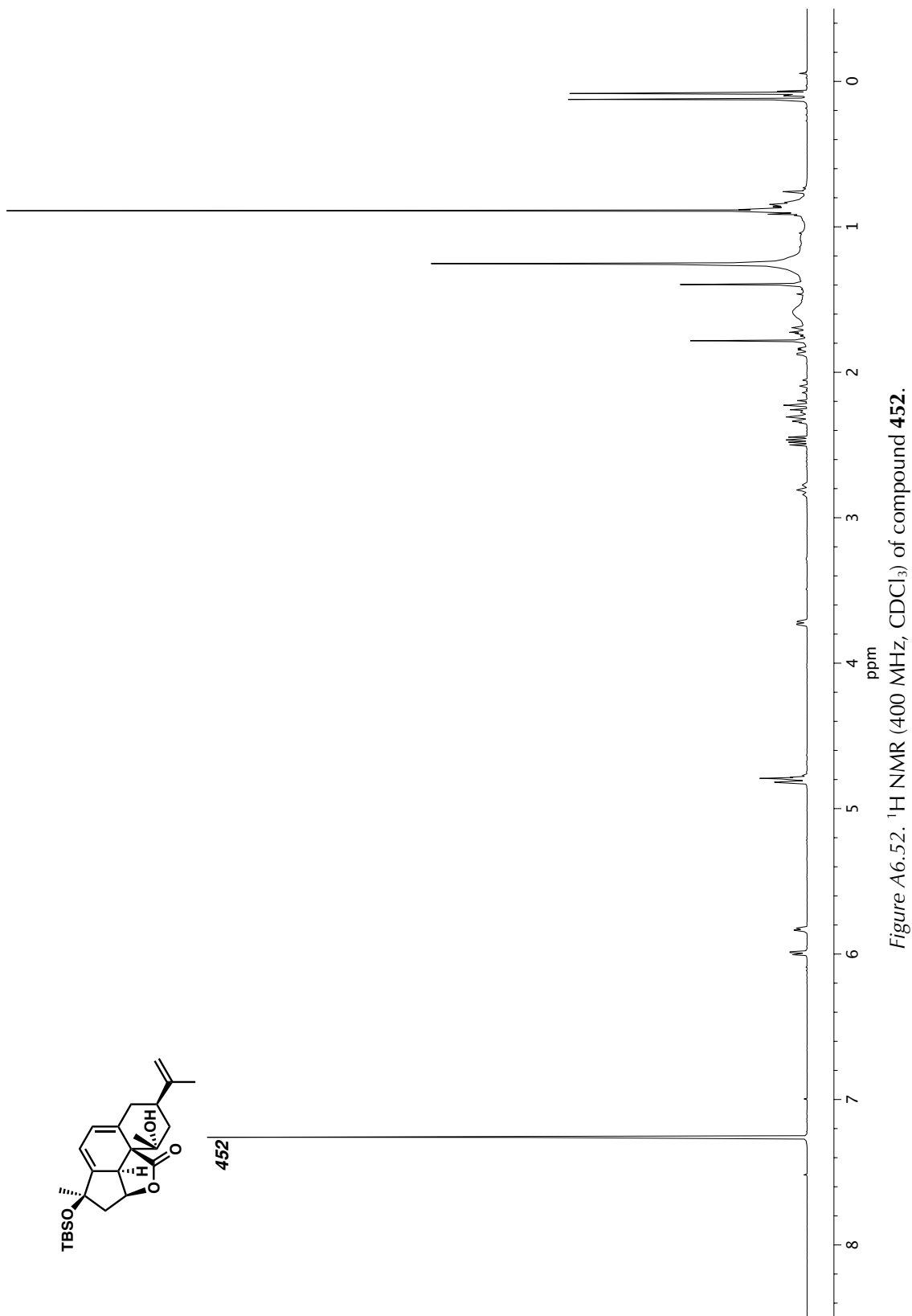
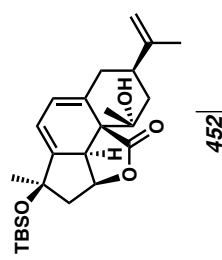


Figure A6.52. ^1H NMR (400 MHz, CDCl_3) of compound 452.

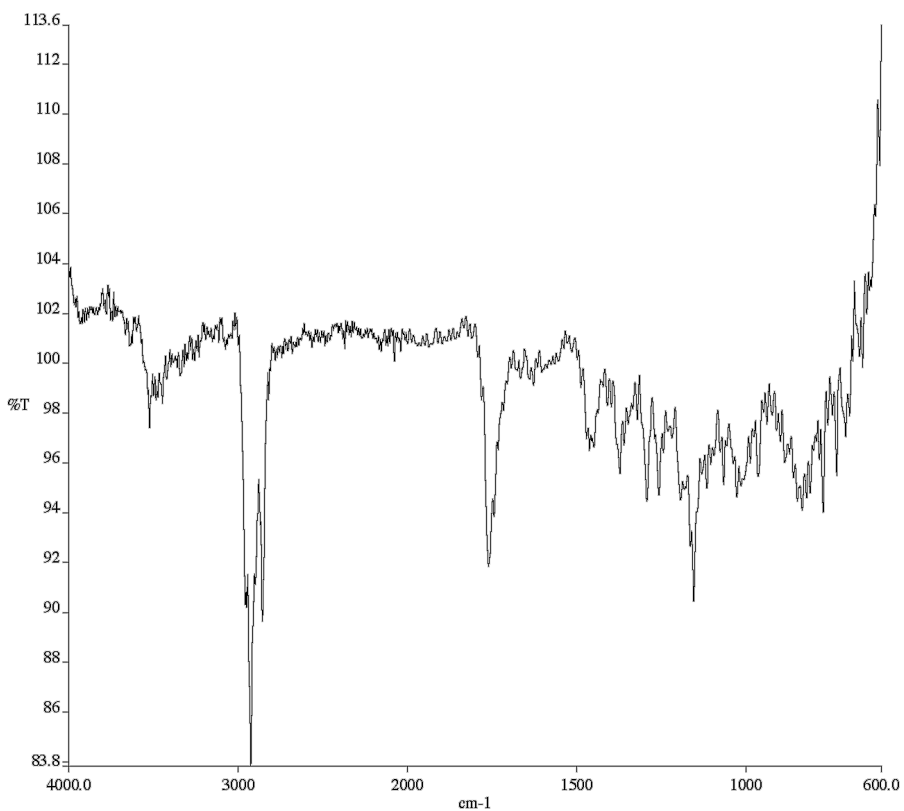


Figure A6.53. Infrared spectrum (Thin Film, NaCl) of compound **452**.

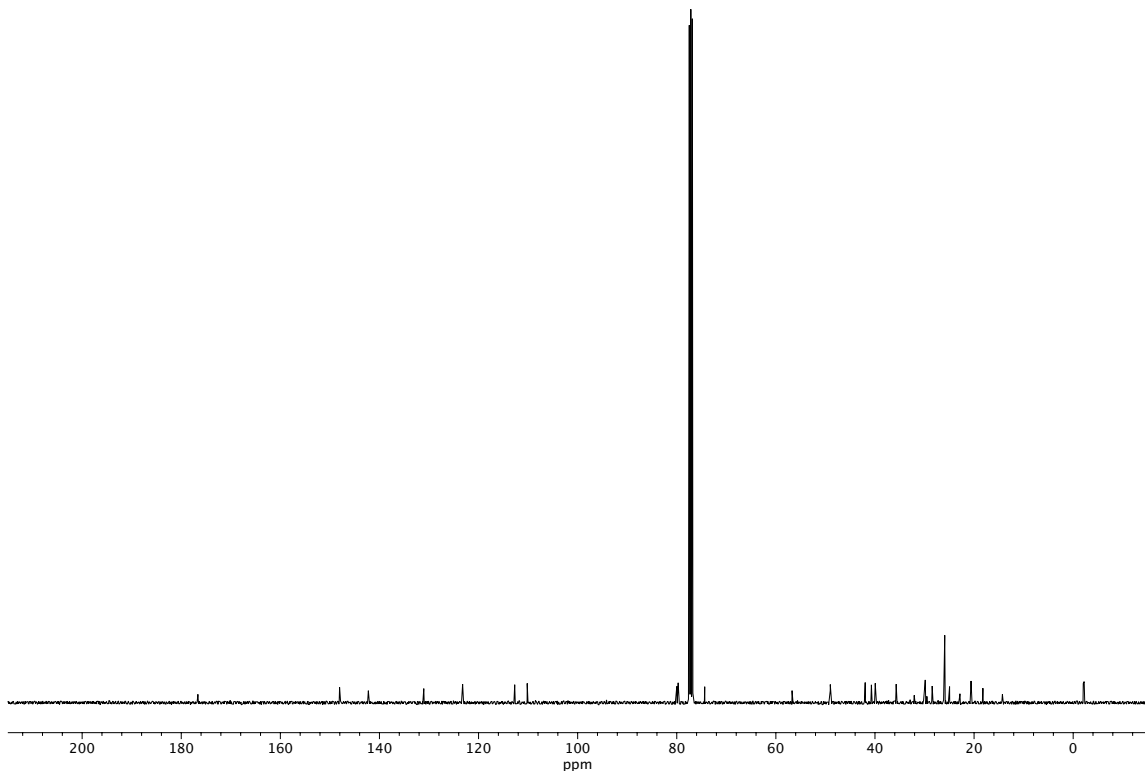


Figure A6.54. ^{13}C NMR (101 MHz, CDCl_3) of compound **452**.

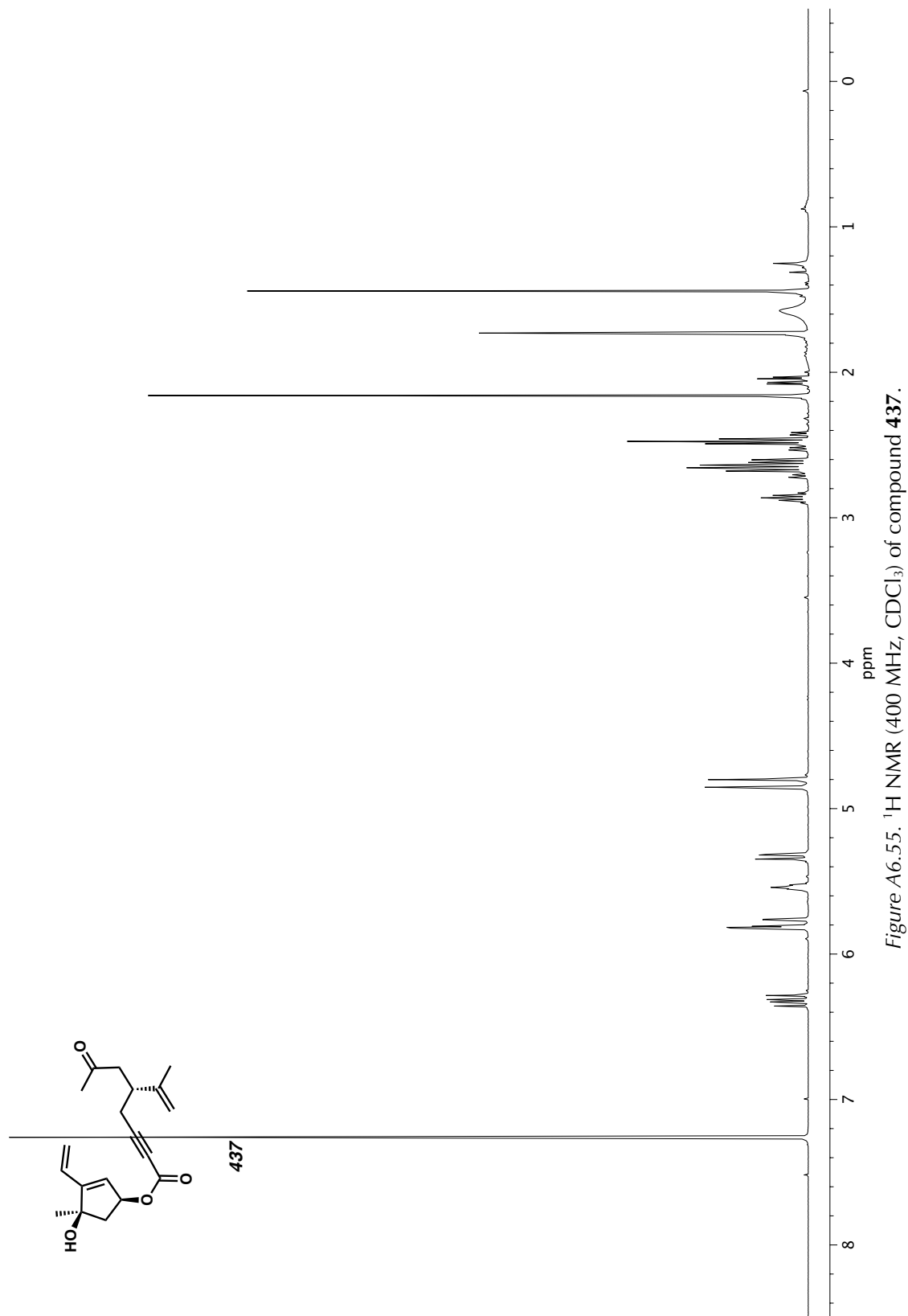


Figure A6.55. ^1H NMR (400 MHz, CDCl_3) of compound 437.

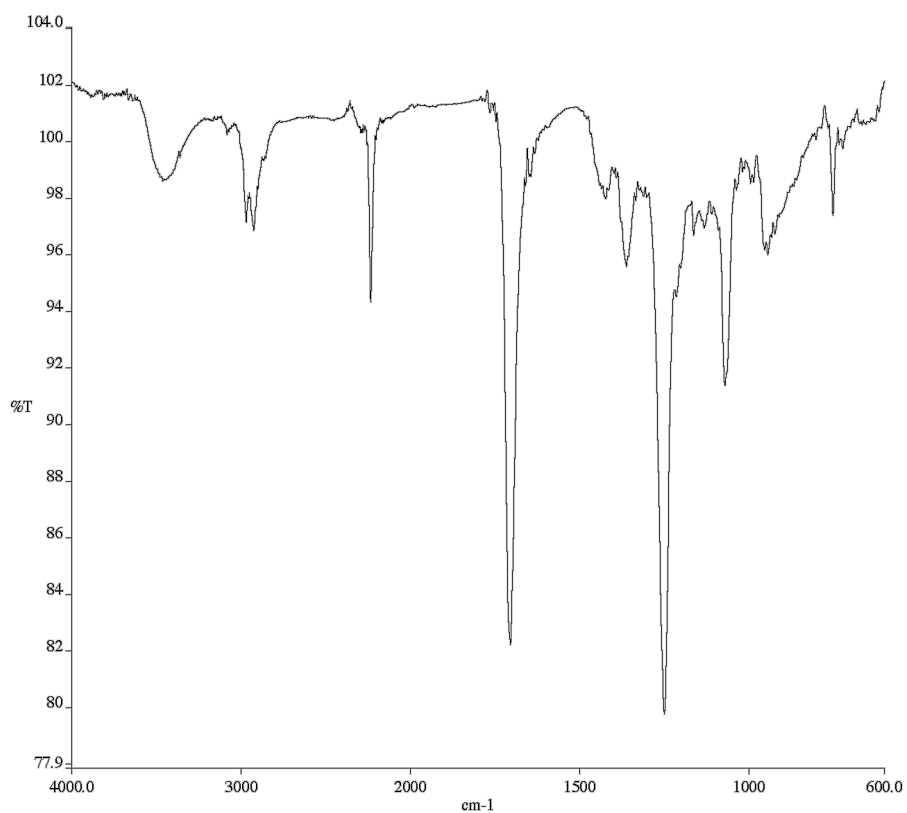


Figure A6.56. Infrared spectrum (Thin Film, NaCl) of compound **437**.

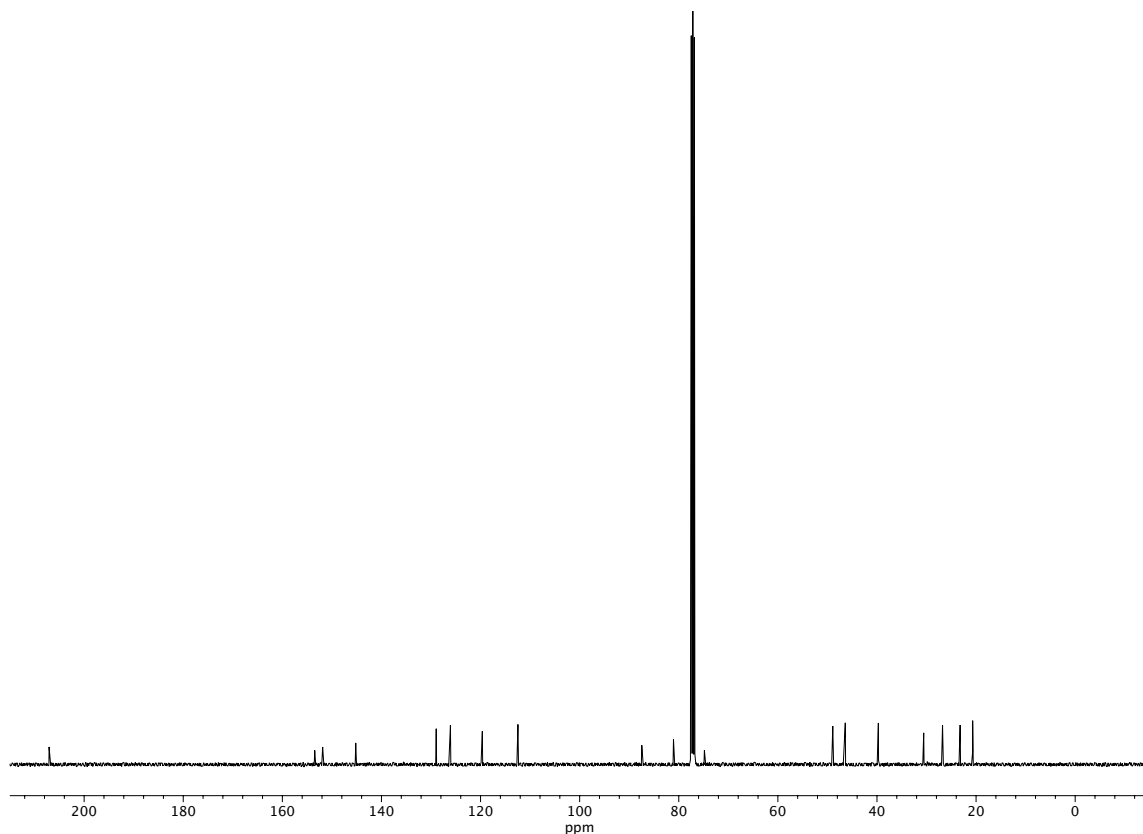


Figure A6.57. ^{13}C NMR (101 MHz, CDCl_3) of compound **437**.

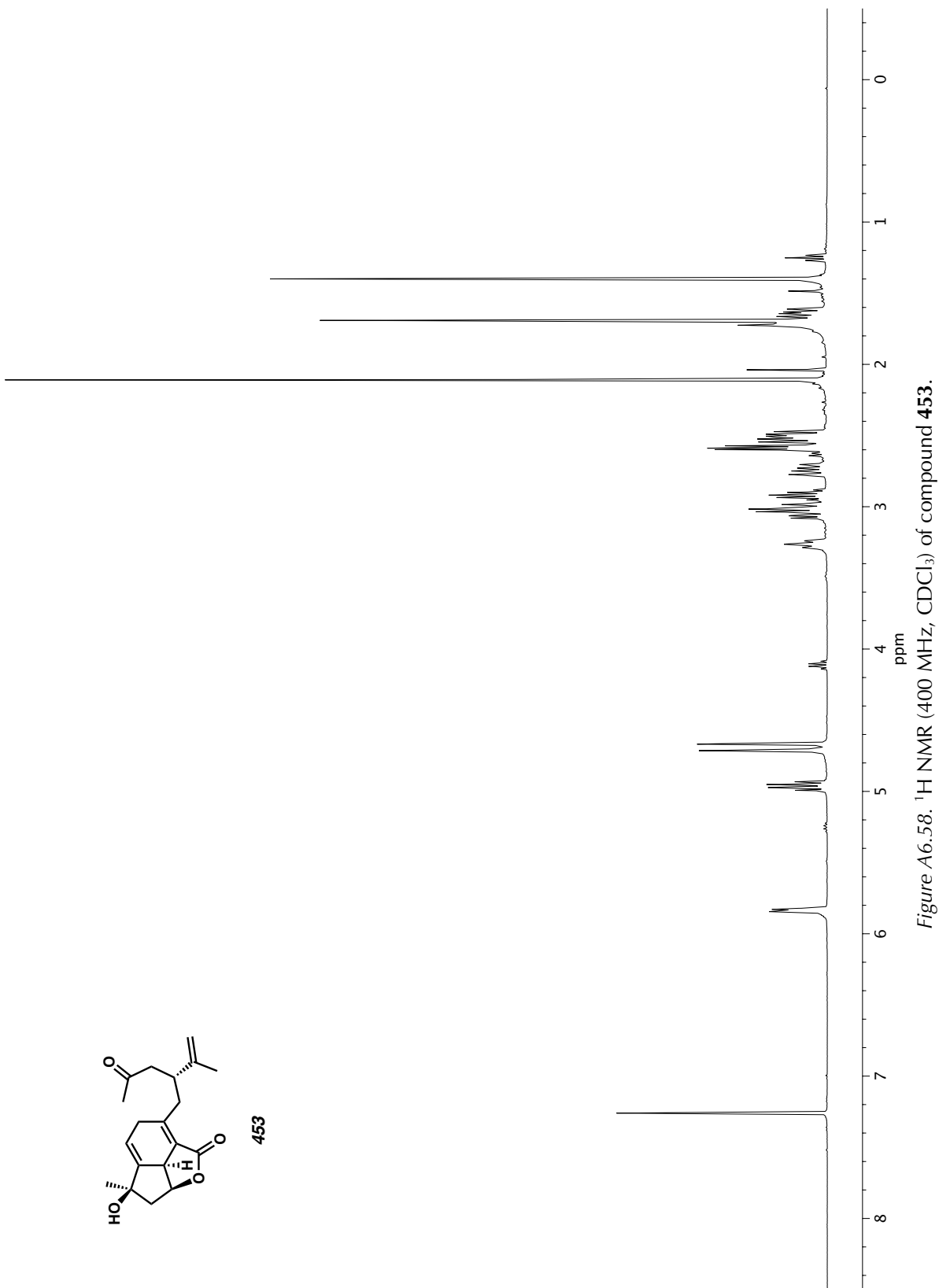


Figure A6.58. ^1H NMR (400 MHz, CDCl_3) of compound 453.

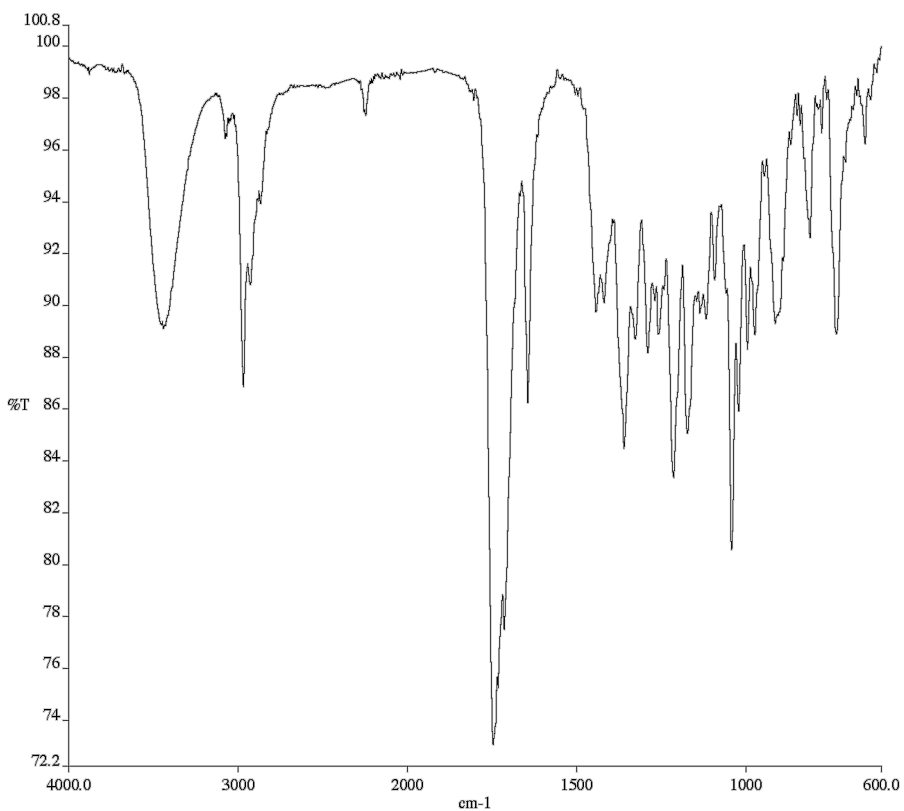


Figure A6.59. Infrared spectrum (Thin Film, NaCl) of compound 453.

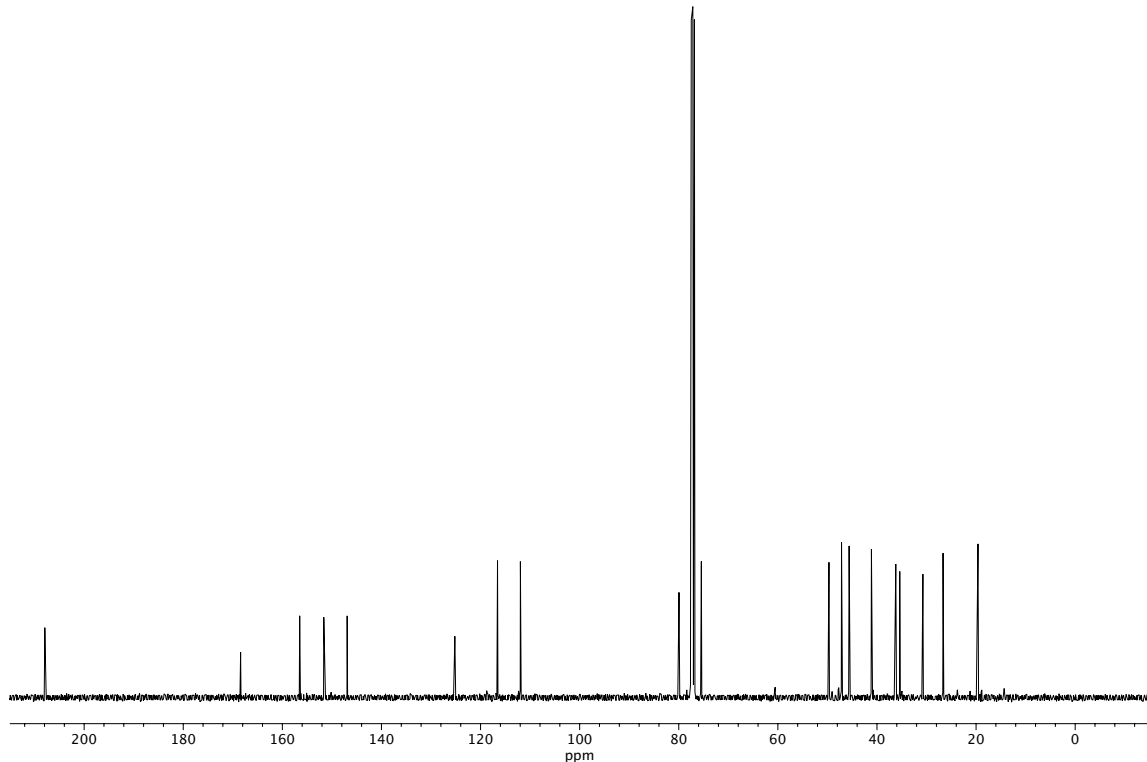


Figure A6.60. ¹³C NMR (101 MHz, CDCl_3) of compound 453.

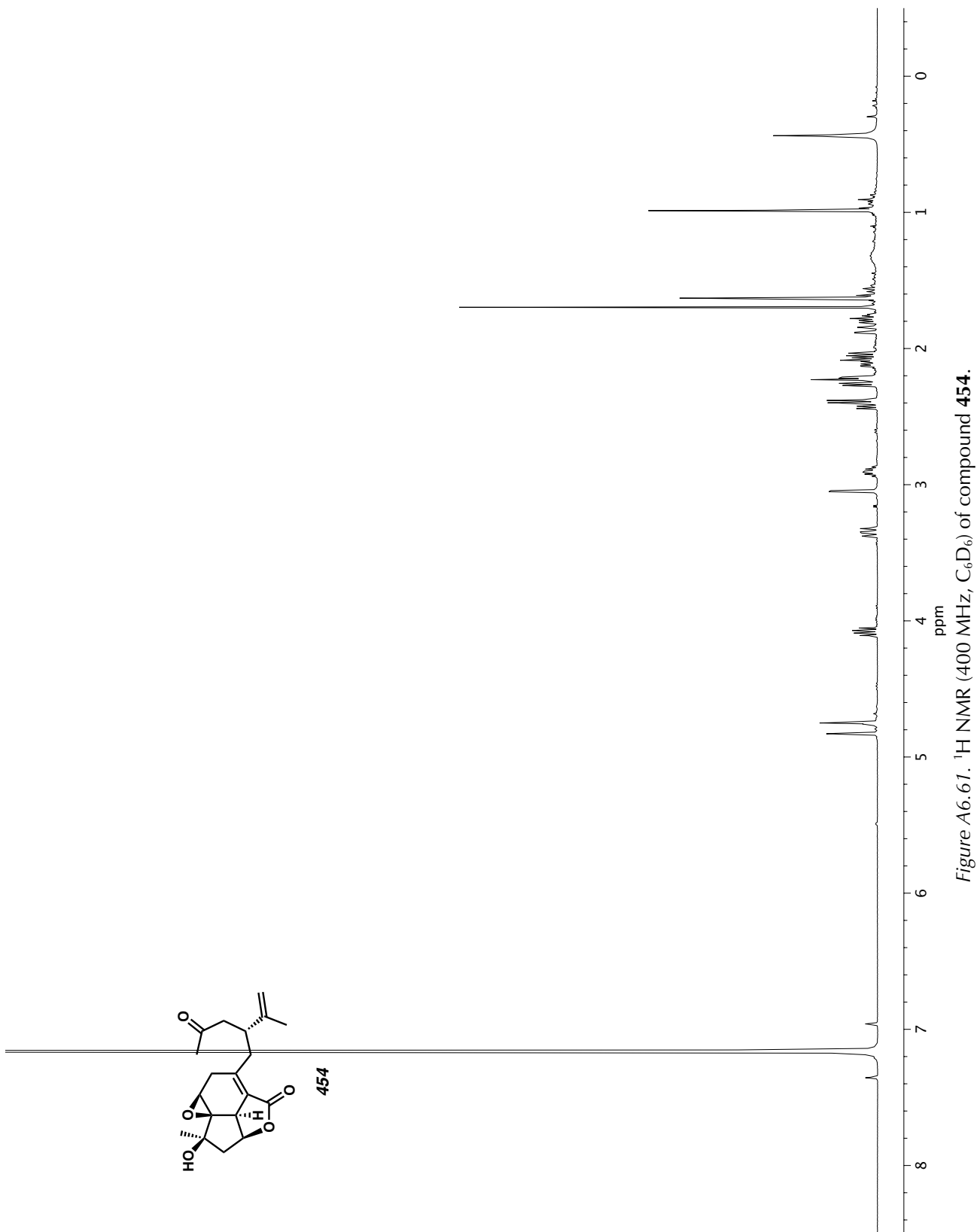


Figure A6.61. ^1H NMR (400 MHz, C_6D_6) of compound 454.

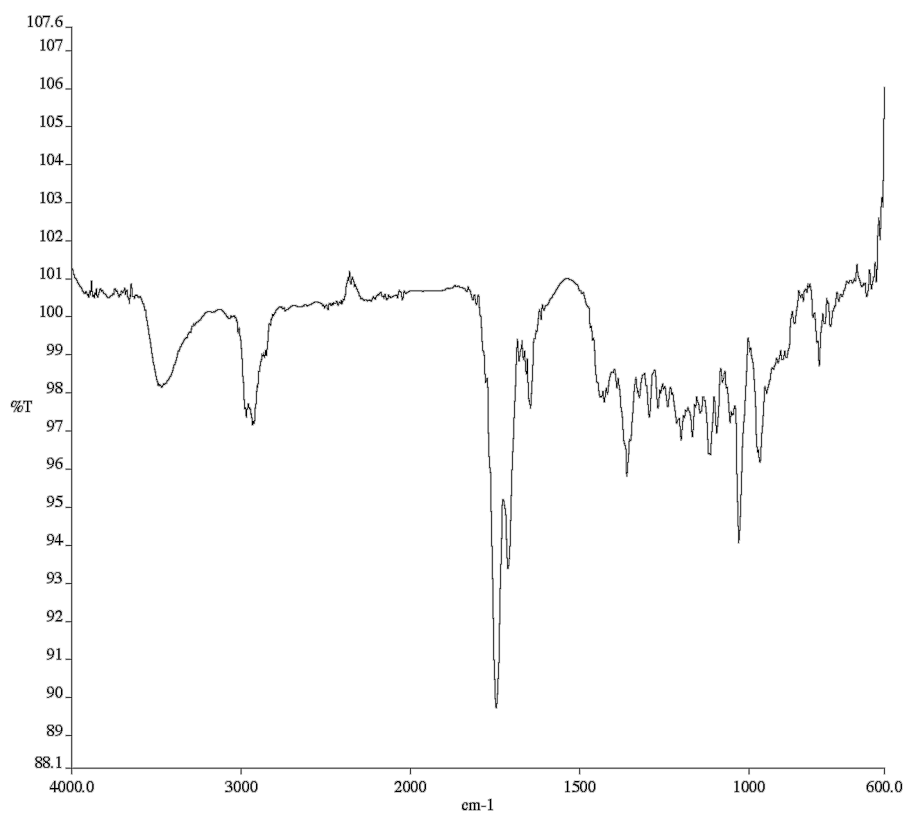


Figure A6.62. Infrared spectrum (Thin Film, NaCl) of compound **454**.

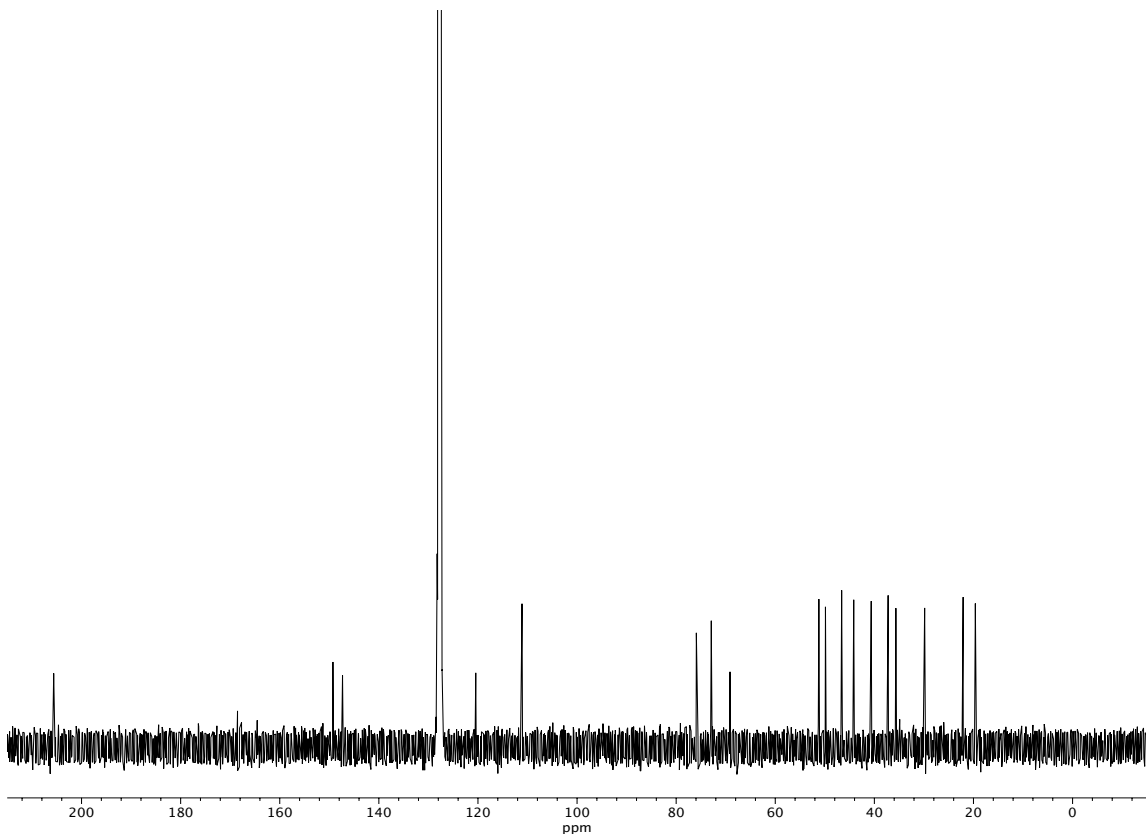


Figure A6.63. ^{13}C NMR (101 MHz, C_6D_6) of compound **454**.

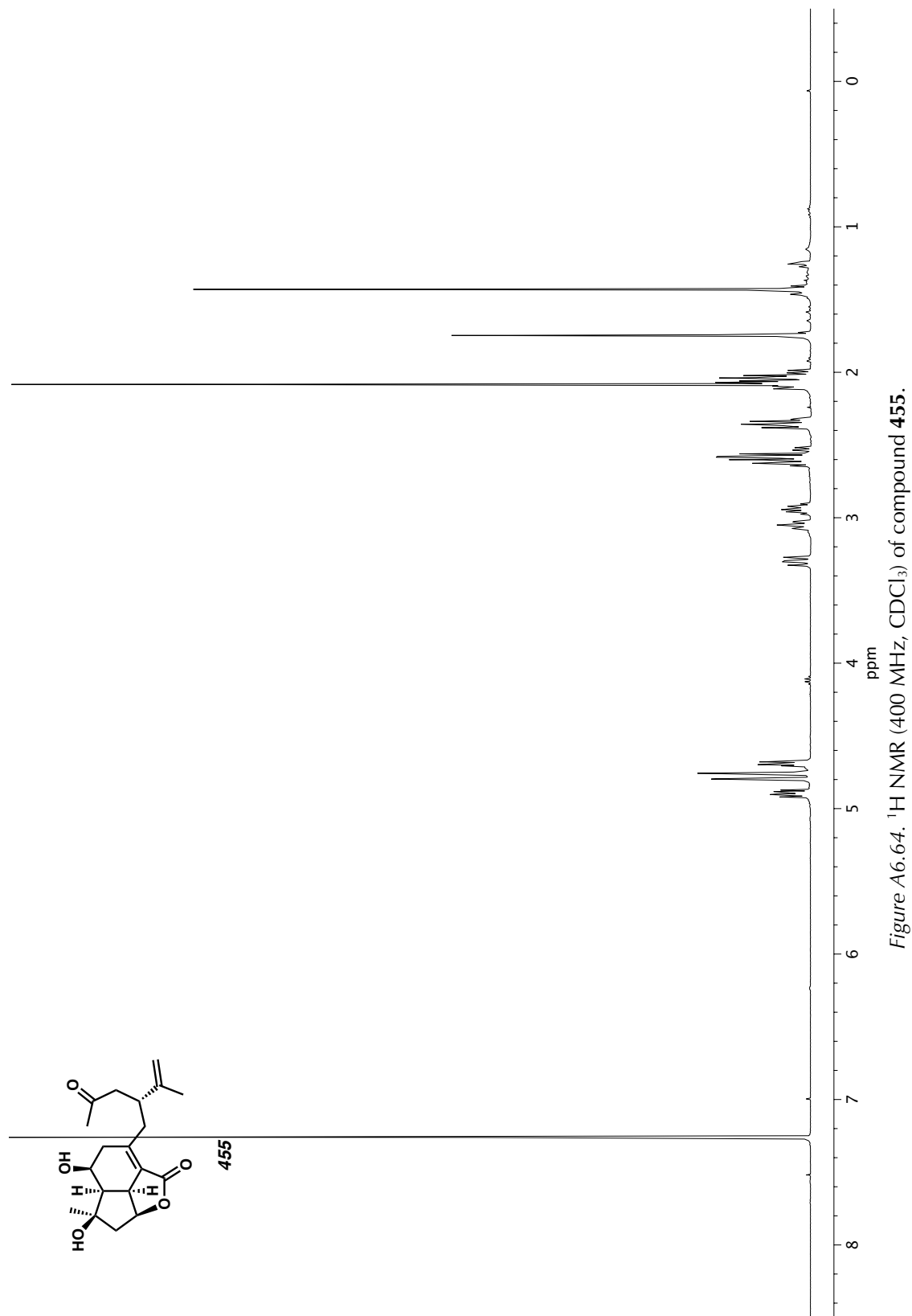


Figure A6.64. ^1H NMR (400 MHz, CDCl_3) of compound 455.

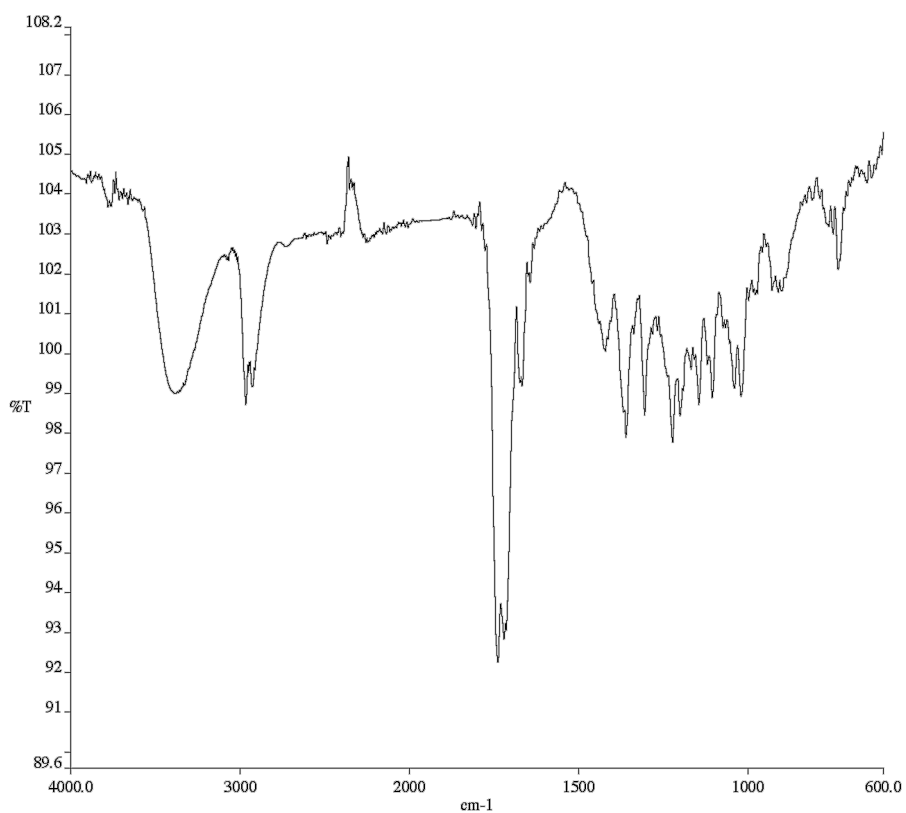


Figure A6.65. Infrared spectrum (Thin Film, NaCl) of compound 455.

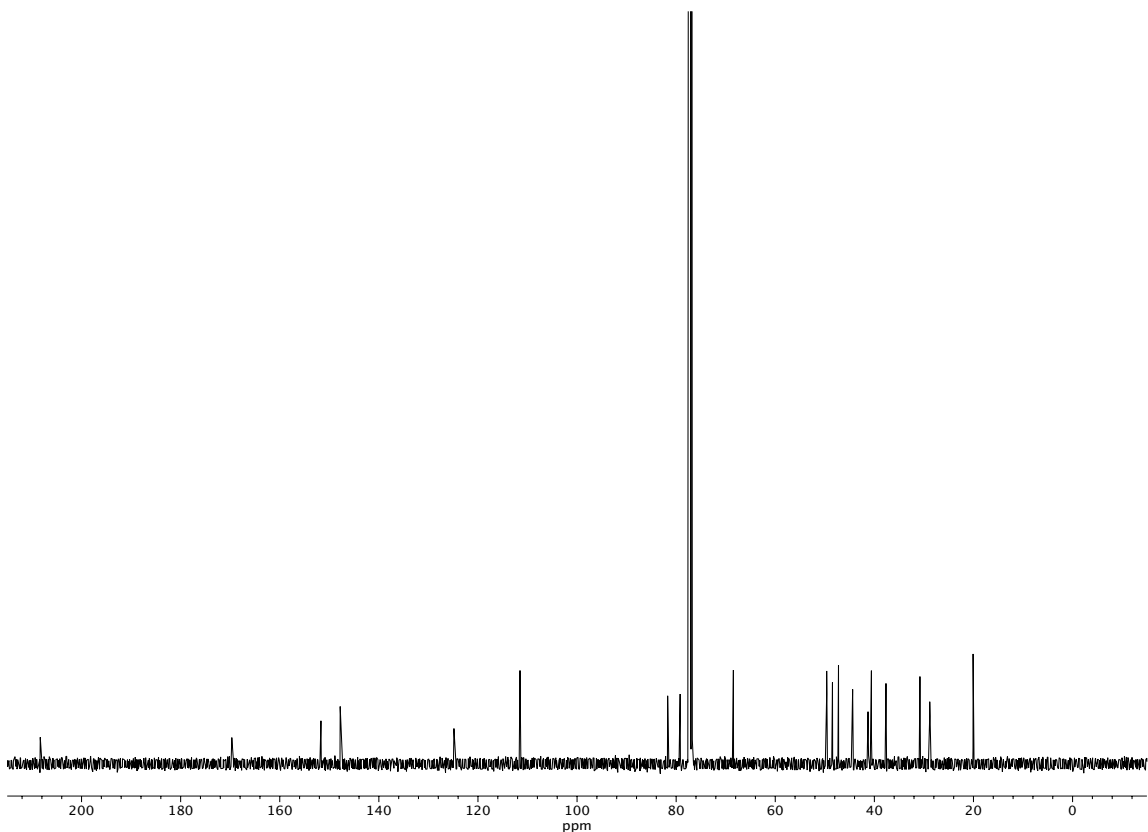


Figure A6.66. ^{13}C NMR (101 MHz, CDCl_3) of compound 455.

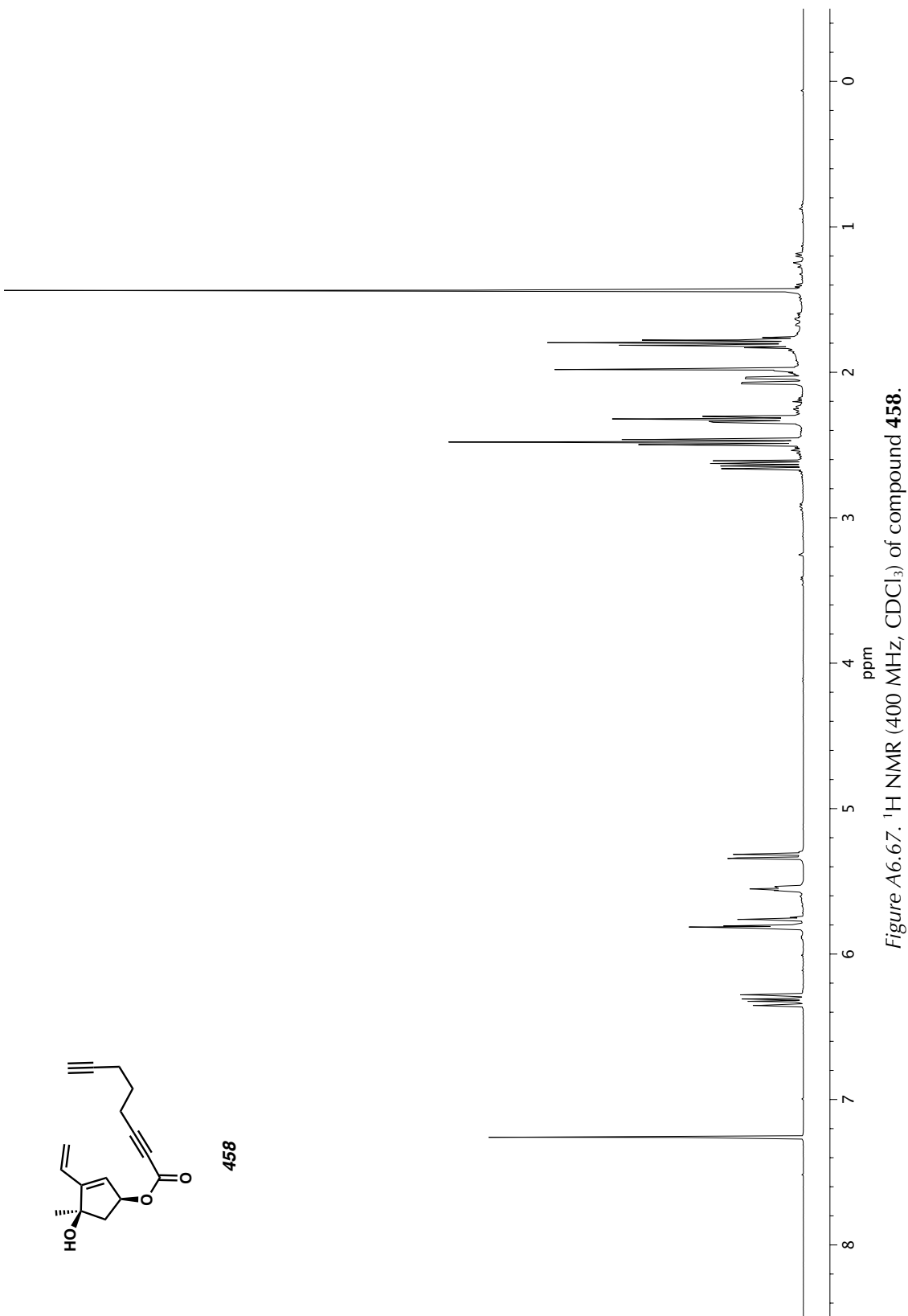


Figure A6.67. ^1H NMR (400 MHz, CDCl_3) of compound 458.

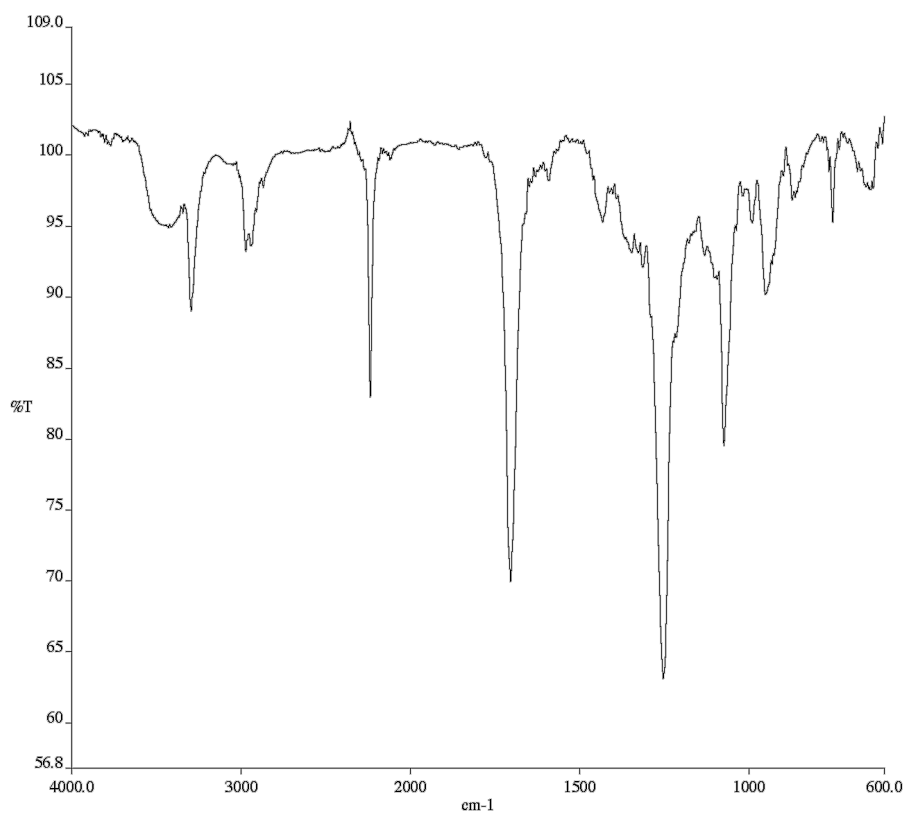


Figure A6.68. Infrared spectrum (Thin Film, NaCl) of compound **458**.

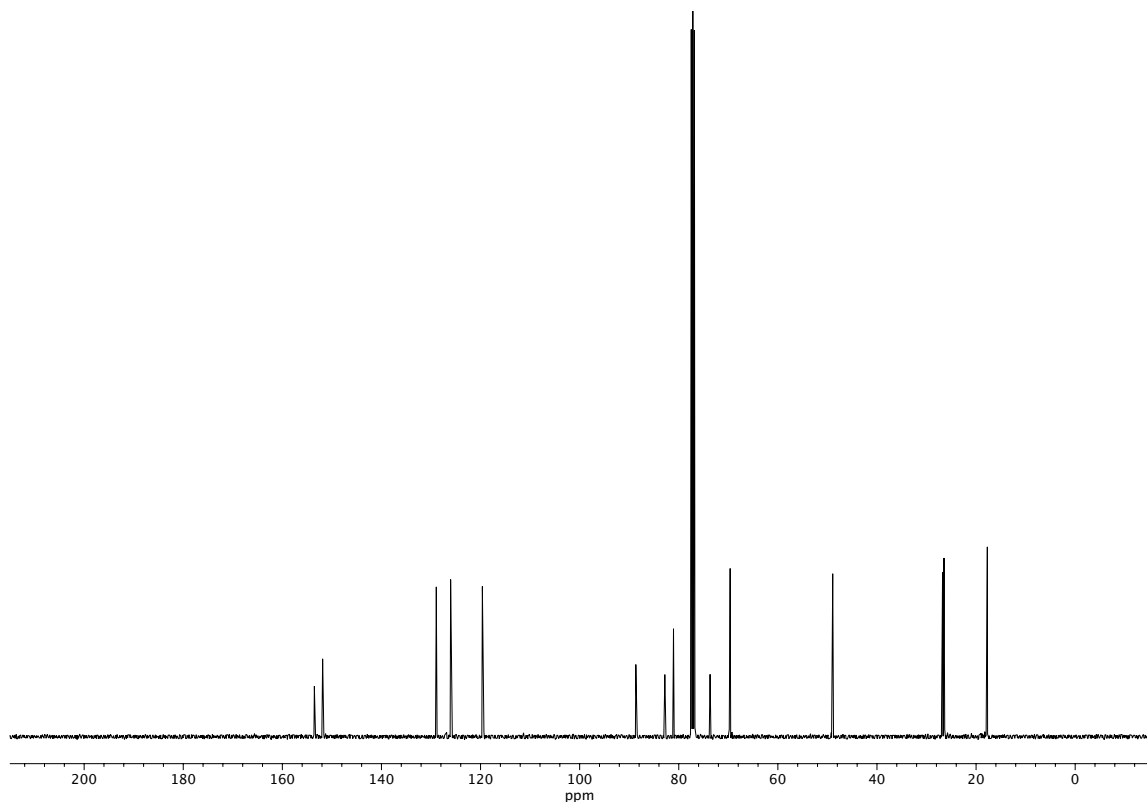


Figure A6.69. ^{13}C NMR (101 MHz, CDCl_3) of compound **458**.

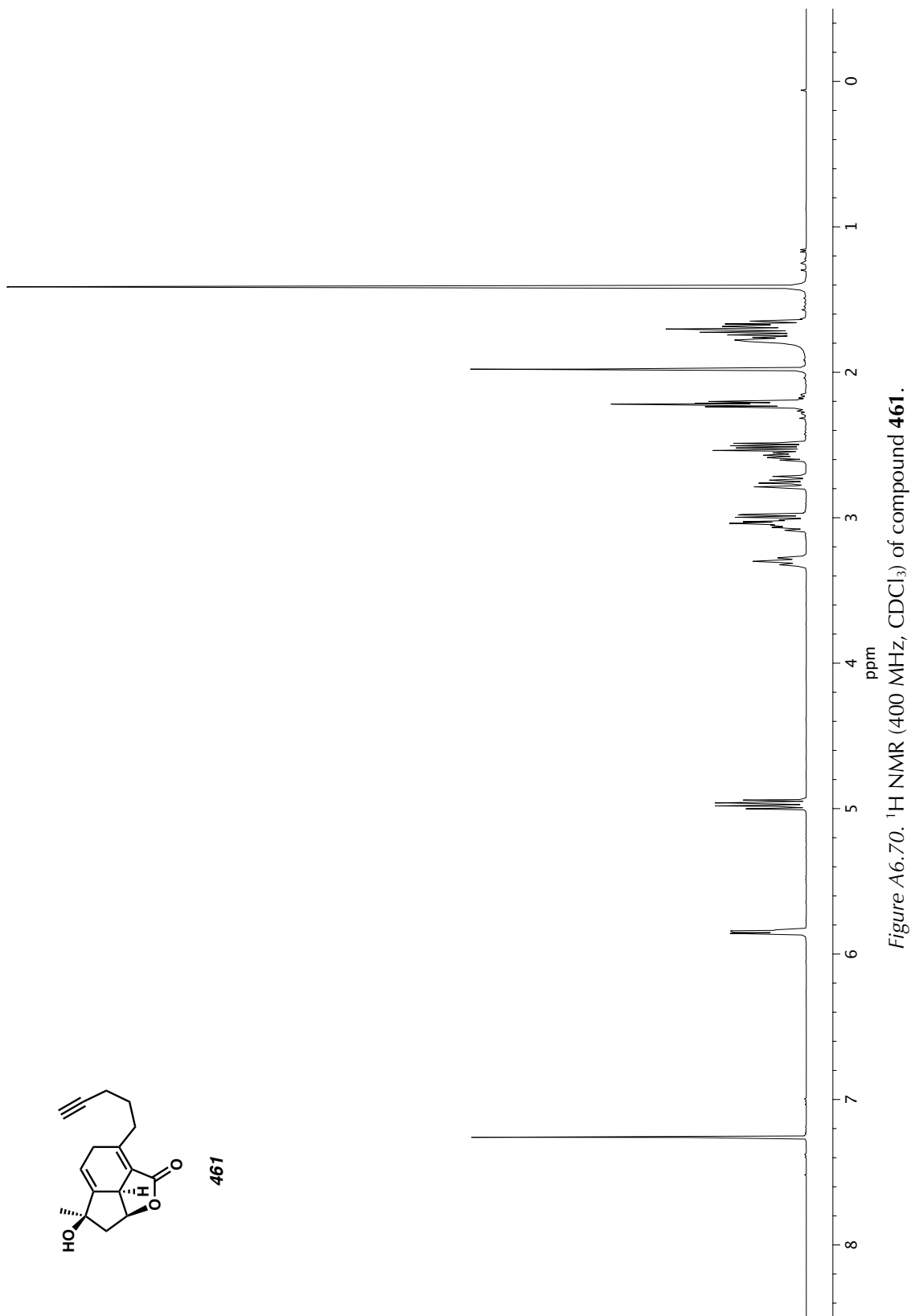


Figure A6.70. ^1H NMR (400 MHz, CDCl_3) of compound 461.

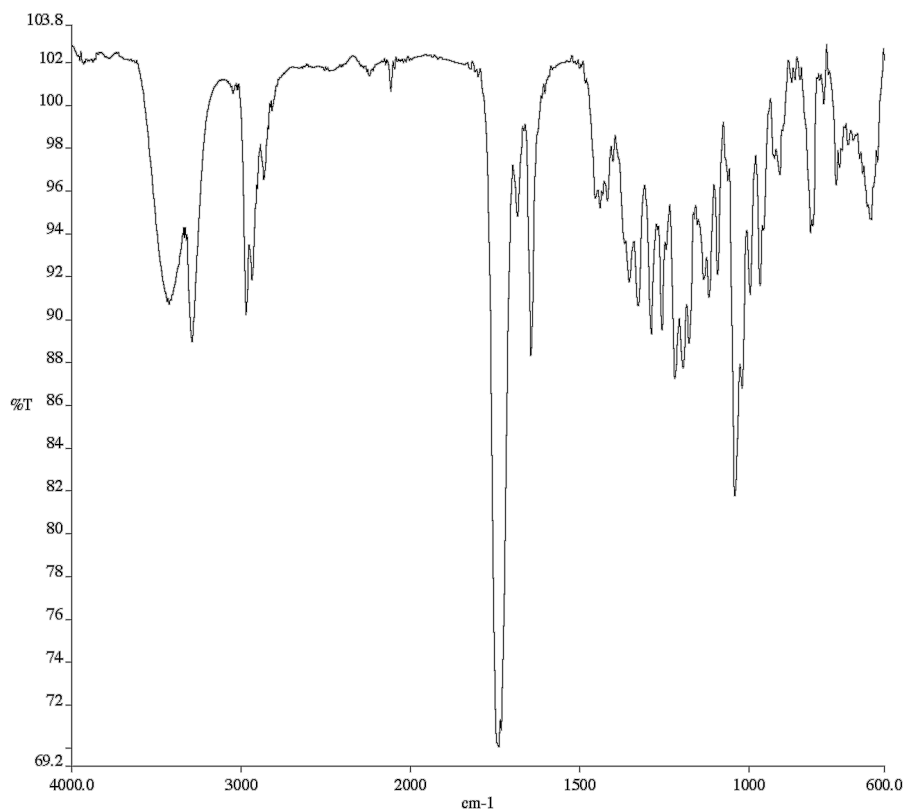


Figure A6.71. Infrared spectrum (Thin Film, NaCl) of compound **461**.

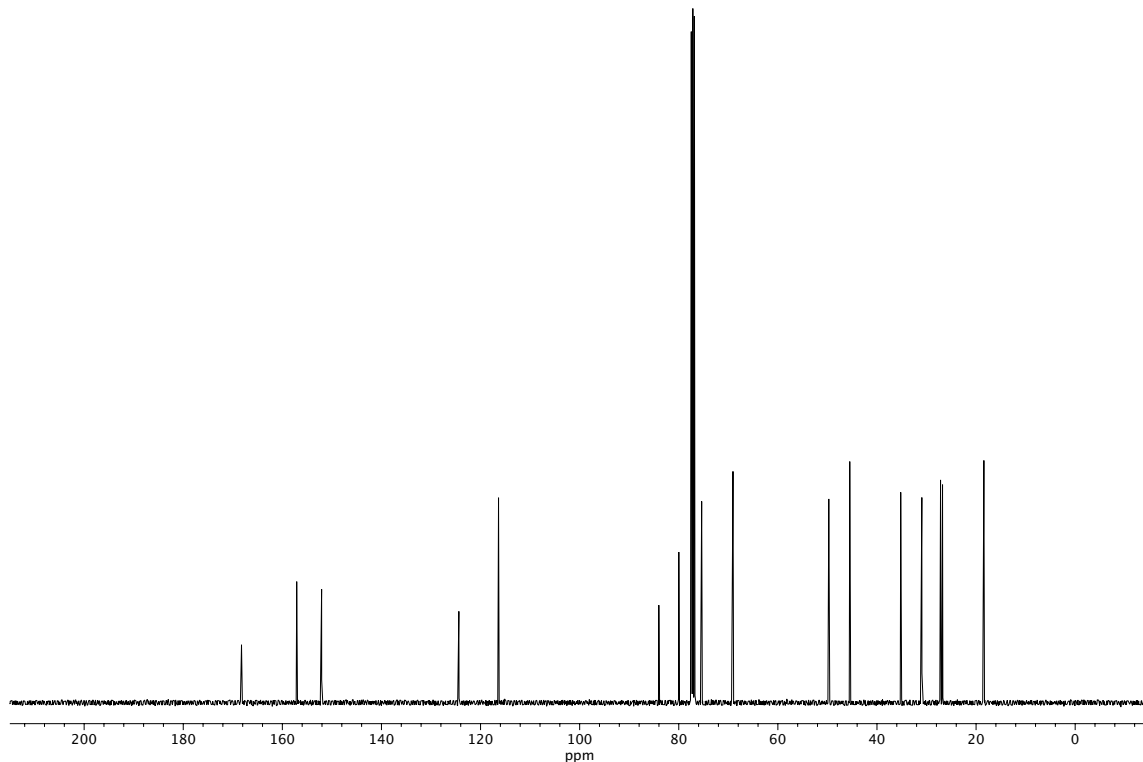


Figure A6.72. ^{13}C NMR (101 MHz, CDCl_3) of compound **461**.

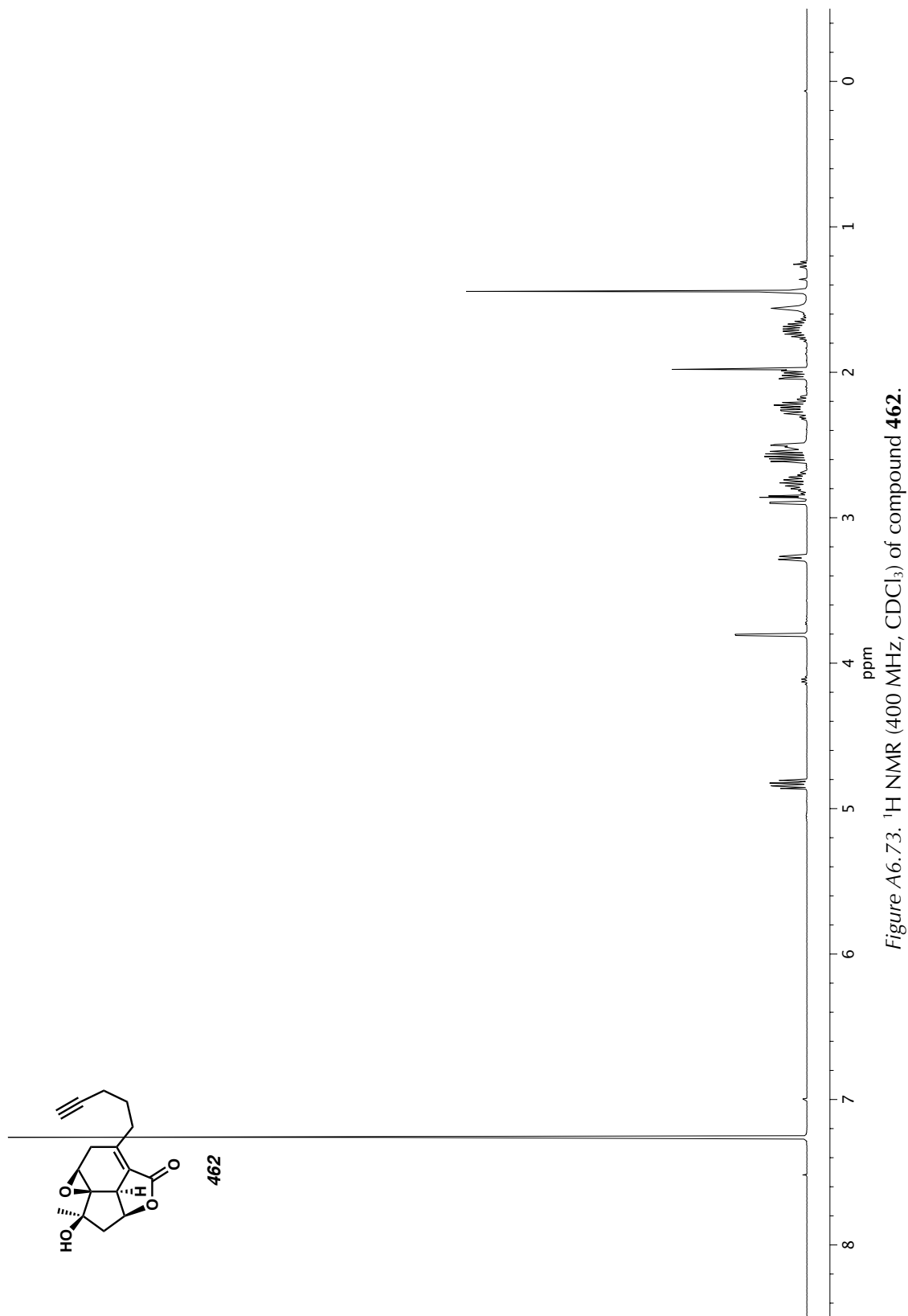


Figure A6.73. ^1H NMR (400 MHz, CDCl_3) of compound 462.

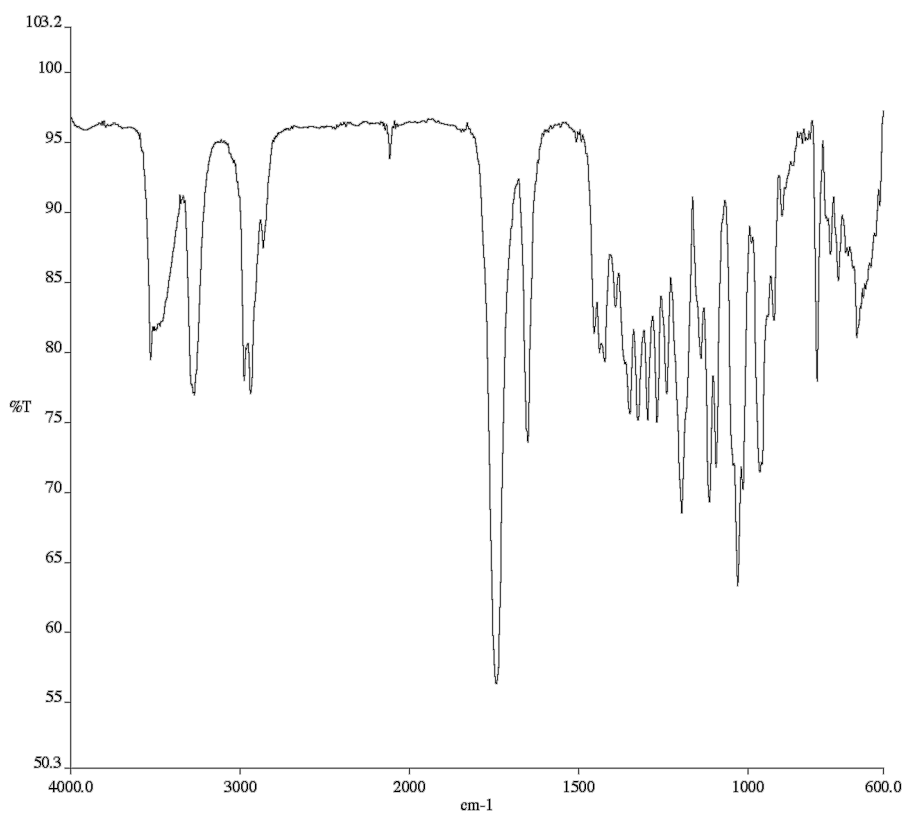


Figure A6.74. Infrared spectrum (Thin Film, NaCl) of compound **462**.

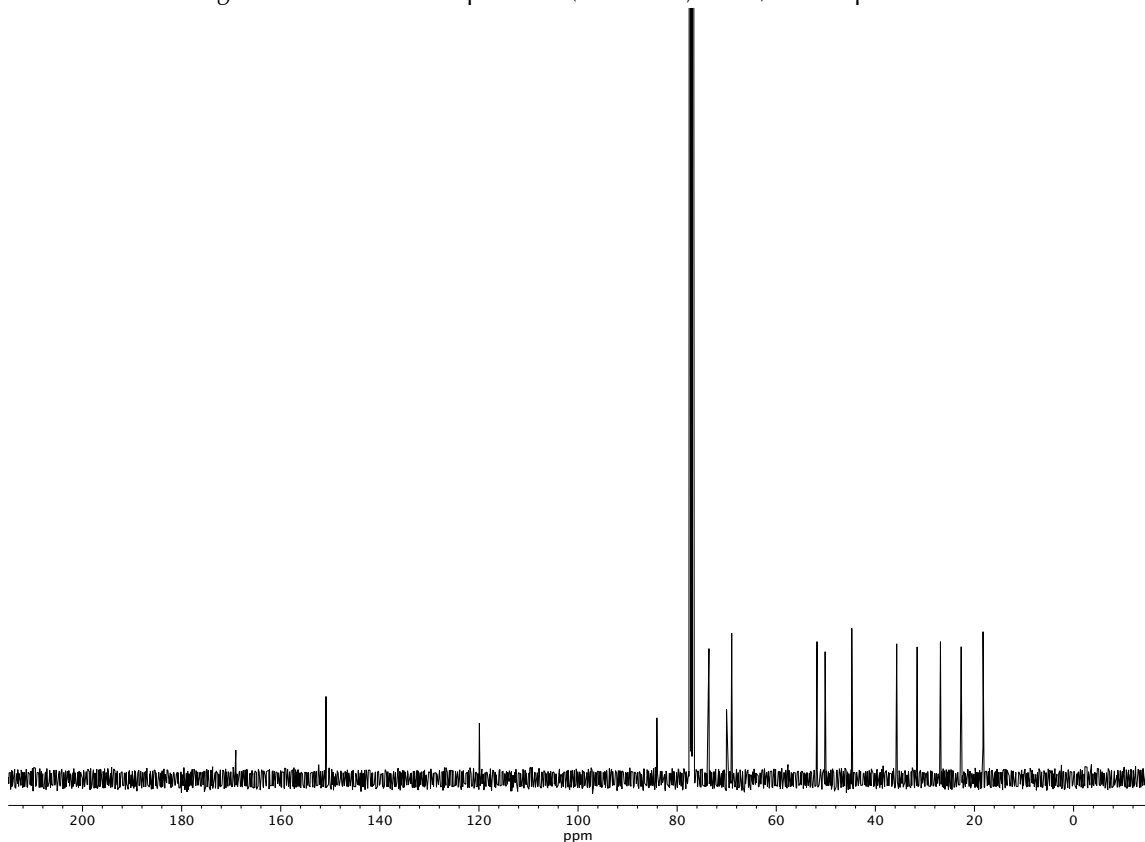


Figure A6.75. ^{13}C NMR (101 MHz, CDCl_3) of compound **462**.

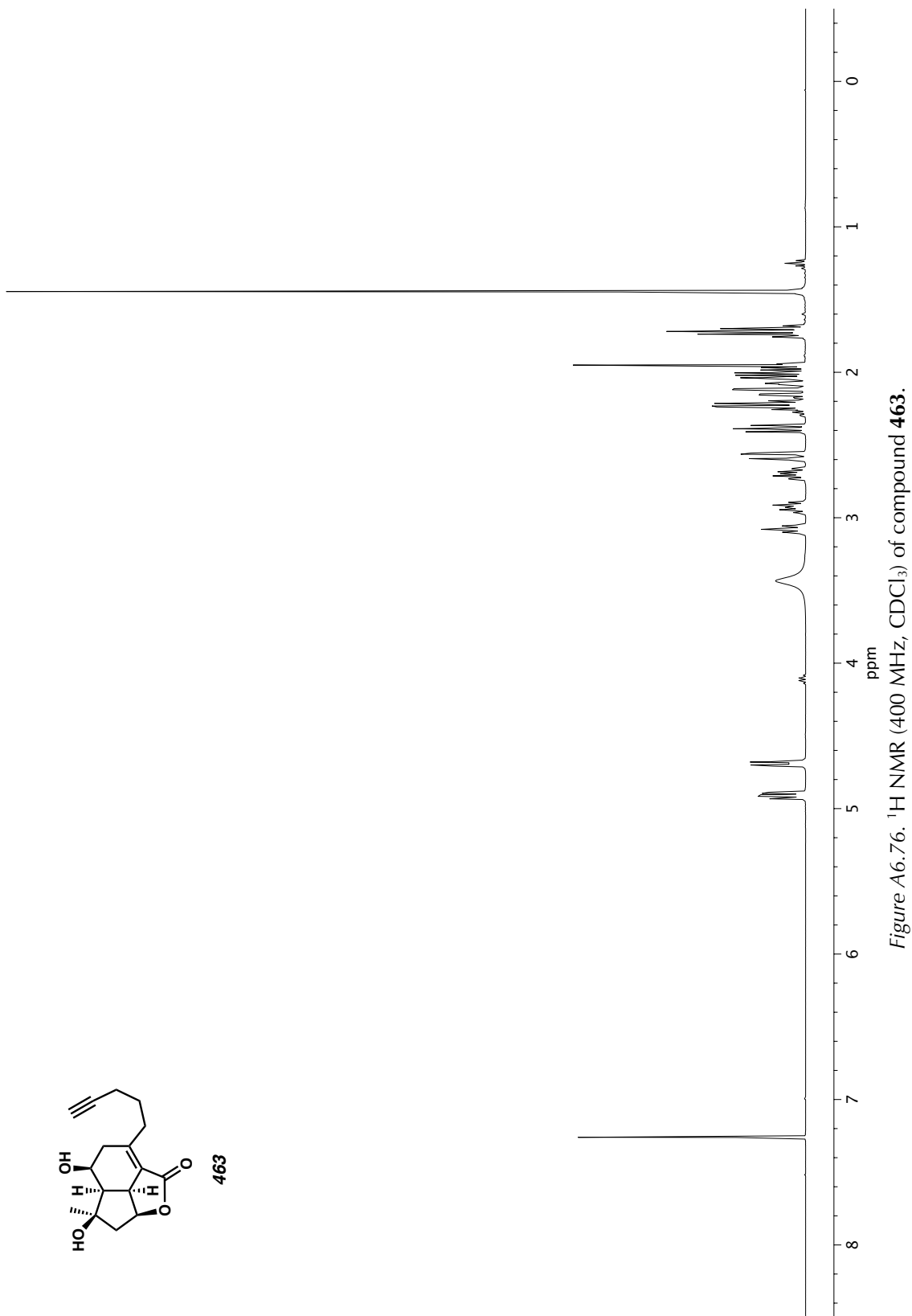
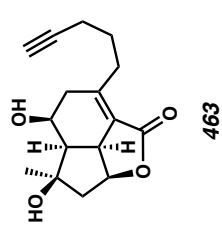


Figure A6.76. ¹H NMR (400 MHz, CDCl₃) of compound 463.

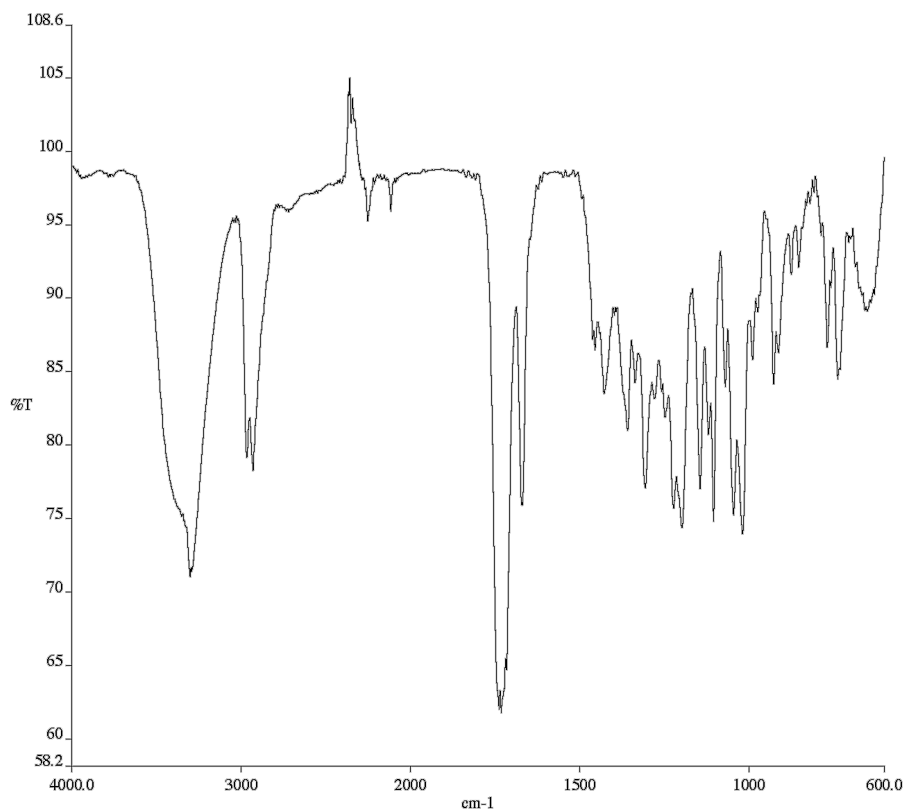


Figure A6.77. Infrared spectrum (Thin Film, NaCl) of compound **463**.

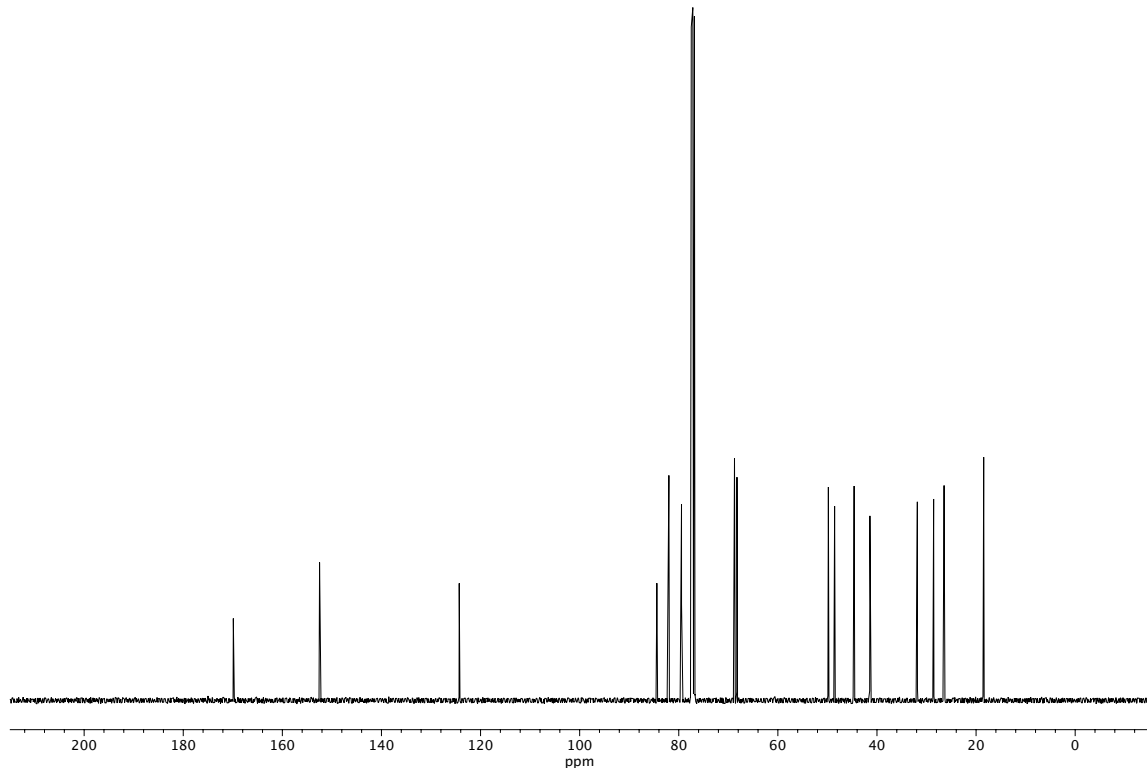


Figure A6.78. ^{13}C NMR (101 MHz, CDCl_3) of compound **463**.

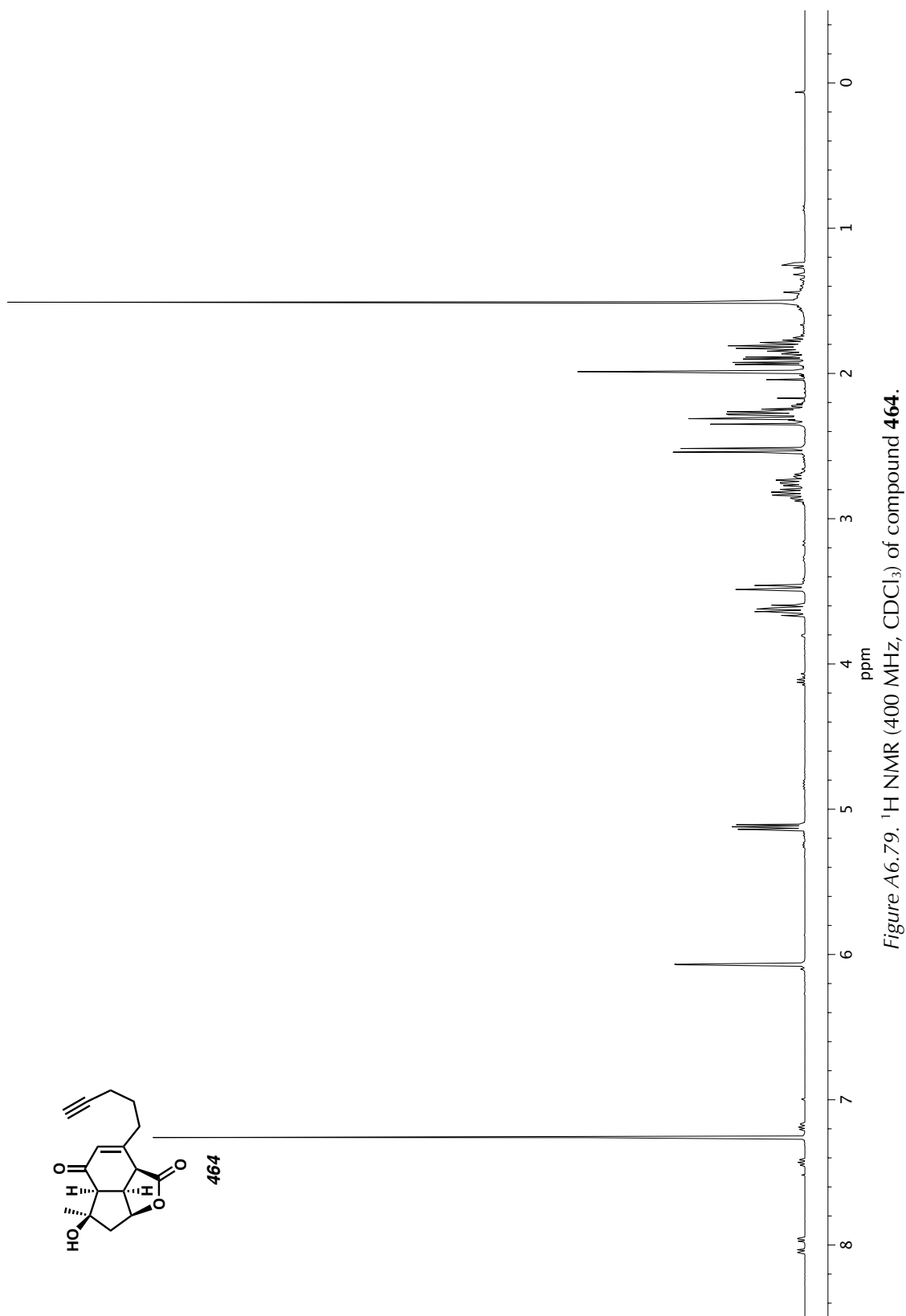
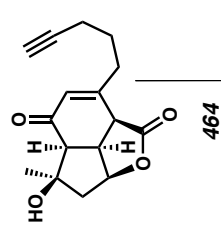


Figure A6.79. ^1H NMR (400 MHz, CDCl_3) of compound 464.

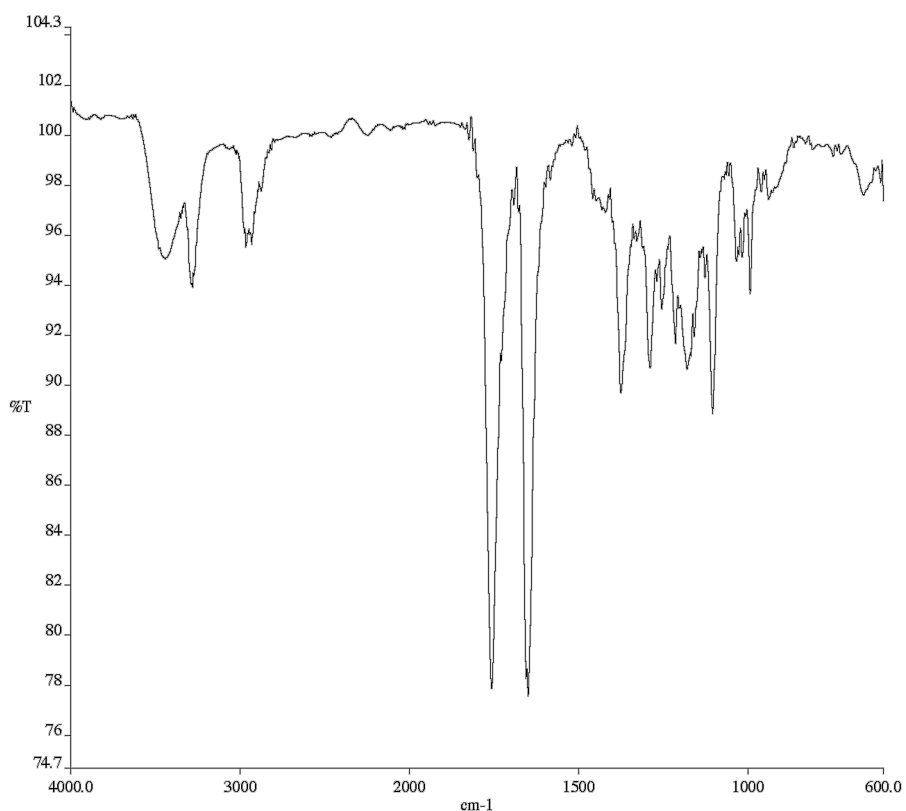


Figure A6.80. Infrared spectrum (Thin Film, NaCl) of compound **464**.

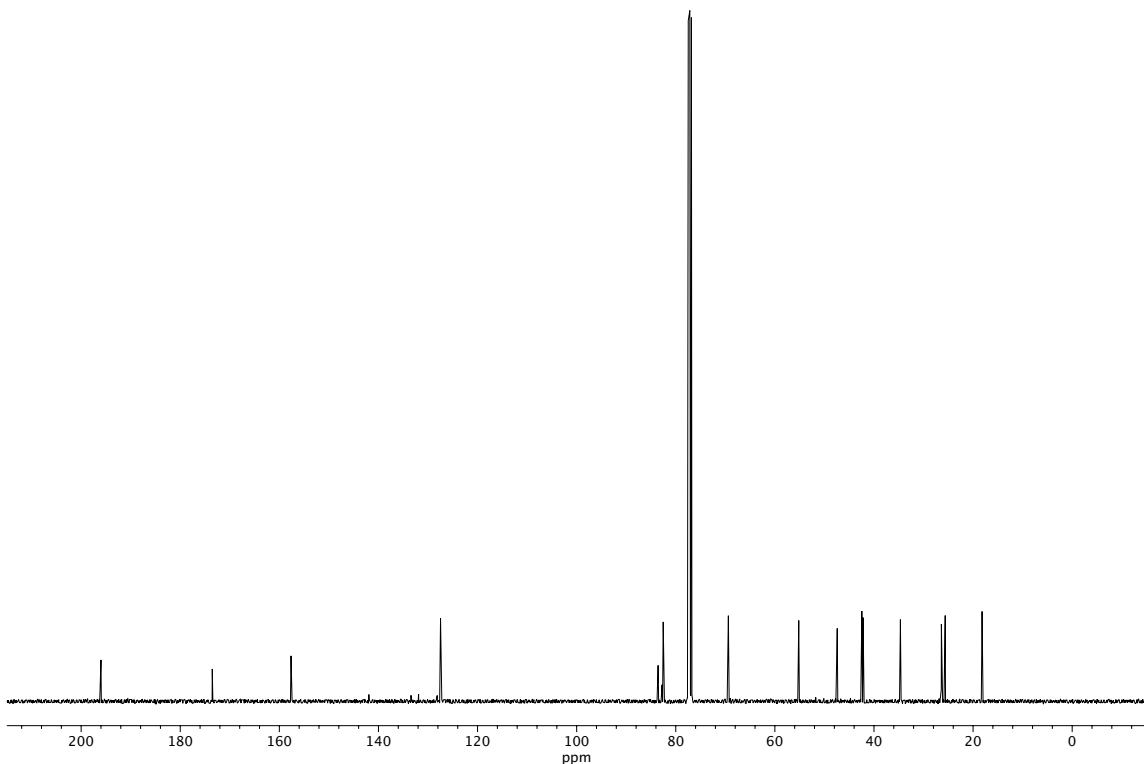


Figure A6.81. ^{13}C NMR (101 MHz, CDCl_3) of compound **464**.

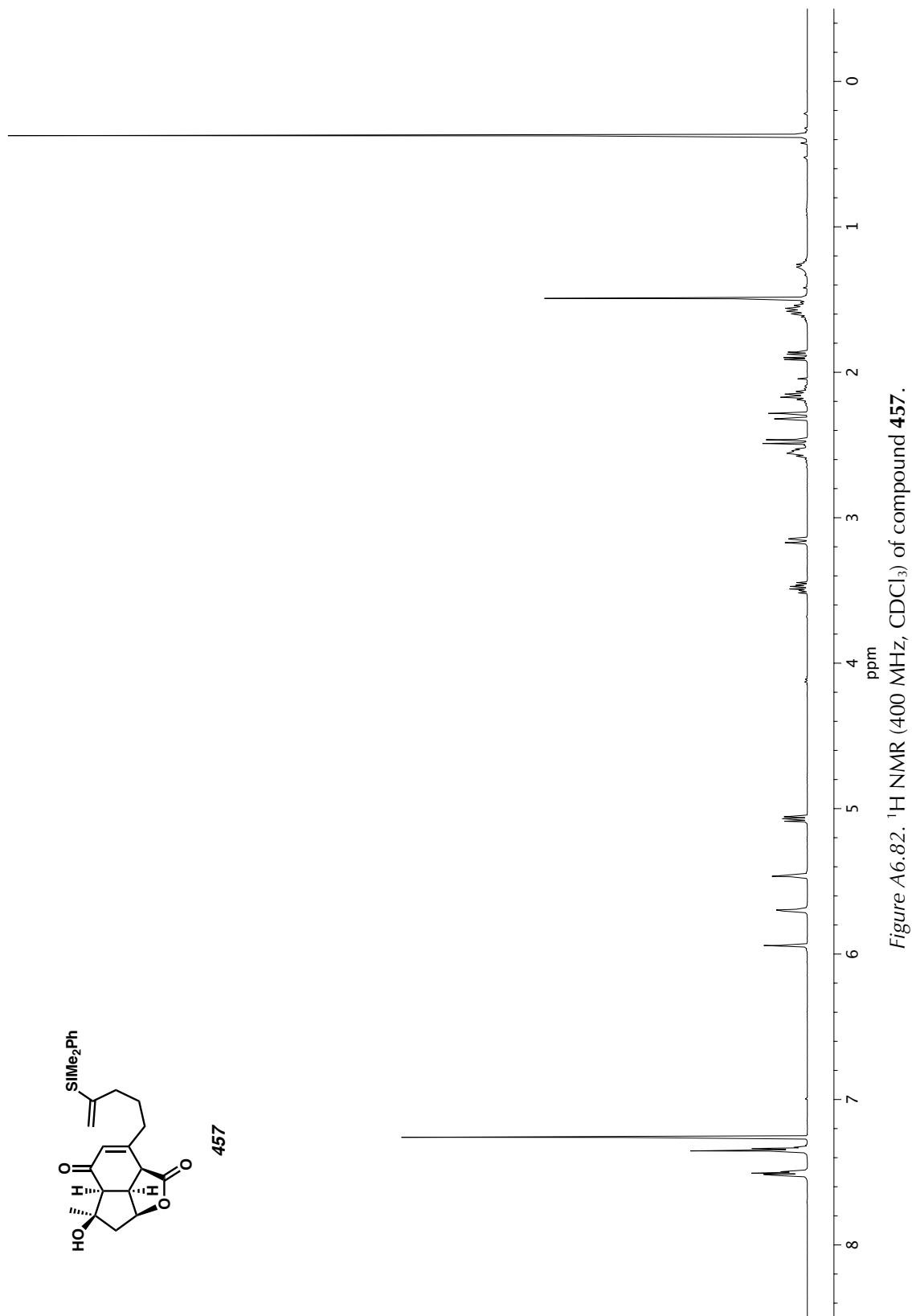
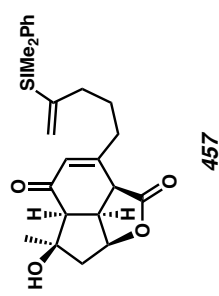


Figure A6.82. ¹H NMR (400 MHz, CDCl₃) of compound 457.

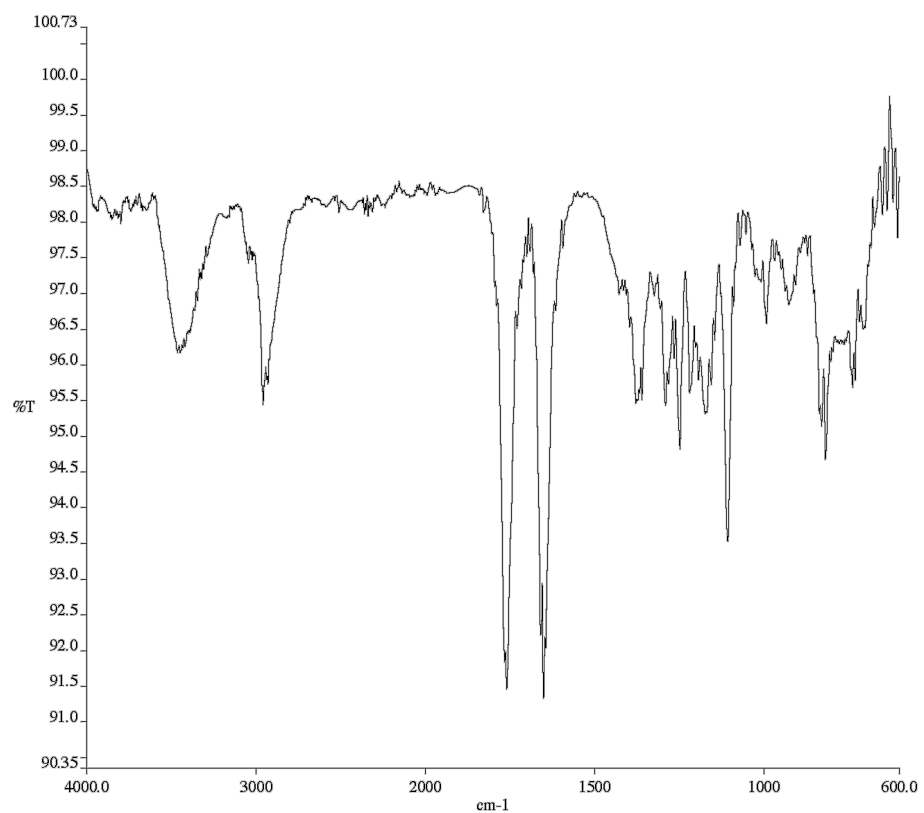


Figure A6.83. Infrared spectrum (Thin Film, NaCl) of compound **457**.

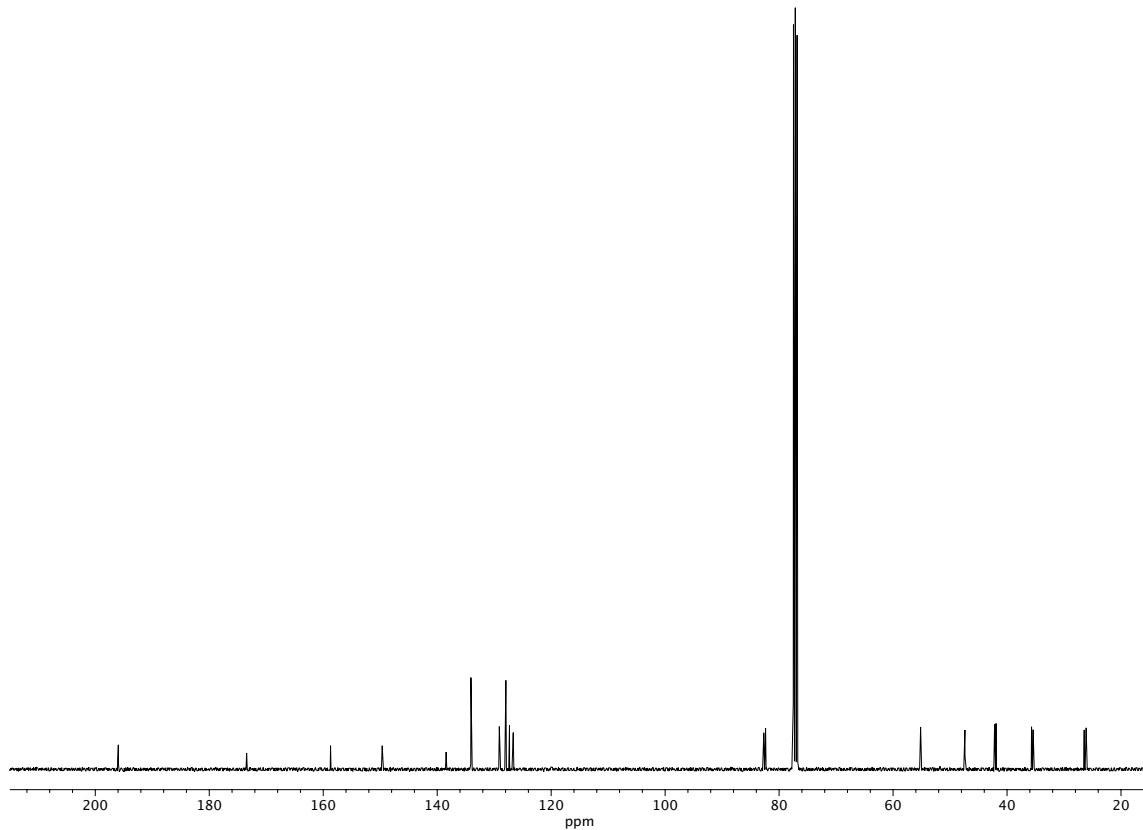


Figure A6.84. ^{13}C NMR (101 MHz, CDCl_3) of compound **457**.

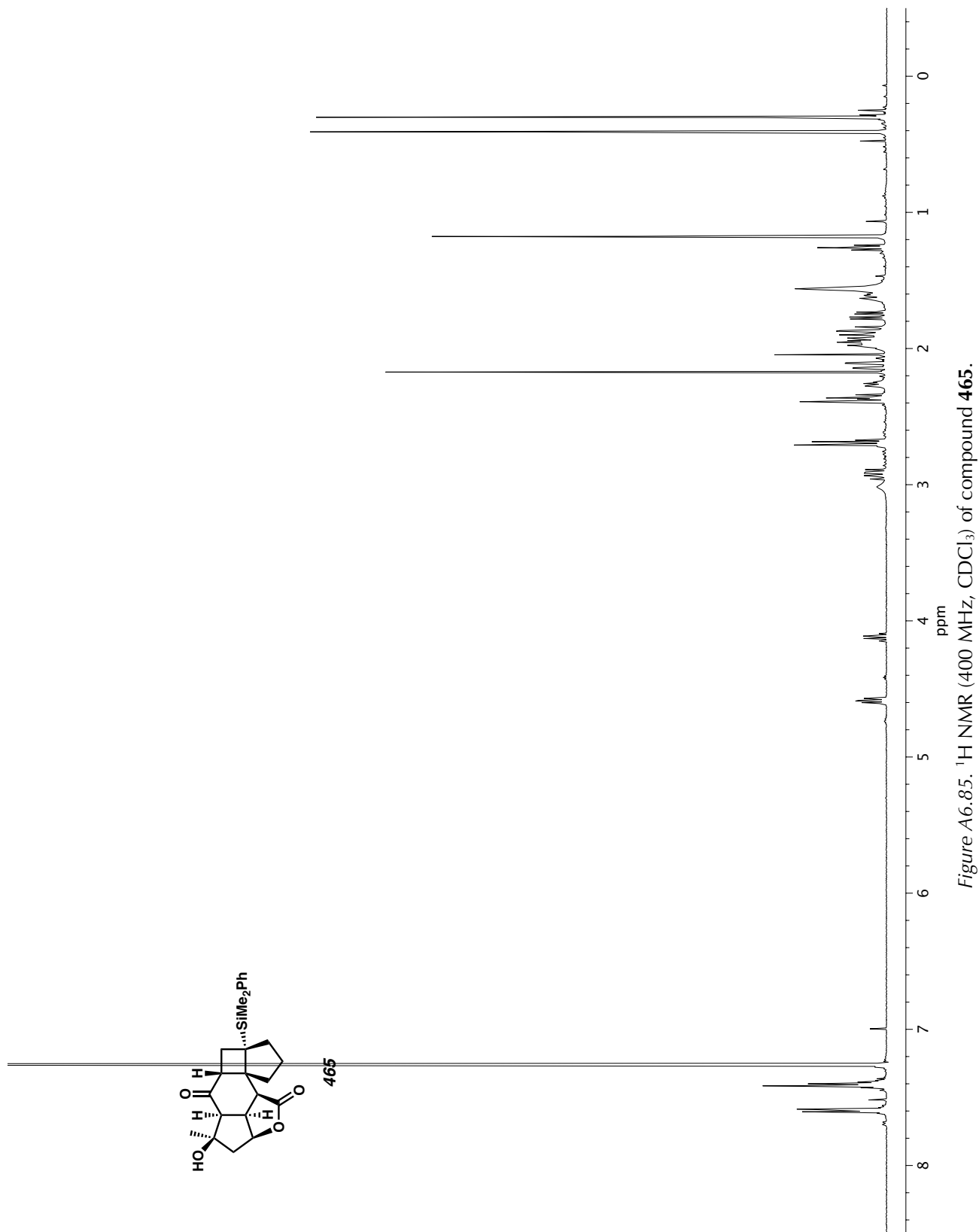


Figure A6.85. ^1H NMR (400 MHz, CDCl_3) of compound 465.

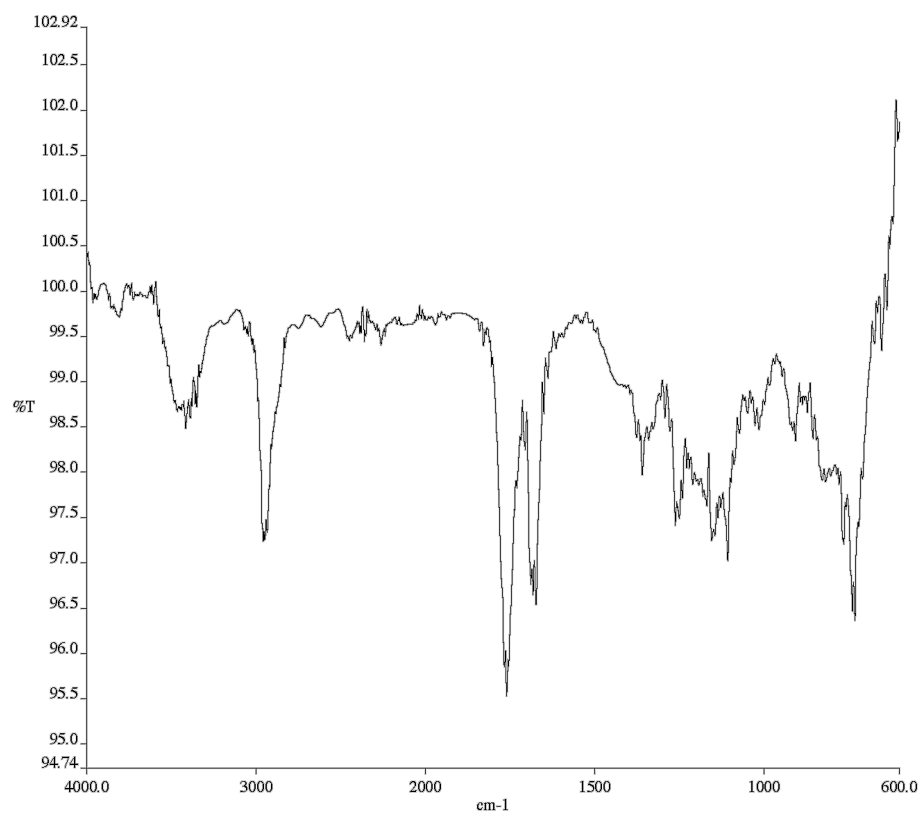


Figure A6.86. Infrared spectrum (Thin Film, NaCl) of compound **465**.

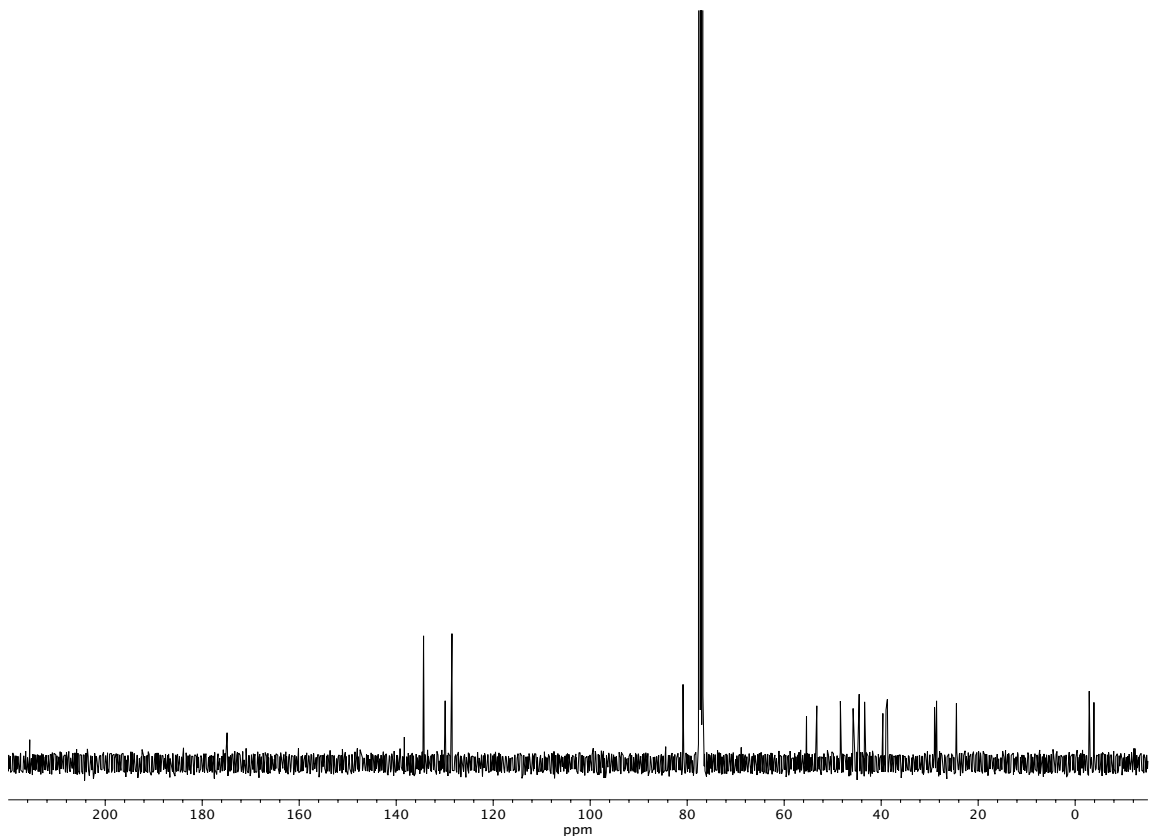


Figure A6.87. ^{13}C NMR (101 MHz, CDCl_3) of compound **465**.

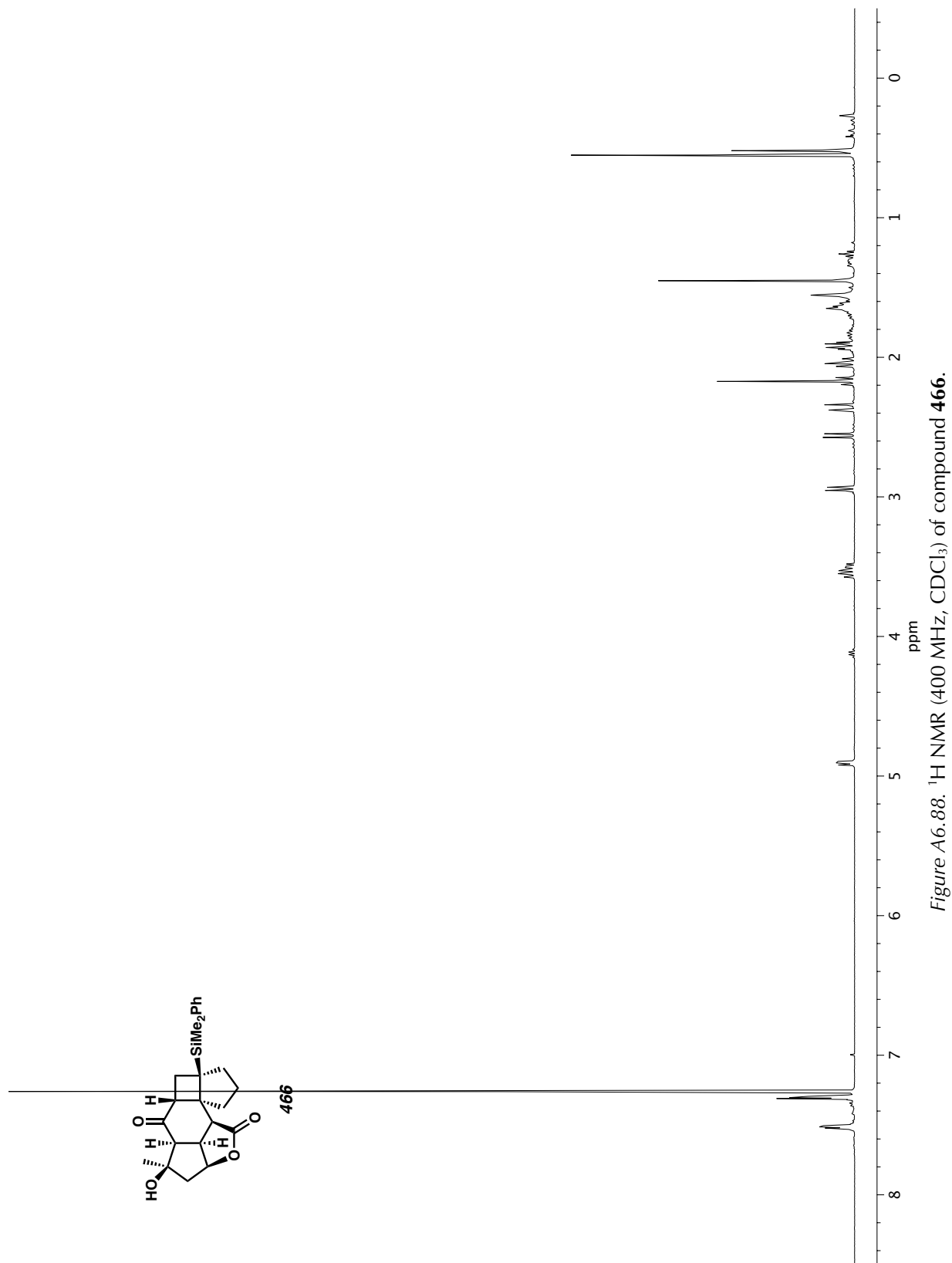


Figure A6.88. ^1H NMR (400 MHz, CDCl_3) of compound 466.

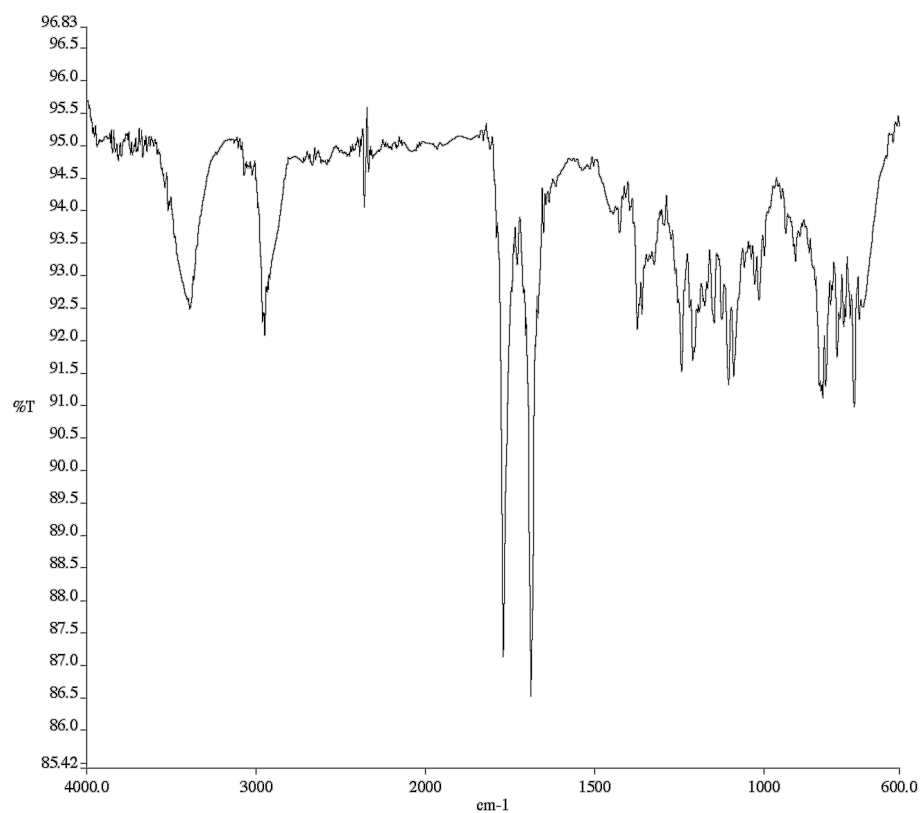


Figure A6.89. Infrared spectrum (Thin Film, NaCl) of compound **466**.

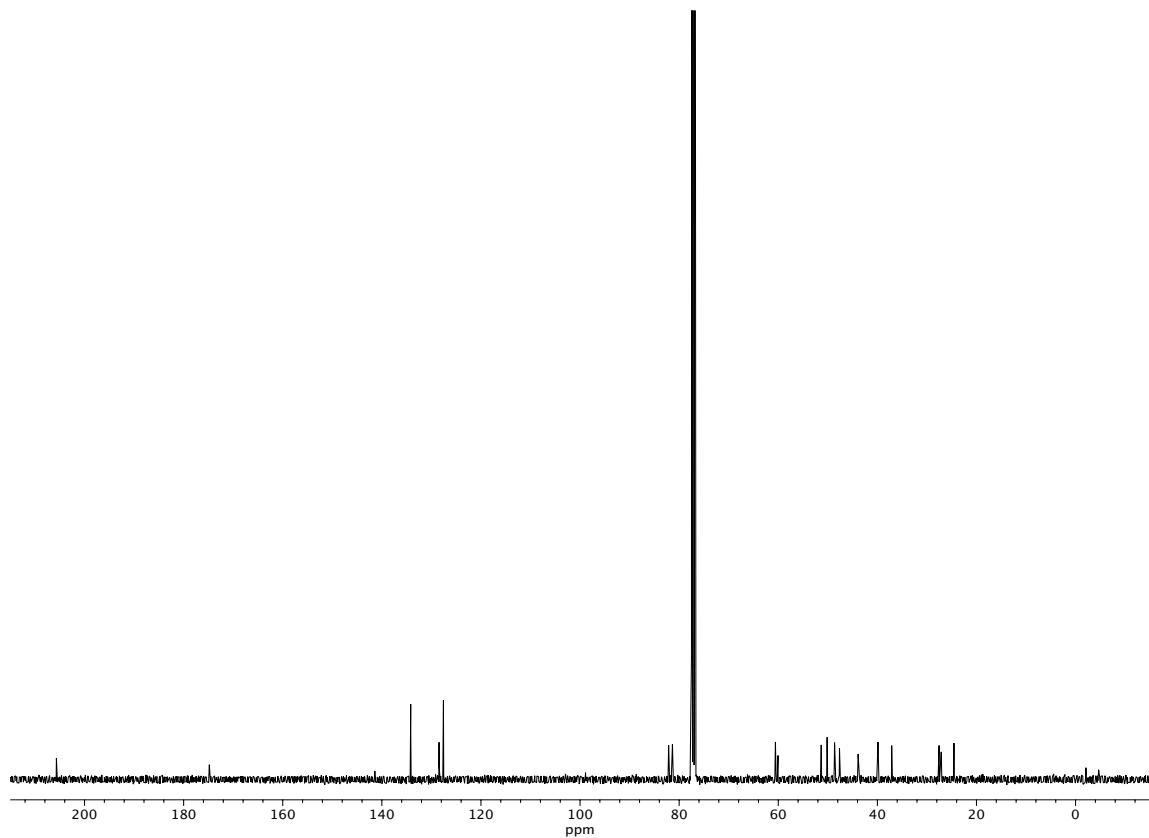


Figure A6.90. ^{13}C NMR (101 MHz, CDCl_3) of compound **466**.

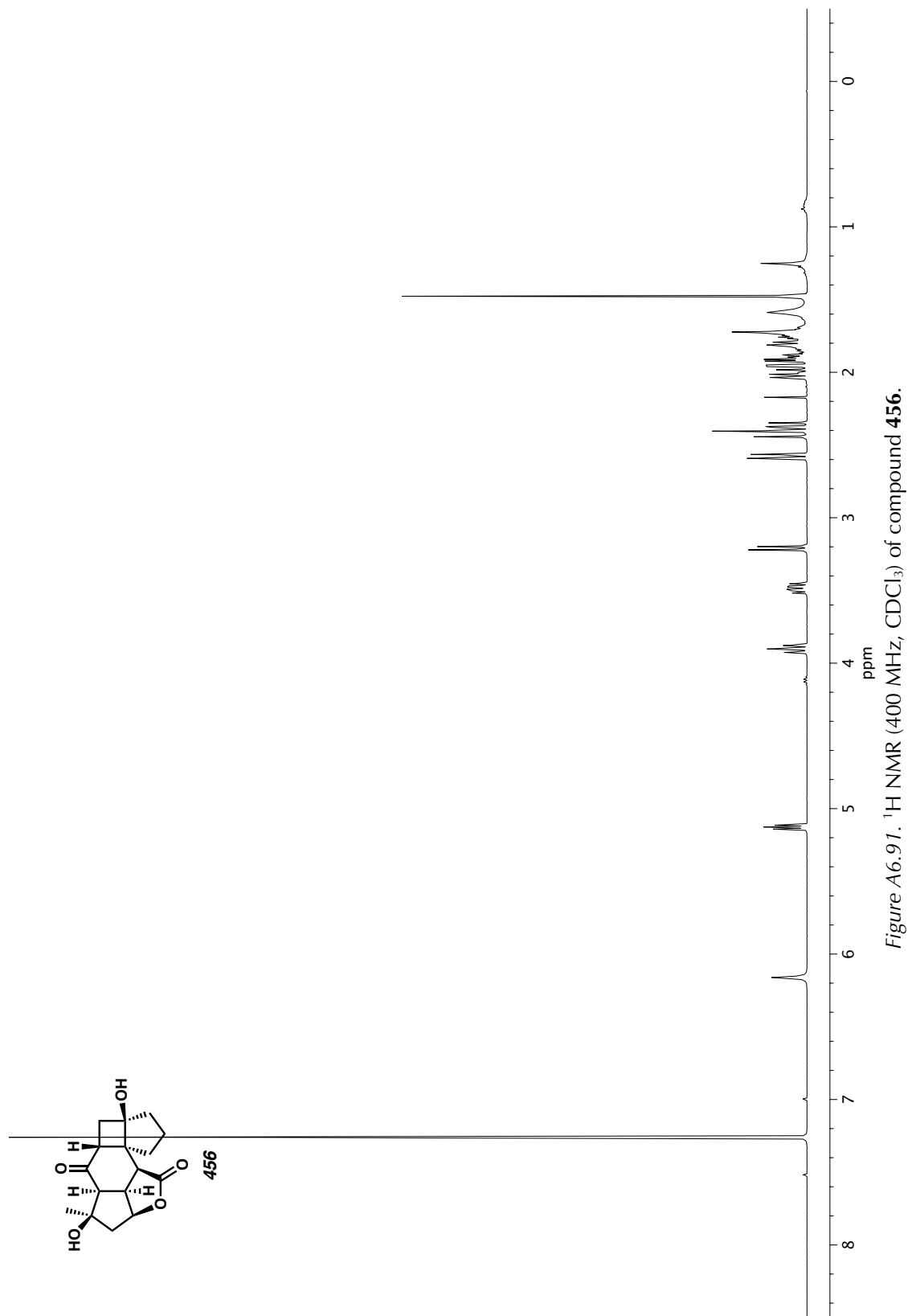


Figure A6.9.1. ^1H NMR (400 MHz, CDCl_3) of compound 456.

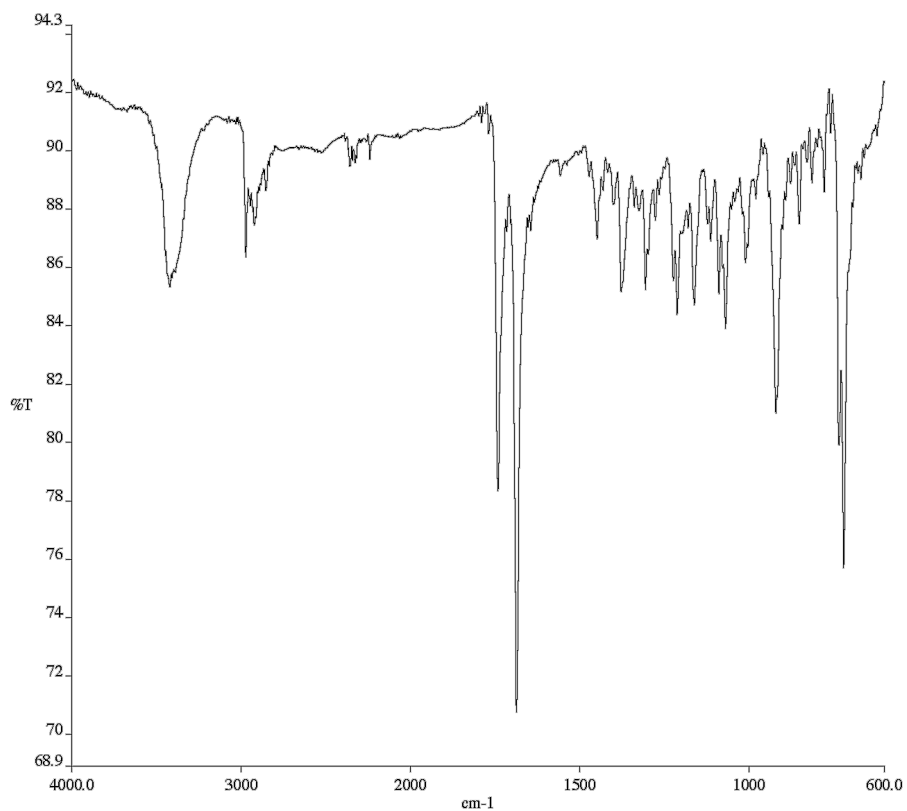


Figure A6.92. Infrared spectrum (Thin Film, NaCl) of compound **456**.

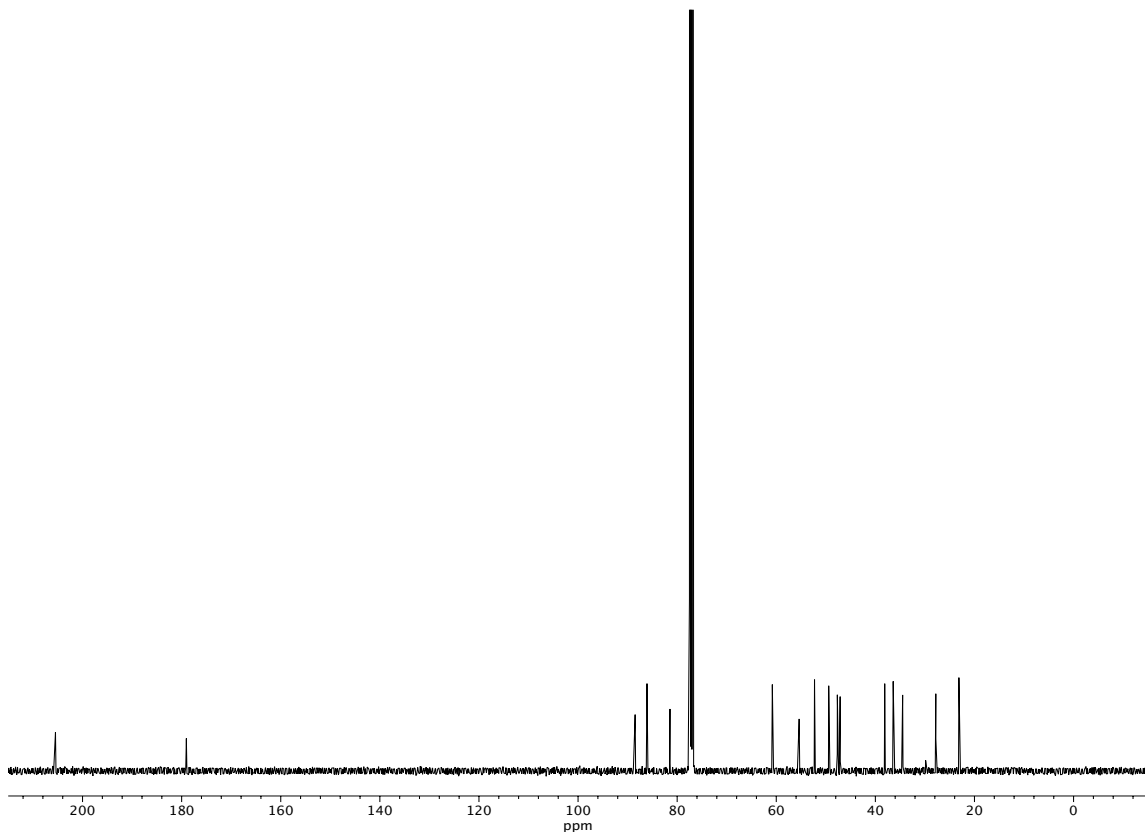
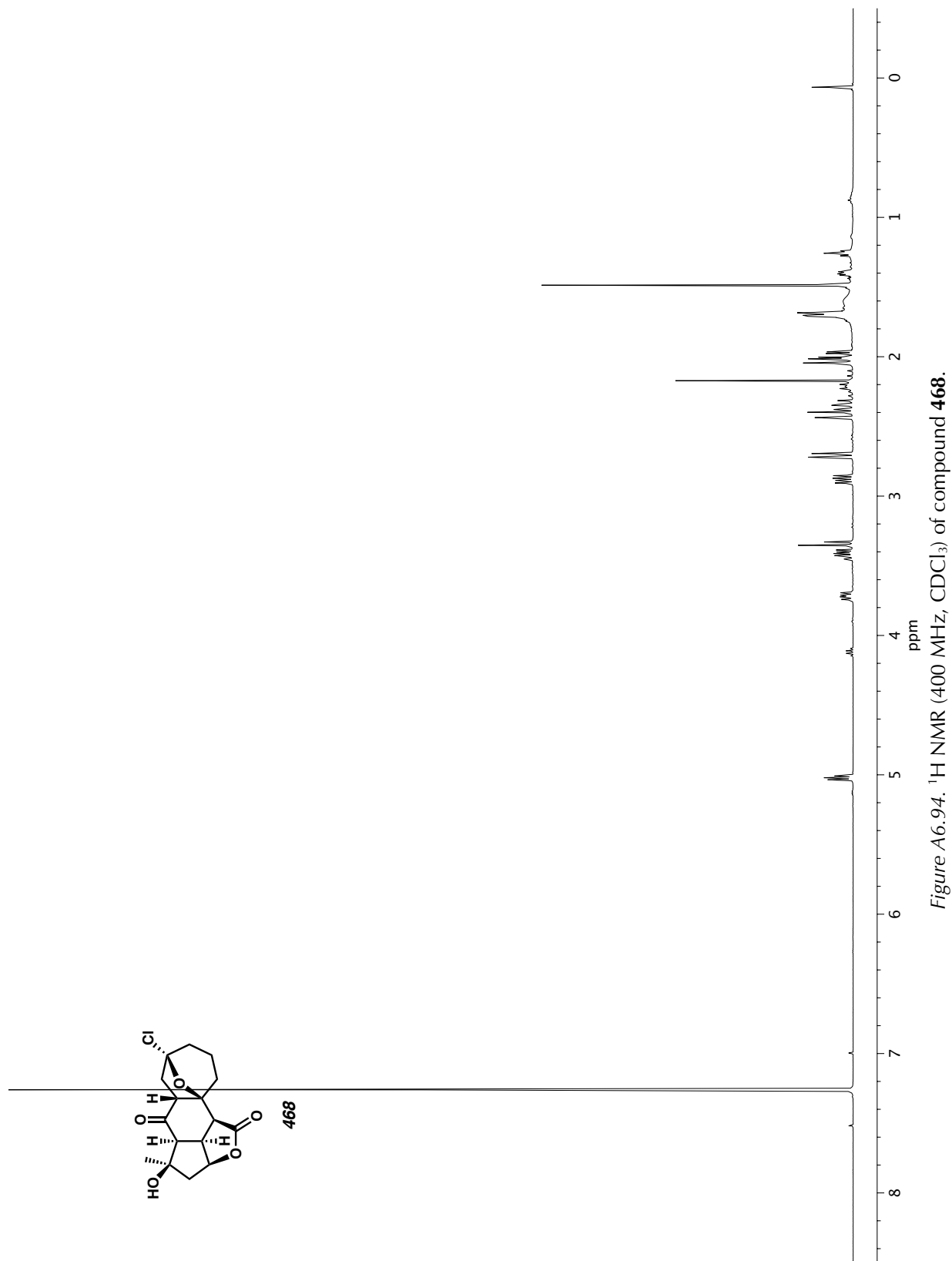


Figure A6.93. ^{13}C NMR (101 MHz, CDCl_3) of compound **456**.



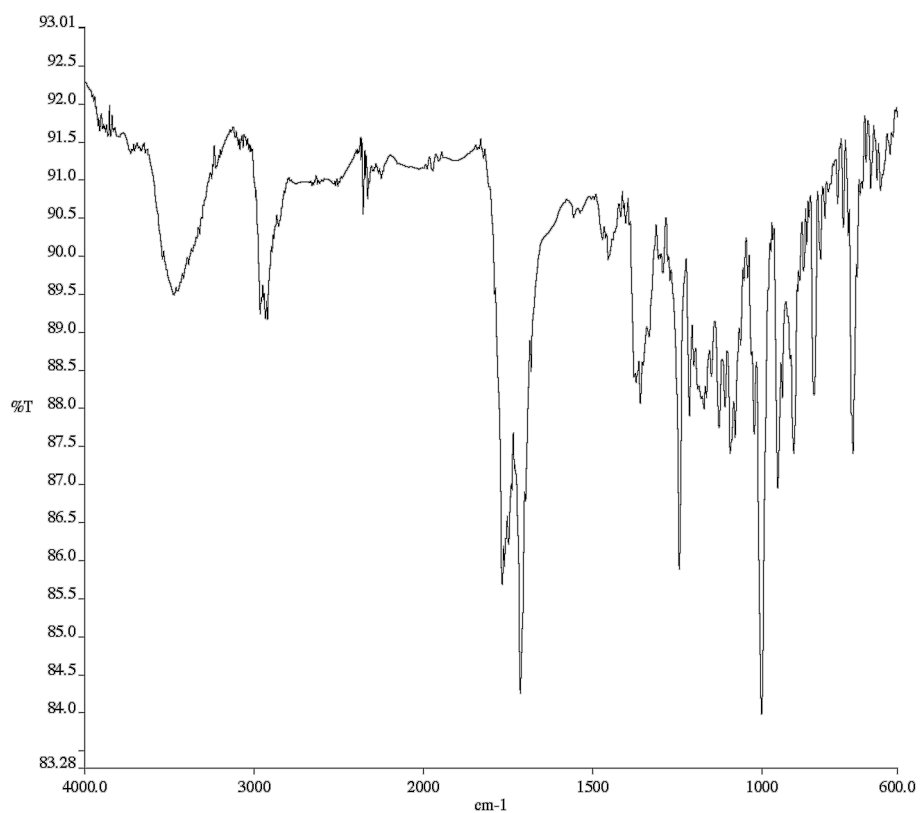


Figure A6.95. Infrared spectrum (Thin Film, NaCl) of compound **468**.

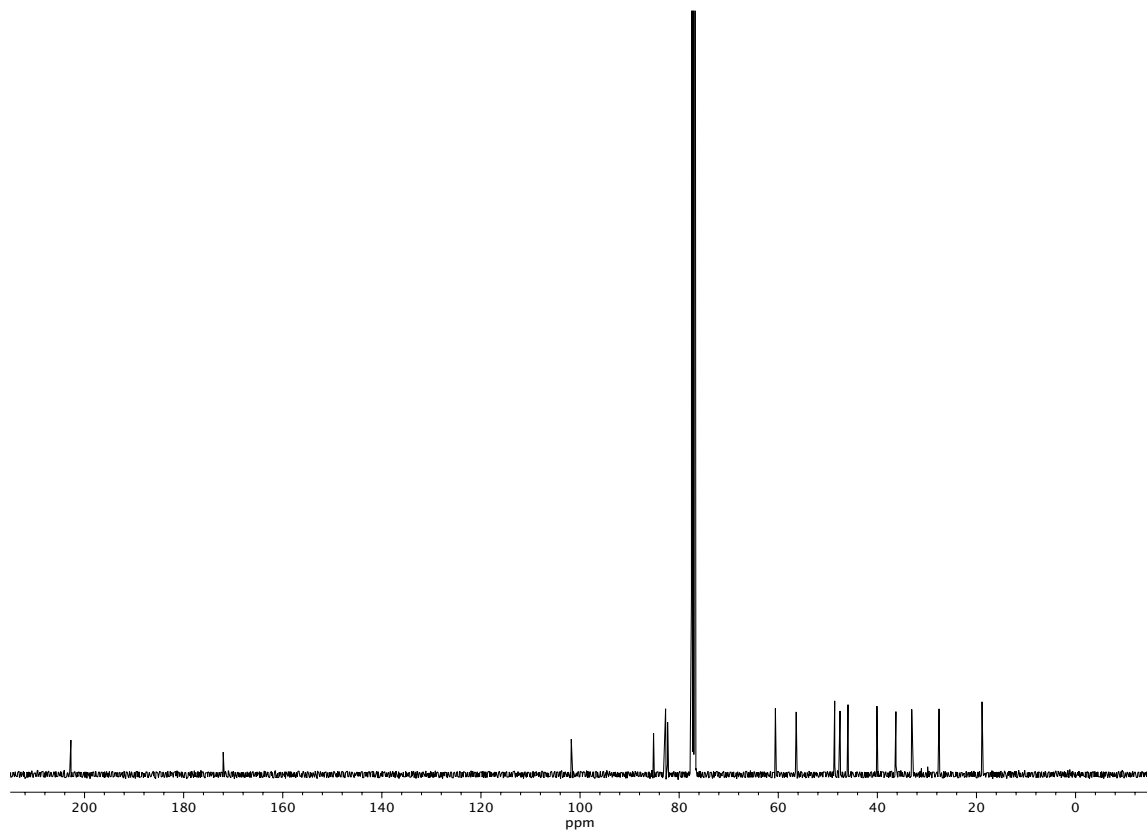


Figure A6.96. ^{13}C NMR (101 MHz, CDCl_3) of compound **468**.

APPENDIX 7

X-Ray Crystallography Reports Relevant to Chapter 4:

Progress Toward the Total Synthesis

of Scabrolide A

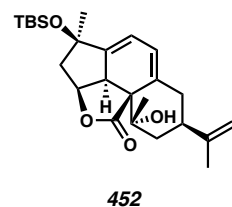
A7.1 X-RAY CRYSTAL STRUCTURE ANALYSIS OF TETRACYCLE 452Contents*Table A7.1.1. Experimental Details**Table A7.1.2. Crystal Data**Table A7.1.3. Atomic Coordinates**Table A7.1.4. Full Bond Distances and Angles**Table A7.1.5. Anisotropic Displacement Parameters**Table A7.1.6. Hydrogen Atomic Coordinates**Table A7.1.7. Torsion Angles**Table A7.1.8. Hydrogen Bond Distances and Angle*

Figure A7.1.1. X-Ray Crystal Structure of Tetracycle 452

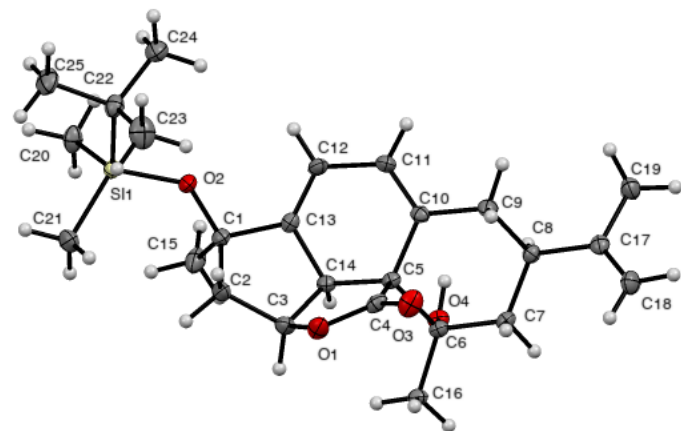


Table A7.1.1. Experimental Details for X-Ray Structure Determination of Tetracycle 452

Low-temperature diffraction data (ϕ -and ω -scans) were collected a Bruker AXS D8 VENTURE KAPPA diffractometer coupled to a PHOTON II CPAD detector with Cu $K\alpha$ radiation ($\lambda = 1.54178 \text{ \AA}$) from an $I\mu\text{S}$ micro-source for the structure of compound V18139. The structure was solved by direct methods using SHELXS¹ and refined against F^2 on all data by full-matrix least squares with SHELXL-2016² using established refinement techniques.³ All non-hydrogen atoms were refined anisotropically. All hydrogen atoms were included into the model at geometrically calculated positions and refined using a riding model. The isotropic displacement parameters of all hydrogen atoms were fixed to 1.2 times the U value of the atoms they are linked to (1.5 times for methyl groups).

Compound **452** crystallizes in the orthorhombic space group $P2_12_12_1$ with one molecule in the asymmetric unit. The coordinates for the hydrogen atom bound to O4 were located in the difference Fourier synthesis and refined semi-freely with the help of a restraint on the O-H distance (0.84(4) \AA).

Table A7.1.2. Crystal Data and Structure Refinement for Tetracycle **452**

Empirical formula	C ₂₅ H ₃₈ O ₄ Si	
Formula weight	430.64	
Temperature	100(2) K	
Wavelength	1.54178 Å	
Crystal system	Orthorhombic	
Space group	P ₂ 12 ₁ 2 ₁	
Unit cell dimensions	a = 6.3347(3) Å	a = 90°.
	b = 12.3768(5) Å	b = 90°.
	c = 30.9537(13) Å	g = 90°.
Volume	2426.87(18) Å ³	
Z	4	
Density (calculated)	1.179 Mg/m ³	
Absorption coefficient	1.064 mm ⁻¹	
F(000)	936	
Crystal size	0.300 x 0.150 x 0.100 mm ³	
Theta range for data collection	2.855 to 74.566°.	
Index ranges	-7<=h<=7, -15<=k<=14, -38<=l<=38	
Reflections collected	25153	
Independent reflections	4954 [R(int) = 0.0480]	
Completeness to theta = 67.679°	99.9 %	
Absorption correction	Semi-empirical from equivalents	
Max. and min. transmission	0.7538 and 0.6036	
Refinement method	Full-matrix least-squares on F ²	
Data / restraints / parameters	4954 / 1 / 282	
Goodness-of-fit on F ²	1.045	
Final R indices [I>2sigma(I)]	R1 = 0.0315, wR2 = 0.0776	
R indices (all data)	R1 = 0.0341, wR2 = 0.0795	
Absolute structure parameter	0.001(10)	
Extinction coefficient	n/a	
Largest diff. peak and hole	0.271 and -0.190 e.Å ⁻³	

*Table A.7.1.3. Atomic Coordinates ($x \cdot 10^4$) and Equivalent Isotropic Displacement Parameters ($\text{\AA}^2 \times 10^3$) for Tetracycle **452**. $U(\text{eq})$ is Defined as One Third of the Orthogonalized U^{ij} Tensor.*

	x	y	z	$U(\text{eq})$
C(1)	2853(3)	1349(2)	3662(1)	17(1)
C(15)	4285(4)	511(2)	3878(1)	27(1)
O(2)	2611(2)	1129(1)	3218(1)	19(1)
Si(1)	1788(1)	60(1)	2947(1)	16(1)
C(20)	4027(3)	-872(2)	2822(1)	24(1)
C(21)	-250(4)	-722(2)	3251(1)	27(1)
C(22)	679(3)	665(2)	2435(1)	22(1)
C(23)	-1264(4)	1358(2)	2539(1)	34(1)
C(24)	2358(4)	1396(2)	2225(1)	27(1)
C(25)	61(4)	-241(2)	2120(1)	31(1)
C(2)	716(3)	1448(2)	3904(1)	23(1)
C(3)	1072(3)	2289(2)	4263(1)	21(1)
O(1)	-488(2)	3141(1)	4231(1)	24(1)
C(4)	390(3)	4128(2)	4204(1)	18(1)
O(3)	-697(2)	4922(1)	4186(1)	26(1)
C(5)	2811(3)	4065(2)	4224(1)	14(1)
C(6)	3546(3)	4471(2)	4685(1)	15(1)
O(4)	5671(2)	4121(1)	4755(1)	17(1)
C(16)	2269(3)	3954(2)	5047(1)	18(1)
C(7)	3408(3)	5707(1)	4721(1)	16(1)
C(8)	4719(3)	6285(2)	4379(1)	16(1)
C(17)	4820(3)	7503(2)	4426(1)	18(1)
C(18)	3432(4)	8079(2)	4649(1)	24(1)
C(19)	6667(4)	8017(2)	4198(1)	24(1)
C(9)	3849(3)	5956(2)	3933(1)	20(1)
C(10)	3843(3)	4750(2)	3871(1)	16(1)
C(11)	4656(3)	4292(2)	3517(1)	20(1)

Table A.7.1.3. Cont'd

C(12)	4409(3)	3144(2)	3418(1)	18(1)
C(13)	3699(3)	2478(2)	3720(1)	15(1)
C(14)	3205(3)	2845(1)	4173(1)	15(1)

Table A7.1.4. Bond Lengths [\AA] and angles [$^\circ$] for Tetracycle **452**

C(1)-O(2)	1.412(2)
C(1)-C(13)	1.507(3)
C(1)-C(15)	1.530(3)
C(1)-C(2)	1.551(3)
C(15)-H(15A)	0.9800
C(15)-H(15B)	0.9800
C(15)-H(15C)	0.9800
O(2)-Si(1)	1.6507(14)
Si(1)-C(21)	1.868(2)
Si(1)-C(20)	1.869(2)
Si(1)-C(22)	1.887(2)
C(20)-H(20A)	0.9800
C(20)-H(20B)	0.9800
C(20)-H(20C)	0.9800
C(21)-H(21A)	0.9800
C(21)-H(21B)	0.9800
C(21)-H(21C)	0.9800
C(22)-C(23)	1.534(3)
C(22)-C(25)	1.537(3)
C(22)-C(24)	1.540(3)
C(23)-H(23A)	0.9800
C(23)-H(23B)	0.9800
C(23)-H(23C)	0.9800
C(24)-H(24A)	0.9800
C(24)-H(24B)	0.9800
C(24)-H(24C)	0.9800
C(25)-H(25A)	0.9800
C(25)-H(25B)	0.9800
C(25)-H(25C)	0.9800
C(2)-C(3)	1.541(3)
C(2)-H(2A)	0.9900
C(2)-H(2B)	0.9900

Table A.7.1.4. Cont'd

C(3)-O(1)	1.448(3)
C(3)-C(14)	1.542(3)
C(3)-H(3)	1.0000
O(1)-C(4)	1.345(3)
C(4)-O(3)	1.201(3)
C(4)-C(5)	1.537(2)
C(5)-C(10)	1.529(2)
C(5)-C(14)	1.538(2)
C(5)-C(6)	1.585(2)
C(6)-O(4)	1.430(2)
C(6)-C(16)	1.522(3)
C(6)-C(7)	1.535(2)
O(4)-H(4O)	0.84(2)
C(16)-H(16A)	0.9800
C(16)-H(16B)	0.9800
C(16)-H(16C)	0.9800
C(7)-C(8)	1.524(3)
C(7)-H(7A)	0.9900
C(7)-H(7B)	0.9900
C(8)-C(17)	1.515(3)
C(8)-C(9)	1.540(3)
C(8)-H(8)	1.0000
C(17)-C(18)	1.326(3)
C(17)-C(19)	1.506(3)
C(18)-H(18A)	0.9500
C(18)-H(18B)	0.9500
C(19)-H(19A)	0.9800
C(19)-H(19B)	0.9800
C(19)-H(19C)	0.9800
C(9)-C(10)	1.505(3)
C(9)-H(9A)	0.9900
C(9)-H(9B)	0.9900
C(10)-C(11)	1.336(3)
C(11)-C(12)	1.462(3)

Table A.7.1.4. Cont'd

C(11)-H(11)	0.9500
C(12)-C(13)	1.325(3)
C(12)-H(12)	0.9500
C(13)-C(14)	1.505(2)
C(14)-H(14)	1.0000
O(2)-C(1)-C(13)	109.48(15)
O(2)-C(1)-C(15)	111.00(16)
C(13)-C(1)-C(15)	111.47(16)
O(2)-C(1)-C(2)	112.91(16)
C(13)-C(1)-C(2)	100.35(15)
C(15)-C(1)-C(2)	111.20(17)
C(1)-C(15)-H(15A)	109.5
C(1)-C(15)-H(15B)	109.5
H(15A)-C(15)-H(15B)	109.5
C(1)-C(15)-H(15C)	109.5
H(15A)-C(15)-H(15C)	109.5
H(15B)-C(15)-H(15C)	109.5
C(1)-O(2)-Si(1)	133.20(12)
O(2)-Si(1)-C(21)	112.17(9)
O(2)-Si(1)-C(20)	111.08(9)
C(21)-Si(1)-C(20)	107.95(10)
O(2)-Si(1)-C(22)	103.08(8)
C(21)-Si(1)-C(22)	111.81(10)
C(20)-Si(1)-C(22)	110.76(10)
Si(1)-C(20)-H(20A)	109.5
Si(1)-C(20)-H(20B)	109.5
H(20A)-C(20)-H(20B)	109.5
Si(1)-C(20)-H(20C)	109.5
H(20A)-C(20)-H(20C)	109.5
H(20B)-C(20)-H(20C)	109.5
Si(1)-C(21)-H(21A)	109.5
Si(1)-C(21)-H(21B)	109.5
H(21A)-C(21)-H(21B)	109.5

Table A.7.1.4. Cont'd

Si(1)-C(21)-H(21C)	109.5
H(21A)-C(21)-H(21C)	109.5
H(21B)-C(21)-H(21C)	109.5
C(23)-C(22)-C(25)	109.66(19)
C(23)-C(22)-C(24)	108.29(18)
C(25)-C(22)-C(24)	109.73(18)
C(23)-C(22)-Si(1)	110.17(15)
C(25)-C(22)-Si(1)	109.73(14)
C(24)-C(22)-Si(1)	109.24(14)
C(22)-C(23)-H(23A)	109.5
C(22)-C(23)-H(23B)	109.5
H(23A)-C(23)-H(23B)	109.5
C(22)-C(23)-H(23C)	109.5
H(23A)-C(23)-H(23C)	109.5
H(23B)-C(23)-H(23C)	109.5
C(22)-C(24)-H(24A)	109.5
C(22)-C(24)-H(24B)	109.5
H(24A)-C(24)-H(24B)	109.5
C(22)-C(24)-H(24C)	109.5
H(24A)-C(24)-H(24C)	109.5
H(24B)-C(24)-H(24C)	109.5
C(22)-C(25)-H(25A)	109.5
C(22)-C(25)-H(25B)	109.5
H(25A)-C(25)-H(25B)	109.5
C(22)-C(25)-H(25C)	109.5
H(25A)-C(25)-H(25C)	109.5
H(25B)-C(25)-H(25C)	109.5
C(3)-C(2)-C(1)	105.86(16)
C(3)-C(2)-H(2A)	110.6
C(1)-C(2)-H(2A)	110.6
C(3)-C(2)-H(2B)	110.6
C(1)-C(2)-H(2B)	110.6
H(2A)-C(2)-H(2B)	108.7
O(1)-C(3)-C(2)	110.00(17)

Table A.7.1.4. Cont'd

O(1)-C(3)-C(14)	105.10(15)
C(2)-C(3)-C(14)	107.37(15)
O(1)-C(3)-H(3)	111.4
C(2)-C(3)-H(3)	111.4
C(14)-C(3)-H(3)	111.4
C(4)-O(1)-C(3)	112.56(15)
O(3)-C(4)-O(1)	120.61(18)
O(3)-C(4)-C(5)	128.00(19)
O(1)-C(4)-C(5)	111.32(17)
C(10)-C(5)-C(4)	111.75(15)
C(10)-C(5)-C(14)	113.68(15)
C(4)-C(5)-C(14)	102.01(15)
C(10)-C(5)-C(6)	109.99(15)
C(4)-C(5)-C(6)	108.18(15)
C(14)-C(5)-C(6)	110.88(14)
O(4)-C(6)-C(16)	105.17(15)
O(4)-C(6)-C(7)	110.16(16)
C(16)-C(6)-C(7)	109.63(15)
O(4)-C(6)-C(5)	108.43(14)
C(16)-C(6)-C(5)	111.94(15)
C(7)-C(6)-C(5)	111.31(15)
C(6)-O(4)-H(4O)	112.7(19)
C(6)-C(16)-H(16A)	109.5
C(6)-C(16)-H(16B)	109.5
H(16A)-C(16)-H(16B)	109.5
C(6)-C(16)-H(16C)	109.5
H(16A)-C(16)-H(16C)	109.5
H(16B)-C(16)-H(16C)	109.5
C(8)-C(7)-C(6)	112.79(15)
C(8)-C(7)-H(7A)	109.0
C(6)-C(7)-H(7A)	109.0
C(8)-C(7)-H(7B)	109.0
C(6)-C(7)-H(7B)	109.0
H(7A)-C(7)-H(7B)	107.8

Table A.7.1.4. Cont'd

C(17)-C(8)-C(7)	115.09(16)
C(17)-C(8)-C(9)	111.31(15)
C(7)-C(8)-C(9)	107.63(15)
C(17)-C(8)-H(8)	107.5
C(7)-C(8)-H(8)	107.5
C(9)-C(8)-H(8)	107.5
C(18)-C(17)-C(19)	122.07(19)
C(18)-C(17)-C(8)	123.84(19)
C(19)-C(17)-C(8)	114.09(17)
C(17)-C(18)-H(18A)	120.0
C(17)-C(18)-H(18B)	120.0
H(18A)-C(18)-H(18B)	120.0
C(17)-C(19)-H(19A)	109.5
C(17)-C(19)-H(19B)	109.5
H(19A)-C(19)-H(19B)	109.5
C(17)-C(19)-H(19C)	109.5
H(19A)-C(19)-H(19C)	109.5
H(19B)-C(19)-H(19C)	109.5
C(10)-C(9)-C(8)	112.16(15)
C(10)-C(9)-H(9A)	109.2
C(8)-C(9)-H(9A)	109.2
C(10)-C(9)-H(9B)	109.2
C(8)-C(9)-H(9B)	109.2
H(9A)-C(9)-H(9B)	107.9
C(11)-C(10)-C(9)	121.61(17)
C(11)-C(10)-C(5)	120.96(17)
C(9)-C(10)-C(5)	117.41(16)
C(10)-C(11)-C(12)	122.87(18)
C(10)-C(11)-H(11)	118.6
C(12)-C(11)-H(11)	118.6
C(13)-C(12)-C(11)	119.56(17)
C(13)-C(12)-H(12)	120.2
C(11)-C(12)-H(12)	120.2
C(12)-C(13)-C(14)	122.60(17)

Table A.7.1.4. Cont'd

C(12)-C(13)-C(1)	127.85(17)
C(14)-C(13)-C(1)	108.49(15)
C(13)-C(14)-C(5)	115.21(15)
C(13)-C(14)-C(3)	102.49(15)
C(5)-C(14)-C(3)	106.08(15)
C(13)-C(14)-H(14)	110.9
C(5)-C(14)-H(14)	110.9
C(3)-C(14)-H(14)	110.9

Symmetry transformations used to generate equivalent atoms:

*Table A7.1.5. Anisotropic Displacement Parameters ($\text{\AA}^2 \times 10^3$) for Tetracycle **452**. The Anisotropic Displacement Factor Exponent Takes the Form: $-2p^2[h^2a^{*2}U^{11} + \dots + 2hka^{*}b^{*}U^{12}]$.*

	U ¹¹	U ²²	U ³³	U ²³	U ¹³	U ¹²
C(1)	20(1)	18(1)	13(1)	-1(1)	0(1)	-3(1)
C(15)	38(1)	19(1)	24(1)	-3(1)	-8(1)	4(1)
O(2)	25(1)	18(1)	14(1)	-2(1)	0(1)	-4(1)
Si(1)	16(1)	15(1)	17(1)	-2(1)	0(1)	-1(1)
C(20)	20(1)	19(1)	34(1)	-5(1)	-2(1)	3(1)
C(21)	28(1)	25(1)	28(1)	-2(1)	4(1)	-10(1)
C(22)	24(1)	21(1)	21(1)	-2(1)	-5(1)	0(1)
C(23)	28(1)	29(1)	47(1)	0(1)	-10(1)	7(1)
C(24)	35(1)	26(1)	20(1)	-1(1)	0(1)	-2(1)
C(25)	38(1)	31(1)	25(1)	-5(1)	-11(1)	-6(1)
C(2)	25(1)	23(1)	22(1)	-4(1)	6(1)	-9(1)
C(3)	22(1)	23(1)	18(1)	-1(1)	5(1)	-6(1)
O(1)	16(1)	28(1)	27(1)	-7(1)	5(1)	-5(1)
C(4)	13(1)	26(1)	15(1)	-5(1)	-1(1)	1(1)
O(3)	16(1)	31(1)	32(1)	-6(1)	-4(1)	6(1)
C(5)	13(1)	17(1)	12(1)	-1(1)	0(1)	1(1)
C(6)	15(1)	19(1)	13(1)	-1(1)	1(1)	1(1)
O(4)	14(1)	21(1)	15(1)	1(1)	-2(1)	2(1)
C(16)	20(1)	21(1)	13(1)	1(1)	3(1)	-1(1)
C(7)	16(1)	18(1)	13(1)	-2(1)	0(1)	2(1)
C(8)	16(1)	16(1)	16(1)	-1(1)	0(1)	2(1)
C(17)	21(1)	18(1)	16(1)	1(1)	-4(1)	0(1)
C(18)	28(1)	17(1)	28(1)	-1(1)	1(1)	2(1)
C(19)	27(1)	18(1)	28(1)	0(1)	3(1)	-3(1)
C(9)	27(1)	18(1)	15(1)	2(1)	0(1)	0(1)
C(10)	16(1)	18(1)	13(1)	2(1)	-2(1)	-1(1)
C(11)	25(1)	20(1)	16(1)	1(1)	5(1)	-5(1)

Table A.7.1.5. Cont'd

C(12)	19(1)	22(1)	15(1)	-4(1)	5(1)	-2(1)
C(13)	13(1)	17(1)	16(1)	-3(1)	-1(1)	2(1)
C(14)	15(1)	16(1)	13(1)	1(1)	1(1)	0(1)

Table A7.1.6. Hydrogen Coordinates ($\times 10^4$) and Isotropic Displacement Parameters ($\text{\AA}^2 \times 10^3$) for Tetracycle 452.

	x	y	z	U(eq)
H(15A)	3655	-209	3848	41
H(15B)	4443	685	4185	41
H(15C)	5674	519	3738	41
H(20A)	5104	-483	2656	37
H(20B)	3507	-1485	2653	37
H(20C)	4646	-1136	3092	37
H(21A)	372	-1007	3517	41
H(21B)	-752	-1323	3072	41
H(21C)	-1437	-247	3322	41
H(23A)	-1856	1647	2270	52
H(23B)	-850	1957	2728	52
H(23C)	-2326	914	2685	52
H(24A)	1858	1638	1942	40
H(24B)	3675	990	2190	40
H(24C)	2611	2026	2410	40
H(25A)	-1010	-704	2254	47
H(25B)	1310	-674	2050	47
H(25C)	-513	76	1855	47
H(2A)	-408	1691	3704	28
H(2B)	300	743	4029	28
H(3)	1053	1945	4555	25
H(4O)	6480(40)	4290(20)	4552(8)	20
H(16A)	2464	3169	5040	27
H(16B)	771	4125	5008	27
H(16C)	2751	4236	5326	27
H(7A)	1914	5930	4691	19
H(7B)	3899	5931	5011	19
H(8)	6195	6004	4400	19

Table A.7.1.6. Cont'd

H(18A)	3586	8841	4669	29
H(18B)	2284	7730	4788	29
H(19A)	6682	8794	4258	36
H(19B)	6537	7900	3886	36
H(19C)	7982	7690	4302	36
H(9A)	2391	6233	3902	24
H(9B)	4723	6293	3705	24
H(11)	5428	4732	3322	24
H(12)	4756	2877	3140	22
H(14)	4310	2591	4380	18

Table A7.1.7. Torsion Angles [°] for Tetracycle **452**.

C(13)-C(1)-O(2)-Si(1)	179.54(13)
C(15)-C(1)-O(2)-Si(1)	56.1(2)
C(2)-C(1)-O(2)-Si(1)	-69.6(2)
C(1)-O(2)-Si(1)-C(21)	31.7(2)
C(1)-O(2)-Si(1)-C(20)	-89.25(19)
C(1)-O(2)-Si(1)-C(22)	152.10(17)
O(2)-Si(1)-C(22)-C(23)	-65.50(17)
C(21)-Si(1)-C(22)-C(23)	55.18(18)
C(20)-Si(1)-C(22)-C(23)	175.62(15)
O(2)-Si(1)-C(22)-C(25)	173.66(15)
C(21)-Si(1)-C(22)-C(25)	-65.66(18)
C(20)-Si(1)-C(22)-C(25)	54.79(18)
O(2)-Si(1)-C(22)-C(24)	53.33(15)
C(21)-Si(1)-C(22)-C(24)	174.01(14)
C(20)-Si(1)-C(22)-C(24)	-65.55(16)
O(2)-C(1)-C(2)-C(3)	-147.14(16)
C(13)-C(1)-C(2)-C(3)	-30.70(19)
C(15)-C(1)-C(2)-C(3)	87.3(2)
C(1)-C(2)-C(3)-O(1)	125.61(17)
C(1)-C(2)-C(3)-C(14)	11.8(2)
C(2)-C(3)-O(1)-C(4)	-125.15(17)
C(14)-C(3)-O(1)-C(4)	-9.8(2)
C(3)-O(1)-C(4)-O(3)	-178.16(17)
C(3)-O(1)-C(4)-C(5)	-0.9(2)
O(3)-C(4)-C(5)-C(10)	-50.1(3)
O(1)-C(4)-C(5)-C(10)	132.92(16)
O(3)-C(4)-C(5)-C(14)	-171.86(19)
O(1)-C(4)-C(5)-C(14)	11.1(2)
O(3)-C(4)-C(5)-C(6)	71.2(2)
O(1)-C(4)-C(5)-C(6)	-105.85(17)
C(10)-C(5)-C(6)-O(4)	-74.73(17)
C(4)-C(5)-C(6)-O(4)	162.96(15)

Table A.7.1.7. Cont'd

C(14)-C(5)-C(6)-O(4)	51.88(19)
C(10)-C(5)-C(6)-C(16)	169.70(15)
C(4)-C(5)-C(6)-C(16)	47.4(2)
C(14)-C(5)-C(6)-C(16)	-63.7(2)
C(10)-C(5)-C(6)-C(7)	46.6(2)
C(4)-C(5)-C(6)-C(7)	-75.7(2)
C(14)-C(5)-C(6)-C(7)	173.21(15)
O(4)-C(6)-C(7)-C(8)	62.5(2)
C(16)-C(6)-C(7)-C(8)	177.78(15)
C(5)-C(6)-C(7)-C(8)	-57.8(2)
C(6)-C(7)-C(8)-C(17)	-174.09(17)
C(6)-C(7)-C(8)-C(9)	61.2(2)
C(7)-C(8)-C(17)-C(18)	-20.2(3)
C(9)-C(8)-C(17)-C(18)	102.6(2)
C(7)-C(8)-C(17)-C(19)	159.28(17)
C(9)-C(8)-C(17)-C(19)	-77.9(2)
C(17)-C(8)-C(9)-C(10)	177.00(17)
C(7)-C(8)-C(9)-C(10)	-56.0(2)
C(8)-C(9)-C(10)-C(11)	-130.3(2)
C(8)-C(9)-C(10)-C(5)	51.3(2)
C(4)-C(5)-C(10)-C(11)	-103.3(2)
C(14)-C(5)-C(10)-C(11)	11.5(3)
C(6)-C(5)-C(10)-C(11)	136.48(19)
C(4)-C(5)-C(10)-C(9)	75.0(2)
C(14)-C(5)-C(10)-C(9)	-170.19(16)
C(6)-C(5)-C(10)-C(9)	-45.2(2)
C(9)-C(10)-C(11)-C(12)	-171.04(19)
C(5)-C(10)-C(11)-C(12)	7.2(3)
C(10)-C(11)-C(12)-C(13)	-12.7(3)
C(11)-C(12)-C(13)-C(14)	-2.5(3)
C(11)-C(12)-C(13)-C(1)	164.33(19)
O(2)-C(1)-C(13)-C(12)	-8.9(3)
C(15)-C(1)-C(13)-C(12)	114.3(2)
C(2)-C(1)-C(13)-C(12)	-127.8(2)

Table A.7.1.7. Cont'd

O(2)-C(1)-C(13)-C(14)	159.42(15)
C(15)-C(1)-C(13)-C(14)	-77.38(19)
C(2)-C(1)-C(13)-C(14)	40.45(18)
C(12)-C(13)-C(14)-C(5)	20.8(3)
C(1)-C(13)-C(14)-C(5)	-148.21(16)
C(12)-C(13)-C(14)-C(3)	135.51(19)
C(1)-C(13)-C(14)-C(3)	-33.52(19)
C(10)-C(5)-C(14)-C(13)	-24.1(2)
C(4)-C(5)-C(14)-C(13)	96.36(18)
C(6)-C(5)-C(14)-C(13)	-148.65(16)
C(10)-C(5)-C(14)-C(3)	-136.71(15)
C(4)-C(5)-C(14)-C(3)	-16.25(18)
C(6)-C(5)-C(14)-C(3)	98.75(17)
O(1)-C(3)-C(14)-C(13)	-104.81(16)
C(2)-C(3)-C(14)-C(13)	12.3(2)
O(1)-C(3)-C(14)-C(5)	16.37(18)
C(2)-C(3)-C(14)-C(5)	133.48(17)

Symmetry transformations used to generate equivalent atoms:

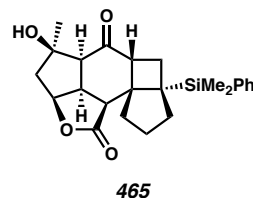
Table A7.1.8. Hydrogen Bonds for Tetracycle **452** [\AA and $^\circ$].

D-H...A	d(D-H)	d(H...A)	d(D...A)	\angle (DHA)
C(3)-H(3)...O(4)#1	1.00	2.52	3.514(2)	171.9
O(4)-H(4O)...O(1)#2	0.84(2)	2.59(3)	3.167(2)	127(2)
O(4)-H(4O)...O(3)#2	0.84(2)	2.25(2)	3.062(2)	162(3)
C(7)-H(7A)...O(3)	0.99	2.59	3.231(2)	122.0

Symmetry transformations used to generate equivalent atoms:

#1 x-1/2,-y+1/2,-z+1 #2 x+1,y,z

A7.2 X-RAY CRYSTAL STRUCTURE ANALYSIS OF CYCLOBUTANE 465



Contents

Table A7.2.1. Experimental Details

Table A7.2.2. Crystal Data

Table A7.2.3. Atomic Coordinates

Table A7.2.4. Full Bond Distances and Angles

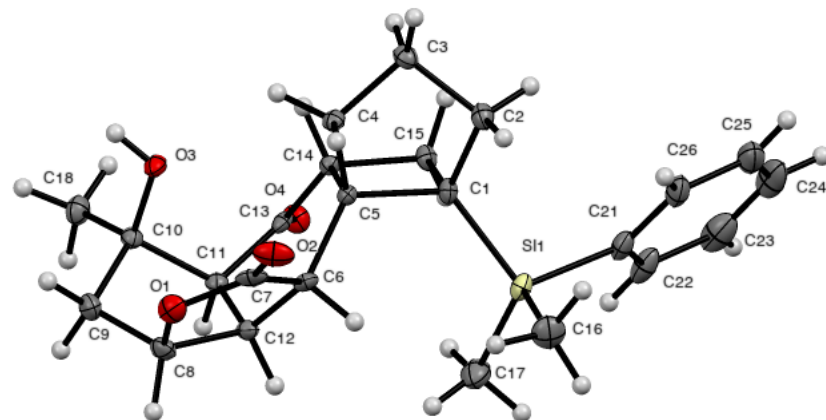
Table A7.2.5. Anisotropic Displacement Parameters

Table A7.2.6. Hydrogen Atomic Coordinates

Table A7.2.7. Torsion Angles

Table A7.2.8. Hydrogen Bond Distances and Angle

Figure A7.2.1. X-Ray Crystal Structure of Cyclobutane 465



*Table A7.2.1. Experimental Details for X-Ray Structure Determination of Cyclobutane***465**

Low-temperature diffraction data (ϕ -and ω -scans) were collected on a Bruker AXS KAPPA APEX II diffractometer coupled to an PHOTON 100 CMOS detector with graphite monochromated Mo $K\alpha$ radiation ($\lambda = 0.71073 \text{ \AA}$) for the structure of compound **465**. The structure was solved by direct methods using SHELXS and refined against F^2 on all data by full-matrix least squares with SHELXL-2017 using established refinement techniques. All non-hydrogen atoms were refined anisotropically. All hydrogen atoms were included into the model at geometrically calculated positions and refined using a riding model. The isotropic displacement parameters of all hydrogen atoms were fixed to 1.2 times the U value of the atoms they are linked to (1.5 times for methyl groups).

Compound **465** crystallizes in the monoclinic space group $P2_1$ with one molecule in the asymmetric unit. The molecule was refined with a disordered hydroxide.

Table A7.2.2. Crystal Data and Structure Refinement for Cyclobutane **465**

Empirical formula	C ₂₄ H ₃₀ O _{4.16} Si	
Formula weight	413.21	
Temperature	100(2) K	
Wavelength	0.71073 Å	
Crystal system	Monoclinic	
Space group	P2 ₁	
Unit cell dimensions	a = 7.267(3) Å	a = 90°.
	b = 9.667(3) Å	b = 99.237(16)°.
	c = 15.436(4) Å	g = 90°.
Volume	1070.3(7) Å ³	
Z	2	
Density (calculated)	1.282 Mg/m ³	
Absorption coefficient	0.138 mm ⁻¹	
F(000)	443	
Crystal size	0.300 x 0.100 x 0.050 mm ³	
Theta range for data collection	2.495 to 30.501°.	
Index ranges	-10<=h<=9, -13<=k<=13, -22<=l<=22	
Reflections collected	16781	
Independent reflections	5995 [R(int) = 0.0322]	
Completeness to theta = 25.242°	99.7 %	
Absorption correction	Semi-empirical from equivalents	
Max. and min. transmission	0.7466 and 0.6535	
Refinement method	Full-matrix least-squares on F ²	
Data / restraints / parameters	5995 / 2 / 280	
Goodness-of-fit on F ²	1.024	
Final R indices [I>2sigma(I)]	R1 = 0.0392, wR2 = 0.0861	
R indices (all data)	R1 = 0.0494, wR2 = 0.0897	
Absolute structure parameter	0.04(4)	
Extinction coefficient	n/a	
Largest diff. peak and hole	0.316 and -0.247 e.Å ⁻³	

*Table A.7.2.3. Atomic Coordinates ($x \cdot 10^4$) and Equivalent Isotropic Displacement Parameters ($\text{\AA}^2 \times 10^3$) for Cyclobutane **465**. $U(\text{eq})$ is Defined as One Third of the Trace of the Orthogonalized U^{ij} Tensor.*

	x	y	z	$U(\text{eq})$
Si(1)	4386(1)	6279(1)	8522(1)	15(1)
C(1)	3245(3)	4685(2)	7973(1)	12(1)
C(2)	3535(3)	3370(2)	8547(1)	17(1)
C(3)	2928(3)	2185(2)	7909(1)	16(1)
C(4)	3789(3)	2600(2)	7113(1)	12(1)
C(5)	3459(3)	4173(2)	7001(1)	10(1)
C(6)	4859(3)	4923(2)	6488(1)	12(1)
O(6B)	6250(11)	5648(9)	7055(5)	9(3)
C(7)	6204(3)	3975(2)	6103(2)	17(1)
O(1)	6138(2)	4182(2)	5238(1)	20(1)
O(2)	7296(2)	3157(2)	6489(1)	24(1)
C(8)	5001(3)	5372(2)	4925(1)	17(1)
C(9)	3445(3)	4958(2)	4187(1)	18(1)
C(10)	1752(3)	4665(2)	4626(1)	13(1)
C(18)	-89(3)	4728(2)	4002(1)	19(1)
O(3)	1978(2)	3371(2)	5078(1)	15(1)
C(11)	1954(3)	5803(2)	5343(1)	12(1)
C(12)	4054(3)	5873(2)	5706(1)	13(1)
C(13)	749(3)	5568(2)	6031(1)	12(1)
O(4)	-691(2)	6223(2)	6041(1)	17(1)
C(14)	1345(3)	4496(2)	6715(1)	11(1)
C(15)	1116(3)	4936(2)	7652(1)	14(1)
C(16)	6926(3)	6088(3)	8901(2)	27(1)
C(17)	3947(4)	7835(3)	7791(2)	26(1)
C(21)	3208(3)	6548(2)	9508(1)	19(1)
C(22)	1903(3)	7607(3)	9547(2)	25(1)
C(23)	1014(4)	7768(3)	10273(2)	35(1)

Table A.7.2.3. Cont'd

C(24)	1401(4)	6871(3)	10974(2)	37(1)
C(25)	2668(4)	5819(3)	10955(2)	30(1)
C(26)	3574(3)	5662(3)	10235(1)	23(1)

Table A7.2.4. Bond Lengths [\AA] and angles [$^\circ$] for Cyclobutane **465**

Si(1)-C(16)	1.853(2)
Si(1)-C(17)	1.877(3)
Si(1)-C(21)	1.881(2)
Si(1)-C(1)	1.886(2)
C(1)-C(2)	1.545(3)
C(1)-C(15)	1.566(3)
C(1)-C(5)	1.611(3)
C(2)-C(3)	1.529(3)
C(2)-H(2A)	0.9900
C(2)-H(2B)	0.9900
C(3)-C(4)	1.520(3)
C(3)-H(3A)	0.9900
C(3)-H(3B)	0.9900
C(4)-C(5)	1.545(3)
C(4)-H(4A)	0.9900
C(4)-H(4B)	0.9900
C(5)-C(14)	1.561(3)
C(5)-C(6)	1.564(3)
C(6)-O(6B)	1.412(8)
C(6)-C(7)	1.529(3)
C(6)-C(12)	1.554(3)
C(6)-H(6)	1.0000
O(6B)-H(6OB)	0.8400
C(7)-O(2)	1.207(3)
C(7)-O(1)	1.343(3)
O(1)-C(8)	1.452(3)
C(8)-C(9)	1.525(3)
C(8)-C(12)	1.558(3)
C(8)-H(8)	1.0000
C(9)-C(10)	1.524(3)
C(9)-H(9A)	0.9900
C(9)-H(9B)	0.9900

Table A7.2.4. Cont'd

C(10)-O(3)	1.430(2)
C(10)-C(18)	1.519(3)
C(10)-C(11)	1.551(3)
C(18)-H(18A)	0.9800
C(18)-H(18B)	0.9800
C(18)-H(18C)	0.9800
O(3)-H(3O)	0.81(2)
C(11)-C(13)	1.499(3)
C(11)-C(12)	1.541(3)
C(11)-H(11)	1.0000
C(12)-H(12)	1.0000
C(13)-O(4)	1.225(2)
C(13)-C(14)	1.492(3)
C(14)-C(15)	1.542(3)
C(14)-H(14)	1.0000
C(15)-H(15A)	0.9900
C(15)-H(15B)	0.9900
C(16)-H(16A)	0.9800
C(16)-H(16B)	0.9800
C(16)-H(16C)	0.9800
C(17)-H(17A)	0.9800
C(17)-H(17B)	0.9800
C(17)-H(17C)	0.9800
C(21)-C(26)	1.403(3)
C(21)-C(22)	1.403(3)
C(22)-C(23)	1.390(3)
C(22)-H(22)	0.9500
C(23)-C(24)	1.380(5)
C(23)-H(23)	0.9500
C(24)-C(25)	1.375(4)
C(24)-H(24)	0.9500
C(25)-C(26)	1.387(3)
C(25)-H(25)	0.9500
C(26)-H(26)	0.9500

Table A7.2.4. Cont'd

C(16)-Si(1)-C(17)	109.50(13)
C(16)-Si(1)-C(21)	108.58(11)
C(17)-Si(1)-C(21)	108.67(11)
C(16)-Si(1)-C(1)	113.85(11)
C(17)-Si(1)-C(1)	111.37(10)
C(21)-Si(1)-C(1)	104.63(10)
C(2)-C(1)-C(15)	110.28(17)
C(2)-C(1)-C(5)	104.92(16)
C(15)-C(1)-C(5)	89.47(14)
C(2)-C(1)-Si(1)	113.87(14)
C(15)-C(1)-Si(1)	110.89(13)
C(5)-C(1)-Si(1)	124.62(14)
C(3)-C(2)-C(1)	104.36(16)
C(3)-C(2)-H(2A)	110.9
C(1)-C(2)-H(2A)	110.9
C(3)-C(2)-H(2B)	110.9
C(1)-C(2)-H(2B)	110.9
H(2A)-C(2)-H(2B)	108.9
C(4)-C(3)-C(2)	102.09(17)
C(4)-C(3)-H(3A)	111.4
C(2)-C(3)-H(3A)	111.4
C(4)-C(3)-H(3B)	111.4
C(2)-C(3)-H(3B)	111.4
H(3A)-C(3)-H(3B)	109.2
C(3)-C(4)-C(5)	105.86(16)
C(3)-C(4)-H(4A)	110.6
C(5)-C(4)-H(4A)	110.6
C(3)-C(4)-H(4B)	110.6
C(5)-C(4)-H(4B)	110.6
H(4A)-C(4)-H(4B)	108.7
C(4)-C(5)-C(14)	110.87(16)
C(4)-C(5)-C(6)	114.26(16)
C(14)-C(5)-C(6)	117.03(16)

Table A7.2.4. Cont'd

C(4)-C(5)-C(1)	103.58(15)
C(14)-C(5)-C(1)	87.97(14)
C(6)-C(5)-C(1)	119.85(16)
O(6B)-C(6)-C(7)	95.7(4)
O(6B)-C(6)-C(12)	109.3(4)
C(7)-C(6)-C(12)	103.69(16)
O(6B)-C(6)-C(5)	112.1(4)
C(7)-C(6)-C(5)	115.31(17)
C(12)-C(6)-C(5)	118.24(16)
C(7)-C(6)-H(6)	106.2
C(12)-C(6)-H(6)	106.2
C(5)-C(6)-H(6)	106.2
C(6)-O(6B)-H(6OB)	109.5
O(2)-C(7)-O(1)	120.3(2)
O(2)-C(7)-C(6)	127.7(2)
O(1)-C(7)-C(6)	111.93(18)
C(7)-O(1)-C(8)	112.11(17)
O(1)-C(8)-C(9)	110.79(18)
O(1)-C(8)-C(12)	106.70(16)
C(9)-C(8)-C(12)	107.08(18)
O(1)-C(8)-H(8)	110.7
C(9)-C(8)-H(8)	110.7
C(12)-C(8)-H(8)	110.7
C(10)-C(9)-C(8)	105.72(17)
C(10)-C(9)-H(9A)	110.6
C(8)-C(9)-H(9A)	110.6
C(10)-C(9)-H(9B)	110.6
C(8)-C(9)-H(9B)	110.6
H(9A)-C(9)-H(9B)	108.7
O(3)-C(10)-C(18)	111.44(17)
O(3)-C(10)-C(9)	110.04(17)
C(18)-C(10)-C(9)	113.72(17)
O(3)-C(10)-C(11)	106.37(15)
C(18)-C(10)-C(11)	113.38(17)

Table A7.2.4. Cont'd

C(9)-C(10)-C(11)	101.23(16)
C(10)-C(18)-H(18A)	109.5
C(10)-C(18)-H(18B)	109.5
H(18A)-C(18)-H(18B)	109.5
C(10)-C(18)-H(18C)	109.5
H(18A)-C(18)-H(18C)	109.5
H(18B)-C(18)-H(18C)	109.5
C(10)-O(3)-H(3O)	110.9(19)
C(13)-C(11)-C(12)	113.93(16)
C(13)-C(11)-C(10)	113.52(17)
C(12)-C(11)-C(10)	105.39(16)
C(13)-C(11)-H(11)	107.9
C(12)-C(11)-H(11)	107.9
C(10)-C(11)-H(11)	107.9
C(11)-C(12)-C(6)	118.97(16)
C(11)-C(12)-C(8)	103.86(16)
C(6)-C(12)-C(8)	105.05(16)
C(11)-C(12)-H(12)	109.5
C(6)-C(12)-H(12)	109.5
C(8)-C(12)-H(12)	109.5
O(4)-C(13)-C(14)	120.14(18)
O(4)-C(13)-C(11)	121.80(18)
C(14)-C(13)-C(11)	118.06(17)
C(13)-C(14)-C(15)	114.11(17)
C(13)-C(14)-C(5)	119.99(17)
C(15)-C(14)-C(5)	92.24(14)
C(13)-C(14)-H(14)	109.7
C(15)-C(14)-H(14)	109.7
C(5)-C(14)-H(14)	109.7
C(14)-C(15)-C(1)	90.25(15)
C(14)-C(15)-H(15A)	113.6
C(1)-C(15)-H(15A)	113.6
C(14)-C(15)-H(15B)	113.6
C(1)-C(15)-H(15B)	113.6

Table A7.2.4. Cont'd

H(15A)-C(15)-H(15B)	110.9
Si(1)-C(16)-H(16A)	109.5
Si(1)-C(16)-H(16B)	109.5
H(16A)-C(16)-H(16B)	109.5
Si(1)-C(16)-H(16C)	109.5
H(16A)-C(16)-H(16C)	109.5
H(16B)-C(16)-H(16C)	109.5
Si(1)-C(17)-H(17A)	109.5
Si(1)-C(17)-H(17B)	109.5
H(17A)-C(17)-H(17B)	109.5
Si(1)-C(17)-H(17C)	109.5
H(17A)-C(17)-H(17C)	109.5
H(17B)-C(17)-H(17C)	109.5
C(26)-C(21)-C(22)	117.0(2)
C(26)-C(21)-Si(1)	120.69(17)
C(22)-C(21)-Si(1)	122.26(19)
C(23)-C(22)-C(21)	121.4(3)
C(23)-C(22)-H(22)	119.3
C(21)-C(22)-H(22)	119.3
C(24)-C(23)-C(22)	120.0(3)
C(24)-C(23)-H(23)	120.0
C(22)-C(23)-H(23)	120.0
C(25)-C(24)-C(23)	120.0(2)
C(25)-C(24)-H(24)	120.0
C(23)-C(24)-H(24)	120.0
C(24)-C(25)-C(26)	120.3(3)
C(24)-C(25)-H(25)	119.9
C(26)-C(25)-H(25)	119.9
C(25)-C(26)-C(21)	121.4(2)
C(25)-C(26)-H(26)	119.3
C(21)-C(26)-H(26)	119.3

Symmetry transformations used to generate equivalent atoms:

Table A7.2.5. Anisotropic Displacement Parameters ($\text{\AA}^2 \times 10^3$) for Cyclobutane **465**.

The Anisotropic Displacement Factor Exponent Takes the Form: $-2p^2[h^2a^{*2}U^{11} + \dots + 2hka^{*}b^{*}U^{12}]$.

	U ¹¹	U ²²	U ³³	U ²³	U ¹³	U ¹²
Si(1)	15(1)	15(1)	14(1)	-4(1)	1(1)	1(1)
C(1)	13(1)	14(1)	10(1)	-1(1)	1(1)	3(1)
C(2)	20(1)	17(1)	13(1)	1(1)	3(1)	2(1)
C(3)	18(1)	14(1)	16(1)	2(1)	5(1)	1(1)
C(4)	14(1)	10(1)	14(1)	-1(1)	3(1)	1(1)
C(5)	11(1)	10(1)	10(1)	-1(1)	1(1)	-1(1)
C(6)	10(1)	10(1)	16(1)	-1(1)	1(1)	-3(1)
O(6B)	4(4)	15(5)	9(4)	-3(3)	2(3)	-1(3)
C(7)	11(1)	14(1)	28(1)	0(1)	7(1)	-5(1)
O(1)	16(1)	22(1)	24(1)	-4(1)	8(1)	1(1)
O(2)	12(1)	21(1)	42(1)	7(1)	8(1)	1(1)
C(8)	17(1)	18(1)	18(1)	1(1)	8(1)	-3(1)
C(9)	22(1)	19(1)	14(1)	-1(1)	6(1)	-2(1)
C(10)	15(1)	11(1)	12(1)	1(1)	2(1)	1(1)
C(18)	21(1)	21(1)	16(1)	0(1)	-1(1)	1(1)
O(3)	21(1)	10(1)	13(1)	-1(1)	1(1)	-1(1)
C(11)	14(1)	9(1)	13(1)	1(1)	2(1)	0(1)
C(12)	14(1)	11(1)	15(1)	-1(1)	5(1)	-2(1)
C(13)	14(1)	8(1)	13(1)	-3(1)	-1(1)	0(1)
O(4)	14(1)	18(1)	18(1)	2(1)	3(1)	5(1)
C(14)	10(1)	11(1)	11(1)	-1(1)	2(1)	0(1)
C(15)	16(1)	15(1)	12(1)	0(1)	3(1)	2(1)
C(16)	16(1)	35(2)	29(1)	-1(1)	2(1)	-2(1)
C(17)	37(2)	18(1)	24(1)	-2(1)	3(1)	-1(1)
C(21)	14(1)	23(1)	18(1)	-10(1)	2(1)	-2(1)
C(22)	16(1)	29(1)	29(1)	-14(1)	0(1)	-1(1)
C(23)	18(1)	41(2)	47(2)	-23(1)	11(1)	-4(1)

Table A7.2.5. Cont'd

C(24)	26(1)	51(2)	38(1)	-24(1)	21(1)	-12(1)
C(25)	32(1)	38(2)	23(1)	-10(1)	11(1)	-13(1)
C(26)	21(1)	29(1)	19(1)	-9(1)	5(1)	-4(1)

Table A7.2.6. Hydrogen Coordinates ($\times 10^4$) and Isotropic Displacement Parameters $(\text{\AA}^2 \times 10^3)$ for Cyclobutane **465**.

	x	y	z	U(eq)
H(2A)	4860	3268	8816	20
H(2B)	2760	3400	9019	20
H(3A)	3424	1287	8151	19
H(3B)	1553	2127	7765	19
H(4A)	3185	2097	6584	15
H(4B)	5140	2390	7209	15
H(6)	5647	5529	6924	15
H(6OB)	6985	6026	6759	90(90)
H(8)	5785	6123	4729	20
H(9A)	3177	5718	3754	21
H(9B)	3801	4124	3881	21
H(18A)	-81	4048	3531	29
H(18B)	-260	5657	3747	29
H(18C)	-1113	4520	4324	29
H(3O)	1630(40)	2740(20)	4749(16)	22
H(11)	1581	6705	5049	15
H(12)	4418	6853	5851	15
H(14)	646	3617	6555	13
H(15A)	297	4314	7928	17
H(15B)	733	5913	7695	17
H(16A)	7531	5787	8409	40
H(16B)	7141	5397	9371	40
H(16C)	7449	6978	9122	40
H(17A)	4148	8677	8147	40
H(17B)	2659	7815	7483	40
H(17C)	4805	7824	7362	40
H(22)	1622	8227	9066	30
H(23)	140	8495	10287	42

Table A7.2.6. Cont'd

H(24)	792	6979	11471	44
H(25)	2924	5197	11436	36
H(26)	4461	4941	10235	27

Table A7.2.7. Torsion Angles [°] for Cyclobutane **465**.

C(16)-Si(1)-C(1)-C(2)	56.33(18)
C(17)-Si(1)-C(1)-C(2)	-179.28(15)
C(21)-Si(1)-C(1)-C(2)	-62.05(17)
C(16)-Si(1)-C(1)-C(15)	-178.59(14)
C(17)-Si(1)-C(1)-C(15)	-54.20(17)
C(21)-Si(1)-C(1)-C(15)	63.02(15)
C(16)-Si(1)-C(1)-C(5)	-74.03(18)
C(17)-Si(1)-C(1)-C(5)	50.4(2)
C(21)-Si(1)-C(1)-C(5)	167.59(16)
C(15)-C(1)-C(2)-C(3)	67.9(2)
C(5)-C(1)-C(2)-C(3)	-27.2(2)
Si(1)-C(1)-C(2)-C(3)	-166.73(14)
C(1)-C(2)-C(3)-C(4)	42.6(2)
C(2)-C(3)-C(4)-C(5)	-42.0(2)
C(3)-C(4)-C(5)-C(14)	-68.47(19)
C(3)-C(4)-C(5)-C(6)	156.67(16)
C(3)-C(4)-C(5)-C(1)	24.6(2)
C(2)-C(1)-C(5)-C(4)	1.8(2)
C(15)-C(1)-C(5)-C(4)	-109.09(16)
Si(1)-C(1)-C(5)-C(4)	135.63(15)
C(2)-C(1)-C(5)-C(14)	112.77(17)
C(15)-C(1)-C(5)-C(14)	1.90(15)
Si(1)-C(1)-C(5)-C(14)	-113.38(16)
C(2)-C(1)-C(5)-C(6)	-126.96(19)
C(15)-C(1)-C(5)-C(6)	122.16(18)
Si(1)-C(1)-C(5)-C(6)	6.9(2)
C(4)-C(5)-C(6)-O(6B)	-102.5(4)
C(14)-C(5)-C(6)-O(6B)	125.6(4)
C(1)-C(5)-C(6)-O(6B)	21.3(4)
C(4)-C(5)-C(6)-C(7)	5.6(2)
C(14)-C(5)-C(6)-C(7)	-126.37(19)
C(1)-C(5)-C(6)-C(7)	129.33(19)

Table A7.2.7. Cont'd

C(4)-C(5)-C(6)-C(12)	129.03(18)
C(14)-C(5)-C(6)-C(12)	-2.9(2)
C(1)-C(5)-C(6)-C(12)	-107.2(2)
O(6B)-C(6)-C(7)-O(2)	60.3(4)
C(12)-C(6)-C(7)-O(2)	171.8(2)
C(5)-C(6)-C(7)-O(2)	-57.4(3)
O(6B)-C(6)-C(7)-O(1)	-116.5(4)
C(12)-C(6)-C(7)-O(1)	-5.0(2)
C(5)-C(6)-C(7)-O(1)	125.80(18)
O(2)-C(7)-O(1)-C(8)	-169.35(19)
C(6)-C(7)-O(1)-C(8)	7.8(2)
C(7)-O(1)-C(8)-C(9)	-123.23(18)
C(7)-O(1)-C(8)-C(12)	-7.0(2)
O(1)-C(8)-C(9)-C(10)	94.2(2)
C(12)-C(8)-C(9)-C(10)	-21.8(2)
C(8)-C(9)-C(10)-O(3)	-74.5(2)
C(8)-C(9)-C(10)-C(18)	159.71(18)
C(8)-C(9)-C(10)-C(11)	37.8(2)
O(3)-C(10)-C(11)-C(13)	-50.7(2)
C(18)-C(10)-C(11)-C(13)	72.2(2)
C(9)-C(10)-C(11)-C(13)	-165.64(17)
O(3)-C(10)-C(11)-C(12)	74.70(19)
C(18)-C(10)-C(11)-C(12)	-162.48(17)
C(9)-C(10)-C(11)-C(12)	-40.28(19)
C(13)-C(11)-C(12)-C(6)	36.0(2)
C(10)-C(11)-C(12)-C(6)	-89.1(2)
C(13)-C(11)-C(12)-C(8)	152.21(17)
C(10)-C(11)-C(12)-C(8)	27.10(19)
O(6B)-C(6)-C(12)-C(11)	-142.6(4)
C(7)-C(6)-C(12)-C(11)	116.25(18)
C(5)-C(6)-C(12)-C(11)	-12.8(3)
O(6B)-C(6)-C(12)-C(8)	101.8(4)
C(7)-C(6)-C(12)-C(8)	0.6(2)
C(5)-C(6)-C(12)-C(8)	-128.44(18)

Table A7.2.7. Cont'd

O(1)-C(8)-C(12)-C(11)	-122.18(17)
C(9)-C(8)-C(12)-C(11)	-3.5(2)
O(1)-C(8)-C(12)-C(6)	3.5(2)
C(9)-C(8)-C(12)-C(6)	122.15(18)
C(12)-C(11)-C(13)-O(4)	135.85(19)
C(10)-C(11)-C(13)-O(4)	-103.5(2)
C(12)-C(11)-C(13)-C(14)	-44.4(2)
C(10)-C(11)-C(13)-C(14)	76.2(2)
O(4)-C(13)-C(14)-C(15)	-42.7(3)
C(11)-C(13)-C(14)-C(15)	137.55(18)
O(4)-C(13)-C(14)-C(5)	-150.63(19)
C(11)-C(13)-C(14)-C(5)	29.6(3)
C(4)-C(5)-C(14)-C(13)	-138.52(18)
C(6)-C(5)-C(14)-C(13)	-5.0(3)
C(1)-C(5)-C(14)-C(13)	117.72(18)
C(4)-C(5)-C(14)-C(15)	101.83(17)
C(6)-C(5)-C(14)-C(15)	-124.68(17)
C(1)-C(5)-C(14)-C(15)	-1.93(15)
C(13)-C(14)-C(15)-C(1)	-122.46(17)
C(5)-C(14)-C(15)-C(1)	1.98(16)
C(2)-C(1)-C(15)-C(14)	-107.64(17)
C(5)-C(1)-C(15)-C(14)	-1.92(15)
Si(1)-C(1)-C(15)-C(14)	125.28(14)
C(16)-Si(1)-C(21)-C(26)	-49.7(2)
C(17)-Si(1)-C(21)-C(26)	-168.77(18)
C(1)-Si(1)-C(21)-C(26)	72.18(19)
C(16)-Si(1)-C(21)-C(22)	131.85(19)
C(17)-Si(1)-C(21)-C(22)	12.8(2)
C(1)-Si(1)-C(21)-C(22)	-106.24(19)
C(26)-C(21)-C(22)-C(23)	-0.1(3)
Si(1)-C(21)-C(22)-C(23)	178.40(18)
C(21)-C(22)-C(23)-C(24)	-0.3(4)
C(22)-C(23)-C(24)-C(25)	0.1(4)
C(23)-C(24)-C(25)-C(26)	0.6(4)

Table A7.2.7. Cont'd

C(24)-C(25)-C(26)-C(21)	-1.0(4)
C(22)-C(21)-C(26)-C(25)	0.8(3)
Si(1)-C(21)-C(26)-C(25)	-177.75(18)

Symmetry transformations used to generate equivalent atoms:

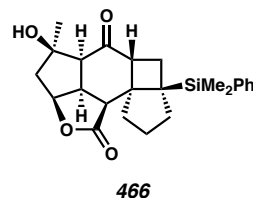
Table A7.2.8. Hydrogen Bonds for Cyclobutane **465** [\AA and $^\circ$].

D-H...A	d(D-H)	d(H...A)	d(D...A)	\angle (DHA)
C(9)-H(9A)...O(2)#1	0.99	2.40	3.280(3)	147.2
C(18)-H(18C)...O(1)#2	0.98	2.64	3.622(3)	175.1
O(3)-H(3O)...O(4)#3	0.81(2)	1.96(2)	2.766(2)	177(3)
C(14)-H(14)...O(2)#2	1.00	2.46	3.182(3)	128.6

Symmetry transformations used to generate equivalent atoms:

#1 -x+1,y+1/2,-z+1 #2 x-1,y,z #3 -x,y-1/2,-z+1

A7.3 X-RAY CRYSTAL STRUCTURE ANALYSIS OF CYCLOBUTANE **466**



Contents

Table A7.3.1. Experimental Details

Table A7.3.2. Crystal Data

Table A7.3.3. Atomic Coordinates

Table A7.3.4. Full Bond Distances and Angles

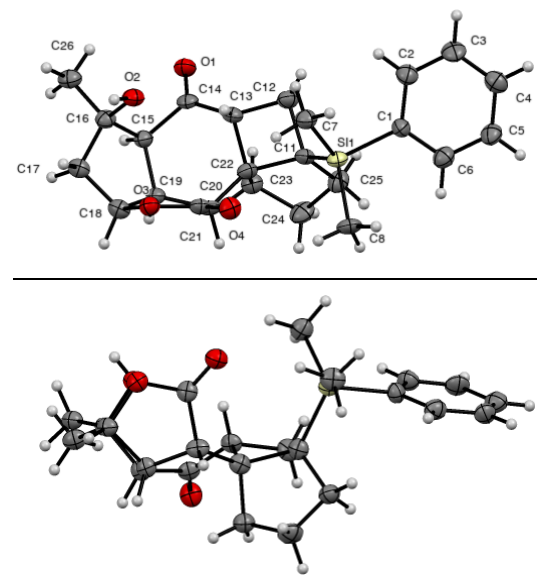
Table A7.3.5. Anisotropic Displacement Parameters

Table A7.3.6. Hydrogen Atomic Coordinates

Table A7.3.7. Torsion Angles

Table A7.3.8. Hydrogen Bond Distances and Angle

*Figure A7.3.1. X-Ray Crystal Structure of Cyclobutane **466***



*Table A7.3.1. Experimental Details for X-Ray Structure Determination of Cyclobutane **466***

Low-temperature diffraction data (ϕ -and ω -scans) were collected on a Bruker AXS D8 VENTURE KAPPA diffractometer coupled to a PHOTON II CPAD detector with Cu $K\alpha$ radiation ($\lambda = 1.54178 \text{ \AA}$) from an $1\mu\text{S}$ micro-source for the structure of compound V19015. The structure was solved by direct methods using SHELXS¹ and refined against F^2 on all data by full-matrix least squares with SHELXL-2017² using established refinement techniques.³ All non-hydrogen atoms were refined anisotropically. Unless otherwise noted, all hydrogen atoms were included into the model at geometrically calculated positions and refined using a riding model. The isotropic displacement parameters of all hydrogen atoms were fixed to 1.2 times the U value of the atoms they are linked to (1.5 times for methyl groups).

Compound **466** crystallizes in the monoclinic space group $P2_1$ with one molecule in the asymmetric unit. The coordinates for the hydrogen atom bound to O2 were located in the difference Fourier synthesis and refined semi-freely with the help of a restraint on the O-H distance (0.84(4) \AA). The structure was refined as a twin [-1 0 0 0 -1 0 1 0 1].

Table A7.3.2. Crystal Data and Structure Refinement for Cyclobutane **466**

Empirical formula	C ₂₄ H ₃₀ O ₄ Si	
Formula weight	410.57	
Temperature	100(2) K	
Wavelength	1.54178 Å	
Crystal system	Monoclinic	
Space group	P2 ₁	
Unit cell dimensions	a = 6.7649(5) Å	a = 90°.
	b = 10.9273(9) Å	b = 103.394(5)°.
	c = 14.4629(14) Å	g = 90°.
Volume	1040.05(15) Å ³	
Z	2	
Density (calculated)	1.311 Mg/m ³	
Absorption coefficient	1.224 mm ⁻¹	
F(000)	440	
Crystal size	0.200 x 0.150 x 0.050 mm ³	
Theta range for data collection	3.141 to 74.630°.	
Index ranges	-7<=h<=8, -13<=k<=13, -18<=l<=17	
Reflections collected	17179	
Independent reflections	4172 [R(int) = 0.0797]	
Completeness to theta = 67.679°	99.7 %	
Absorption correction	Semi-empirical from equivalents	
Max. and min. transmission	0.7504 and 0.5626	
Refinement method	Full-matrix least-squares on F ²	
Data / restraints / parameters	4172 / 2 / 269	
Goodness-of-fit on F ²	1.071	
Final R indices [I>2sigma(I)]	R1 = 0.0880, wR2 = 0.2288	
R indices (all data)	R1 = 0.0893, wR2 = 0.2312	
Absolute structure parameter	0.03(6)	
Extinction coefficient	n/a	
Largest diff. peak and hole	0.686 and -0.364 e.Å ⁻³	

*Table A.7.3.3. Atomic Coordinates ($x \times 10^4$) and Equivalent Isotropic Displacement Parameters ($\text{\AA}^2 \times 10^3$) for Cyclobutane **466**. $U(\text{eq})$ is Defined as One Third of the Trace of the Orthogonalized U^{ij} Tensor.*

	x	y	z	$U(\text{eq})$
Si(1)	5500(3)	3644(2)	3733(2)	26(1)
C(1)	5454(13)	4028(8)	5009(6)	28(2)
C(2)	3622(15)	4276(9)	5275(7)	34(2)
C(3)	3582(16)	4570(10)	6208(8)	38(2)
C(4)	5409(17)	4598(10)	6909(8)	37(2)
C(5)	7217(15)	4334(10)	6668(7)	35(2)
C(6)	7249(16)	4064(9)	5719(7)	34(2)
C(7)	3130(15)	2738(10)	3256(7)	34(2)
C(8)	7879(13)	2754(9)	3754(8)	33(2)
C(11)	5539(13)	5208(8)	3156(6)	26(2)
C(12)	3363(14)	5841(9)	3012(7)	32(2)
C(13)	2992(13)	5596(8)	1937(6)	26(2)
C(14)	2128(13)	6460(8)	1150(6)	26(2)
O(1)	1187(12)	7376(6)	1210(5)	34(2)
C(15)	2743(13)	6116(8)	223(6)	27(2)
C(16)	1075(14)	5330(8)	-431(6)	28(2)
C(26)	-690(15)	6100(9)	-971(7)	34(2)
O(2)	321(10)	4436(6)	135(5)	31(1)
C(17)	2279(15)	4700(8)	-1074(6)	28(2)
C(18)	4326(15)	4391(8)	-447(6)	29(2)
C(19)	4824(13)	5439(8)	283(6)	26(2)
C(20)	5848(13)	4788(8)	1237(6)	27(2)
C(21)	5101(13)	3456(8)	1047(6)	27(2)
O(3)	4251(10)	3301(6)	116(5)	30(1)
O(4)	5290(12)	2622(6)	1593(5)	34(2)
C(22)	5312(13)	5490(8)	2053(6)	27(2)
C(23)	6384(15)	6755(8)	2115(7)	30(2)

Table A.7.3.3. Cont'd

C(24)	8208(15)	6643(10)	2960(8)	39(2)
C(25)	7315(15)	5980(9)	3715(7)	34(2)

Table A7.3.4. Bond Lengths [\AA] and angles [$^\circ$] for Cyclobutane **466**

Si(1)-C(8)	1.874(9)
Si(1)-C(7)	1.875(10)
Si(1)-C(1)	1.900(9)
Si(1)-C(11)	1.905(9)
C(1)-C(6)	1.397(13)
C(1)-C(2)	1.406(13)
C(2)-C(3)	1.393(14)
C(2)-H(2)	0.9500
C(3)-C(4)	1.406(15)
C(3)-H(3)	0.9500
C(4)-C(5)	1.378(15)
C(4)-H(4)	0.9500
C(5)-C(6)	1.409(14)
C(5)-H(5)	0.9500
C(6)-H(6)	0.9500
C(7)-H(7A)	0.9800
C(7)-H(7B)	0.9800
C(7)-H(7C)	0.9800
C(8)-H(8A)	0.9800
C(8)-H(8B)	0.9800
C(8)-H(8C)	0.9800
C(11)-C(25)	1.535(12)
C(11)-C(12)	1.596(12)
C(11)-C(22)	1.598(12)
C(12)-C(13)	1.541(13)
C(12)-H(12A)	0.9900
C(12)-H(12B)	0.9900
C(13)-C(14)	1.489(12)
C(13)-C(22)	1.544(12)
C(13)-H(13)	1.0000
C(14)-O(1)	1.201(12)
C(14)-C(15)	1.541(12)
C(15)-C(16)	1.552(12)

Table A.7.3.4. Cont'd

C(15)-C(19)	1.574(12)
C(15)-H(15)	1.0000
C(16)-O(2)	1.441(11)
C(16)-C(26)	1.521(13)
C(16)-C(17)	1.534(12)
C(26)-H(26A)	0.9800
C(26)-H(26B)	0.9800
C(26)-H(26C)	0.9800
O(2)-H(2A)	0.83(3)
C(17)-C(18)	1.508(13)
C(17)-H(17A)	0.9900
C(17)-H(17B)	0.9900
C(18)-O(3)	1.450(11)
C(18)-C(19)	1.541(12)
C(18)-H(18)	1.0000
C(19)-C(20)	1.565(12)
C(19)-H(19)	1.0000
C(20)-C(22)	1.520(12)
C(20)-C(21)	1.544(12)
C(20)-H(20)	1.0000
C(21)-O(4)	1.193(11)
C(21)-O(3)	1.347(11)
C(22)-C(23)	1.554(13)
C(23)-C(24)	1.527(13)
C(23)-H(23A)	0.9900
C(23)-H(23B)	0.9900
C(24)-C(25)	1.545(14)
C(24)-H(24A)	0.9900
C(24)-H(24B)	0.9900
C(25)-H(25A)	0.9900
C(25)-H(25B)	0.9900
C(8)-Si(1)-C(7)	112.9(5)
C(8)-Si(1)-C(1)	107.8(4)

Table A.7.3.4. Cont'd

C(7)-Si(1)-C(1)	105.7(4)
C(8)-Si(1)-C(11)	111.9(4)
C(7)-Si(1)-C(11)	114.2(4)
C(1)-Si(1)-C(11)	103.4(4)
C(6)-C(1)-C(2)	117.7(9)
C(6)-C(1)-Si(1)	120.9(7)
C(2)-C(1)-Si(1)	121.4(7)
C(3)-C(2)-C(1)	121.7(9)
C(3)-C(2)-H(2)	119.2
C(1)-C(2)-H(2)	119.2
C(2)-C(3)-C(4)	119.5(10)
C(2)-C(3)-H(3)	120.2
C(4)-C(3)-H(3)	120.2
C(5)-C(4)-C(3)	119.7(10)
C(5)-C(4)-H(4)	120.1
C(3)-C(4)-H(4)	120.1
C(4)-C(5)-C(6)	120.4(9)
C(4)-C(5)-H(5)	119.8
C(6)-C(5)-H(5)	119.8
C(1)-C(6)-C(5)	121.0(9)
C(1)-C(6)-H(6)	119.5
C(5)-C(6)-H(6)	119.5
Si(1)-C(7)-H(7A)	109.5
Si(1)-C(7)-H(7B)	109.5
H(7A)-C(7)-H(7B)	109.5
Si(1)-C(7)-H(7C)	109.5
H(7A)-C(7)-H(7C)	109.5
H(7B)-C(7)-H(7C)	109.5
Si(1)-C(8)-H(8A)	109.5
Si(1)-C(8)-H(8B)	109.5
H(8A)-C(8)-H(8B)	109.5
Si(1)-C(8)-H(8C)	109.5
H(8A)-C(8)-H(8C)	109.5
H(8B)-C(8)-H(8C)	109.5

Table A.7.3.4. Cont'd

C(25)-C(11)-C(12)	114.6(7)
C(25)-C(11)-C(22)	107.6(7)
C(12)-C(11)-C(22)	85.0(6)
C(25)-C(11)-Si(1)	110.5(6)
C(12)-C(11)-Si(1)	109.9(6)
C(22)-C(11)-Si(1)	127.1(6)
C(13)-C(12)-C(11)	89.2(7)
C(13)-C(12)-H(12A)	113.8
C(11)-C(12)-H(12A)	113.8
C(13)-C(12)-H(12B)	113.8
C(11)-C(12)-H(12B)	113.8
H(12A)-C(12)-H(12B)	111.0
C(14)-C(13)-C(12)	127.2(8)
C(14)-C(13)-C(22)	109.9(7)
C(12)-C(13)-C(22)	88.8(7)
C(14)-C(13)-H(13)	109.5
C(12)-C(13)-H(13)	109.5
C(22)-C(13)-H(13)	109.5
O(1)-C(14)-C(13)	126.4(8)
O(1)-C(14)-C(15)	121.4(8)
C(13)-C(14)-C(15)	111.9(7)
C(14)-C(15)-C(16)	111.1(7)
C(14)-C(15)-C(19)	119.0(7)
C(16)-C(15)-C(19)	106.8(7)
C(14)-C(15)-H(15)	106.4
C(16)-C(15)-H(15)	106.4
C(19)-C(15)-H(15)	106.4
O(2)-C(16)-C(26)	109.1(8)
O(2)-C(16)-C(17)	110.3(7)
C(26)-C(16)-C(17)	113.6(7)
O(2)-C(16)-C(15)	109.4(7)
C(26)-C(16)-C(15)	112.3(7)
C(17)-C(16)-C(15)	101.8(7)
C(16)-C(26)-H(26A)	109.5

Table A.7.3.4. Cont'd

C(16)-C(26)-H(26B)	109.5
H(26A)-C(26)-H(26B)	109.5
C(16)-C(26)-H(26C)	109.5
H(26A)-C(26)-H(26C)	109.5
H(26B)-C(26)-H(26C)	109.5
C(16)-O(2)-H(2A)	106(10)
C(18)-C(17)-C(16)	106.2(7)
C(18)-C(17)-H(17A)	110.5
C(16)-C(17)-H(17A)	110.5
C(18)-C(17)-H(17B)	110.5
C(16)-C(17)-H(17B)	110.5
H(17A)-C(17)-H(17B)	108.7
O(3)-C(18)-C(17)	112.0(7)
O(3)-C(18)-C(19)	104.9(7)
C(17)-C(18)-C(19)	105.7(7)
O(3)-C(18)-H(18)	111.3
C(17)-C(18)-H(18)	111.3
C(19)-C(18)-H(18)	111.3
C(18)-C(19)-C(20)	104.4(7)
C(18)-C(19)-C(15)	105.1(7)
C(20)-C(19)-C(15)	118.0(7)
C(18)-C(19)-H(19)	109.7
C(20)-C(19)-H(19)	109.7
C(15)-C(19)-H(19)	109.7
C(22)-C(20)-C(21)	119.2(7)
C(22)-C(20)-C(19)	108.6(6)
C(21)-C(20)-C(19)	102.2(7)
C(22)-C(20)-H(20)	108.8
C(21)-C(20)-H(20)	108.8
C(19)-C(20)-H(20)	108.8
O(4)-C(21)-O(3)	121.4(8)
O(4)-C(21)-C(20)	128.5(8)
O(3)-C(21)-C(20)	110.1(7)
C(21)-O(3)-C(18)	113.3(7)

Table A.7.3.4. Cont'd

C(20)-C(22)-C(13)	111.9(7)
C(20)-C(22)-C(23)	107.6(7)
C(13)-C(22)-C(23)	112.9(8)
C(20)-C(22)-C(11)	133.8(7)
C(13)-C(22)-C(11)	89.0(6)
C(23)-C(22)-C(11)	100.2(7)
C(24)-C(23)-C(22)	104.8(8)
C(24)-C(23)-H(23A)	110.8
C(22)-C(23)-H(23A)	110.8
C(24)-C(23)-H(23B)	110.8
C(22)-C(23)-H(23B)	110.8
H(23A)-C(23)-H(23B)	108.9
C(23)-C(24)-C(25)	103.1(8)
C(23)-C(24)-H(24A)	111.1
C(25)-C(24)-H(24A)	111.1
C(23)-C(24)-H(24B)	111.1
C(25)-C(24)-H(24B)	111.1
H(24A)-C(24)-H(24B)	109.1
C(11)-C(25)-C(24)	105.8(8)
C(11)-C(25)-H(25A)	110.6
C(24)-C(25)-H(25A)	110.6
C(11)-C(25)-H(25B)	110.6
C(24)-C(25)-H(25B)	110.6
H(25A)-C(25)-H(25B)	108.7

Symmetry transformations used to generate equivalent atoms:

Table A7.3.5. Anisotropic Displacement Parameters ($\text{\AA}^2 \times 10^3$) for Cyclobutane **466**.

The Anisotropic Displacement Factor Exponent Takes the Form: $-2p^2[h^2a^{*2}U^{11} + \dots + 2hka^{*}b^{*}U^{12}]$.

	U ¹¹	U ²²	U ³³	U ²³	U ¹³	U ¹²
Si(1)	19(1)	29(1)	32(1)	0(1)	7(1)	-1(1)
C(1)	26(4)	33(4)	24(4)	2(3)	7(3)	0(3)
C(2)	31(5)	36(5)	35(4)	3(4)	11(4)	-4(4)
C(3)	26(4)	44(5)	44(5)	-1(4)	10(4)	-13(4)
C(4)	42(6)	32(4)	39(5)	-4(4)	15(4)	-2(4)
C(5)	27(4)	41(5)	34(5)	2(4)	4(4)	-8(4)
C(6)	30(4)	34(5)	37(5)	2(3)	5(4)	-2(4)
C(7)	27(4)	41(5)	37(5)	-3(4)	10(4)	-1(4)
C(8)	20(4)	34(5)	47(5)	1(4)	11(4)	7(3)
C(11)	21(4)	31(4)	30(4)	-2(3)	10(3)	4(3)
C(12)	26(4)	32(4)	37(5)	3(4)	10(4)	7(4)
C(13)	21(4)	29(4)	31(4)	-1(3)	11(3)	0(3)
C(14)	15(3)	30(4)	34(4)	-1(3)	7(3)	-2(3)
O(1)	32(3)	38(4)	36(3)	0(3)	12(3)	9(3)
C(15)	22(4)	31(4)	28(4)	2(3)	7(3)	2(3)
C(16)	24(4)	28(4)	31(4)	2(3)	7(3)	-3(4)
C(26)	26(4)	35(5)	42(5)	-2(4)	9(4)	-1(4)
O(2)	25(3)	34(3)	35(3)	1(2)	12(3)	0(3)
C(17)	30(4)	24(4)	34(4)	-1(3)	12(3)	-1(3)
C(18)	30(4)	26(4)	33(4)	-2(3)	13(3)	-2(4)
C(19)	21(4)	29(4)	29(4)	0(3)	8(3)	2(3)
C(20)	20(4)	22(4)	40(4)	-2(3)	10(3)	5(3)
C(21)	22(4)	29(4)	31(4)	-1(3)	9(3)	6(3)
O(3)	27(3)	29(3)	32(3)	-1(2)	7(2)	2(2)
O(4)	35(4)	31(3)	37(3)	3(3)	9(3)	-1(3)
C(22)	20(4)	28(4)	33(4)	3(3)	6(3)	5(3)
C(23)	29(4)	28(4)	34(4)	0(3)	7(4)	0(4)
C(24)	26(5)	41(5)	48(6)	2(4)	4(4)	-9(4)
C(25)	32(4)	31(4)	35(4)	1(4)	3(4)	-6(4)

Table A7.3.6. Hydrogen Coordinates ($\times 10^4$) and Isotropic Displacement Parameters $(\text{\AA}^2 \times 10^3)$ for Cyclobutane **466**.

	x	y	z	U(eq)
H(2)	2380	4242	4806	40
H(3)	2330	4751	6369	45
H(4)	5397	4799	7547	44
H(5)	8449	4333	7144	42
H(6)	8510	3903	5559	41
H(7A)	1946	3280	3161	52
H(7B)	3004	2092	3709	52
H(7C)	3201	2367	2647	52
H(8A)	8045	2119	4244	50
H(8B)	9051	3307	3897	50
H(8C)	7785	2371	3133	50
H(12A)	2417	5398	3324	38
H(12B)	3426	6721	3180	38
H(13)	2354	4772	1789	31
H(15)	2817	6900	-124	32
H(26A)	-1691	5569	-1381	51
H(26B)	-188	6704	-1362	51
H(26C)	-1329	6524	-518	51
H(2A)	-100(200)	3860(90)	-230(80)	46
H(17A)	1573	3948	-1357	34
H(17B)	2433	5255	-1594	34
H(18)	5385	4317	-825	35
H(19)	5814	6014	96	31
H(20)	7355	4806	1316	32
H(23A)	6832	6932	1524	36
H(23B)	5462	7416	2222	36
H(24A)	8746	7459	3189	47
H(24B)	9308	6156	2792	47

Table A.7.3.6. Cont'd

H(25A)	8353	5450	4119	40
H(25B)	6829	6579	4125	40

Table A7.3.7. Torsion Angles [$^{\circ}$] for Cyclobutane **466**.

C(8)-Si(1)-C(1)-C(6)	23.2(9)
C(7)-Si(1)-C(1)-C(6)	144.2(8)
C(11)-Si(1)-C(1)-C(6)	-95.5(8)
C(8)-Si(1)-C(1)-C(2)	-156.3(8)
C(7)-Si(1)-C(1)-C(2)	-35.2(9)
C(11)-Si(1)-C(1)-C(2)	85.1(8)
C(6)-C(1)-C(2)-C(3)	1.2(15)
Si(1)-C(1)-C(2)-C(3)	-179.4(8)
C(1)-C(2)-C(3)-C(4)	-1.3(15)
C(2)-C(3)-C(4)-C(5)	-0.1(16)
C(3)-C(4)-C(5)-C(6)	1.5(16)
C(2)-C(1)-C(6)-C(5)	0.3(15)
Si(1)-C(1)-C(6)-C(5)	-179.2(8)
C(4)-C(5)-C(6)-C(1)	-1.6(16)
C(25)-C(11)-C(12)-C(13)	127.8(8)
C(22)-C(11)-C(12)-C(13)	20.7(6)
Si(1)-C(11)-C(12)-C(13)	-107.0(6)
C(11)-C(12)-C(13)-C(14)	-135.6(8)
C(11)-C(12)-C(13)-C(22)	-21.4(7)
C(12)-C(13)-C(14)-O(1)	-17.2(15)
C(22)-C(13)-C(14)-O(1)	-121.5(10)
C(12)-C(13)-C(14)-C(15)	157.4(8)
C(22)-C(13)-C(14)-C(15)	53.1(10)
O(1)-C(14)-C(15)-C(16)	-89.6(11)
C(13)-C(14)-C(15)-C(16)	95.4(8)
O(1)-C(14)-C(15)-C(19)	145.8(9)
C(13)-C(14)-C(15)-C(19)	-29.2(11)
C(14)-C(15)-C(16)-O(2)	-42.2(10)
C(19)-C(15)-C(16)-O(2)	89.0(8)
C(14)-C(15)-C(16)-C(26)	79.1(9)
C(19)-C(15)-C(16)-C(26)	-149.6(8)
C(14)-C(15)-C(16)-C(17)	-159.0(7)

Table A.7.3.7. Cont'd

C(19)-C(15)-C(16)-C(17)	-27.8(8)
O(2)-C(16)-C(17)-C(18)	-77.6(9)
C(26)-C(16)-C(17)-C(18)	159.5(7)
C(15)-C(16)-C(17)-C(18)	38.5(8)
C(16)-C(17)-C(18)-O(3)	79.1(8)
C(16)-C(17)-C(18)-C(19)	-34.6(9)
O(3)-C(18)-C(19)-C(20)	22.3(8)
C(17)-C(18)-C(19)-C(20)	140.8(7)
O(3)-C(18)-C(19)-C(15)	-102.6(7)
C(17)-C(18)-C(19)-C(15)	16.0(9)
C(14)-C(15)-C(19)-C(18)	134.4(8)
C(16)-C(15)-C(19)-C(18)	7.8(9)
C(14)-C(15)-C(19)-C(20)	18.7(11)
C(16)-C(15)-C(19)-C(20)	-107.9(8)
C(18)-C(19)-C(20)-C(22)	-147.5(7)
C(15)-C(19)-C(20)-C(22)	-31.4(10)
C(18)-C(19)-C(20)-C(21)	-20.7(8)
C(15)-C(19)-C(20)-C(21)	95.4(8)
C(22)-C(20)-C(21)-O(4)	-51.9(12)
C(19)-C(20)-C(21)-O(4)	-171.5(9)
C(22)-C(20)-C(21)-O(3)	132.0(8)
C(19)-C(20)-C(21)-O(3)	12.4(8)
O(4)-C(21)-O(3)-C(18)	-174.6(8)
C(20)-C(21)-O(3)-C(18)	1.9(9)
C(17)-C(18)-O(3)-C(21)	-129.8(7)
C(19)-C(18)-O(3)-C(21)	-15.7(9)
C(21)-C(20)-C(22)-C(13)	-59.4(10)
C(19)-C(20)-C(22)-C(13)	57.0(9)
C(21)-C(20)-C(22)-C(23)	176.1(7)
C(19)-C(20)-C(22)-C(23)	-67.6(8)
C(21)-C(20)-C(22)-C(11)	51.8(13)
C(19)-C(20)-C(22)-C(11)	168.1(9)
C(14)-C(13)-C(22)-C(20)	-71.5(10)
C(12)-C(13)-C(22)-C(20)	159.0(7)

Table A.7.3.7. Cont'd

C(14)-C(13)-C(22)-C(23)	50.1(10)
C(12)-C(13)-C(22)-C(23)	-79.4(8)
C(14)-C(13)-C(22)-C(11)	150.8(7)
C(12)-C(13)-C(22)-C(11)	21.3(7)
C(25)-C(11)-C(22)-C(20)	105.0(10)
C(12)-C(11)-C(22)-C(20)	-140.7(10)
Si(1)-C(11)-C(22)-C(20)	-29.5(13)
C(25)-C(11)-C(22)-C(13)	-134.9(7)
C(12)-C(11)-C(22)-C(13)	-20.6(7)
Si(1)-C(11)-C(22)-C(13)	90.6(8)
C(25)-C(11)-C(22)-C(23)	-21.8(8)
C(12)-C(11)-C(22)-C(23)	92.4(7)
Si(1)-C(11)-C(22)-C(23)	-156.3(7)
C(20)-C(22)-C(23)-C(24)	-103.1(8)
C(13)-C(22)-C(23)-C(24)	132.9(8)
C(11)-C(22)-C(23)-C(24)	39.6(9)
C(22)-C(23)-C(24)-C(25)	-43.1(10)
C(12)-C(11)-C(25)-C(24)	-96.0(9)
C(22)-C(11)-C(25)-C(24)	-3.4(10)
Si(1)-C(11)-C(25)-C(24)	139.2(7)
C(23)-C(24)-C(25)-C(11)	28.0(10)

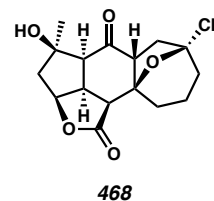
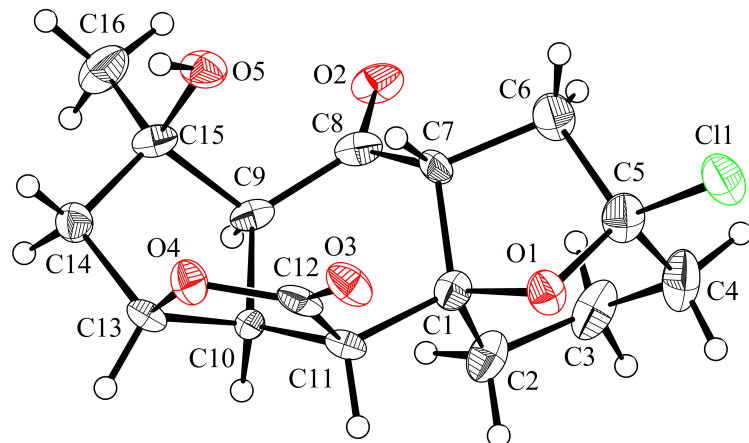
Symmetry transformations used to generate equivalent atoms:

Table A7.3.8. Hydrogen Bonds for Cyclobutane **466** [\AA and $^\circ$].

D-H...A	d(D-H)	d(H...A)	d(D...A)	\angle (DHA)
C(13)-H(13)...O(2)	1.00	2.49	3.079(11)	116.9
C(15)-H(15)...O(3)#1	1.00	2.50	3.246(11)	130.8
O(2)-H(2A)...O(1)#2	0.83(3)	2.16(3)	2.996(10)	178(15)
C(17)-H(17A)...O(1)#2	0.99	2.58	3.430(11)	143.8
C(19)-H(19)...O(3)#1	1.00	2.52	3.267(11)	131.5

Symmetry transformations used to generate equivalent atoms:

#1 -x+1,y+1/2,-z #2 -x,y-1/2,-z

A7.4 X-RAY CRYSTAL STRUCTURE ANALYSIS OF CYCLOHEPTANE **468**Contents*Table A7.4.1. Experimental Details**Table A7.4.2. Crystal Data**Table A7.4.3. Atomic Coordinates**Table A7.4.4. Full Bond Distances and Angles**Table A7.4.5. Anisotropic Displacement Parameters**Table A7.4.6. Hydrogen Atomic Coordinates**Table A7.4.7. Torsion Angles**Table A7.4.8. Hydrogen Bond Distances and Angle**Figure A7.4.1. X-Ray Crystal Structure of Cycloheptane **468***

*Table A7.4.1. Experimental Details for X-Ray Structure Determination of Cycloheptane **468***

Refinement details

A crystal was mounted on a polyimide MiTeGen loop with STP Oil Treatment and placed under a nitrogen stream. Low temperature (100K) X-ray data were collected with a Bruker AXS D8 VENTURE KAPPA diffractometer running at 50 kV and 1mA ($\text{Cu } K_{\alpha} = 1.54178 \text{ \AA}$; PHOTON II CPAD detector and Helios focusing multilayer mirror optics). All diffractometer manipulations, including data collection, integration, and scaling were carried out using the Bruker APEX3 software. An absorption correction was applied using SADABS. The space group was determined and the structure solved by intrinsic phasing using XT. Refinement was full-matrix least squares on F^2 using XL. All non-hydrogen atoms (except the carbon of a disordered chloroform) were refined using anisotropic displacement parameters. Hydrogen atoms were placed in idealized positions and refined using a riding model. The isotropic displacement parameters of all hydrogen atoms were fixed at 1.2 times (1.5 times for methyl groups) the U_{eq} value of the bonded atom.

Special refinement details

Compound **468** crystallizes in the monoclinic space group *C*2 with two molecules, one water molecule, and 38% of a chloroform in the asymmetric unit. The structure was refined as a two-component twin (refined ratio of 85:15) on an HKLF 5 file generated by PLATON.

Table A7.4.2. Crystal Data and Structure Refinement for Cycloheptane **468**

Empirical formula	C16.19 H20.19 Cl1.59 O5.50	
Formula weight	359.09	
Temperature	100 K	
Wavelength	1.54178 Å	
Crystal system	Monoclinic	
Space group	C 1 2 1	
Unit cell dimensions	a = 34.102(5) Å	a = 90°
	b = 14.485(2) Å	b = 94.960(10)°
	c = 6.6087(11) Å	g = 90°
Volume	3252.2(9) Å ³	
Z	8	
Density (calculated)	1.467 g/cm ³	
Absorption coefficient	3.208 mm ⁻¹	
F(000)	1507	
Crystal size	0.11 x 0.04 x 0.03 mm ³	
Theta range for data collection	3.317 to 76.122°.	
Index ranges	-41 ≤ h ≤ 40, -17 ≤ k ≤ 17, 0 ≤ l ≤ 8	
Reflections collected	6144	
Independent reflections	6144 [R(int) = ?]	
Completeness to theta = 67.679°	98.9 %	
Absorption correction	Semi-empirical from equivalents	
Max. and min. transmission	0.9904 and 0.7072	
Refinement method	Full-matrix least-squares on F ²	
Data / restraints / parameters	6144 / 4 / 434	
Goodness-of-fit on F ²	1.065	
Final R indices [I>2sigma(I)]	R1 = 0.0840, wR2 = 0.2207	
R indices (all data)	R1 = 0.0969, wR2 = 0.2291	
Absolute structure parameter [Flack]	0.163(12)	
Extinction coefficient	n/a	
Largest diff. peak and hole	0.708 and -0.538 e.Å ⁻³	

*Table A.7.4.3. Atomic Coordinates ($x \cdot 10^4$) and Equivalent Isotropic Displacement Parameters ($\text{\AA}^2 \times 10^3$) for Cycloheptane **468**. $U(\text{eq})$ is Defined as One Third of the Trace of the Orthogonalized U^{ij} Tensor.*

	x	y	z	$U(\text{eq})$
Cl(1)	6462(1)	349(2)	11229(4)	36(1)
O(1)	6294(2)	1950(4)	12668(10)	25(1)
O(2)	5281(2)	2980(5)	8327(10)	29(2)
O(3)	6853(2)	3559(5)	11901(10)	28(1)
O(4)	6508(2)	4844(4)	11323(10)	25(1)
O(5)	6000(2)	4396(5)	7538(10)	27(1)
C(1)	6013(2)	2698(6)	12313(13)	23(2)
C(2)	5664(3)	2506(7)	13588(15)	31(2)
C(3)	5480(3)	1561(8)	13098(18)	38(2)
C(4)	5790(3)	823(7)	12868(19)	40(3)
C(5)	6094(3)	1208(7)	11574(16)	30(2)
C(6)	5924(3)	1617(7)	9532(16)	32(2)
C(7)	5919(3)	2650(6)	10038(12)	21(2)
C(8)	5562(3)	3240(7)	9446(13)	25(2)
C(9)	5591(2)	4203(6)	10287(12)	21(2)
C(10)	5876(3)	4396(6)	12246(13)	19(2)
C(11)	6178(2)	3656(6)	12938(13)	20(2)
C(12)	6543(3)	3974(7)	12019(13)	23(2)
C(13)	6124(2)	5226(6)	11765(12)	20(2)
C(14)	5911(3)	5671(6)	9851(14)	24(2)
C(15)	5723(2)	4889(7)	8647(13)	23(2)
C(16)	5371(3)	5187(8)	7186(16)	37(2)
Cl(1B)	5600(1)	7225(2)	14099(5)	54(1)
O(1B)	6287(2)	7010(5)	16090(11)	35(2)
O(2B)	7121(2)	8559(5)	12394(11)	41(2)
O(3B)	6650(2)	5146(5)	15897(10)	31(2)
O(4B)	7290(2)	5266(6)	15553(12)	43(2)

Table A.7.4.3. Cont'd

O(5B)	7372(2)	6411(5)	11759(11)	33(2)
C(1B)	6692(4)	7307(8)	16092(16)	42(3)
C(2B)	6754(5)	8185(9)	17260(18)	64(4)
C(3B)	6466(5)	8945(9)	16450(19)	65(4)
C(4B)	6047(5)	8570(9)	15850(20)	63(4)
C(5B)	6081(3)	7679(8)	14762(17)	42(3)
C(6B)	6326(3)	7773(7)	12972(15)	33(2)
C(7B)	6725(3)	7396(7)	13782(13)	30(2)
C(8B)	7108(3)	7877(7)	13444(13)	32(2)
C(9B)	7466(3)	7454(8)	14569(15)	40(3)
C(10B)	7409(3)	6845(10)	16518(15)	46(3)
C(11B)	6992(3)	6573(9)	16972(16)	42(3)
C(12B)	6950(3)	5610(8)	16141(16)	36(2)
C(13B)	7614(3)	5924(10)	16200(20)	55(4)
C(14B)	7873(3)	6067(10)	14504(19)	51(3)
C(15B)	7675(3)	6800(8)	13096(15)	35(2)
C(16B)	7962(3)	7313(9)	11897(15)	44(3)
O(6)	7478(2)	4630(5)	10479(12)	41(2)
Cl(2)	5193(2)	-332(5)	7527(14)	100(5)
Cl(3)	4852(3)	-647(9)	11220(19)	169(12)
Cl(4)	5237(3)	-2147(5)	9390(20)	147(9)
C(17)	4947(2)	-1158(6)	8908(16)	130(30)

Table A7.4.4. Bond Lengths [\AA] and angles [$^\circ$] for Cycloheptane **468**

Cl(1)-C(5)	1.796(10)
O(1)-C(1)	1.452(10)
O(1)-C(5)	1.435(11)
O(2)-C(8)	1.217(11)
O(3)-C(12)	1.224(11)
O(4)-C(12)	1.343(11)
O(4)-C(13)	1.473(10)
O(5)-H(5)	0.8400
O(5)-C(15)	1.434(10)
C(1)-C(2)	1.542(12)
C(1)-C(7)	1.512(12)
C(1)-C(11)	1.541(12)
C(2)-H(2A)	0.9900
C(2)-H(2B)	0.9900
C(2)-C(3)	1.528(15)
C(3)-H(3A)	0.9900
C(3)-H(3B)	0.9900
C(3)-C(4)	1.521(15)
C(4)-H(4A)	0.9900
C(4)-H(4B)	0.9900
C(4)-C(5)	1.505(15)
C(5)-C(6)	1.540(13)
C(6)-H(6A)	0.9900
C(6)-H(6B)	0.9900
C(6)-C(7)	1.533(13)
C(7)-H(7)	1.0000
C(7)-C(8)	1.511(13)
C(8)-C(9)	1.501(13)
C(9)-H(9)	1.0000
C(9)-C(10)	1.576(12)
C(9)-C(15)	1.564(12)
C(10)-H(10)	1.0000

Table A.7.4.4. Cont'd

C(10)-C(11)	1.528(12)
C(10)-C(13)	1.520(12)
C(11)-H(11)	1.0000
C(11)-C(12)	1.504(12)
C(13)-H(13)	1.0000
C(13)-C(14)	1.544(12)
C(14)-H(14A)	0.9900
C(14)-H(14B)	0.9900
C(14)-C(15)	1.497(13)
C(15)-C(16)	1.534(13)
C(16)-H(16A)	0.9800
C(16)-H(16B)	0.9800
C(16)-H(16C)	0.9800
Cl(1B)-C(5B)	1.788(13)
O(1B)-C(1B)	1.447(13)
O(1B)-C(5B)	1.448(13)
O(2B)-C(8B)	1.210(12)
O(3B)-C(12B)	1.223(12)
O(4B)-C(12B)	1.350(14)
O(4B)-C(13B)	1.495(14)
O(5B)-H(5B)	0.8400
O(5B)-C(15B)	1.416(12)
C(1B)-C(2B)	1.494(16)
C(1B)-C(7B)	1.546(13)
C(1B)-C(11B)	1.553(18)
C(2B)-H(2C)	0.9900
C(2B)-H(2D)	0.9900
C(2B)-C(3B)	1.54(2)
C(3B)-H(3C)	0.9900
C(3B)-H(3D)	0.9900
C(3B)-C(4B)	1.55(2)
C(4B)-H(4D)	0.9900
C(4B)-H(4C)	0.9900
C(4B)-C(5B)	1.487(18)

Table A.7.4.4. Cont'd

C(5B)-C(6B)	1.513(15)
C(6B)-H(6C)	0.9900
C(6B)-H(6D)	0.9900
C(6B)-C(7B)	1.519(15)
C(7B)-H(7B)	1.0000
C(7B)-C(8B)	1.514(13)
C(8B)-C(9B)	1.504(16)
C(9B)-H(9B)	1.0000
C(9B)-C(10B)	1.586(14)
C(9B)-C(15B)	1.572(16)
C(10B)-H(10B)	1.0000
C(10B)-C(11B)	1.531(15)
C(10B)-C(13B)	1.53(2)
C(11B)-H(11B)	1.0000
C(11B)-C(12B)	1.502(17)
C(13B)-H(13B)	1.0000
C(13B)-C(14B)	1.503(18)
C(14B)-H(14C)	0.9900
C(14B)-H(14D)	0.9900
C(14B)-C(15B)	1.531(16)
C(15B)-C(16B)	1.510(13)
C(16B)-H(16D)	0.9800
C(16B)-H(16E)	0.9800
C(16B)-H(16F)	0.9800
O(6)-H(6E)	0.8689
O(6)-H(6F)	0.9962
Cl(2)-Cl(3)#1	0.969(17)
Cl(2)-C(17)	1.7602
Cl(3)-Cl(4)#1	2.227(5)
Cl(3)-C(17)	1.7534
Cl(4)-C(17)	1.7546
C(17)-H(17)	0.9198
C(5)-O(1)-C(1)	101.4(6)

Table A.7.4.4. Cont'd

C(12)-O(4)-C(13)	109.9(7)
C(15)-O(5)-H(5)	109.5
O(1)-C(1)-C(2)	107.9(7)
O(1)-C(1)-C(7)	102.0(7)
O(1)-C(1)-C(11)	114.1(7)
C(7)-C(1)-C(2)	115.3(8)
C(7)-C(1)-C(11)	110.5(7)
C(11)-C(1)-C(2)	107.3(7)
C(1)-C(2)-H(2A)	109.3
C(1)-C(2)-H(2B)	109.3
H(2A)-C(2)-H(2B)	108.0
C(3)-C(2)-C(1)	111.5(8)
C(3)-C(2)-H(2A)	109.3
C(3)-C(2)-H(2B)	109.3
C(2)-C(3)-H(3A)	109.2
C(2)-C(3)-H(3B)	109.2
H(3A)-C(3)-H(3B)	107.9
C(4)-C(3)-C(2)	112.1(8)
C(4)-C(3)-H(3A)	109.2
C(4)-C(3)-H(3B)	109.2
C(3)-C(4)-H(4A)	110.0
C(3)-C(4)-H(4B)	110.0
H(4A)-C(4)-H(4B)	108.4
C(5)-C(4)-C(3)	108.3(8)
C(5)-C(4)-H(4A)	110.0
C(5)-C(4)-H(4B)	110.0
O(1)-C(5)-Cl(1)	105.9(6)
O(1)-C(5)-C(4)	108.2(9)
O(1)-C(5)-C(6)	106.3(8)
C(4)-C(5)-Cl(1)	109.7(7)
C(4)-C(5)-C(6)	114.6(8)
C(6)-C(5)-Cl(1)	111.7(7)
C(5)-C(6)-H(6A)	111.5
C(5)-C(6)-H(6B)	111.5

Table A.7.4.4. Cont'd

H(6A)-C(6)-H(6B)	109.3
C(7)-C(6)-C(5)	101.2(8)
C(7)-C(6)-H(6A)	111.5
C(7)-C(6)-H(6B)	111.5
C(1)-C(7)-C(6)	104.9(7)
C(1)-C(7)-H(7)	106.9
C(1)-C(7)-C(8)	109.2(7)
C(6)-C(7)-H(7)	106.9
C(8)-C(7)-C(6)	121.3(7)
C(8)-C(7)-H(7)	106.9
O(2)-C(8)-C(7)	123.7(9)
O(2)-C(8)-C(9)	122.4(9)
C(9)-C(8)-C(7)	113.8(7)
C(8)-C(9)-H(9)	107.2
C(8)-C(9)-C(10)	119.0(7)
C(8)-C(9)-C(15)	110.3(7)
C(10)-C(9)-H(9)	107.2
C(15)-C(9)-H(9)	107.2
C(15)-C(9)-C(10)	105.3(7)
C(9)-C(10)-H(10)	109.2
C(11)-C(10)-C(9)	118.3(7)
C(11)-C(10)-H(10)	109.2
C(13)-C(10)-C(9)	106.4(7)
C(13)-C(10)-H(10)	109.2
C(13)-C(10)-C(11)	104.2(7)
C(1)-C(11)-H(11)	108.9
C(10)-C(11)-C(1)	109.3(7)
C(10)-C(11)-H(11)	108.9
C(12)-C(11)-C(1)	117.6(7)
C(12)-C(11)-C(10)	103.0(7)
C(12)-C(11)-H(11)	108.9
O(3)-C(12)-O(4)	119.4(8)
O(3)-C(12)-C(11)	128.7(9)
O(4)-C(12)-C(11)	111.8(7)

Table A.7.4.4. Cont'd

O(4)-C(13)-C(10)	105.3(7)
O(4)-C(13)-H(13)	111.5
O(4)-C(13)-C(14)	110.9(7)
C(10)-C(13)-H(13)	111.5
C(10)-C(13)-C(14)	105.8(7)
C(14)-C(13)-H(13)	111.5
C(13)-C(14)-H(14A)	110.6
C(13)-C(14)-H(14B)	110.6
H(14A)-C(14)-H(14B)	108.7
C(15)-C(14)-C(13)	105.7(7)
C(15)-C(14)-H(14A)	110.6
C(15)-C(14)-H(14B)	110.6
O(5)-C(15)-C(9)	106.2(7)
O(5)-C(15)-C(14)	112.1(7)
O(5)-C(15)-C(16)	109.3(7)
C(14)-C(15)-C(9)	104.4(7)
C(14)-C(15)-C(16)	113.5(8)
C(16)-C(15)-C(9)	111.1(7)
C(15)-C(16)-H(16A)	109.5
C(15)-C(16)-H(16B)	109.5
C(15)-C(16)-H(16C)	109.5
H(16A)-C(16)-H(16B)	109.5
H(16A)-C(16)-H(16C)	109.5
H(16B)-C(16)-H(16C)	109.5
C(1B)-O(1B)-C(5B)	102.4(8)
C(12B)-O(4B)-C(13B)	108.3(10)
C(15B)-O(5B)-H(5B)	109.5
O(1B)-C(1B)-C(2B)	110.3(11)
O(1B)-C(1B)-C(7B)	100.1(8)
O(1B)-C(1B)-C(11B)	113.2(8)
C(2B)-C(1B)-C(7B)	114.9(9)
C(2B)-C(1B)-C(11B)	109.3(11)
C(7B)-C(1B)-C(11B)	109.0(9)
C(1B)-C(2B)-H(2C)	109.3

Table A.7.4.4. Cont'd

C(1B)-C(2B)-H(2D)	109.3
C(1B)-C(2B)-C(3B)	111.7(12)
H(2C)-C(2B)-H(2D)	107.9
C(3B)-C(2B)-H(2C)	109.3
C(3B)-C(2B)-H(2D)	109.3
C(2B)-C(3B)-H(3C)	109.1
C(2B)-C(3B)-H(3D)	109.1
C(2B)-C(3B)-C(4B)	112.7(11)
H(3C)-C(3B)-H(3D)	107.8
C(4B)-C(3B)-H(3C)	109.1
C(4B)-C(3B)-H(3D)	109.1
C(3B)-C(4B)-H(4D)	110.0
C(3B)-C(4B)-H(4C)	110.0
H(4D)-C(4B)-H(4C)	108.3
C(5B)-C(4B)-C(3B)	108.7(11)
C(5B)-C(4B)-H(4D)	110.0
C(5B)-C(4B)-H(4C)	110.0
O(1B)-C(5B)-Cl(1B)	106.8(7)
O(1B)-C(5B)-C(4B)	110.0(10)
O(1B)-C(5B)-C(6B)	105.2(9)
C(4B)-C(5B)-Cl(1B)	109.2(10)
C(4B)-C(5B)-C(6B)	111.8(10)
C(6B)-C(5B)-Cl(1B)	113.5(8)
C(5B)-C(6B)-H(6C)	111.1
C(5B)-C(6B)-H(6D)	111.1
C(5B)-C(6B)-C(7B)	103.3(8)
H(6C)-C(6B)-H(6D)	109.1
C(7B)-C(6B)-H(6C)	111.1
C(7B)-C(6B)-H(6D)	111.1
C(1B)-C(7B)-H(7B)	106.9
C(6B)-C(7B)-C(1B)	103.8(8)
C(6B)-C(7B)-H(7B)	106.9
C(8B)-C(7B)-C(1B)	108.8(8)
C(8B)-C(7B)-C(6B)	122.6(8)

Table A.7.4.4. Cont'd

C(8B)-C(7B)-H(7B)	106.9
O(2B)-C(8B)-C(7B)	122.5(10)
O(2B)-C(8B)-C(9B)	123.2(9)
C(9B)-C(8B)-C(7B)	114.3(8)
C(8B)-C(9B)-H(9B)	107.8
C(8B)-C(9B)-C(10B)	118.5(9)
C(8B)-C(9B)-C(15B)	109.3(8)
C(10B)-C(9B)-H(9B)	107.8
C(15B)-C(9B)-H(9B)	107.8
C(15B)-C(9B)-C(10B)	105.1(9)
C(9B)-C(10B)-H(10B)	108.9
C(11B)-C(10B)-C(9B)	118.9(9)
C(11B)-C(10B)-H(10B)	108.9
C(13B)-C(10B)-C(9B)	106.6(9)
C(13B)-C(10B)-H(10B)	108.9
C(13B)-C(10B)-C(11B)	104.2(10)
C(1B)-C(11B)-H(11B)	108.6
C(10B)-C(11B)-C(1B)	110.1(9)
C(10B)-C(11B)-H(11B)	108.6
C(12B)-C(11B)-C(1B)	117.4(9)
C(12B)-C(11B)-C(10B)	103.2(10)
C(12B)-C(11B)-H(11B)	108.6
O(3B)-C(12B)-O(4B)	119.2(10)
O(3B)-C(12B)-C(11B)	127.7(10)
O(4B)-C(12B)-C(11B)	113.0(9)
O(4B)-C(13B)-C(10B)	105.1(9)
O(4B)-C(13B)-H(13B)	111.6
O(4B)-C(13B)-C(14B)	109.9(11)
C(10B)-C(13B)-H(13B)	111.6
C(14B)-C(13B)-C(10B)	106.6(10)
C(14B)-C(13B)-H(13B)	111.6
C(13B)-C(14B)-H(14C)	110.3
C(13B)-C(14B)-H(14D)	110.3
C(13B)-C(14B)-C(15B)	107.0(11)

Table A.7.4.4. Cont'd

H(14C)-C(14B)-H(14D)	108.6
C(15B)-C(14B)-H(14C)	110.3
C(15B)-C(14B)-H(14D)	110.3
O(5B)-C(15B)-C(9B)	106.4(8)
O(5B)-C(15B)-C(14B)	111.3(9)
O(5B)-C(15B)-C(16B)	109.8(8)
C(14B)-C(15B)-C(9B)	104.0(9)
C(16B)-C(15B)-C(9B)	112.2(9)
C(16B)-C(15B)-C(14B)	112.8(9)
C(15B)-C(16B)-H(16D)	109.5
C(15B)-C(16B)-H(16E)	109.5
C(15B)-C(16B)-H(16F)	109.5
H(16D)-C(16B)-H(16E)	109.5
H(16D)-C(16B)-H(16F)	109.5
H(16E)-C(16B)-H(16F)	109.5
H(6E)-O(6)-H(6F)	111.1
Cl(3)#1-Cl(2)-C(17)	28.3(8)
Cl(2)#1-Cl(3)-Cl(4)#1	125.8(10)
Cl(2)#1-Cl(3)-C(17)	176.6(7)
C(17)-Cl(3)-Cl(4)#1	57.4(6)
Cl(2)-C(17)-Cl(4)#1	170.4(6)
Cl(2)-C(17)-H(17)	109.8
Cl(3)-C(17)-Cl(2)	107.2
Cl(3)#1-C(17)-Cl(2)	26.9(11)
Cl(3)#1-C(17)-Cl(3)	86.6(10)
Cl(3)#1-C(17)-Cl(4)#1	146.3(17)
Cl(3)#1-C(17)-Cl(4)	103.7(6)
Cl(3)-C(17)-Cl(4)#1	73.5(5)
Cl(3)-C(17)-Cl(4)	109.3
Cl(3)#1-C(17)-H(17)	134.5
Cl(3)-C(17)-H(17)	109.0
Cl(4)-C(17)-Cl(2)	111.4
Cl(4)-C(17)-Cl(4)#1	60.1(6)
Cl(4)#1-C(17)-H(17)	78.5

Table A.7.4.4. Cont'd

Cl(4)-C(17)-H(17)	110.1
-------------------	-------

Symmetry transformations used to generate equivalent atoms:

#1 -x+1,y,-z+2

Table A7.4.5. Anisotropic Displacement Parameters ($\text{\AA}^2 \times 10^3$) for Cycloheptane **468**.

The Anisotropic Displacement Factor Exponent Takes the Form: $-2p^2[h^2a^{*2}U^{11} + \dots + 2hka^{*}b^{*}U^{12}]$.

	U ¹¹	U ²²	U ³³	U ²³	U ¹³	U ¹²
Cl(1)	36(1)	26(1)	42(1)	-7(1)	-7(1)	4(1)
O(1)	21(3)	22(3)	31(3)	-2(3)	-3(3)	3(2)
O(2)	21(3)	42(4)	22(3)	2(3)	-10(2)	-9(3)
O(3)	24(3)	28(3)	33(4)	-11(3)	1(3)	6(3)
O(4)	24(3)	20(3)	32(3)	-2(3)	2(3)	3(3)
O(5)	28(3)	32(4)	22(3)	-4(3)	10(3)	-6(3)
C(1)	22(4)	22(4)	23(4)	2(4)	3(3)	1(4)
C(2)	27(5)	30(5)	36(5)	11(4)	8(4)	3(4)
C(3)	30(5)	38(6)	47(6)	20(5)	5(4)	4(4)
C(4)	41(6)	24(5)	56(7)	10(5)	-2(5)	-5(4)
C(5)	25(5)	28(5)	36(5)	3(4)	-9(4)	-1(4)
C(6)	32(5)	26(5)	34(5)	-2(4)	-16(4)	2(4)
C(7)	27(4)	15(4)	19(4)	-5(3)	-4(3)	-2(4)
C(8)	24(5)	35(5)	17(4)	0(4)	1(3)	-2(4)
C(9)	18(4)	31(5)	14(4)	2(4)	0(3)	1(4)
C(10)	28(4)	14(4)	14(4)	1(3)	-1(3)	4(3)
C(11)	20(4)	24(4)	16(4)	-7(3)	2(3)	-1(3)
C(12)	23(4)	28(5)	18(4)	-12(4)	-4(3)	1(4)
C(13)	21(4)	21(4)	18(4)	-8(3)	1(3)	0(3)
C(14)	26(4)	21(4)	24(5)	0(4)	-2(4)	1(3)
C(15)	22(4)	32(5)	15(4)	1(4)	3(3)	-1(4)
C(16)	37(5)	42(6)	30(5)	12(5)	-6(4)	-1(5)
Cl(1B)	45(2)	40(2)	77(2)	16(2)	14(1)	11(1)
O(1B)	44(4)	32(4)	31(4)	9(3)	9(3)	-5(3)
O(2B)	65(5)	26(4)	34(4)	-2(3)	13(4)	-15(3)
O(3B)	27(3)	37(4)	27(3)	5(3)	-3(3)	-5(3)
O(4B)	20(3)	52(5)	55(5)	28(4)	-6(3)	-6(3)

Table A7.4.5. Cont'd

O(5B)	35(4)	26(4)	37(4)	0(3)	-9(3)	-1(3)
C(1B)	58(7)	38(6)	29(5)	-10(5)	4(5)	-19(5)
C(2B)	122(13)	46(7)	27(6)	-11(6)	20(7)	-34(8)
C(3B)	129(14)	37(7)	32(6)	-17(5)	28(8)	-16(8)
C(4B)	97(11)	37(7)	59(8)	7(6)	39(8)	10(7)
C(5B)	50(6)	35(6)	42(6)	5(5)	8(5)	1(5)
C(6B)	50(6)	19(5)	28(5)	2(4)	3(4)	-6(4)
C(7B)	42(5)	32(6)	17(4)	-6(4)	7(4)	-12(4)
C(8B)	50(6)	32(5)	12(4)	2(4)	2(4)	-15(5)
C(9B)	50(6)	45(7)	23(5)	-2(5)	-2(4)	-32(5)
C(10B)	43(6)	75(9)	19(5)	4(5)	-8(4)	-38(6)
C(11B)	45(6)	59(8)	23(5)	2(5)	5(4)	-29(6)
C(12B)	29(5)	47(7)	31(5)	14(4)	-7(4)	-13(4)
C(13B)	34(6)	79(10)	50(7)	32(7)	-12(5)	-24(6)
C(14B)	30(6)	75(9)	46(7)	27(6)	-10(5)	-20(6)
C(15B)	36(5)	43(6)	25(5)	13(4)	-4(4)	-14(5)
C(16B)	53(7)	59(8)	20(5)	5(5)	6(4)	-22(6)
O(6)	39(4)	37(4)	49(5)	-11(4)	14(3)	-6(3)
Cl(2)	78(8)	64(7)	162(16)	5(8)	34(9)	31(6)
Cl(3)	74(10)	310(40)	120(15)	28(19)	16(10)	-12(15)
Cl(4)	100(10)	200(20)	148(15)	93(14)	27(10)	74(12)

*Table A7.4.6. Hydrogen Coordinates ($\times 10^4$) and Isotropic Displacement Parameters ($\text{\AA}^2 \times 10^3$) for Cycloheptane **468**.*

	x	y	z	U(eq)
H(5)	6187	4747	7314	40
H(2A)	5756	2532	15049	37
H(2B)	5462	2991	13313	37
H(3A)	5316	1380	14197	46
H(3B)	5307	1603	11821	46
H(4A)	5916	646	14219	49
H(4B)	5667	266	12218	49
H(6A)	6096	1485	8433	38
H(6B)	5656	1381	9136	38
H(7)	6145	2937	9406	25
H(9)	5321	4391	10601	25
H(10)	5717	4553	13399	23
H(11)	6226	3680	14452	24
H(13)	6152	5671	12926	24
H(14A)	5710	6117	10229	29
H(14B)	6101	5999	9056	29
H(16A)	5464	5588	6130	56
H(16B)	5182	5525	7941	56
H(16C)	5244	4640	6555	56
H(5B)	7454	5921	11262	49
H(2C)	7028	8401	17168	77
H(2D)	6719	8068	18709	77
H(3C)	6568	9239	15249	78
H(3D)	6451	9426	17506	78
H(4D)	5906	8475	17082	75
H(4C)	5896	9019	14961	75
H(6C)	6347	8427	12557	39
H(6D)	6213	7408	11798	39

Table A7.4.6. Cont'd

H(7B)	6744	6755	13237	36
H(9B)	7653	7965	14989	48
H(10B)	7542	7158	17739	55
H(11B)	6981	6547	18479	51
H(13B)	7768	5712	17474	66
H(14C)	7903	5483	13754	61
H(14D)	8138	6279	15048	61
H(16D)	8113	6870	11152	66
H(16E)	8143	7671	12826	66
H(16F)	7818	7732	10933	66
H(6E)	7684	4303	10257	62
H(6F)	7299	4281	11315	62
H(17)	4712	-1315	8203	155

Table A7.4.7. Torsion Angles [°] for Cycloheptane **468**.

Cl(1)-C(5)-C(6)-C(7)	-135.7(7)
O(1)-C(1)-C(2)-C(3)	-56.0(10)
O(1)-C(1)-C(7)-C(6)	36.0(9)
O(1)-C(1)-C(7)-C(8)	167.4(7)
O(1)-C(1)-C(11)-C(10)	172.7(7)
O(1)-C(1)-C(11)-C(12)	55.9(10)
O(1)-C(5)-C(6)-C(7)	-20.7(10)
O(2)-C(8)-C(9)-C(10)	159.3(8)
O(2)-C(8)-C(9)-C(15)	-78.9(10)
O(4)-C(13)-C(14)-C(15)	81.2(8)
C(1)-O(1)-C(5)-Cl(1)	162.9(6)
C(1)-O(1)-C(5)-C(4)	-79.5(8)
C(1)-O(1)-C(5)-C(6)	44.0(9)
C(1)-C(2)-C(3)-C(4)	41.8(12)
C(1)-C(7)-C(8)-O(2)	-131.9(9)
C(1)-C(7)-C(8)-C(9)	50.8(10)
C(1)-C(11)-C(12)-O(3)	-49.2(12)
C(1)-C(11)-C(12)-O(4)	133.0(8)
C(2)-C(1)-C(7)-C(6)	-80.7(10)
C(2)-C(1)-C(7)-C(8)	50.8(10)
C(2)-C(1)-C(11)-C(10)	-67.8(8)
C(2)-C(1)-C(11)-C(12)	175.4(8)
C(2)-C(3)-C(4)-C(5)	-45.3(12)
C(3)-C(4)-C(5)-Cl(1)	-179.1(8)
C(3)-C(4)-C(5)-O(1)	65.8(11)
C(3)-C(4)-C(5)-C(6)	-52.5(12)
C(4)-C(5)-C(6)-C(7)	98.7(10)
C(5)-O(1)-C(1)-C(2)	72.7(8)
C(5)-O(1)-C(1)-C(7)	-49.1(8)
C(5)-O(1)-C(1)-C(11)	-168.2(7)
C(5)-C(6)-C(7)-C(1)	-9.4(9)
C(5)-C(6)-C(7)-C(8)	-133.5(8)
C(6)-C(7)-C(8)-O(2)	-9.8(14)

Table A7.4.7. Cont'd

C(6)-C(7)-C(8)-C(9)	172.9(8)
C(7)-C(1)-C(2)-C(3)	57.1(11)
C(7)-C(1)-C(11)-C(10)	58.6(9)
C(7)-C(1)-C(11)-C(12)	-58.2(10)
C(7)-C(8)-C(9)-C(10)	-23.3(11)
C(7)-C(8)-C(9)-C(15)	98.5(8)
C(8)-C(9)-C(10)-C(11)	13.5(11)
C(8)-C(9)-C(10)-C(13)	130.2(8)
C(8)-C(9)-C(15)-O(5)	-36.7(9)
C(8)-C(9)-C(15)-C(14)	-155.2(7)
C(8)-C(9)-C(15)-C(16)	82.1(9)
C(9)-C(10)-C(11)-C(1)	-29.8(10)
C(9)-C(10)-C(11)-C(12)	96.0(8)
C(9)-C(10)-C(13)-O(4)	-102.0(7)
C(9)-C(10)-C(13)-C(14)	15.5(8)
C(10)-C(9)-C(15)-O(5)	93.0(7)
C(10)-C(9)-C(15)-C(14)	-25.6(9)
C(10)-C(9)-C(15)-C(16)	-148.3(8)
C(10)-C(11)-C(12)-O(3)	-169.4(8)
C(10)-C(11)-C(12)-O(4)	12.8(9)
C(10)-C(13)-C(14)-C(15)	-32.4(9)
C(11)-C(1)-C(2)-C(3)	-179.4(7)
C(11)-C(1)-C(7)-C(6)	157.5(7)
C(11)-C(1)-C(7)-C(8)	-71.0(9)
C(11)-C(10)-C(13)-O(4)	23.8(8)
C(11)-C(10)-C(13)-C(14)	141.3(7)
C(12)-O(4)-C(13)-C(10)	-16.8(8)
C(12)-O(4)-C(13)-C(14)	-130.7(7)
C(13)-O(4)-C(12)-O(3)	-175.7(7)
C(13)-O(4)-C(12)-C(11)	2.4(9)
C(13)-C(10)-C(11)-C(1)	-147.6(7)
C(13)-C(10)-C(11)-C(12)	-21.9(8)
C(13)-C(14)-C(15)-O(5)	-78.7(9)
C(13)-C(14)-C(15)-C(9)	35.7(9)

Table A7.4.7. Cont'd

C(13)-C(14)-C(15)-C(16)	156.8(7)
C(15)-C(9)-C(10)-C(11)	-110.8(8)
C(15)-C(9)-C(10)-C(13)	5.9(8)
Cl(1B)-C(5B)-C(6B)-C(7B)	-135.5(7)
O(1B)-C(1B)-C(2B)-C(3B)	-55.2(13)
O(1B)-C(1B)-C(7B)-C(6B)	37.4(10)
O(1B)-C(1B)-C(7B)-C(8B)	169.4(8)
O(1B)-C(1B)-C(11B)-C(10B)	168.1(9)
O(1B)-C(1B)-C(11B)-C(12B)	50.5(12)
O(1B)-C(5B)-C(6B)-C(7B)	-19.1(10)
O(2B)-C(8B)-C(9B)-C(10B)	155.9(10)
O(2B)-C(8B)-C(9B)-C(15B)	-83.8(11)
O(4B)-C(13B)-C(14B)-C(15B)	83.0(13)
C(1B)-O(1B)-C(5B)-Cl(1B)	165.3(7)
C(1B)-O(1B)-C(5B)-C(4B)	-76.3(11)
C(1B)-O(1B)-C(5B)-C(6B)	44.3(10)
C(1B)-C(2B)-C(3B)-C(4B)	39.5(14)
C(1B)-C(7B)-C(8B)-O(2B)	-126.1(11)
C(1B)-C(7B)-C(8B)-C(9B)	52.1(11)
C(1B)-C(11B)-C(12B)-O(3B)	-48.0(15)
C(1B)-C(11B)-C(12B)-O(4B)	129.5(9)
C(2B)-C(1B)-C(7B)-C(6B)	-80.8(13)
C(2B)-C(1B)-C(7B)-C(8B)	51.3(15)
C(2B)-C(1B)-C(11B)-C(10B)	-68.5(12)
C(2B)-C(1B)-C(11B)-C(12B)	173.9(9)
C(2B)-C(3B)-C(4B)-C(5B)	-42.0(14)
C(3B)-C(4B)-C(5B)-Cl(1B)	179.0(9)
C(3B)-C(4B)-C(5B)-O(1B)	62.0(12)
C(3B)-C(4B)-C(5B)-C(6B)	-54.5(14)
C(4B)-C(5B)-C(6B)-C(7B)	100.3(11)
C(5B)-O(1B)-C(1B)-C(2B)	71.4(11)
C(5B)-O(1B)-C(1B)-C(7B)	-50.0(10)
C(5B)-O(1B)-C(1B)-C(11B)	-165.8(9)
C(5B)-C(6B)-C(7B)-C(1B)	-11.2(10)

Table A7.4.7. Cont'd

C(5B)-C(6B)-C(7B)-C(8B)	-134.6(9)
C(6B)-C(7B)-C(8B)-O(2B)	-5.0(14)
C(6B)-C(7B)-C(8B)-C(9B)	173.2(9)
C(7B)-C(1B)-C(2B)-C(3B)	57.0(15)
C(7B)-C(1B)-C(11B)-C(10B)	57.7(11)
C(7B)-C(1B)-C(11B)-C(12B)	-59.9(11)
C(7B)-C(8B)-C(9B)-C(10B)	-22.3(13)
C(7B)-C(8B)-C(9B)-C(15B)	98.0(9)
C(8B)-C(9B)-C(10B)-C(11B)	10.3(16)
C(8B)-C(9B)-C(10B)-C(13B)	127.5(10)
C(8B)-C(9B)-C(15B)-O(5B)	-33.4(10)
C(8B)-C(9B)-C(15B)-C(14B)	-151.0(8)
C(8B)-C(9B)-C(15B)-C(16B)	86.7(10)
C(9B)-C(10B)-C(11B)-C(1B)	-27.7(14)
C(9B)-C(10B)-C(11B)-C(12B)	98.3(12)
C(9B)-C(10B)-C(13B)-O(4B)	-101.6(9)
C(9B)-C(10B)-C(13B)-C(14B)	15.1(11)
C(10B)-C(9B)-C(15B)-O(5B)	94.9(9)
C(10B)-C(9B)-C(15B)-C(14B)	-22.7(10)
C(10B)-C(9B)-C(15B)-C(16B)	-145.0(9)
C(10B)-C(11B)-C(12B)-O(3B)	-169.2(10)
C(10B)-C(11B)-C(12B)-O(4B)	8.2(11)
C(10B)-C(13B)-C(14B)-C(15B)	-30.4(13)
C(11B)-C(1B)-C(2B)-C(3B)	179.8(10)
C(11B)-C(1B)-C(7B)-C(6B)	156.3(8)
C(11B)-C(1B)-C(7B)-C(8B)	-71.6(10)
C(11B)-C(10B)-C(13B)-O(4B)	25.0(11)
C(11B)-C(10B)-C(13B)-C(14B)	141.7(9)
C(12B)-O(4B)-C(13B)-C(10B)	-20.7(11)
C(12B)-O(4B)-C(13B)-C(14B)	-135.1(11)
C(13B)-O(4B)-C(12B)-O(3B)	-174.5(9)
C(13B)-O(4B)-C(12B)-C(11B)	7.8(11)
C(13B)-C(10B)-C(11B)-C(1B)	-146.2(9)
C(13B)-C(10B)-C(11B)-C(12B)	-20.1(11)

Table A7.4.7. Cont'd

C(13B)-C(14B)-C(15B)-O(5B)	-81.1(12)
C(13B)-C(14B)-C(15B)-C(9B)	33.1(12)
C(13B)-C(14B)-C(15B)-C(16B)	154.9(10)
C(15B)-C(9B)-C(10B)-C(11B)	-112.2(12)
C(15B)-C(9B)-C(10B)-C(13B)	5.0(10)
Cl(3)#1-Cl(2)-C(17)-Cl(3)	41.5(13)
Cl(3)#1-Cl(2)-C(17)-Cl(4)	-78.0(13)
Cl(4)#1-Cl(3)-C(17)-Cl(2)	-170.0(7)
Cl(4)#1-Cl(3)-C(17)-Cl(3)#1	-152.5(14)
Cl(4)#1-Cl(3)-C(17)-Cl(4)	-49.2(7)

Symmetry transformations used to generate equivalent atoms:

#1 -x+1,y,-z+2

Table A7.4.8. Hydrogen Bonds for Cycloheptane **468** [\AA and $^\circ$].

D-H...A	d(D-H)	d(H...A)	d(D...A)	\angle (DHA)
O(5)-H(5)...O(3B)#2	0.84	1.99	2.772(9)	154.9
O(5B)-H(5B)...O(6)	0.84	1.94	2.749(10)	160.2
O(6)-H(6E)...O(2B)#3	0.87	2.21	2.886(10)	134.6
O(6)-H(6F)...O(3)	1.00	1.91	2.858(9)	157.8

Symmetry transformations used to generate equivalent atoms:

#1 -x+1,y,-z+2 #2 x,y,z-1 #3 -x+3/2,y-1/2,-z+2

A7.5 NOTES AND REFERENCES

1. Sheldrick, G. M. *Acta Cryst.* **1990**, A46, 467-473.
2. Sheldrick, G. M. *Acta Cryst.* **2015**, C71, 3-8.
3. Müller, P. *Crystallography Reviews* **2009**, 15, 57-83.

Appendix 8

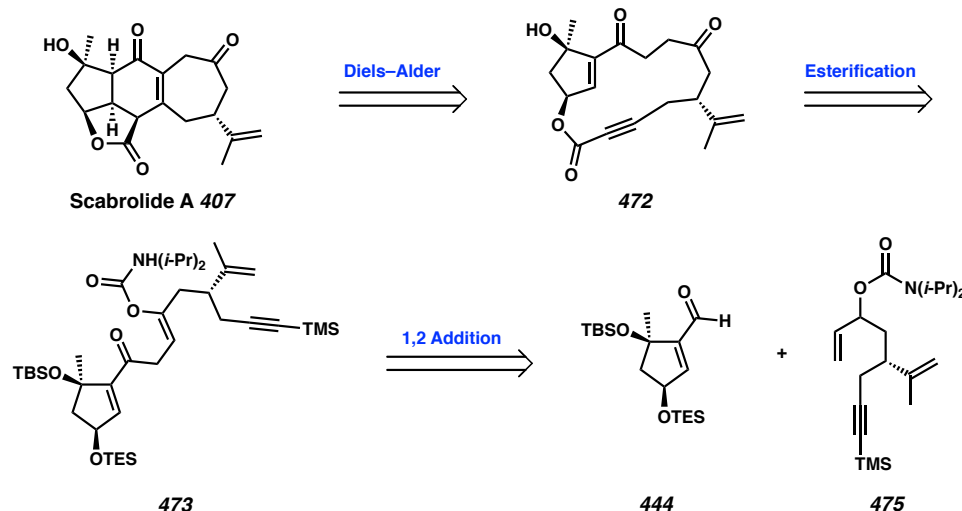
Alternative Strategy Toward the

Total Synthesis of Scabrolide A

A8.1 ALTERNATIVE APPROACH TO SCABROLIDE A

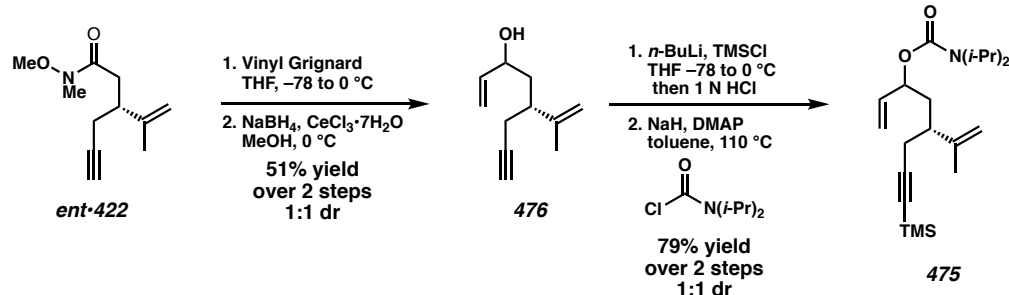
During the development of the ultimately successful ring expansion of a small-membered ring for the synthesis of the cycloheptanone ring in the core of scabrolide A, we concurrently investigated numerous alternative routes (Scheme A8.1.1). Retrosynthetically, we envisioned access to scabrolide A **407** through an intramolecular transannular Diels–Alder reaction from intermediate **472**. We believed intermediate **472** could be formed through a Yamaguchi macrolactonization from masked 1,4-diketone **473**. The key masked 1,4 diketone moiety of **473** is believed to be generated from an umpolung 1,2 addition of allyl carbamate **475** and aldehyde **444**.

Scheme A8.1.1. Retrosynthetic Analysis of Scabrolide A



A8.2 SYNTHESIS OF DIISOPROPYL CARBAMATE

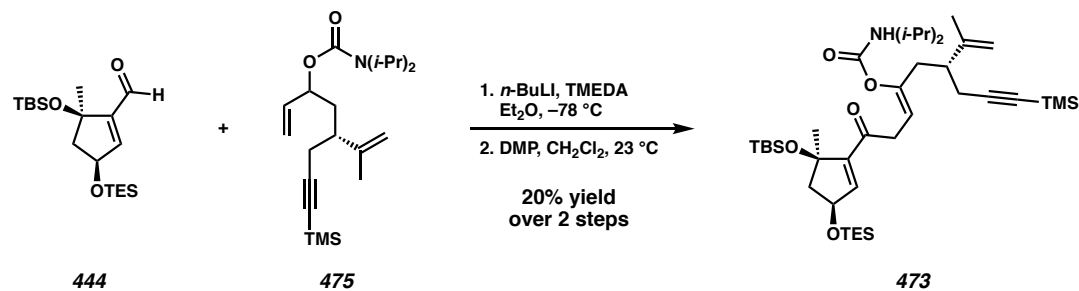
Exploration of the proposed synthetic route began with the derivatization of key carvone derived Weinreb amide **ent•422** (Scheme A8.2.1). Single addition of vinyl Grignard followed by subsequent Luche reduction of the resultant ketone, afforded allylic alcohol **476** in 51% yield over 2 steps as a 1:1 mixture of diastereomers. The mixture of diastereomers can then be TMS protected at the terminal alkyne followed by the carbamoylation of the allylic alcohol generating carbamate **475** in a 70% yield over 2 steps in a 1:1 mixture of diastereomers. Ultimately, silyl protection of the alkyne is required to avoid statistical mixtures of the desired carbamate and the undesired acetylated alkyne.

Scheme A8.2.1. Derivatization of Weinreb Amide **ent•422** to Carbamate **475**

A8.3 UMPOLUNG ALDEHYDE ADDITION

Successful synthesis of allylic carbamate **475**, allows for the investigation of the synthesis of the 1,4-diketone moiety of scabrolide A. Deprotonation of the allylic carbamate **475** with *n*-BuLi in the presence of TMEDA at low temperatures, generates a stabilized allylic carbanion, which are known to undergo selective 1,2 additions into aldehydes (Scheme A8.3.1).¹ Addition of previously synthesized aldehyde **444** to the stabilized allylic anion followed by an oxidation with DMP affords our desired masked 1,4-diketone **473** in 20% yield over 2 steps. While we were able to selectively generate enol carbamate **473**, albeit in low yield, we were unable to progress this intermediate toward macrocycle **472**. Attempts to deprotect the alkyne and affect Yamaguchi esterification resulted in decomposition. Deprotection of the enol carbamate moiety similarly resulted in decomposition. Ultimately we were unable to advance this interesting intermediate any further in the synthesis.

*Scheme A8.3.1. Coupling of Carbamate **475** and Aldehyde **444***



A8.4 EXPERIMENTAL METHODS AND ANALYTICAL DATA

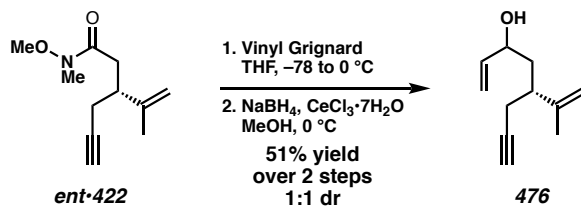
A8.4.1 MATERIALS AND METHODS

Unless stated otherwise, reactions were performed at ambient temperature (23°C) in flame-dried or oven-dried glassware under an argon or nitrogen atmosphere using dry,

deoxygenated solvents (distilled or passed over a column of activated alumina).² Commercially obtained reagents were used as received. Triethylamine (Et_3N) and trimethylsilyl chloride (TMSCl) were distilled over potassium hydride prior to use. Reactions requiring external heat were modulated to the specified temperatures using an IKAmag temperature controller. Reaction progress was monitored by thin-layer chromatography (TLC), which was performed using E. Merck silica gel 60 F254 precoated glass plated (0.25 mm) and visualized by UV fluorescence quenching, potassium permanganate, *p*-anisaldehyde, or iodine staining. Silicycle SiliaFlash® P60 Academic Silica gel (particle size 40-63 nm) was used for column chromatography. ^1H and ^{13}C NMR spectra were recorded on a Varian Inova 500 (500 MHz and 126 MHz, respectively), Varian Mercury 300 spectrometer (300 MHz and 75 MHz, respectively), Varian 600 MHz Spectrometer (600 MHz), and a Bruker AV III HD spectrometer equipped with a Prodigy liquid nitrogen temperature cryoprobe (400 MHz and 101 MHz, respectively) and are reported in terms of chemical shift relative to CHCl_3 (δ 7.26 and δ 77.16, respectively) and C_6H_6 (δ 7.16 and δ 128.4 respectively). Data for ^1H NMR are reported as follows: chemical shift (δ ppm) (multiplicity, coupling constant (Hz), integration). Multiplicities are reported as follows: s = singlet, d = doublet, t = triplet, q = quartet, p = pentet, sext = sextet, sept = septet, m = multiplet, and br s = broad singlet. Infrared (IR) spectra were recorded on a Perkin Elmer Paragon 1000 spectrometer using thin films deposited on NaCl plates and are reported in frequency of absorption (cm^{-1}). Optical rotations were measured with a Jasco P-2000 polarimeter operating on the sodium D-line (589 nm), using a 100-mm path-length cell and are reported as: $[\alpha]_D^T$ (concentration in g/100 mL, solvent). High resolution mass spectra were obtained from the Caltech Mass Spectral Facility using a JEOL JMS-600H

High Resolution Mass Spectrometer in fast atom bombardment (FAB+) ionization mode or a Agilent 6200 Series TOF with an Agilent G1978A Multimode source in electrospray ionization (ESI+), atmospheric pressure chemical ionization (APCI+), or mixed (ESI/APCI) ionization mode.

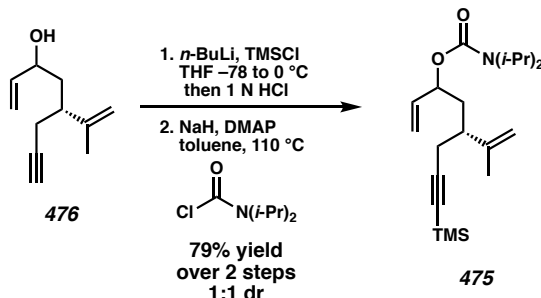
A8.4.2 EXPERIMENTAL PROCEDURES



(5*R*)-5-(prop-1-en-2-yl)oct-1-en-7-yn-3-ol (476): In a flame dried round bottom flask, amide **ent-422** (250 mg, 1.3 mmol, 1.0 equiv) was dissolved in THF (4.2 mL, 0.3 M) and cooled to -78 °C. Allyl magnesium bromide (2.6 mL, 2.6 mmol, 1.0 M, 2.0 equiv) was added dropwise to the reaction solution. The reaction was allowed to stir for 15 min at -78 °C and then warmed to 0 °C and stirred for 16 h. Upon complete consumption of starting material (determined by TLC analysis, 9:1 hexanes:EtOAc), the reaction was quenched with a saturated solution of NH_4Cl and the product was extracted from the biphasic mixture with EtOAc (3 x 10 mL). The combined organic layers were washed with brine, dried over MgSO_4 , filtered, and concentrated in vacuo. The crude product was purified by flash chromatography (SiO_2 , 9:1 hexanes:EtOAc) to generate an intermediate enone (128 mg, 62% yield) as a pale yellow oil which was used without further characterization.

In a round bottom flask, crude enone (490 mg, 3 mmol, 1 equiv) was dissolved in methanol (30 mL, 0.1 M). The solution was stirred for 5 min followed by the addition of $\text{CeCl}_3 \cdot 7\text{H}_2\text{O}$ (1.1 g, 3.3 mmol, 1.1 equiv). Once the reaction is homogeneous, the solution is cooled to -78 °C and allowed to stir for 1 h. NaBH_4 (164 mg, 3 mmol, 1 equiv) was

added slowly in portions to the reaction and was allowed to stir until completion (as determined by TLC analysis 4:1 hexanes:EtOAc). Upon complete consumption of starting material, the reaction was quenched with a saturated solution of NH₄Cl (30 mL) and the biphasic mixture was allowed to warm to room temperature. The biphasic mixture was extracted with 2:1 Et₂O:hexanes (3 x 30 mL) and the combined organic layers were dried over Na₂SO₄, filtered and concentrated in vacuo. The crude product was assumed to have quantitative conversion and was used directly into the next reaction without further purification. Alcohol **476** could be purified by column chromatography (SiO₂, 9:1 hexanes:EtOAc) to afford pure alcohol **476** as a colorless oil; R_f = 0.44 (4:1 hexanes:EtOAc); ¹H NMR (400 MHz, CDCl₃) δ = 5.89 (ddd, J = 17.2, 10.4, 5.8 Hz, 1H), 5.23 (dt, J = 17.2, 1.5 Hz, 1H), 5.10 (dt, J = 10.4, 1.4 Hz, 1H), 4.84 (ddt, J = 5.6, 2.0, 1.1 Hz, 2H), 2.58 (dtd, J = 9.6, 7.1, 4.9 Hz, 1H), 2.31 (d, J = 1.4 Hz, 1H), 2.29 (s, 1H), 1.69 (dd, J = 1.5, 0.8 Hz, 3H), 1.68–1.63 (m, 2H), 1.25 (s, 2H); 5.84 (ddd, J = 17.0, 10.4, 6.5 Hz, 1H), 5.24 (dt, J = 17.2, 1.4 Hz, 1H), 5.13 (dt, J = 10.4, 1.3 Hz, 1H), 4.84–4.78 (m, 2H), 4.19 – 4.11 (m, 2H), 2.45–2.34 (m, 1H), 2.32 (d, J = 2.3 Hz, 1H), 2.30 (d, J = 3.8 Hz, 1H), 1.77–1.69 (m, 5H); ¹³C NMR (101 MHz, CDCl₃) δ = 146.7, 146.1, 141.3, 140.7, 115.5, 114.4, 113.0, 112.6, 82.8, 82.8, 71.9, 70.9, 69.7, 69.6, 42.9, 42.5, 39.5, 39.4, 23.8, 23.5, 19.1, 18.8; IR (thin film, NaCl) 3305, 3076, 2972, 2935, 2117, 1645, 1429, 1376, 1122, 992, 924, 895, 633 cm⁻¹; HRMS (ESI) m/z calc'd C₁₁H₁₇O [M+H]⁺: 165.1279, found: 165.1299; [a]_D²³ +17.3 (c 0.125, CHCl₃).

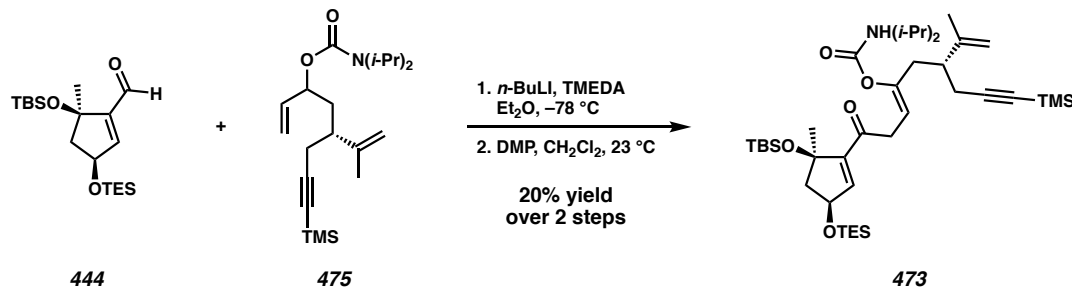


(5*R*)-5-(prop-1-en-2-yl)-8-(trimethylsilyl)oct-1-en-7-yn-3-yl diisopropylcarbamate (475):

To a stirred solution of alcohol **476** (58 mg, 0.35 mmol, 1.0 equiv) in THF (2.2 mL, 0.15 M) at -78 °C has *n*-BuLi (0.35 mL, 0.812 mmol, 2.16 M, 2.3 equiv) added. The reaction was warmed to 0 °C, stirred for 10 min, and cooled back to -78 °C. TMSCl (89 µL, 0.71 mmol, 2 equiv) was added and allowed to stir for 1 h. Upon complete consumption of starting material (as determined by TLC analysis, 4:1 hexanes:EtOAc), 1 N HCl (1.8 mL, 0.2 M) was added and allowed to stir for 20 min. The organic layer was separated and the aqueous layer was extracted with Et₂O (3 X 5 mL). The combined organic layers were washed with brine, dried over MgSO₄, filtered, and concentrated in vacuo. The crude product was purified by column chromatography (SiO₂, 4:1 hexanes:EtOAc) and carried onto the next reaction without further purification.

To a stirred solution of alcohol (68 mg, 0.29 mmol, 1 equiv) in toluene (2.9 mL, 0.1 M) had NaH (23 mg, 0.58 mmol, 2 equiv), DMAP (3.5 mg, 0.03 mmol, 0.1 equiv), and diisopropyl carbamoyl chloride (118 mg, 0.72 mg, 2.5 equiv) added. The reaction was sealed and heated to 110 °C. Upon complete consumption of starting material (as determined by TLC analysis, 4:1 hexanes:EtOAc), the reaction was cooled to 23 °C and quenched with a saturated solution of NH₄Cl (5 mL). The biphasic mixture was extracted

with Et₂O (3 x 5 mL) and the combined organic layers were dried over Na₂SO₄, filtered and concentrated in vacuo. The crude product was purified by column chromatography (SiO₂, 9:1 hexanes:EtOAc) to afford carbamate **475** (86 mg, 98%) as a viscous colorless oil (R_f = 0.57, 4:1 hexanes:EtOAc). ¹H NMR (400 MHz, CDCl₃) δ = 5.79 (ddd, J = 17.3, 10.4, 6.9 Hz, 1H), 5.26 (dt, J = 17.2, 1.4 Hz, 1H), 5.20–5.05 (m, 2H), 4.82–4.73 (m, 2H), 4.20–3.64 (bd, 1H), 2.36–2.24 (m, 3H), 2.06 (s, 1H), 1.93–1.75 (m, 2H), 1.71 (dd, J = 1.5, 0.8 Hz, 3H), 1.20 (dd, J = 7.0, 2.9 Hz, 12H), 0.13 (s, 9H); 6.00–5.65 (m, 1H), 5.33–5.07 (m, 3H), 4.84 (q, J = 1.6 Hz, 1H), 4.76–4.73 (m, 1H), 4.06 (bs, 1H), 3.80 (bs, 1H), 2.45 (dddd, J = 10.4, 8.0, 6.1, 4.1 Hz, 1H), 2.38–2.18 (m, 2H), 2.07–1.91 (m, 1H), 1.74–1.57 (m, 4H), 1.32–1.16 (m, 12H), 0.13 (s, 9H); ¹³C NMR (101 MHz, CDCl₃) δ = 155.12, 145.77, 137.20, 117.01, 112.61, 105.71, 86.41, 73.82, 69.76, 46.24, 42.50, 36.87, 25.19, 21.26, 19.17, 0.22; 155.05, 145.52, 138.16, 137.12, 117.09, 115.45, 112.87, 112.83, 105.84, 86.10, 73.00, 42.77, 37.30, 25.42, 19.31, 0.23; IR (thin film, NaCl) 3076, 2967, 2175, 1742, 1693, 1646, 1435, 1368, 1285, 1249, 1157, 1133, 1048, 842, 760, 694 cm⁻¹; HRMS (FAB+) m/z calc'd C₂₁H₃₇NO₂SiNa [M+Na]⁺: 386.2486, found: 386.2470; $[\alpha]_D^{23}$ +5.6 (*c* 0.305, CHCl₃).



(*R,Z*)-1-((3*S*,5*R*)-5-((tert-butyldimethylsilyl)oxy)-5-methyl-3-((triethylsilyl)oxy)cyclopent-1-en-1-yl)-1-oxo-6-(prop-1-en-2-yl)-9-(trimethylsilyl)non-3-en-8-yn-4-yl diisopropylcarbamate (473):

To a stirred solution of carbamate **475** (16 mg, 0.0275 mmol, 1 equiv) and TMEDA (6 µL, 0.04225 mmol, 1.3 equiv) in Et₂O (0.33 mL, 0.1 M) was cooled to -78 °C. *n*-BuLi (0.02 mL, 0.04 mmol, 2.16 M, 1.3 equiv) was added and stirred for 2 h. Aldehyde **444** (27.4 mg, 0.98 mmol, 2.2 equiv) in a solution of Et₂O (0.33 mL, 0.1 M) was added dropwise and allowed to stir for 2 h. Upon complete consumption of starting material (as determined by TLC, 9:1 hexanes:EtOAc) the reaction was quenched with H₂O (3 mL) and extracted with Et₂O (3 x 5 mL). The combined organic layers were dried over Na₂SO₄, filtered, and concentrated in vacuo. The crude product was purified by column chromatography (SiO₂, 9:1 hexanes:EtOAc) and carried on to the next reaction.

The crude alcohol product (8 mg, 0.011 mmol, 1 equiv) in wet CH₂Cl₂ (0.55 mL, 0.02 M) had DMP (9 mg, 0.022 mmol, 2 equiv) added. The reaction was allowed to stir for 2 h, at which time complete consumption of starting material was observed (by TLC analysis, 9:1 hexanes:EtOAc). The reaction was quenched with Na₂S₂O₃, poured into a saturated solution of NaHCO₃, and extracted with Et₂O (3 x 5 mL). The combined organic layers were dried over Na₂SO₄, filtered, and concentrated in vacuo. The crude product was purified by column chromatography (SiO₂, 9:1 hexanes:EtOAc) to afford enone **473** (4 mg,

20% over 2 steps) as a colorless oil ($R_f = 0.46$); ^1H NMR (400 MHz, CDCl_3) δ = 6.33 (d, J = 1.8 Hz, 1H), 5.34 (t, J = 6.5 Hz, 1H), 4.79 (q, J = 1.6 Hz, 1H), 4.75 (d, J = 1.6 Hz, 1H), 4.60 (td, J = 7.0, 1.8 Hz, 1H), 3.93 (s, 2H), 3.45 (dd, J = 18.7, 6.5 Hz, 1H), 3.26 (dd, J = 18.8, 6.7 Hz, 1H), 2.55 – 2.26 (m, 6H), 2.03 – 1.96 (m, 1H), 1.69 (dd, J = 1.5, 0.9 Hz, 3H), 1.52 – 1.43 (m, 3H), 1.26 (d, J = 6.7 Hz, 12H), 0.96 (t, J = 7.9 Hz, 9H), 0.82 (s, 9H), 0.67 – 0.56 (m, 6H), 0.12 (s, 9H), 0.08 (s, 3H), 0.05 (s, 3H); ^{13}C NMR (101 MHz, CDCl_3) δ = 196.0, 152.5, 149.3, 148.5, 145.9, 141.9, 112.2, 110.3, 105.8, 86.2, 81.9, 72.6, 53.9, 46.6, 43.4, 37.8, 37.2, 28.6, 25.9, 24.4, 21.7, 20.7, 19.9, 18.2, 6.9, 4.9, 0.3, 0.2, -2.3, -2.4; HRMS (FAB+) m/z calc'd $\text{C}_{40}\text{H}_{74}\text{NO}_5\text{Si}_3$ [M+H] $^+$: 732.4875, found: 732.4869.

A8.5 NOTES AND REFERENCES

1. Hoppe, D. *Synthesis*, **2009**, 43–55.
2. Pangborn, A. M.; Giardello, M. A.; Grubbs, R. H.; Rosen, R. K.; Timmers, F. J. *Organometallics* **1996**, *15*, 1518–1520.

APPENDIX 9

Spectra Relevant to Appendix 8:

Alternative Strategy Toward the

Total Synthesis of Scabrolide A

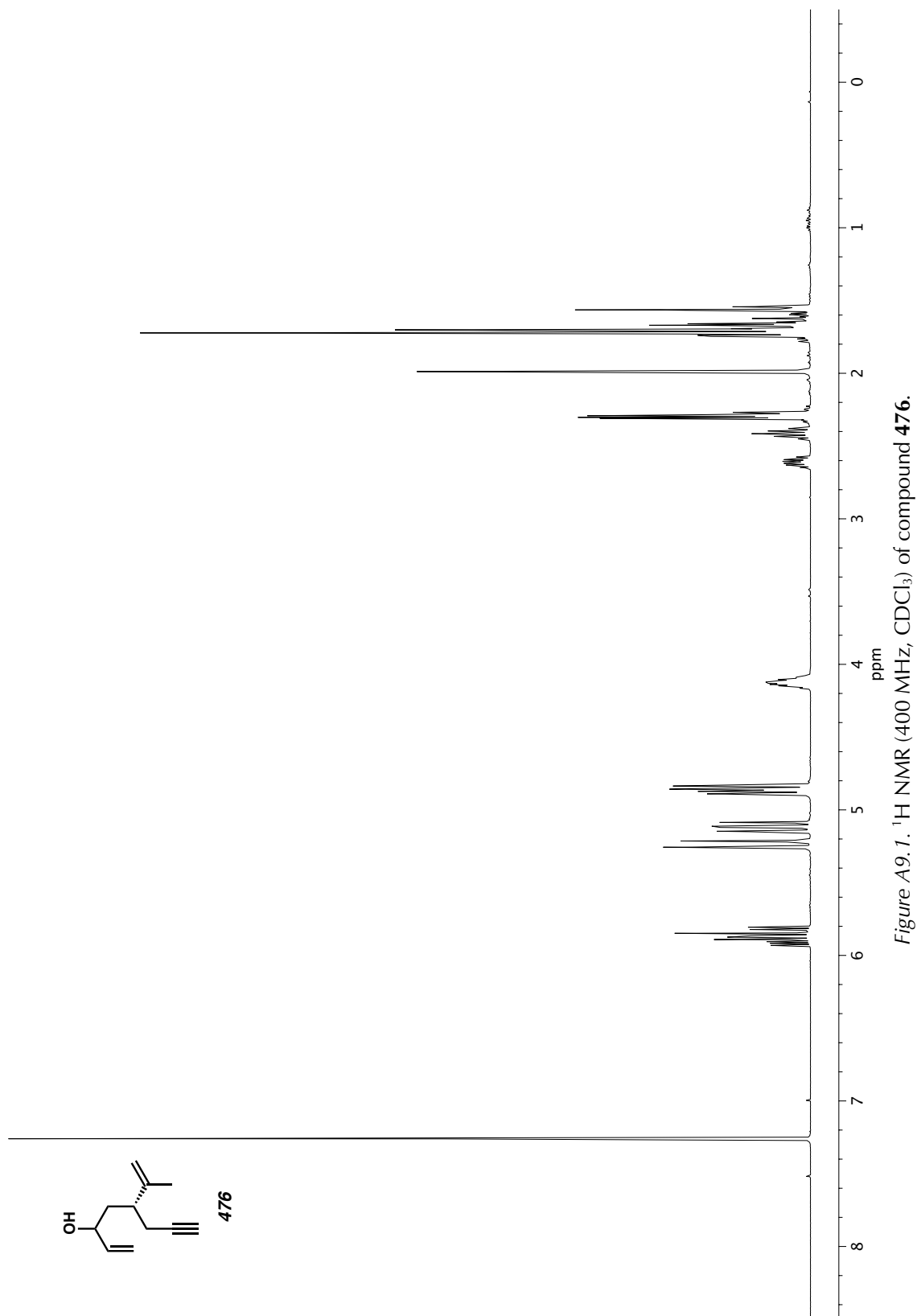


Figure A9.1. ^1H NMR (400 MHz, CDCl_3) of compound 476.

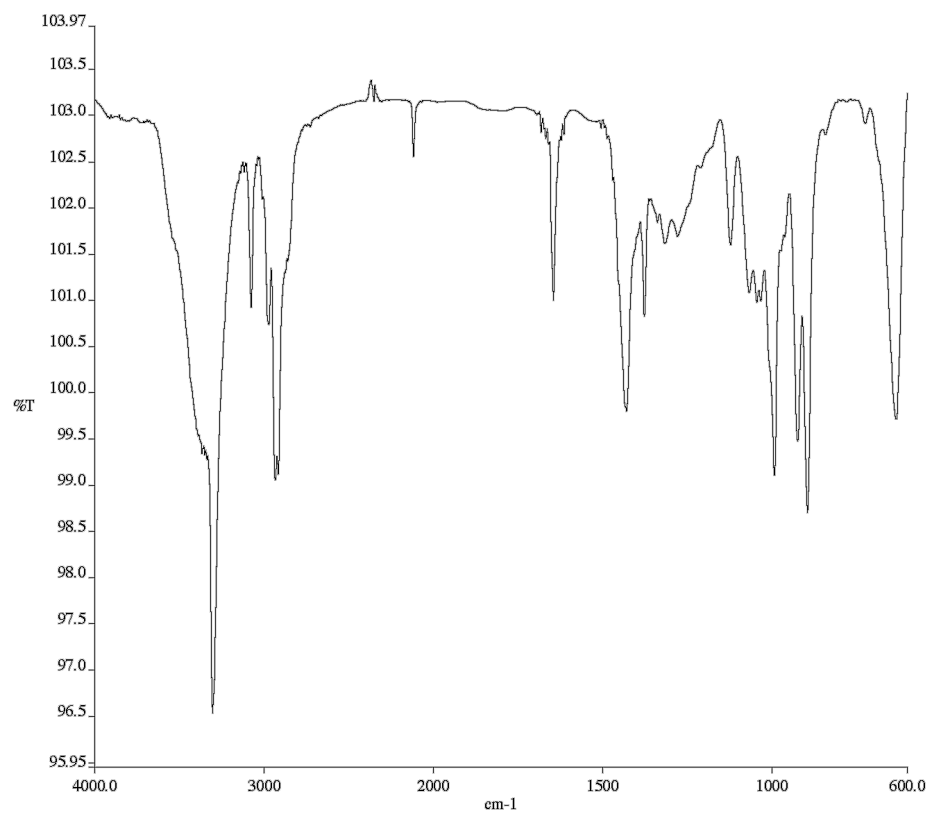


Figure A9.2. Infrared spectrum (Thin Film, NaCl) of compound **476**.

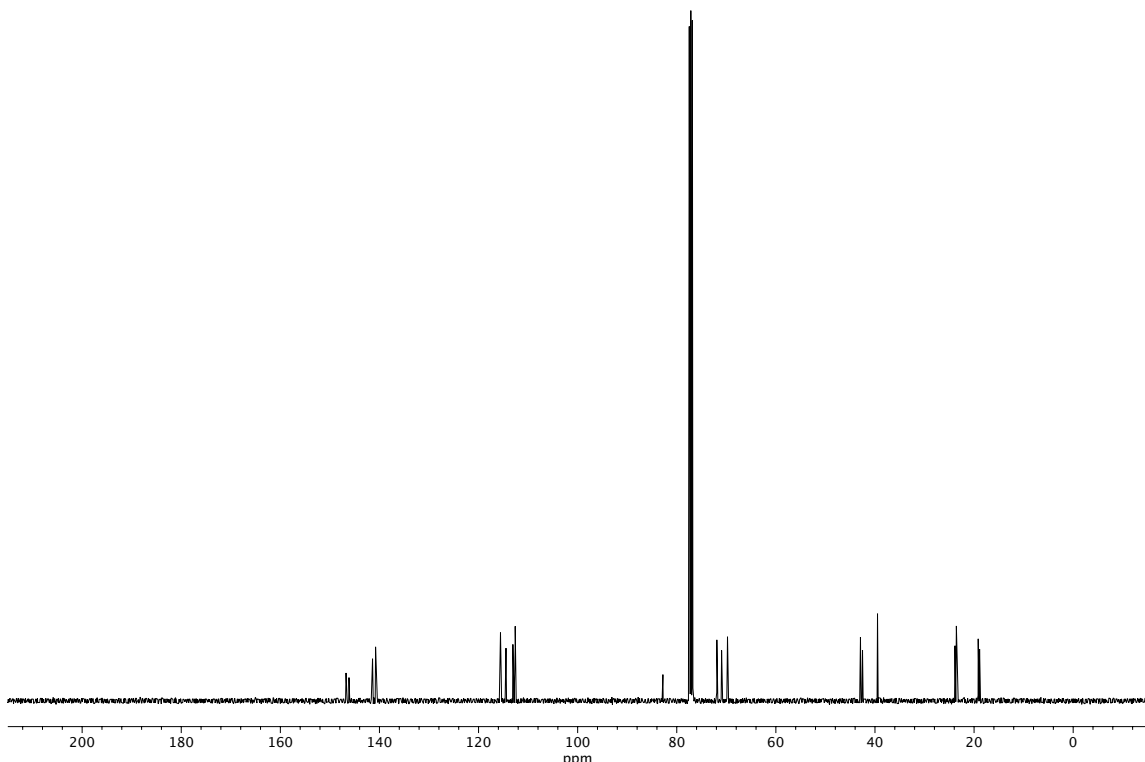


Figure A9.3. ^{13}C NMR (101 MHz, CDCl_3) of compound **476**.

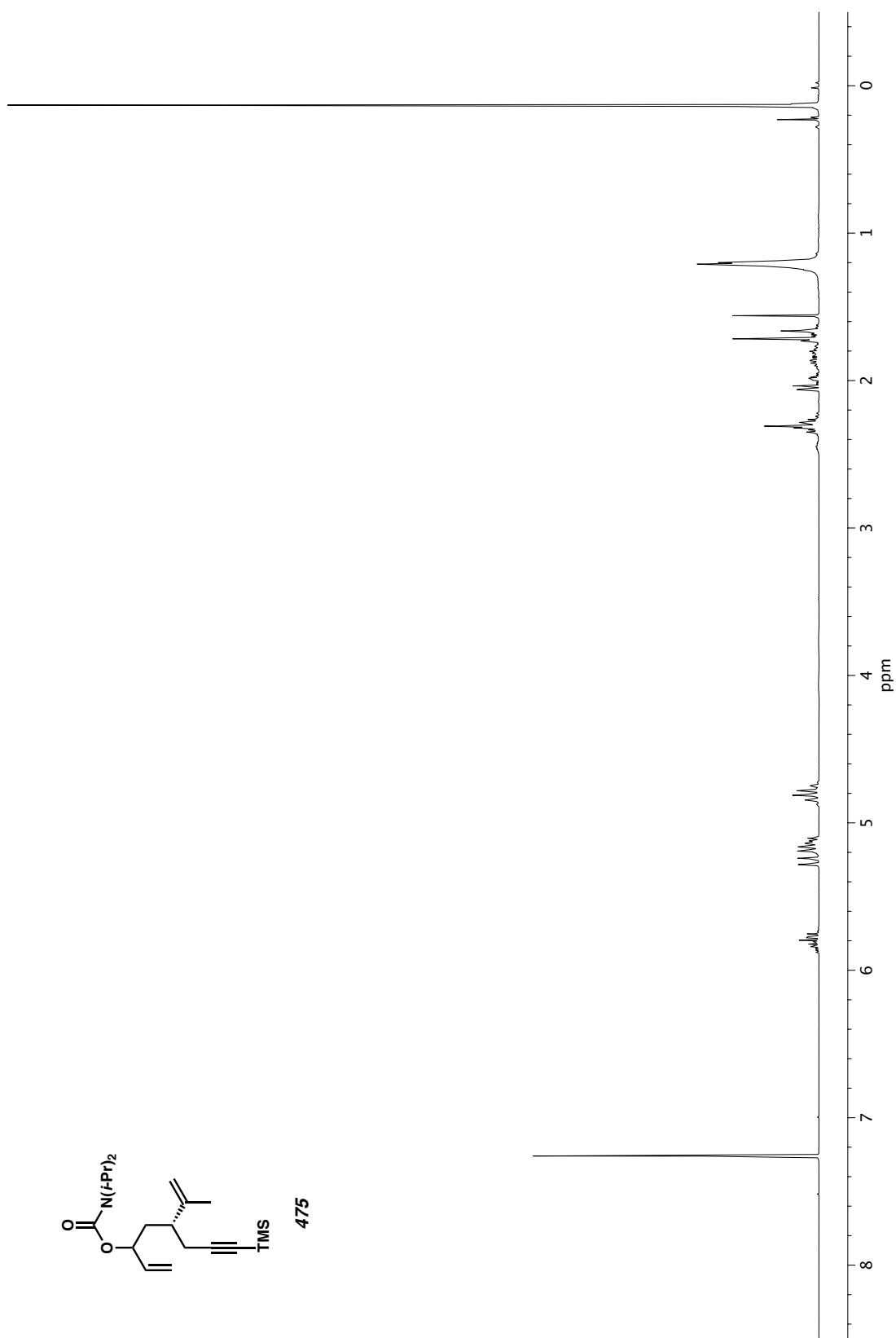
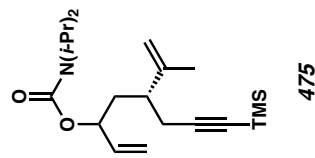


Figure A9.4. ¹H NMR (400 MHz, CDCl₃) of compound 475.

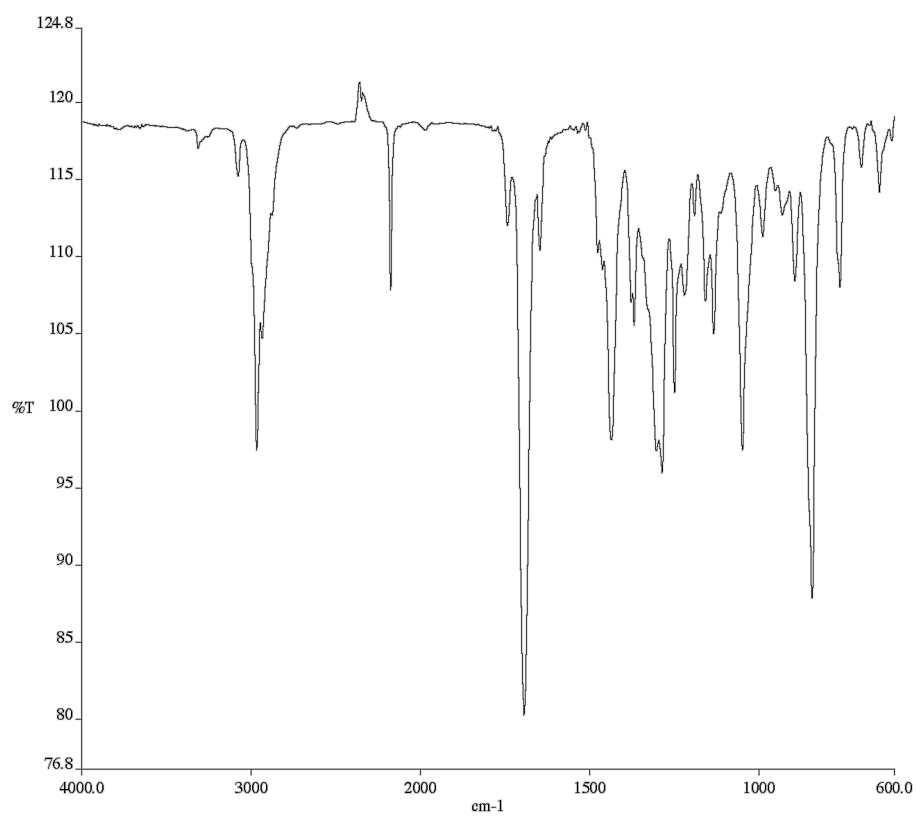


Figure A9.5. Infrared spectrum (Thin Film, NaCl) of compound 475.

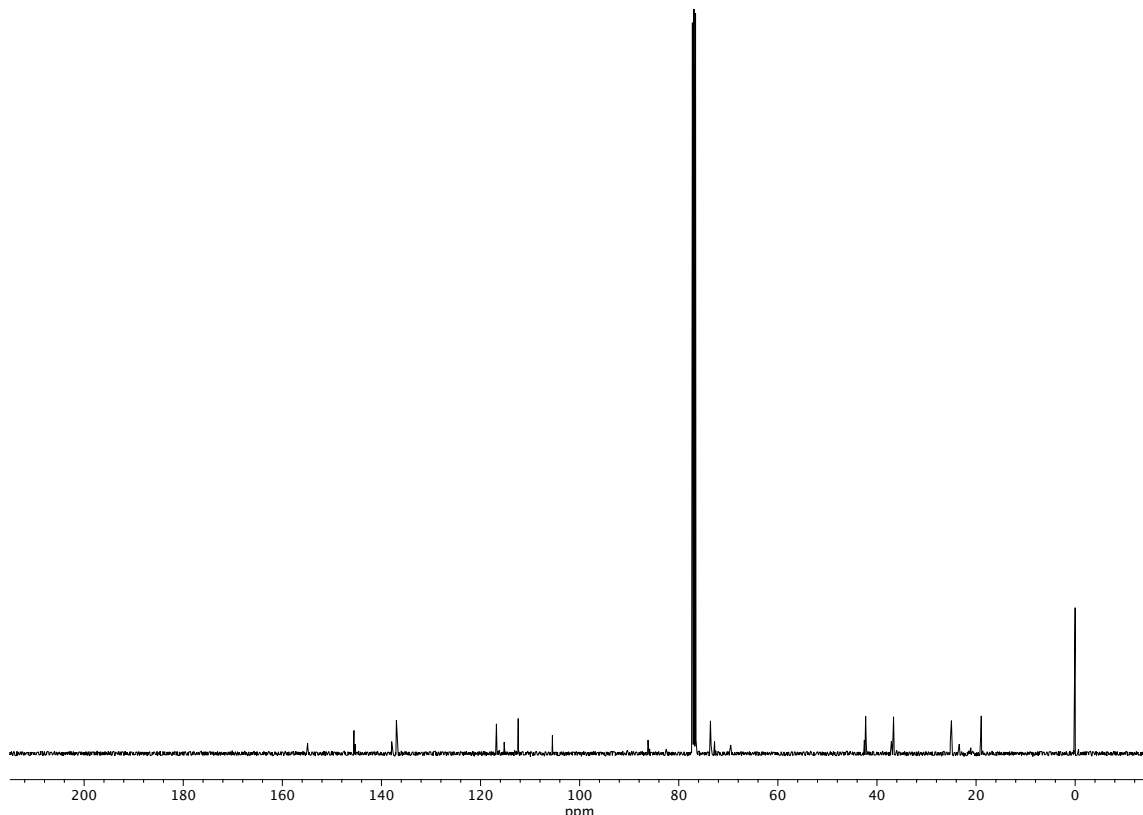


Figure A9.6. ¹³C NMR (101 MHz, CDCl₃) of compound 475.

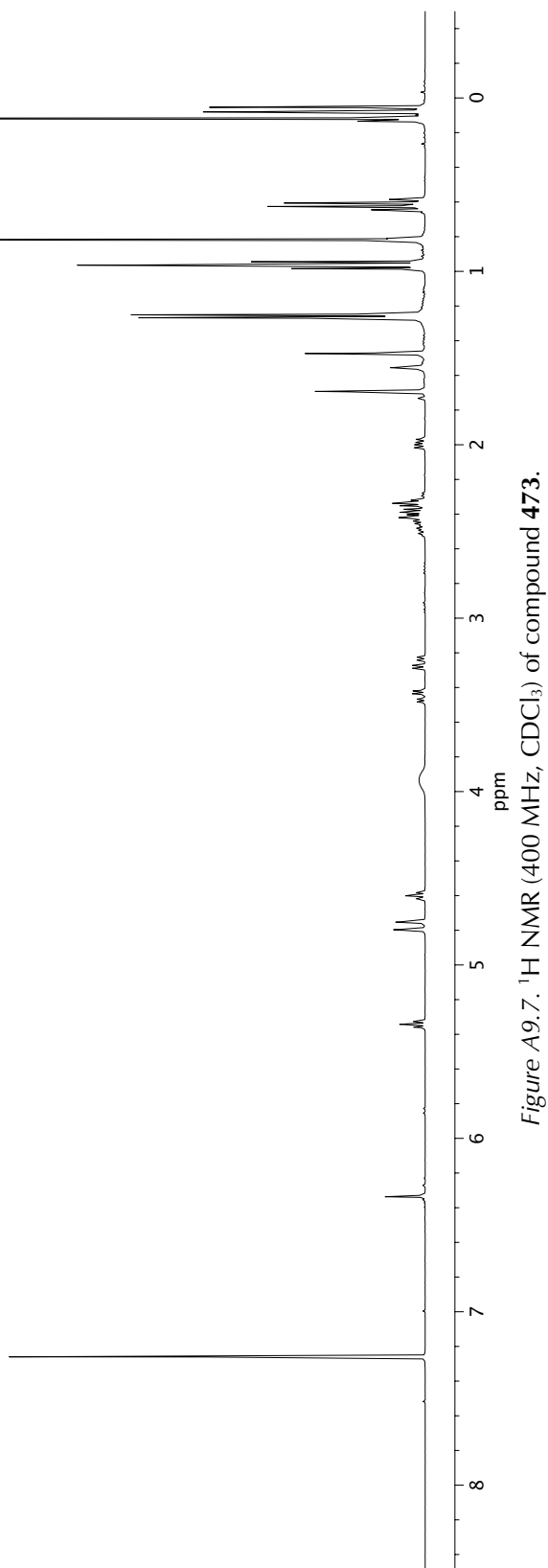
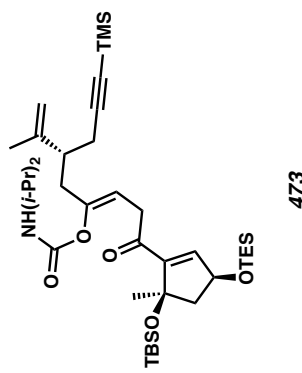


Figure A9.7. ^1H NMR (400 MHz, CDCl_3) of compound 473.

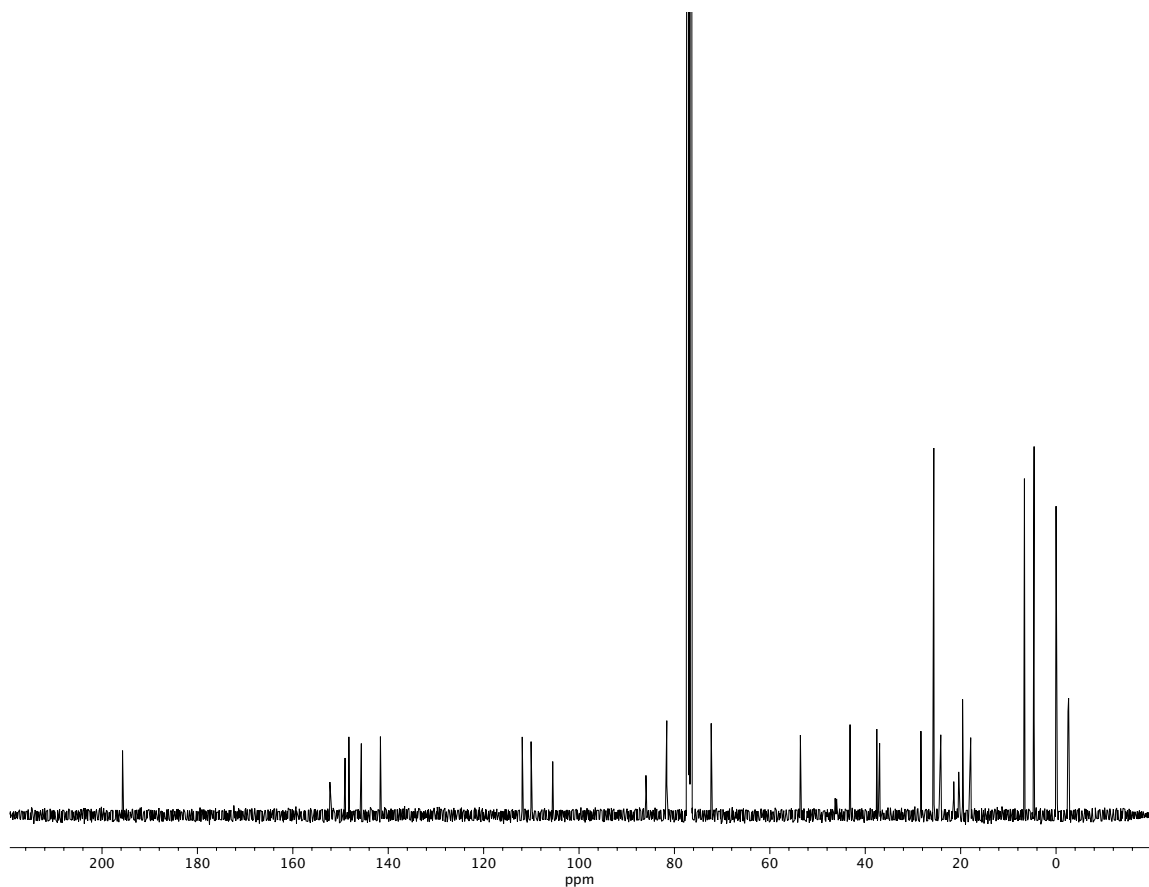


Figure A9.8. ^{13}C NMR (101 MHz, CDCl_3) of compound 473.

APPENDIX 10

Notebook Cross-Reference for New Compounds

A10.1 CONTENTS

The following notebook cross-reference provides the file name for all original spectroscopic data obtained for new compounds presented within this thesis. The information is organized by chapter or appendix and sequentially by compound number. All ^1H NMR, ^{13}C NMR, as well as ^{19}F NMR and any two-dimensional NMR data, if applicable, are electronically stored on the Caltech NMR laboratory server (mangia.caltech.edu, most typically under the usernames ‘sloskot’, ‘nhafeman’, ‘bpritche’, or ‘rcraig’) and on the Stoltz group server. Electronic copies of all IR spectra can also be found on the Stoltz group server. All laboratory notebooks are stored in the Stoltz group archive.

A10.2 NOTEBOOK CROSS-REFERENCE TABLES

Table A10.2.1. Notebook Cross-Reference For Compounds in Chapter 2

Compound	^1H NMR (instrument)	^{13}C NMR (instrument)	IR	Yield and Procedure
331	RAC-XIII-165 (Florence)	RAC-XIII-165 (Florence)	RAC-XIII-165	JTM-VII-237
332	RAC-XIII-141 (Florence)	RAC-XIII-141 (Florence)	RAC-XIII-141	RAC-XIII-141

Compound	¹ H NMR (instrument)	¹³ C NMR (instrument)	IR	Yield and Procedure
336	RAC-XIII-175 (Florence)	RAC-XIII-175 (Florence)	RAC-XIII-175	RAC-XIII- 175
339	RAC-XIII-179 (Florence)	RAC-XIII-179 (Florence)	RAC-XIII-179	RAC-XIII- 179
346	SAL-II-149 (Florence)	SAL-II-149 (Florence)	SAL-II-149	SAL-II-149
347	SAL-II-151 (Florence)	SAL-II-151 (Florence)	SAL-II-151	SAL-II-151
348	SAL-II-187 (Florence)	SAL-II-187 (Florence)	SAL-II-187	SAL-II-187
349	SAL-II-191 (Florence)	SAL-II-191 (Florence)	SAL-II-191	SAL-II-191
351	SAL-II-131 (Florence)	SAL-II-131 (Florence)	SAL-II-131	SAL-II-131
353	SAL-II-121 (Florence)	SAL-II-121 (Florence)	SAL-II-121	SAL-II-121
354	SAL-II-141 (Florence)	SAL-II-141 (Florence)	SAL-II-141	SAL-II-141
355	SAL-II-125 (Florence)	SAL-II-125 (Florence)	SAL-II-125	SAL-II-125
359	SAL-III-161 (Florence)	SAL-III-161 (Florence)	SAL-III-161	SAL-III-161
361	SAL-III-169 (Florence)	SAL-III-169 (Florence)	SAL-III-169	SAL-III-169
363	SAL-JAE-X- 167B (Florence)	SAL-JAE-X- 167B (Florence)	SAL-JAE-X- 167B	JAE-X-167B
364	SAL-II-133 (Florence)	SAL-II-133 (Florence)	SAL-II-133	SAL-II-133
365	SAL-II-135 (Florence)	SAL-II-135 (Florence)	SAL-II-135	SAL-II-135
366	SAL-II-179 (Florence)	SAL-II-179 (Florence)	SAL-II-179	SAL-II-179
367	SAL-II-181 (Florence)	SAL-II-181 (Florence)	SAL-II-181	SAL-II-181
370	RAC-XIII-CH- CH ₂ CH ₂ CO ₂ Et (Florence)	RAC-XIII-CH- CH ₂ CH ₂ CO ₂ Et (Florence)	RAC-XIII-CH- CH ₂ CH ₂ CO ₂ Et	RAC-XIII- 167
377	SAL-II-123 (Florence)	SAL-II-123 (Florence)	SAL-II-123	SAL-II-123
378	SAL-III-167 (Florence)	SAL-III-167 (Florence)	SAL-III-167	SAL-III-167

Compound	¹ H NMR (instrument)	¹³ C NMR (instrument)	IR	Yield and Procedure
379	SAL-III-165 (Florence)	SAL-III-165 (Florence)	SAL-III-165	SAL-III-165
380	SAL-III-173 (Florence)	SAL-III-173 (Florence)	SAL-III-173	SAL-III-173
382	SAL-II-169 (Florence)	SAL-II-169 (Florence)	SAL-II-169	SAL-II-169
383	SAL-II-173 (Florence)	SAL-II-173 (Florence)	SAL-II-173	SAL-II-173
384	SAL-II-177 (Florence)	SAL-II-177 (Florence)	SAL-II-177	SAL-II-177

Table A10.2.2. Notebook Cross-Reference For Compounds in Chapter 3

Compound	¹ H NMR (instrument)	¹³ C NMR (instrument)	IR	Yield and Procedure
385	SAL-V-271-3 (Florence)	SAL-V-271-3 (Florence)	SAL-V-271	SAL-VI-241
389	SAL-IV-177 (Florence)	SAL-IV-177 (Florence)	SAL-IV-177	SAL-VI-075
390	SAL-IV-063 (Florence)	SAL-IV-063 (Florence)	SAL-IV-063	SAL-IV-193
391	SAL-IV-111 (Florence)	SAL-IV-111 (Florence)	SAL-IV-111	SAL-IV-155
392	SAL-I-101 (Indy)	SAL-I-101 (Indy)	SAL-VI-037	SAL-V-265
393	SAL-I-073 (Indy)	SAL-I-073 (Indy)	SAL-VI-023	SAL-VI-023
395	SAL-I-289 (Florence)	SAL-I-289 (Florence)	SAL-IV-107	SAL-IV-107
396	SAL-I-061 (Indy)	SAL-I-061 (Indy)	SAL-I-061	SAL-IV-191
397	SAL-IV-101 (Florence)	SAL-IV-101 (Florence)	SAL-IV-101	SAL-VI-021
400	SAL-IV-061 (Florence)	SAL-IV-061 (Florence)	SAL-IV-061	SAL-V-281
401	SAL-IV-169 (Florence)	SAL-IV-169 (Florence)	SAL-IV-169	SAL-VI-051

Table A10.2.3. Notebook Cross-Reference For Compounds in Chapter 4

Compound	¹ H NMR (instrument)	¹³ C NMR (instrument)	IR	Yield and Procedure
422	BPP-V-287 (Indy)	BPP-V-287 (Indy)	BPP-V-287	NJH-II-221
416	BPP-V-295 (Indy)	BPP-V-295 (Indy)	BPP-V-295	SAL-VI-245
423	SAL-VII-051 (Florence)	SAL-VII-051 (Florence)	SAL-VII-051	SAL-VII- 051
430	BPP-VI-197 (Florence)	BPP-VI-197 (Florence)	BPP-VI-197	SAL-VI-261
432	SALVI-267 (Florence)	SALVI-267 (Florence)	SALVI-267	SALVI-267
434	BPP-VI-197- coll-A (Florence)	BPP-VI-197- coll-A (Florence)	BPP-VI-197-coll- A	SAL-VI-279
437	SAL-IX-263 (Florence)	SAL-IX-263 (Florence)	SAL-IX-263	SAL-IX-197
441	NJH-II-083 (Florence)	NJH-II-083 (Florence)	NJH-II-083	SAL-VIII- 279
442	SAL-VIII- NJH-enone- CN (Florence)	SAL-VIII- NJH-enone- CN (Florence)	SAL-VIII-enone- CN	SAL-VIII- 143
443	SAL-VIII-153 (Florence)	SAL-VIII-153 (Florence)	SAL-VIII-153	SAL-IX-141
444	NJH-II-089 (Florence)	NJH-II-089 (Florence)	NJH-II-089	SAL-VIII- 043
445	SAL-TBSTES- (Florence)	SAL-TBSTES- (Florence)	SAL-VII- doubleprotecteddiol	SAL-VIII- 245
446	SAL-TBSOH- (Florence)	SAL-TBSOH- (Florence)	SAL-VIII- monoprotecteddiol	SAL-VIII- 219
447	SAL-VIII-155 (Florence)	SAL-VIII-155 (Florence)	SAL-VIII-155	SAL-VIII- 155
448	SAL-X-203 (Florence)	SAL-X-203 (Florence)	SAL-X-203	NJH-II-093
449	SAL-VIII-229 (Florence)	SAL-VIII-229 (Florence)	SAL-VII-229	SAL-VIII- 229
450	SAL-VIII-195 (Florence)	SAL-VIII-195 (Florence)	SAL-VIII-195	SAL-VIII- 233
451	SAL-VIII-215 bottom (Florence)	SAL-VIII-215 bottom (Florence)	SAL-VIII-215	SAL-VIII- 209

Compound	¹ H NMR (instrument)	¹³ C NMR (instrument)	IR	Yield and Procedure
452	SAL-VIII-209 crystals Florence	SAL-VIII-209 crystals Florence	SAL-VIII-209- toptbsaldol	SAL-VIII- 209
453	SAL-IX-267 (Florence)	SAL-IX-267 (Florence)	SAL-IX-267	SAL-IX-197
454	SAL-IX-271-2 (Florence)	SAL-IX-271-2 (Florence)	SAL-IX-271-2	SAL-IX-241
455	SAL-IX-243 (Florence)	SAL-IX-243 (Florence)	SAL-IX-243	SAL-IX-031
456	SAL-X-201 (Florence)	SAL-X-201 (Florence)	SAL-X-201	SAL-X-201
457	SAL-X-197 (Florence)	SAL-X-197 (Florence)	SAL-X-197	SAL-X-197
458	SAL-X-183 (Florence)	SAL-X-183 (Florence)	SAL-X-183	SAL-X-183
461	SAL-X-185 (Florence)	SAL-X-185 (Florence)	SAL-X-185	SAL-X-185
462	SAL-X-189 (Florence)	SAL-X-189 (Florence)	SAL-X-189	SAL-X-189
463	SAL-X-193 (Florence)	SAL-X-193 (Florence)	SAL-X-193	SAL-X-079
464	SAL-X-195 (Florence)	SAL-X-195 (Florence)	SAL-X-195	SAL-X-091
465	SAL-X-199-1 (Florence)	SAL-X-199-1 (Florence)	SAL-X-199-1	SAL-X-119
466	SAL-X-199-2 (Florence)	SAL-X-199-2 (Florence)	SAL-X-199-2	SAL-X-119
468	SAL-X-163 (Florence)	SAL-X-163 (Florence)	SAL-X-163	SAL-X-163
470	SAL-VIII- NJH-alcohol- CN (Florence)	SAL-VIII- NJH-alcohol- CN (Florence)	SAL-VIII-NJH- alcohol-CN	SAL-IX-139

Table A10.2.4. Notebook Cross-Reference For Compounds in Appendix 8

Compound	¹ H NMR (instrument)	¹³ C NMR (instrument)	IR	Yield and Procedure
473	SAL-VIII-091- 4 (Florence)	SAL-VIII-091- 4 (Florence)	–	SAL-VIII- 091
475	SAL-VIII-121 (Florence)	SAL-VIII-121 (Florence)	SAL-VIII-121	SAL-VIII- 087
476	SAL-VIII-117 (Florence)	SAL-VIII-117 (Florence)	SAL-VIII-117	SAL-VIII- 117

COMPREHENSIVE BIBLIOGRAPHY

- Abbas, H. K.; Mirocha, C. J. *Appl. Environ. Microbiol.* **1988**, *54*, 1268–1274.
- Abreu, M.; Alvaro-Benito, M.; Sanz-Aparicio, J.; Plou, F. J.; Fernandez-Lobato, M.; Alcalde, M. *Adv. Synth. Catal.* **2013**, *355*, 1698–1702.
- Åhman, J.; Wolfe, J. P.; Troutman, M. V.; Palucki, M.; Buchwald, S. L. *J. Am. Chem. Soc.* **1998**, *120*, 1918–1919.
- Alexy, E. J.; Zhang, H.; Stoltz, B. M. *J. Am. Chem. Soc.* **2018**, *140*, 10109–10112.
- Allais, C.; Tsai, A. S.; Nuhant, P.; Roush, W. R. *Angew. Chem. Int. Ed.* **2013**, *52*, 1288–12891.
- Allen, J. G.; Danishefsky, S. J. *J. Am. Chem. Soc.* **2001**, *123*, 351–352.
- Anderson, N. H.; Uh, H.-S. *Synth. Commun.* **1973**, *3*, 125–128.
- d'Angelo J. *Tetrahedron* **1976**, *32*, 2979–2990.
- Arao, T.; Kondo, K.; Aoyama, T. *Chem. Pharm. Bull.* **2006**, *54*, 1743–1744.
- Arao, T.; Kondo, K.; Aoyama, T. *Tetrahedron Lett.* **2006**, *47*, 1417–1420.
- Arend, M.; Westermann, B.; Risch, N. *Angew. Chem. Int. Ed.* **1998**, *37*, 1044–1070.
- Arnold, F. H. *Acc. Chem. Res.* **1998**, *31*, 125–131.
- Arrayás, R. G.; Carretero, J. C. *Chem. Soc. Rev.* **2009**, *38*, 1940–1948.

Asai, R.; Mitsuhashi, S.; Shigetomi, K.; Miyamoto, T.; Ubukata, M. *J. Antibiot.* **2011**, *64*, 693–696.

Bassner, S. L.; Morrison, E. D.; Geoffroy, G. L.; Rheingold, A. L. *J. Am. Chem. Soc.* **1986**, *108*, 5358–5359.

Bauta, W.; Booth, J.; Bos, M. E.; DeLuca, M.; Diorazio, L.; Donohoe, T.; Magnus, N.; Magnus, P.; Mendoza, J.; Pye, P.; Tarrant, J.; Thom, S.; Ujjainwalla, F. *Tetrahedron Lett.* **1995**, *36*, 5327–5330.

Behenna, D. C.; Liu, Y.; Yurino, T.; Kim, J.; White, D. E.; Virgil, S. C.; Stoltz, B. M. *Nature Chemistry* **2012**, *4*, 130–133.

Behenna, D. C.; Mohr, J. T.; Sherden, N. H.; Marunescu, S. C.; Harned, A. M.; Tani, K.; Seto, M.; Ma, S.; Novak, Z.; Krout, M. R.; McFadden, R. M.; Roizen, J. L.; Enquist Jr., J. A.; White, D. E.; Levine, S. R.; Petrova, K. V.; Iwashita, A.; Virgil, S. C.; Stoltz, B. M. *Chem. – Eur. J.* **2011**, *17*, 14199–14223.

Behenna, D. C.; Stoltz, B. M. *J. Am. Chem. Soc.* **2004**, *126*, 15044–15045.

Bellina, F.; Rossi, R. *Chem. Rev.* **2010**, *110*, 1082–1146.

Bisai, V.; Bisai, A.; Singh, V. K. *Tetrahedron* **2012**, *68*, 4541–4580.

Bhanushali, M.; Zhao, C.-G. *Synthesis* **2011**, 1815–1830.

Blacker, A. J.; Clarke, M. L.; Loft, M. S.; Mahon, M. F.; Williams, J. M. *Organometallics* **1999**, *18*, 2867–2873.

Bloch, R.; Le Perche, P.; Rouessac, F.; Conia, J.-M. *Tetrahedron*, **1968**, *24*, 5971–5989.

- Boechman, Jr., R. K.; Chinn, R. L. *Tetrahedron*, **1985**, *26*, 5005–5008.
- Bonadies, F.; Lattanzi, A.; Orelli, L. R.; Pesci, S.; Scettri, A. *Tetrahedron Lett.* **1993**, *34*, 7649–7650.
- Botteghi, C.; Paganelli, S.; Schionate, A.; Boga, C.; Fava, A. *J. Mol. Catal.* **1991**, *66*, 7–21.
- Botteghi, C.; Schionanto, A.; Rosini, C.; Salvadori, R. P. *J. Mol. Catal.* **1990**, *63*, 155–165.
- Brill, Z. G.; Grover, H. K.; Maimone, T. J. *Science* **2016**, *27*, 1078–1082.
- Brodmann, T.; Lorenz, M.; Schäckel, R.; Simsek, S.; Kalesse, M. *Synlett* **2009** 174–192.
- Brown, H. C.; Dhar, R. K.; Bakshi, R. K.; Pandiarajan, P. K.; Singaram, B. *J. Am. Chem. Soc.* **1989**, *111*, 3441–3442.
- Brown, H. C.; Ganesan, K.; Dhar, R. K. *J. Org. Chem.* **1993**, *58*, 147–153.
- Brunel, J. M.; Tenaglia, A.; Buono, G. *Tetrahedron: Asymmetry* **2000**, *11*, 3585–3590.
- Brunner, H.; Kraus, J. *J. Mol. Catal.* **1989**, *49*, 133–142.
- Brunner, H.; Krumey, C. *J. Mol. Catal. A: Chem.* **1999**, *142*, 7–15.
- Brunner, H.; Hammer, B. *Angew. Chem. Int. Ed.* **1984**, *23*, 312–313.
- Bruno, N. C.; Tudge, M. T.; Buchwald, S. L. *Chem. Sci.* **2013**, *4*, 916–920.
- Burger, E.; Barron, B.; Tunge, J. *Synlett* **2006**, *17*, 2824–2826.
- Burkhardt, E. R.; Bergman, R. G.; Heathcock, C. H. *Organometallics* **1990**, *9*, 30–44.

Burkhardt, E. R.; Doney, J. J.; Slough, G. A.; Stack, J. M.; Heathcock, C. H.; Bergman, R. G. *Pure Appl. Chem.* **1998**, *60*, 1–6.

Burtoloso, A. C. B. *Synlett* **2009**, 320–327.

Castro, A. M. M. *Chem. Rev.* **2004**, *104*, 2939–3002.

Cazeau, P.; Moulines, F.; Laporte, O.; Duboudin, F. *J. Organomet. Chem.* **1980**, *201*, C9–C13.

Chan, T. H.; Zheng, G. Z. *Tetrahedron Lett.* **1993**, *34*, 3095–3098.

Chantani, N. Murai, S.; Sonoda, N. *J. Am. Chem. Soc.* **1983**, *105*, 1370–1372.

Chen, G.; Kwong, F. Y.; Chan, H. O.; Yu, W.-Y.; Chan, A. S. C. *Chem. Commun.* **2006**, 1413–1415.

Chen, M. S.; Prabagaran, N.; Labenz, N. A.; White, C. M. *J. Am. Chem. Soc.* **2005**, *127*, 6970–6971.

Chen, Z.; Morimoto, H.; Matsunaga, S.; Shibasaki, M. *J. Am. Chem. Soc.* **2008**, *130*, 2170–2171.

Chen, Q. B.; Xin, X. L.; Yang, Y.; Lee, S. S.; Aisa, H. A. *J. Nat. Prod.* **2014**, *77*, 807–812.
b) Zhang, S.; Zhang, Z. Y. *Drug Discovery Today* **2007**, 373–381.

Chieffi, A.; Kamikawa, K.; Åhman, J.; Fox, J. M.; Buchwald, S. L. *Org. Lett.* **2001**, *3*, 1897–1900.

Christoffers, J. *Eur. J. Org. Chem.* **1998**, 1259–1266.

Christoffers, *J. Prakt. Chem. (Weinheim, Ger.)*, **1999**, *341*, 495.

Christoffer, J.; Baro, A. *Angew. Chem. Int. Ed.* **2003**, *42*, 1688–1690.

Christoffers, J.; Mann, A. *Eur. J. Org. Chem.* **1999**, 1475–1479.

Christoffers, J.; Mann, A.; Pickardt, J. *Tetrahedron*, **1999**, *55*, 5377–5388.

Christoffers, J.; Rößler, U.; Werner, T. *Eur. J. Org. Chem.* **2000**, 701–705.

Claisen, L. *Chem. Ber.*, **1912**, *45*, 3157–3166.

Collman, J. P. *J. Org. Chem.* **1961**, *26*, 3162–3166.

Conia, J.-M.; Le Perche, P. *Synthesis* **1975**, 1–19.

Corbin, N. C.; Fraher, P.; McChesney, J. D. *J. Pharm. Sci.* **1979**, *68*, 1501–1504.

Córdova, A. *Acc. Chem Res.* **2004**, *37*, 102–112.

Córdova, A. in *Stereoselective Organocatalysis: Bond Formation Methodologies and Activation Modes*, 1st Edition (Ed. R. R. Torres), Chap. 4, Wiley, 2013, p. 129–146

Corey, E. J.; Enders, D. *Tetrahedron Lett.* **1976**, *17*, 3–6.

Corey, E. J.; Kania, R. S. *J. Am. Chem. Soc.* **1996**, *118*, 1229–1230.

Corey, E. J.; Lee, D. H. *J. Am. Chem. Soc.* **1991**, *113*, 4026–4028.

Corey, E. J.; Roberts, B. E.; Dixon, B. R. *J. Am. Chem. Soc.* **1995**, *117*, 193–196.

Corkey, B. K.; Toste, F. D. *J. Am. Chem. Soc.* **2005**, *127*, 17168–17169.

Cowden, C. J.; Paterson, I. in *Organic Reactions*, Vol. 51, Chap. 1, Wiley, 1997, p. 1–200.

Craig, II, R. A.; Loskot, S. A.; Mohr, J. T.; Behenna, D. C.; Harned, A. M.; Stoltz, B. M. *Org. Lett.* **2015**, *17*, 5160–5163.

Craig, II, R. A.; Roizen, J. L.; Smith, R. C.; Jones, A. C.; Virgil, S. C.; Stoltz, B. M. *Chem. Sci.* **2017**, *8*, 507–514.

Craig, II, R. A.; Stoltz, B. M. *Tetrahedron Lett.* **2015**, *56*, 4670–4673.

Cram, D. J.; Sogah, G. D. Y. *J. Chem. Soc., Chem. Commun.* **1981**, 625–628.

Culkin, D. A.; Hartwig, J. F. *Acc. Chem. Res.* **2003**, *36*, 234–245.

Dalko, P. I.; Moisan, L. *Angew. Chem. Int. Ed.* **2004**, *43*, 5138–5175.

Das, J. P; Marek, I. *Chem. Commun.* **2011**, *47*, 4593–4623.

Dauben, H. J.; McCoy, L. L. *J. Am. Chem. Soc.* **1959**, *81*, 4863–4873.

Davies, H. M. L.; Manning, J. R. *Nature* **2008**, *451*, 417–424.

Davis, F. A.; Lal, G. S.; Wei, J. *Tetrahedron Lett.* **1988**, *29*, 4269–4272.

Dawson, G. J.; Frost, C. G.; Williams, J. M. J.; Coote, S. J. *Tetrahedron Lett.* **1993**, *34*, 3149–3150.

- Day, J. J.; McFadden, R. M.; Virgil, S. C.; Kolding, H.; Alleva, J. L.; Stoltz, B. M. *Angew. Chem., Int. Ed. Engl.* **2011**, *50*, 6814–6818.
- Denard, C. A.; Ren, H.; Zhao, H. *Curr. Opin. Chem. Biol.* **2015**, *25*, 55–64.
- Desimoni, G.; Dusi, G.; Faita, G.; Quadrelli, P.; Righetti, P. P. *Tetrahedron* **1995**, *51*, 4131–4144.
- Desimoni, G.; Quadrelli, P.; Righetti, P. P. *Tetrahedron* **1990**, *46*, 2927–2934.
- Dias, D. A.; Urban, S.; Roessner, U. *Metabolites* **2012**, *2*, 303–336.
- Dimitrov, V.; Kostova, K.; Genov, M. *Tetrahedron Lett.* **1996**, *37*, 6787–6790.
- Doering, W. V. E.; Yamashita, Y. *J. Am. Chem. Soc.* **1983**, *105*, 5368–5372.
- Doran, R.; Guiry, P. J. *J. Org. Chem.* **2014**, *79*, 9112–9124.
- Douglas, C. J.; Overman, L. E. *Proc. Natl. Acad. Sci.* **2004**, *101*, 5363–5367.
- Doyle, A. G.; Jacobsen, E. N. *J. Am. Chem. Soc.* **2005**, *127*, 62–63.
- Doyle, A. G.; Jacobsen, E. N. *Angew. Chem. Int. Ed.* **2007**, *46*, 3701–3705.
- Egger, H.; Reinshagen, H. *J. Antibiot.* **1976**, *29*, 923–927.
- Enders, D.; Knopp, M.; Schiffers, R. *Tetrahedron: Asymmetry* **1996**, *7*, 1847–1882.
- Engle, K. M.; Mei, T.-S.; Wasa, M.; Yu, J.-Q. *Acc. Chem. Res.* **2012**, *45*, 788–802.
- Evans, D. A.; Nelson, J. V.; Taber, T. R., *Top. Stereochem.*, **13**, 1 (1982)

- Evans, W. J.; Dominguez, R.; Hanusa, T. P. *Organometallics*, **5**, 1291–1296.
- Fossey, J. S.; Russell, M. L.; Malik, K. M. A.; Richards, C. J. *J. Organomet. Chem.* **2007**, *692*, 4843–4848.
- Fox, J. M.; Huang, X.; Chieffi, A.; Buchwald, S. L. *J. Am. Chem. Soc.* **2000**, *122*, 1360–1370.
- Freixa, Z.; van Leeuwen, P. W. N. M. *Coord. Chem. Rev.* **2008**, *252*, 1755–1786.
- Frostick, F. C.; Hauser, C. R. *J. Am. Chem. Soc.* **1949**, *71*, 1350–1352.
- Fujimura, O. *J. Am. Chem. Soc.* **1998**, *120*, 10032–10039.
- Fukuchi, I.; Hamashima, Y.; Sodeoka, M. *Adv. Synth. Catal.* **2007**, *349*, 509–512.
- Galarini, R.; Musco, A.; Pontellini, R.; Santi, R. *J. Mol. Catal.* **1992**, *72*, L11–L13.
- García-Fortanet, J.; Buchwald, S. L. *Angew. Chem. Int. Ed.* **2008**, *47*, 8108–8111.
- Garzan, A.; Jaganathan, A.; Salehi Marzijarani, N.; Yousefi, R.; Whitehead, D. C.; Jackson, J. E.; Borhan, B. *Chem. – Eur. J.* **2013**, *19*, 9015–9021.
- Ge, S.; Hartwig, J. F. *J. Am. Chem. Soc.* **2011**, *133*, 16330–16333.
- Giner, J.-L.; Kehbein, K. A.; Cook, J. A.; Smith, M. C.; Vlahos, C. J.; Badwey, J. A. *Bioorg. Med. Chem. Lett.* **2006**, *16*, 2518–2521.
- Glorius, F.; Altenhoff, G.; Goddard, R.; Lehmann, C. *Chem. Commun.* **2002**, 2704–2705.

- Göricke, F.; Schneider, C. *Angew. Chem. Int. Ed.* **2018**, *57*, 14736–14741.
- Gonda, J. *Angew. Chem. Int. Ed.* **2004**, *43*, 3516–3524.
- González, M. A.; Ghosh, S.; Rivas, F.; Fischer, D.; Theodorakis, E. A. *Tetrahedron Lett.* **2004**, *45*, 5039–5041.
- Gopalaiah, K. *Chem. Rev.* **2013**, *113*, 3248–3296.
- Gradillas, A.; Pérez-Castells, J. *Angew. Chem. Int. Ed.* **2006**, *45*, 6086–6101.
- Greco, S. J.; Lacerda, V. Jr.; dos Santos, R. B. *Aldrichimica Acta*, **2011**, *44*, 15–24.
- Grubbs, R. H. *Tetrahedron* **2004**, *60*, 7117–7140.
- Gulias, M.; Rodriguez, J. R.; Castedo, L.; Mascarenas, J. L. *Org. Lett.* **2003**, *5*, 1975–1977.
- Gutekunst, W. R.; Baran, P. S. *Chem. Soc. Rev.* **2011**, *40*, 1976–1991.
- Hama, T.; Culkin, D. A.; Hartwig, J. F. *J. Am. Chem. Soc.* **2006**, *128*, 4976–4985.
- Hamada, T.; Chieffi, A.; Åhman, J.; Buchwald, S. L. *J. Am. Chem. Soc.* **2002**, *124*, 1261–1268.
- Hamada, T.; Buchwald, S. L. *Org. Lett.* **2002**, *4*, 999–1001.
- Hamann, B. C.; Hartwig, J. F. *J. Am. Chem. Soc.* **1997**, *119*, 12382–12383.
- Hamashima, Y.; Hotta, D.; Sodeoka, M. *J. Am. Chem. Soc.* **2002**, *124*, 11240–11241.

Hamashima, Y.; Sasamoto, N.; Hotta, D.; Somei, H.; Umebayashi, N.; Sodeoka, M. *Angew. Chem. Int. Ed.* **2005**, *44*, 1525–1529.

Hamashima, Y.; Hotta, D.; Umebayashi, N.; Tsuchiya, Y.; Suzuki, T.; Sodeoka, M. *Adv. Synth. Catal.* **2005**, *347*, 1576–1586.

Hamashima, Y.; Sodeoka, M. *Chem. Rec.* **2004**, *4*, 231–242.

Hamashima, Y.; Takano, H.; Hotta, D.; Sodeoka, M. *Org. Lett.* **2003**, *5*, 3225–3228.

Han, Y.-Y.; Wu, Z.-J.; Chen, W.-B.; Du, X.-L.; Zhang, X.-M.; Yuan, W.-C. *Org. Lett.* **2011**, *13*, 5064–5067.

Hansen, M. M.; Bartlett, P. A.; Heathcock, C. H. *Organometallics*, **1987**, *6*, 2069–2074.

Harris, R. K.; Becker, E. D.; Cabral de Menezes, S. M.; Goodfellow, R.; Granger, P. *Pure Appl. Chem.* **2001**, *73*, 1795–1818.

Harris, R. K.; Becker, E. D.; Cabral de Menezes, S. M.; Granger, P.; Hoffman, R. E.; Zilm, K. W. *Pure Appl. Chem.* **2008**, *80*, 59–84.

Hatano, M.; Horibe, T.; Ishihara, K. *J. Am. Chem. Soc.* **2010**, *132*, 56–57.

Hayashi, T.; Kanehira, K.; Hagihara, T.; Kumada, M. *J. Org. Chem.* **1988**, *53*, 113–120.

Heathcock, C. H. in *Asymmetric Synthesis*, Vol. 3 (Ed. J. D. Morrison), Chap. 2, Academic Press, 1984, p. 111–212.

Heravi, M. M.; Asadi, S. *Tetrahedron: Asymmetry* **2012**, *23*, 1431–1465.

Heravi, M. M.; Zadsirjan, V. *Tetrahedron: Asymmetry* **2013**, *24*, 1149–1188.

- Heravi, M. M.; Zadsirjan, V. *Tetrahedron: Asymmetry* **2014**, *25*, 1061–1090.
- Herrmann, A. T.; Smith, L. L.; Zakarian, A. *J. Am. Chem. Soc.* **2012**, *134*, 6976–6979.
- Hirano, M.; Ito, Y.; Hirai, M.; Fukuoka, A.; Komiya, S. *Chem. Lett.* **1993**, *22*, 2057–2060.
- Hiroshi, S.; Masahito, I.; Kazuhiro, K. *Chem. Lett.* **1987**, *16*, 1527–1530.
- Hoffmeister, D.; Yang, J.; Liu, L.; Thorson, J. S. *Proc. Natl. Acad. Sci. U. S. A.* **2003**, *100*, 13184–13189.
- Hong, A. Y.; Bennett, N. B.; Krout, M. R.; Jensen, T.; Harned, A. M.; Stoltz, B. M. *Tetrahedron*, **2011**, *67*, 10234–10248.
- Hoover, J. M.; Stahl, S. S. *J. Am. Chem. Soc.* **2011**, *133*, 16901–16910.
- Hoppe, D. *Synthesis*, **2009**, 43–55.
- Horn, E. J.; Rosen, B. R.; Chen, Y.; Tang, J.; Chen, K.; Eastgate, M. D.; Baran, P. S. *Nature* **2016**, *533*, 77–81.
- House, H. O.; Czuba, L. J.; Gall, M.; Olmstead, H. D. *J. Org. Chem.* **1969**, *34*, 2324–2336.
- Hoye, T. R.; Jeffrey, C. S.; Tennakoon, M. A.; Wang, J.; Zhao, H. *J. Am. Chem. Soc.* **2004**, *126*, 10210–10211.
- Huang, F.-Q., Sun J.-G.; Wang, Y.-W.; Dong, X.; Qi, L.-W.; Zhang, B. *Org. Lett.* **2016**, *18*, 684–687.

- Huang, J. Z.; Jie, X. K.; Wei, K.; Zhang, H.; Wang, M. C.; Yang, Y. R. *Synlett* **2013**, *24*, 1303–1306.
- Inagaki, K.; Nozaki, K.; Takaya, H. *Synlett*, **1997**, 119–120.
- Inanaga, J.; Hirata, K.; Saeki, H.; Katsuki, T.; Yamaguchi, M. *Bull. Chem. Soc. Jpn.* **1979**, *52*, 1989–1993.
- Ireland, R. E.; Liu, L. *J. Org. Chem.* **1993**, *58*, 2899–2899.
- Ireland, R. E.; Mueller, R. H.; Willard, A. K. *J. Am. Chem. Soc.* **1976**, *98*, 2868–2877.
- Ireland, R. E.; Norbeck, D. W. *J. Org. Chem.* **1985**, *50*, 2198–2200.
- Ireland, R. E.; Willard, A. K. *Tetrahedron Lett.* **1975**, *16*, 3975–3978.
- Ireland, R. E.; Wipf, P.; Armstrong, J. D. III. *J. Org. Chem.* **1991**, *56*, 650–657.
- Ishikawa, S.; Hamada, T.; Manabe, K.; Kobayashi, S. *J. Am. Chem. Soc.* **2004**, *126*, 12236–12237.
- Ito, H.; Taguchi, T. *Chem. Soc. Rev.* **1999**, *28*, 43–50.
- Janocha, S.; Schmitz, D.; Bernhardt, R. *Adv. Biochem. Eng./Biotechnol.* **2015**, *148*, 215–250.
- Jasiczak, J. *J. Chem. Soc., Perkin Trans. I* **1988**, 2687–2692.
- Jay, A. in *Dictionary of Chemistry*, 2nd Edition (Ed. E Geller), McGraw-Hill, 2003, p. 317.

Jette, C. I.; Geibel, I.; Bachman, S.; Hayashi, M.; Sakurai, S.; Shimizu, H.; Morgan, J. B.; Stoltz, B. M. *Angew. Chem. Int. Ed.* **2019**, *58*, 1–6

Jiménez, T.; Campaña, A. G.; Bazdi, B.; Paradas, M.; Arráez-Román, D.; Segura-Carretero, A.; Fernández-Gutiérrez, A.; Oltra, J. E.; Robles, R.; Justicia, J.; Cuerva, J. M. *Eur. J. Org. Chem.* **2010**, 4288–4295.

Johansson, C. C. C.; Colacot, T. J. *Angew. Chem. Int. Ed.* **2010**, *49*, 676–707.

Jung, M. E.; Nishimura, N. *Org. Lett.* **2001**, *3*, 2113–2115.

Jung, S. T.; Lauchli, R.; Arnold, F. H. *Curr. Opin. Biotechnol.* **2011**, *22*, 809–817.

Kalek, M.; Himo, F. *J. Am. Chem. Soc.* **2012**, *134*, 19159–19169.

Kamel, H. N.; Slattery, M. *Pharmaceutical Biology* **2005**, *43*, 253–269.

Kanayama, T.; Yoshida, K.; Miyabe, H.; Takemoto, Y. *Angew. Chem. Int. Ed.* **2003**, *42*, 2054–2056.

Kantorowski, E. J.; Kurth, M. J. *Tetrahedron* **2000**, *56*, 4317–4353

Karimi, B.; Ender, D.; Jafari, E. *Synthesis*, **2013**, *45*, 2769–2812.

Kato, Y.; Furutachi, M.; Chen, Z.; Mitsunuma, H.; Matsunaga, S.; Shibasaki, M. *J. Am. Chem. Soc.* **2009**, *131*, 9168–9169.

Keana, J. F.; Seyedrezai, S. E. *J. Org. Chem.* **1982**, *42*, 347–352.

Keith, J. A.; Behenna, D. C.; Mohr, J. T.; Ma, S.; Marinescu, S. C.; Oxgaard, J.; Stoltz, B. M.; Goddard, W. A. *J. Am. Chem. Soc.* **2007**, *129*, 11876–11877.

- Kennedy-Smith, J. J.; Staben, S. T.; Toste, F. D. *J. Am. Chem. Soc.* **2004**, *126*, 4526–4527.
- Kille, S.; Zilly, F. E.; Acevedo, J. P.; Reetz, M. T. *Nat. Chem.* **2011**, *3*, 738–743.
- Kim, E. J.; Kang, Y. K.; Kim, D. Y. *Bull. Korean Chem. Soc.* **2009**, *30*, 1437–1438.
- Kim, Y. S.; Matsunaga, S.; Das, J.; Sekine, A.; Ohshima, T.; Shibasaki, M. *J. Am. Chem. Soc.* **2000**, *122*, 6506–6507.
- Kobayashi, S.; Mori, Y.; Fossey, J. S.; Salter, M. M. *Chem. Rev.* **2011**, *111*, 2626–2704.
- Korch, K. M.; Eidamshaus, C.; Behenna, D. C.; Nam, S.; Horne, D.; Stoltz, B. M. *Angew. Chem. Int. Ed.* **2015**, *54*, 179–183.
- Krause, N.; Hoffmann-Röder, A. *Synthesis* **2001**, 171–196.
- Krebs, A.; Kazmaier, U. *Tetrahedron Lett.* **1996**, *37*, 7945–7946.
- Krout, M. R.; Mohr, J. T.; Stoltz, B. M. *Org. Synth.* **2009**, *86*, 181–205.
- Kündig, E. P.; Seidel, T. M.; Jia, Y.; Bernardinelli, G. *Angew. Chem. Int. Ed.* **2007**, *46*, 8484–8487.
- Kumaraswamy, G.; Jena, N.; Sastry, M. N. V.; Padmaja, M.; Markondaiah, B. *Adv. Synth. Catal.* **2005**, *347*, 867–871.
- Kuwano, R.; Miyazaki, H.; Ito, Y. *Chem Commun.* **1998**, 71–72.
- Kuwano, R.; Miyazaki, H.; Ito, Y. *J. Organomet. Chem.* **2000**, *603*, 18–29.

Långström, B.; Göran, B. *Acta Chem. Scand.* **1973**, *27*, 3118–3119.

Lee, S.; Hartwig, J. F. *J. Org. Chem.* **2001**, *66*, 3402–3415.

Leonard, J.; Díez-Barra, E.; Merino, S. *Eur. J. Org. Chem.* **1998** 2051–2061.

Lewis, J. C.; Bastian, S.; Bennett, C. S.; Fu, Y.; Mitsuda, Y.; Chen, M. M.; Greenberg, W. A.; Wong, C.-H.; Arnold, F. H. *Proc. Natl. Acad. Sci. U. S. A.* **2009**, *106*, 16550–16555.

Lewis, J. C.; Mantovani, S. M.; Fu, Y.; Snow, C. D.; Komor, R. S. Wong, C.-H.; Arnold, F. H. *ChemBioChem* **2010**, *11*, 2502–2505.

Ley, S. V.; Norman, J.; Griffith, W. P.; Marsden, S. P. *Synthesis* **1994**, 639–666.

Liao, X.; Weng, Z.; Hartwig, J. F. *J. Am. Chem. Soc.* **2008**, *130*, 195–200.

Liu, W.-B.; Reeves, C. M.; Virgil, S. C.; Stoltz, B. M. *J. Am. Chem. Soc.* **2013**, *135*, 10626–10629.

Liu, W.-B.; Reeves, C. M.; Stoltz, B. M. *J. Am. Chem. Soc.* **2013**, *135*, 17298–17301.

Liu, X.; Lin, L.; Feng, X. *Acc. Chem. Res.* **2011**, *44*, 574–587.

Liu, Y.; Han, S. J.; Lui, W. B.; Stoltz, B. M. *Acc. Chem. Res.* **2015**, *48*, 740–751.

Liu, Y.; Liniger, M.; McFadden, R. M.; Roizen, J. L.; Malette, J.; Reeves, C. M.; Behenna, D. C.; Seto, M.; Kim, J.; Mohr, J. T. *Beilstein J. Org. Chem.* **2014**, *10*, 2501–2512.

Liu, Z.; Shi, M. *Organometallics*, **2010**, *29*, 2831–2834.

- Lyons, T. W.; Sanford, M. S. *Chem. Rev.* **2010**, *110*, 1147–1169.
- Majima, K.; Tosaki, S.-Y.; Ohshima, T.; Shibasaki, M. *Tetrahedron Lett.* **2005**, *46*, 5377–5381.
- Malherbe, R.; Belluš, D. *Helv. Chim. Acta* **1978**, *61*, 3096–3099.
- Malherbe, R.; Rist, G.; Belluš, D. *J. Org. Chem.* **1983**, *48*, 860–869.
- Manuel, M.; Marques, M. B. *Angew. Chem. Int. Ed.* **2006**, *45*, 348–352.
- Marigo, M.; Kjærsgaard, A.; Juhl, K.; Gathergood, N.; Jørgensen, K. A. *Chem. Eur. J.* **2003**, *9*, 2359–2367.
- Marinescu, S. C.; Nishimata, T.; Mohr, J. T.; Stoltz, B. M. *Org. Lett.* **2008**, *10*, 1039–1042.
- Martin, N. J. A.; List, B. *J. Am. Chem. Soc.* **2006**, *128*, 12268–13369.
- Martin, S. F. *Tetrahedron* **1980**, *36*, 419–460.
- Marziale, A. N.; Duquette, D. C.; Craig, II, R. A.; Kim, K. E.; Liniger, M.; Numajiri, Y.; Stoltz, B. M. *Adv. Synth. Catal.* **2015**, *357*, 2238–2245.
- Masamune, S.; Choy, W.; Kerdesky, F. A. J.; Imperiali, B. *J. Am. Chem. Soc.* **1981**, *103*, 1566–1568.
- Masahiro, M.; Masahiko, I.; Michinori, S.; Yoshihiko, I. *Bull. Chem. Soc. Jpn.* **1988**, *61*, 3649–3652.
- Masdeu-Bultó, A. M.; Diéguez, M.; Martin, E.; Gómez, M. *Coord. Chem. Rev.* **2003**, *242*, 159–201.

- Matsunaga, S.; Ohshima, T.; Shibasaki, M. *Adv. Synth. Catal.* **2002**, *344*, 3–15.
- Matsuzawa, A.; Mashiko, T.; Kumagai, N.; Shibasaki, M. *Angew. Chem. Int. Ed.* **2011**, *50*, 7616–7619.
- Mazet, C. *Synlett* **2012**, *23*, 1999–2004.
- McDougal, N. T.; Virgil, S. C.; Stoltz, B. M. *Synlett* **2010**, *11*, 1712–1716.
- McDougal, N. T.; Streuff, J.; Mukherjee, H.; Virgil, S. C.; Stoltz, B. M. *Tetrahedron Lett.* **2010**, *51*, 5550–5554.
- Mehta, G.; Shinde, H. M. *J. Org. Chem.* **2012**, *77*, 8056–8070.
- Mekelburger, H. B.; Wilcox, C. S. in *Comprehensive Organic Synthesis*, 2nd Edition (Eds. Knochel, P. and Molander, G. A.), Chap. 2, Elsevier, 2014, p. 243–272.
- Meyer, T. Y.; Garner, L. R.; Baenziger, N. C.; Messerie, L. *Inorg. Chem.* **1990**, *29*, 4045–4050.
- Mikiko, S.; Yoshitaka, H. *Bull. Chem. Soc. Jpn.* **2005**, *78*, 941–956.
- Miller, R. D.; McKean, D. R. *Synthesis*, **1979**, 730–732.
- Minko, Y.; Pasco, M.; Lercher, L.; Botoshansky, M.; Marek, I. *Nature*, **2012**, *490*, 522–526.
- Mino, T.; Masuda, S.; Nishio, M.; Yamashita, M. *J. Org. Chem.* **1997**, *62*, 2633–2635.
- Missakian, M. G.; Burreson, B. J.; Scheuer, P. J. *Tetrahedron* **1975**, *31*, 2513–2515.

- Mohr, J. T.; Behenna, D. C.; Harned, A. M.; Stoltz, B. M. *Angew. Chem. Int. Ed.* **2005**, *44*, 6924–6927.
- Mouri, S.; Chen, Z.; Matsunaga, S.; Shibasaki, M. *Chem Commun.* **2009**, 5138–5140.
- Müller, P. *Crystallography Reviews* **2009**, *15*, 57–83.
- Müller, S.; Liepold, B.; Roth, G. J.; Bestmann, H. J. *Synlett* **1996**, 521–522.
- Mukaiyama, T.; Matsuo, J.-I. in *Modern Aldol Reactions*, 1st Edition (Ed. R. Mahrwald), Chap. 3, Wiley, 2004, p. 127–160.
- Mukherjee, S.; Yang, J. W.; Hoffmann, S.; List, B. *Chem. Rev.* **2007**, *107*, 5471–5569.
- Murahashi, S.-I.; Take, K.; Naota, T.; Takaya, H. *Synlett* **2000**, 1016–1018.
- Muratake, H.; Hayakawa, A.; Natsume, M. *Tetrahedron Lett.* **1997**, *38*, 7577–7580.
- Muratake, H.; Natsume, M. *Tetrahedron Lett.* **1997**, *38*, 7581–7582.
- Nahra, F.; Macé, Y.; Boreux, A.; Billard, F.; Riant, O. *Chem. – Eur. J.* **2014**, *20*, 10970–10981.
- Nahra, F.; Macé, Y.; Lambin, D.; Riant, O. *Angew. Chem. Int. Ed.* **2013**, *52*, 3208–3212.
- Nakajima, M.; Yamaguchi, Y.; Hashimoto, S. *Chem. Commun.* **2001**, 1596–1597.
- Nakajima, M.; Yamamoto, S.; Yamaguchi, Y.; Nakamura, S.; Hashimoto, S. *Tetrahedron*, **2003**, *59*, 7307–7313.

Nakamura, M.; Hajra, A.; Endo, K.; Nakamura, E. *Angew. Chem. Int. Ed.* **2005**, *44*, 7248–7251.

Nakamura, A.; Nakada, M. *Synthesis* **2013**, *45*, 1421–1451.

Nahra, F.; Macé, Y.; Lambin, D.; Riant, O. *Angew. Chemie Int. Ed.* **2013**, *52*, 3208–3212.

Nemoto, T.; Matsumoto, T.; Masuda, T.; Hitoma, T.; Hatano, K.; Hamada, Y. *J. Am. Chem. Soc.* **2004**, *126*, 3690–2691.

Nerz-Stormes, M.; Thronton, E. R. *J. Org. Chem.* **1991**, *56*, 2489–2498.

Nestl, B. M.; Hammer, S. C.; Nebel, B. A.; Hauer, B. *Angew. Chem., Int. Ed. Engl.* **2014**, *53*, 3070–3095.

Newman, D. J.; Cragg, G. M.; Snader, K. M. *Nat Prod. Rep.* **2000**, *17*, 215–234.

Ngamnithiporn, A.; Jette, C. I.; Bachman, S.; Virgil, S. C.; Stoltz, B. M. *Chem. Sci.* **2018**, *9*, 2547–2551.

Noda, D.; Sunada, Y.; Hatakeyama, T.; Nakamura, M.; Nagashima, H. *Chem. Commun.* **2012**, *48*, 12231–12233.

Nojiri, A.; Kumagai, N.; Shibasaki, M. *J. Am. Chem. Soc.* **2008**, *130*, 5630–5631.

Notz, W.; Tanaka, F.; Barbas, C. F. *Acc. Chem. Res.* **2004**, *37*, 580–591.

Numajiri, Y.; Pritchett, B. P.; Chiyoda, K.; Stoltz, B. M. *J. Am. Chem. Soc.* **2015**, *137*, 1040–1043.

Oh, H.; Swenson, D. C.; Gloer, J. B.; Wicklow, D. T.; Dowd, P. F. *Tetrahedron Lett.* **1998**, *39*, 7633–7636.

Ohtsuka, Y.; Ikeno, T.; Yamada, T. *Tetrahedron: Asymmetry*, **2003**, *14*, 967–970.

Oisaki, K.; Suto, Y.; Kanai, M.; Shibasaki, M. *J. Am. Chem. Soc.* **2003**, *125*, 5644–5645.

Palucki, M.; Buchwald, S. L. *J. Am. Chem. Soc.* **1997**, *119*, 11108–11109.

Pangborn, A. M.; Giardello, M. A.; Grubbs, R. H.; Rosen, R. K.; Timmers, F. J. *Organometallics* **1996**, *15*, 1518–1520.

Panish, R.; Selvaraj, R.; Fox, J. M. *Org. Lett.* **2015**, *17*, 3978–3981.

Petrova, K. V.; Mohr, J. T.; Stoltz, B. M. *Org. Lett.* **2009**, *11*, 292–295.

Piers, E.; Wong, T.; Ellis, K. A. *Can. J. Chem.* **1992**, *70*, 2058–2064.

Prakash, J.; Marek, I. *Chem. Commun.* **2011**, *47*, 4593–4623.

Quinn, R. K.; Könst, Z. A.; Michalak, S. E.; Schmidt, Y.; Szklarski, A. R.; Flores, A. R.; Nam, S.; Horne, D. A.; Vanderwal, C. D.; Alexanian, E. *J. Am. Chem. Soc.* **2016**, *138*, 696–702.

Rambla, M.; Duroure, L.; Chabaud, L.; Guillou, C. *Eur. J. Org. Chem.* **2014**, 7716–7720.

Reetz, M. T. *Angew. Chem., Int. Ed. Engl.* **2001**, *40*, 284–310.

Reetz, M. T. *J. Am. Chem. Soc.* **2013**, *135*, 12480–12496.

Reetz, M. T.; Peter, R. *Tetrahedron Lett.* **1981**, *22*, 4691–4694.

- Reeves, C. M.; Behenna, D. C.; Stoltz, B. M. *Org. Lett.* **2014**, *16*, 2314–2317.
- Reeves, C. M.; Eidamshaus, C.; Kim, J.; Stoltz, B. M. *Angew. Chem. Int. Ed.* **2013**, *52*, 6718–6721.
- Rehbein, J.; Hiersemann, M. *Synthesis* **2013**, *45*, 1121–1159.
- Reich, H. J.; Holtan, R. C.; Borkowsky, S. L. *J. Org. Chem.* **1987**, *52*, 312–314.
- Renata, H.; Zhou, Q.; Dünstl, G.; Felding, J.; Merchant, R., R.; Yeh, C.-H.; Baran, P. S. *J. Am. Chem. Soc.* **2015**, *137*, 1330–1340.
- Rentmeister, A.; Arnold, F. H.; Fasan, R. *Nat. Chem. Biol.* **2009**, *5*, 26–28.
- Roiban, G.-D.; Reetz, M. T. *Chem. Commun.* **2015**, *51*, 2208–2224.
- Salmond, W. G.; Barta, M. A.; Havens, J. L. *J. Org. Chem.* **1978**, *43*, 2057–2059.
- Sasai, H.; Arai, T.; Shibasaki, M. *J. Am. Chem. Soc.* **1994**, *116*, 1571–1572.
- Sasai, H.; Emori, E.; Arai, T.; Shibasaki, M. *Tetrahedron Lett.* **1996**, *37*, 5561–5564.
- Sasai, H.; Itoh, N.; Suzuki, T.; Shibasaki, M. *Tetrahedron Lett.* **1993**, *34*, 855–858.
- Sasai, H.; Suzuki, T.; Arai, S.; Arai, T.; Shibasaki, M. *J. Am. Chem. Soc.* **1992**, *114*, 4418–4420.
- Sasai, H.; Suzuki, T.; Itoh, N.; Arai, S.; Shibasaki, M. *Tetrahedron Lett.* **1993**, *34*, 2657–2660.

Sasai, H.; Suzuki, T.; Itoh, N.; Shibasaki, M. *Tetrahedron Lett.* **1993**, *34*, 851–854.

Sasai, H.; Suzuki, T.; Itoh, N.; Tanaka, K.; Date, T.; Okamura, K.; Shibasaki, M. *J. Am. Chem. Soc.* **1993**, *115*, 10372–10373.

Satoh, T.; Kawamura, Y.; Miura, M.; Nomura, M. *Angew. Chem. Int. Ed.* **1997**, *36*, 1740–1742.

Sawamura, M.; Hamashima, H.; Ito, Y. *J. Am. Chem. Soc.* **1992**, *114*, 8295–8296.

Sawamura, M.; Hamashima, H.; Ito, Y. *Tetrahedron*, **1994**, *50*, 4439–4454.

Sawamura, M.; Hamashima, H.; Shinoto, H.; Ito, Y. *Tetrahedron Lett.* **1995**, *36*, 6479–6482.

Sawamura, M.; Nagata, H.; Sakamoto, H.; Ito, Y. *J. Am. Chem. Soc.* **1992**, *114*, 2586–2592.

Schetter, B.; Mahrwald, R. *Angew. Chem. Int. Ed.* **2006**, *45*, 7506–7525.

Schmuff, N. R.; Trost, B. M. *J. Org. Chem.* **1983**, *48*, 1404–1412.

Sears, J. E.; Boger, D. L. *Acc. Chem. Res.* **2015**, *48*, 653–662.

Seebach, S. *Angew. Chem. Int. Ed. Engl.* **1988**, *27*, 1624–1654.

Semmelhack, M. F.; Chong, B. P.; Stauffer, R. D.; Rogerson, T. D.; Chong, A.; Jones, L. D. *J. Am. Chem. Soc.* **1975**, *97*, 2507–2516.

Semmelhack, M. F.; Stauffer, R. D.; Rogerson, T. D. *Tetrahedron Lett.* **1973**, *14*, 4519–4522.

Shaw, S.; White, J. D. *J. Am. Chem. Soc.* **2014**, *136*, 13578–135

Sheldrick, G. M. *Acta Cryst.* **1990**, A46, 467–473.

Sheldrick, G. M. *Acta Cryst.* **2008**, A64, 112–122.

Shen, K.; Liu, X.; Wang, W.; Wang, G.; Cao, W.; Li, W.; Hu, X.; Lin, L.; Feng, X. *Chem. Sci.* **2010**, *1*, 590–595.

Shen, K.; Liu, X.; Zheng, K.; Li, W.; Hu, X.; Lin, L.; Feng, X. *Chem. Euro. J.* **2010**, *16*, 3736–3742.

Sherden, N. H.; Behenna, D. C.; Virgil, S. C.; Stoltz, B. M. *Angew. Chem. Int. Ed.* **2009**, *48*, 6840–6843.

Shibasaki, M.; Sasai, H.; Arai, T. *Angew. Chem. Int. Ed.* **1997**, *36*, 1236–1256.

Shibasaki, M.; Yoshikawa, N. *Chem Rev.* **2002**, *102*, 2187–2210.

Shimizu, S.; Tsubogo, T.; Xu, P.; Kobayashi, S. *Org. Lett.* **2015**, *17*, 2006–2008.

Shrestham R.; Dorn, S. C. M.; Weix, D. J. *J. Am. Chem. Soc.* **2013**, *135*, 751–762.

Shockley, S. E.; Hethcox, J. C.; Stoltz, B. M. *Angew. Chem. Int. Ed.* **2017**, *56*, 11545–11548.

Sibi, M. P.; Manyem, S. *Tetrahedron*, **2000**, *56*, 8033–8061

Sibi, M. P.; Tatamidani, H.; Patil, K. *Org. Lett.* **2005**, *7*, 2571–2573.

- Sladojevich, F.; Fuentes de Arriba, Á. L.; Ortín, I.; Yang, T.; Ferrali, A.; Paton, R. S.; Dixon, D. J. *Chem. Eur. J.* **2013**, *19*, 14286–14295.
- Sparling, B. A.; Moebius, D. C.; Shair, M. D. *J. Am. Chem. Soc.* **2013**, *135*, 644–647.
- Spielvogel, D. J.; Buchwald, S. L. *J. Am. Chem. Soc.* **2002**, *124*, 3500–3501.
- Spielvogel, D. J.; Davis, W. M.; Buchwald, S. L. *Organometallics* **2002**, *21*, 3833–3836.
- Sprinz, J.; Helmchen, G. *Tetrahedron Lett.* **1993**, *34*, 1769–1772.
- Staben, S. T.; Kennedy-Smith, J. J.; Toste, F. D. *Angew. Chem. Int. Ed.* **2004**, *43*, 5350–5352.
- Stark, M. A.; Jones, G.; Richards, C. J. *Organometallics*, **2000**, *19*, 1282–1291.
- Stoltz, B. M.; Kano, T.; Corey, E. J. *J. Am. Chem. Soc.* **2000**, *122*, 9044–9045.
- Stork, G.; Danheiser, R. L. *J. Org. Chem.* **1973**, *38*, 1775–1776.
- Streuff, J.; White, D. E.; Virgil, S. C.; Stoltz, B. M. *Nature Chem.* **2010**, *2*, 192–196.
- Subramaniapillai, S. G. *J. Chem. Sci.* **2013**, *125*, 467–482.
- Sun, Y.-W.; Zhu, P.-L.; Xu, Q.; Shi, M. *RSC Adv.* **2013**, *3*, 3153–3168.
- Suzuki, H.; Koyama, Y. *Tetrahedron Lett.* **1979**, *20*, 1415–1418.
- Suzuki, T.; Torii, T. *Tetrahedron: Asymmetry* **2001**, *12*, 1077–1081.

- Takahashi, K.; Ishiyama, T.; Miyaura, N. *J. Organomet. Chem.* **2001**, *47*–53.
- Takasu, K.; Nagao, S.; Ihara, M. *Tetrahedron Lett.* **2005**, *46*, 1005–1008.
- Takayama, H.; Katakawa, K.; Kitajima, M.; Yamaguchi, K.; Aimi, N. *Tetrahedron Lett.* **2002**, *43*, 8307–8311.
- Takenaka, K.; Minakawa, M.; Uozumi, Y. *J. Am. Chem. Soc.* **2005**, *127*, 12273–12281.
- Takenaka, K.; Uozumi, Y. *Org. Lett.* **2004**, *6*, 1833–1835.
- Taylor, A. M.; Altman, R. A.; Buchwald, S. L. *J. Am. Chem. Soc.* **2009**, *131*, 9900–9901.
- Taylor, R. J. K. *Synthesis* **1985**, 364–392.
- Thominiaux, C.; Roussé, S.; Desmaële, D.; d'Angelo, J.; Riche, C. *Tetrahedron: Asymmetry* **1999**, *10*, 2015–2021.
- Ting, A.; Schaus, S. E. *Eur. J. Org. Chem.* **2007**, 5797–5815.
- Trost, B. M. *Tetrahedron* **2015**, *71*, 5708–5733.
- Trost, B. M.; Ball, Z. T. *J. Am. Chem. Soc.* **2001**, *123*, 12726–12727.
- Trost, B. M.; Bream, R. N.; Xu, J. *Angew. Chem. Int. Ed.* **2006**, *45*, 3109–3112.
- Trost, B. M.; Frederiksen, M. U. *Angew. Chem. Int. Ed.* **2005**, *44*, 308–310.
- Trost, B. M.; Pissot-Soldermann, C.; Chen, I. *Chem. Eur. J.* **2005**, *11* 951–959.
- Trost, B. M.; Radinov, R.; Grenzer, E. M. *J. Am. Chem. Soc.* **1997**, *119*, 7879–7880.

- Trost, B. M.; Schroeder, G. M. *J. Am. Chem. Soc.* **1999**, *121*, 6759–6760.
- Trost, B. M.; Schroeder, G. M. *Chem. Eur. J.* **2005**, *11*, 174–184.
- Trost, B. M.; Schroeder, G. M.; Kristensen, J. *Angew. Chem. Int. Ed.* **2002**, *41*, 3492–3495.
- Trost, B. M.; Van Vranken, D. L. *Chem. Rev.* **1996**, *96*, 395–422. (b) Trost, B. M. *J. Org. Chem.* **2004**, *69*, 5813–5837.
- Trost, B. M.; Xu, J. *J. Am. Chem. Soc.* **2005**, *127*, 2846–2847.
- Trost, B. M.; Xu, J.; Schmidt, T. *J. Am. Chem. Soc.* **2009**, *131*, 18343–18357.
- Trost, B. M.; Zhang, Y. *J. Am. Chem. Soc.* **2006**, *128*, 4590–4591.
- Trost, B. M.; Zhang, Y. *J. Am. Chem. Soc.* **2007**, *129*, 14548–14549.
- Tsuji, J.; Minami, I.; Shimizu, I. *Tetrahedron Lett.* **1983**, *24*, 1793–1796.
- Turner N. *J. Nat. Chem. Biol.* **2009**, *5*, 567–573.
- Verkade, J. M. M.; van Hemert, L. J. C.; Quaedflieg, P. J. L. M.; Rutjes, F. P. J. T. *Chem. Soc. Rev.* **2008**, *37*, 29–41.
- Von Matt, P.; Pfaltz, A. *Angew. Chem., Int. Ed. Engl.* **1993**, *32*, 566–568.
- Wang, Y.; Kuang, Y.; Wang, Y. *Chem. Commun.* **2015**, *51*, 5852–5855.
- Wang, Z.; Yang, Z.; Chen, D.; Liu, X.; Lin, L.; Feng, X. *Angew. Chem. Int. Ed.* **2011**, *50*, 4928–4932.

- Weaver, J. D.; Recio, A.; Grenning, A. J.; Tunge, J. A. *Chem. Rev.* **2011**, *111*, 1846–1913.
- Wehmeyer, R. M.; Rieke, R. D. *J. Org. Chem.* **1987**, *52*, 5056–5057.
- Weidmann, V.; Maison, W. *Synthesis* **2013**, *45*, 2201–2221.
- Wellington, K. D.; Cambie, R. C.; Rutledge, P. S.; Bergquist, P. R. *J. Nat. Prod.* **2000**, *63*, 79–85.
- Wencel-Delord, J.; Dröge, T. *Chem. Soc. Rev.* **2011**, *40*, 4740–4761.
- Wendlandt, A. E.; Suess, A. M.; Stahl, S. S. *Angew. Chem., Int. Ed. Engl.* **2011**, *50*, 11062–11087.
- Whitehouse, C. J. C.; Bell, S. G.; Tufton, H. G.; Kenny, R. J. P.; Ogilvie, L. C. I.; Wong, L. L. *Chem. Commun.* **2008**, 966–968.
- Whitehouse, C. J.; Bell, S. G.; Wong, L. L. *Chem. Soc. Rev.* **2012**, *41*, 1218–1260.
- Wilde, N. C.; Isomura, M.; Mendoza, A.; Baran, P. S. *J. Am. Chem. Soc.* **2014**, *136*, 4909–4912.
- Wohlgemuth, R. *Curr. Opin. Biotechnol.* **2010**, *21*, 713–724.
- Wolberg, M.; Hummel, W.; Wandrey, C.; Müller, M. *Angew. Chem., Int. Ed. Engl.* **2000**, *39*, 4306–4308.
- Wright, T. B.; Evans, P. A. *J. Am. Chem. Soc.* **2016**, *138*, 1503–15306.
- Wu, Q.-F.; He, H.; Liu, W.-B.; You, S.-L. *J. Am. Chem. Soc.* **2010**, *132*, 11418–11419.

- Wu, Q.-F.; Zheng, C.; You, S.-L. *Angew. Chem. Int. Ed.* **2012**, *51*, 1680–1683.
- Wurtz, A. C. *Bull. Soc. Chim. Fr.* **1872**, *17*, 436–442.
- Xie, X.; Chen, Y.; Ma, D. *J. Am. Chem. Soc.* **2006**, *128*, 16050–16051.
- Xing, X.; O'Connor, N. R.; Stoltz, B. M. *Angew. Chem., Int. Ed. Engl.* **2015**, *54*, 11186–11190.
- Yamaguchi, J.; Yamaguchi, A. D.; Itami, K. *Angew. Chem. Int. Ed. Engl.* **2012**, *51*, 8960–9009.
- Yamashita, Y.; Odashima, K.; Koga, K. *Tetrahedron Lett.* **1999**, *40*, 2803–2806.
- Yanagisawa, A.; Lin, Y.; Miyake, R.; Yoshida, K. *Org. Lett.* **2014**, *16*, 86–89.
- Yang, T.; Ferrali, A.; Sladojevich, F.; Campbell, L.; Dixon, D. J. *J. Am. Chem. Soc.* **2009**, *131*, 9140–9141.
- Yasufumi, T.; Atsushi, K.; Eiji, K.; Sotaro, M. *Chem. Lett.* **1995**, *24*, 957–958.
- Yoon, T. P.; Dong, V. M.; MacMillan, D. W. C. *J. Am. Chem. Soc.* **1999**, *121*, 9726–9727.
- Yoon, T. P.; MacMillan, D. W. C. *J. Am. Chem. Soc.* **2001**, *123*, 2911–2912.
- Yoshikai, N.; Zhang, S.-L.; Yamagata, K.-I.; Tsuji, H.; Nakamura, E. *J. Am. Chem. Soc.* **2009**, *131*, 4099–4109.
- You, S.-L.; Dai, L.-X. *Angew. Chem. Int. Ed.* **2006**, *45*, 5246–5248.

Young, W. B.; Masters, J. J.; Danishefsky, S. *J. Am. Chem. Soc.* **1995**, *117*, 5228–5234.

Yu, J.-Q.; Corey, E. *J. Org. Lett.* **2002**, *4*, 2727–2730.

Yu, K.; Jackson, J. J.; Nguyen, T. D.; Alvatado, J.; Stivala, C. E.; Ma, Y.; Mack, K. A.; Hayton, T. W.; Collum, D. B.; Zakarian, A. *J. Am. Chem. Soc.* **2017**, *139*, 527–533.

Yusuke, I.; Isao, S.; Akio, Y. *Bull Chem. Soc. Jpn.* **2004**, *77*, 2033–2045.

Zhang, K.; Shafer, B. M.; Demars, M. D., II; Stern, H. A.; Fasan, R. *J. Am. Chem. Soc.* **2012**, *134*, 18695–18704.

Zhang, P.-P.; Yan, Z.-M.; Li, Y.-H.; Gong, J.-X.; Yang, Z. *J. Am. Chem. Soc.* **2017**, *139*, 13989–13992.

Zhang, T. Y.; Zhang, H. *Tetrahedron Lett.* **2002**, *43*, 1363–1365.

Zhao, Y.; Yeung, Y.-Y. *Org. Lett.* **2010**, *12*, 2128–2131.

Zhu, J.; Germain, A. R.; Porco, J. A. Jr. *Angew. Chem., Int. Ed. Engl.* **2004**, *43*, 1239–1243.

Ziegler, F. E. *Chem. Rev.* **1988**, *88*, 1423–1452.

Zou, Y.; Millar, J. G. *J. Org. Chem.* **2009**, *74*, 7207–7209.

INDEX

#

- 1,3 dicarbonyl..... 19, 23-24, 28, 30, 32, 37,

α

- | | |
|----------------------------------|------------------|
| α -alkenylation | 67 |
| α - arylation..... | 67–84, 105 |
| α -bromo | 6, 221, 320, 325 |
| α -vinylation..... | 68–72 |
| α,β -unsaturated..... | 6–7, 17, 86, 219 |

β

- β -ketoester 13–15, 19–21, 23, 26, 29, 35–46, 49–53, 56, 58, 61, 64, 83, 89–90,
92, 111–117, 123–125, 128–147, 151–152, 219–221, 235–237
 β -scission 332

π

- π -allyl..... 11, 53

A

- | | |
|--------------------|---|
| acetone | 321 |
| acyclic | 23–24, 35, 38, 44, 54, 62–65, 67 |
| ADH | 227–228, 244, 257 |
| aldimine | 20, 22–25 |
| aldol | 4, 9–10, 12–13, 15–18, 36, 95, 220–221, 321, 328–329, 375 |
| alkylation | 11, 18, 51–67, 109–119, 219–221, 227–228, 253, 320, 324 |
| alkyne | 88–90, 222, 240–241, 318, 320–321, 327, 336–337, 365, 530–531 |
| allylic alkylation | 51–57, 59–64–109–161, 219–221, 228, 253, 320, 324 |
| allylic anion | 531 |
| amide | 3–6, 17, 22, 34, 72–73, 87, 90–91, 319–320, 327, 336–337, 349–350, 530, 533 |

- aminophosphine ligand 52, 68–70, 73
 asymmetric 1–108, 219–221, 228, 253, 320, 324, 446, 466, 486, 504

B

- bidentate ligand 16, 80
 BINAP 20, 33, 40–41, 45, 67–68, 71–72, 80–82
 BINOL 23–24, 36–40, 49–50, 61, 63–64
 bioactive 18, 110, 317
 boron 9–10, 17, 84–85, 219, 222–223, 229, 241–242
 BOX ligand 19, 25, 87–88

C

- calcium 25, 49–50
 carbon monoxide 231, 327
 carboxylic acid 32, 48, 63, 65, 84, 91, 119, 121–122, 148, 150, 222, 225, 231, 240, 319
 carvone 319–320, 327–328, 330, 333–334, 373, 530
 cerium 228, 232, 326, 344, 374, 530, 533
 chelate (chelation) 21, 28, 30, 37–38, 43, 46, 85, 87
 chromium 64–65
 Claisen 84–88
 co-catalyst 89
 cobalt 26–28
 Conia-ene 88–93
 conjugate addition 6–7, 11, 25, 30–31, 37, 46, 50–51, 333–334
 copper 11, 19, 31–32, 83–84, 88, 90–91, 229
 cross-coupling 219–223
 cyanoketones 20, 22
 cyclic 12, 20–24, 26, 29, 35–36, 38–41, 44–45, 49, 52, 56–58, 61, 64–66
 69, 78, 81, 109–113
 cycloaddition, [2+2] 330–332
 cyclohexadiene 318, 327
 cyclopentanone 68, 70, 109–161
 cyclopentene 127, 318, 320–321, 325–326, 328

D

- decarboxylative 53–54, 109–161
 desamino ligand 69–70
 diamine ligand 26–27, 29–31, 35
 diastereoselective 4, 12, 21, 39, 325, 333–334
 DIBAL 321, 326, 346, 374
 Dieckmann 123–124
 Diels–Alder 318–319, 323–324, 327–328, 330–331, 375, 529–530
 dienone 219, 221, 223
 directed epoxidation 328, 331
 diyne 330
 DMAP 122, 148, 321, 327, 330, 339, 351–352, 3550, 360, 373, 375–376, 530, 535
 DMP 227–229, 244–245, 257, 321, 334, 364, 276, 531, 537

E

- enantioselective 39, 41, 43, 53, 63, 75, 79, 84, 109–161, 217–256, 258, 285, 320, 325
 enolate 1–109, 159, 220, 320, 324, 329
 enzymatic 218, 220, 225, 228, 246, 254
 epoxidation 319, 328, 331
 epoxide 319, 328, 331, 357–358, 362–363
 europium 32

F

- ferrocenylphosphine ligand 59

G

- gold 89
 Grignard 6, 530, 533

H

- HMDS 5, 8, 56–57, 63–64, 79, 81–82, 85–86
 homologation 90
 hydroboration 17, 222, 241

hydrolysis.....	220, 319
hydrosilylation.....	7–8, 331, 370

I

ineleganolide	317–318, 320
ionic liquid	44–45
iridium.....	35, 60–63
iron.....	41, 88, 92–92, 101
isocarvone	319

J

Jonphos	69
---------------	----

K

ketal	320
ketalization.....	46

L

lactam.....	53–54, 64, 79
lactone.....	24, 64, 81–82, 367
lanthanum.....	36–38, 40, 88
LDA.....	5–6, 56–57, 221–222, 234, 240, 257
Lewis acid.....	3, 24, 56–57, 81, 87, 89, 91
ligand screen.....	28, 31, 42, 69, 71, 75–77, 89, 91–92, 112–113, 226
linalool	325–326, 374
low catalyst loading.....	14, 43, 54, 70, 118–119, 151–152
Luche	325, 530

M

macrocycle	318, 321, 323, 531
manganese.....	50–51
Mannich reaction.....	19–25, 45, 54

- metathesis 318, 321, 323, 531
- methyl vinyl ketone 26, 28–29, 31–32, 35–36, 38–39, 40–42, 45, 47, 49
- Michael addition 25–50, 333–334
- molybdenum 59–60
- monophosphine ligand 71
- MOP ligand 70–71

N

- N*-heterocyclic carbene (NHC) 21, 45, 73, 75–76
- N,N'*-dioxide ligand 17, 47–48
- NADPH 227, 246–247
- natural product 2, 110–111, 119, 219, 227, 317
- neodymium 15, 17
- nickel 11, 13, 15, 23, 28–31, 64, 78–83
- nigelladine A 217–258, 285
- norcembranoid 317, 318, 323

O

- Ohira–Bestmann 320, 336, 373
- olefin isomerization 8, 223, 248, 318, 320, 324
- oxa–Michael 333–334
- oxidation 217–256, 258, 285, 318, 321, 324–325, 327–329, 331–334, 531
- oxidative enolate coupling 324, 329
- oxindole 15, 17, 19, 25, 30–31, 50, 58–59, 71–75

P

- P-PHOS (ligand) 64, 80, 82–83
- palladium 11, 13, 14, 19–22, 42–46, 51–59, 67–79, 88–89, 109–161, 228, 327, 350
- Pavidolide 317
- Pericyclic reaction 84
- phosphinooxazoline (PHOX) 52–54, 77, 109–114, 116–119, 139, 151–152
221, 229, 237, 253, 257, 321
- photocycloaddition 331
- pincer complex ligand 42–43

platinum 13–14, 41

Q

quaternary center 1–114, 118–119, 128, 159, 219, 221, 228

R

rearrangement 7–8, 84–88, 107–108, 222
 reduction 84, 321, 325–326, 530
 regioselective 3, 225–226
 retrosynthetic analysis 219–220, 318–319, 324, 329–330, 530
 rhodium 12–13, 33–36, 63–64
 ring expansion 329–334, 376, 529

S

saponification 222, 327, 330
 scabrolide A 317–372, 377, 444, 529–539
 scabrolide B 317–318
 scandium 15–16, 22–23, 47–48
 SEGPHOS ligand 20, 80, 89
 selectivity 3, 5–6, 9–10, 13–14, 20–27, 29–35, 38–41, 43–44, 46, 48, 50, 54, 58, 62, 65–66
 68–70, 80–81, 85–87, 89, 91–92, 217–219, 224–228, 246–247, 249, 322, 325
 silver 92, 332
 silyl enol ether 6–8, 52, 66, 127, 152–153, 159, 320
 sinolochmodin C 317–318
 Stork–Danheiser 220

T

tautomerization 88
 transition state 2–5, 12–13, 17–18, 21–22, 46
 TRAP ligand 12–13, 33–34
 Trost ligand 56–59

U

UHPLC 225, 227, 248, 249

V

vinylogous 58, 232, 325

W

Wacker oxidation 159, 220–221

Wittig olefination 321, 326

X

XPhos ligand 222–223, 242, 257

X-ray 222, 253, 285–316, 328, 331–333, 444–528

Y

Yamaguchi esterification 321, 529, 531

yonarolide 317–318

yttrium 47–48

Z

Zimmerman–Traxler transition state 4

zwitterionic 13, 86

ABOUT THE AUTHOR

Steven Anthony Loskot was born in San Jose, California on October 7th, 1991 to Victor and Annette Loskot. Steven was raised in San Jose with his older brother, Daniel Loskot. Steven's love for science and engineering stemmed from his father, who was an engineer. Originally Steven was interested in biology thanks to his AP biology teacher, Mr. Wong, at Bellarmine College Preparatory, but was convinced by him to pursue a degree in biochemistry.

In the fall of 2010, Steven moved to Seattle, Washington to attend the University of Seattle, a small Jesuit, liberal arts college for a B.S. in biochemistry. After the first organic chemistry class taken, instructed by Professor Joe Langenhan, Steven immediately fell in love with it and sought to perform research with Professor Langenhan. Under the tutelage of Professor Langenhan, Steven performed research in a number of subfields of organic chemistry, specifically with natural product total synthesis being is favorite area of research.

In the summer of 2013, Steven solidified his interest and intent to study the field of organic synthesis when he conduct research under Professor Neil Garg at UCLA as an Amgen Scholar. During his time there, he learned what it was truly like to be on the forefront of research in pursuit of the total synthesis of the complex natural product tubingensin A.

Following his undergraduate education, Steven moved to Pasadena, California to pursue his doctoral studies at the California Institute of Technology with Professor Brian Stoltz. His doctoral research has focused on the pursuit of the asymmetric total synthesis

of alkaloids and terpenoids. Upon completion of his doctoral research in May, 2019, Steven will begin his professional career as a medicinal chemist at Janssen, San Diego.